



UNIVERSITAT DE
BARCELONA

Syntaxin-1A, a synaptic-related protein in breast and head and neck cancer progression and prognosis

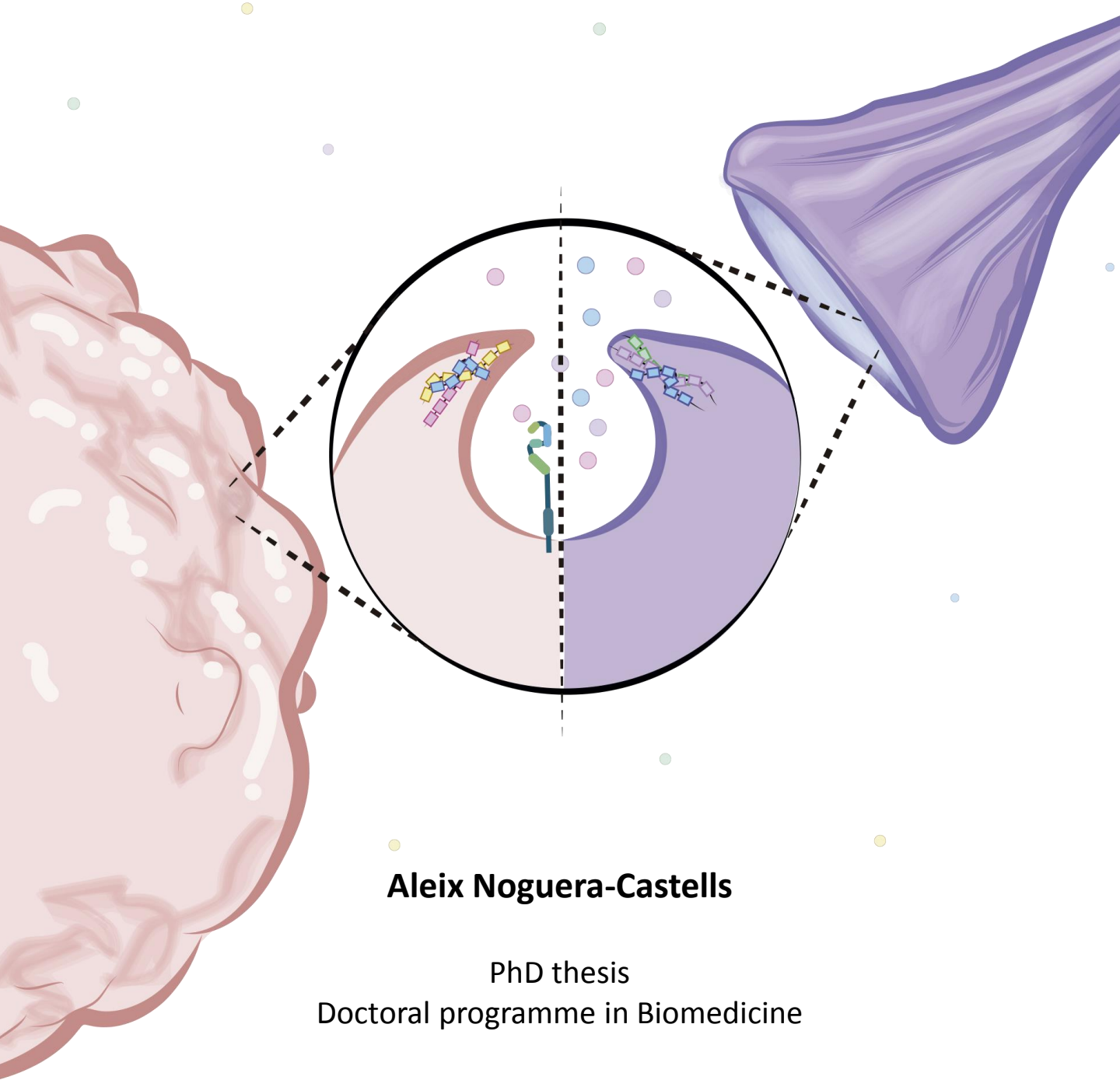
Aleix Noguera-Castells

ADVERTIMENT. La consulta d'aquesta tesi queda condicionada a l'acceptació de les següents condicions d'ús: La difusió d'aquesta tesi per mitjà del servei TDX (www.tdx.cat) i a través del Dipòsit Digital de la UB (diposit.ub.edu) ha estat autoritzada pels titulars dels drets de propietat intel·lectual únicament per a usos privats emmarcats en activitats d'investigació i docència. No s'autoritza la seva reproducció amb finalitats de lucre ni la seva difusió i posada a disposició des d'un lloc aliè al servei TDX ni al Dipòsit Digital de la UB. No s'autoritza la presentació del seu contingut en una finestra o marc aliè a TDX o al Dipòsit Digital de la UB (framing). Aquesta reserva de drets afecta tant al resum de presentació de la tesi com als seus continguts. En la utilització o cita de parts de la tesi és obligat indicar el nom de la persona autora.

ADVERTENCIA. La consulta de esta tesis queda condicionada a la aceptación de las siguientes condiciones de uso: La difusión de esta tesis por medio del servicio TDR (www.tdx.cat) y a través del Repositorio Digital de la UB (diposit.ub.edu) ha sido autorizada por los titulares de los derechos de propiedad intelectual únicamente para usos privados enmarcados en actividades de investigación y docencia. No se autoriza su reproducción con finalidades de lucro ni su difusión y puesta a disposición desde un sitio ajeno al servicio TDR o al Repositorio Digital de la UB. No se autoriza la presentación de su contenido en una ventana o marco ajeno a TDR o al Repositorio Digital de la UB (framing). Esta reserva de derechos afecta tanto al resumen de presentación de la tesis como a sus contenidos. En la utilización o cita de partes de la tesis es obligado indicar el nombre de la persona autora.

WARNING. On having consulted this thesis you're accepting the following use conditions: Spreading this thesis by the TDX (www.tdx.cat) service and by the UB Digital Repository (diposit.ub.edu) has been authorized by the titular of the intellectual property rights only for private uses placed in investigation and teaching activities. Reproduction with lucrative aims is not authorized nor its spreading and availability from a site foreign to the TDX service or to the UB Digital Repository. Introducing its content in a window or frame foreign to the TDX service or to the UB Digital Repository is not authorized (framing). Those rights affect to the presentation summary of the thesis as well as to its contents. In the using or citation of parts of the thesis it's obliged to indicate the name of the author.

Syntaxin-1A, a synaptic-related protein in breast and head and neck cancer progression and prognosis

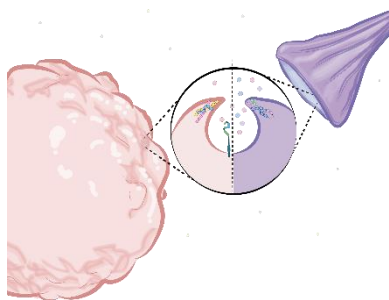


Aleix Noguera-Castells

PhD thesis
Doctoral programme in Biomedicine



UNIVERSITAT DE
BARCELONA



- Cover designed by Darya Kulyk -



UNIVERSITAT DE
BARCELONA

PhD thesis

Doctoral programme in Biomedicine

Syntaxin-1A, a synaptic-related protein in breast and head and neck cancer progression and prognosis

Aleix Noguera-Castells

A thesis to obtain the degree of

Doctor in Philosophy by the Universitat de Barcelona

This thesis has been performed under the direction of Dr. M. Neus Carbó Carbó and Dr. Mario Mancino, in the laboratory of Molecular and Translational Oncology (IDIBAPS-Fundació Clínic, Faculty of Medicine, Medicine department, Universitat de Barcelona) and New Strategies against Cancer (Faculty of Biology, Biochemistry and Molecular Biomedicine department, Universitat de Barcelona).

M. Neus Carbó Carbó
Director

Maria Neus
Carbo Carbo -
DNI
79285171P
(TCAT)

Signat digitalment
per Maria Neus
Carbo Carbo - DNI
79285171P (TCAT)
Data: 2021.09.29
17:43:05 +02'00'

Mario Mancino
Director

Aleix Noguera-Castells
PhD candidate

ALEIX
NOGUERA
CASTELLS - DNI
39389075B

Firmado digitalmente
por ALEIX NOGUERA
CASTELLS - DNI
39389075B
Fecha: 2021.09.29
15:07:38 +02'00'

Francesc Cardellach López
Tutor

FRANCESC
CARDELLACH
LOPEZ - DNI
39121893C
(TCAT)

Firmado digitalmente por
FRANCESC CARDELLACH LOPEZ -
DNI 39121893C (TCAT)
Nombre de reconocimiento (DNI):
cs-ES_o=Universitat de Barcelona,
2.5.4.97=VATES-Q0818001J,
ou=Empleat public de nivell mig,
sn=CARDELLACH LOPEZ - DNI
39121893C,
givenName=FRANCESC,
serialNumber=IDCES-39121893C,
cn=FRANCESC CARDELLACH LOPEZ
- DNI 39121893C (TCAT)
Fecha: 2021.09.29 14:19:59 +02'00'

Faculty of Medicine
2021

The work presented in this doctoral dissertation has been developed with the financial support from Fundació per a la Recerca en Oncologia i Immunologia (FROI) and from Universitat de Barcelona (UB) (*Ajuts de personal investigador predoctoral en formació (APIF)* and *ajuts per a la finalització de la tesi doctoral*) predoctoral fellowships. Moreover, the research project has been funded by Fundació Cellex (Barcelona, Spain), Carlos III Health Institute from the Ministry of Economy and Competitiveness of the Spanish Government (PI15/00661). The research team belongs to the 2017SGR01305 from the AGAUR (Agència de Gestió d'Ajuts Universitaris i de Recerca de Catalunya) and to the Institute of Biomedicine of UB (IBUB).

The international internship in Dr. Marc Coppolino's laboratory at the University of Guelph (Guelph, Canada) was funded by Universitat de Barcelona APIF travel grant. Furthermore, assistance to congresses and workshops was financed by Eurolife, Meeting Bursary Award for the Metastasis Research Society and by Fundació Cellex.



UNIVERSITAT DE
BARCELONA

IDIBAPS

Institut
D'Investigacions
Biomèdiques
August Pi i Sunyer

Fundació Privada
CELLEX

FUNDACIÓ
CLÍNIC
BARCELONA



Agència
de Gestió
d'Ajuts
Universitaris
i de Recerca


eurolife
network of european universities in life sciences



MRS METASTASIS
RESEARCH SOCIETY

UNIVERSITY
of GUELPH

Syntaxin-1A, a synaptic related protein in breast and head and neck cancer progression and prognosis



*Gràcies a tothom qui ha fet possible que un heatmap
i unes corbes Kaplan-Meier es convertissin en el que s'han convertit:*

*Pere, Neus, Mario, Paloma, Gemma, Patri, Anna, Leire, Núria, Alba, Darya, Patri J.,
Javi, Raúl, Marc C., Míriam, Àngels i al laboratori del Dr. Soriano i als
otorrinolaringòlegs de l'Hospital Clínic i de l'Hospital de la Santa Creu i Sant Pau.*

Gràcies als meus pares, avis i a tu, Queralt.

*Aquí tens el meu desig: camina.
Camina lluny.
Camina com qui vol saber-ho tot.
Camina fins a trencar-te:
Camina*

- Txarango -



Syntaxin-1A, a synaptic related protein in breast and head and neck cancer progression and prognosis

SUMMARY

ABBREVIATIONS	1
ABSTRACT.....	11
INTRODUCTION	15
1. CANCER.....	17
1.1. HALLMARKS OF CANCER	18
1.1.1. SUSTAINING PROLIFERATIVE SIGNALLING	19
1.1.2. EVADING GROWTH SUPPRESSORS	19
1.1.3. AVOIDING IMMUNE DESTRUCTION	20
1.1.4. ACTIVATING INVASION AND METASTASIS	20
1.1.5. TUMOUR-PROMOTING INFLAMMATION	20
1.1.6. ENABLING REPLICATIVE IMMORTALITY	21
1.1.7. INDUCING ANGIOGENESIS	21
1.1.8. GENOME INSTABILITY AND MUTATION.....	21
1.1.9. RESISTING CELL DEATH	22
1.1.10. DEREGULATING CELL ENERGETICS.....	22
1.2. TUMOUR MICROENVIRONMENT	22
1.3. COMPONENTS OF THE TUMOUR MICROENVIRONMENT	23
1.3.1. IMMUNE CELLS	23
1.3.2. CANCER-ASSOCIATED FIBROBLASTS	24
1.3.3. CANCER-ASSOCIATE ADIPOCYTES.....	25
1.3.4. EXTRACELLULAR MATRIX.....	25
1.3.5. BLOOD VESSELS	25
1.3.6. LYMPHATIC VESSELS	26
1.3.7. NERVOUS SYSTEM	26
1.4. NERVOUS SYSTEM AND CANCER.....	28
1.5. NEONEUROGENESIS.....	29
1.6. INTERACTION WITH SOLUBLE FACTORS.....	30
1.7. THE INFLUENCE OF THE NERVOUS SYSTEM IN TUMOUR PROGRESSION	33
1.8. THE INFLUENCE OF THE NERVOUS SYSTEM IN TUMOUR INVASION AND DISSEMINATION	34

1.9.	THE NERVOUS SYSTEM AS A THERAPEUTIC TOOL IN CANCER TREATMENT.....	35
2.	SNARE PROTEINS.....	38
2.1.	SNARE PROTEINS STRUCTURE.....	39
2.1.1.	SNARE MOTIF.....	39
2.2.	SNARE PROTEINS CLASSIFICATION.....	41
2.3.	REGULATION OF SNARE COMPLEX ASSEMBLY AND FUNCTION.....	42
2.3.1.	Sec1/Munc18 PROTEIN FAMILY.....	43
2.3.2.	TETHERING FACTORS.....	43
2.4.	SNARE LOCALIZATION AND SPECIFICITY.....	45
2.4.1.	LOCALIZATION.....	45
2.4.2.	SPECIFICITY.....	45
2.5.	SNARE HYPOTHESIS: FROM THE BEGINNING TO THE MOST RECENT RESEARCH.....	46
2.5.1.	SNARE CYCLING IN MEMBRANE FUSION.....	47
2.6.	SNARE ROLE IN CANCER.....	50
2.6.1.	ROLE OF SNARE PROTEINS IN TUMOUR PROLIFERATION.....	51
2.6.2.	ROLE OF SNARE PROTEINS IN RESISTANCE TO CELL DEATH AND AUTOPHAGY.....	51
2.6.3.	ROLE OF SNARE PROTEINS IN INVASION AND METASTASIS.....	52
2.6.4.	SNARE PROTEINS AS BIOMARKERS.....	53
3.	SYNTAXIN-1A.....	54
3.1.	SYNTAXIN FAMILY AND DOMAINS.....	54
3.2.	ROLE OF SYNTAXIN-1A IN NEURONS.....	56
3.3.	SYNTAXIN-1A IN NON-NEURONAL TISSUES.....	58
3.4.	SYNTAXIN-1A ROLE IN CANCER.....	60
4.	BREAST CANCER.....	62
4.1.	EPIDEMIOLOGY OF BREAST CANCER.....	62
4.2.	BREAST CANCER SUBTYPES.....	63
4.2.1.	HISTOPATHOLOGICAL CLASSIFICATION.....	63
4.2.2.	CLINICAL CLASSIFICATION.....	64
4.2.3.	MOLECULAR INTRINSIC CLASSIFICATION.....	65
4.2.1.	DIFFERENTIAL EXPRESSION OF NEUROGENES AMONG BREAST CANCER SUBTYPES	69
4.3.	HER2-POSITIVE BREAST CANCER SUBTYPES.....	70
4.3.1.	HER FAMILY OF RECEPTORS.....	70
4.3.2.	HER2 SIGNALLING.....	72
4.3.3.	HER2 INTERNALIZATION.....	73
4.3.4.	HER2 IN CANCER THERAPIES.....	74

4.4.	HER2-NEGATIVE BREAST CANCER SUBTYPES	78
4.4.1.	LUMINAL A BREAST CANCER SUBTYPE	78
4.4.2.	TRIPLE NEGATIVE BREAST CANCER SUBTYPE.....	81
4.5.	BREAST CANCER DIAGNOSIS AND TREATMENT	83
4.5.1.	DIAGNOSIS	83
4.5.2.	BREAST CANCER THERAPY FOR NON-METASTATIC BREAST CANCER.....	85
4.5.3.	BREAST CANCER THERAPY FOR ADVANCED AND METASTATIC BREAST CANCER ...	87
5.	HEAD AND NECK CANCER.....	90
5.1.	EPIDEMIOLOGY	90
5.2.	PATHOPHYSIOLOGY	91
5.2.1.	INITIATION AND EARLY EVENTS IN HPV-NEGATIVE HEAD AND NECK CANCER	93
5.2.2.	INITIATION AND EARLY EVENTS IN HPV-POSITIVE HEAD AND NECK CANCER.....	93
5.3.	MOLECULAR CHARACTERISTICS.....	94
5.3.1.	TP53/RB PATHWAY	94
5.3.2.	NOTCH PATHWAY	95
5.3.3.	PI3K/AKT/MTOR PATHWAY	95
5.3.4.	EGFR PATHWAY	95
5.3.5.	MET PATHWAY	96
5.3.6.	JAK/STAT PATHWAY.....	96
5.3.7.	RAS/RAF/MAPK PATHWAY	97
5.4.	DIAGNOSIS AND TREATMENT	97
5.4.1.	DIAGNOSIS	97
5.4.2.	TREATMENT	98
	<u>HYPOTHESIS AND OBJECTIVES.....</u>	103
	<u>MATERIALS AND METHODS.....</u>	109
1.	PATIENT SAMPLES	110
2.	BIOINFORMATIC TOOLS	110
2.1.	ANALYSIS OF BC AND HNSCC PATIENTS DATABASE	110
2.1.	ANALYSIS OF STX1A AND OTHER SNARE GENES EXPRESSION IN BREAST CANCER CELL LINES DATABASE	112
2.2.	ANALYSIS OF STX1A GENE	112
3.	CELL CULTURES.....	114
3.1.	CELL LINES AND 2D CULTURES	114

4. PROTEIN EXPRESSION MODULATION	116
4.1. OBTENTION OF CANCER CELL LINES WITH NON-FUNCTIONAL STX1A	116
4.1.1. COMPETENT CELLS TRANSFORMATION AND PLASMID AMPLIFICATION	116
4.1.2. PLASMID TRANSFECTION	117
4.1.3. RETROVIRAL PARTICLES PRODUCTION	118
4.1.4. RETROVIRAL PARTICLES TITRATION	119
4.1.5. RETROVIRAL INFECTION.....	120
4.2. OBTENTION OF TRANSIENT BC CELLS DOWN-REGULATED BY STX1A	120
4.3. OBTENTION OF STABLE BC CELLS DOWN-REGULATED BY STX1A.....	121
4.3.1. LENTIVIRAL INFECTION	122
4.3.2. SORTING OF GFP+ shRNA STX1A AND NON-TARGET shRNA BREAST CANCER CELL LINES	122
4.4. CRISPR-Cas9	123
4.4.1. LENTIVIRAL PARTICLES PRODUCTION	124
4.4.2. OBTENTION OF CAS9-POSITIVE CELLS	125
4.4.3. gRNAs DESIGN.....	126
4.4.4. OBTENTION OF CRISPR-Cas9 CELLS FOR STX1A	127
5. RNA EXPRESSION.....	128
5.1. RNA ISOLATION AND QUANTIFICATION.....	128
5.2. QUANTITATIVE REAL TIME PCR.....	128
6. PROTEIN DETECTION	129
6.1. WESTERN BLOT ANALYSIS	129
6.2. IMMUNOPRECIPITATION	131
6.3. IMMUNOFLUORESCENCE IN COVERSLEIPS	132
6.4. IMMUNOFLUOROHISTOCHEMISTRY.....	132
7. FUNCTIONAL ASSAYS.....	133
7.1. CELL VIABILITY ASSAYS	133
7.1.1. PROLIFERATION ASSAY	133
7.1.2. CELL CYCLE ANALYSIS.....	133
7.1.3. CITOTOXICITY ASSAY	134
7.1.4. ANNEXIN V ASSAY	134
7.2. COLONY FORMATION ASSAY.....	136
7.3. MIGRATION AND INVASION ASSAYS	136
7.3.1. WOUND HEALING ASSAY	136
7.3.2. INVASION TRANSWELL ASSAY	136
7.3.3. CELL ADHESION ASSAY.....	137

7.3.4. CELL SPREADING ASSAY	137
7.3.5. GELATIN FLUORESCENT ASSAY	138
7.3.6. ZYMOGRAM	138
8. IN VIVO EXPERIMENTS	139
8.1. CHICKEN CHORIOALLANTOIC MEMBRANE ASSAY	140
8.2. IMMUNODEFICIENT MICE XENOGRAPTS	141
9. STATISTICAL ANALYSIS AND GRAPHICAL REPRESENTATION	141
10. ADDITIONAL INFORMATION ON REAGENTS USED	142
<u>RESULTS</u>	<u>149</u>
1. SYNTAXIN-1A IN BREAST CANCER AND HEAD AND NECK CANCER PATIENT DATABASES	151
1.1. <i>SYNTAXIN-1A</i> IN ALL BREAST CANCER SUBTYPES	151
1.1.1. <i>SYNTAXIN-1A</i> IS DIFFERENTIALLY EXPRESSED AMONGST BC SUBTYPES AND OVEREXPRESSED IN HER2-POSITIVE PATIENTS	151
1.1.2. <i>SYNTAXIN-1A</i> EXPRESSION CORRELATES WITH WORSE PROGNOSIS AND TUMOUR PROGRESSION MARKERS	153
1.1.3. <i>STX1A</i> EXPRESSION CORRELATES WITH THE EXPRESSION OF OTHER SYNTAXIN AND SNARE-RELATED GENES AND IMPROVES <i>STX1A</i> PROGNOSTIC VALUE	156
1.2. <i>SYNTAXIN-1A</i> IN HER2-POSITIVE BREAST CANCER SUBTYPES	162
1.2.1. <i>SYNTAXIN-1A</i> EXPRESSION CORRELATES WITH WORSE PROGNOSIS IN HER2- POSITIVE TUMOURS	162
1.2.2. <i>SYNTAXIN-1A</i> EXPRESSION CORRELATES WITH THE EXPRESSION OF OTHER SNARES AND EGFR/HER RECEPTORS GENES IN HER2-POSITIVE TUMOURS	164
1.2.3. G ₂ /M CHECKPOINT AND PI3K/AKT/mTOR SIGNALLING PATHWAYS ARE UP- REGULATED IN TUMOURS WITH <i>STX1A^{HIGH}/HER2^{HIGH}</i> HER2-POSITIVE BC TUMOURS	171
1.3. <i>SYNTAXIN-1A</i> IN HER2-NEGATIVE BREAST CANCER	173
1.3.1. <i>SYNTAXIN-1A</i> EXPRESSION CORRELATES WITH WORSE PROGNOSIS IN HER2- NEGATIVE BC TUMOURS	173
1.3.2. <i>SYNTAXIN-1A</i> EXPRESSION CORRELATES WITH THE EXPRESSION OF OTHER SNARES AND EGFR/HER FAMILY MEMBERS IN HER2-NEGATIVE BC TUMOURS	174
1.3.3. <i>STX1A^{HIGH}</i> BASAL TUMOURS UP-REGULATE IMPORTANT SIGNALLING PATHWAYS	181
1.3.4. SUMMARY OF THE RELATIONSHIP OF <i>SYNTAXIN-1A</i> EXPRESSION AND SYNTAXIN, SNARE AND EGFR/HER GENE EXPRESSION IN BC PATIENTS	189

1.4.	<i>SYNTAXIN-1A</i> IN HEAD AND NECK CANCER	191
1.4.1.	<i>SYNTAXIN-1A</i> AND <i>SNAP-25</i> GENES ARE OVEREXPRESSED IN HEAD AND NECK TUMOURS	191
1.4.2.	HIGH <i>SYNTAXIN-1A</i> EXPRESSION CORRELATES WITH SHORTER RECURRENCE AND SPECIFIC OVERALL SURVIVAL AND <i>SNAP-25</i> EXPRESSION CORRELATES WITH LOCAL RECURRENCE	193
1.4.3.	HIGH <i>SYNTAXIN-1A</i> AND LOW <i>SNAP-25</i> GENE EXPRESSION CORRELATE WITH WORSE SPECIFIC OVERALL SURVIVAL	196
2.	<i>SYNTAXIN-1A</i> CHARACTERIZATION IN BREAST AND HEAD AND NECK CANCER CELL LINES	200
2.1.	<i>SYNTAXIN-1A</i> AND RELATED PROTEINS CHARACTERIZATION IN BREAST CANCER CELL LINES	200
2.1.1.	<i>SYNTAXIN-1A</i> IS OVEREXPRESSED IN HER2-POSITIVE BREAST CANCER CELL LINES	200
2.1.2.	OTHER SNARES ARE DIFFERENTIALLY EXPRESSED AMONG BREAST CANCER SUBGROUPS	202
2.1.3.	<i>SYNTAXIN-1A</i> IS LOCALIZED INTO THE SMALL CLUSTERS IN BREAST CANCER CELL LINES	212
2.1.	<i>SYNTAXIN-1A</i> CHARACTERIZATION IN HEAD AND NECK CANCER CELL LINES	215
2.1.1.	<i>SYNTAXIN-1A</i> EXPRESSION IN HEAD AND NECK CANCER CELL LINES	215
2.2.	<i>SYNTAXIN-1A</i> TRANSCRIPTIONAL MECHANISMS CHARACTERIZATION IN BREAST AND HEAD AND NECK CANCER CELL LINES	217
2.2.1.	HUMAN <i>SYNTAXIN-1A</i> GENE REGULATORY ELEMENTS ARE SIMILAR TO THOSE IN THE RAT GENOME	217
2.2.2.	<i>SYNTAXIN-1A</i> TRANSCRIPTION IS REGULATED BY HISTONE DEACETYLASES IN BREAST AND HEAD AND NECK CANCER AND BY SP1 TRANSCRIPTION FACTOR AND PKA IN HER2-NEGATIVE BREAST CANCER SUBTYPE	220
2.3.	STRATEGIES TO IMPAIR <i>SYNTAXIN-1A</i> FUNCTION OR DOWN-REGULATE ITS EXPRESSION	224
2.3.1.	<i>SYNTAXIN-1A</i> EXPRESSION WAS DOWN-REGULATED BY shRNA TECHNOLOGY....	226
2.3.2.	<i>SYNTAXIN-1</i> INFLUENCES THE TRANSCRIPTION OF ITS OTHER SNARE PARTNERS	229
3.	FUNCTIONAL CHARACTERIZATION OF <i>SYNTAXIN-1A</i> IN BREAST AND HEAD AND NECK CANCER MODELS	231
3.1.	ROLE OF <i>SYNTAXIN-1A</i> IN BREAST AND HEAD AND NECK CANCER CELL PROLIFERATION	231
3.1.1.	<i>SYNTAXIN-1A</i> REPRESSES BC AND HNSCC CELL CYCLE PROGRESSION AND PROLIFERATION	231

3.1.2.	SYNTAXIN-1A INHIBITS BC AND HNSCC CLONOGENIC CAPACITY	235
3.2.	STUDY OF THE RELATIONSHIP BETWEEN SYNTAXIN-1A, THE EGFR/HER FAMILY OF RECEPTORS AND TREATMENT RESPONSES	236
3.2.1.	EGFR, HER2 AND HER3 RECEPTORS ARE INVERSELY REGULATED IN BC AND HNSCC WHEN SYNTAXIN-1 FUNCTION IS IMPAIRED	237
3.2.2.	EGF INDUCES SYNTAXIN-1A CLUSTERING IN BC AND HNSCC CELL LINES.....	243
3.2.3.	SYNTAXIN-1A MODULATES EGFR/HER FAMILY MEMBERS RESPONSIVENESS TO EGF AND LAPATINIB.....	246
3.2.4.	HNSCC CELL LINES WITH NON-FUNCTIONAL SYNTAXIN-1A ARE MORE SENSITIVE TO LAPATINIB TREATMENT	249
3.2.5.	HNSCC CELL LINES WITH DOWN-MODULATION OF SYNTAXIN-1 ACTIVITY ARE MORE SENSITIVE TO CISPLATIN TREATMENT	256
3.3.	ROLE OF SYNTAXIN-1A IN BREAST AND HEAD AND NECK CANCER CELL MIGRATION AND INVASION	258
3.3.1.	SYNTAXIN-1A PROMOTES MIGRATION IN BC AND HNSCC CELLS.....	259
3.3.2.	SYNTAXIN-1A PROMOTES CELL ADHESION AND SPREADING IN BC AND HNSCC CELL LINES.....	262
3.3.3.	SYNTAXIN-1A PROMOTES CELL INVASION IN BC AND HNSCC CELL LINES.....	268
3.4.	ROLE OF SYNTAXIN-1A IN TUMOUR GROWTH AND THERAPY RESISTANCE <i>IN VIVO</i> .	272
3.4.1.	SYNTAXIN-1A SUPPRESSES TUMOUR GROWTH <i>IN VIVO</i>	272
<u>DISCUSSION.....</u>		291

1.	SYNTAXIN-1A, AND OTHER SNARE-RELATED GENES, AS NOVEL OVERALL SURVIVAL PREDICTORS IN BREAST AND HEAD AND NECK CANCERS.....	295
2.	STX1A CHARACTERIZATION IN BREAST AND HEAD AND NECK CANCER CELL LINES ..	300
3.	EPIGENETICALLY MODULATION OF SNARE GENES	302
4.	STRATEGIES TO INHIBIT STX1A EXPRESSION OR TO IMPAIR ITS FUNCTION	305
5.	STX1A ACTS AS A GROWTH REPRESSOR IN BREAST AND HEAD AND NECK CANCER .	306
6.	SYNTAXIN-1A CONTROLS EGFR/HER FAMILY OF RECEPTORS TRAFFICKING INTO THE PLASMA MEMBRANE	308
7.	SYNTAXIN-1A PROMOTES LAPATINIB, AN EGFR/HER2 TARGETED THERAPY, RESISTANCE IN BREAST CANCER	312
8.	SYNTAXIN-1A PROMOTES LAPATINIB RESISTANCE IN HEAD AND NECK CANCER	313
9.	SYNTAXIN-1A PROMOTES CISPLATIN AND ADRIAMYCIN RESISTANCE IN HEAD AND NECK CANCER	316

10. SYNTAXIN-1A PROMOTES INVASION AND MIGRATION OF BREAST AND HEAD AND NECK CANCER CELLS	318
11. STX1A IS A PROMISING TARGET TO INCREASE OVERALL AND METASTASIS FREE SURVIVAL OF BREAST AND HEAD AND NECK CANCER PATIENTS	324
<u>CONCLUSIONS</u>	<u>329</u>
<u>BIBLIOGRAPHY.....</u>	<u>335</u>
<u>ANNEX.....</u>	<u>353</u>
1. FIGURES	355
2. TABLES.....	375



Syntaxin-1A, a synaptic related protein in breast and head and neck cancer progression and prognosis

ABBREVIATIONS

#

5-FU 5-fluorouracil

A

A Ampere
ACP Adamantinomatous craniopharyngioma
AECC Asociación Española Contra el Cáncer
aFGF/bFGF Acidic/basic fibroblast growth factor
AMP Adenosine monophosphate
APP Amyloid Precursor Protein
AR Androgen receptor
AREG Amphiregulin
ARTN Artemin
ATCC American Type Culture Collection
ATP Adenosine triphosphate
ATP Adenosine triphosphate

B

BC Breast Cancer
BL1 Basal-like subtype 1
BL2 Basal-like subtype 2
BoNT Botulinum neurotoxins
BSA Bovine Serum Albumin
BTC Betacellulin

C

CAA Cancer-associated adipocyte
CAF Cancer-associated fibroblast
CAM Chicken chorioallantoic membrane
CCL Cancer Cell Line Encyclopedia
CCND1 Cyclin-D1
CD Cluster of differentiation

cDNA	Complimentary DNA
CEEA	Comitè Ètic d'Experimentació Animal
CFTR	Cystic Fibrosis transmembrane regulator
CK	Cytokeratin
cm	Centimetre
CNTF	Ciliary neurotrophic factor
CO₂	Carbon dioxide
CPLX	Complexin
CPS	Combined positive score
CRISPR-Cas9	Clustered regularly interspaced short palindromic repeats-associated protein 9 system
CT	Computed tomography
CTC	Circulating tumour cell

D

DALY	Disability-adjusted life years
DALY	Cause-specific disability-adjusted life year
DCC	Deleted in colorectal cancer
DCIS	Ductal carcinoma <i>in situ</i>
DMEM	Dulbecco's Modified Eagle Medium
DMFS	Distant metastasis-free survival
DN	Syntaxin-1 Dominant negative
DNA	Deoxyribonucleic Acid
DSB	Double-strand break
DTT	Dithiothreitol

E

<i>E. Coli</i>	<i>Escherichia coli</i>
ECM	Extracellular matrix
EDTA	Ethylenediaminetetraacetic acid
EFNB1	Ephrin-B1
EGF	Epidermal growth factor
EGFR	Epidermal growth factor receptor
EMT	Epithelial-to-mesenchymal transition
ENaC	Epithelial Sodium Channel

EPR	Epiregulin
ER	Oestrogen receptors
ERK	Extracellular regulated kinase

F

FAK	Focal adhesion kinase
FBS	Foetal Bovine Serum
FDA	Food and Drug Administration
FDR	False discovery rate
FGF	Fibroblast growth factors
FNA	Fine needle aspiration
FRSK	Foetal rat skin keratinocyte
FSC-A	Forward scatter area
FSC-H	Forward scatter height
FSK	Forskolin

G

g	Grams
G-418	Geneticin
G-CSF	Granulocyte colony-stimulating factor
GDNF	Glial cell line-derived neurotrophic factor
GFP	Green Fluorescent Protein
GH	Growth hormone
GLUT	Glucose transporter
GOBO	Gene expression-based outcome for breast cancer
GRF/GHRF/GHRH	Growth hormone-releasing factor
gRNA	Guide RNA
GSEA	Gene set enrichment analysis

H

h	Hour
HB-EGF	Heparin-binding EGF-like growth factor
hCTR1	Human copper transporter 1
HER2-4	Human Epidermal Growth Factor Receptor 2-4
HGF	Hepatocyte growth factors

HNSCC	Head and neck squamous cell carcinoma
HPV	Human papillomavirus
HR	Hormone receptors
HRH1	Histamine Receptor 1

I

IDC	Invasive ductal carcinoma
IFNγ	Interferon- γ
IGF	Insulin-like growth factor
IL	Interleukin
ILC	Invasive lobular carcinoma
IRNA	Interference RNA

K

kg	Kilograms
KLK1	Kallikrein 1
KO	Knock-out

L

l	Litre
Lab	Laboratory
LAR	Luminal androgen receptor
LB	Luria-Bertani
LC3	Microtubule-associated protein light chain 3
LCIS	Lobular carcinoma <i>in situ</i>
LIF or CDF/LIF	Leukemia inhibitory factor
LOH	Loss of heterozygosity

M

M	Molar
M	Mock
mAb	Monoclonal antibody
MAPK	Mitogen-activated protein kinase
μg	Microgram
mg	Milligrams

min	Minute
μl	Microliter
ml	Millilitre
μM	Micromolar
mm	Millimetres
MMA	Mithramycin A
MMP	Metalloprotease
MMP	Matrix metalloproteinase
MOI	Multiplicity of Infection
MRI	Magnetic Resonance Imaging
mRNA	Messenger RNA
MT1-MMP	Membrane type 1-matrix metalloproteinase
MTC	Multi-subunit tethering complex
MTC	Multi-subunit tethering complexes
mTOR	Mammalian target of rapamycin
MTT	3-(4,5-Dimethylthiazol-2-yl)-2,5-diphenyltetrazolium bromide
Mw	Multi-well

N

N-pep	N-peptide
ng	Nanogram
NGF	Nerve growth factor
NGFR	Nerve growth factor receptor
NGS	Normal goat serum
NHEJ	Non-homologous end joining
NK	Natural killer cells
NKR	Neurokinin receptor
nM	Nanomolar
NRG	Neuregulin
NRP2	Neuropilin 2
NSF	N-ethylmaleimide-Sensitive Factor
NT	Neurotrophin
NTN	Neurturin

O

OS	Overall survival
-----------	------------------

P	
----------	--

P-gp	P-glycoprotein
PAH	Polycyclic aromatic hydrocarbon
PAM	Protospacer adjacent motif
PAM50	Prediction Analysis of Microarray of 50 genes
PARP	Poly-ADP ribose polymerase
PBS	Phosphate-buffered saline
PC-12	Rat adrenal gland cell line
PCR	Polymerase chain reaction
PD-1	Programmed death-1
PD-L1	Programmed death ligand 1
PDGF	Platelet-derived growth factor
PE	Phosphatidylethanolamine
Pen/Strep	Fungizone-penicillin-streptomycin
PET	Positron Emission Tomography
PFA	Paraformaldehyde
PI	Propidium iodide
PI3K	Phosphatidylinositol-3-kinase
PKD	Protein kinase domain
PR	Progesterone receptors
PSP	Persephin
PVDF	Polyvinylidene fluoride

Q	
----------	--

qPCR	Quantitative real-time PCR
-------------	----------------------------

R	
----------	--

RASSF1A	Ras association domain family 1 isoform A
Rb	Retinoblastoma
RIPA	Radio-immunoprecipitation assay
RNA	Ribonucleic acid
RNAi	RNA Interference
ROBO	Roundabout

Rpm Revolution per minute

S

SCF	Stem cell factor
SDS-PAGE	Sodium Dodecyl Sulphate Polyacrylamide Gel electrophoresis
SERD	Selective oestrogen receptor down-regulators
SERM	Selective oestrogen modifiers
SGK1	Serine/threonine-protein kinase-1/serum and glucocorticoid-regulated kinase 1
shRNA	Short hairpin RNA
SM	Sec1/Munc18
SNAP	Synaptosome-associated protein
SNARE	Soluble NSF Attachment Protein Receptor
SP	Substance P
SPECT	Single Photon Emission Computed Tomography
STX1-DN	Syntaxin-1 Dominant Negative
STX1A	Syntaxin-1A
SYT	Synaptotagmin

T

T-DM1	Ado-trastuzumab emtansine
TBS-T	Tris Buffered Saline with tween
TCGA	The Cancer Genome Atlas
TEMED	Tetrametyletilendiamina
TGA	The Cancer Genome Atlas
TGFβ	Transforming growth factor- β
TGN	Trans-Golgi network
TKI	Tyrosine kinase inhibitor
TNBC	Triple-negative breast cancer
TNF	Tumour necrosis factor
Trk	Tropomyosin receptor kinase
TSA	Trichostatin A
TSS	Transcription start site

U

UB	Universitat de Barcelona
UCM	Universidad Complutense de Madrid
UCSC	University of California, Santa Cruz
USA	United States of America

V

V	Volts
VAMP	Vesicle-associated membrane protein
VEGF	Vascular endothelial growth factor

W

WHO	World Health Organization
------------	---------------------------

Y

YY1	Yin-Yang 1
------------	------------

Syntaxin-1A, a synaptic related protein in breast and head and neck cancer progression and prognosis

ABSTRACT

Modern oncology conceives solid tumours as organs by themselves, meaning that not only should the behaviour of cancer cells to be considered and evaluated therapeutically, but also the so-called tumour microenvironment. Even though much research has been done on the influence of several cellular and molecular components of the microenvironment on tumour progression, only a few studies have focused on the direct influence of neurons and tumour innervation in promoting tumour growth and metastasis, or the role of neural-related proteins, expressed in cancer cells, on the different cancer hallmarks. In the context of this second line of research, our group published in 2016 an article demonstrating the differential expression of neurogenes in breast cancer (BC) subtypes and their correlation with patient overall survival. Among them, Syntaxin-1A (STX1A), a synaptic-related protein and a member of the SNARE family of proteins, was found overexpressed in HER2-positive (HER2-enriched and luminal B) in comparison to the HER2-negative (luminal A and basal) BC subtypes. This project is focused on BC but also studies STX1A in head and neck squamous cell carcinoma (HNSCC), considering that the BC is the first cancer-related death in women and that the incidence of HNSCC is expected to increase by 30% in 2030.

Understanding the role of STX1A in the tumour biology of BC and HNSCC may lead to proposing this neurogene as a prognostic biomarker and as a targetable candidate to treat these cancers. Particularly, the expression of STX1A and other SNARE-family members has been investigated in BC and HNSCC patient databases, as well as whether STX1A could be involved in cell proliferation, treatment sensitivity and invasion and metastasis processes in BC and HNSCC.

On one hand, STX1A has been found overexpressed in BC and HNSCC tumours in comparison to healthy tissues, and high expression of this neurogene correlates with a poorer overall survival of BC and HNSCC patients and with a shorter metastasis-free period in BC. On the other hand, STX1A suppresses cell proliferation by enhancing G₂/M checkpoint and decreasing Cyclin D1 expression *in vitro*. Also, STX1A expression restrains BC and HNSCC tumour growth *in vivo*, in comparison to tumours with impaired STX1A function. Moreover, a functional link between STX1A and the EGFR/HER family of receptors is described. EGF induces STX1A clustering and STX1A is involved in EGFR and HER2 plasma membrane turnover and

signal transduction. Also, in HER2-positive BC and HNSCC, STX1A modulates sensitivity to lapatinib, an anti-HER2 targeted therapy, likely due to the differential expression of EGFR and HER2 at the plasma membrane. Non-functional STX1A cells become more sensitive to lapatinib *in vitro* and *in vivo*. Finally, STX1A promotes invasion and metastasis by facilitating cell adhesion and spreading in BC and HNSCC cells *in vitro*.

In conclusion this novel research work has unveiled the role of STX1A in BC and HNSCC cancer progression and prognosis, positioning STX1A as a putative survival biomarker and as a promising therapeutic target to sensitize to lapatinib treatment and to suppress invasion and metastasis events in BC and HNSCC tumours.

Syntaxin-1A, a synaptic related protein in breast and head and neck cancer progression and prognosis

INTRODUCTION

Syntaxin-1A, a synaptic related protein in breast and head and neck cancer progression and prognosis

1. CANCER

Cancer comprises a diverse class of diseases in which cells undergo uncontrolled growth with the potential to become malignant through the acquisition of mutations arisen as a consequence of genome damage (1–3). Cancer cells acquire a series of aberrant characteristics such as self-sufficiency on growth signals, insensitivity to anti-growth signals, evasion from apoptosis and immune surveillance, or genetic instability, among others, as a result of genetic or environmental factors. The acquisition of these characteristics will give the tumour cells the ability to infiltrate, destruct and transform the surrounding stroma resulting in the spreading of cancer cells through lymphatic and circulatory systems to other organs of the body, leading to metastasis (1–4).

Cancer poses a major public health problem to our society. Amongst all illnesses, cancer represents the most relevant clinical, social and economic burden in terms of cause-specific disability-adjusted life years (DALYs). Even more, it is the second cause of death worldwide, after heart ischemic disease. For this reason, almost every year all the epidemiological data from cancer patients are collected and analysed to estimate cancer incidence and mortality and to evaluate how the disease is evolving in our population (5,6). However, it is worth mentioning that in 2020 diagnosis and treatment of cancer has been hampered by the coronavirus (COVID-19) pandemic, which has brought delays in diagnosis and treatment that may lead to an apparent cancer incidence reduction, followed by an uptick in advanced stage disease and increase in mortality (5,7,8).

Among these high amounts of data, the most interesting indicator is the one that reflects mortality. Analysis of mortality rates and 5-year survival rates help research community to better estimate the advances on scientific knowledge, cancer prevention, early diagnosis and treatment (9). The impact of these advances is clearly shown in *Figure 1* where an estimation of 2,902,200 cancer deaths have been averted in the USA thanks to these new knowledge and technical advances (8,9).

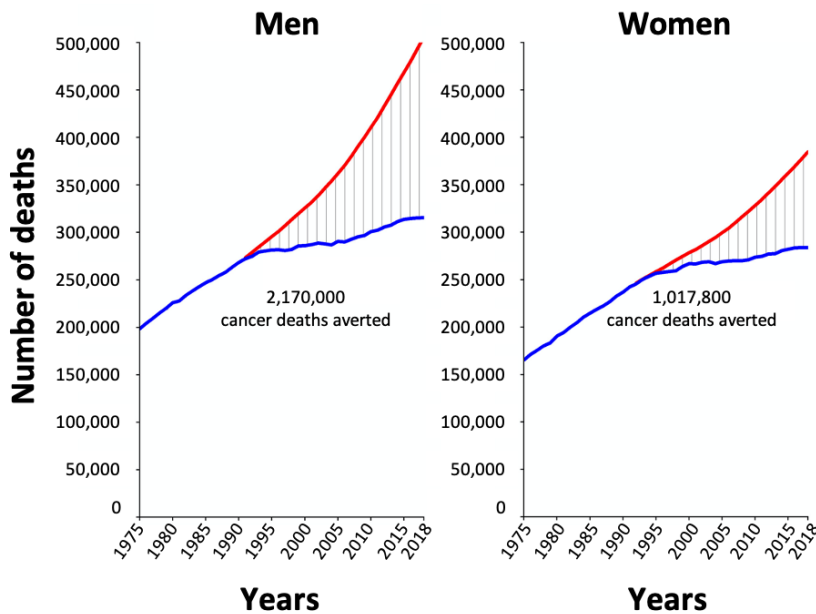


Figure 1 – Total number of cancer deaths averted in men and in women in the U.S.A. The blue line represents the actual number of deaths recorded each year, and the red line represents the number of deaths that would have been expected if cancer death rates had remained at their peak. Data from men is recorded from 1991 to 2018 whereas data from women is recorded from 1992 to 2018. Adapted from (8).

1.1. HALLMARKS OF CANCER

Cancer is considered as an evolving, dynamic and heterogenous system. However, in order to simplify this complex and interrelated system, it is possible to assume that all cancer types share many features: among them, their origin from normal cells, their increase in proliferation rate, their loss of differentiation characteristics and their acquired capability to invade and to metastasize to other organs. Acknowledging that cancer is a very complex research field, Hanahan and Weinberg (3) were able to highlight some features of cancer, shared by most or perhaps all types of human cancers, which globally describe how a cell can become cancerous. These common traits were designed as the hallmarks of cancer that in 2000 they were just six, but as the research in cancer field progressed and more knowledge was gained, two emerging hallmarks and two enabling characteristics were added in 2011 (2–4). The complete and updated hallmarks of cancer described by Hannah and Weinberg are shown in *Figure 2* and briefly described below.

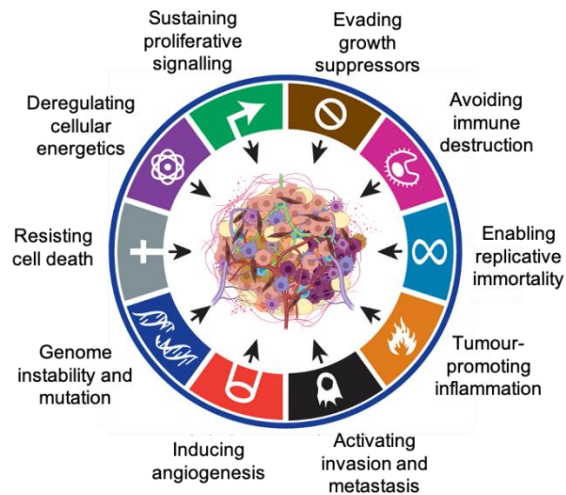


Figure 2 – Hallmarks of cancer described by Hannah and Weinberg. Representation of the updated hallmarks of cancer described by Hannah and Weinberg with the objective to rationalize neoplastic diseases. Figure adapted from (2).

1.1.1. SUSTAINING PROLIFERATIVE SIGNALLING

Sustaining proliferative signalling is probably the most fundamental trait of cancer cells.

Normal cells tightly control the production and release of growth factors to enter the cell cycle in a regulated manner and to ensure the homeostasis of the cell within the tissue. However, cancer cells gain the ability to deregulate these signals, becoming self-sufficient and entering the cell cycle and dividing without control. Cancer cells gain the ability to sustain their proliferative signals in a number of alternative ways: displaying an autocrine signalling by producing growth factors and (over)expressing their specific receptors; stimulating the microenvironment to produce supplies or dysregulate cancer cell receptors or by structural alterations which could facilitate the activation of the receptors in a ligand-independent way. At the end, the cancer cell can become growth factor independent by constitutively activating their down-stream signalling pathways (2,3,10).

1.1.2. EVADING GROWTH SUPPRESSORS

In concordance to the previous hallmark, the cell has to be able to evade counteracting signals, such as growth suppressors known as tumour suppressor genes. Two canonical suppressors of proliferation are p53 and Rb (retinoblastoma-associated). These proteins have their main role in regulatory circuits that decide if the cell is ready to proliferate or not, and are able to activate apoptotic and senescence programs. Moreover, these proteins, in cancer

cells, are able to overcome the mechanisms by which cell-cell contact inhibits proliferation as well (2,3,11).

1.1.3. AVOIDING IMMUNE DESTRUCTION

Normally, tumours arise in immune-competent organisms. That fact indicates that tumour cells are able to evade the immune system. The theory proposed is that immune system constantly recognize and eliminates antigenic tumour cells, but through acquired mutations and genome instability, some cancer cells manage to avoid their detection by the immune system and eventually grow, thereby evading eradication (2,12). The process by which the immune system can attack and promote tumour development is called immunoediting (13).

1.1.4. ACTIVATING INVASION AND METASTASIS

During tumour progression, cancer cells acquire the ability to invade and metastasize through the blood, lymph vessels and nerves to distant organs. Probably the most differential characteristic is that disseminating or metastatic cells undergo the epithelial-to-mesenchymal transition (EMT). This transition is driven by a complex regulatory and transcriptional network which involves several transcription factors such as SNAI1, SNAI2, ZEB1 and ZEB2, TWIST and E12/E47. Not only transcription factors are important in this transition, but also non-coding RNAs, chromatin remodelling and epigenetic modifications, alternative splicing and post-translational regulation will play an important role in orchestrating this phenotype change (2,3,14–16).

This a multistep process termed as the invasion-metastasis cascade which consists in acquiring the ability of surviving without attachment, and detaching from the tumour bulk. Then, cancer cells invade locally and intravasate into the blood and lymphatic vessels surrounding the tumour. Once there, they travel through blood or lymph and extravasate from the vessels to distant tissues and form small nodules of cells (micrometastasis). Once the cells have colonized the tissue and established a positive microenvironment, they are able to grow and form macrometastasis (2,3,15).

1.1.5. TUMOUR-PROMOTING INFLAMMATION

As research evolved, it was evidenced that immune cells infiltrate tumours. However, this infiltration rather than triggering an immune response against tumour cells, induces a tumour-associated inflammatory response. Paradoxically, this response is able to enhance tumour

progression by helping cancer cells to acquire more malignant capabilities. For example, inflammation can provide the tumour growth factors, proliferation signalling, proangiogenic factors or invasion and metastasis precursor molecules, among others (2,17).

1.1.6. ENABLING REPLICATIVE IMMORTALITY

In a healthy tissue, the majority of cell types are not able to divide unlimitedly. On the opposite, cancer cells do not have this limitation, enabling the formation of macroscopic tumours starting only with few cancer cells. This means that cancer cells have to be able to escape different barriers to proliferate: senescence and crisis, among others. The first one is typical of a cell which is viable but has entered a non-proliferative state. The second takes place- in cells that have overcome the senescence stage, which enter in a crisis phase where they end up dying (2,18).

The basis of this replicative immortality seems to relay in telomeres, DNA structures composed by multiple nucleotides repeats that normally shorten after each cell division. In mortal cells, once telomeres are short enough to not protect DNA from fusion, their ends create dicentric chromosomes which would threaten cell viability and induce the cell to enter in apoptosis. In the 90% of human cancer cells telomerase, an enzyme that add telomere repeat segments to avoid telomere shorten, is expressed, to prevent senescence and/or apoptosis (2,3).

1.1.7. INDUCING ANGIOGENESIS

In order to grow, tumours as normal cells require nutrients and oxygen. This means that they need blood vessels to obtain these supplies. Moreover, blood vessels would be useful to eliminate cancer cells metabolic waste and to migrate to invade other organs. The adult normal vasculature system usually remains quiescent, but in some situations, such as wound healing or during the female reproductive cycle, it is turned on transiently. However, in cancer is aberrantly activated to be able to sustain tumour growth (2,3,19).

1.1.8. GENOME INSTABILITY AND MUTATION

Changes in cancer cell genome due to epigenetic dysregulation or DNA mutations lead to genome instability conferring selective advantage and outgrowth to certain cancer cells which will eventually dominate the tumour bulk. These spontaneous mutations happen because the

DNA-maintenance machinery is dysregulated in cancer cells, displaying defects in detecting DNA damage and in activating DNA repairing machinery. Normally, the problem relays on the DNA-repairing proteins themselves or problems in inactivating or intercepting mutagenic molecules that can potentially damage the DNA. It is thought that genome instability helps tumour progression because accelerates tumour evolution to a more malignant stage (3,18).

1.1.9. RESISTING CELL DEATH

Usually, the apoptotic machinery is able to sense damage from two different sources: there is one circuit that is able to detect death-inducing signals from the extracellular space (extrinsic apoptotic program) and another circuit that senses DNA damage and cellular stress (intrinsic apoptotic program). Each circuit culminates in activating an intracellular cascade driven by caspases which trigger apoptosis, ending up with the cell progressively disassembled and then consumed by neighbour cells and phagocytic cells. Tumour cells have been able to develop different strategies in order to avoid apoptosis. The most common is the loss of *TP53* which, besides regulating the cell cycle, it also senses the DNA damage of the cell triggering the apoptosis event in case of huge damage. Moreover, p53 can also increase the levels of anti-apoptotic proteins, decrease the levels of other pro-apoptotic proteins or by short-circuiting the ligand-induced death pathway (2,3,21).

1.1.10. DEREGULATING CELL ENERGETICS

As previously mentioned, cancer cells proliferate at a high rate. This means that they have a huge demand of metabolic energy to sustain cell growth and division. In order to do that, cancer cells make metabolic adjustments to be able to complete all the processes that need to maintain. Otto Warburg was the first to observe this characteristic: even in aerobic conditions, cancer cells switch their glucose metabolism into anaerobic glycolysis. After this discovery, more metabolic switches have been described to occur in cancer cells. Moreover, it is important to note, that as tumour mass increases, oxygen will not be able to reach all cancer cells, and some of them will have to produce energy under hypoxic conditions. This metabolic switch is favoured by some oncoproteins and mutant tumour suppressors and also by the overexpression of important glucose transporters, such as GLUT1 (3,19).

1.2. TUMOUR MICROENVIRONMENT

At the beginning cancer research was focused only on cancer cells that composed the tumour bulk. However, later cancer was comprehended not only as cell mass, but an organ itself, meaning that many other cells types are present which can be influenced by cancer cells and play an important role in tumour progression. The established crosstalk between cancer cells and non-transformed cells conforms the stroma and the microenvironment of the tumour. Non-transformed cells will provide physical and chemical sustainment to the tumour to promote its growth and progression. The intercellular communication between cancer cells and the stromal cells that are part of the microenvironment will be through a dynamic network of chemokines, cytokines, growth factors, inflammatory signals and matrix remodelling enzymes (22–24).

However, when the tumour microenvironment is considered, it is important not to fail in the assumption that the tumour microenvironment is only the non-transformed cells directly found surrounding the tumour. In fact, the entire organism influences the development of the tumour, and the tumour influences distant organs as well. Some of these evidences point out at the relevant role of the immune and the nervous systems. Hence, some researchers have named this phenomenon as tumour organismal environment (24).

1.3. COMPONENTS OF THE TUMOUR MICROENVIRONMENT

The tissue microenvironment of a developing tumour is composed mainly by proliferating tumour cells and their stroma which includes the extracellular matrix (ECM), blood, lymphatic vessels and nerves, but also a variety of tissue cells, such as immune cells, fibroblasts and adipocytes that would promote tumour expansion (*Figure 3*) (22–24).

1.3.1. IMMUNE CELLS

In the tumour microenvironment it is possible to find immune cells involved in the adaptative immunity such as T lymphocytes, dendritic cells and B lymphocytes, as well as effectors of the innate immunity like macrophages, polymorphonuclear leukocytes and natural killer (NK) cells. Nevertheless, in the tumour microenvironment not all cell types will help the tumour to progress. Among all the immune cell types, there will be a few with tumour antagonising functions such as effector T cells, NK cells, dendritic cells, M1-polarized macrophages and N1-polarized neutrophils. Dendritic cells will work as professional antigen-presenting cells and will provide co-stimulatory signals for T cell activation, triggering a cytotoxic immune response against tumour cells. On the other side, there are immune cells

with a tumour-promoting role such as regulatory T cells or myeloid-derived suppressor cells. The function of these cells will rely on suppressing the immune response and to induce angiogenesis, two actions that would facilitate tumour growth and dissemination (12,22,23).

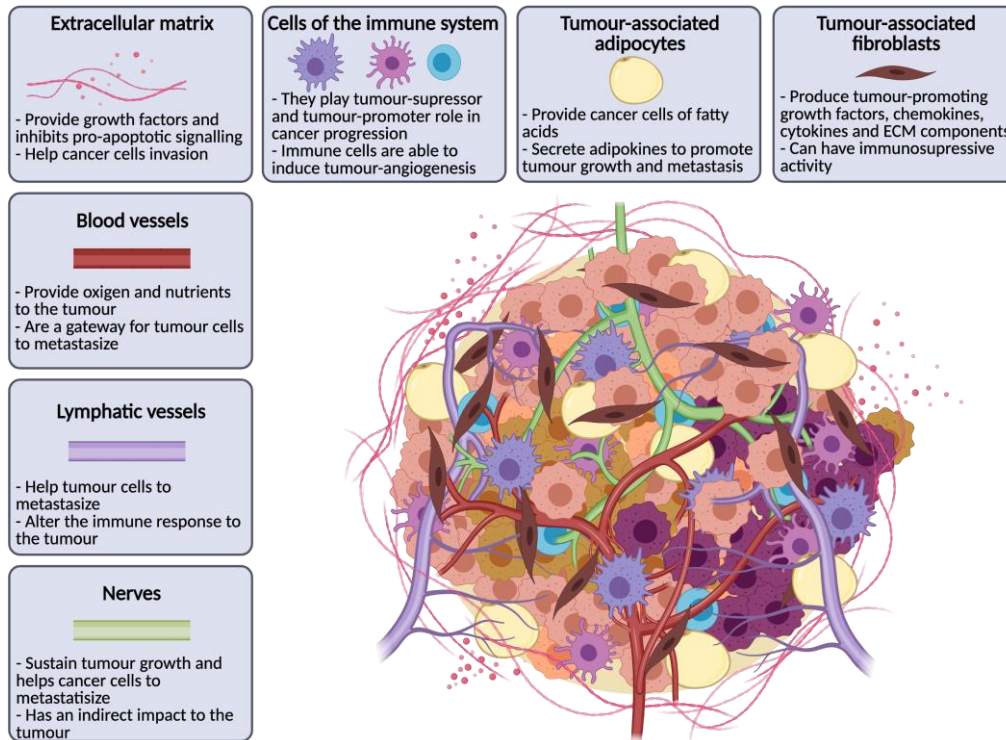


Figure 3 – Components of the tumour microenvironment. Tumour cells are found in a microenvironment composed of extracellular matrix, blood and lymphatic vessels, nerves, cells of the immune system, tumour-associated adipocytes and tumour-associated fibroblasts which promote and control tumour progression and invasion.

1.3.2. CANCER-ASSOCIATED FIBROBLASTS

Cancer-associated fibroblasts (CAFs) are a very heterogeneous population of fibroblasts within a tumour. This heterogeneity seems to relay in their origin. A significant proportion of CAFs seems to emerge from mesoderm-derived precursor cells, however, it is also described that they can originate from endothelial cells, adipocytes or epithelial cells as well. Moreover, quiescent fibroblasts, residing in the host tissue can be transformed to CAFs in response to the injury caused by the developing neoplasm (22,25,26).

CAFs, as immune cells do, can play two opposite roles in tumour progression. On the one hand, they display an anti-tumour capability by orchestrating the antitumour immunity regulating and avoiding the presence of regulatory T cells. Moreover, they will enhance the response of anti-tumour immune cells such as macrophages, NK cells and T cells by secreting Interleukin-10 (IL-10), transforming growth factor β (TGF β), interferon γ (IFN γ) and IL-6. On

the other hand CAFs will promote tumour progression mainly through their altered secretome. CAFs will secrete paracrine growth factors, cytokines such as CXCL12, fibroblast growth factors (FGFs) and hepatocyte growth factors (HGF) among others factors, that will directly impact on tumour progression by enhancing cancer cells survival, proliferation, stemness, metastasis-initiating capacity and also therapy resistance (22,25,26).

1.3.3. CANCER-ASSOCIATE ADIPOCYTES

Adipose tissue is highly regulated by environmental factors. As a consequence of the released tumour-secreted factors, adipocytes acquire an activated phenotype, becoming cancer-associated adipocytes (CAAs). The main characteristic of CAAs is that they have a high lipolysis rate by which they will provide energy in the form of fatty acids to cancer cells. Moreover, they overexpress and secrete adipokines, glutamine, ketone bodies that will influence cancer cells leading to tumour growth, metastasis and treatment resistance (22,27,28).

1.3.4. EXTRACELLULAR MATRIX

The homeostatic ECM is composed of different components that give rise to different ECM properties. The most common components are collagen, proteoglycans, laminin and fibronectin. ECM main function in a homeostatic tissue is to regulate tissue development and maintain tissue homeostasis and architecture. However, in cancer ECM composition and organization is altered contributing to the tumorigenic process (29,30). As an example, an increased collagen deposition leads to an increase in mammographic density, correlating with an elevated risk of developing breast cancer (BC) (31). So important the ECM is in cancer, that it has been implicated in all the hallmarks of cancer. For instance, the ECM could be the source of growth factors for the cancer cells and also cancer cells adhesion to the ECM inactivates its pro-apoptotic signalling cascade. Moreover, its consistence is essential for the activation of the invasion and metastatic processes. Cancer cells need a stiff ECM to promote invadopodia formation which enhances cancer cell invasion by driving focal adhesion assembly (29,30,32).

1.3.5. BLOOD VESSELS

The formation of new blood vessels within a tumour is an essential step for tumour progression. These new blood vessels will supply the tumour with nutrients and oxygen and

remove waste products from the tumour, also providing a gateway for tumour cells to metastasize (19,22,33).

The tumour microenvironment and cancer cell themselves will send angiogenic signals, such as vascular endothelial growth factor (VEGF) or hypoxia signals that will induce the formation of new blood vessels. However, this new vasculature is abnormal in comparison to a homeostatic blood vessel. It has a chaotic branching and uneven vessel lumen. The vessels are also leaky which raises tumour interstitial pressure and cause an irregular blood flow, oxygenation, nutrient and drug distribution within the tumour and tumour microenvironment (19,22,33).

An important role of pericytes have also been described. One of the functions of these cells is to provide structural support to the blood vessels. Clinical studies demonstrate that low pericyte coverage of the vasculature correlates with poor prognosis and increased metastasis. Also, *in vivo* studies supported the hypothesis that normal pericyte coverage of the tumour vasculature might act as a key negative regulator of metastases (19,22).

1.3.6. LYMPHATIC VESSELS

Tumours also induce lymphangiogenesis. The presence of new lymph vessels within a tumour is proved to be a mechanism to metastasize to lymphatic nodes and to distant organs. It is believed that tumour cells will enter to the lymph vessels following a chemokine gradient. To enhance lymphangiogenesis tumour cells secrete VEGF-C and VEGF-A that will induce the growth of the lymphatic endothelium. Inflammation of the lymphatic endothelium induces an immunosuppressive tumour microenvironment due to the inhibition of dendritic cells maturation and limiting the cytotoxic activity of lymphocytes. However, if this inflammation is not present, dendritic cells could be able to present tumour antigens, generating antitumour immunity into the lymphatic nodes (22,34,35).

1.3.7. NERVOUS SYSTEM

The nervous system also plays a very important role in tumour progression and metastasis. As in the other systems, there is a crosstalk between tumour cells and nerves fibers. On the one hand, tumour cells secrete neurotrophic factors that will promote neurogenesis. On the other hand, nerve fibers will release neurotransmitters and neuromodulators that would modulate cancer cell survival, proliferation and metastasis. Moreover, tumour innervation is

not the only to be considered, but also the indirect impact of the whole nervous system in tumour progression, as a relationship between stress and cancer has recently been recognized (24,36–38).

1.4. NERVOUS SYSTEM AND CANCER

As explained in the previous section, cancer is not an isolated entity within an organism. In fact, cancer is a tissue that interacts not only with the cells in its environment, but also with the vasculature and lymphatic vessels that surround it. These vessels do not expand alone, instead, they are found in tandem with nerve fibers, all three structures being necessary for the well maintenance of the organ. Owing to the fact that a tumour can be considered as an organ, and that the blood and lymphatic vessels influence tumour progression, it makes sense that nerves could play a very important role in tumour progression as well. However, it has only been in the past decade, thanks to new technological improvements, that researchers have been able to prove the molecular mechanisms by which nerves contributes to cancer progression (22,24,37).

The first studies trying to reveal the role of the nervous system in cancer were focused on its indirect function. They proved that the immunological response is under control of the nervous system, and by incidence of negative stimulus such as chronic stress, anxiety or depression, the nervous system supresses the immune response, which could facilitate tumour development. Later, more studies in the nervous system and cancer field proved that it did exist a direct relationship between nervous system and the development of cancer. Initially, this direct effect was thought to be only a mechanic effect, where the nerves fibres behave as paths to the cancer cells to allow them to migrate to other organs. However, further research elucidated that nerves secrete neurotransmitters and neuromodulators that are affecting the transcription and translation processes within the cancer cell, changing cytoskeletal dynamics and promoting cancer cell survival, migration and invasion capacity (*Figure 4*). However, it was not only a unidirectional relationship but, but also It was proved the existence of a crosstalk between tumour cells and nerves. While nerves secrete neural factors which promote tumour growth, cancer cells secrete neurotrophic factors and axon guidance molecules which stimulate nerve growth to infiltrate the tumour, a process also known as neoneurogenesis.

Another clue to understand the importance of innervation and its contribution to tumour progression relies on the fact that tumours nearly double their own innervation in comparison to age-matched non-neoplastic tissue controls (39). Moreover, it has been found that there is a direct relationship between nerve density within a tumour and tumour aggressivity in prostate, colon and rectum, pancreas, stomach, head and neck and BC (40,41). Targeting

communication between tumour cells and nerve fibers could be the basis of an innovative anti-tumour therapy. The advantage of these therapies is that there are currently some therapeutical approaches developed to modulate the nervous system function, so it is worth thinking that with further investigation similar approaches could be useful in controlling cancer progression and metastasis.

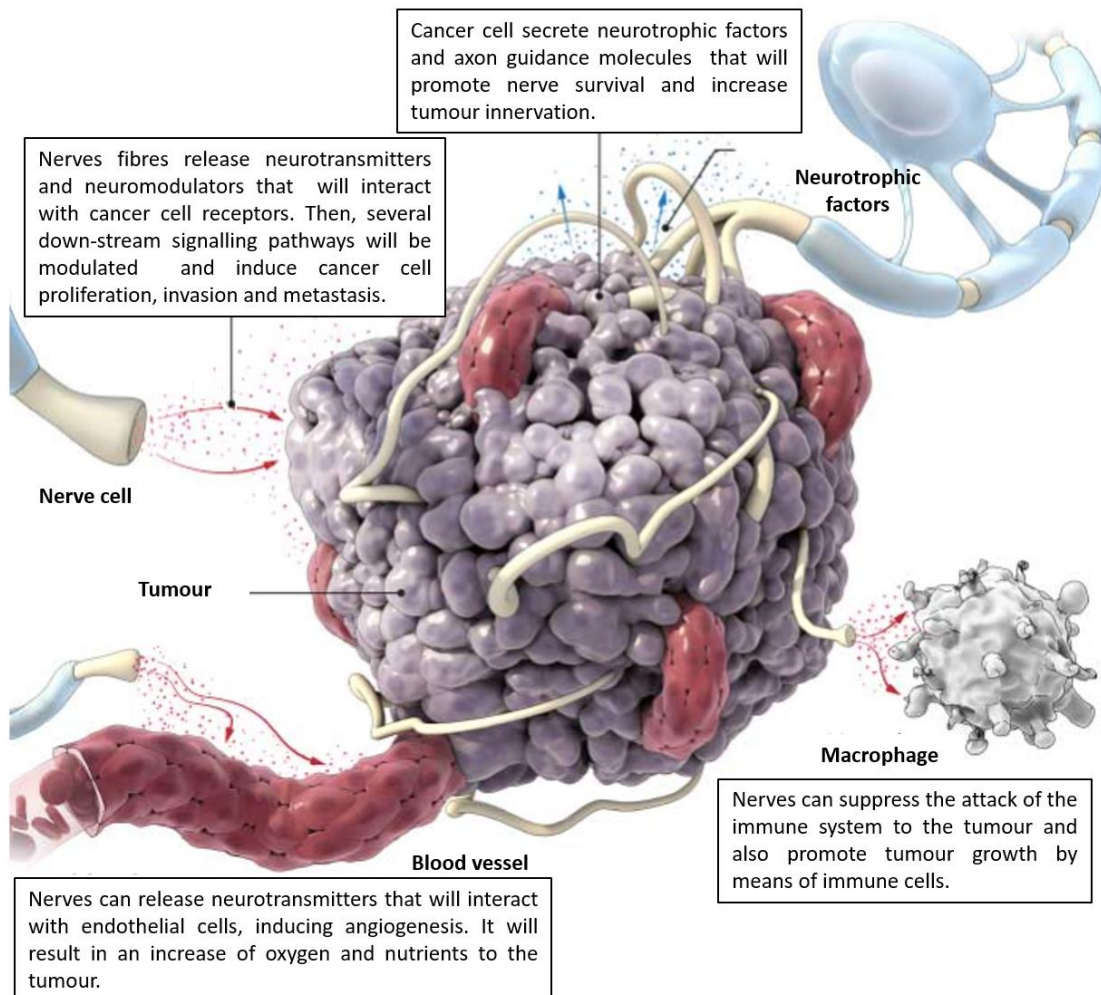


Figure 4 – Cross-talk between nerve fibres and a tumour. The nervous system is actively involved in tumour progression and dissemination, but also tumours induce neoneurogenesis promoting spreading of nerves within the tumour. Modified from (42).

1.5. NEONEUROGENESIS

The stimulation of innervation is referred as neoneurogenesis. Tumours release soluble components and induce cell-to-cell signalling which is found to promote tumour innervation. Targeting these components opens an important window of opportunities to the discovery of molecules that could be pharmacological targets for regulating nerve fibres-dependent tumour progression (37,43,44).

Only few studies have been focused on neurogenesis in cancer, most of them in prostate cancer. One of them described that prostate tumour cells, in comparison to normal and benign hyperplastic prostate epithelial cells, overexpressed pro-nerve growth factor (proNGF). Moreover, overexpression of this precursor of NGF correlated with a poorer overall survival of the patients. *In vitro*, they discovered that prostate cells secreted proNGF which stimulate neuron outgrowth. This study also demonstrated that proNGF/NGF could be a potential driver of nerve infiltration (45). Another study in prostate cancer demonstrates that also semaphorin-4F is overexpressed in prostate tumour cells, in comparison to normal prostate cells, and that induces neurogenesis. Moreover, *in vivo* experiments in mice proved that G-CSF (granulocyte colony-stimulating factor) promotes the survival of sympathetic nerve fibers and induces the aberrant outgrowth of parasympathetic nerves in transgenic or xenogeneic prostate tumour models (39). Neurons and cancer cells also express neurotrophic growth factor receptors and neurotransmitter receptors, such as β -adrenergic, acetylcholine or histamine receptors among others, which highlight their potential to be used to develop new oncology treatments (36,46–48).

1.6. INTERACTION WITH SOLUBLE FACTORS

The crosstalk between tumour cells and nerves is driven by soluble factors secreted by both of them. Although several neurotrophic factors, axon guidance molecules, neuropeptides and neurotransmitters have been described to play important roles in the tumour-nerve interaction, the complete network of these soluble factors and their actions on the tumour and the nerves biology is largely unknown. Further comprehension of the effect of these soluble factors lead to a new area of therapeutical target discovery (37,44,49,50).

On the one hand, cancer cells, as explained before, are able to support the neuronal growth and survival through the release of neurotrophic factors. They include a large family of proteins that can be subdivided, among others, into neurotrophins, neuropoietins, insulin-like growth factors and transforming growth factors (*Table 1*). Moreover, to promote axon growth to a certain area of the tumour, cancer cells secrete axon guidance molecules which would act as chemoattractant guiding the nerve to the tumour. There are several families of proteins that work as axon guidance molecules, some of them are netrins, ephrins, semaphorins and silts (*Table 2*)(37,44,50).

Table 1 – Summary of the neurotrophic factors family members and their receptors.

Family	Member	Signalling receptor
Neurotrophins	Nerve growth factor (NGF)	TrkA
	Brain-derived neurotrophic factor (BDNF)	TrkB
	Novel neurotrophin-1 (NT-1)	gp130
	Neurotrophin-3 (NT-3)	TrkC > TrkA and TrkB
	Neurotrophin-4/5 (NT-4/5)	TrkB
Neuropoietins	Ciliary neurotrophic factor (CNTF)	CNTF receptor complex (CNTRFa, gp130, LIFRb subunits)
	Leukemia inhibitory factor (LIF or CDF/LIF)	LIF receptor complex (gp130, LIFRb subunits)
Insulin-like growth factors	Insulin-like growth factor-I (IGF-I)	IGF type I receptor (IGF1R) > insulin receptor (IR)
	Insulin-like growth factor-II (IGF-II)	IGF1R, less than IR
Transforming growth factor	Transforming growth factor α (TGF α)	TGF α receptor
	Transforming growth factor β (TGF β 1, TGF β 2, TGF β 3)	TGF β type I, II and III receptors
GDNF ligands	Glial cell line-derived neurotrophic factor (GDNF)	GFRA2, GFRA1
	Neurturin (NTN)	GFRA2, GFRA1
	Persephin (PSP)	GFR α 4
	Artemin (ARTN)	RET receptor, GFR α 3 as co-receptor
Fibroblast growth factors	Acidic fibroblast growth factor (aFGF or FGF-1)	FGF receptors 1-4 (FGFR 1-4)
	Basic fibroblast growth factor (bFGF or FGF-2)	FGFR-1-3
	Fibroblast growth factor 5 (FGF-5)	FGFR-1, FGFR-2
Other growth factors	Platelet-derived growth factor (PDGF: AA, BB and BB isoforms)	PDGF a- and b- receptors
	Stem cell factor (mast cell growth factor) (SCF)	c-kit

Table 2 - Summary of some axon guidance molecules and their receptors known to be related with tumour progression

Family	Member	Signalling receptor
Netrins	Netrin-1	Deleted in colorectal cancer (DCC), Uncoordinated-5 (UNC5)
	Netrin-3/NTN12	
	Netrin-4/ β	
	Netrin-G	
Ephrins	Ephrin A ligand	EphA receptor
	Ephrin B ligand	EphB receptor
Semaphorin	Semaphorins 1-7	Plexins, Neuropilins
Slit	Slit 1-3	Roundabout 1-4 (ROBO 1-4)

Some researchers think that this paracrine communication between nerve fibres and cancer cells could take place into a neuro-neoplastic synapse, by which the neuron and the cancer cell would be in a close contact, facilitating the interaction between the receptors and the neurotransmitters and neuromodulators released by the neurons (summarized in [Table 3](#)) or the tumour cells (46,50,51). However, the neuro-neoplastic synapse is only an hypothesis made according to the functional aspects described, although there is no morphological characterization so far (50).

Table 3 - Summary of the most relevant neurotransmitters and neuromodulators related to tumour progression.

	Family	Member	Signalling receptor
Neurotransmitters	Amino acids	Aspartate	NMDA receptor
		Glutamate (Glutamic acid)	Metabotropic glutamate receptor, NMDA receptor, Kainate receptor, AMPA receptor
		Gamma-aminobutyric acid	GABAB receptor, GABAA and GABAA-p receptor
		Glycine	Glycine receptor
	Acetylcholine	Acetylcholine	Muscarinic acetylcholine receptor, nicotinic acetylcholine receptor
	Monoamine (Phe/Tyr)	Dopamine	Dopamine 1-5 (D1-5) receptors
		Borepinephrine (noradrenaline)	α - β Adrenergic receptors
		Epinephrine (adrenaline)	
	Monoamine (Trp)	Serotonin (5-hydroxytryptamine)	5-HT1-7 receptors
		Melatonin	MTNR1 A-B-C receptors
Monoamine (His)	Histamine	H 1-4 receptors	
Neuromodulators	Neurohypophyseals	Vasopressin	Vasopressin receptor
		Oxytocin	Oxytocin receptor
		Neurophysin I	?
		Neurophysin II	?
	Neuropeptide Y	Neuropeptide Y	Neuropeptide Y receptors (NPY1R, NPY2R, PPYR1, NPY5R)
		Pancreatic polypeptide	PPYR1
		Peptide YY	NPY2R
	Corticotropin-releasing factor	Corticotropin (adrenocorticotrophic hormone)	Corticotropin receptor
	Opioids	Dynorphin	κ -opioid receptors
		Endorphin	μ 1 opioid receptor > μ 2 and δ opioid receptors > κ 1 opioid receptors
		Enkephaline	Enkephaline receptors
		Secretin	Secretin receptor
		Motilin	Motilin receptor

Family	Member	Signalling receptor
Secretins	Glucagon	Glucagon receptor
	Vasoactive intestinal peptide	Vasoactive intestinal peptide receptor
	Growth hormone-releasing factor (GRF/GHRF/GHRH)	Growth hormone-releasing factor receptor
Somatostatins	Somatostatin	Somatostatin receptor
Tachykinins	Substance P	NK1 > NK2 > NK3
	Neurokinin A	NK2 > NK3 > NK1
	Neurokinin B	NK3 > NK2 > NK1
Other neuropeptides	Bombesin	BB 1-4
	Gastrin releasing peptide	BB2

1.7. THE INFLUENCE OF THE NERVOUS SYSTEM IN TUMOUR PROGRESSION

The nervous system plays an active role in tumour progression. Several studies in different types of cancer demonstrate, through different denervation techniques, that the impairment of the nerves signalling to tumours result in the inhibition of cancer initiation, progression and metastasis (50,52).

Nowadays this has been studied in several cancer types, however first studies were developed in prostate cancer due to its easy manipulation and given that is an organ which is anatomically distinct for its sympathetic and parasympathetic nerve system. Magnon and colleagues went beyond to demonstrate the influence of the nerves in tumour progression. On the one hand, their experiments showed that sympathetic nervous system plays its main role during the early stages of tumour progression (41). Signalling impairment of the parasympathetic nervous system chemically, surgically or by genetic deletion of β_2 - and β_3 -adrenergic receptors resulted in no tumour growth. On the other hand, they demonstrated, by enhancing parasympathetic nervous system signalling or by blocking pharmacologically or genetically stromal type 1 muscarinic receptor, that parasympathetic cholinergic fibers surrounding the prostate tumour promote cancer dissemination (41). Another study from Zhao *et al.* (53) demonstrated in three separate mouse models that bilateral or specific vagotomy of the anterior part of the stomach resulted in a markedly reduction of tumour incidence and progression, whereas if a unilateral vagotomy was performed in the posterior part of the stomach gastric tumours continued to develop. Moreover, they proved that a local injection of botulinum neurotoxin type A also reduced tumour incidence in mice (53). Similarly

as in prostate and gastric cancer, in breast, head and neck or melanoma cancer the huge impact that the nervous system has in tumour progression has also been confirmed (40,44,54).

Not only nervous system plays a dramatic role in tumour progression, but also it has a high impact in treatment response. In gastric cancer, denervated tumours showed an increased efficacy of chemotherapy (53). Similar results were seen in pancreatic cancer, where denervation of the superior mesenteric ganglia resulted in an increase of the efficacy of chemotherapy, as well (40).

1.8. THE INFLUENCE OF THE NERVOUS SYSTEM IN TUMOUR INVASION AND DISSEMINATION

Furthermore, studies have demonstrated how the nervous system facilitates tumour migration through the release of neural-related factors such as neurotrophins, neurotransmitters and neuromodulators, regulating the metastatic cascade. Some researchers stated that the nervous system has a clear impact in the beginning of the metastatic process by promoting the EMT and enhancing the production of extracellular matrix (37,52). Overexpression of TrkB or BDNF stimulation results in altered expression of EMT markers (TWIST-1, Snail, E-cadherin and N-cadherin) in human endometrial cancer cell lines. Moreover, exogenous expression of TrkB results in an increased capacity to resist anoikis *in vitro*. Furthermore, *in vivo* experiments enforced the role of TrkB, since TrkB-depleted endometrial cells underwent mesenchymal-to-epithelial transition and anoikis, and also there was a decrease of their peritoneal dissemination (55). Other study supported the role of the nervous system and its relationship to tumour invasion by demonstrating that treatment with recombinant human BDNF inhibited anoikis and stimulated cellular proliferation, invasion and migration in gastric cancer cells (56). Others researchers have focused on the influence of the nervous system in MMPs secretion. Two research groups found that NGF and GDNF stimulated the expression and activity of MMP-2 and MMP-9, respectively in human pancreatic cell lines *in vitro* (57,58). Moreover, MMP-9 is also stimulated by norepinephrine in *in vitro* studies in HNSCC (59).

Finally, the whole effect the nervous system exerts on tumour metastasis is also proved in prostate cancer. Magnon *et al.* demonstrated that overstimulation of the parasympathetic nervous system resulted in an increase of positive lymph nodes metastases and that poor

clinical patient outcomes associated with the densities of sympathetic and parasympathetic nerve fibres in tumour and surrounding normal tissue, respectively (41).

Overall, these studies clearly show the influence of the nervous system and the nervous system-related factors in cancer invasion and metastasis.

1.9. THE NERVOUS SYSTEM AS A THERAPEUTIC TOOL IN CANCER TREATMENT

Regarding all these studies performed *in vitro* and *in vivo*, it is clear that the nervous system plays a key role in tumour progression. Clinical data in humans support this fact, retrospective studies in colon and prostate cancer patients have evidenced a direct correlation between neural density and advanced tumour stages (41,53). Moreover, in gastric cancer there is a positive correlation between neural density and activation of Wnt, neurotrophin and axonal guidance signalling pathways. Moreover, the same researchers found that patients who underwent surgical vagotomy had a reduced risk of gastric cancer (53). Immunohistochemical analysis of endometrial tumours revealed that TrkB and its secreted ligand (BDNF) are overexpressed in comparison to normal endometrium. Moreover, in endometrial tumours TrkB levels positively correlate with lymph node metastasis (55).

This existing cross-talk between nerves and cancer makes feasible a therapeutic intervention to improve the prognosis of cancer patients. Furthermore, the fact that nerve removal or the inhibition of their signalling, results in slow cancer progression and less metastasis, makes local inhibition of the nervous system a feasible strategy to treat cancer. The great advantage is that nowadays several drugs to treat various neurological illnesses are already available, and as neurons and cancer cells have some common receptors, these drugs could exert a similar effect in cancer cells as they have in the neural system. On the one hand, epidemiological data seems to confirm this statement. Patients with schizophrenia treated long-term with antipsychotics have a significant lower risk of gastric cancer (60). Tricyclic antidepressants also have a similar effect in cancer incidence, they are antagonists of serotonergic, adrenergic, glutamatergic and histaminergic receptors, and patients treated with these antidepressants have a reduced incidence of colorectal cancer and glioma (61,62). On the other hand, it is important to be careful because these treatments are not cancer-specific, and there are currently much better and more specific treatments to treat cancer. Also, some of these drugs have serious secondary effects therefore in some cases the risk would overcome the benefit in the risk/benefit balance. Also, the experiments mentioned

above are performed using chemicals and surgeries that are unlikely to be of clinical use. Nevertheless, these findings and associations open the window to start thinking for some specific therapeutical strategies to treat tumours considering the influence of the nervous system in the tumour and on its microenvironment. An example of these molecular tools could be neurotoxins such as botulinum neurotoxins (63,64).

Botulinum neurotoxins (BoNTs) are produced by bacteria of the genus *Clostridium*. BoNTs are MMPs, their targets being Soluble N-ethylmaleimide-Sensitive Factor (NSF) Attachment Protein Receptor (SNARE) proteins. The main role of SNARE proteins, initially described in the neurons, is the contribution to vesicle trafficking and neurotransmitters release during the synaptic process (63–65). Consequently, BoNTs bind with high affinity to peripheral cholinergic nerve terminals of the skeletal and autonomic nervous system, on which by specific SNARE cleavage inhibit the release of acetylcholine, causing the flaccid paralysis of botulism. However, nowadays the binding mechanism of BoNTs is still unclear, some researchers claiming that is due to hydrophobic interactions (66,67).

There are several BoNTs serotypes, each one targeting specific SNARE proteins (63,66–68) (Table 4). Currently, BoNTs are used in the clinic to treat some disorders such as muscular dystonia, strabismus or hyperhidrosis, among others (63,65). The use of BoNTs in cancer is not so common, however several manuscripts have been published explaining the likely use of BoNT in cancer, but all for treating and trying to relieve the secondary effects of cancer, such as pain or muscle spasms. There are only a few research articles focused on cancer cells and BoNT treatment as an anti-cancer drug, but they suggest that BoNT reduced cancer cells growth and proliferation but also cancer cell sensitivity to drugs (63).

Table 4– Neurotoxin serotypes and their cellular protein targets.

Neurotoxins	Intracellular target proteins
BoNT/A	SNAP-25
BoNT/B and tetanus toxin	VAMP-1, VAMP-2 and VAMP-3
BoNT/C1	SNAP-25, STX1A and STX1B
BoNT/D	VAMP-1, VAMP-2 and VAMP-3
BoNT/E	SNAP-25
BoNT/F	
BoNT/G	VAMP-1, VAMP-2 and VAMP-3

Overall, these data reflect the possibility of treating cancer with drugs directed to the nervous system or to nervous system-related proteins. However, much research is needed because the approved drugs are not specific for tumours, and the tools used in experimental models are not feasible to be translated into the clinical practice.

2. SNARE PROTEINS

Crosstalk between cancer cells themselves or between cancer cells and stromal or immune cells is essential to promote tumour progression and dissemination. Communication between cells is driven either by direct cell interactions through membrane receptors and ligands, or by the release of extracellular vesicles, soluble molecules, such as growth factors, cytokines, chemokines, neurotransmitters and microRNAs (69,70).

The release of extracellular vesicles or soluble molecules usually start with the generation of a vesicle from a precursor membrane, then the vesicle is transferred to its destination and, finally, it is fused together with the target compartment. These processes are called trafficking and membrane fusion, and it has been proved that even there is an enormous diversity in size and shape of the vesicles, these events are carried out by certain multiprotein complexes. These complexes consist of protein families that have been conserved throughout eukaryotic evolution (71–79). One of this multiprotein complexes are SNARE proteins, discovered in the late 1980s (Figure 5) and described for the first time as a superfamily of small proteins (100–300 amino acids in length) really well conserved among species. Initially, their main function was found to be involved in eukaryotic membrane fusion events, in all of the trafficking steps of the secretory pathway (71–73).

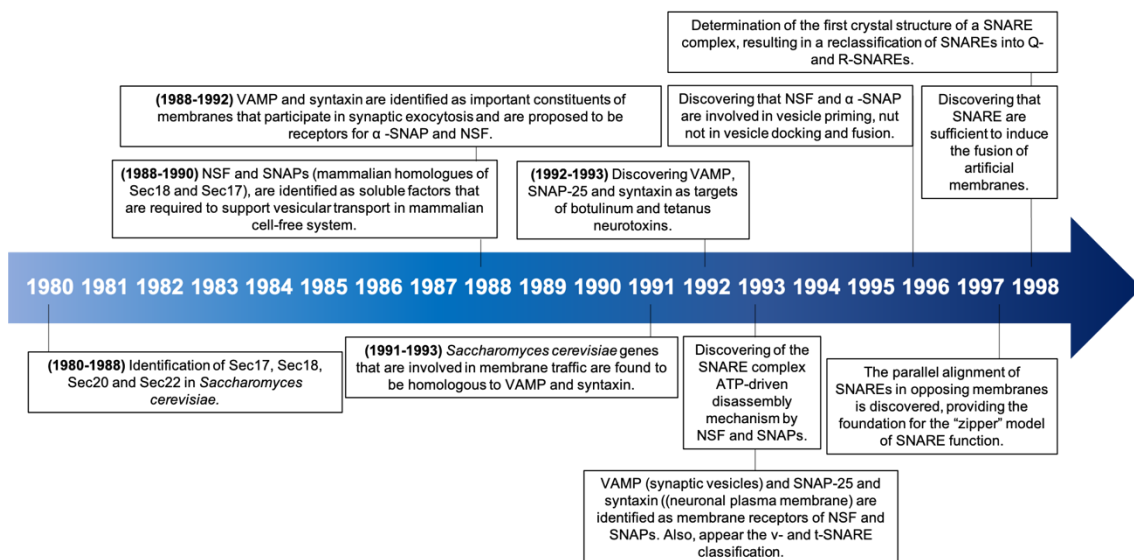


Figure 5 - Discovery of SNAREs and the role of SNARE cycling in membrane fusion. Timeline indicating the different discoveries surrounding SNARE proteins and their role in membrane fusion from 1980 to 1998. Modified from (71).

2.1. SNARE PROTEINS STRUCTURE

Since the discovery of SNARE proteins at late 1980s, there has been a lot of research focused on these proteins that lead to the discovery of new SNAREs. Nowadays, 38 SNARE proteins have been described in humans. Through crystallography experiments it has been possible to identify their structure and their protein motifs. Most SNARE contain one SNARE motif, whereas four SNAREs (Synaptosome-associated protein-23 (SNAP-23), SNAP-25, SNAP-29/GS32 and SNAP-47) contain two SNARE motifs (*Figure 6*) (71,76).

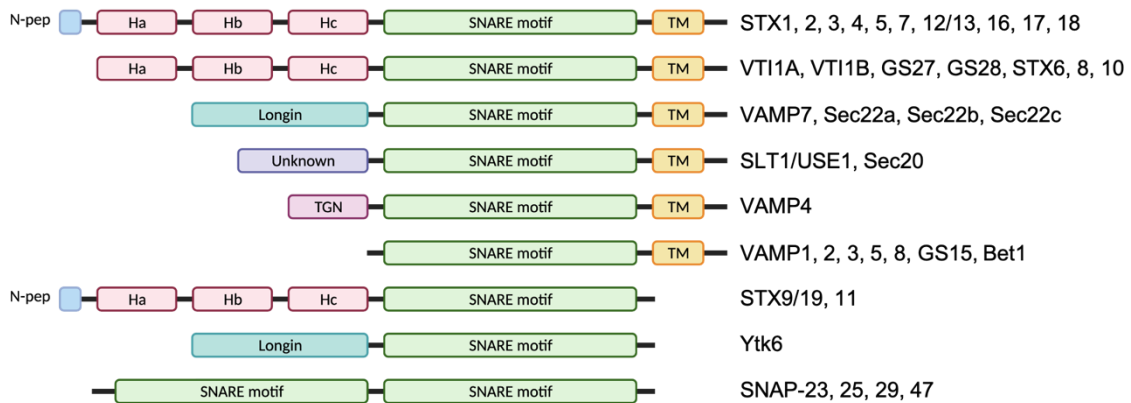


Figure 6 – Domain organization of human SNAREs proteins. Protein graphic indicates the different SNAREs described and their corresponding domains. Abbreviations: N-pep (N-peptide), TM (transmembrane domain) TGN (Trans-Golgi network). Modified from (73).

2.1.1. SNARE MOTIF

The SNARE proteins structure is really evolutionally-conserved (71,73,74,76), mainly its SNARE motif or H3 motif. This motif consists of 60 residues present in all SNARE proteins. As described before, all the SNARE proteins have one single SNARE domain except four SNARE proteins (SNAPs) that have two (*Figure 6*). The SNARE complex is mediated by these SNARE motifs, and is associated with conformational and free energy changes. When SNARE proteins are found as monomers, SNARE motifs are unstructured. However, when appropriate sets of SNAREs are combined, SNARE motifs spontaneously associate to form a helical core complex with extraordinary stability. These core complexes are formed by elongated coiled coils of four interlace parallel α -helices provided each one from a different SNARE motif. The centre of the bundle formed by the SNARE complex contains several layers of interacting side chains from the SNARE proteins (*Figure 7*). These layers are largely hydrophobic, except for a central “zero” layer that contains one highly conserved hydrophilic arginine (R) and three highly conserved glutamines (Q) (*Figure 7*). These residues normally come from one R-SNARE, one Qa-SNARE,

one Qb/Qc-SNARE (the classification of SNARE proteins will be explained in point 2.2) (71,74,80).

The SNARE complex is widely described and characterized during the synapsis process in the neurons, where the release of neurotransmitters is essential for the crosstalk between neurons. The first SNARE complex identified in the presynaptic neuron contained 3 SNAREs: STX1A, SNAP-25 (Q-SNAREs) and VAMP-1 (R-SNARE) (74). In this situation when the SNARE complex is formed, it is arranged in parallel forming the four helix-bundle. This specific pairing will contribute to the SNARE complex with four SNARE motifs (STX1A and VAMP-1 which will bear one motif each one, whereas SNAP-25 will contribute with two), this process will drive both membranes into fusion. Following the classification based on the crystal structure (Figure 7), this complex is formed by one Qa-SNARE (STX1A), one Qb/Qc-SNARE (SNAP-25) and one R-SNARE (VAMP-1) contributing with a total of three glutamines (Q) and one arginine(R) at the “zero” layer of the central bundle of the SNARE complex (71,74,75,77,80).

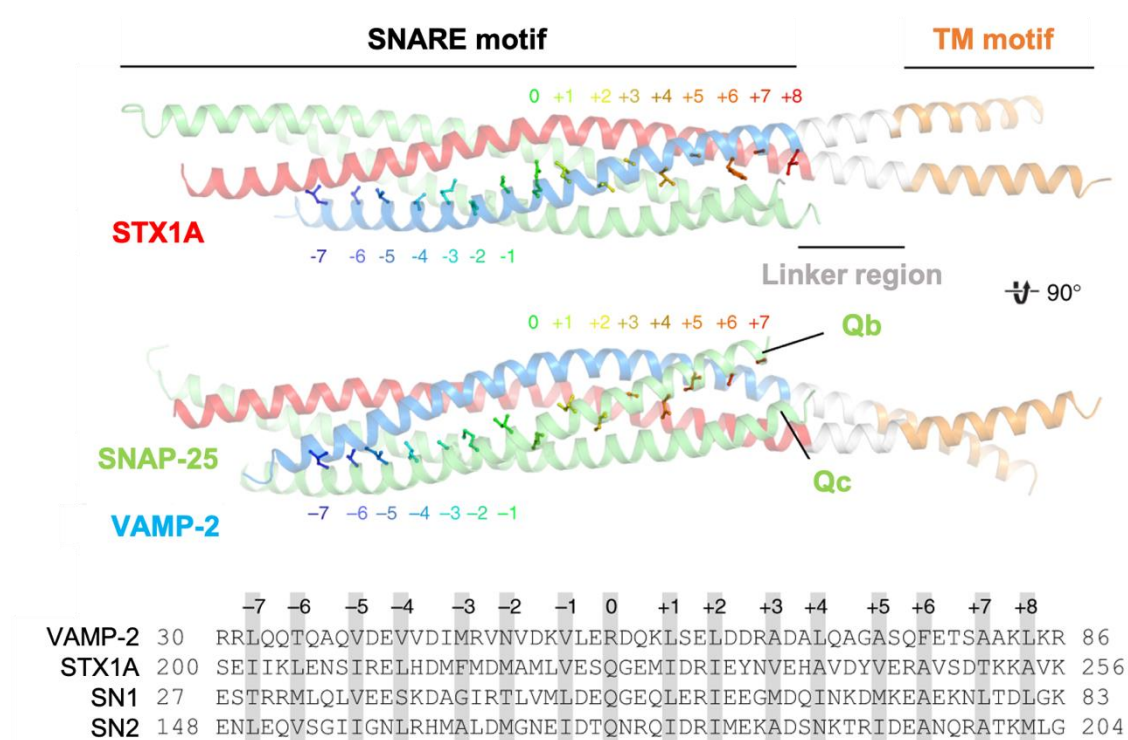


Figure 7 – SNARE core complex. On the top, crystal structure of the SNARE complex (PDB: 3HD7) showing the different interaction side chains within the different layers (indicated in rainbow colours). On the bottom, sequence of the SNARE motifs of VAMP-2, STX1A, SNAP-25 (with his two SNARE motifs Qb and Qc). Indicated shaded in grey, the hydrophobic binding layers. Modified from (80).

However, SNARE proteins do not have only the SNARE motif, they also have other motifs and regions that characterized their function in the cell:

- **Linker region:** it connects the SNARE motif with the transmembrane domain. The linker region is positively charged, a condition required for lipid mixing and the transition from hemifusion to full fusion into the plasma membrane. The linker region serve as a force toward the membrane interface that triggers the membrane fusion (72).
- **Transmembrane motif:** the majority of the SNARE proteins have at its C-terminal a hydrophobic region that functions as a membrane anchor. However, some SNARE proteins do not have this transmembrane domain, but even so, they are also attached to the membrane due to some posttranslational and lipidic modifications such as prenylation, palmitoylation and/or interaction with other SNAREs that are anchored to the membrane by their C-terminal tails (*Figure 6*) (73,76).
- **N-terminal chain:** Most SNARE proteins have also an extended N-terminal domain with coiled coil regions (*Figure 6*). When present, these regions have different functions. Collectively, N-terminal domains are involved in several regulations of SNARE protein function. Some of these domains are able to interact with other regulatory factors (such as Munc18-1) to modulate the SNARE complex. Others are able to interact with the SNARE motif at C-terminal and endorse a closed conformation of the protein, thereby preventing its assembly into SNARE complex. Also, the N-terminal domain of some SNARE proteins have a profilin-like structure, which role has not been well elucidated. It seems that it could regulate the open or closed conformation of the SNARE protein. The N-terminal extension of VAMP-4 contains a dileucine motif and acidic clusters that mediate its recycling from the endosome to the trans-Golgi network (TGN). However N-terminal domain of these SNARE proteins can play other roles that remain to be defined (73,76).

2.2. SNARE PROTEINS CLASSIFICATION

Initially, SNARE proteins were subclassified according to its subcellular localization: SNARE proteins found into the target membrane were termed as t-SNARE. The ones present into the membrane of the vesicle were termed as v-SNARE (73,76). The SNARE hypothesis, first introduced in 1993 by Rothman and colleagues (further explained later, point 2.5) suggested that v-SNARE pairs with a cognate t-SNAREs on the target membrane, forming a complex that not only determined the specificity of the fusion but also catalysed the fusion process.

However, many SNAREs can be found on both vesicles and target membranes, therefore an alternative classification based on the crystal structure of the synaptic SNARE complex (or SNAREpin) was formulated (*Table 5*). The R-SNARE are the SNARE proteins that contribute with an arginine to the SNARE complex ionic layer, while the Q-SNAREs proteins are the ones which contribute with a glutamine to the ionic layer. It is important to note that this last subgroup of SNARE proteins, the Q-SNARE, is also subdivided into three more subgroups called Qa, Qb and Qc. This subclassification of the Q-SNARE is based on the SNARE motif of the Q-SNARE proteins family. Most SNAREs (34 out of the 38 in humans) contain only one SNARE motif near the C-terminal tail anchor or the C-terminus, but 4 of these (SNAP-23, SNAP-25, SNAP-29/GS32 and SNAP-47) contain two tandem SNARE motifs separated by a linker region (*Figure 6*). Both N-terminal SNARE motifs of these four SNAREs are more homologous to each other than to the C-terminal SNARE motif of the same protein. The same is also true for their C-terminal SNARE motif. Accordingly, the N-terminal SNARE motif of SNAP-25 defines a subfamily (S25N) of SNARE domains, while the C-terminal SNARE motif of SNAP-25 defines another subfamily (S25C). The other SNARE proteins are classified according to the homology with the SNARE motifs of Syntaxin (Qa) or SNAP-25 (Qb if they are similar to S25N or Qc if they are similar to S25C) (*Figure 6*) (71,73,76).

Table 5 – Human SNARE classification based to crystal structure of the synaptic SNARE complex and according to its location in the cell. SNAREs marked in blue correspond to v-SNAREs while marked in green correspond to t-SNAREs

SNARE subtypes	SNARE Proteins
R	Sec22b, Ykt6, VAMP-1, VAMP-2, VAMP-3, VAMP-4, VAMP-5, VAMP-7 and VAMP-8
Qa	STX1, STX2, STX3, STX4, STX5, STX7, STX11, STX13, STX16, STX17 and STX18
Qb	GS27, GS28, Vti1a, Vti1b, SNAP-23N, SNAP-25N, SNAP-29N
Qc	Sit1, GS15, Bet1, STX8, STX6, STX10, SNAP-23C, SNAP-25C, SNAP-29C
?	Sec20, Sec22a, Sec22c

2.3. REGULATION OF SNARE COMPLEX ASSEMBLY AND FUNCTION

The SNARE proteins hypothesis is recognized now as the core mechanism for membrane fusion. However, this complex process is not only regulated by the SNARE proteins themselves,

but also is highly regulated by multiple auxiliary machineries such as tethering factors, Sec1/Munc18 family (SM) proteins, NSF and α -SNAP (75,78).

2.3.1. Sec1/Munc18 PROTEIN FAMILY

SM proteins family are, as SNARE proteins, evolutionarily conserved. Instead of SNARE proteins, mostly found anchored into a membrane, SM proteins are found soluble into the cell cytosol, peripherally to membrane proteins and are considered key universal components of the fusion machinery. Even they are located into different subcellular compartments, their main role is to physically interact with SNARE proteins and regulate several transport steps. *In vitro* studies showed that SM proteins strongly accelerate the rate of SNARE-mediated fusion and contribute to the specificity of various fusion events by endorsing the opening of the fusion core or by enhancing the activity of the SNARE complex. For example MUNC18-1 seems to have a specificity in regulating STX1 function, while STXBP2, also known as MUNC18-2 seems to regulate STX1 (81). SM proteins can work individually on SNARE proteins or in SNARE complexes, suggesting that this family of proteins can interact with their cognate SNARE through distinct mechanisms and at different stages in the SNARE assembly and disassembly cycle. This fact demonstrates the important regulatory roles of SM proteins in cell trafficking mechanisms. Consequently, *in vitro* binding assays suggest that the interactions of SM proteins with SNARE prevent the formation of non-physiological SNARE complexes, stimulating specific SNARE pairing (73–75,78).

2.3.2. TETHERING FACTORS

As described for SM proteins, tethering factors also play an important role in regulating SNARE proteins. Two groups of tethering factors can be distinguished, one comprised of long coiled-coil proteins, the other formed by several multi-subunit tethering complexes (MTCs). These tethering factors are able to associate with different cellular compartments to mediate specific membrane trafficking ([Table 6](#)) (73–75,78).

It is thought that coiled-coil tethers mediate vesicle targeting to membranes over longer distances, while MTCs modulate vesicle targeting to target membranes over shorter distances. As SM proteins do, tethering factors can also regulate vesicle docking and SNARE function. Mechanistically, these factors can interact directly with SNARE proteins (through multiple structural motifs in SNARE proteins) or through SM proteins to regulate specific assembly and SNARE complex stabilization. In this context, tethering factors play a role in fine-tuning the

specific availability and accessibility of SNAREs promoting the formation of the correct SNARE complexes. Also, specific interaction of MTCs can inhibit promiscuous assembly of non-functional or premature SNARE complexes in biological membranes. Moreover, they are able to protect SNAREs from degradation by inducing conformational changes in SNAREs, as SM proteins could also do. However, it appears that SNARE-tether interactions have bidirectional effects, and in some cases, SNARE proteins can influence the localization of tethering factors (73–75,78).

All these observations indicates that the interactions between tethering factors, SM proteins and SNARE proteins are crucial in order to coordinate spatial and temporal regulation of intracellular membrane fusion and vesicle trafficking through SNARE complex assembly (73–75,78).

Table 6 – Tethering factors and their SNARE family interactors. Abbreviations: ER (endoplasmic reticulum), TGN (trans-Golgi network), PM (plasma membrane).

Tethering factors		Subcellular association	SNARE interaction	Function
DSL1		ER	Use1, Sec20	Golgi to ER retrograde transport
COG		Golgi	STX5, STX6, STX16, GS28	Transport within the Golgi apparatus and Golgi to ER retrograde transport
GARP		TGN	STX6, STX16, VAMP-4	Endosome to TGN retrograde transport
HOPS		Late endosome	VAMP-3, VAMP-7, Nyv1	Late endosome to lysosome transport
CORVET		Early endosome		Early endosome to late endosome transport
EXOCYST		PM	Sec9, Snc2	Secretory vesicle fusion with PM
TRAPP	TRAPP-I	ER, Golgi	Unknown	ER to Golgi transport, autophagy
	TRAPP-II	Golgi		
	TRAPP-III	TGN		
p115		Cis-Golgi	STX5, GS28, GS15, Sec22, GS27, Ykt6	ER to Golgi transport
Giantin		Golgi		ER to Golgi transport
CASP		Golgi		Retrograde transport within the Golgi
GM130		Cis-Golgi		ER to Golgi transport
Golgin-97		TGN		TGN to endosome transport
Golgin-245		TGN		TGN to endosome transport
GCC185		TGN		Endosome to TGN-trafficking
EEA1		Early endosome		Transport through the early endosome

2.4. SNARE LOCALIZATION AND SPECIFICITY

In a cell there are a lot of membrane trafficking processes resulting into membrane fusion events, which require specific and highly regulated SNARE complexes. Some of these SNARE complexes will be specific of certain cell traffic reactions (73,76).

2.4.1. LOCALIZATION

There must be sorting mechanisms that ensure that each intracellular membrane have its appropriate SNAREs proteins, even after completing fusion reactions where some SNARE proteins should be displaced from the original subcellular compartment. This means that SNARE proteins not only reside in their organelle where membrane fusion took place, but also they can be identified through their recycling pathway. This fact makes difficult to deduce in which fusion step a certain SNARE protein is involved, due to the fact that SNARE localization will depend on the steady state among SNARE biosynthesis, fusion and recycling (73,76).

In this scenario, accessory proteins that can bind to free SNARE would play a role in SNARE sorting and localization. It has been proved that cytoplasmatic domains of SNAREs are essential for their correct sorting (with few specialized exceptions), nevertheless no defined sorting signals have been identified into the SNARE proteins themselves (73,76).

2.4.2. SPECIFICITY

Under normal and homeostatic conditions, only the appropriate organelles fuse with each other. This means that the traffic and secretory machinery of eukaryotes has to be tightly organized and regulated because membrane fusion is the final and irreversible step of each trafficking route (73,76).

After several research works a picture has been drawn, and even though some SNARE proteins seem to be promiscuous, it is also certain that some combinations are more stable than others. The main SNARE complexes involved into the secretory and endocytic pathway of a mammalian cell are shown in *Figure 8*.

Regarding evolution, it is possible to picture which SNAREs have acquired specificity, but this degree of specificity seems variable. Some observations demonstrate that the depletion of a specific SNARE protein does not prevent both membranes to fuse. These observations

indicate that SNAREs can functionally replace each other to a certain extent. This fact is not overly surprising considering the extraordinary degree of structural conservation between SNARE complexes. However, even though such promiscuity has been proved, cells manage themselves to select a specific set of SNAREs for an upcoming fusion step. Although there is no currently general answer to this question, it is conceivable that tethering complexes play an important role in this step (73,76).

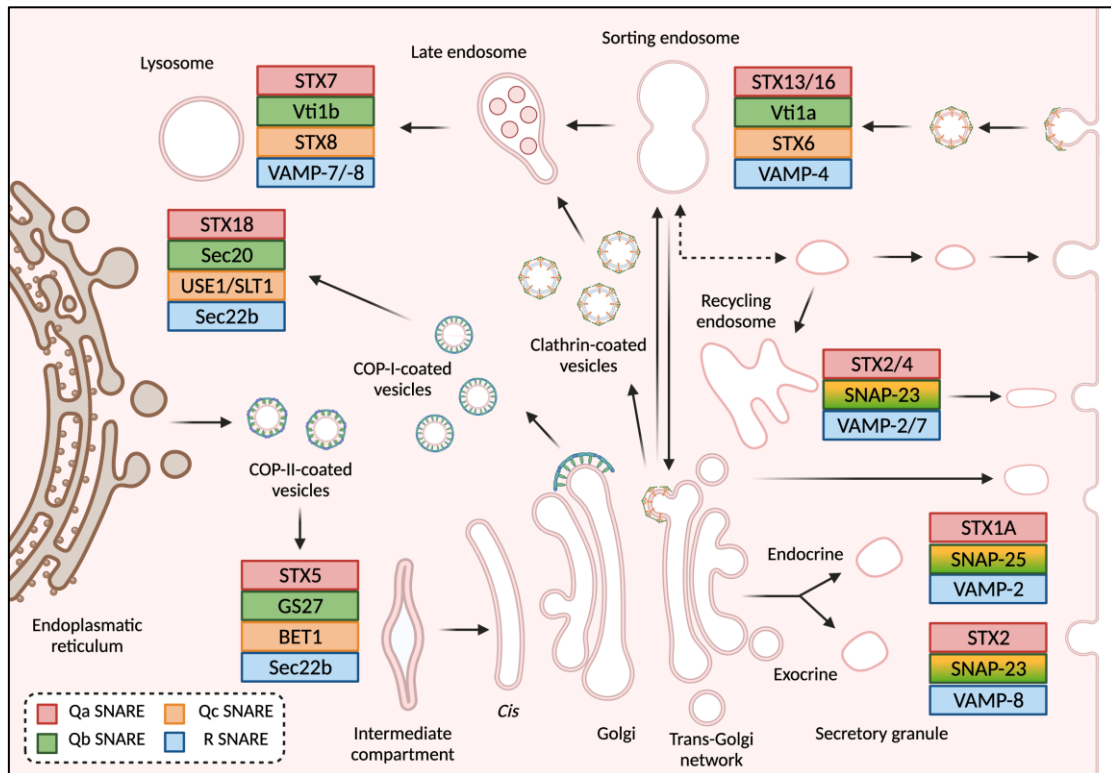


Figure 8 – SNARE complexes along the secretory and endocytic pathways. Schematic summary of known SNARE complexes and their action sites along exocytic and endocytic pathways in mammal cells. Modified from (71,73,75).

2.5. SNARE HYPOTHESIS: FROM THE BEGINNING TO THE MOST RECENT RESEARCH

The SNARE hypothesis was first postulated at 1993 by Rothman *et al.* (82), nevertheless a lot of research and findings have been going on since then. The SNARE hypothesis initially proposed that v-SNAREs interact with t-SNAREs to form a *trans*-SNARE complex. The pairing of these SNARE proteins brings the vesicle membrane to the target membrane close enough to fuse, and the assembly of SNARE complex generates enough energy to overcome the energy barrier of the two opposing lipid bilayers and to catalyze/mediate membrane fusion. As a consequence of this fusion the *trans*-SNARE complex becomes *cis*-SNARE complex on the target membrane, which binds to NSF through α -SNAP to form a transient (20S) complex. Subsequently, the ATPase of NSF hydrolyses ATP, resulting in the disassembly of SNARE

complex to allow the v-SNARE and t-SNARE to be used for the next round of fusion (Figure 9) (71,74).

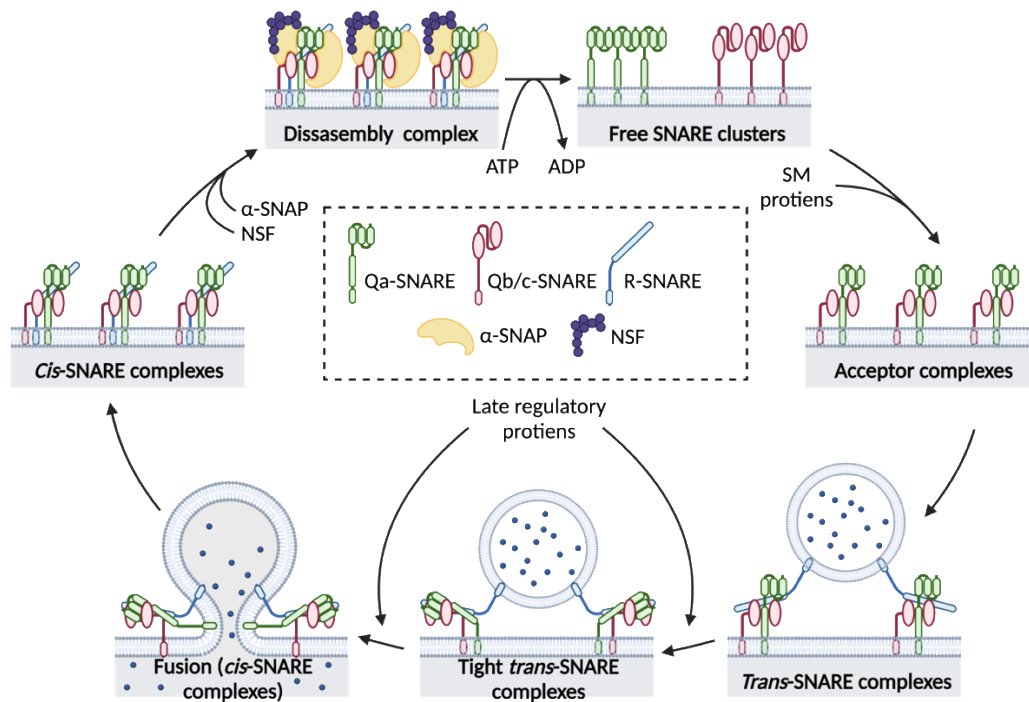


Figure 9 - The SNARE conformational cycle during vesicle docking and fusion. Schematic representation of how free Qa and Qb/c SNAREs assemble to a SNARE complex with other SM proteins. The complex will end up with the interaction with an R-SNARE located into the vesicle membrane. Then, the SNARE complex, together with other regulatory proteins will induce vesicle and plasma membrane fusion and the release of the vesicle content. After the fusion event, the SNARE complex will be recycled to their initial free form thanks to α -SNAP and NSF proteins. Modified from (71).

2.5.1. SNARE CYCLING IN MEMBRANE FUSION

Initially it was thought that membrane fusion through SNARE proteins was mediated by NSF. However, later discoveries lead to the demonstration that are the SNARE protein themselves with the regulatory activity of tethering and SM proteins, which drive the fusion process. In accordance to that statement, SNARE motifs, that will be part of the SNARE complex, will “zipper” between themselves from their N-terminal end towards their C-terminal membrane anchors and initiate the fusion process, acting directly as catalytic proteins (71,75).

Even though this model is still controversial, it has gained wide acceptance, and it is the one which will be discussed:

- 1. Free SNAREs in membrane.** Initially SNARE proteins are found free in the membrane thanks to the activity of the NSF. However, finding SNARE protein freely it would not

indicate that these proteins are not able to interact with other proteins. During the free state, they can be involved in SNARE sorting and recycling as well. Furthermore, they can recruit other SNARE into trafficking vesicles. They can also be involved in the formation of docking complexes or finally, they can play a role in regulating the capability of SNARE motifs to enter SNARE complexes (*Figure 9*) (71).

It is important to note that plasma membrane SNAREs are not uniformly distributed in the membrane, but are clustered in nanodomains, the stability of which normally depends on cholesterol. SNAREs clustering will define docking and fusion sites for exocytosis (71,72).

- 2. Formation and maintenance of trans-SNARE complexes.** SNAREs must assemble in a *trans* configuration. This means that the two membranes that have to fuse, each one has to have a SNARE protein with a transmembrane domain attached to it. Assembly starts at the N-terminal of the SNARE motifs, proceeding in a zipper-like fashion towards the C-terminal membrane anchors. These SNARE motifs transit from a partially unstructured conformation into a fully coiled-coil structure. Due to the rigidity of the α -helical linker region between the Habc domains and the transmembrane domain of the SNAREs, zippering pulls the transmembrane domains into closer proximity and finally aligns with each other. This results in a mechanical force exerted on the membranes, which might overcome the energy barrier for fusion. Moreover, it is important to note that at this step SNARE proteins are regulated by other factors. One of these factors, as it is widely described in neuronal exocytosis, would be Ca^{2+} . The cation presence will be sensed by synaptotagmin (SYT) proteins, which contain two Ca^{2+} - binding C2 domains. When Ca^{2+} is bound to this protein family, membrane fusion is promoted. Other factors that will contribute to the fusion process will be complexin (CPLX) proteins, small helical proteins that bind to the surface of SNARE complexes, that also are sensitive to Ca^{2+} and help to the fusion process (*Figure 9*) (71,74,75,78,79).

However, the fact that *trans*-SNARE complexes are transient makes really difficult to study them *in vitro*, and more research has to be done in order to identify how free SNAREs assembles to *trans*-SNARE complexes (71).

3. **Fusion.** In this process, opposing membranes contact and proceeds through a series of intermediates, which, at the end will result in an aqueous pore that will connect the distal leaflets of the fusing membranes while maintaining a lipidic seal between the distal and the proximal leaflets during the reaction. The best-supported model indicates that SNARE assembly exerts a mechanical force on membranes, which directly causes fusion. SNARE proteins will work as linkers that will bend both membranes and disturb the hydrophilic-hydrophobic boundary, deforming the membranes and forming fusion stalks. Nevertheless, before the total fusion and the pore formation, it is believed that an hemifusion state takes place, defined experimentally as a state in which the lipids of the proximal leaflets are already exchanging, but an aqueous connection between the structures that are undergoing fusion has not yet formed (*Figure 9*) (71,72,78).

Although this model is intuitively satisfying, many details are still unknown. For example, it is not certainly known how many SNARE complexes are needed for a single fusion event. Moreover, even that a large body of evidence supports that SNAREs functions as fusion catalyst, they also bring fusion to completion. However, researchers have suggested that further proteins are required to operate downstream of SNAREs, such as vacuolar H⁺-ATPase (71,72,75).

4. **Disassembly and recycling.** Once the fusion is done, SNARE complexes are transformed from *trans*-configuration to *cis*-configuration, in which all of the SNAREs forming the complex reside together in the resulting fused membrane. The configuration of this SNARE complex results in the lowest point in terms of potential energy, and it is thought that these complexes are biologically inactive until the complex dissociation. To disassemble the SNARE complex, a high amount of metabolic energy is needed. This energy will be provided by NSF, a member of a type II AAA+ ATPases that will work as “unfoldase” and will disentangle this protein complex. However, NSF is not able to interact with SNARE complex by itself, which means that will need the help of some cofactors such as SNAPs (which include three isoforms termed as α -SNAP, β -SNAP and γ -SNAP). Therefore, three SNAP molecules bind to the middle of *cis*-SNARE complex, approximately centred around the hydrophilic “zero” layer. Once the SNAP proteins have been settled, they bind to the N-domain of NSF, forming a 20S supercomplex. However, the mechanism regulating the disassembly of this supercomplex remains elusive. Once NSF is recruited it is also activated and after

several catalytic cycles of NSF with numerous ATP-hydrolysis events, SNARE complex dissociates (Figure 9) (71,74,75,79).

Before concluding this general consideration about SNARE cycle, it is important to note that the SNARE cycle model explained is the heterotypic model, where the SNARE complex is formed by one v-SNARE/R-SNARE protein in the vesicle and two or three SNARE proteins in the target membrane (Q-SNARES) (Figure 10, left). However, there is also the homotypic membrane fusion model, where the SNARE proteins located at the target membrane and the vesicle are of the same type, and even they fuse together (Figure 10, right). In general terms, the homotypic model functions as the heterotypic model, whereas once the *cis*-SNARE complex has been formed, they have to be disassembled by NSF and SNAP proteins in order to assemble the *trans*-SNARE complex (74).

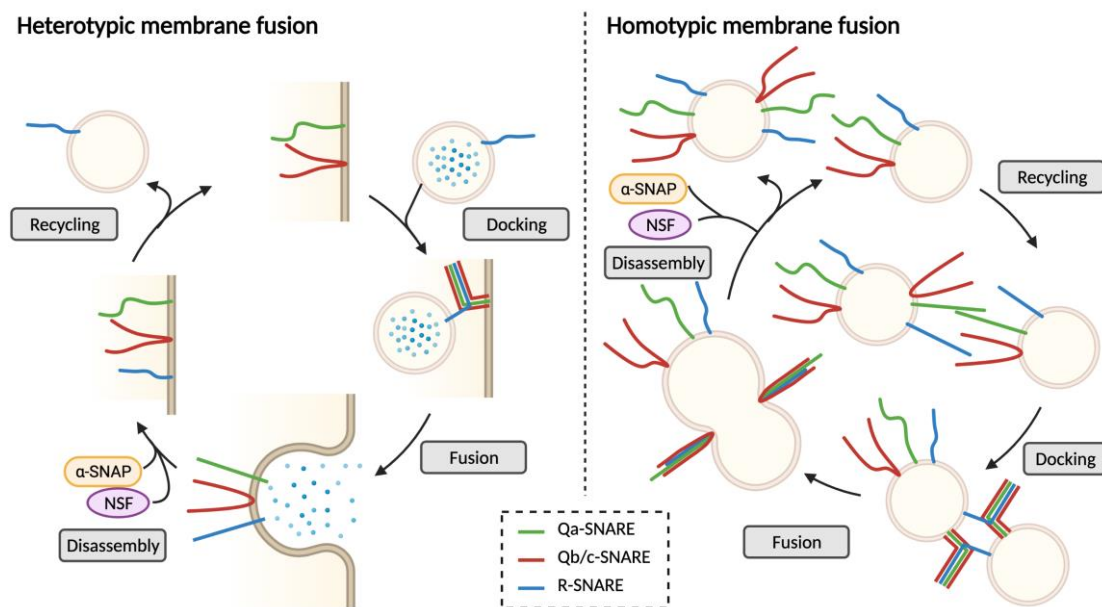


Figure 10 – Cycles of SNARE assembly and disassembly according to the heterotypic or homotypic membrane fusion model. On the left, heterotypic membrane fusion model where the v-SNARE is found into the vesicle and two or three t-SNAREs are located into the plasma membrane. On the right, an example of the homotypic membrane fusion model where v-SNARE and t-SNAREs are found together into the same vesicle membrane resulting into the fusion of two vesicles due to a v-SNARE from one vesicle interacting with t-SNAREs from the other vesicle. Adapted from (74).

2.6. SNARE ROLE IN CANCER

SNARE proteins are key proteins which mediates a wide range of cellular processes. Besides its well-characterized role in synaptic vesicle fusion and neurotransmitter release, they are also involved in cell growth, migration, cytokinesis and protein transport (83,84). Recent findings have identified SNARE and SNARE-related proteins as very important elements

during the process of tumorigenesis in cancer signalling, progression and onset (44,64). They are directly involved in several hallmarks of cancer, such as sustaining proliferative signalling and evading growth suppressor, resisting cell death and in invasion and metastatic processes. Moreover, SNARE proteins have been also proposed as biomarkers for certain cancers (44,64).

2.6.1. ROLE OF SNARE PROTEINS IN TUMOUR PROLIFERATION.

One of the most fundamental traits of cancer cells is that they are able to overcome the strict proliferation control exerted in normal cells, by deregulating proliferative and anti-proliferative signals. Several studies have proved that SNARE proteins are highly involved in this dysregulation (85–87).

In glioblastomas, a highly proliferative and malignant type of brain cancer, blocking the function of STX1 results in a higher proportion of cells at the G₂/M cell cycle phase in comparison to control cells (86). Interestingly, knockdown of VAMP-8 attenuated tumour growth by arresting glioma cells at the G₀/G₁ phase of the cell cycle (87).

Despite further research is needed to explain how SNARE proteins are able to control the cell cycle, it is proved that another member of the Syntaxin family, STX16, plays an important role in the regulation of cytokinesis. Song and colleagues have demonstrated that STX16 interacts with the tumour suppressor RASSF1A (Ras association domain family 1 isoform A) at the midzone and midbody during late mitosis, enabling and regulating the cytokinesis step (85).

Altogether, these findings show that SNARE proteins play important roles regulating tumour cell proliferation and tumour growth and that their impairment could result in tumour growth attenuation.

2.6.2. ROLE OF SNARE PROTEINS IN RESISTANCE TO CELL DEATH AND AUTOPHAGY

Cell death is a natural brake to avoid aberrant cell population. However, if the signals that make the cells to enter into apoptosis are misled, cells can continue living and dividing, maintaining the tumour bulk and even expanding it. To this regard, it has been proved that the SNARE protein α -SNAP can deactivate the AMPK pathway, protecting cancer cells from mitochondrial mediated apoptosis (88). In ovarian cancer, downregulation of SNAP-23 resulted in an increase of apoptosis (89).

Another key cellular process that can contribute to cell death is autophagy, an important cell-physiologic response to cellular stress. The autophagic programme enables cells to breakdown organelles and cell components, such as ribosomes or mitochondria, or to envelope them into intracellular vesicles called autophagosomes which at the end will fuse with lysosomes where the organelle degradation will take place. VAMP-7, VAMP-3 and the ATPase NSF are involved in the fusion of the multivesicular bodies with the autophagosomes and the lysosomes in chronic myeloid leukaemia cells (90).

The role of autophagy in cancer treatment is controversial, most anticancer drugs or ionizing radiation affect autophagy. In most, but not all cases, these treatments increase autophagy in tumour cells, and autophagy affects the ability of tumour cells to die after drug treatment. Depending on the context, it has been seen that the effect of autophagy may be to promote or inhibit cell death (91). To this respect, VAMP-8 and STX17 have been involved in temozolamide resistance in the treatment of gliomas, through the activation of autophagy. STX17 located into the autophagosome interacts with VAMP-8 located into the lysosome/endosome, inducing membrane fusion of both vesicles (87,92).

Finally, STX6 and VAMP-4 have been found to confer cisplatin resistance in human ovarian cancer cell lines by co-localizing both with a P-type ATPase and contributing to the secretory vesicular transport of cisplatin from Golgi to the plasma membrane of the cell (93).

2.6.3. ROLE OF SNARE PROTEINS IN INVASION AND METASTASIS

SNARE proteins are involved in cell invasion and metastasis as well. As explained above, SNARE proteins function mainly relies in vesicle trafficking. Some of the proteins that they transport to the membrane are integrins, which are closely involved in migration and invasion (94–97). It has been proved by several authors that SNARE proteins, through integrin trafficking, contribute to the formation of invadopodia (protrusions, generally formed at the site of cell invasion, that enhances the ability of the cancer cell to invade) (94–97). SNARE proteins also promote secretion of MMP facilitating cell migration (64,96). SNAP-23, STX4 and VAMP-7 are associated in invadopodia to mediate trafficking of membrane type 1-matrix metalloproteinase (MT1-MMP) in BC cell lines (96).

In addition, SNARE proteins are able to modulate migration and invasion by regulating cancer cells junctions. In that field, different SNARE proteins have been described as focal adhesion regulators, among them, NSF and SNAP-23 regulate focal adhesion kinase (FAK): in

CHO-K1 cells, when NSF and SNAP-23 are not functional, FAK/SRV/PI3K-dependent pathway is downregulated, resulting in a lower focal adhesion turnover and less integrin trafficking to the plasma membrane (98,99). Moreover overexpression of STX4 abrogates E-cadherin function in mammary epithelial cells, activating the Smad pathway and contributing to an asymmetric mammary epithelial cells morphogenesis, acquiring an invasive phenotype (100,101).

2.6.4. SNARE PROTEINS AS BIOMARKERS

In some cases, SNARE proteins are very low expressed in the healthy tissue but high in the tumour, their expression being significantly correlated with a poorer overall and metastases free survival. It is the case of STX3 that is expressed in BC but not in the healthy tissue and its higher expression correlates with a poorer overall and metastasis-free survival (102). SNAP-25 and STX1A are not expressed in the parathyroid tissue but are overexpressed in parathyroid carcinoma samples (103). In addition, our research group has demonstrated that STX1A expression correlates with a poorer overall and distant-metastasis free survival in BC (104).

Together these findings open the possibility to use SNARE proteins expression in tumours in order to classify patients' outcomes in terms of overall and distant metastasis free survival.

3. SYNTAXIN-1A

3.1. SYNTAXIN FAMILY AND DOMAINS

Vesicular transport mediates the traffic between intracellular membrane compartments and the plasma membrane through the concerted action of several cytosolic proteins: the SNAP receptors also known as SNARE proteins. According to the SNARE hypothesis, synaptic vesicles dock to the target membrane through the interactions of NSF protein (an ATPase), NSF-attachment proteins, α/γ SNAP (synaptosomal-associated proteins), and vesicular (VAMP or synaptobrevin) and target (syntaxins and SNAP-25) membrane proteins (v- and t-SNARE, respectively) (77,105).

Syntaxin-like sequences have been found in all eukaryotes examined to date, which demonstrate the importance of these proteins into the different organisms and along the whole evolutionary process (106). Syntaxin proteins conform a big family which consist of 15 different genes in mammals and 7 genes in yeasts (*Figure 11 and Table 7*).

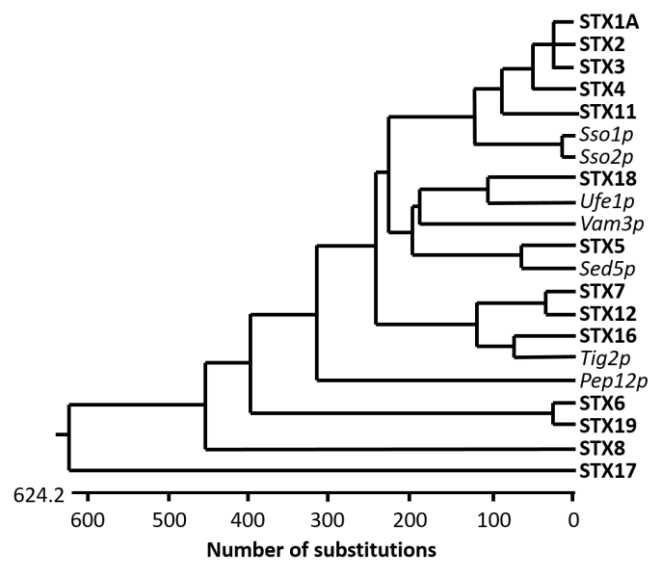


Figure 11 – Dendrogram of the nearest-neighbour syntaxins of the 7 *S.cerevisiae* and 15 mammalian syntaxins. This dendrogram is generated with DNASTAR and published in (106). Yeast syntaxins are marked in italics and are not in bold.

In general, all mammalian syntaxins (except STX9/19 and STX11) are transmembrane proteins that are anchored into the plasma membrane or into vesicle's membrane through its carboxyl-terminal tail (73,106) (*Figure 12*). Focusing on the domain structure of STX1A, the first syntaxin to be identified together with STX1B, has a transmembrane domain, and next to it, a coiled-coil H3 domain or SNARE domain which is characteristic and conserved in all

syntaxins. This domain is thought to be involved in membrane fusion, and is where the other SNARE proteins do interact. This motif is connected with a flexible linker to the autonomously folded Habc domain, located at the N-terminal part and at the end of the protein, near its short N-terminal peptide (Npep) (107). Differently from others syntaxins who have these N-terminal domains and are also involved in vesicle exocytosis and neurotransmitter release, STX1A Npep is Ca^{2+} sensitive and able to bind to the v-SNARE SYT1 in a Ca^{2+} -dependent manner. Moreover, specific point mutations in these motifs resulted into an impairment of vesicle docking and granule recruitment highlighting their importance in STX1A activity (95,107–109).

Table 7– Syntaxins isoforms and chromosome, cellular and tissue localization with their known function.

Syntaxins	Chromosome	Cellular localization	Tissue distribution	Known function
STX1A (A and C)	7q11.23	Presynaptic PM	Neuronal and secretory cells	Neuronal exocytosis, regulated secretion
STX1B	16p11.2	Presynaptic PM	Neuronal and secretory cells	Neuronal exocytosis, regulated secretion
STX2 (A - D)	7	PM	Ubiquitous	Exocytosis, morphoregulator during development
STX3 (A - D)	11cent-11q12.3	PM	Ubiquitous	Exocytosis, morphoregulator during development
STX4	16p13.13-16p12.3	PM	Ubiquitous	Glut4 translocation
STX5	11cen-11q12.1	ER-Golgi boundary	Ubiquitous	ER-Golgi transport
STX6	1	TGN	Ubiquitous	TGN-endosome transport, endosome-TGN transport, fusion of immature secretory granules
STX7	6	Endosome	Ubiquitous	Late endosome fusion, late endosome-lysosome fusion
STX8	17p12	Endosome	Ubiquitous	Late endosome fusion
STX10	19p13.2	TGN	Ubiquitous	?
STX11	6q23.1-6q25.3	TGN/late endosome	Ubiquitous	?
STX12/13	1	Endosome	Ubiquitous	Recycling of surface protein, early endosome fusion
STX16 (A - C)	10p1.23-20p11.21	Golgi/TGN	Ubiquitous	Early endosome-TGN transport

Syntaxin-1A, a synaptic related protein in breast and head and neck cancer progression and prognosis

Syntaxins	Chromosome	Cellular localization	Tissue distribution	Known function
STX17	?	Smooth ER	Ubiquitous	Trafficking to smooth ER
STX18	4	ER	Steroidogenic tissues	ER-Golgi transport, ER homotypic fusion

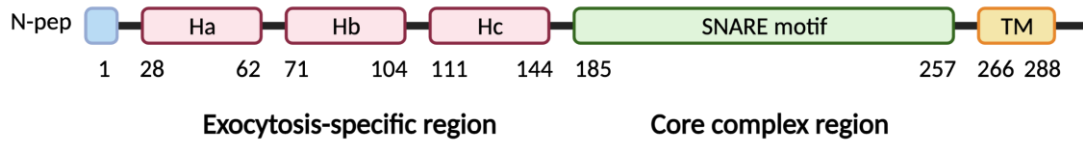


Figure 12 – Structure of STX1A protein. Schema of the different domains that conforms the human STX1A protein.

3.2. ROLE OF SYNTAXIN-1A IN NEURONS

Neuronal synapse is a well-orchestrated process where through a stimulus, a pre-synaptic neuron is able to release the content of synaptic vesicles (containing neurotransmitters and/or neuromodulators) into the synaptic cleft where they will be able to trigger a response to the target cell (post-synaptic neuron or cell). During this process the synaptic vesicles fuse with the target membrane (*Figure 13*) (107,108,110).

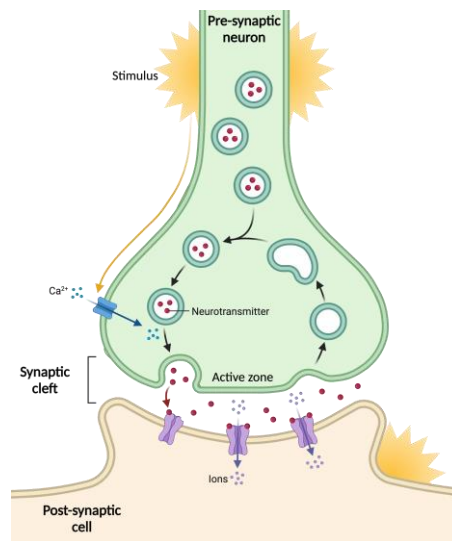


Figure 13 – Neuronal synapse. Scheme representing the different parts of a neuronal synapse: the pre-synaptic neuron that under some stimulus opens the voltage-gated Ca^{2+} channels. Ca^{2+} entrance together with the formation of the SNARE complex (not represented) leads to the fusion of the vesicles with the cell membrane and the neurotransmitter release and/or neuromodulators into the synaptic cleft that will interact with the receptors of the post-synaptic neuron or cell.

In a neuron three distinct pools of vesicles exist:

- A pool of vesicles that are ready to be released, located at the active zone.
- A recycling pool used to supply the ready releasable pool.
- A large reserve pool, that will supply vesicles for the recycling pool.

Under resting conditions, STX1A is located along the active zones of the presynaptic neuron, forming small clusters ready to dock with the readily releasable pool of vesicles once the neuron reaches the action potential (107,108,110). In this resting state, STX1A is bound to MUNC18-1, a cytosolic protein, member of the SM family, which induces a close-conformation of STX1A by binding to its N-peptide, and hiding its H3 and Habc domains, making STX1A inaccessible to interact with other SNARE proteins (105,111–113). When the neuron receives an input, the vesicles in the recycling pool start to relocate to the readily releasable pool that will tether into the target membrane to fuse and release their cargo. This process is called tethering and facilitates the interaction between the target membrane and the exocytic synaptic vesicle. In this step, STX1A will start the transition from a closed-conformation to an open-conformation (*Figure 14, tethering*). How this transition is made, is still not clear. Recent studies reveal that MUNC13 would be the protein in charge to induce the open conformation to STX1A. First of all, MUNC13 recruits VAMP-2 from the synaptic vesicles, approaching them towards the target membrane. Doing that, the SNARE motif of VAMP-2 becomes accessible for STX1A. To interact with VAMP2, STX1A needs a conformational change that occurs after its interaction with SNAP-25, MUNC18-1 and MUNC13. Interaction among all these proteins leads, at the end, to the SNARE complex formation (*Figure 14, docking*) (80,114). In this step, the interactions of the t-SNARE proteins with the v-SNARE protein are weak and calcium-independent. In the next step in the docking stage the SNARE proteins come in contact with each other via the SNARE motifs, also in a calcium-independent manner, and the interactions between the vesicle and the plasma membrane become stronger due to Syntaxins and the recruitment of other SNARE proteins, and will increase cluster size (105,107,108). Docking is followed by the priming step (*Figure 14, priming*): the SNARE complex recruits other SNAREs such as complexins which help SNARE proteins stabilization and prepare the synaptic vesicles for fusion. In this step the action potential depolarizes the neuron membrane and induces the opening of the voltage-gated Ca^{2+} channels, Ca^{2+} binding to some SNAREs, such as SYT1 and the increase of the concentration of intracellular Ca^{2+} into the microdomain surrounding the pre-synapse. Then, the vesicles fuse with the target membrane (*Figure 14, fusion*), this fusion is calcium-dependent. Finally, once the neurotransmitters and/or neuromodulators are released into the pre-synaptic space, the synaptic vesicle has to be recycled and the SNARE complex disassembled. In this part NSF and α -SNAP proteins will play their role, ending up with STX1A in its closed-conformation, bound with MUNC18-1 and spread along the active zone, ready to re-enter the exocytosis cycle of the neuron (105,108,114).

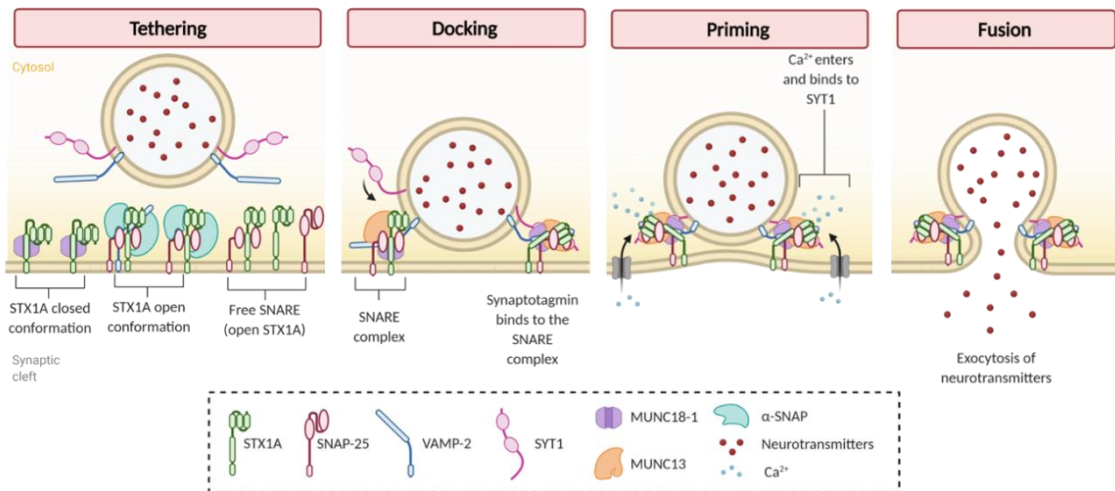


Figure 14 – Role of STX1A and their SNARE partners in neuron exocytosis. Scheme of the different stages of vesicle exocytosis in human neurons. In the tethering step, STX1A can be found in different conformations: closed due to MUNC18-1 interaction, open conformation interacting with other SNAREs and α -SNAP or in an open conformation free in the plasma membrane. Then, once the vesicle is approaching, in the docking step, the SNARE complex starts forming by interaction of STX1A with SNAP-25 and VAMP-2 and also with the soluble SNAREs MUNC18-1 and MUNC13. The interaction with SYT1 strengthens the interaction, that after calcium entrance and interaction with SYT1 in the priming step, the process ends up with the fusion of the exocytic vesicle with the plasma membrane and the release of the neurotransmitters and/or neuromodulators into the synaptic cleft. Adapted from (71,115)

3.3. SYNTAXIN-1A IN NON-NEURONAL TISSUES

Even though STX1A function is widely described and studied in neurons, it also plays an important role in other tissues altogether with other SNARE proteins. However, in other tissues, STX1A not only contributes in regulating exocytosis events, but also is able to modulate ion channels.

One example of its role in non-neuronal cells is its importance in fertilization. STX1A is expressed in mammalian sperm, where it plays a pivotal role regulating the acrosome reaction (*Figure 15*) (116). The acrosome is a membrane-bound organelle originated at Golgi apparatus and located at the anterior part of the mature sperm head. The acrosome contains hydrolytic enzymes that, once secreted, will help to penetrate the oocyte's zona pellucida to achieve fertilization (117). The acrosome will be released due to the acrosome reaction, a type of exocytosis with special characteristics because it is an all or nothing secretion of a single granule that is not able to be recycled. STX1A together with other SNARE proteins such as SNAP-25 and VAMP-2 regulate this type of exocytosis. As in neural synapses, the exocytosis is triggered by an increase of intracellular calcium, followed by a relocation of STX1A and other SNARE proteins into the exocytosis site (116,118–120). Finally, thanks to the MUNC18-1 chaperoning of STX1A and its interaction with SNAP-25 and VAMP-2, the acrosome membrane

ends up fusing to the plasma membrane of the sperm, and all the proteins are released into the oocyte zona pellucida enabling the sperm to go through oocyte extracellular matrix and fertilize it (118,120).

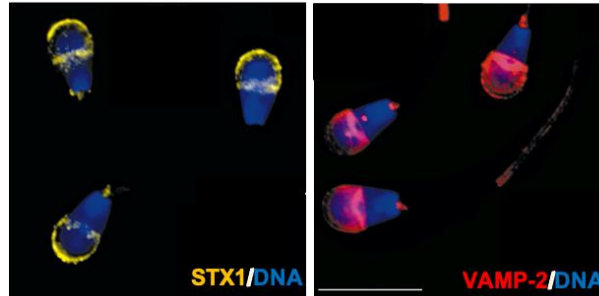


Figure 15 – STX1 and VAMP-2 are expressed in mammalian sperm. Image of bull sperm stained with STX1 (left image) and VAMP-2 (right image) demonstrating the expression of these SNARE proteins in sperm and their possible role in the acrosome reaction. Adapted from (116).

Other example where STX1A plays an essential role is in the regulation of Cystic Fibrosis transmembrane regulator (CFTR) channel. CFTR channel is found into the apical membranes of epithelial cells located into the airways, intestine and exocrine glands. It is a cAMP-activated chloride channel and mediates salt and water secretion in submucosal glands and intestinal crypts. CFTR final function is to lubricate the mucosal surface and to help deliver secreted proteins out of the gland or crypt. CFTR protein has a regulatory domain (R domain) which is the target of multiple phosphorylation and it is where STX1A is able to bind, through its N-terminal tail, and inhibit CFTR function. However, is by a hydrophilic interaction that STX1A interacts with CFTR channel, in comparison to the hydrophobic interactions that STX1A uses to interact with other SNARE proteins (121). Nevertheless, STX1A is regulated in a similar way than in neurons as MUNC18-1 also regulates the open or closed-conformation of STX1A. Open STX1A interacts with SNAP-23 (a SNAP-25 homologue) and both proteins bind to the R domain of CFTR, inhibiting its function. STX1A has also been linked to the regulation of CFTR and Epithelial Sodium Channel (ENaC) density into the plasma membrane (122). Mutations in CFTR channels or ENaC have been associated to cystic fibrosis disease, the most common sever autosomal-recessive disorder in Caucasians. This disease is characterized by a progressive decline of lung function as a consequence of a sustained inflammatory response to pathogens accompanied by pancreatic insufficiency. The cystic fibrosis genotype has been widely characterized, however sometimes was difficult to determine the mutation causing a cystic fibrosis phenotype. After some bioinformatic research, it was found that STX1A variants influence the functionality of CFTR channels by reducing their function (123,124).

Finally, STX1A also plays a very important role in insulin secretion and in the regulation of some ion channels in pancreatic β -cells. On the one hand, using the same mechanism seen in neurons and sperm, STX1A regulates insulin exocytosis forming part of the SNARE core that facilitates the fusion of the insulin vesicles to the plasma pancreatic β -cells. Briefly, STX1A is recruited in its close-conformation by MUNC-18-1, and once there is a trigger to induce insulin secretion, MUNC13 approaches the insulin vesicles inducing the open conformation of STX1A, that interacts with SNAP-25 into the exocytosis site. Finally, once both membranes are fused, insulin is secreted into the bloodstream (125–127). On the other hand, STX1A and other SNARE proteins (MUNC18-1 and SNAP-25) regulate some ion channels involved in insulin secretion: it has been proved that the open conformation of STX1A inhibits the opening of the K^+ voltage gated Kv2.1 channel (128,129) and regulates the opening of ATP-sensitive K^+ channels and the L-type calcium channel (130,131). Through the regulation of these ion channels, STX1A modulates the membrane repolarization, optimizing insulin release (129,132). To this respect, it has been shown that diabetic patients have decreased levels of STX1A, miR-29a seeming to be responsible for its down-regulation (125,132–134). Moreover, a single nucleotide polymorphism in STX1A gene seems to correlate with insulin requirement in type II diabetic patients (135).

3.4. SYNTAXIN-1A ROLE IN CANCER

As previously explained, even if it is an ongoing research, there is increasing scientific evidences that SNARE proteins play a very important role in cancer progression and metastasis. Moreover, it has been stated that syntaxins in particular also have a high impact in tumour development by helping in the formation of invadopodia or being involved into tumorigenic factors secretion. Particularly, little is known about the specific role of STX1A in cancer. After an exhaustive search in Pubmed, only a few articles appeared describing STX1A as a possible biomarker for some types of cancer and only one research article is focused on the tumourogenic effects of this protein.

Ulloa *et al.* (2015) describe the role of STX1A in glioblastoma, a nervous-related tumour. The authors found that the blockade of STX1A resulted into lower glioblastoma cells proliferation *in vitro*. Moreover, impairing STX1A function *in vivo* resulted in a reduction of tumour growth into the brain of immune compromised mice (86). Additionally, they postulated that STX1A could be involved in the metastatic process as well, as other authors

found similar results in osteosarcoma metastasis, proposing STX1A as a possible target for the treatment for this type of metastasis (86,136). Other published articles are focused on describing STX1A as a good biomarker to diagnose a specific type of cancer or as a prognostic predictor. It has been postulated that determining STX1A expression could be useful as a diagnostic tool for adamantinomatous craniopharyngioma (ACP), where a low expression of this gene is found in this benign epithelial tumour (137). Contrarily, others authors proved STX1A to be a robust neuroendocrine marker for its sensitivity and specificity for only being positive in neuroendocrine tumour samples in comparison to non-neuroendocrine tumours (138). Finally, overexpression of STX1A have been correlated to a poorer overall survival in patients suffering from lung cancer, bladder cancer or BC (104,139,140).

Overall, the fact that STX1A is overexpressed in some tumours in comparison to non-tumoral samples, and that is a targetable protein, for example by BoNTs, make worth exploring its role in cancer, such as in breast and head and neck tumours.

4. BREAST CANCER

4.1. EPIDEMIOLOGY OF BREAST CANCER

BC was the second most incident cancer worldwide in 2020 (considering both sexes and all ages) and the most common between women (all ages) with 2,088,849 new cases diagnosed. In terms of mortality BC was the fifth cancer-related death worldwide in 2020 (both sexes and all ages), however, it was the first cancer-related death between women (all ages) with 626,679 deaths (7,8). As represented in *Table 8*, the same epidemiological data is seen specifically for U.S.A, Europe, Spain and Catalonia, where BC is the most incident cancer in women and the first (except for the U.S.A) cause of cancer-related deaths (7,8,141).

Table 8 – BC incidence and mortality worldwide, U.S.A., Europe, Spain and in Catalonia in both sexes or specifically in women.

	Both sexes		Women		Year	Source
	Incidence	Mortality	Incidence	Mortality		
World	2 nd	5 th	1 st (2,088,849 new cases)	1 st (626,679 deaths)	2018	WHO
U.S.A	3 rd	4 th	1 st (281,550 new cases)	2 nd (62,470 deaths)	2021	Cancer Statistics, 2021
Europe	1 st	3 rd	1 st (522,513 new cases)	1 st (137,707 deaths)	2018	Globocan
Spain	2 nd	4 th	1 st (33,307 new cases)	1 st (6,625 deaths)	2019	AECC
Catalonia	2 nd	4 th	1 st	1 st (1,066 deaths)	2019	AECC

Interestingly, in Spain women from Barcelona and Madrid represent the 25% of the total incidence of BC. Comparing these data with data from other European countries in 2018, BC estimated age-standardized incidence and mortality rates in Spain are lower than in Netherlands, Germany, Switzerland, France or United Kingdom (7,142).

An increase in BC incidence in Catalonia has been stated among the years. Scientists try to explain that fact according to changes in reproductive factors, such as postmenopausal hormone therapy. It could also be explained by an increase in BC screening programs or an increase of older women population (141).

4.2. BREAST CANCER SUBTYPES

As previously mentioned, cancer has not to be considered as a single disease. BC is not an exception, it is a complex disease with a high grade of heterogeneity related to different histopathological and biological features, clinical outcomes and treatment protocols. Due to this high diversity, there is a need to classify BC tumours into more homogenous entities which will enable a better understanding of the tumour biology to ultimately apply the best treatment protocol to the patients. A suitable classification needs to be clinically useful, easily applicable and widely reproducible. Currently, despite all the efforts made to achieve the perfect classification, there is still room for improvement. Considering an historical point of view, there are two types of classifications: the histopathological and the molecular classification (143,144).

4.2.1. HISTOPATHOLOGICAL CLASSIFICATION

The histopathological classification is based on the diversity of morphological features of the BC tumours. Even though some difficulties exist due to the lack of markers defining hyperplasia, BC tumours can be divided according to their invasiveness, distinguishing between *in situ* and invasive tumours (144,145). Breast carcinoma *in situ* can also be subclassified into ductal carcinoma *in situ* (DCIS) and lobular carcinoma *in situ* (LCIS), being the first one the most common of the *in situ* carcinomas. The same happens with the invasive carcinoma, it can be subclassified into invasive ductal carcinoma (IDC) and invasive lobular carcinoma (ILC) (144,145):

- **Ductal carcinoma *in situ*:** is a non-invasive pre-malignant BC lesion. It is located inside the mammary ducts surrounded by a myoepithelial cell layer and by an intact basement membrane. Although featured by clonal proliferation, cancer epithelial cells do not have the capability to spread into the mammary stroma. It is considered a non-obliged precursor lesion of IDC (143,145,146) (*Figure 16*).
- **Invasive ductal carcinoma:** is a highly heterogeneous lesion that evolve differently in each patient. In this BC subtype the clonal proliferating epithelial cells are no longer maintained within the ducts and are able to spread to the surrounding tissues thanks to the disruption of the myoepithelial cell layer and also of the basement membrane (143,146) (*Figure 16*).

- **Lobular carcinoma *in situ*:** the clonal proliferation of epithelial cells is located in the terminal ductal lobular units. These cells will fill and expand in more than 50% of the acini. In this BC subtype, mitotic activity is absent or exceedingly rare (143,145,147) (Figure 16).
- **Invasive lobular carcinoma:** this type of BC tends to appear in older women than IDC. It has a better prognosis than IDC, it is well-differentiated, shows low-to-moderate proliferation index and the majority have a good response to endocrine therapy. ILC presents a loss of epithelial markers (such as E-cadherin), acquiring a more mesenchymal phenotype which does not lead to a more aggressive phenotype (143,148,149) (Figure 16).

However, histopathological classification has not been proved to be able to distinguish correctly between BC tumours subtypes. In each BC histopathological subtype there is still high degree of heterogeneity, comprising different biological and clinical profiles within (144).

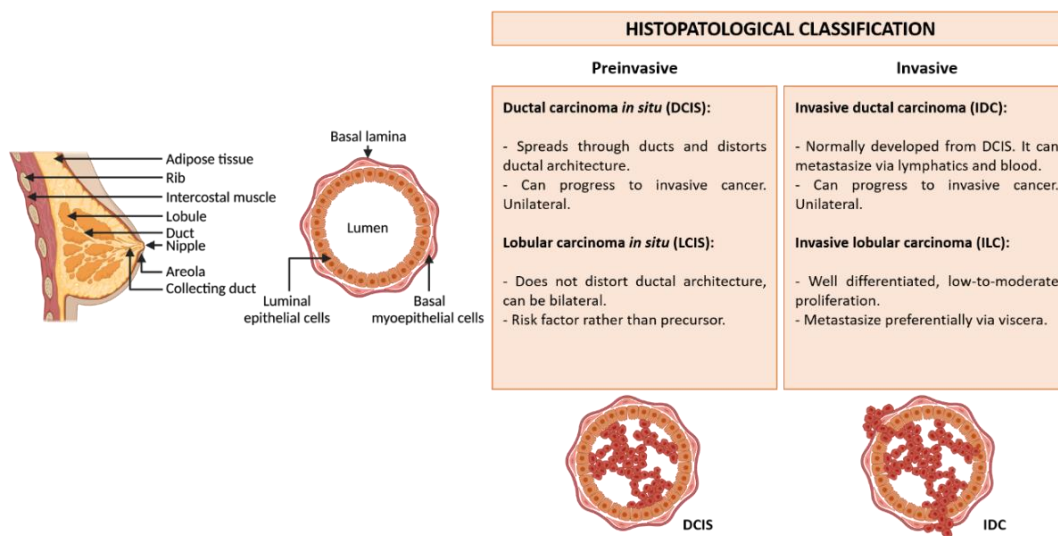


Figure 16 – Healthy breast anatomy and characteristics of histopathological classification of BC. On the left, anatomy of a healthy breast with a sagittal cut where it is possible to see the cell components of the duct. On the right, characteristics of the preinvasive and invasive stages of the histopathological classification of BC. Adapted from (143).

4.2.2. CLINICAL CLASSIFICATION

Later, the finding that some BC tumours do express hormone receptors (HR) such as oestrogen receptors (ER) and progesterone receptors (PR) and the discovery of the distinct patten of expression of the epidermal growth factors receptors (mainly HER2) give rise to a new classification of BC tumours and also new treatment approaches based on hormonal and

targeted therapies against them. This new clinical classification is based, among other criteria, on the expression levels of ER, PR and HER2 receptors (*Figure 17*). The expression of the above mentioned receptors can be used as biomarkers, which are able to predict patient's outcome, and is also useful to determine the treatment strategy to face the tumour (144,150).

According to that, the clinical classification distinguishes the following BC subtypes:

- **Hormone receptor positive BC subtypes:** it is the most frequent subtype, it includes HR positive but HER2-negatives tumours. They have the best prognosis and generally respond to hormonal treatment, the response varying according to a gradient of HR expression (144,150).
- **HER2 positive BC subtype:** it corresponds to the 20-25% of all BC and includes HR-negative and HER2-positive tumours. Most of these tumours have an overexpression of the HER2 protein due to chromosomal amplification of the HER2 gene. They have an intermediate-poor prognosis and respond poorly to chemotherapy and endocrine therapy but are optimal candidates to anti-HER2 treatment, which will increase patients survival rates (144,150,151).
- **ER-positive, PR-positive and HER2-positive or Triple positive BC subtype:** they are tumours that are HR-positive and HER2-positive. Their prognosis is intermediate and they can be treated with a combination of hormone therapy, chemotherapy and/or anti-HER2 targeted therapies (144,150,151).
- **Triple negative BC subtype:** they express neither HR nor HER2 receptors clinically relevant levels. This subtype has the worst prognosis. Nowadays, there is no specific treatment for this BC subtype, the only drug treatment available is chemotherapy. At least, it has been shown that this subtype respond better to this treatment than others BC subtypes (144,150,151).

4.2.3. MOLECULAR INTRINSIC CLASSIFICATION

Even if the previous classification was useful in predicting the clinical outcome and in choosing between therapeutical strategies, significant variations in treatment response and survival were still present in the BC subgroups defined by the clinical classification. To solve this drawback, and taking advantage of technological progresses, Perou *et al.* in 2000

conducted a gene expression profile study in BC tumours that enabled their classification into four gene clusters, finally distinguishing four intrinsic BC subtypes according to their gene expression patterns (ER+/luminal-like, HER2-enriched, basal-like and normal breast-like) (152). One year later, Sørbye *et al.* corroborated the previous findings, but also subdivided the luminal group in two distinct luminal types, luminal A and luminal B (153). According to this intrinsic molecular classification some diagnostic tools have been developed and, in 2009, it was possible to robustly classify BC tumours analysing a minimum of 50 genes without compromising accuracy, naming this gene molecular classifier as PAM50 (154). Finally, in 2012 The Cancer Genome Atlas (TCGA) confirmed that the four intrinsic subtypes, luminal A, luminal B, HER2-Enriched and basal-like BC subtypes could explain the phenotypic diversity present in BC tumours. However, they excluded the normal-like subgroup because it shows a low number of somatic mutations and is considered to be enriched for benign breast tissue markers (155). According to the final classification, the four intrinsic molecular subtypes are (*Figure 17 and Table 9*):

- **Luminal A:** It is the most common subtype (50-60% of the total BC). This subgroup is characterized by low-grade tumours that have high expression of luminal epithelial genes, ER, PR and low expression of HER2. Luminal A tumours usually have a good prognosis and respond well to hormone/endocrine treatments (143–145,150,151,156,157).
- **Luminal B:** It comprises to the 10-20% of BC and is characterized by high grade tumours with low expression of ER and PR in comparison to luminal A tumours. In luminal B tumours, there is a subgroup that overexpresses HER2 receptors and is associated with a worse overall survival in comparison to luminal B HER2-negative tumours. Prognosis of luminal B tumours is intermediate, and they can be treated with a combination of chemotherapy and hormone treatment. Luminal B HER2-positive tumours can also be treated with anti-HER2 targeted therapies (143–145,150,151,156,157).
- **HER2-enriched:** 15-20% of BC tumours correspond to HER2-enriched BC subtype. These tumours overexpress the HER2 receptor and they do not express luminal epithelial genes. They have a high proliferation rate and a poorer prognosis than luminal B. Currently, HER2-enriched tumours are treated with HER2-targeted therapies, to block HER2 signalling (143–145,150,151,156,157).

- **Basal-like:** It represents the 10-20% of all breast tumours. This breast carcinoma subtype expresses genes that are typically found in basal (myoepithelial) cells. In this subtype there is often an increased activation of WNT and EGFR pathway-related genes, and TP53 and BRCA1 tumour suppressor genes are frequently mutated. Basal-like tumours are highly proliferative, they have the worst prognosis among BC subtypes and a high risk of relapse as well. According to the fact that basal-like tumours do not express PR, ER or HER2 receptors, normally they are treated with chemotherapy (143–145,150,151,156,157).

Nowadays, this intrinsic classification is not an alternative to the clinical classification, it is often integrated with the clinical classification to achieve a better prognostic score and to be able to establish the most suitable treatment protocol (150).

In 2007, a new intrinsic BC subtype was identified, termed as claudin-low BC subtype. This BC subtype is characterized by low expression of tight junctions and intercellular adhesions genes such as claudin-3, claudin-4 or claudin-7 or E-cadherin, among others. Its hierarchical cluster is located near basal BC subtypes. Moreover, this BC subtype overexpresses 40 genes related to immune response, which is related to a high infiltration of immune cells. The claudin-low subtype overexpresses genes related to mesenchymal differentiation, which altogether, makes them very aggressive tumours with a poor prognosis. As the basal subtype, claudin-low subtype tumours normally do not overexpress PR, ER or HER2 receptors (considered a triple-negative BC subtype) which means that the only drug treatment option is chemotherapy (156,158).

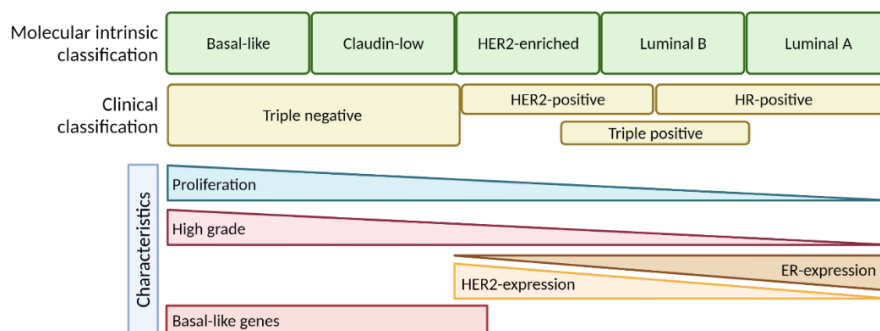


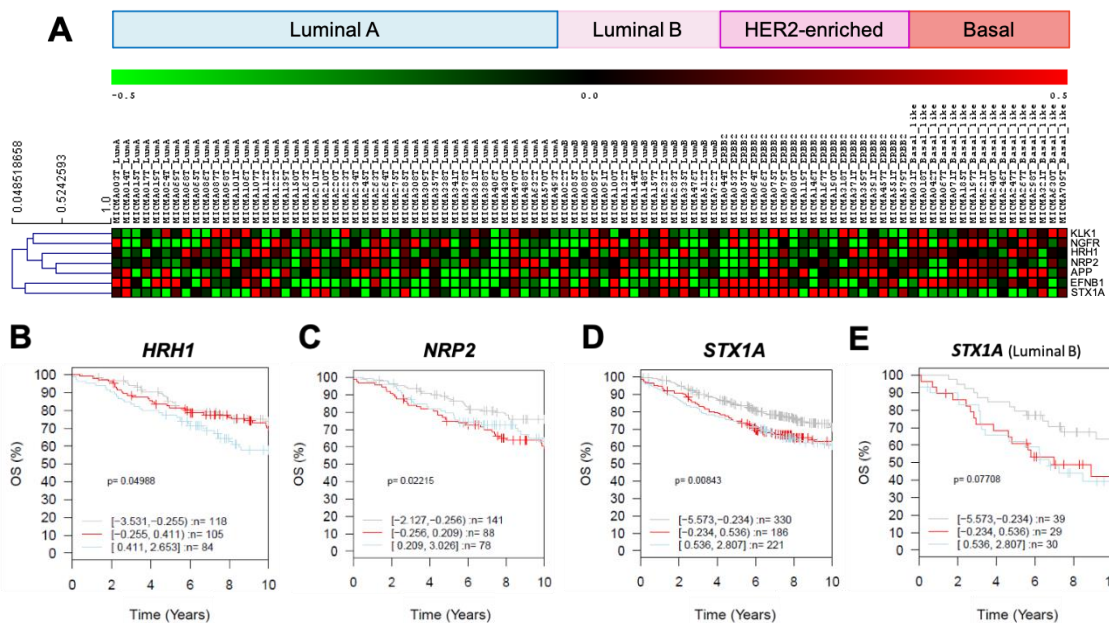
Figure 17 – Clinical and molecular intrinsic classification of BC and their characteristics. On the top, the molecular intrinsic and the clinical classifications of BC. On the bottom, some of the characteristics of BC along each BC subtype. Adapted from (143).

Table 9 – Features of the microarray gene expression profiling for defined molecular subtypes. Abbreviations: IHC (immunohistochemistry), GI/II/III (histological grade I/II/III, pCR (pathological complete response after neoadjuvant chemotherapy, +/- (predominantly negative), +/- (predominantly positive). Adapted from (151).

	IHC markers	Histological grade	Proliferation cluster	Other markers	Outcome	Benefit from chemotherapy
Luminal A	ER+: 91-100%	GI/GII: 70-87% GIII: 13-30%	Low	FOXA1 high	Good	Low (0-5% pCR)
	PR+: 70-74%					
	HER2+: 8-11%					
	Ki67: low					
	Basal markers: -					
Luminal B	ER+: 91-100%	GI/GII: 38-59% GIII: 41-62%	High	FGFR1 and ZIC3 amp	Intermediate or poor	Intermediate (10-20% pCR)
	PR+: 41-53%					
	HER2+: 15-24%					
	Ki67: high					
	Basal markers: -					
HER2-enriched	ER+: 29-59%	GI/GII: 11-45% GIII: 55-89%	High	GRB7: high	Poor	Intermediate (20-40% pCR)
	PR+: 25-30%					
	HER2+: 66-71%					
	Ki67: high					
	Basal markers: +/-					
Claudin-low	ER+: 12%-33%	GI/GII: 62-23% GIII:38-77%	Intermediate/high	CDH1: low/ Claudin: low	Intermediate	Intermediate (25-40% pCR)
	PR+: 22-23%					
	HER2+: 6-22%					
	Ki67: low/intermediate					
	Basal markers: +/-					
Basal-like	ER+: 0-19%	GI/GII: 7-12% GIII:88-93%	High	RB1: low/ CDKN2A: high BRCA1: low/ FGFR2: amp	Poor	High (>40% pCR)
	PR+: 6-13%					
	HER2+: 9-13%					
	Ki67: high					
	Basal markers: +					
Normal breast like	ER+: 44%-100%	GI/GII: 37-80% GIII: 20-63%	Low/intermediate		Intermediate	Low (0-5% pCR)
	PR+: 22-63%					
	HER2+: 0-13%					
	Ki67: low/intermediate					
	Basal markers: +/-					

4.2.1. DIFFERENTIAL EXPRESSION OF NEUROGENES AMONG BREAST CANCER SUBTYPES

In 2016, our group published an article revealing 6 neurogenes differentially expressed among BC subtypes. This discovery opened the possibility to use those genes as biomarkers. Briefly, three different databases of human genes (GeneGo, GeneCards and Eugenes) were interrogated to obtain a list of human neurogenes. Then, using a bioinformatic approach, the neurogenes list was crossed with two published BC patient's database, obtaining a short list of 7 human neurogenes differentially expressed among BC subtypes: Histamine Receptor 1 (*HRH1*), Neuropilin 2 (*NRP2*), Ephrin-B1 (*EFNB1*), Neural Growth Factor Receptor (*NGFR*), Kallikrein 1 (*KLK1*), *STX1A* and Amyloid Precursor Protein (*APP*). Among them, *KLK1*, *HRH1*, *NRP2*, *EFNB1*, *NGFR* and *APP* were differentially overexpressed in basal and HER2-enriched tumour samples, while *STX1A* was overexpressed in HER2-enriched and luminal B tumours (*Figure 18A*). Then, the correlation between neurogenes expression and the patient's clinical response was investigated to prove if they could be used as biomarkers. Using the GOBO patient's database, it was found that 6 of 7 initial neurogenes correlated with BC patient's prognosis. High or medium expression of the neurogenes correlated with worse overall survival than low expression (*Figure 18B -Figure 18I*). Moreover, *HRH1*, *NRP2* and *STX1A* gene set expression significantly correlate with a shorter overall survival ($p < 0.0001$) and distant metastasis-free survival ($p < 0.0001$) (*Figure 18J and Figure 18K*). Overall, our group proposed that *HRH1*, *NRP2* and *STX1A* targeted therapies could improve the outcome of BC patients, and even though more research is needed, they can be likely used as biomarkers (159).



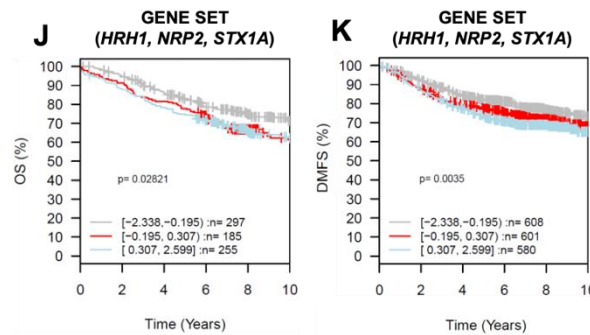


Figure 18 – Differential neurogenes expression in BC subtypes correlate with overall survival and distant metastasis free survival. (A) Selected neurogenes (*KLK1*, *NRP2*, *EFNB1*, *STX1A*, *NGFR*, *HRH1*, *APP*) expression levels for 96 patients with different BC subtypes. Rows represent microarray probes corresponding to the selected genes and columns represent patients. Red and green indicate high and low expression levels, respectively. (B-I) Kaplan-Meier analysis using overall survival (OS) in GOBO: *HRH1*, all tumours (B); *NRP2*, all tumours (C); *STX1A*, all tumours (D); *STX1A*, luminal B tumours (E), *STX1A*, HER2-enriched tumours (G); *NGFR*, all tumours (H); *EFNB1*, all tumours (I). (J) *HRH1*, *NRP2*, *STX1A* gene set OS analysis GOBO database. (H) *HRH1*, *NRP2*, *STX1A* gene set DMFS analysis from GOBO database.

4.3. HER2-POSITIVE BREAST CANCER SUBTYPES

HER2-positive BC subtypes include HER2-enriched and some Luminal B subtypes, the ones that overexpress HER2 besides ER and PR (143).

4.3.1. HER FAMILY OF RECEPTORS

HER2 receptor (also known as ERBB2 receptor) is a tyrosine kinase receptor from the family of EGFR. This family consist of four members: epidermal growth factor receptor 1 (EGFR/EGFR1/HER1), HER2, HER3 and HER4 and are ubiquitously expressed in epithelial, mesenchymal and neuronal cells and their progenitors (143,160,161).

These family of kinases present an extracellular domain by which they interact with their ligands. This extracellular domain is divided into four parts: domain I and III participating in ligand-binding, and domain II and IV participating in disulphide bond formation between other receptors, forming homodimers or heterodimers. Next to this domain, there is a transmembrane domain and an intracellular domain formed by a juxtamembrane segment, a protein kinase domain and finally, a carboxyterminal tail (*Figure 19*) (143,160,161). This is the general structure of the receptors of the HER family, however there are two exceptions:

- HER2 does not have any known ligand, which means that probably its extracellular domain (domain I and III) does not work properly (161,162), showing always an open (active) conformation .
- HER3 lacks the intracellular protein kinase domain (161,162).

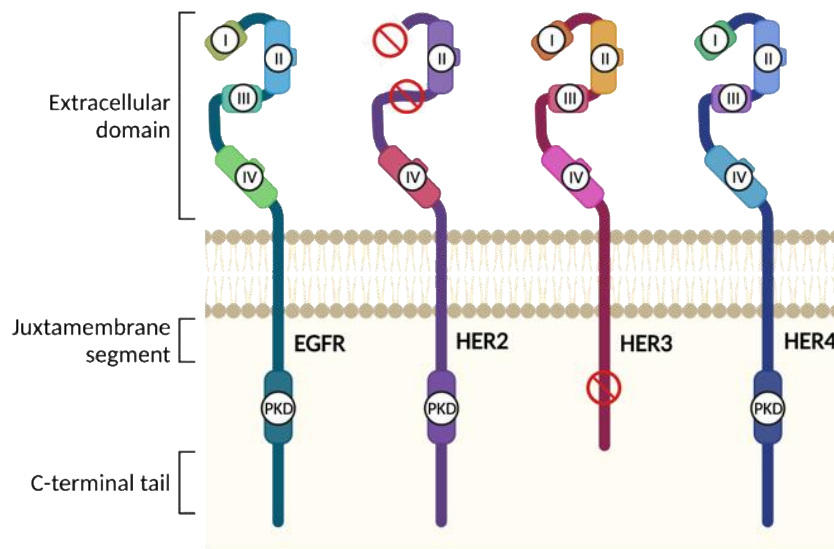


Figure 19 - Domains of the human EGFR/HER family of receptors. Scheme of the four receptors of the EGFR/HER family where it is possible to identify the four domains in the extracellular segment. Note that HER2 receptor lacks domain I and III which participate in ligand binding. The protein kinase domain (PKD) is also indicated, which is lacking in the HER3 receptor. Adapted from (161).

Like all protein-tyrosine kinase receptors, HER family receptors do not work alone, they need to form dimers (homodimers or heterodimers) or even, higher oligomers once they are bound to a ligand. There are several ligands that are likely to bind the extracellular domain of HER receptors, as seen in [Figure 20](#). Taking into consideration that 11 growth factors are able to interact with the HER receptors and that a combination of 28 HER dimers is possible, there are 614 possible combinations of active receptors. Nevertheless, it is important to note that not all the ligands are expressed near the cell that expose the receptors, so the number of potential combinations is reduced, but still a high number is possible (161). Since HER2 and HER3 monomers are not functional, under physiological conditions HER2 tends to form heterodimers with EGFR1 or HER3, which trigger a robust signalling activity. However, under non-physiological situations, such as in cancer, there is the possibility for HER2 and HER3 monomers to be activated without any ligand, or phosphorylate proteins without the PKD domain. For example, when there is an overexpression of HER2 receptors, HER2 homodimers are able to activate themselves and to trigger a signalling cascade. More difficult is to imagine the fact that HER3 homodimers, having their kinase domain impaired, would be able to trigger an intracellular signal. However, even that it is difficult there is the possibility that these monomers auto-phosphorylate themselves and activate a cellular response (161). Finally, it is also important to consider the diversity of ligands that can activate and modulate this family of receptors, described in [Figure 20](#). As an example, EGF can activate EGFR homodimers, but

also EGFR-HER2 heterodimers, but epiregulin (EPR) is able to activate EGFR and HER4 homodimers and EGFR-HER2 and HER3-HER2 heterodimers leading to a different response in each condition (161,163).

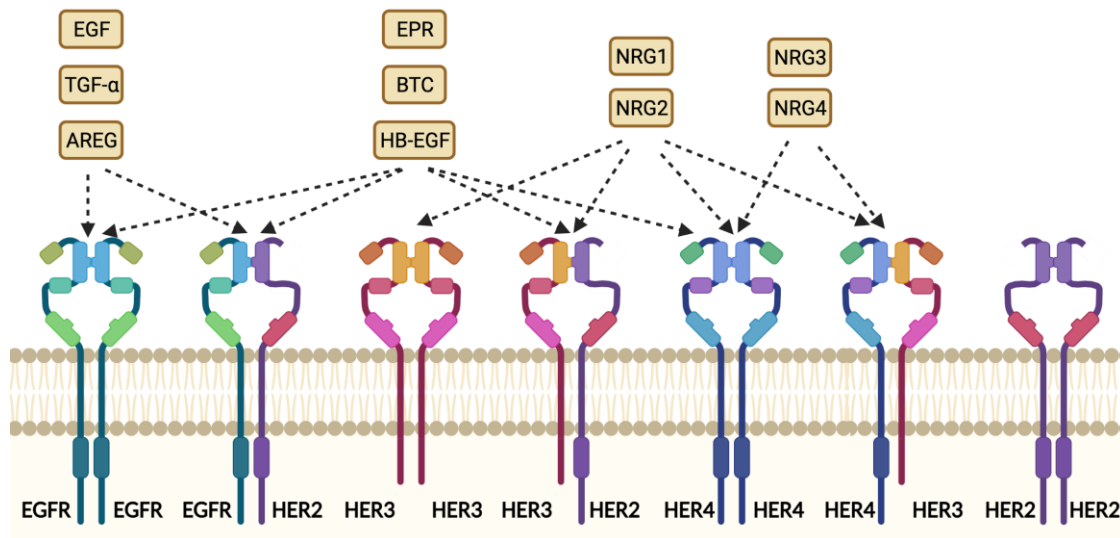


Figure 20 – Most frequent combinations of EGFR/HER family of receptors dimerization and their corresponding ligands. Representation of the four members of EGFR/HER family of receptors and their different dimerization combinations, together with their agonists. Abbreviations: AREG (amphiregulin), BTC (betacellulin), EGF (epidermal growth factor), EPR (epiregulin), HB-EGF (heparin-binding EGF-like growth factor) NRG (neuregulin) and TGF (transforming growth factor). Modified from: (161,163).

4.3.2. HER2 SIGNALLING

HER2 signalling pathway is a complex network of interactions between ligands and membrane receptors, protein kinases and transcription factors that regulate various key cellular functions. HER2 is the dominant tyrosine kinase receptor in BC, and due to the fact that it does not have any specific ligand, it can interact with the others three HER receptors. Once HER2 heterodimers with another HER receptor bound to a ligand, HER2 intracellular kinase domain is phosphorylated and several intracellular pathways activated. Some of these pathways will be Ras/Raf/mitogen-activated protein and PI3K/AKT/mTOR signalling pathways, which are master regulators of cell growth and survival. Moreover, its dimerization promotes mislocalization and degradation of the cell cycle inhibitor p27, enhancing cell cycle progression. Also, activation of the PI3K/AKT/mTOR pathway results in activation of NFκB, MDM2 and p53 which inhibits apoptosis. However, since HER2 receptor cannot work alone and its homodimerization is rare, the heterodimer HER2-HER3 is the most potent stimulator of the downstream pathways, particularly of the PI3K/AKT/mTOR (Figure 21). It is important to consider that HER2 receptor not only can heterodimerize with their family receptors but

also with others membrane receptors such as insulin-like growth factor receptor, increasing the complexity of HER2-triggered signalling (160,161,164).

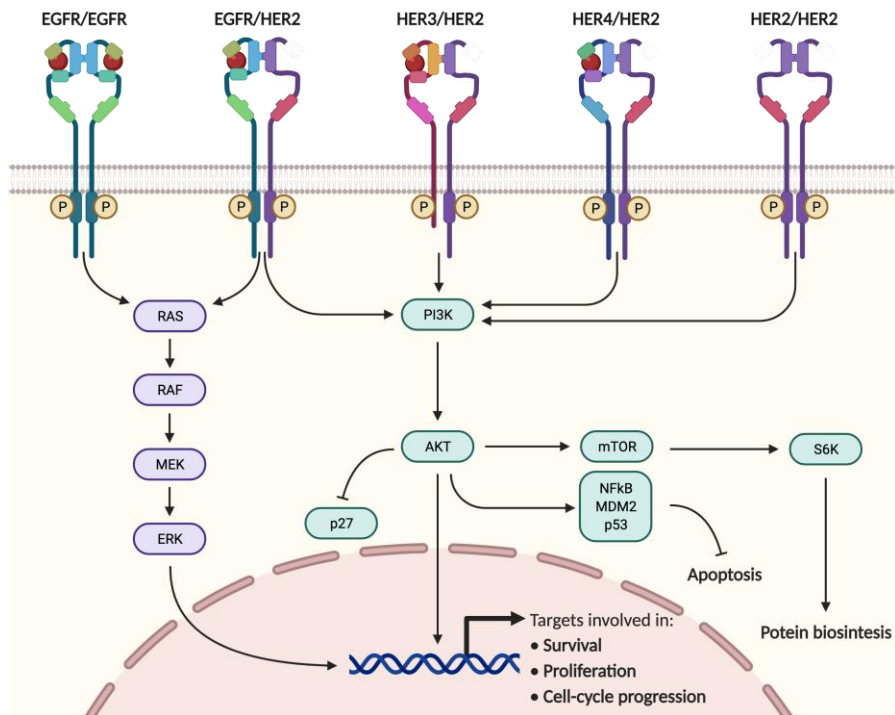


Figure 21 – HER2 signalling pathway. Representation of the most common signalling pathways activated when HER2 receptors hetero or homodimerize upon ligand activation. Adapted from (160,161,164).

4.3.3. HER2 INTERNALIZATION

Even there are evidences of how EGFR, HER3 and HER4 are internalized and degraded, HER2 seems not to follow the same path. EGFR internalization and degradation are very well studied and understood processes. Briefly, it is known that depending on the ligand bound to EGFR, the ligand concentration, the extent of EGFR ubiquitination and the cell type, EGFR will be internalized by a clathrin-dependent pathway or by a clathrin-independent pathway. Once the receptor is internalized it can be recycled and returned to the plasma membrane or degraded into the lysosomes. The pathway that receptor will take will depend on the ligand and the extent of phosphorylated and ubiquitinated EGFR (165). HER3 plasma membrane down-regulation is determined by endocytosis of the receptor in a clathrin-dependent manner and degraded by the ER-associated degradation pathway (166,167). Internalization of HER4 is not well characterized but it seems that its internalization is led by ubiquitination (165).

In contrast to other HER receptors, HER2 seems to be resistant to internalization, and as a consequence, to degradation. It remains at the cell surface signalling for prolonged periods

once activated, normally localizing in lipid rafts on cellular protrusions (168–170). Nowadays, some controversial regarding HER2 still exist. Several studies point out that HER2 is endocytosis-resistant or deficient because it lacks internalization signals or suffers from an active retention. Other studies indicate that HER2 is internalized but very efficiently recycled (165,169).

Sorkin and colleagues constructed a chimeric protein consisting of the extracellular domain of EGFR and the intracellular domain of HER2 receptor. This chimeric protein was able to activate its kinase domain, but even it was activated, their endocytosis rate was significantly slower than wild-type EGFR, concluding that the carboxyl-terminal domain of HER2 is internalization-impaired (169). Another study wanted to find out if overexpression of the protein resulted in an increased HER2 internalization, but they concluded that, like in BC, in cells overexpressing HER2 it remains into the cell membrane, so a stimulation of HER2 internalization and degradation does not occur (165). Another study aimed to determine if the heterodimerization of the receptor with EGFR or HER3 induced HER2 internalization. They found that in cells with HER2 overexpression, HER2 worked as a dominant negative slowing the rate of EGFR and HER3 internalization and degradation. Worthylake *et al.* also found that HER2 did not slow down EGFR internalization, but once EGFR was internalized HER2 re-routed internalized EGFR back to the plasma membrane instead of being degraded (171). One of the mechanisms proposed to maintain HER2 into the plasma membrane seems to be through interaction with the chaperone HSP90 and the calcium pump PMCA2 within the plasma membrane protrusions where HER2 is signalling (168,169).

Although the internalization and degradation mechanism of EGFR is well studied and comprehended, there is still a lot of work to do in HER2 internalization and degradation signalling to be able to elucidate HER2 turnover.

4.3.4. HER2 IN CANCER THERAPIES

HER2 receptors are expressed in normal tissues but at low levels at the plasma membrane, however, some cancers, such as breast, ovarian or gastric cancer, tend to overexpress it. HER2 overexpression could be as a result of gene amplification (chromosome amplification of the region 17q) or somatic mutations, normally in the extracellular domain or in the tyrosine kinase domain, which can result in a permanent activation leading to an overactivation of

HER2 regulated pathways such as proliferation, cell survival, metastasis and adhesion (143,172).

HER2 amplification confers some biological particularities to the breast tumour from which physicians can take advantage to treat BC. HER2 positive tumours are more resistant to hormonal therapies and HER2 tumours caused by 17q amplification normally are more sensitive to doxorubicin, because in the same chromosomal region the topoisomerase-2 gene (doxorubicin molecular target) is located. This fact makes really important to test if HER2 is present or not in a breast tumour biopsy to facilitate the selection of a potential curative therapy (143,172).

Nowadays, there are different therapies that act against the HER2 receptor. The introduction of these drugs lead to a better clinical management of the disease which results in a dramatic improvement in BC patients' outcome. In the past 20 years five HER2-targeted therapies have been approved by the Food and Drug Administration (FDA): trastuzumab, lapatinib, neratinib, pertuzumab and ado-trastuzumab emtansine (T-DM1) (*Table 10*) (143,172).

Table 10 – Anti-HER2 targeted therapies and their mechanism of action. Adapted from (160).

Drug name	Class of drug	Mechanism of action
Trastuzumab	Monoclonal antibody	Binds to extracellular domain, effective against HER2 homodimers
Lapatinib	Small molecule TKI-reversible	Selective inhibitor of EGFR and HER2 intracellular tyrosine kinase
Neratinib	Small molecule TKI-irreversible	Pan-HER TKI
Pertuzumab	Monoclonal antibody	Binds to different part of extracellular domain than trastuzumab and inhibits heterodimerization.
T-DMI	Antibody-drug conjugate	Trastuzumab conjugated to an anti-microtubule agent (a maytansine derivative called emtansine)

Trastuzumab is a monoclonal antibody that binds specifically to the extracellular part of HER2 receptor. It is a cytostatic agent that blocks Ras/Maf/MEK/ERK and PI3K/AKT/mTOR signalling pathway resulting in cell cycle arrest at G₁ phase. Moreover, it promotes HER2 ubiquitination, endocytosis and degradation leading to plasma membrane down-regulation of HER2 receptor. Additionally, owing to the fact that is an antibody, it enhances the immune response to the tumour thanks to its antibody-dependent cellular-mediated cytotoxicity. Once bound to HER2 receptors, immune cells are able to recognize the Fc region of the antibody and trigger an immune response. Initially, trastuzumab was approved to treat metastasis from

HER2-positive tumours, in addition to standard chemotherapy, but it also was proved to be effective in increasing pathologic complete response and disease-free survival in combination with chemotherapy as a neoadjuvant therapy in early BC patients. Also, it was beneficial as adjuvant therapy when it was prescribed for 1 year after chemotherapy (combined or alone) (143,164,172–176).

Another HER2-targeted drug is Lapatinib, a small molecule tyrosine-kinase inhibitor of EGFR and HER2 receptors. The inhibition of EGFR and HER2 receptors results in a reversible blockade of the intracellular signalling pathways, inhibiting downstream proliferation and survival signalling and inducing tumour cells apoptosis. Lapatinib down-regulates the activation of HER2, EGFR and ERK and promotes mutant p53 degradation. Moreover, delays DNA repair mechanism resulting in an increase sensitivity to radiation. Usually, it is used as a second-line therapy in tumours with a shorter form of HER2 receptor (p95HER2) which do not have the trastuzumab binding site. Besides the advantage that it is administered orally (in comparison to trastuzumab) it has the capacity of crossing the blood-brain-barrier which means that it could act in BC brain metastasis, as well (161,176,177).

Lapatinib and Trastuzumab were the first anti-HER2 targeted therapies to be approved by the FDA and with their commercialization the overall survival of HER2 positive BC patients dramatically increased. However, with long-term treatments, even though at the beginning tumours responded to the treatment, they became resistant and after some years tumour recurred. That was the main reason why new strategies needed to be developed and new drugs were approved by the FDA. Among them, pertuzumab, a novel antibody was developed. It targets a different extracellular region of HER2 which inhibits its heterodimerization. It is able to inhibit HER2-EGFR and HER2-HER3 dimers formation. In BC metastasis this drug showed that in combination with Trastuzumab, and in some cases with chemotherapy, resulted in a better progression-free survival and with a higher pathologic complete response. After pertuzumab, T-DM1 was approved by the FDA. It consists of a trastuzumab molecule conjugated with a microtubule agent that, thanks to the specificity of trastuzumab to bind HER2, it is able to act only in BC cells expressing HER2 receptors. This therapy showed better results in terms of progression-free survival and overall response rate than the combination of capecitabine and lapatinib. Finally, the last HER2-targeted therapy drug approved by the FDA was neratinib, that like lapatinib is a small molecule that inhibits the tyrosine kinase domain of HER receptors, but in that case, irreversibly. It was approved for early BC patients since a better disease-free survival rates were seen when compared to treated with

trastuzumab. Moreover, in HR positive patients neratinib is beneficial as well, in comparison to pertuzumab and lapatinib that had no effect in them (160,178).

- **HER2-TARGETED THERAPIES RESISTANCE**

Although HER2-targeted therapies have improved drastically the overall and the disease-free survival rate of HER2-positive BC patients, there is still a major problem concern: resistance to these therapies. There are two types of resistance to these therapies, it can be an intrinsic resistance or *de novo* resistance. For example, it has been proved that trastuzumab does not work equally in all early-stage BC tumours. Around 45%-62% of these tumours do not respond to the neoadjuvant combination of trastuzumab and chemotherapy, which indicates an intrinsic resistance. Otherwise, some patients respond initially to the treatment, but after some time they relapse and the tumour do not longer respond to the treatment, indicating a *de novo* resistance achieved by a drug-induced selection of tumour cells that have acquired resistance to the drug (164,179,180). A study performed in patients with metastatic BC determined that after treatment with trastuzumab and chemotherapy, the median duration of a partial or complete response was around 9 months, indicating that in less than a year the tumour acquired resistance to the treatment (181).

After years of research some mechanisms of resistance have been elucidated:

- **Gene amplification:** several studies identified that gene amplification could be a process related to HER2-targeted therapies resistance. Gene amplification would not be directly in HER2 genes but in genes that would play an important role in HER2 signalling. An example is amplification of NIBP (TRAPPC9, trafficking protein particle complex 9) which seems to be involved in the activation of NFκB pathway. Inhibition of NIBP resulted in sensitization of lapatinib-resistant BC cells to the drug (164,177,182).
- **Receptor mutation:** the receptor itself acquires some mutations that makes it no longer recognizable for the drug. Examples of this type of mutations have been seen in tumours treated with trastuzumab and lapatinib. Trastuzumab-acquired resistance through receptor mutations is typically characterized by a truncated HER2 isoform (p95HER2) in which its extracellular domain, where trastuzumab binds to, is cleaved proteolytically rendering it insensitive to the drug and constitutively

activated. In lapatinib resistance, mutations in the tyrosine-kinase domain have also been reported (164,177,182).

- **Activation of compensatory pathways:** probably the most common mechanism of acquired resistance. Its bases rely on the possibility that other receptors or intracellular kinases activate the downstream signals that are usually activated by HER2. On the one hand, trastuzumab specifically inhibits HER2 receptor but does not prevent HER3 dimerization. In some resistant BC tumours an overexpression of HER3 receptors has been reported, which could explain how the tumour cells overcome HER2 inhibition. On the other hand, in lapatinib BC resistance the majority of studies converge in the alteration of the PI3K/Akt/mTOR pathway and SRC family of non-receptor tyrosine kinase pathways as the main involved in the acquisition of lapatinib resistance (164,177,182).

There is no discussion about the importance of HER2-targeted therapies in HER2-positive BC treatment. However, the most important challenge that these targeted therapies have to face is the intrinsic and acquired resistance. That is the reason why it is important to continue on the study of HER2 receptor biology and therapy resistance mechanisms to be able to unravel relevant molecular and cellular mechanisms to design specific therapies able to overcome these obstacles (164,177,182).

4.4. HER2-NEGATIVE BREAST CANCER SUBTYPES

HER2-negative BC subtypes include luminal A, triple-negative BC (which includes basal-like subtype) and claudin-low. (143).

4.4.1. LUMINAL A BREAST CANCER SUBTYPE

Luminal A BC subtype is the most common BC subtype, representing 50-60% of the total. In terms of prognosis and mortality, patients with this BC subtype have the best prognosis of the other BC subtypes, considering a relapse rate around 28% being significantly lower than other BC subtypes and also a longer survival time after relapse (median of 2.2 years) (156,157,183). Focusing in their molecular characteristics, luminal A BC subtype expresses ER in the luminal epithelium, PR, Bcl-2 and cytokeratin CK8/18. Histologically, Ki67 (a proliferative marker) is also evaluated and normally associated with low expression of Ki67, indicating that luminal A tumours have a low proliferation rate. Moreover, GATA3 transcription factor is

overexpressed in luminal A BC subtype in comparison to other subtypes (143,156). GATA3 stimulates expression of ER, and ER stimulates expression of GATA3, establishing a positive feedback loop. Also, GATA3 has been identified as a repressor of tumour features associated with poor prognosis. It has been described that GATA3 suppressed expression of factors critical to EMT and metastasis (ref - GATA3 in BC: tumor suppressor or oncogene?). The treatment of this BC subtype is focused on targeting the hormonal need for the tumour to survive by third generation hormonal aromatase inhibitors and also targeting the oestrogen and progesterone receptors (156,157).

- OESTROGEN AND PROGESTERONE RECEPTORS

Oestrogen and progesterone receptors are hormonal receptors that are critical for the normal development of the breast. ER and PR belong to the nuclear receptor family of receptors which are activated by specific ligands and regulate cellular gene expression by working as transcription factors, activating or suppressing transcription (184,185). The structure of these receptors consists of a central DNA-binding domain, containing tandem zinc fingers motifs responsible of the specific DNA binding. The ligand-specificity is driven by the carboxyl terminal region of the receptors. Hormone binding to the receptors, which takes place in the cytosol, induces receptor dimerization and activates its transcription factor activity (184–186).

Epidemiological studies demonstrate that high exposure to oestrogen and progesterone throughout an individual's lifetime increases the likelihood of developing BC. It can be explained because during repeated menstrual cycles, there is a recurrent activation of the ER and PR and its potentially oncogenic downstream signalling pathways (184,187). For instance, experimental data demonstrated that ER is essential in the progression and proliferation of BC cells by upregulating the proliferation pathways and downregulating the pro-apoptotic and quiescence signals. Similar results have been found in *in vitro* studies of PR in BC, aberrant signalling promotes up-regulation of cyclin D1, Wnt4 and RANKL proteins which are involved in proliferation signalling pathways. In addition, PR receptors are also involved in stem cell regulation (184,187).

These receptors are often co-expressed in BC so it is becoming increasingly evident that it does exist a crosstalk between them and that their actions are mutually dependent on their expression and activity (186,188)

Because of this important role that ER and PR have in tumour growth and progression, the ER and PR signalling network has served as an attractive target for the development of the therapeutic agents and anti-hormonal therapies have been developed. There are three classes of endocrine therapy (185):

- **Selective oestrogen modifiers (SERMs):** they have a direct impact into ER and PR activity. For example, tamoxifen blocks transcriptional activity of ER by binding to and inhibiting the receptor binding to the DNA (185,189,190).
- **Selective oestrogen receptor down-regulators (SERDs):** these drugs block directly the function of the receptor. On example is Fulvestrant which down-regulates the expression of ER (185,191).
- **Aromatase inhibitors:** they block the conversion of androgens to oestrogens in peripheral tissues, limiting the ligand amount for the ER (185).

However, as described in HER2-targeted therapies, some tumours are resistant (intrinsic resistance) or develop resistance to these treatments (acquired resistance) (189,192,193). Some of these resistance mechanisms are directly related to:

- **Oestrogen receptor:** intrinsic resistance to hormonal therapies could be due to mutations or deletions in the ER gene, even though these are rarely found (mutation less than 1%). However, after treatment some patients loss ER expression which is explained by aberrant methylation mechanisms in ER gene promoter or deletion of exon 5 in the ER gene (189).
- **ER co-factors:** ER function is tightly regulated by several co-factors. Overexpression of some of these co-factors, such as AIB1 (amplified in some BC) can contribute to tamoxifen resistance. Not only dysregulation of co-factors is due to gene overexpression, but also to reprogrammed chromatin landscapes as it happens with an enhanced expression of EZH2. This protein is a methyltransferase that suppresses GREB1, an ER co-factor, conferring resistance to tamoxifen (189,192,193).

- **Cross-talk with signalling pathways:** overexpression of different tyrosine kinases such as EGFR or IGF1R, phosphorylate ER and activate it in a ligand-independent manner making cells refractory to tamoxifen action (189,192).

Given the fact that BC tumours adapt to the treatment and become resistant to the endocrine therapy, more research is needed to overcome this intrinsic or acquired resistance. Combining endocrine therapies with other molecularly targeted agents could increase the response, however more research is needed to design specific therapies to treat these BC subtypes (189,192).

4.4.2. TRIPLE NEGATIVE BREAST CANCER SUBTYPE

Triple negative BC (TNBC) is molecularly defined as the BC subtype that do not express ER, PR or HER2 receptors. Focusing on the gene profile classification, TNBC is often considered into the basal-like subtype. It has been proved that the genetic profile overlap ratio between TNBC and basal like subtype can be as high as 60-90% compared to only 11.5% between non-TNBC and basal-like BC subtype (194).

Epidemiologically, TNBC mostly occurs in premenopausal young women under 40 years old, accounting for 10-20% of invasive BC. Compared with other BC patients, the TNBC is the most aggressive BC subtype with the shortest overall survival (mortality rate of 40% within the 5 first years) and also with the highest rates of recurrence (25% after surgery). 46% of TNBC patients will develop distant metastasis with a median survival time after metastasis of 13.3 months. TNBC distant metastasis normally involves brain, lung and visceral organs (143,194–197).

TNBCs are highly heterogenous tumours with different clinical outcomes and without a standard treatment protocol. These are the main reasons why several scientists tried to subclassify TNBCs. After several attempts (153,198), the most comprehensive and used subclassification was proposed by Lehmann *et al.* which subdivided TNBC into 7 different molecular subtypes (199) and 5 years after they refined the subclassification into four subgroups (200):

- **Basal-like subtype 1 (BL1):** there is an abnormal expression of genes involved in cell-cycle regulation and DNA repair-related genes. Possible therapeutic drugs for this

subtype could be poly (ADP-ribose) polymerase (PARP) inhibitors and genotoxic agents, such as cisplatin (194,200).

- **Basal-like subtype 2 (BL2):** in this TNBC subtype there is a differential regulation of EGFR, MET, NGF, Wnt/ β -catenin and IGF1R pathway. The alterations in these signalling pathways make the patients to be treated with mTOR inhibitors and growth factor inhibitors (lapatinib, gefitinib and cetuximab) (194,200).
- **Mesenchymal subtype:** TNBC tumours classified as mesenchymal overexpress cell migration-related signalling pathways, ECM-receptor interaction pathways and differentiation pathways. This BC subtype is prone to develop resistance to chemotherapeutic agents. However, these patients could be treated with mTOR inhibitors or drugs targeting the EMT pathway (194,200).
- **Luminal androgen receptor (LAR) subtype:** even though this subtype does not express ER receptor, it does have highly activated hormonal-related signalling pathways (steroid synthesis, androgen/oestrogen metabolism). This TNBC subtype overexpresses androgen receptor (AR) which make it suitable to treat with anti-AR therapy (194,200).

As mentioned before, TNBC tumours do not have a standard of care approach but thanks to this subclassification scientists are starting to identify potential molecular targets (143,201). Currently, the options that oncologists have to treat these tumours are based on four strategies (*Figure 22*):

- **Immunotherapy:** BC is not an immunogenic tumour, but tumour-infiltrating lymphocytes are present within the tumours. That is the main reason why immune checkpoint inhibitors and programmed death-1 (PD-1) and programmed death ligand 1 (PD-L1) therapies are being used to treat TBNC (143,201).
- **PARP inhibitors:** Normally used in TNBC with defective homologous recombination DNA repair, such TNBC with BRCA1 and BRCA2 mutations. Inhibition of another DNA damage repair enzyme such are PARP enzymes will leave the tumour without DNA repair machinery and make it more sensitive to chemotherapeutic agents (143,201).

- **Antibody drug conjugates:** these are novel strategies to treat TNBC and promising results are arising from clinical trials. The basis of this treatment is to conjugate a cytotoxic agent into an antibody directed to a target BC cell surface molecule. The antibody will recognize specifically the BC cell, and there the cytotoxic agent will have an specific effect to the cancer cell (143,201).
- **AKT pathway inhibition:** considering that hyperactivation of the PI3K/AKT/mTOR pathway is relatively frequent in TNBC, targeting this pathway is an attractive option to treat these tumours. Normally, it is used in combination with a chemotherapeutic agent (143,201).

Finally, it is important to mention that despite there are several novel therapies to treat TNBC, chemotherapy is still the backbone therapy for the advanced TNBC (201).

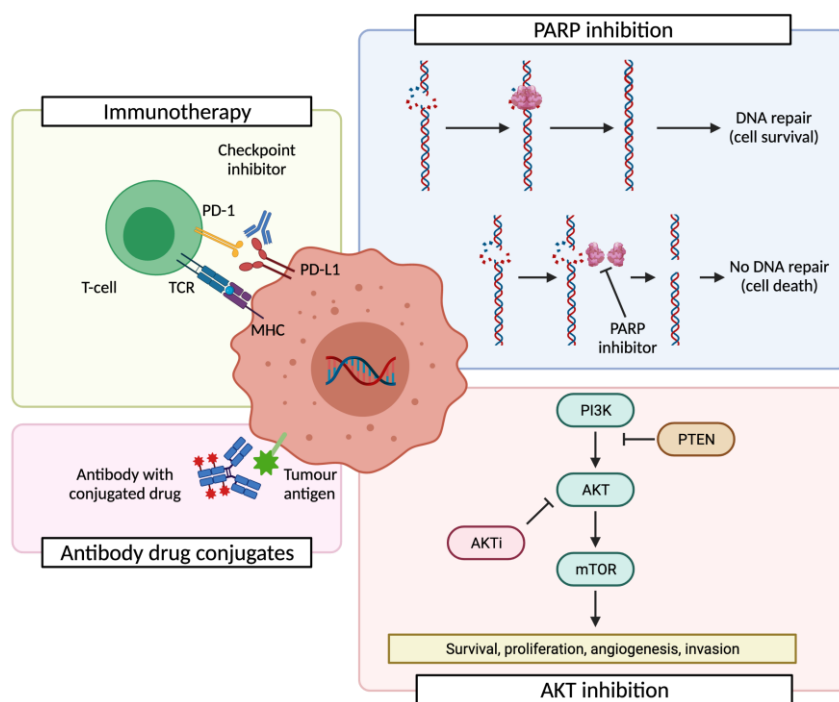


Figure 22 – Principal therapeutic strategies to TNBC tumours. Schema of the main targeted-therapies to treat TNBC tumours (immunotherapy, PARP inhibition, AKT inhibition and antibody drug conjugates). Adapted from (201).

4.5. BREAST CANCER DIAGNOSIS AND TREATMENT

4.5.1. DIAGNOSIS

Currently, more than half of BC are diagnosed thanks to screening programs and people self-awareness, because one third are detected as a palpable breast mass. Palpable axillary

mass, nipple discharge, nipple inversion, breast asymmetry, breast skin erythema and breast skin thickening (peau d'orange) are less common presentations of BC. Due to this awareness, 62% of BC in the USA are detected confined in the breast at diagnosis, the additional 31% have spread to the regional lymph nodes while only the 6% has spread to distant sites (143,202,203).

At time of diagnosis, BC could be diagnosed with various techniques, imaging techniques, which are very useful for monitoring tumour progression and response to therapy as well. The most used imaging techniques are (203):

- **Mammography:** it is known as the gold-standard technique with high sensitivity and specificity, it is not expensive and it is well tolerated among BC patients. However, there are some disadvantages of this technique such as pain and anxiety, false positives and radiation risks. The use of this technique is able to reduce the BC mortality by a 19% (203) .
- **Ultrasound:** It is useful to diagnose and to follow-up BC progression. The main advantage of this technique is that it is able to diagnose breast pathology without using ionizing radiation. Normally is used in young women, pregnant or breastfeeding women (203).
- **Magnetic Resonance Imaging (MRI):** this technique is mostly used in order to monitor response to therapy, monitoring high-risk patients, the assessment of BC metastasis and the study of BC recurrence (203).
- **Positron Emission Tomography (PET) and Single Photon Emission Computed Tomography (SPECT):** PET technique uses radioactive isotopes which emits positrons and SPECT also uses isotopes that emit gamma photons. They are mainly used to detect metastasis, mainly in bone where this techniques are more sensitive (203).

This wide panel of imaging techniques enables physicians to detect and diagnose BC in early stages and be able to obtain morphology and metabolic information of the tumour to correctly monitor the BC response to the treatment (203). Also, it is very important to determine the mammographic density, considered a risk factor in the development of BC, which can help for their potential therapeutic implications for BC patients (31). After the

morphological diagnosis, a biochemical diagnosis is needed to decide which treatment would be more beneficial for the patient. As explained before, this type of diagnosis is based normally in three molecular markers: ER, PR and HER2 receptor which will enable to classify the tumour into four different subtypes and assign therapeutic choice (203).

4.5.2. BREAST CANCER THERAPY FOR NON-METASTATIC BREAST CANCER

The main goal for nonmetastatic BC is to eradicate the tumour from the breast and regional lymph nodes and to prevent metastatic recurrence. To do that, local and systemic therapies are applied. On the one side, local therapy mainly consists in surgically remove the tumour from the breast and sampling or removing axillary lymph nodes, with consideration of postoperative radiation. On the other side, systemic therapy could be preoperative (neoadjuvant) or postoperative (adjuvant) and it would differ according to the BC subtype (143,202).

- LOCAL THERAPY

Surgical treatment has evolved drastically in the past decades to avoid total mastectomy, being breast conservation the primary goal. Currently, advances have minimized the long-term cosmetics and functional sequelae of surgical resection. Considering tumour size, tumour to breast size relationship, tumour biology, comorbidities and patient choice, surgery would be the first treatment or the second, if a neoadjuvant therapy is needed. Once the surgery has to be done, the surgical extent would be oriented to the tumour burdens. Nowadays if mastectomy is oncologically required, breast reconstruction can be offered as an immediate or delayed procedure, depending on the oncological situation and patient preference (143,202).

In some cases, lymphatic nodes are also removed to determine cancer cells presence in the node. If cancer cells are detected, this would mean that the tumour has already spread. This also could be used to determine patient's long-term locoregional relapse and outcome (143,202).

Together with surgery, postoperative radiation therapy improves disease-free and overall survival for patients with early BC with lymph node involvement and/or with breast conserving therapy. Radiation can be delivered to the whole breast or only to a portion of it and/or to the regional nodes. The objective of the radiotherapy is to eliminate residual tumour cells and/or

induce an abscopal effect (143,202). The abscopal effect is produced when radiation treatment (or another type of local therapy) not only reduces primary tumour volume, but also affects to untreated tumours elsewhere in the body. It is believed that its main effect is driven by the immune system cells, which as a cause of irradiated-cancer cell destruction, are able to recognize cancer cell antigens and attack other distant cancer cells (204).

- **SYSTEMIC THERAPY**

The systemic therapy depends on the intrinsic BC subtype, tumour burden and risk of recurrence and it can be administered as a neoadjuvant or as an adjuvant therapy. Usually, neoadjuvant therapy is only administered if a reduction of tumour size is warranted (143,202). The systemic therapy used to treat non-metastatic BC patients can be:

- **Chemotherapy:** several types of chemotherapeutic drugs are used. For example, anthracyclines, inhibitors of DNA/RNA synthesis, are used to treat luminal tumours with high risk of recurrence and as a neoadjuvant therapy for triple negative and HER2-enriched BC subtypes with poor prognosis. Also, taxanes such as docetaxel, are used for the same type of tumours. Another taxane, paclitaxel is used in combination for treating HER2-enriched BC tumours with good prognosis. Its mechanism of action consists on inhibiting cell proliferation by inducing microtubule destabilization (143,202).
- **Endocrine therapy:** is used only in luminal BC subtypes which are ER positive and have high risk of recurrence. The most used endocrine therapy is aromatase inhibitors, such as tamoxifen, or selective ER inhibitors such as fulvestrant (143,191,202,205).
- **HER2-targeted therapy:** it is only used as a neoadjuvant therapy for HER2-enriched BC tumours with poor prognosis and HER2-enriched tumours with good prognosis as adjuvant therapy. In non-metastatic BC tumours trastuzumab, a monoclonal antibody that binds specifically to HER2 receptors and inhibits its intracellular signalling, is usually administered (143,164,202).

4.5.3. BREAST CANCER THERAPY FOR ADVANCED AND METASTATIC BREAST CANCER

Advanced BC comprises tumours that are inoperable and are locally advanced even though there is no metastasis or metastatic BC. Each intrinsic subtype of BC tumour has a metastatic organ preference (shown in [Figure 23](#)), with bone, lungs, brain and liver as the most common sites. Even if the patient presents a *de novo* metastasis (metastasis at the time of diagnosis) or a recurrent metastatic disease (presented after diagnosis and treatment of early BC) both are difficult to treat. In these situations, the aim of the treatment would focus in relieving the symptoms of the primary tumour or metastasis and to prolong quality-adjusted life expectancy. Nowadays, advanced BC is treatable, but virtually incurable. Epidemiological studies determined a median overall survival of 2-3 years in patients with BC metastasis (143,202).

In these advanced stages of the tumour decisions are made with a multidisciplinary evaluation of the possible interactions between local and systemic treatments, evaluating the final outcome (patient's survival and toxicity of the treatments) (143,202).

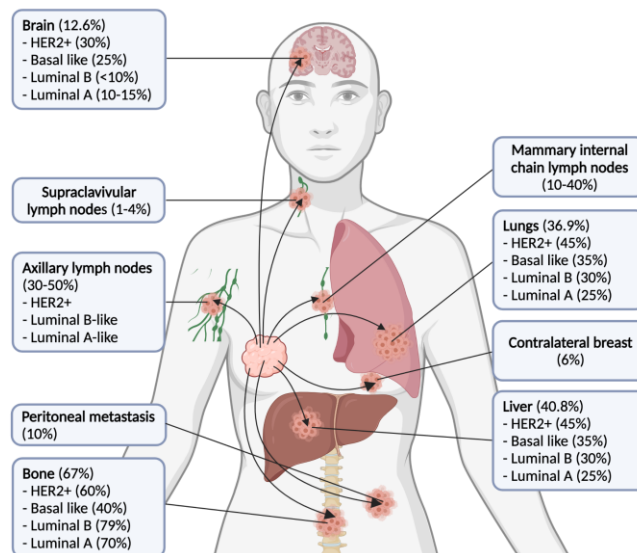


Figure 23 – Common metastatic sites in BC. Picture of the most common sites where BC tends to metastasize according to the molecular subtype. Adapted from (143).

- LOCAL THERAPY

In cases of advanced BC sometimes is difficult to apply local therapy. Surgery or radiotherapy are not the first line of treatments, even though that it can be very useful in some situations like in bone or brain metastasis (143,202).

Usually there is no surgical resection of the primary tumour, except for cases in which the patient presents an excellent response to the systemic treatment. Sometimes a patient can undergo surgery if it is considered as a palliative cure that will provide an adequate control of the tumour growth. The resection of metastasis is controversial, only it would be done if it can increase patient's quality of life. Radiotherapy is useful in case of bone, brain and soft tissues metastases because it alleviates the symptoms. However, it will be prescribed only according to the severity of the lesions and live expectancy (143,202).

- **SYSTEMIC THERAPY**

For the clinical oncologist, to prescribe the treatment for an advanced and metastatic BC, is key to know the receptor status and which BC subtype is dealing with. A biopsy to assess receptor expression and to identify potential changes in tumour biology in comparison to primary tumour would be necessary. In this BC stage, the most important systemic therapies are:

- **Chemotherapy:** chemotherapy is administered in advanced TNBC and luminal BC that do not respond to endocrine therapies. In that stage platinum derivatives and also anthracyclines are used. However, it can be possible to combine chemotherapy with targeted therapies such as anti-VEGF antibodies to increase the therapeutic response (143,202).
- **Endocrine therapy:** in this stage endocrine therapy is prescribed in luminal patients but usually it is combined with targeted-therapies such as cyclin dependent kinases inhibitors or mTOR signalling pathway inhibitors (e.g., everolimus) (143,202).
- **Targeted therapies:** in BC patients with BRCA germline mutations PARP inhibitors are used. They inhibit the enzyme PARP which is in charge of repairing single strand breaks in the DNA. The inhibition of PARP increases cell cytotoxicity by inhibiting DNA repair damaged by chemotherapy (143,202,206). Another targeted therapy is lapatinib. According to the general treatment pipeline, this drug should be used as a third-line therapy for BC tumours that are HER2-enriched (143,177,202).

Even though it has been an impressive increase in knowledge in the field of molecular biology, there is still room for improvements and to discover better treatments directed to specific targets of metastatic and advanced BC (143,202).

5. HEAD AND NECK CANCER

5.1. EPIDEMIOLOGY

Head and neck cancers include cancers derived from the mucosal epithelium in the oral cavity, which comprises the salivary glands and the paranasal sinuses, in the pharynx (nasopharynx, oropharynx and hypopharynx) and in the larynx, collectively known as head and neck squamous cell carcinoma (HNSCC) (207,208). These types of carcinomas are the sixth most common cancer type worldwide with more than 900,000 cases diagnosed the past 2020 and with more than 450,000 deaths (*Figure 24*). The estimated crude incidence (*Figure 24A*) and mortality (*Figure 24B*) of HNSCC in both sexes (all ages) are shown (GLOBOCAN) (7). However, the incidence and mortality of HNSCC varies across regions considering that normally these types of carcinomas are originated due to risk factors exposure, such as tobacco-derived carcinogens and excessive alcohol consumption. Another risk factor is a previous infection with oncogenic serotypes of human papillomavirus (HPV), being the most frequent causing HNSCC the serotypes HPV-16 and HPV-18 (208,209). In Europe, in 2020, 168,498 new cases were diagnosed being the sixth cancer more incident and the seventh more deathly with 73,484 deaths (GLOBOCAN) (7). In Spain, it follows the same trend in cancer incidence, being the sixth most incident with 19,663 new cases, but it dropped to the ninth within the most cancer-related deaths with 3,875 deaths (GLOBOCAN) (7). More specifically, in 2020 in Catalonia 1,173 new cases were diagnosed and 350 died of HNSCC (AECC)(210)(211).

In general, men are a two to four-fold higher risk to develop HNSCC than women and taking into account the HPV status, diagnosis of HPV-negative HNSCC is around 66 years, whereas HPV-positive patients and Epstein-Barr virus positive is around 50 years. Over the past decades 5-year survival has increased, but is thought to be influenced by the emergence of HPV-associated HNSCC that has a better prognosis, rather than a better treatment of HNSCC. In addition to deaths directly caused by HNSCC, survivors of this cancer have the second highest rate of suicide only after pancreatic cancer. In these suicide cases, it seems that psychological distress and compromised quality of life are the main risk factors (208).

Even though HNSCC is not one of the most incident cancers, it is expected to increase by 30% by 2030. That is the reason why measures to reduce tobacco use and alcohol consumption are essential to try to decrease the incidence. Moreover, more research is needed to design new treatment strategies and new drugs that will help to gain a better quality of life for patients suffering from HNSCC (208).

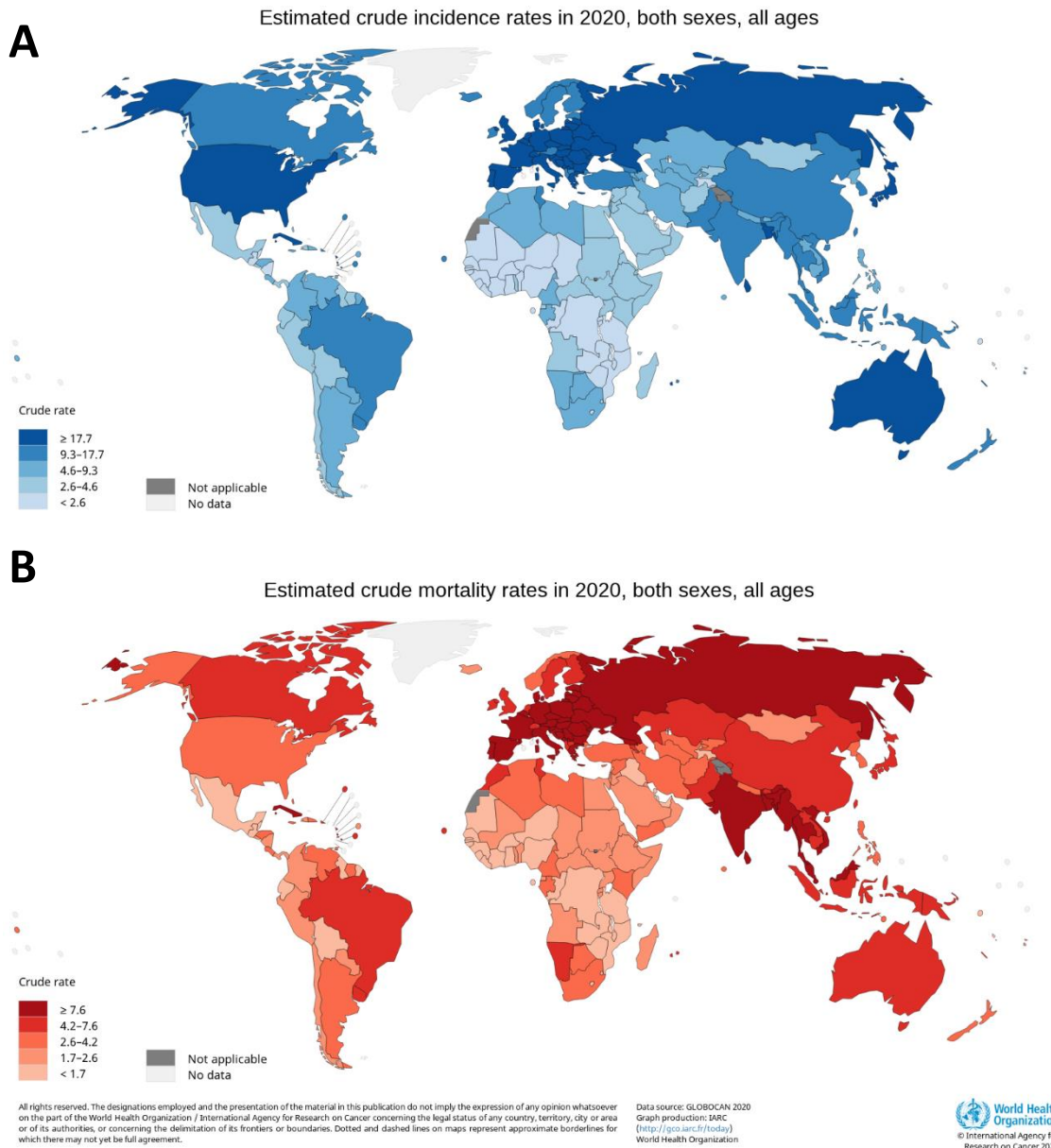


Figure 24 – Estimated crude incidence and mortality rates of HNSCC worldwide in 2020, both sexes and all ages. (A) GLOBOCAN data of estimated crude incidence rates of HNSCC worldwide in 2020, both sexes, the darker the blue, the higher the incidence. (B) GLOBOCAN data of estimated crude mortality rates of HNSCC worldwide in 2020, both sexes, the darker the orange, the higher the mortality.

5.2. PATHOPHYSIOLOGY

HNSCC originates into the mucosa epithelia of the oral cavity, pharynx, larynx and its progression follows an ordered series of events. Histologically, it begins with a hyperplasia of epithelial cells, followed by mild, moderate and severe dysplasia that could develop into an *in situ* carcinoma which can evolve to invasive carcinoma. Each progression step is characterized with different gene alterations (*Figure 25*). The main problem relies on the lack of an effective

screening strategies because patients diagnosed with HNSCC do not have a history of antecedent pre-malignant regions and normally are diagnosed as advanced carcinoma (207–209).

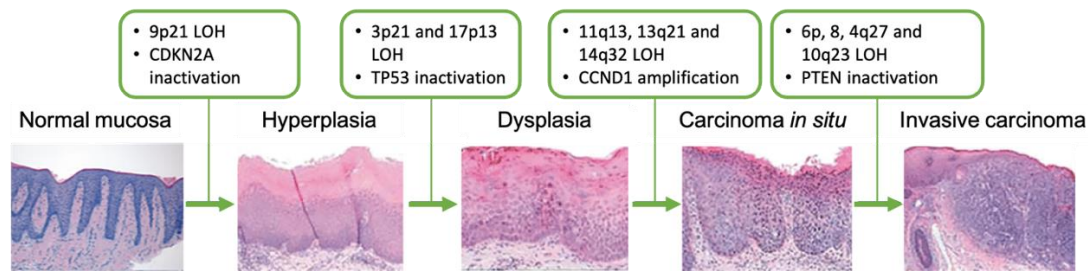


Figure 25 – Progression of HNSCC and key genetic events. Model of ordered histological progression of HNSCC. Normally transition from normal mucosa to hyperplasia is triggered by 9p21 loss of heterozygosity (LOH) and the inactivation of the tumour suppressor gene CDKN2A. Hyperplasia can turn into dysplasia after normally 3p21 and 17p13 LOH and TP53 inactivation which in turn will lead to carcinoma *in situ* after specific gene events such as LOH of detrimental genes and also CCND1 amplification. Finally, some carcinoma *in situ* will evolve to invasive carcinoma where normally this transition is characterized by other specific genes LOH and PTEN inactivation. Adapted from (208).

HNSCC is an heterogeneous cancer in which the cell of origin will depend on the anatomical location and aetiological agent, normally a carcinogen or a virus. Even though HNSCC cancer stem cells constitute a minor fraction of the cells in primary tumours, they are thought to be the cells of origin of HNSCC. An important phenomenon to consider when it is looked for the cell of origin of HNSCC is the development of second primary tumours that could be synchronous (at the same time of diagnosis) and/or metachronous (later than the time of diagnosis). In HNSCC is really frequent the appearance of second primary tumours at the time of diagnosis of the primary tumour or after, that can be localized at the same or distinct anatomical sites in the head and neck region, oesophagus or larynx. The high rate of second primary tumours is thought to be due to the concept of “field cancerization”, suggesting that carcinogens damage a large anatomical structure which could develop cancer with the same odds in all these head and neck field. Considering this fact, it is possible that primary tumour and second primary tumour reflects distinct cancer stem cells because they have raised from independent oncogenic transformation (208).

Normally HNSCC are classified according to their HPV status taking in consideration each subtype as a different entity with different gene expression, mutational landscape and distinct immune profile, which confer diverse clinical and biological behaviour (208,212,213).

5.2.1. INITIATION AND EARLY EVENTS IN HPV-NEGATIVE HEAD AND NECK CANCER

Normally HPV-negative HNSCCs are initiated due to the exposure to carcinogens. Tobacco consumption is the first risk factor associated to HPV-negative HNSCC due to the fact that it consists of more than 5,000 different chemicals of which dozens of them have carcinogenic activity. Smokeless tobacco, areca nut and betel quid are also carcinogens that used to cause HNSCC. Polycyclic aromatic hydrocarbons (PAHs) and nitrosamines are ones of the chemicals that are thought to be more carcinogenic in tobacco. PAHs and nitrosamines undergo metabolic activation and require detoxification enzymes and excretion pathways to try to eliminate them from the organism. Nevertheless, sometimes reactive metabolites of these carcinogens can also form covalent DNA adducts, which, if not properly repaired, can lead to mutations or other genetic abnormalities. The balance between metabolic activation and detoxification and DNA repair will determine the propensity of the carcinogen to induce cancer. Moreover, tobacco induces inflammation in the exposed tissues, which will induce production of local cytokines, chemokines and growth factors can promote carcinogenesis by inducing proliferation and angiogenesis. Another important risk factor is alcohol consumption that can act synergistically with tobacco. It is metabolized to acetaldehyde, that can form DNA adducts, enhancing the exposition of epithelial cells to carcinogens (208,209).

5.2.2. INITIATION AND EARLY EVENTS IN HPV-POSITIVE HEAD AND NECK CANCER

HPV infection is associated with more than 70% of oropharyngeal cancers (normally arise from deep-crypts in the palatine and lingual tonsils) and a minority in other head and neck anatomical sites. Infection of HPV is an early event and the most common causative HPV serotype is HPV-16, although other high-risk HPV could be detected in a minority of cases (HPV-18, HPV-31, HPV-33 and HPV-52). The genome of these double-stranded, circular DNA viruses consists of seven early genes (E1-E7) and two late genes (L1 and L2). Once they infect the cell, the viral genome is integrated at a single genomic site, which can be different among infected cells. The oncogenic mechanism of the virus could be explained by the interaction of the viral proteins with the cell proteins (*Figure 26*). E6 protein forms a complex with the cellular ubiquitylation protein (MDM2) and the tumour suppressor gene p53, MDM2 promotes p53 ubiquitylation and degradation through proteosome pathway. By doing so, p53 is not usually mutated in HPV-positive HNSCC because is already degraded, in comparison to HPV-negative HNSCC in which p53 is frequently found deleted or mutated. Another HPV protein that confers oncogenic capacity is E7, which binds to the cell cycle regulator RB, promoting its proteosomal destruction and in consequence, E2F proteins are released and free

to drive the cell cycle to the S phase. E7 also affect the control of other cell cycle regulators such as Myc or RAS (207–209,212,213).

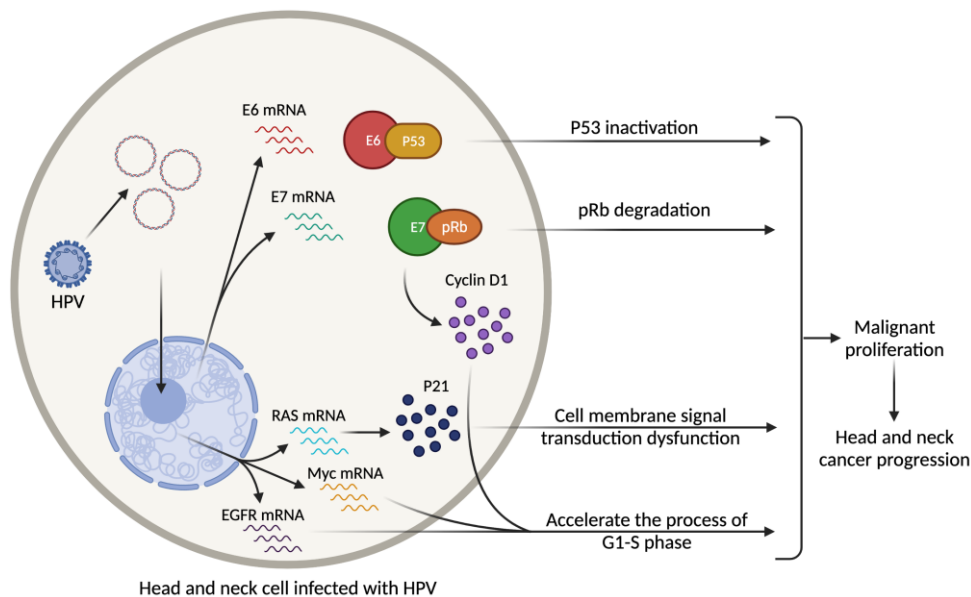


Figure 26 – Carcinogenesis of HPV infection and how it triggers the development of HNSCC. After HPV infects HNSCC cells, its DNA is integrated into the host genome. It results in expression of virus protein that alter the expression of cell proto-oncogenes proteins and tumour suppressor genes leading to a malignant proliferation and therefore cancer progression. Image adapted from (212).

5.3. MOLECULAR CHARACTERISTICS

5.3.1. TP53/RB PATHWAY

TP53 is a tumour suppressor gene that encodes for the protein p53 which its main role is in maintaining genomic stability in the cell by regulating the cell cycle, DNA repair, apoptosis and senescence. Normally p53 detects DNA damage and in a MDM2-dependent manner activates cell cycle checkpoint kinases CHK1 and CHK2 resulting in cell cycle arrest and apoptosis. As it is explained before, mutations in this gene are typical of HPV-negative HNSCC patients. Over 80% of this HNSCC subtype have mutations in *TP53* and is thought to occur early in cancer development. In both HNSCC subtypes (HPV-positive and HPV-negative), mutations in *TP53* are correlated with poor overall survival, therapy resistance and an increased rate of recurrence (209,213).

RB protein is another tumour suppressor that is mutated early in the carcinogenic process. As p53, RB also regulates cell-cycle progression controlling the transition point between early and late G_1 by sequestering the E2F transcription factor. That is the reason why mutations in p53 and RB pathways result in an unlimited replication potential for cancer cells (209,213).

Several strategies to restore both pathways have been studied and some adenoviral p53 therapies have been developed. However, no efficacy has been proved in clinical trials (209,213).

5.3.2. NOTCH PATHWAY

NOTCH pathway mutations have been detected in 17% of HPV-positive and 26% of HPV-negative HNSCCs, predominantly in NOTCH1, a tumour suppressor gene. NOTCH pathway activates the Wnt and β -catenin pathway which has been related to promotion of tumorigenesis, a process which seems to be closely related to their regulatory role in CSC (208,209,213).

5.3.3. PI3K/AKT/MTOR PATHWAY

PI3K/AKT/mTOR pathway is one of the most commonly activated pathways in cancer, regulating cell proliferation, cell survival and differentiation. This pathway is frequently activated by tyrosine-kinase receptors such as EGFR. The downstream signalling pathway includes the mTOR complex (mTORC1 and mTORC2) in which mTORC2 is responsible of AKT and SGK1 activation. Aberrant activation in HNSCC through mutations in *PIK3CA* (gene encoding for the catalytic subunit of PI3K) has been detected in around 16% of HNSCC. Mutations in this catalytic subunit have been associated with an advanced tumour, with an increased vascular invasion and lymph nodes metastasis. Another mutation found in HNSCC is in the negative regulator of PI3K, PTEN, found mutated in 7% of HNSCC (208,209,213).

Currently rapamycin, an mTOR inhibitor, has been approved for the treatment of some types of cancers and is under clinical trial investigation for HNSCC. Although inhibition of the PI3K/AKT/mTOR is promising in HNSCC, this pathway is characterized by multiple cross-talk and compensatory pathways which make more difficult to inhibit the whole pathway targeting only a single component. Further investigation is needed in order to incorporate these treatments into the clinical routine for treating HNSCC (208,209,213).

5.3.4. EGFR PATHWAY

As explained before, EGFR is activated by several ligands such as EGF, TGF- α , amphiregulin and β -cellulin. Ligand binding induces receptor dimerization and autophosphorylation in its tyrosine-kinase domains, activating down-stream signalling pathways. Activated EGFR can also

translocate to the nucleus and function as a transcription factor or coactivate other transcription factors. This is translated into proliferation and survival signalling pathways activation. In cancer, the HER2 pathway regulates cell cycle progression, metastasis, resistance to radiotherapy and angiogenesis (161,208,209,213).

In HNSCC EGFR is an established oncogene where mutations and overexpression are reported in 80-90% of HNSCC. Higher levels of EGFR will lead to spontaneous dimerization of receptors which will result into a constitutive activated pathway. In cancer, overexpression of EGFR correlates with poor prognosis and treatments outcomes. However, in HNSCC, due to the heterogeneity of HNSCC it is not clear if overexpression of this oncogene confers a poorer prognostic in patients. Cetuximab, a chimeric monoclonal antibody (mAb) is approved to treat HNSCC patients which overexpress EGFR. This mAb targets the extracellular ligand binding domain of EGFR, blocking its downstream signalling. Cetuximab improves overall survival in locally advanced and recurrent or metastatic HNSCC cancer in combination with radiotherapy and chemotherapy respectively. However, this treatment is not free from acquisition of resistance, which means that new strategies to control the cancer growth will be needed (208,209,213).

5.3.5. MET PATHWAY

MET pathway is related to an increase of migration, invasion and metastasis in cancer. Cancer patients overexpressing this receptor have a worse prognosis and lower overall survival. Moreover, it has been proposed as a resistance mechanism to EGFR therapies. EGFR and c-MET share down-stream pathways such as RAS/RAF/MAPK or PI3K/AKT/mTOR, so dual blockade of EGFR and c-MET receptor could represent a promising therapy for patients that became resistant to EGFR inhibition (213).

5.3.6. JAK/STAT PATHWAY

Janus kinases (JAKs) are part of a protein family of non-receptor tyrosine kinases activated by cytokines when binding to their receptors. These receptors do not have an intrinsic tyrosine-kinase capacity but they are bound constitutively to JAK proteins that transphosphorylate cytokine receptors after cytokine binding. Then, activated cytokine receptors phosphorylate STAT proteins, inducing their dimerization and translocation into the nucleus, where they work as transcription factors.

In both HNSCC subtypes an aberrant activation of JAK/STAT pathway has been detected, and upregulation of STAT3 and its gene targets seems to happen in an early stage of tumorigenesis. JAK/STAT pathway seems to promote cell survival and growth, angiogenesis and is considered to be immunosuppressive, protecting the cancer cells to be recognized and destroyed by the immune cells. Nowadays there is an FDA approved JAK inhibitor for myelofibrosis treatment (ruxoblitinib), but its use in solid tumours is still under clinical trials validation (207,209,213).

5.3.7. RAS/RAF/MAPK PATHWAY

The MAPK pathway comprises four sub-pathways which phosphorylate and modify several cytoskeletal proteins, kinases and transcription factors, such as NFκB that will control cell proliferation, differentiation, apoptosis, angiogenesis, invasion and metastasis. However, in HNSCC mutations only represent 4% of cases. There are some MEK inhibitors such as trametinib, approved for melanoma treatment, that are under clinical trials for HNSCC (213).

5.4. DIAGNOSIS AND TREATMENT

5.4.1. DIAGNOSIS

Clinical presentation of HNSCC will depend on the anatomical site where cancer is located. Head and neck tumours located into the oral cavity are easy to detect in their early stages because patients themselves are able to detect them. Normally are presented as a non-healing mouth sore or ulcer and the most frequent symptoms would be difficulties in eating or chewing and speaking (dysarthria). Primary tumours of the oropharynx are more difficult to detect at early stages and often are detected when some symptoms such as dysphagia (difficulty eating), odynophagia (pain when swallowing) or otalgia (ear pain) appear. Symptoms of larynx tumours normally are detected when patients manifest dyspnoea (difficulty breathing) and at late-stages airway obstruction leading to tracheostomy (208).

The diagnostic is based on histopathology of the primary tumour and/or neck mass. The biopsy method will depend on the location of the lesion which could vary among cup forceps, incisional biopsy (only a small portion of the mass is removed) or excisional biopsy (the whole mass is removed). Usually, the incisional biopsy is performed by fine needle aspiration (FNA) and excisional biopsy will be performed only if the FNA is non-diagnostic, otherwise it is not recommended. Once the sample is obtained, the histopathological spectrum will be characterized by the extent of cellular atypia and squamous differentiation. On the one hand,

a well-differentiated tumour is characterized by a stratified epithelium with mature-appearing cells organized in two layers and manifesting a keratin pearl. On the other hand, a poorly differentiated tumour has immature cells with nuclear pleomorphism and atypical mitoses and keratinization is not organized by stratifications. Moreover, squamous differentiation is also associated with HNSCC aetiology, HPV-negative tumours are often moderately or well differentiated, whereas HPV-positive tumours are poorly differentiated and display basaloid morphology. Normally the histopathological analysis is done by haematoxylin and eosin staining, but in cases of poor differentiation other markers are needed in order to confirm the epithelial origin. The antibodies used to detect the epithelial origin are pancytokeratin and markers of squamous differentiation such as CK5, CK6 and p63 (209,213,214).

Following histopathological analysis HPV status is needed being considered as a prognosis factor. Moreover, a complete evaluation of the head and neck area is indicated to determine if there are second primary tumours. Also, a cross-sectional imaging of the head and neck anatomy by computed tomography (CT) or MRI is essential to establish the extent of the tumour. It is recommended, if available, to perform a PET-CT scan in order to look for distant metastasis in patients with locally advanced tumours or nodal disease (209,213,214).

5.4.2. TREATMENT

It is possible to decrease HNSCC incidence by applying a primary prevention by reducing the exposure of the patients to modifiable risk factors such as tobacco, alcohol and areca nuts consumption. To prevent HPV-positive, vaccination against several HPV serotypes, the most oncogenic is a feasible strategy. Secondary prevention is mainly based on screening programs to detect latent and asymptomatic disease to avoid progression. Oral pre-malignant regions such as leucoplakia (white patches) or erythroplakia (red patches) are associated with an increased risk of HPV-negative HNSCC, but not all of them progress to a malignant tumour, here relies the importance to detect the pre-malignant lesions to try to prevent their progression (208).

Treatment of HNSCC patients will vary to every individual according to several characteristics of the tumour and the patient: anatomical subsite, stage, disease characteristics, functional considerations, age of the patient and patient wishes. Currently, the only curative therapy for HNSCC patients is the locally or locoregionally confined tumour resection. In some cases, resection is not possible since it could impair organ function.

Therefore, an alternative of surgery should be radiotherapy. Surgery is normally used for oral cavity cancers, whereas radiation is commonly used for pharyngeal and laryngeal cancers. In late-stage tumours or tumours that have spread to the node, postoperative radiation or chemoradiation, guided by pathological risk factors, reduces risk of recurrence and improves overall survival. Pathological features that indicate increased risk of recurrence are extra-nodal extension, close or involved surgical margins or perineural invasion. The presence of these pathological features is currently treated with high-dose of cisplatin chemotherapy combined with radiation, which has been seen to improve disease-free survival and ameliorate overall survival.

In patients with advanced tumours (stage 3 or more) that have one or more positive nodes and need organ function preservation, chemoradiation with cisplatin is the first-treatment option (208,214). Chemotherapy could be combined with cetuximab, an EGFR-directed antibody that is effective as a radiation sensitizer (207,208,213,214). Cisplatin is a chemotherapeutic drug used to radiosensitive HNSCC tumours. It induces DNA crosslinking, preventing its repair by DNA repairing mechanisms, causing DNA damage, and as a consequence, cell death (208,214).

The last option is immunotherapy, a type of systemic therapy for patients which cannot be cured with salvage resection, re-irradiation or resection of metastases and do not have an autoimmune disorder. The first-line immunotherapy treatment is pembrolizumab, an immune checkpoint inhibitor which efficacy has been proved in combination with chemotherapy to improve the overall survival in comparison to chemotherapy plus cetuximab. For patients who are not candidates for first-line immunotherapy the best treatment option is cetuximab and a combination of chemotherapy with a platinating agent and either 5-fluorouracil (5-FU) or paclitaxel (208,214,215). 5-FU is an analogue of uracil which rapidly enter the cell and is metabolised to several active metabolites which will misincorporate to the DNA and RNA, and also it inhibits the enzyme thymidylate synthase (216). Paclitaxel is a microtubule-stabilizing agent that cause cell death. The mechanism by which it is caused it is not completely clear, some studies demonstrate that it is caused by mitotic arrest, while others claimed that intratumoral concentration of paclitaxel caused cell death due to chromosome missegregation on multipolar bodies (217).

After some time, the tumour can reappear at the same site or metastasize. After the diagnosis it is important to decide if the patient is candidate to local therapy, radiation or

limited-volume radiation and subject to observation. However, in patients that are not subject to local therapy, systemic therapy is applied (208).

As it was explained before, HNSCC is only classified according to HPV status, there are not any biomarkers approved to stratify these patients to predict the prognosis or the treatment response either. Therefore, biomarkers to stratify patients could help to improve HNSCC treatment and prognosis (208,209,213).

Syntaxin-1A, a synaptic related protein in breast and head and neck cancer progression and prognosis

HYPOTHESIS AND OBJECTIVES

Syntaxin-1A, a synaptic related protein in breast and head and neck cancer progression and prognosis

Recently, the influence of the nervous system on cancer biology has been shown to be detrimental since it promotes tumour progression and invasion (36,37,44,218). The avenue of knowledge provided by this new oncological field could result in the development of new antitumor therapeutic strategies, by altering tumour innervation and modulating nerve-related proteins expressed in tumours, to inhibit invasion and metastatic processes.

The former group leader, Pere Gascón (MD, PhD), when appointed as Head of the Oncology Service at the Hospital Clinic de Barcelona, established a new translational oncology team mainly focused on the role of neurogenes in BC, a research team which he led for more than 25 years until his retirement in 2019. Among the results obtained in this field, they showed that inhibition of NK-1R, a substance P (SP) receptor, reduced BC tumour growth and EGFR and HER2 receptors expression in BC tumours (219–221). Later, a panel of six other neurogenes differentially expressed between BC subtypes and whose expression correlates with the overall survival of the patients were identified (104). Two doctoral theses (222,223) and an article (224) have already been published by our group showing the biological role of three of these neurogenes (HRH1, SEMA3F and NRP2) in BC and HNSCC.

The present project focuses on STX1A, one of the six neurogenes previously identified by the group. Its high expression correlates with poorer overall survival in several cancers (225,226), however, little is still known about the molecular alterations driven by STX1A in non-neural tumours, a knowledge which could provide clues for its applications as tumour biomarker and/or therapeutic target.

Our initial **hypothesis** has been that **STX1A levels might be used as a biomarker to predict BC and HNSCC overall and distant-metastasis survival** and also that STX1A could be used **as a therapeutical target to treat BC and HNSCC advanced tumours**.

Consequently, the **main objectives** of this project have been **to characterize STX1A expression in BC and HNSCC patients to determine its potential as a biomarker and to understand its biological function in regulating cell growth, sensitivity to treatments and invasion and metastasis processes in BC and HNSCC cells**. To answer these two general questions, we have developed the following **specific aims**:

1. To study STX1A expression in BC and HNSCC patient public databases or patient cohorts, focusing on its relationship with patient overall and metastasis free survival.

2. To assess whether BC and HNSCC cell lines are good models to study the role of STX1A *in vitro* and *in vivo*.
3. To initially characterize and understand the epigenetic and transcriptional regulation of STX1A between BC cell subtypes and in HNSCC cells.
4. To study the biological role of STX1A, by modulating either STX1A levels or activity, in BC and HNSCC *in vitro* and *in vivo* models:
 - 4.1. To determine STX1A role in BC and HNSCC cell proliferation and tumour growth.
 - 4.2. To determine STX1A biological relationship with EGFR/HER family of receptors in BC and HNSCC cell lines and tumours.
 - 4.3. To determine STX1A role in HER2-targeted and chemotherapeutic therapies sensitivity in BC and HNSCC cell lines and tumours.
 - 4.4. To determine STX1A role in cell migration and invasion capabilities.

Syntaxin-1A, a synaptic related protein in breast and head and neck cancer progression and prognosis

MATERIALS AND METHODS

1. PATIENT SAMPLES

HNSCC patient samples used in this study were obtained in collaboration with otorhinolaryngologists either from the Hospital Clínic de Barcelona (IDIBAPS) or the Hospital de la Santa Creu i Sant Pau (Barcelona) under the approval of their correspondent institutional ethics committee. Samples from Hospital Clínic de Barcelona were obtained from healthy and tumoral tissue from HNSCC patients before undergoing surgery. Samples were processed to obtain RNA (protocol in section 5.1) from tumoral and healthy samples and SNAREs expression of these samples was analysed by qPCR (protocol in section 5.2). Samples from Hospital de la Santa Creu i Sant Pau were processed and analysed in collaboration with the otorhinolaryngologists Dra. Mercedes Camacho and Dr. Xavier León from the same hospital.

2. BIOINFORMATIC TOOLS

2.1. ANALYSIS OF BC AND HNSCC PATIENTS DATABASE

To interrogate the role of *STX1A* in BC and HNSCC patients, public databases were used. cBioPortal (<http://cbioportal.org>) platform was used to download clinical and gene expression data from METABRIC (Nature) (227,228) database for BC patients and from The Cancer Genome Atlas (TGA) database (229) for HNSCC patients. The methodology used in order to obtain the clinical and genomic data, and how the results are represented in the database can be found in the methodology section of the above referred articles.

The analysis has mainly been focused on gene expression of *STX1A* but other SNAREs and EGFR/HER receptor family genes have been also considered in BC and HNSCC patients. Relative mRNA expression of these genes has been used to correlate with several clinical data. Some analysis in METABRIC and TGA databases have been performed separating the level of expression of a particular gene of interest in different groups. The division has been made with the decision tree algorithm of the IBM®SPSS® software which helps to find specific subgroups and relationships between data. It classifies cases into groups based on values or predictor variables. In this analysis gene expression data has been used as cases and the vital status of the patient as a predictor variable in order to identify possible biomarkers in predicting patient outcome. After the establishment of two (high or low gene expression) or three (high, medium or low gene expression) subgroups, Kaplan-Meier curves have been performed to analyse the correlation of gene expression levels with specific patient survival.

Furthermore, with METABRIC database a gene set enrichment analysis (GSEA) was performed (230). This type of analysis consists on separating the data from the database in two or more groups, given that one of the two states is considered primary (high expression) and the other groups secondary (medium and low expression). Then all groups are compared using the GSEA method and a list of differentially expressed genes between subgroups and grouped according to biological processes was generated. These genes are ordered according to their statistical importance in these biological processes considering four statistical parameters:

- Enrichment score (ES): it represents the degree to which a gene set is overrepresented at the top or bottom of a ranked list of genes. The magnitude of the increment depends on the correlation of the gene with the phenotype. A positive ES indicates gene set enrichment at the top of the ranked list; a negative ES indicates gene set enrichment at the bottom of the ranked list.
- ES p value: calculation of significance of the ES represented by the value of p.
- Normalized ES (NES): this parameter is the primary statistic for examining gene set enrichment results. By normalizing the ES, GSEA accounts for differences in gene set size and in correlations between gene sets and the expression dataset; therefore, the normalized enrichment scores (NES) can be used to compare analysis results across gene sets.
- False discovery rate (FDR): it is the estimated probability that a gene set with a given NES represents a false positive finding.

In our analysis, to determine if a biological process is different between both subgroups, it was considered a p value lower than 0.05 and an FDR equal or lower than 0.25 as GSEA recommends.

Finally, gene expression-based outcome for BC (GOBO) (<http://co.bmc.lu.se/gobo>) database has been used to obtain data on the expression of our genes of interest and correlate them with distant-free metastasis. GOBO database contains 1881 BC patients samples and 51 BC cell lines that allows for various analyses such as looking at the gene expression of a

particular gene in these samples or relating this expression to the overall survival, metastasis free survival, disease free survival of patients (231).

2.1. ANALYSIS OF STX1A AND OTHER SNARE GENES EXPRESSION IN BREAST CANCER CELL LINES DATABASE

To further analyse STX1A and other SNARE genes expression at the Cancer Cell Line Encyclopedia (CCLE), a public database containing transcriptome analysis of approximately 1,000 cell lines (235), was used to . The mRNA expression levels of *STX1A* and other SNARE genes was downloaded from the database and only BC cell lines were selected. Then, BC cell lines were grouped according to HER2 status (HER2-positive or HER2-negative) or considering BC subtypes in three groups (HER2-positive, HER2-negative/luminal or HER2-negative/basal). Comparison between groups were made in order to find statistical differences on STX1A/Snare gene expression between subgroups.

2.2. ANALYSIS OF STX1A GENE

To further study *STX1A* gene expression and its regulatory mechanisms, UCSC genome browser (<http://genome.ucsc.edu>) software was used. This database provides to the research community genome annotations and visualisation of several genetic mechanisms alongside the genome of different species. The analysis of *STX1A* gene has been performed using the UCSC genome browser, together with *in vitro* data from two articles by Takahiro Nakayama and colleagues which demonstrated several regulatory mechanisms of *STX1A* gene (232–234).

First of all, *STX1A* gene is located into human genome GRCh37/hg17 region. Together with data from Nakayama's articles (232–234) and public databases, the regulatory sequences described in the article (promoter region, transcription factor binding site and enhancer regions) were identified. Throughout Blat alignment the *in vitro* data from Nakayama was represented in the genome browser to be able to compare it within the UCSC genome browser database. Regulatory element tracks (see [Table 11](#)) were activated in order to further study and confirm epigenetic regulatory mechanisms of *STX1A* gene.

Table 11 – List of the tracks used in UCSC Genome Browser database.

Track	Subtrack	Description	Reference
NCBI Reference Sequences (RefSeq)	-	The track shows human protein-coding and non-protein coding genes from the NCBI RNA RefSeq collection.	NCBI Reference Sequence (RefSeq): a curated non-redundant sequence database of genomes, transcripts and proteins (236)
GeneHancer	-	The track is from GeneHancer database of human regulatory elements (enhancers and promoters). This track was created by integrating more than 1 million regulatory elements from multiple genome-wide databases. We use this database to identify enhancers and promoter regions.	GeneHancer: genome-wide integration of enhancers and target genes in GeneCards (237)
CpG islands track	-	The track shows predicted CpG islands. CpG islands are commonly located near transcription start sites and may be associated with promoter regions.	CpG islands in vertebrate genomes (238)
Integrated regulation from ENCODE tracks	DNaseI hypersensitive clusters	The track shows DNase hypersensitive areas in a large collection of cell types (125). These clusters are normally located into promoter regions.	ENCODE portal (239)
	H3K4Me1	The track shows the levels of enrichment of the H3K4Me1 histone mark across the genome determined by ChIP-seq assay in 7 cell types. Usually, these marks are associated to regulatory elements, normally enhancers and with DNA regions downstream of transcription starts.	
	H3K4Me3	The track shows the levels of enrichment of the H3K4Me3 histone mark across the genome determined by ChIP-seq assay in 7 cell types. Usually, these marks are found near active promoters.	
	H3K27Ac	The track shows the levels of enrichment of the H3K27Ac histone mark across the genome determined by ChIP-seq assay in 7 cell types. Usually, these marks are found near active regulatory elements.	
	Txn Factr ChIP E3	The track shows regions of transcription factors binding derived from a large collection of ChIP-seq experiments. This track allows you to select all the transcription factors proved, or select the ones that you are interested in. In our case, SP1 was the selected transcription factor according to published literature.	

3. CELL CULTURES

3.1. CELL LINES AND 2D CULTURES

A wide panel of human BC and HNSCC cell lines purchased from the American Type Culture Collection (ATCC, Rockville, MD) were used. BC cell lines used along the project were: SK-BR-3, MDA-MB-453, BT-474, HCC1954, ZR-75-1, MCF-7, T-47D, MDA-MB-231, MDA-MB-468, Hs 578T, BT-549 and HCC70 ([Table 12](#)). HNSCC cell lines used were: FaDu, SCC090 and SCC-25 ([Table 13](#)). The cells were cultured following the ATCC instructions: incubated at 37°C in humidified 5% CO₂ atmosphere, SK-BR-3, MDA-MB-453, BT-474, MCF-7, MDA-MB-468, and SCC25 in DMEM/F12 media (Gibco, #21331-020); HCC1954, ZR-75-1, T-47D, BT-549, HCC70, Hs 578T, FaDu and SCC090 in RPMI media (Gibco, #A10491-01). All media was supplemented with 10% foetal bovine serum (FBS) (Gibco, #10270-106), 5% Glutamax (Gibco, #3550-038) and 5% fungizone-penicillin-streptomycin (Pen/Strep) mixture (Invitrogen, #15070-063). In addition, 10 µg/ml of insulin (Sigma, #I9278) was added to BT-474 and MCF-7 cell lines media.

Moreover, a non-transformed mammary epithelial cell line, MCF10A, was used. This cell line is cultured under the same conditions than BC cell lines (incubated at 37°C in humidified 5% CO₂ atmosphere) but with DMEM/F12 media supplemented with 5% horse serum (Gibco, Life Technologies), 20 ng/ml EGF (Peprotech, AF10015), 0.5 µg/ml hydrocortisone (Sigma, H2270), 10 µg/ml insulin, 2 mM L-GlutaMAX, 100 ng/ml choleric toxin (from *Vibrio cholera*, Sigma, C8052) and 1% Pen/Strep mixture. Tumorigenic-HEp3 (T-HEp3) cells were also used in some experiments, other HNSCC cells, provided by our collaborator, Dra. Paloma Bragado from the Universidad Complutense de Madrid (UCM). T-HEp3 cells were derived from a lymph node metastasis from a HNSCC patient as it is described previously by Ossowski *et al.* (240) and must be kept in *in vivo* models such as CAM or mice. These cells can be cultured *in vitro* for a low number of passages (usually four) at 37°C in humidified 5% CO₂ atmosphere with DMEM/F12 media supplemented with 10% foetal bovine serum (Gibco, #16140071), 5% Glutamax and 5% Pen/Strep mixture. Finally, HEK 293 and HEK 293T-Phoenix cancer cell lines were also used for lentiviral and retroviral particles productions, respectively. These cell lines were cultivated in DMEM/F12 media with 5% FBS, 5% Glutamax and 5% Pen/Strep mixture

All the experiments in which cells need to be treated have been performed by incubating the cells overnight with serum-free media and the treatment has been diluted in serum-free media as well.

Table 12 – Summary of BC cell line properties and BC subtypes according to ATCC and Dai *et al.* (241).

BC subtype	HER2 status	Cell line	Tissue	Disease	Media
HER2-enriched	HER2 +	SK-BR-3	mammary gland/breast; derived from metastatic site: pleural effusion	adenocarcinoma	DMEM/F12
		MDA-MB-453	mammary gland/breast; derived from metastatic site: pericardial effusion	metastatic carcinoma	DMEM/F12
		HCC1954	mammary gland; breast/duct	ductal carcinoma	RPMI
Luminal B		BT-474	mammary gland; breast/duct	ductal carcinoma	DMEM/F12 + insulin
Luminal A	HER2 -	ZR-75-1	mammary gland; breast/duct; derived from metastatic site: ascites	ductal carcinoma	RPMI
		MCF-7	mammary gland; breast	ductal carcinoma	DMEM/F12 + insulin
		T-47D	mammary gland; derived from metastatic site: pleural effusion	ductal carcinoma	RPMI
Basal	HER2 -	MDA-MB-468	mammary gland/breast; derived from metastatic site: pleural effusion	adenocarcinoma	DMEM/F12
		BT-549	mammary gland; breast	ductal carcinoma	RPMI + insulin
		MDA-MB-231	mammary gland/breast; derived from metastatic site: pleural effusion	adenocarcinoma	DMEM/F12
		HCC70	mammary gland; breast/duct	ductal carcinoma	RPMI
		Hs 578T	mammary gland/breast	carcinoma	RPMI

Table 13 – Summary of HNSCC cell lines properties according to ATCC.

Cell line	Tissue	Disease	Media
FaDu	pharynx	squamous cell carcinoma	RPMI
SCC090	derived from metastatic site: tongue	squamous cell carcinoma	RPMI
SCC25	tongue	squamous cell carcinoma	DMEM/F12

4. PROTEIN EXPRESSION MODULATION

4.1. OBTENTION OF CANCER CELL LINES WITH NON-FUNCTIONAL STX1A

The strategy followed to obtain cells with non-functional STX1A was the expression of a Syntaxin-1 Dominant Negative (STX1-DN) protein. To do that, two STX1-DN plasmids were kindly provided by the collaborators from Dr. Soriano's lab from the Universitat de Barcelona (UB), along with their corresponding control plasmid (MOCK). One plasmid was to directly transfect the desired cells in a transient form, and a retroviral plasmid to produce retroviral particles to infect cancer cells and obtain a stable expression of the STX1-DN protein. Both plasmids codified for a non-functional STX1A protein which competed with the wild-type STX1A form for its ligands, with already proved efficacy in impairing STX1 function as published in several articles (83,84,86,242).

4.1.1. COMPETENT CELLS TRANSFORMATION AND PLASMID AMPLIFICATION

DH5- α^{TM} competent cells were used for plasmid amplification according to manufacturer's protocol (Invitrogen #18263012). Briefly, DH5- α^{TM} competent *E.coli* were thawed on ice and then mixed with 1 to 5 μl (1 to 10 ng) of plasmid DNA. After 30 min of incubation on ice and a heat shock of 20 seconds in a 42°C water bath (without shaking) followed by 2 min on ice, 950 μl of pre-warmed Terrific Broth (Table 14) was added. Later, cells were incubated at 37°C for 1 hour at 225 rpm shaking. After that time, 50 μl of transformed bacteria were spread into pre-warmed selective bacteria plates (Table 14) and incubated overnight at 37°C facedown. After culturing transformed cells into selective plates, amplification of these selected bacteria was performed to increase the amount of the plasmid of interest. For this procedure, a bacteria colony is picked with a tip and let grow into a 15 ml tube with 1 ml of Terrific Broth with its correspondent antibiotic for the whole day at 37°C at 225 rpm. At the end of the day 4.5 ml of Terrific Broth with the correspondent antibiotic was added and bacteria culture was further incubated overnight at 37°C at 225 rpm shaking.

The next day, when the media became turbid, indicating that the bacteria have proliferated and the extraction procedure could start using the QIAGEN plasmid mini-kit (Quiagen, #12125), following the manufacturer's protocol. Finally, purified plasmid was quantified using Nanodrop® spectrophotometer (Thermo-Scientific).

Table 14 – Terrific broth and bacteria culture media recipe.

Terrific Broth (1.5 l)		Bacteria culture media
YTG base (1.35 l)	18 g bacto-tryptone	40 g/l Luria Agar
	36 g bacto-yeast extract	
	6 ml glycerol	
Potassium phosphate base (150 ml)	3.5 g KH ₂ PO ₄ monobasic	25 µg/ml kanamycin or
	18.8 g KH ₂ PO ₄ dibasic	100 µg/ml ampicillin

4.1.2. PLASMID TRANSFECTION

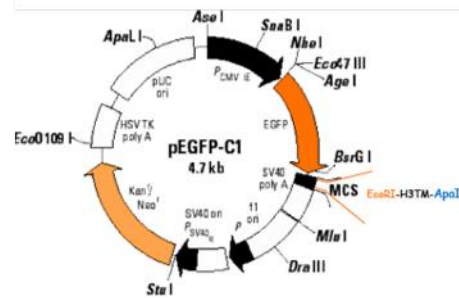
BC and HNSCC cells were seeded under sub-confluent conditions with complete media with antibiotics in a p60 dish. After 24 hours media was replaced with 2 ml of complete media without antibiotics. MOCK (plasmid without the insert) and STX1-DN plasmids ([Table 15](#)) were transfected to BC cell lines following the manufacturer's protocol of the Lipofectamine 3000™ transfection reagent (ThermoFisher #L3000008). Briefly, for each condition, 275 µl of OptiMEM media and 16,5 µl of Lipofectamine 3000 were mixed in a tube. In another tube, 275 µl of OptiMEM media, 22 µl of p3000 transfection reagent and 4 µg of the plasmid of interest were mixed. Both tubes were incubated for 5 minutes at room temperature, and afterwards both tubes were mixed and incubated at room temperature for 20 min. Finally, 550 µl of the mixture were added dropwise into the cell culture. After 4 hours media with Lipofectamine was removed and new fresh complete media without antibiotics was added.

The experiments were performed at least 24 hours after transfection and always taking into account the transfection efficiency, looking for GFP expression under a fluorescent microscope.

Syntaxin-1A, a synaptic related protein in breast and head and neck cancer progression and prognosis

Table 15 – STX1-DN plasmid information.

Backbone: pEGFP-C1 (Clontech)
Insert: H3TM (syntaxin-1)
Specie: Rattus Norvegicus
Selection in bacteria: Kanamycin
Selection in mammal cells: Neomycin
Nucleotide sequence: ATCTCGAAGCAGGCCCTCAG TGAGTCGAGACCAGGCACAGTGAGATCATCAAGTTG GAGAACAGACTCCGGGAGCTACACGATATGTTACAT GGACATGGCCATGCTGGTGGAGAGCCAGGGGGAGA TGATTGACAGGATCGAGTACAATGTGGAACACGCTG TGGACTACGTGGAGAGGGCCGTGTCTGACACCAAGA AGGCCGTCAAGTACCAGAGCAAGGCACGCAGGAAG AAGATCATGCATCATCTTTGCTGTGTGATTCTGGGC ATCATCATCGCTGCACCATCGGG



4.1.3. RETROVIRAL PARTICLES PRODUCTION

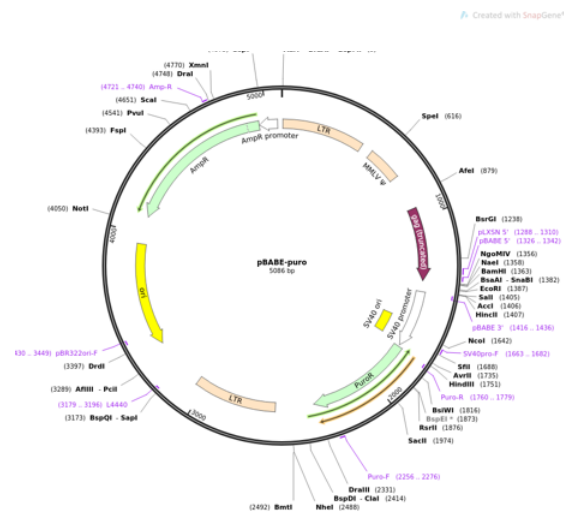
HEK 293T-Phoenix, a second-generation retrovirus producer cell lines, were used. This cell lines have already integrated the gag-pol and envelope constructs for producing retroviral particles. HEK 293T-Phoenix cells were seeded in a 6-mw plate with DMEM/F12 complete media and the next day the transfection protocol was performed as described in the previous section (section 4.1.2), adding 4 µg of MOCK or STX1-DN plasmid (*Table 16*). 24 hours after the media containing retroviral particles was collected and new fresh media was added. The collected media containing retroviral particles was centrifuged at 500 g for 5 min to discard unattached HEK 293T-Phoenix cells, and the supernatant is filtered using a 0.45µm PES filter, aliquoted and frozen at -80°C. Next day, this last step was repeated. Considering that the peak of retroviral production by HEK 293T-Phoenix cells were the first 48 hours after plasmid transfection, cells were discarded at that time point. Next step is to tritiate the retroviral particles.

Table 16 – Retroviral STX1A-DN plasmid.**Backbone: pBABE (Addgene)****Insert: H3TM (syntaxin-1)****Specie: Rattus Norvegicus****Selection in bacteria: Ampicillin****Selection in mammal cells:****Puromycin****Nucleotide sequence:**

```

ATCTCGAAGCAGGCCCTCAGTGAGATCGA
GAAGTTGGAGAACAGACTCCGGGAGCTAC
ACGATATGTTACATGGACATGGCCATGCTG
GTGGAGAGCCAGGGGGAGATGATTGACAG
GATCGAGTACAATGTGGAACACGCTGTGGA
CTACGTGGAGAGGGCCGTGTCTGACACCAAG
AAGGCCGTCAAGTACCAGAGCAAGGCACGC
AGGAAGAAGATCATGCACATCATTTGCTGTG
TGATTCTGGGCATCATCATCGCCTGCACATCG
GGATCGGG

```



4.1.4. RETROVIRAL PARTICLES TITRATION

After obtaining retroviral particles, the next step is to determine their concentration. It is important to note that this protocol also works for lentiviral particles. To do that, HEK 293 cells were seeded to obtain a 60% of confluence into a 6-mw plate. Next day, HEK 293 were infected with different dilutions of the retroviral media stock. The dilution was made in media without antibiotics. After 24 hours media was changed with complete media with antibiotics, and the next day the selection antibiotic was added. 3 days after media was aspirated and cells fixed and stained with crystal violet (Sigma Aldrich, #V5265). The smaller viral concentration where there were approximately 50% of resistant cells will be the one used for the infection of our cells of interest (*Figure 27*).

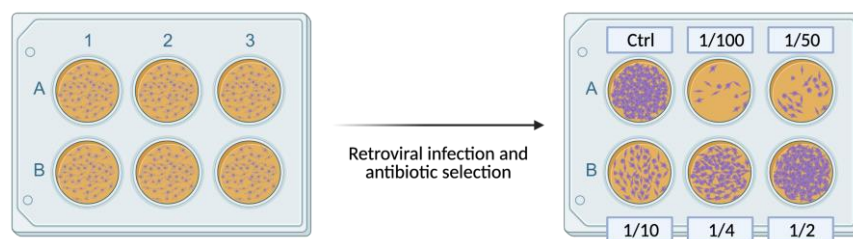


Figure 27- Retroviral particles tritration protocol. On the left, HEK 293 cells after retroviral infection. On the right, after infection, antibiotic selection and crystal violet staining, the retroviral dilution which works better for infecting our cells of interest can be appreciated. In this case the dilution that worked better was 1/4.

4.1.5. RETROVIRAL INFECTION

SK-BR-3 and MDA-MB-231 (HER2-positive BC cell lines), BT-549 and MDA-MB-231 (basal/HER2 negative BC cell lines) and FaDu and SCC090 (HNSCC cell lines) were infected with MOCK and STX1-DN retroviral particles. All BC and HNSCC were seeded in different 6-mw plates with their corresponding complete media with antibiotics (see [Table 12](#) and [Table 13](#)). The day after, media was removed and the dilution of retroviral particles, previously determined by retroviral particle tritration (section 4.1.4), was added into complete media without antibiotics. After 24 hours of the retroviral infection, media was changed to complete media with antibiotics. Next day, the selection antibiotic (puromycin) was added at a concentration of 500 µg/ml to the infected cells. The day after media was changed to newly fresh media with puromycin and the cell cultures were let grow, maintaining the selection pressure of puromycin.

4.2. OBTENTION OF TRANSIENT BC CELLS DOWN-REGULATED BY STX1A

To obtain BC cells down-regulated by STX1A siRNA technology was used. siRNA molecules are delivered to the cell by a transfection reagent and there they will bind and activate the RNA-induced silencing complex, or RISC, which will recognize the mRNA complementary sequence of the siRNA, cleaving the target mRNA sequence and promoting its degradation. The main disadvantage of this approach is that the down-regulation achieved is not stable because the siRNA cannot be inserted into the cell genome.

Cells were plated into 60% of confluence and incubated overnight to allow the cells to adhere. Next day, the siRNA transfection protocol was started according to manufacturer's protocol (243). Briefly, siRNA - (Dharmacon, D-001810-10-05) and siRNA STX1A (Dharmacon, L-012677-00-0005) was diluted with serum free media without antibiotics, considering a final siRNA concentration of 50 µM. In a separate tube, DharmaFECT reagent 1 (Dharmacon, T-2001-01), was diluted in serum-free media without antibiotics. Then, both tubes were incubated for 5 minutes at room temperature. After that, both tubes were mixed and incubated for 20 min at room temperature and then, complete media without antibiotics was added to the mix. Cells media was removed and the siRNA media was added. Finally, cells were incubated for 72 hours to analyse STX1A down-regulation by different strategies.

4.3. OBTENTION OF STABLE BC CELLS DOWN-REGULATED BY STX1A

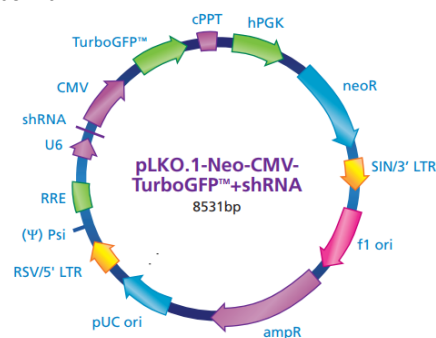
To obtain BC cell lines specifically and long-term down-regulated by STX1A, the lentiviral short hairpin (shRNA) RNA interference (RNAi) strategy was chosen. Briefly, this strategy consists of infecting cells with lentiviral particles bearing shRNA codifying construct that would integrate into the target cell genome. shRNA gene will be transcribed and processed by the enzyme Dicer, producing a RNAi which will assemble and activate the RISC complex. Finally, the activated RISC complex will recognize mRNA sequences complementary to RNAi and cleave them. This will end up with no translation of the mRNA and protein down-regulation (*Figure 28*) (244).

Lentiviral-delivered short hairpin RNA (shRNA)-RNA interference (RNAi) were used to impair STX1A expression in BC cell lines. This approach was chosen because lentiviral vectors can infect both non-dividing and actively dividing cells and also, integrate their genome into host cells genome, achieving a stable inhibition of the target gene. Two types of lentiviral particles carrying the shRNA against SXT1A were purchased from Sigma-Aldrich (Sigma-Aldrich, clone ID: TRCN0000065008 and TRCN0000065009). Given that STX1A shRNA constructs were cloned into pLKO.1-neo-CMV-tGFP vector (*Table 17*), lentiviral-infected cells acquired resistance to Neomycin and derivatives, such as G-418, and could also be sorted by TurboGFP tracking (*Table 17*). MISSION[®] pLKO.1-neo-CMV-tGFP Non-Target shRNA transduction particles (Sigma-Aldrich, # SHC216V-1EA) were used to generate Non-target shRNA-infected control cell lines.

Table 17 – shRNA STX1A plasmids information.

Backbone: pLKO.1 (Clontech)	
Insert: shRNA STX1A	
Specie: Homo Sapiens	
Selection in bacteria: Ampicillin	
Selection in mammal cells: Neomycin	
TRCN0000065008	Nucleotide sequence:
	CCGGAAGAACTCATGTCCGACATACTCGAGT
	ATGTCGGACATGAGTTCTTCTTTTG
TRCN0000065009	Nucleotide sequence:
	CCGCCAGAAAAGTTTGTGGAGGTCACCTCGAG
	GCCACAACTTCTGGTTTTTG

Lentiviral plasmid:



Genomic lentiviral particle structure:



4.3.1. LENTIVIRAL INFECTION

Four BC cell lines resembling different BC subtypes were infected: SK-BR-3, MDA-MB-453 and BT-474 (HER2-positive) and MDA-MB-231 (HER2-negative/basal). As shown in [Figure 28](#) BC cell lines were seeded in a 96-mw plate (5×10^4 cells per well) with 100 μ l of complete DMEM/F-12 media without antibiotics. The day after, cells were infected with lentiviral particles using two Multiplicity of Infection (MOI): 2,5 and 5 in duplicates. The lentiviral particles were added to the BC cells media with DMEM/F-12 complete media without antibiotics. Each cell line was infected with the two lentiviral particles purchased, plus an additional Non-Target lentiviral shRNA. At 20 hours post-infection media was removed and 200 μ l of fresh new complete DMEM/F12 media with 1% Pen/Strep mixture was added. After 48 hours-post infection, infected cells were selected with 200 μ l of complete DMEM/F-12 media with G-418, an analogue of Neomycin (Enzo Life Sciences, ALX-380-013) (1 mg/ml for MDA-MB-453 and MDA-MB-231, 400 μ g/ml for BT-474 and 300 μ g/ml for SK-BR-3). 96 hours post-infection media was replaced with fresh complete DMEM/F-12 media with G-418. Cells were examined under fluorescent microscopy to determine the presence of the TurboGFP reporter gene. Cell culture were let grown, maintaining the selection pressure of G-418. Once amplified, we analysed the efficiency of our experiment assaying the expression of STX1A at mRNA and/or protein levels.

4.3.2. SORTING OF GFP+ shRNA STX1A AND NON-TARGET shRNA BREAST CANCER CELL LINES

To increase the efficiency of STX1A down-regulation in shRNA STX1A BC cell lines, the infected cells were sorted according to GFP expression, thus isolating cells with a major probability of being highly transduced. Only one clone for each condition was sorted (the ones that expressed less STX1A at mRNA/protein level).

Briefly, shRNA Non-Target and shRNA STX1A BC cell lines were trypsinised, washed twice in phosphate-buffered saline (PBS) and finally resuspended with filtered PBS + 1% FBS. Cells were sorted using a BD Biosciences FACS Aria III cell sorter. Wild-type BC cell lines were used as control cells to determine autofluorescence setting. Live cells were gated tacking into account forward and side scattered lights, and single cells were gated according to forward scatter height (FSC-H) and forward scatter area (FSC-A). Gates were determined by analysis of high GFP+ and single cells. Finally, sorted cells were collected in PBS + 1% FBS and kept on ice until plated.

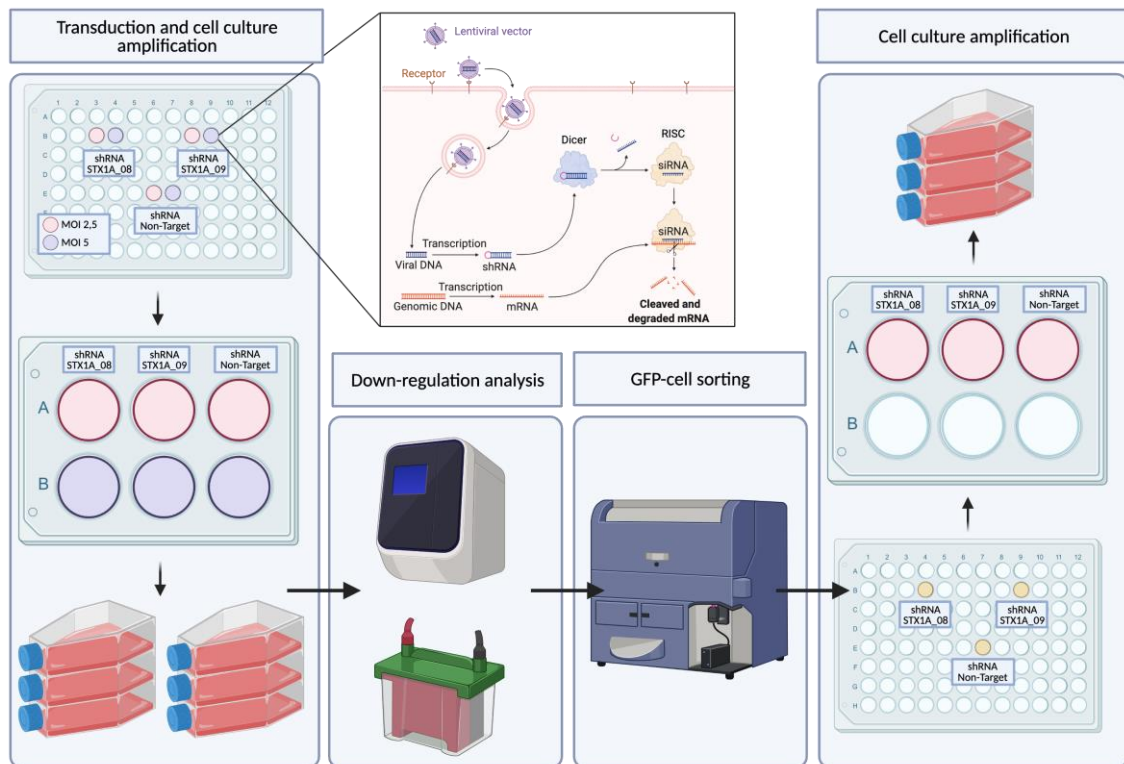


Figure 28- shRNA lentiviral particles transduction protocol. 24 hours after cell seeding each BC cell line was infected with two different MOI (2.5 and 5) with shRNA STX1A_8 (TRCN0000065008), shRNA STX1A_9 (TRCN0000065009) and shRNA Non-target lentiviral particles. After 24 hours media was changed, and the next day the selection antibiotic, G-418, was added to the media. The antibiotic-selected cells were amplified, and down-regulation of STX1A was assessed by Western blot and qPCR assay. After, cells with the highest STX1A down-regulation were GFP-sorted in order to obtain higher efficiency of down-regulation. Finally, GFP-sorted cells were amplified and used for the experiments.

4.4. CRISPR-Cas9

Clustered regularly interspaced short palindromic repeats-associated protein 9 system (CRISPR-Cas9) was used to obtain stable BC and HNSCC cell lines with *STX1A* Knock Out (KO) gene. This technique is based on a bacterial defence mechanism against phage infection and plasmid transfer in nature. Briefly, this system consists of two principal components: Cas9 endonuclease and guide RNA (gRNA). The gRNA sequence consists of 17-21 bases long of single stranded RNA that must be complementary to the target DNA sequence. Cas9 protein is a DNA endonuclease enzyme that binds to gRNA forming a ribonucleoprotein. This ribonucleoprotein would be able to recognize a specific DNA target homologous to the gRNA and cleave both strands of the target DNA where Cas9 enzyme recognizes a protospacer adjacent motif (PAM) sequence (the canonical PAM is the sequence 5'-NGG-3', where "N" is any nucleobase). Thus will create a double-strand break (DSB) at the genome (245,246). The DSB would be repaired via the non-homologous end joining (NHEJ) mechanism which will lead to random insertions or deletions within the open reading frame of the cleaved gene. This repairing mechanism will

often introduce a frameshift, which would cause a premature stop codon and/or a non-sense transcript that will be degraded. In some cases, the transcript can be translated but resulting in an abnormally short and non-functional protein (245,246) (Figure 30).

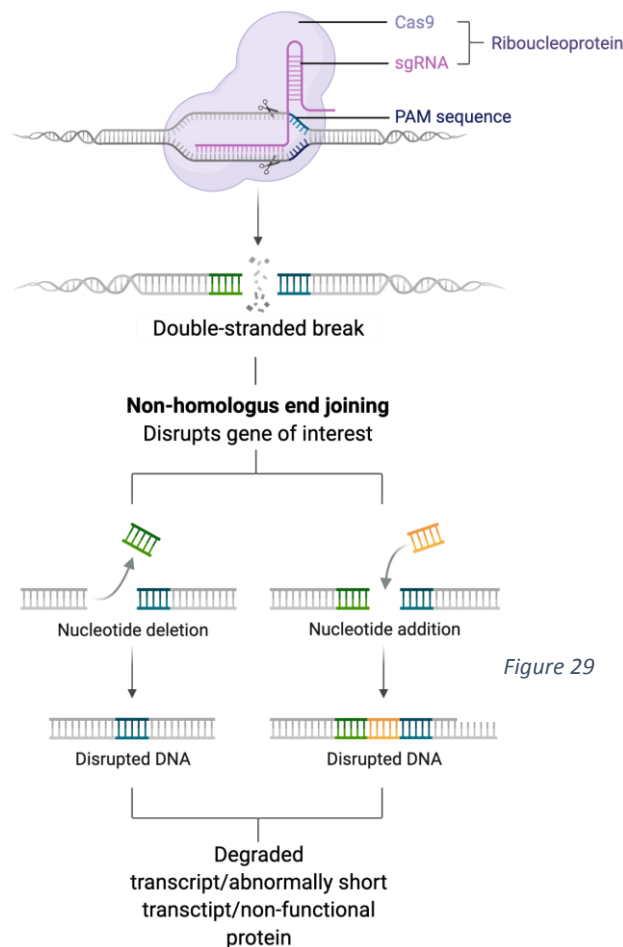


Figure 29

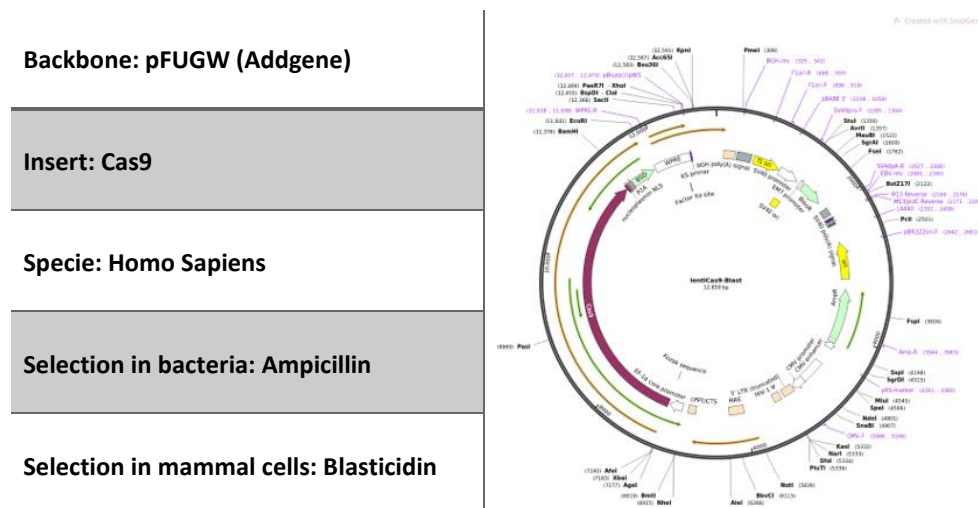
Figure 30 – CRISPR-Cas9 scheme. The specificity to the target DNA strand is driven by the gRNA. When gRNA recognizes the complementary sequence next to a PAM motif, Cas9 endonucleases cut the double strand of the DNA. The genomic DNA is repaired by non-homologous end joining that will end up into no protein production or a non-functional protein.

4.4.1. LENTIVIRAL PARTICLES PRODUCTION

Cas9 lentiviral particles had to be produced in order to infect BC and HNSCC cells to express Cas9 enzyme. This protocol is similar to retroviral particles production (described in 4.1.3). However, in this case, instead of using HEK 293T-Phoenix, wild-type HEK 293 cell line was used. These cells were seeded in a 6-mw plate with DMEM/F12 complete media and let them at the incubator (37°C in humidified and 5% CO₂ atmosphere) overnight. The next day, the transfection protocol was started as described in section 4.1.2. It was added 4.5 µg of Cas9 plasmid (Addgene, #52962,) (Table 18), 3 µg of pMDLg/pRRE plasmid (Addgene, #12251) and 1.5 µg of pRSV-Rev (Addgene, #12253) (Annex figure 1). The cells were let on the incubator for

the following 24 hours, and then the media was changed. Media was collected 48 hours after transfection and new fresh media was added. The media containing lentiviral particles was centrifuged at 500 g for 5 min to discard unattached HEK 293 cells, and it was stored at 4°C. Next, media from 48 hours was recollected as well, and then 24 and 48 hours media which contained lentiviral particles were concentrated. To do that, it was added 1 volume of Lenti-X concentration reagent (Takara, #PT4421-2) to 3 volumes of media containing lentiviral particles. The mixture was incubated overnight at 4°C. Next day the mix was centrifuged at 1,500 g for 45 min at 4°C. The supernatant was removed and the pellet was resuspended with PBS, aliquoted and stored at -80°C. Next, the lentiviral stock was titrated as explained in section 4.1.4 for retroviral particles.

Table 18 – Cas9 lentiviral plasmid information.



4.4.2. OBTENTION OF CAS9-POSITIVE CELLS

To obtain Cas9-positive cells lentiviral particles bearing Cas9 insert were used. It was used the same protocol described in section 0. Briefly, the day before the infection, BC cell lines (MDA-MB-453 and MDA-MB-231) and T-HEp3 (HNSCC) were plated into 96-mw plates with complete media with antibiotics. The next day, media was removed and changed to complete media without antibiotics. Then, cells were infected with lentiviruses bearing the Cas9 insert and the following day media was changed to discard remaining viruses. Finally, 48 hours after the infection the selection process was started by adding 10 µg/ml of blasticidin into the media. Cas9 cells were expanded and checked for Cas9 expression, determined by Western blot (protocol in section 6.1).

4.4.3. gRNAs DESIGN

Specific STX1A gRNAs were designed using three bioinformatical on-line softwares: Integrated DNA technologies (IDT) (<https://eu.idtdna.com>), Synthego (<https://design.synthego.com>) and Benchling (<https://benchling.com>). The first one was used in order to look for recommended human STX1A exons to be targeted with the gRNA sequence. The software recommendation was to design the gRNAs against exon 2, 6 or 10. Then, Synthego software was used to identify recommended gRNA sequences. Synthego software has an algorithm that considers several important aspects about gRNA design. Some of these aspects to consider are:

- The designed gRNA has to target the initial part of the exon to make sure that there is no transcript.
- The exon targeted by the gRNA has to be common to all transcriptional variants of the gene.
- The gRNA designed has to combine a high on-target activity and low off-target potential.

The Synthego software only recommended gRNAs from the exon 6. Considering that the human STX1A gene has 10 exons, we also compared recommended gRNA from exon 2, as IDT software recommended. Then, exon 6 gRNA sequences recommended for Synthego and exon 2 sequences were entered into Benchling in order to compare the on-target and off-target score. Finally, after several comparison the chosen gRNAs were from exon 2 and from exon 6 (*Table 19*).

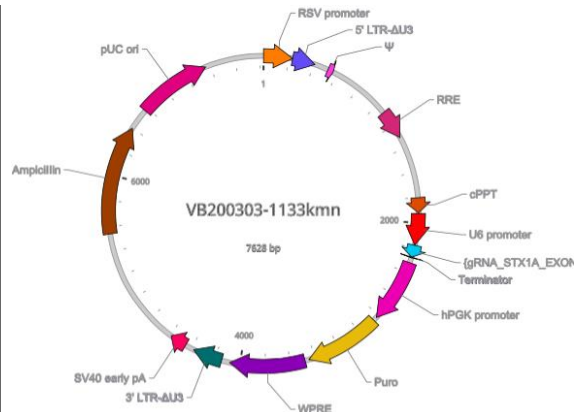
Table 19 – Designed STX1A gRNAs.

gRNA	PAM sequence	Strand	Exon	On-Target Score	Off-Target Score
TGATGATGTCGCTGTCACCG	TGG	+	2	70.8	45.0
CACAACTTTCTGGACAGCG	TGG	-	6	62.8	43.6

Finally, gRNAs were purchased from VectorBuilder (<https://en.vectorbuilder.com>) as lentiviral plasmids (*Table 20*). Plasmids arrived as glycerinates, so they should have to be amplified and purified according to protocols in section 4.1.1 to be able to produce lentiviral particles (protocol in section 4.4.1). Moreover, non-targeting control lentiviral particles were also produced to infect BC and HNSCC cells and use them as controls, the plasmid used was non-targeting control pLentiGuide-Puro plasmid (#52963, Addgene).

Table 20 – Lentiviral gRNA plasmids.

Backbone: pLV[gRNA]-Puro-U6 (VectorBuilder)
Specie: Homo Sapiens
Selection in bacteria: Ampicillin
Selection in mammal cells: Puromycin
gRNA exon 2: TGATGATGTCGCTGTCACCG
gRNA exon 6: CACAACTTTCTGGACAGCG



4.4.4. OBTENTION OF CRISPR-Cas9 CELLS FOR STX1A

To obtain CRISPR-Cas9 cells, Cas-9 positive BC cell lines (MDA-MB-453 and MDA-MB-231) and T-HEp3 (HNSCC) cells were infected with lentiviruses bearing the gRNAs. Duplicates for each gRNA were performed and the lentiviral infection protocol described before (sections 0 and 4.4.2) was strictly followed. However, the selection process, in this step was performed by adding 10 µg/ml blasticidin and 500 µg/ml puromycin to the cells. Cells were expanded and checked for STX1A expression by Western blot assay (protocol in section 6.1).

After the Western blot analysis, no inhibition of STX1A by protein expression was seen. Considering that our cells did not express any tag, the cell culture was subcloned to try to obtain a single cell with *STX1A* KO and select that clone. Only one of the duplicates was subcloned, but it was done for each gRNA. Cells were detached with trypsin and counted and then diluted in complete media (containing 10 µg/ml blasticidin and 500 µg/ml puromycin) considering that it was needed a single cell in each well of a 96-mw plate. After seeding the cells, they were let to attach and grow for 2 days. Then, each well was checked with the aim to identify those wells that had only one cell, discarding those without or with more than one cell. Cells were let grown under selective media until 70-80% of confluence, when cells were detached and seeded in 12-mw plates. This procedure was repeated until there were enough cells to run a Western blot to analyse STX1A expression.

5. RNA EXPRESSION

5.1. RNA ISOLATION AND QUANTIFICATION

RNA was extracted with TRItidy G (PanReac AppliChem, #A4051). Once the cells were collected, 0.5 ml of TRItidy G (Life Technologies, #15596026) was added and the cell pellets resuspended by repetitive pipetting. After that, 0.2 ml of chloroform was added and the tube was shaken vigorously and incubated for 3 min at 4°C. Then, it was centrifuged at 12,000 g for 15 min at 4°C and the mixture was separated into a lower red (phenol-chloroform phase), an interphase and a colourless upper aqueous phase. The RNA remained exclusively in the aqueous phase, so it was transferred into a new tube and the RNA was precipitated with the addition of 0.5 isopropyl alcohol. The samples were incubated at -20°C for 2 hours and then centrifuged at 12,000 g for 10 min at 4°C. The supernatant was removed and the pellets were washed with 1 ml of 75% ethanol, mixed by vortexing and centrifuged at 7,500 g for 5 min at 4°C. Finally, the ethanol was discarded and the RNA pellets were air-dried for 10 min and dissolved into 20 µl of RNase-free water.

Total RNA concentration and quality were assessed by Nanodrop® spectrophotometer (Thermo-Scientific) following the 260/280 and 260/230 rules.

5.2. QUANTITATIVE REAL TIME PCR

First of all, 1 µg of RNA for each experimental condition was reverse transcribed into cDNA using High-Capacity cDNA Reverse Transcription Kit (Life-technologies #4368813) following the reagent proportions of the manufacturer's recommendations (*Table 21, left*). To start the retrotranscription process, the prepared samples were loaded into the thermocycler (model 2720, Applied Biosystems) with the program described in *Table 21, right*.

Table 21 – High-capacity cDNA reverse transcription (left) and reverse transcription program (right).

Mix component	Quantity	Steps	Temperature	Time
10x Reverse transcription buffer	2 µl	Step 1	25°C	10 min
10x Primers	2 µl	Reverse transcription reaction	37°C	2 h
25 dNTPs Mix 100 mM	0.8 µl	Reverse transcriptase inactivation	85°C	5 min
Reverse transcriptase 50 U/µl	1 µl	Storage	4°C	∞
RNA	1 µg			
H ₂ O	Up to 20 µl			

Gene expression quantification and analysis were performed using the quantitative real-time PCR (qRT-PCR) technique and carried out by using a 7900HT Fast Real Time PCR system (Applied Biosystems) and validated Taqman® Gene Expression Assays (Applied Biosystems) probes (see [Table 27](#) in section 10) The PCR reaction mixture was done in a final volume of 10 µl for each sample, including 0.5 µl of each sample probe, 5 µl of master mix (TaqMan Universal PCR Master Mix, ThermoFisher, #4367846), 2 µl of RNase-free water and 2 µl of cDNA per well. Each sample was performed in duplicate and transcript levels were normalized to β-actin used as an endogenous control. The qPCR program is described in [Table 22](#).

Table 22 – qPCR program.

Steps	Temperature	Time	Number of cycles
Pre-heating	50 °C	2 min	1 cycle
Initial denaturalisation	95 °C	10 min	1 cycle
Denaturalisation	95 °C	15 s	40 cycles
Amplification and hybridisation	60 °C	1 min	

6. PROTEIN DETECTION

6.1. WESTERN BLOT ANALYSIS

Cell pellets were obtained by harvesting cells after 5 minutes treatment with trypsin/EDTA followed by a complete media serum-containing wash to inactivate trypsin and two centrifugation (2,200 rpm for 5 min at 4°C) steps with a PBS wash. Then, cells were enzymatically lysed using ice-cold radio-immunoprecipitation assay (RIPA) buffer ([Table 23](#)). Briefly, the samples with RIPA buffer were incubated for 20 min at 4°C and finally centrifuged at 13,000 rpm for 15 min at 4°C. Supernatants containing the protein fraction were collected and quantified by Pierce™ BCA Protein Assay Kit (Thermo-Scientific, #23225) following the manufacturer's instructions.

For each sample, 50 µg of protein mixed with protein loading buffer ([Table 23](#)), were boiled for 5 min at 95°C and loaded into the Sodium Dodecyl Sulphate Polyacrylamide Gel electrophoresis (SDS-PAGE) gels prepared at different concentration of Acrylamide/Bis-Acrylamide (10%, 12% or 15%) depending on the molecular weight of the proteins of interest ([Table 24](#)). Protein electrophoresis was carried out at a constant voltage of 120 mV (Mini-Protean, Bio-Rad) for approximately 2h (depending on the size of the protein of interest). Running buffer used for the electrophoresis is described in [Table 23](#). Polyvinylidene fluoride

(PVDF) membranes were activated with methanol for 1 min, and then the resolved protein was transferred into the PVDF membrane. Wet transference was performed at constant amperage of 350 mA for 90 min. After the transference, Ponceau staining ([Table 23](#)) was done to determine if the protein have been properly transferred into the PVDF membrane. Blotted membrane was blocked with Tris Buffered Saline with tween 20 (TBS-T, recipe in [Table 23](#)) 5% non-fat dry milk for 1 hour at room temperature. Finally, the membranes were incubated with the corresponding primary antibodies (see [Table 28](#) in section 10) overnight at 4°C. To confirm equal protein loading, internal housekeeping control antibodies were used (GAPDH, β -actin or α -tubulin).

The next day, membranes were washed 3 times with TBS-T and then incubated with the secondary antibody horseradish peroxidase-conjugated (1:2,500 with TBS-Tween 5% non-fat dry fat milk) (see [Table 29](#) in section 10) for 1 hour at room temperature. To capture the chemo-luminescence image, membranes were incubated for 1 min with ECL Western Blotting Detection reagent (GE Healthcare, #RPN2209). The chemo-luminescent signal was detected by LAS-4000 (FujiFilm, Japan) by means of ImageReader software (version 2.2, FujiFilm). Images were treated with the densitometric analysis software, Multi-gauge (FujiFilm Corporation), and densitometric data was normalized to the housekeeping gene (GAPDH, β -actin or α -tubulin).

Table 23 – Western blot buffer recipes.

Buffer	Components	Buffer	Components
RIPA buffer	50 mM Tris-HCl (pH 7,4)	TBS-T (1x)	Add 1ml/l Tween-20 to PBS 1x
	150 mM NaCl		0.25 M Tris-HCl pH6.8
	1% Triton X-100	Sample buffer (5x)	0.35 mM SDS
	1% Sodium Deoxycolate		7.5 mM Bromophenol Blue
	0.1% SDS		50% Glycerol
	0.2% NaF		4% β -Mercapotoethanol
	0.25 mM EDTA		Running buffer (10x)
	1 mM Na_3VO_4	2 M Glycine	
5 $\mu\text{l/ml}$ protease inhibitor cocktail	35 mM SDS		

Buffer	Components	Buffer	Components
PBS (10x)	1.37 M NaCl	Transfer buffer (10x)	0.25 M Tris
	27 mM KCl		2 M Glycine
	100 mM Na ₂ HPO ₄	Transfer buffer (1x)	10% Transfer Buffer 10x
	18 mM KH ₂ PO ₄		20% Methanol
TBS (10x)	0.2 M Tris	70% distilled H ₂ O	
	1.5 M NaCl	Ponceau staining	0.5% Ponceau staining
	Adjust at pH 7.5		1% acetic acid

All buffers are dissolved in distilled water

Table 24 - SDS-PAGE gels recipe.

Separating gel	Acrylamide/Bis-Acrylamide (stock: 30%) (will depend on the gel)	Stacking gel	5% of Acrylamide/Bis-Acrylamide (stock: 30%)
	375 mM Tris (pH 8.8)		190 mM Tris (pH 6.8)
	0.1% SDS		0.1% SDS
	0.1% APS		0.1% APS
	0.4 µl/ml TEMED		1 µl/ml TEMED

6.2. IMMUNOPRECIPITATION

The protocol followed was from Dr. Coppolino's lab (Ontario, Guelph). The immunoprecipitation antibodies were coupled to protein G Dynabeads (Bio-Rad, #161-4023) according to the instructions of the manufacturer and let in a rocking platform at 4 °C overnight. Cells were lysed with cold lysis buffer ([Table 25](#)) and cell lysate was quantified. 500-1.000 µg of cell lysate was incubated with antibody-bound protein G Dynabeads overnight in a rocking platform at 4 °C. The next day, beads were washed three times with cold PBS, and eluted with 2.5X Laemmli loading buffer ([Table 25](#)) and heated to 95 °C for 20 min. Proteins were separated using SDS-PAGE and analysed by Western blot (section 6.1).

Table 25 – Immunoprecipitation recipes.

Buffer	Components	Buffer	Components
Immuno-precipitation lysis buffer	1% Nonidet P-40	Laemmli buffer 1X (reducing)	60 mM Tris-HCl (pH 6.8)
	10% glycerol		2% SDS
	0.5% sodium deoxycholate		10% glycerol
	137 mM NaCl		5% β-Mercapotoethanol
	20 mM Tris-HCl (pH 8.0)		0.01 mM Bromophenol Blue
	10 mM NaF	All buffers are dissolved with distilled water	
	10 mM Na ₂ HPO ₄		
	0.2 mM Na ₃ VO ₄		
5 µl/ml protease inhibitor cocktail			

6.3. IMMUNOFLUORESCENCE IN COVERSGLIPS

The cells were seeded in coverslips always in sub-confluent conditions, the exact number depending on the experimental settings for each assay. At the set time point, cells were washed with cold PBS and fixed for 15 min with 4% paraformaldehyde (PFA) (Sigma Aldrich, #1004968350) at 4°C for 20 min. After three washes, the coverslips could be stored at 4°C for 3 weeks until the immunofluorescence protocol continues.

If necessary, cells were permeabilized with 0.5% Triton X-100 in PBS for 5 min and blocked for 1 hour with blocking buffer (3% BSA and 1.5% normal goat serum (NGS) in PBS). After that time, cells were incubated with the corresponding primary antibody (see [Table 28](#) in section 10) in blocking buffer overnight at 4°C in a humidified chamber. The next day, coverslips were washed 5 times with PBS and then incubated for 1 hour at room temperature with the corresponding secondary antibody labelled with fluorochrome (see [Table 29](#) in section 10). Nuclei were counterstained with Hoechst (Thermo Fisher Scientific, #33342) for 15 min and coverslips were mounted on glass with Prolong Gold Antifade reagent (Thermo Fisher Scientific, # P36930).

Samples were visualized using an inverted epifluorescence microscope (Leica SP2) using Leica LAS AF Lite 4.0 software or by a confocal microscope (Leica SP5) with ZEN 3.1 Blue edition software. Image assembly, processing and quantification were performed using ImageJ software (U.S. National Institutes of Health, Bethesda, Maryland, USA, <https://imagej.nih.gov/ij/>, 1997-2018).

Co-immunofluorescences were performed in the same way, using two primary antibodies from different animal host.

6.4. IMMUNOFLUOROHISTOCHEMISTRY

Immunohistochemistry was performed in 4 µm thickness paraffin-embedded tissues. Paraffin was removed at 60°C for 30 min. Afterwards, the slides were put in xylene (10 min) and in an ethanol series (100%-90%-80%-70%) for 5 min each. After washing the slides for 5 min with deionized water, they were put in boiling citrate buffer (pH 6) (10 mM Trisodium citrate (dihydrate) in distilled water) for 45 min to unmask antigens. After tempering the slides, they were rinsed with PBS for 10 min and tissues were blocked for 1 hour at room temperature

with blocking buffer. Tissues were incubated with their corresponding primary antibodies (see [Table 28](#) in section 10) overnight at 4°C in a humidified chamber.

The next day, after washing twice the slides with PBS, they were incubated with the corresponding secondary antibody conjugated with a fluorochrome (see [Table 29](#) in section 10) for 1 hour at room temperature. Nuclei were counterstained with Hoechst for 15 min, and coverslips were mounted on glass with Prolong Gold Antifade reagent. Samples were visualized using an inverted epifluorescence microscope (Leica SP2) with LAS AF Lite 4.0 software. Image assembly, processing and quantification were performed using the ImageJ software.

7. FUNCTIONAL ASSAYS

7.1. CELL VIABILITY ASSAYS

7.1.1. PROLIFERATION ASSAY

To determine differences in proliferation between MOCK and STX1-DN BC and HNSCC cell lines, proliferation assays following the 3-(4,5-Dimethylthiazol-2-yl)-2,5-diphenyltetrazolium bromide (MTT) assay protocol (Promega #G8081) were performed.

First MOCK and STX1-DN BC and HNSCC cells were seeded under sub-confluent conditions in sextuplicate in five different 96-mw plates in 200 µl DMEM/F12 or RPMI media with only 2% FBS. The plates were returned to the incubator. After 6 hours, 80 µl of media was removed from one plate and 20 µl of tetrazolium MTT was added to each well. Then, the plate was incubated for 1 hour at 37°C and read on a microplate spectrophotometer (Molecular Dynamics) at 490 nm wavelength (test wavelength) and at 620 nm (reference wavelength), for background correction. This lecture was used as time 0. During the following four days, every 24 hours this procedure was repeated.

Once all measurements were obtained, the absorbances were normalized to time 0 and represented as cell proliferation rate.

7.1.2. CELL CYCLE ANALYSIS

This assay was done to check for differences in cell cycle distribution between MOCK and STX1-DN BC and HNSCC cell lines. Cells were seeded in sub-confluence conditions in 60 mm diameter dishes in complete growth media. Then, the media was changed to media with

2%FBS for 24 hours. If treatment is needed, cells are treated at this time point as well. Then, attached cells and cells from the supernatant are collected, centrifuged at 1,500 rpm, resuspended in 200 µl of cold PBS and fixed with cold 70% ethanol added dropwise in slight rotational movement. At this point samples could be stored at 4°C until flow cytometry analysis is performed. Finally, fixed cells were incubated for 15 min at 4°C with PI/RNase Staining Buffer (BD Pharmigen, 550825) adding 500 µl of buffer for every 10⁶ cells. After staining, cells are washed with cold PBS, and centrifuged. Finally, once the supernatant is discarded, they are resuspended in cold PBS and analysed using flow cytometry (Fortessa LSR). 10,000 cells were analysed for each sample and duplicates were performed for each experiment condition. The results were analysed using the FlowJo software v10 (BD Biosciences).

7.1.3. CITOTOXICITY ASSAY

To determine the effects of anticancer treatments in STX1-DN BC and HNSCC cell lines cell cytotoxicity assays were performed. The effect of the drugs in BC and HNSCC cell lines were assessed following the MTT assay protocol, as well.

MOCK and STX1-DN BC and HNSCC cell lines were cultured under sub-confluent conditions with 100 µl of complete DMEM/F-12 or RPMI media into 96-mw plate. After 24 hours, cancer cell lines were treated with the particular drug (lapatinib, Adriamycin or cetuximab) in a final volume of 200 µl in serum free media. Treatments were carried out in triplicate. After 72 hours, 80 µl of media was removed, 20 µl of tetrazolium MTT was added to each well and the plate was incubated for 30-45 min at 37°C. Finally, the plate was read on a microplate spectrophotometer (Molecular Dynamics) at 490 and 620 nm wavelength. Afterwards, each measurement was normalised with the absorbance in the control situation where no treatment was added. Three wells with no cells where only culture media was added were also processed for developing the blank measurements.

Determination of half maximal inhibitory concentration (IC₅₀), curve fitting and statistical analysis were performed with GraphPad Prism® Software.

7.1.4. ANNEXIN V ASSAY

To study apoptosis in MOCK and STX1-DN HNSCC cells Annexin-V staining assay was performed using the Annexin V-FITC detection kit (eBiosciences, B45500FI). This assay detects

early and late apoptosis events, based on the flipping of phosphatidylserine of the plasma membrane from the inner surface to the outer layer, when a cell is entering apoptosis. Phosphatidylserine on the outer surface will be specifically recognized and bound by annexin V. If the cell loses its cell membrane integrity due to late apoptosis, the PI will be able to enter into the cell, and the cell will be stained with annexin V and PI. Finally, if the cell is necrotic, the cellular structure is lost, and therefore, phosphatidylserine will not be detected, and the cell will only be stained for PI. This way, it is possible to discriminate between early apoptosis (annexin V staining), from late apoptosis (annexin V and PI staining) and from necrotic events (PI staining) (Figure 31).

Cells were seeded in 60 mm diameter dishes at sub-confluence in complete culture media. After 24 hours media was changed to serum-free and cells were treated with lapatinib. After 24 hours, both attached cells and cells from supernatant were collected and incubated for 15 min at 4°C in dark conditions with Annexin V-FITC and PI solution diluted in 1X binding buffer. Finally, cells were washed with cold PBS and resuspended with binding buffer to be analysed by flow cytometry. Control conditions such as the non-stained (binding buffer only), Annexin V-FITC only and PI only conditions were also performed to calibrate properly the cytometer (Fortessa LSR). 10,000 cells were analysed for each sample and duplicates were performed for each experimental condition. Results were analysed by FACSDiva software (Becton-Dickinson).

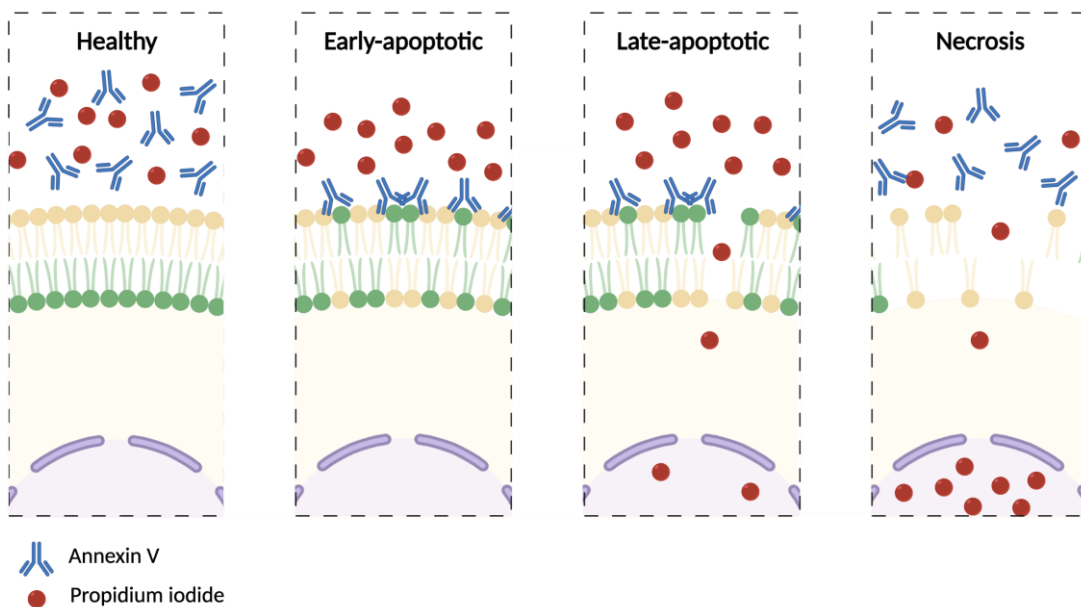


Figure 31 – Schematic representation of Annexin-V assay. Cells which are alive have their plasma membrane intact and Annexin V cannot bind phosphatidylserine. In early-apoptotic cells, phosphatidylserine starts to flip to the outer layer of the plasma membrane where Annexin V can bind it, but the plasma membrane is still intact and PI cannot reach into the DNA. At late apoptotic stages

the cell starts to disrupt, enabling the entrance of PI into the nucleus, and still there is Annexin staining. Finally in the necrosis stage the membrane is disrupted and Annexin-V binding is not detected, but there is PI signal.

7.2. COLONY FORMATION ASSAY

500 cells/well of shRNA Non-target and shRNA STX1A BC cells were seeded into 6 cm diameter cell culture plates with complete DMEM/F-12 media. Cells were allowed to grow at 37°C in humidified 5% CO₂ atmosphere until the colonies were visible to the naked eye (the time can vary among cell lines). Media was removed and the plates were washed 2 times with PBS. Then, colonies were stained with crystal violet 1% aqueous solution for 5 minutes and scanned to obtain representative images. Experiments were performed in triplicate to ensure reproducibility of the data. Number of colonies and area of colonies were analysed by ImageJ software.

7.3. MIGRATION AND INVASION ASSAYS

7.3.1. WOUND HEALING ASSAY

BC or HNSCC cell lines were plated in 12-mw plates with complete media to reach a confluence of 90% 24 hours later. The next day a linear scratch was performed using a 1,000 µl tip. Cells were washed twice with PBS and then serum-free media was added. Image was captured at time 0, which was used as a control image to determine the migration capability of cancer cells. Then, cells were incubated at 37°C in humidified 5% CO₂ atmosphere. Images were captured at the indicated time points using a LEICA DFC295/DMIL LED microscope and ZEISS AXIOVERT200 at 4X magnifications from five randomly selected fields in each condition. The wound area of the scratch was measured in µm by ImageJ software.

7.3.2. INVASION TRANSWELL ASSAY

BC and HNSCC cell lines transfected with MOCK plasmid as a control, or with STX1-DN plasmid for impairing STX1A cell function were used. After 24 hours of BC cells transfection, 24-mw transwell chambers inserts (Merck, #MCEP24H48) were coated with 20 µl serum free media with 1:6 Matrigel (BD Bioscience, #10429212) dilution. After 20 min cells (MOCK and STX1-DN) were harvested with PBS/EDTA (Cultek, #H3BE02-017F) (to avoid disruption of focal adhesion proteins) and seeded at a concentration of 7x10⁴ cells in a volume of 200 µL of serum free media on the chamber insert. The lower chambers were filled with 600 µl of medium containing 10% FBS. 24 hours later, the chamber inserts were washed with PBS and fixed with 4% PFA for 20 min. After that, the cells were dyed with 0.1% crystal violet for 30 min, and then

washed with PBS twice. Cells were observed by light microscope and different areas were randomly selected image captured and quantified with ImageJ software.

7.3.3. CELL ADHESION ASSAY

BC and HNSCC cells were detached with PBS/EDTA and counted. Then 1×10^5 cells were seeded in a 24-mw plate in 250 μ l complete media. Cells were incubated at different times (15 min, 30 min, 1.5 h and 2 h) and after the required time media was carefully removed with a pipette and cells were fixed and stained with crystal violet for 20 min at room temperature. The excess of staining was removed with water. Pictures were taken with Leica SP2 microscope with LAS AF Lite 4.0 software and the images were analysed with ImageJ software.

7.3.4. CELL SPREADING ASSAY

These experiments were performed following Dr. Coppolino's lab protocol (Ontario, Guelph). Coverslips were coated with 20 μ g/ml laminin/PBS (Sigma Aldrich, #L4544) overnight. The next day, BC or HNSCC cancer cell lines were seeded at a very low confluence (10,000 cells/well in a 24-mw plate) and let them attach for 2 hours. After that time, cells were fixed and stained with Phalloidin (Cell Signaling, 8953S) following the immunofluorescence protocol (section 6.3) and the images were captured by a confocal microscopy.

The quantification of the cell area was done by ImageJ software, and cell invadopodia was quantified modifying the measurement plugin of the ImageJ to count only circular cell structures around 5 nm^2 . Cell morphology was also considered by grouping cell morphology into three groups: high sphericity, low sphericity (circular) and low sphericity (angular) which are represented in [Figure 32](#). High sphericity cells were completely spherical, which commonly did not have invadopodia or invadopodia were located in the centre of the cell. Usually, these cells did not have stress fibers. Low sphericity cells were considered the cells that were starting to elongate, but without losing its spherical morphology. Actin filaments redistribution was present and stress fibers started to appear. Also, invadopodia were sprouting from central position of the cell. Finally, low spherical and angular cells were ones that had lost its sphericity and were elongated, with several cell protrusions covered with F-actin filaments. Usually, in these protrusions is where the invadopodia were located.

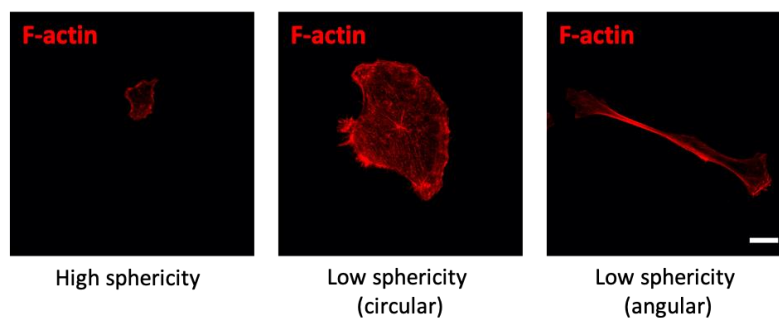


Figure 32 – Cell morphology groups. Representative images of a cell spreading assay and its corresponding cell classification considering the three groups of cell morphology: high sphericity, low sphericity (circular) and low sphericity (angular). Scale bar = 2 μ m.

7.3.5. GELATIN FLUORESCENT ASSAY

These experiments were performed at Dr. Coppolino's lab during my internship in his lab (Ontario, Guelph). Briefly, glass coverslips were coated with 50 μ g/ml Poly-L-lysine (Sigma Aldrich, P4707) diluted in PBS for 20 min, followed by cross-linking with 0.5% glutaraldehyde (Sigma Aldrich, #G5882) diluted in PBS for 10 min. Coverslips were then inverted onto 70 μ l of Alexa Fluor 594 – labeled gelatin (Invitrogen, #A10239) for 10 min. The coated coverslips were then incubated with 5 mg/ml NaBH₄ (Sigma Aldrich, #45882) diluted in PBS for 15 min and subsequently washed with PBS. Then, 5x10⁴ cells were plated and incubated for 4 hours to allow gelatin degradation. Finally, the coverslips were fixed following an immunofluorescence protocol (section 6.3) and the images were captured by the confocal microscopy and analysed by ImageJ software.

7.3.6. ZYMOGRAM

To analyse MMP activity, cells were cultured at 70% of confluence and 24 hours after, cells were serum-starved for 48 hours. After that time, media was collected and centrifuged 2 min at 800 rpm to eliminate unattached cells. Then, media was centrifuged at 4,000 g for 10 min with concentrator tubes (Amicon Ultra-4, Milipore, UFC801096) and protein was quantified using Pierce™ BCA Protein Assay Kit following the manufacturer's instructions. Then, the MMPs analysis could be done via Western blot assay (section 6.1) to see MMPs expression or via zymogram assay to check MMPs activity.

To perform a zymogram assay, an electrophoresis was performed in 8% SDS-PAGE gel (Table 24) containing gelatin (0.1%) (Sigma, G9391), under non-reducing conditions. Samples were prepared in β -mercaptoethanol-free and DTT-free Laemmli buffer 4X (Table 26) and they

were not boiled. Electrophoreses were carried out at a constant voltage (80 V to avoid heating of the proteins and as a consequence, protein denaturalisation. Next, gels were washed with zymogram washing buffer (*Table 26*) for 30 min and incubated overnight in substrate buffer (*Table 26*) at 37°C. Enzymatic activity was proportional to gelatine degradation in the gel, which was visualized by gel staining with Coomassie Brilliant Blue (BioRad, 161-0400) as clear bands over dark background. Band intensity was determined using ImageJ software and data were referred to the control sample in each experiment.

Table 26 – Zymogram buffers recipes.

	40 mM Tris-HCl (pH 7.6)		50 mM Tris (pH 7.5)
Laemmli buffer 4X (non-reducing)	10% Glycerol	Substrate buffer	0.2M NaCl
	1% SDS		2.5 mM CaCl ₂
	0.002% Bromophenol blue		1% Triton X-100
Wash buffer	2.5% Tryton		0.02% NaN ₃
All buffers are dissolved in distilled water			

8. *IN VIVO* EXPERIMENTS

In vivo experiments were performed using two animal experimental models, the chicken chorioallantoic membrane (CAM) assay and immunodeficient mice xenografts.

The CAM is a highly vascularized extra-embryonic membrane connected to the embryo through the circulatory system. It is easily accessible for experimental manipulation such as tumour cell engraftment or treatments effect. The CAM assay is a low-cost model that allows the growth of cancer cell lines on CAM and can be used to assess the efficacy of anticancer drugs, monitoring tumour growth. This assay is significantly faster than mice models, and the tumour grafts became easily vascularized, which enables tumour growth in fewer days than others models do. Nevertheless, the main disadvantages are that the *in vivo* experiments can only last 7 days to avoid the chicken to hatch the egg. Moreover, if the experiment would take longer, the approval of an animal experimental protocol will be required. These are the main reasons why this short treatment observation time.

On the other side, mice experiments are more reliable because mice are phylogenetically closer to humans, and thus it is possible to use orthotopic tumour engraftment. Also, you can monitor the effects of treatment in larger periods of time compared to CAM experiments.

That is the reason why these two techniques have been combined. CAM assay was used for screening a possible differential effect of lapatinib in BC with functionally impaired STX1A, and mice to determine STX1A down-regulation effects in tumour growth in a large period of time, orthotopically and within a species genetically closer to humans.

8.1. CHICKEN CHORIOALLANTOIC MEMBRANE ASSAY

For the CAM xenografts we used premium specific pathogen-free, fertile and embryonated chicken eggs supplied by Gibert farmers (Cambrils, Spain). The eggs were incubated in a humidified incubator at 37°C in 90° rotation every hour. At day 10 post-fertilisation a small window into the eggshell was made to move the egg air chamber and be able to inoculate the cells. BC or HNSCC cancer cells were diluted in a 1:1 relation Matrigel:PBS++ (supplemented with 1 mM CaCl₂ and 0.5 mM MgCl₂). 50 µl of cell suspension was inoculated per egg. The number of cells inoculated varied depending on the cell line: 3x10⁶ cell/egg for MDA-MB-453, 1x10⁶ for MDA-MB-231, 2x10⁶ for FaDu and SCC090 cell lines. Then the eggs were incubated without rotation. Also, if needed, the plasmid transfection was performed *in vitro* 24 hours prior to cells inoculation. When treatment was necessary, tumours were let to settle for 2 days and then treated with the treatment diluted in a final volume of 50 µl of PBS++. The number of days (5 or 6) the experiments lasted depended on the experiment, and it is specified in the results section. At the end, tumours were excised and weighted and then processed to RNA, protein extraction or fixed in 4% PFA for 20 min at 4°C (Figure 33). Then, fixed tumours were embedded in paraffin for further immunofluorohistochemistry studies.

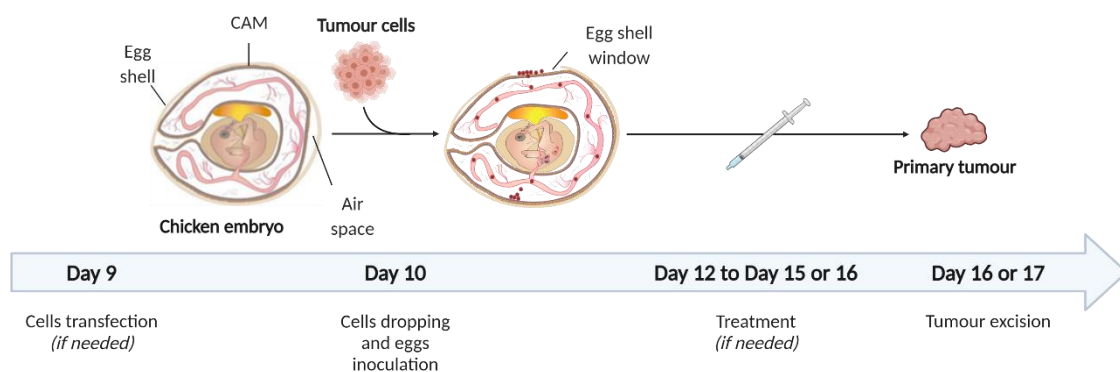


Figure 33 – Schematic representation of CAM *in vivo* model timings. Cell transfection takes place 24 hours before egg cell inoculation. At day 10 post-fertilisation cell dropping is into the CAM. If the tumours have to be treated, the treatment starts at day 12 post-fertilisation until day 15 (if the experiment is with transfected cells) or until day 16. Tumours are excised at day 16 post-fertilisation if the cells have been transfected or at day 17.

8.2. IMMUNODEFICIENT MICE XENOGRAFTS

Mice experiments were performed in accordance with the Catalan Government Animal Experimentation Ethics Committee regulations (Comitè Ètic d'Experimentació Animal (CEEAA)) and the UB ethics committee. Mice were purchased from Janvier Labs (France, Europe) and bred at the Medical School (UB) animal facilities laboratories. They were kept under specific pathogen-free conditions at constant ambient temperature (22°C-24°C) and humidity (30-50%). Mice had access to sterilized food and tap water *ad libitum*. After each experiment, mice were anesthetized and euthanized in accordance with institutional ethics commission guidelines.

Five-week-old female athymic nude Foxn1 *nu/nu* mice were obtained from Janvier Labs. 24 hours before starting the inoculation protocol, mice that had to be inoculated with BT-474 BC cells were surgically inserted with a 17 β -estradiol biodegradable carrier-binder (innovative research of America, #SE-121) 0,72 mg/pellet 60-day release. Before cell injection, mice were anesthetized and then BC cells (STX1A or their correspondent shRNA Non-Target) were inoculated orthotopically into one mammary fat pad of each animal (2×10^6 MDA-MB-453, 5×10^6 BT-474 or 5×10^5 BC cells). BC cells were inoculated in PBS:Matrigel (1:1) with a total volume of 150 μ l into the mouse mammary fat pad.

Tumour growth was measured twice a week with a digital calliper, and the tumour volume was calculated as $V = (D \cdot d^2) / 2$ (D: long diameter; d: short diameter). After 1 (BT-474), 2 (MDA-MB-231) and 3 months (MDA-MB-453) mice were sacrificed, and tumours were surgically recovered, measured, fixed in 4% PFA and embedded in paraffin for further immunofluorohistochemistry analysis.

9. STATISTICAL ANALYSIS AND GRAPHICAL REPRESENTATION

Data obtained during this thesis was analysed and graphed (plotted) by GraphPad Prism 8 and SPSS software. Depending on the type of the study, several statistical analyses have been applied. Each set of data has been analysed whether or not it followed a normal distribution by Kolmogorov-Smirnov test if $n > 50$ or by Shapiro-Wilk test if $n < 50$. If data followed a normal distribution it was analysed with Student *t*-test and if not, it was analysed by U Mann-Whitney test. Statistical analysis of more than two groups were analysed by one-way ANOVA when they had one variable or by two-way ANOVA when they had two variables. Correlation analyses were performed by Spearman correlation analysis, and Kaplan-Meier curves were analysed

using the log-rank test. Differences between two conditions were considered statistically significant when p-value were lower than 0.05. The p-values are marked on the graphs by asterisks: *, **, ***, ****. These values correspond to p-values smaller than 0.05, 0.01, 0.001 and 0.0001, respectively.

10. ADDITIONAL INFORMATION ON REAGENTS USED

Table 27 - Taqman® Gene Expression Assays (Applied Biosystems) probes.

Gene	Catalogue number	Gene	Catalogue number
BACTIN	Hs00946916_m1	STX1B	Hs01041315_m1
CCND1	Hs00765553_m1	STX2	Hs00181827_m1
CPLX1	Hs00362510_m1	STX3	Hs00188210_m1
EGFR	Hs01076088_m1	STX6	Hs01057343_m1
ERBB2 (HER2)	Hs01001580_m1	STX17	Hs00215603_m1
ERBB3 (HER3)	Hs00176538_m1	STXBP1	Hs01119036_m1
FOXO3	Hs00818121_m1	STXBP2	Hs00199557_m1
ITGA6	Hs01041011_m1	SYT1	Hs00194572_m1
MMP7	Hs00159163_m1	TWIST1	Hs00361186_m1
SNAI1	Hs00195591_m1	UNC13B	Hs01066405_m1
SNAI2	Hs00950344_m1	VIM	Hs05024057_m1
SNAP23	Hs01047496_m1	VAMP1	Hs04399177_m1
SNAP25	Hs00938962_m1	VAMP2	Hs00360269_m1
STX1A	Hs00270282_m1	VAMP4	Hs01002031_m1

Table 28 – List of primary antibodies and their applications.

Antibody	Provider	Catalogue number	Origin	Dilution	Application
α-Tubulin	Cell Signaling	3873S	Mouse	1/1000	WB
β-actin	Cell Signaling	3700	Mouse	1/1000	WB
AKT	Cell Signaling	9272	Rabbit	1/500	WB
pAKT (Ser473)	Cell Signaling	4060	Rabbit	1/500	WB
ERK	Cell Signaling	9192	Rabbit	1/500	WB
pERK (Thr202/Tyr204)	Cell Signaling	9101	Rabbit	1/500	WB
EGFR	Cell Signaling	54359	Rabbit	1/500 1/50	WB IP
pEGFR (Tyr1068)	Cell Signaling	2234	Rabbit	1/1000	WB
GAPDH	Cell Signaling	2118	Rabbit	1/1000	WB
HER2	Dako	A0485	Rabbit	1/200 1/100	IF IP
HER2	Cell Signaling	2243	Rabbit	1/500	WB
pHER2 (Tyr1221/1222)	Cell Signaling	2243	Rabbit	1/500	WB
Integrin- α6	Upstate	CBL4548P	Mouse	1/100	IF
Integrin- β1	Cell Signaling	9699	Rabbit	1/50	IF
Ki67	Dako	M7240	Mouse	1/200	IF
MMP2	Abcam	Ab37150	Rabbit	1/1000	WB
MMP3	Abcam	Ab18898	Sheep	1/1000	WB
MMP9	GeneTex	GTX100458	Rabbit	1/1000	WB
MMP14	Millipore	MAB3328	Mouse	1/1000	WB
MUNC18	Cell Signaling	13414	Rabbit	1/500	WB
SNAP-23	Synaptic Systems	111 203	Rabbit	1/500	WB
SNAP-25	Synaptic Systems	111 111	Mouse	1/500	WB
STX1A	Abcam	Ab41453	Rabbit	1/50	IF
STX1A	Synaptic Systems	110 111	Mouse	1/500	WB
Vimentin	Cell Signaling	5741	Rabbit	1/500	WB
Phalloidin	Cell Signaling	8953S		1/1000	IF

Table 29 - List of secondary antibodies and their applications.

Antibody	Provider	Catalogue number	Origin	Dilution	Application
Alexa Fluor 488 anti-mouse IgG	Invitrogen	A21121	Goat	1/500	IF
Alexa Fluor 488 anti-rabbit IgG	Invitrogen	A11034	Goat	1/500	IF
Alexa Fluor 555 anti-mouse IgG	Invitrogen	A21422	Goat	1/500	IF
Alexa Fluor 555 anti-rabbit IgG	Invitrogen	A21422	Goat	1/500	IF
Anti-sheep HRP conjugated	Invitrogen	618620	Rabbit	1/2500	WB
ECL Mouse IgG HRP-linked	GE Healthcare	NXA931	Sheep	1/2500	WB
ECL Rabbit IgG HRP-linked	GE Healthcare	NA934	Donkey	1/2500	WB

Table 30 – List of STX1A-related products.

Reagent	Provider	Catalogue number	Application
ON-TARGET plus Non-targeting pool	Dharmacon	D-001810-10-05	siRNA
ON-TARGET plus Human STX1A siRNA	Dharmacon	L-012677-00-0005	siRNA
TRCN0000065008 (shRNA8 STX1A LV particles)	Sigma-Aldrich	NM_004603.1-227s1c1	shRNA
TRCN0000065009 (shRNA9 STX1A LV particles)	Sigma-Aldrich	NM_004603.1-372s1c1	shRNA
MISSION [®] pLKO.1-neo-CMV-tGFP Non-Target shRNA control LV transduction particles	Sigma-Aldrich	SHC216V-1EA	shRNA
Cas9 plasmid	Addgene	52962	Plasmid
pLV[gRNA]-Puro-U6 (exon 2 customized)	VectorBuilder	VB200303-1067srt	gRNA plasmid
pLV[gRNA]-Puro-U6 (exon 6 customized)	VectorBuilder	VB200303-1133kmn	gRNA plasmid
Non-targeting control pLentiGuide-Puro	Addgene	52963	gRNA plasmid

Table 31 – List of reagents used and their application.

Reagent	Provider	Catalogue number	Application
17- β oestradiol biodegradable carrier-binder	Innovative research of America	5E-121	In vivo mice
24-mw transwell chambers	Merck	MCEP24H48	Transwell assay
Acetic acid	Sigma-Aldrich	A6283	Buffers
Acrylamide/Bis-Acrylamide solution (30%)	Panreac	A4983	Western blot
Agar	Sigma-Aldrich	A7002	Bacteria culture
Alexa Fluor™ 594 labelling kit	Invitrogen	A10239	Invadopodia formation
Amicon Ultra-4	Millipore	UFC801096	Zymogram
Ampicillin	Sigma-Aldrich	A5354	Bacteria selection
Annexin V-FITC apoptosis detection kit	eBiosciences	B45500FI	Apoptosis detection
APS	Sigma-Aldrich	A3678	Western blot
Bacto tryptone	Thermo Fisher	211705	Bacteria culture
Bacto-yeast extract	Thermo Fisher	212750	Bacteria culture
Blasticidin	Biochemica	A3784	Cell selection
Bovine Serum Albumin	Sigma-Aldrich	A7906	Cell culture/IF
Bromophenol blue	Sigma-Aldrich	B0126	Buffers
CaCl₂	Millipore	208291	Zymogram
Choleric toxin	Sigma	C8052	Cell culture
Coomassie brilliant blue	Bio-Rad	161-0400	Zymogram
Crystal violet 1% Aqueous Solution	Sigma-Aldrich	V5265	Cell staining
Dharmafect Transfection Reagent 1	Horizon	T-2001-01	Cell transfection
DMEM-F12 media	Gibco	21331020	Cell culture
DMSO	Sigma-Aldrich	D2650	Cell culture
ECL Western Blotting Detection Kit	GE Healthcare	RPN2209	Western blot
EDTA	Sigma-Aldrich	E6511	Buffers
EGF	Sigma	H2270	Cell treatment
Ethanol	Panreac	212899	Buffers
FBS (North America)	Gibco	16140071	Cell culture
FBS (South America)	Gibco	10270106	Cell culture
Fibronectin	Sigma-Aldrich	F4759	Cell culture
Forskolin	Sigma-Aldrich	F6886	Cell treatment
G-418	Enzo Life Sciences	ALX-380-013	Cell selection
Glutamax	Gibco	3550038	Cell culture

Reagent	Provider	Catalogue number	Application
Glutaraldehyde	Sigma-Aldrich	G5882	Invadopodia formation
Glycerol	Sigma-Aldrich	G9012	Buffers
Glycine	Panreac	A1067	Buffers
HCl	Panreac	257097	Buffers
High-Capacity cDNA Reverse Transcription Kit	Life Technologies	4368814	RNA analysis
Hoechst	Thermo Fisher	33342	IF
Horse serum	Gibco	16050130	Cell culture
Hydrocortisone	Sigma	H2270	Cell culture
Insulin	Sigma-Aldrich	I9278	Cell culture
Kanamycin	Sigma-Aldrich	K4000	Bacteria selection
KCl	Sigma-Aldrich	P9541	Buffers
KH ₂ PO ₄ monobasic	Sigma-Aldrich	1551139	Bacteria culture
Laminin	Sigma-Aldrich	L4544	Cell culture
Lapatinib	Sigma-Aldrich	SML2259	Cell treatment
Lenti-X concentration	Takara	631232	Virus production
Lipofectamine 3000	Invitrogen	L3000015	Cell transfection
Luria agar	Sigma-Aldrich	L3272	Bacteria culture
Matrigel	BD Bioscience	10429212	Cell culture
Methanol	Panreac	141091	Buffers
MMA	Sigma-Aldrich	M6891	Cell treatment
MTT reagent	Promega	G8081	Functional assays
Na ₂ PO ₄ dibasic	Sigma-Aldrich	S3264	Bacteria culture
Na ₃ VO ₄	Sigma-Aldrich	450243	Buffers
NaBH ₄	Sigma-Aldrich	45882	Invadopodia formation
NaCl	Sigma-Aldrich	S9888	Buffers
NaF	Sigma-Aldrich	201154	Buffers
NaN ₃	Sigma-Aldrich	S2002	Zymogram
Nonidet P-40	Sigma-Aldrich	74385	Buffers
Normal Goat Serum	Sigma-Aldrich	G9023	IF
PBS	Gibco	14190169	Cell culture
PBS/EDTA	Cultek	H3BE02-017	Cell culture
Penicillin - Streptomycin	Invitrogen	15140122	Cell culture
PFA	Sigma-Aldrich	1004968350	Fixation
PI/RNase staining buffer	BD Pharmigen	550825	Cell cycle
Pierce BCA Protein Assay Kit	Thermo Fisher	23225	Protein quantification
pMDLg/pPRE	Addgene	12251	Plasmid
Poly-L-lysine	Sigma-Aldrich	P4707	Invadopodia formation

Reagent	Provider	Catalogue number	Application
Ponceau staining	Sigma-Aldrich	P3504	Western blot
Prolong Gold Antifade Reagent	Thermo Fisher	P36930	IF
Protease inhibitor cocktail	Sigma-Aldrich	P8340	Buffers
Protein G Dynabeads	Bio-Rad	1614023	Immunoprecipitation
pSRV-Rev	Addgene	12253	Plasmid
Puromycin	Calbiochem	540411	Cell selection
QIAGEN plasmid mini kit	Qiagen	1212S	Plasmid purification
RPMI media	Gibco	31870074	Cell culture
SDS	Sigma-Aldrich	L3771	Buffers
siRNA buffer	Dharmacon	B-00200-UB-100	Cell transfection
Sodium deoxycolate	Sigma-Aldrich	30970	Buffers
Taqman Universal PCR Master Mix	Thermo Fisher	4367846	RNA analysis
TEMED	Sigma-Aldrich	T9281	Western blot
Trastuzumab	Selleckchem	A2007	Cell treatment
Tris base	Panreac	2264	Buffers
Trisodium citrate dihydrate	Sigma-Aldrich	1006448	IF
TRItidy G	Panreac	A4051	RNA analysis
Triton X-100	Sigma-Aldrich	T8787	Buffers
Trypsin-EDTA 25%	Gibco	2520072	Cell culture
TSA	Selleckchem	S1045	Cell treatment
Tween-20	Sigma-Aldrich	P1379	Buffers
Xylene	Panreac	131769	IF
β -mercaptoethanol	Millipore	4444203	Buffers

Syntaxin-1A, a synaptic related protein in breast and head and neck cancer progression and prognosis

RESULTS

Syntaxin-1A, a synaptic related protein in breast and head and neck cancer progression and prognosis

1. SYNTAXIN-1A IN BREAST CANCER AND HEAD AND NECK CANCER PATIENT DATABASES

In 2016, an article published by our research group stated that 6 neurogenes, differentially expressed among BC subtypes, had a prognostic value for BC patients. Among them, *STX1A* was overexpressed in HER2-positive BC subtype (HER2-enriched and luminal B) in comparison to HER2-negative BC subtype (luminal A and basal). Moreover, *STX1A* expression analysis from GOBO BC patient's database showed that poorer prognosis of the patients was associated with high *STX1A* expression in all BC subtypes, and specifically into HER2-enriched and luminal B BC subtypes.

Considering all published results, other public patients databases was used to further confirm the published results and to determine if *STX1A* expression correlated with other clinical cancer markers. To do that it was used TNM plot, a public database which compares the expression of a gene of interest in healthy tissue, tumour and metastasis (247). Another public database, METABRIC (227,228) was used to obtain clinical data from long-term follow-up BC patients and also gene expression profiles of their breast tumours. Moreover, Kaplan Meier plotter database (248) was analysed to obtain data from metastases in BC patients. To study HNSCC patients it was looked TCGA, another public database, which enabled us to download clinical data and some gene expression information of HNSCC tumours. Also thanks to a collaboration with Dr. Vilaseca and Dr. Avilés otorhinolaryngologists from Hospital Clínic de Barcelona and Dr. León and Dr. Camacho otorhinolaryngologists Hospital de la Santa Creu i Sant Pau de Barcelona it was possible to gain access to HNSCC samples where it was possible to analyse gene expression patterns of genes of interest in several cohorts.

1.1. SYNTAXIN-1A IN ALL BREAST CANCER SUBTYPES

1.1.1. SYNTAXIN-1A IS DIFFERENTIALLY EXPRESSED AMONGST BC SUBTYPES AND OVEREXPRESSED IN HER2-POSITIVE PATIENTS

First of all, considering that it was not known if *STX1A* expression was upregulated in comparison to healthy tissues, its expression was compared between normal breast tissue and tumour or metastasis in the TNM plot database. The analysis of RNA-seq data of the particular *STX1A* gene resulted in an up-regulation of *STX1A* expression in tumour samples in comparison to healthy ones (*Figure 34A*). Also, metastasis samples expressed higher levels of *STX1A* in comparison to healthy tissues even though the number of samples were very low (*Figure 34A*).

Then, to determine if the data obtained previously in GOBO patients' database (104) was comparable with data obtained in other BC patient cohorts, the public BC database METABRIC (227,228) was analysed. First, it was determined if the METABRIC BC cohort was representative of the frequency of BC subtypes in the population. BC patients with "normal-like" BC subtype were considered as basal (*Annex figure 2A*). The frequency of BC subtypes was similar to the ones described in the literature (198), validating this patients' cohort for further studies.

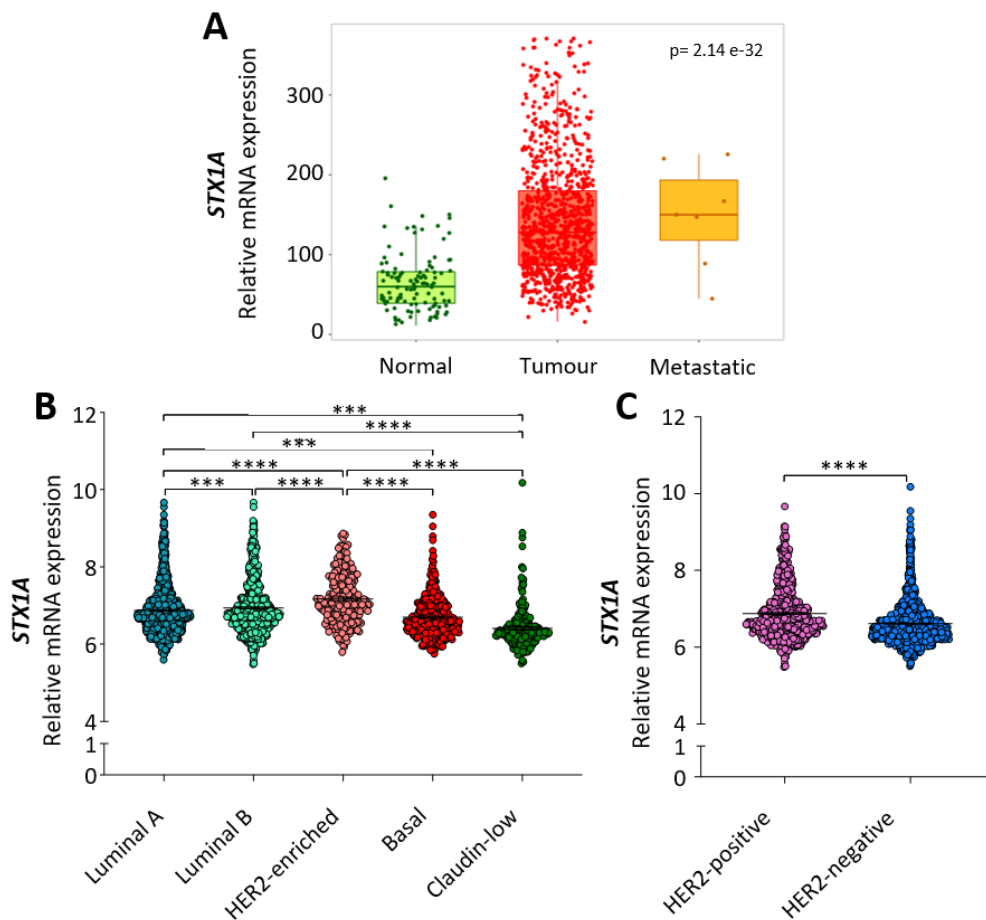


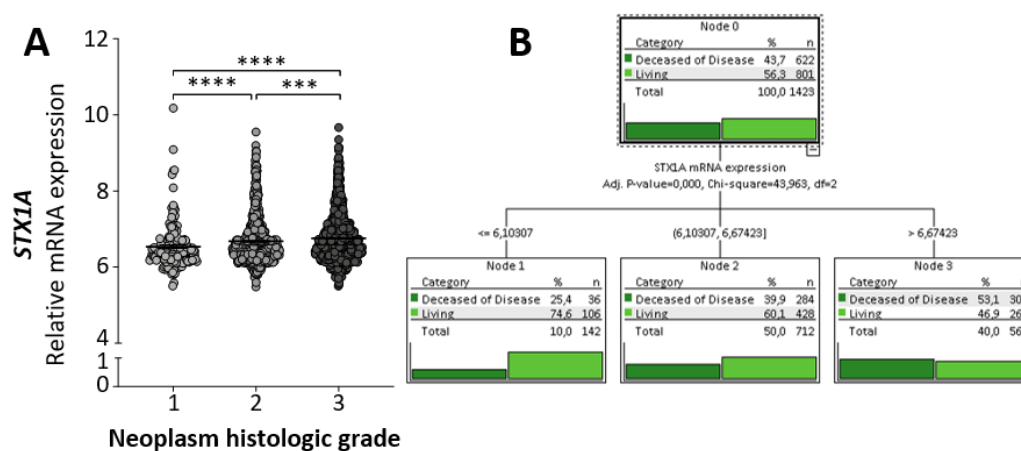
Figure 34 - *STX1A* is overexpressed in breast tumours, its expression differentially expressed amongst BC subtypes and overexpressed in HER2-positive patients. (A) *STX1A* mRNA expression in healthy breast tissue, tumour and metastatic BC expressed as normalized data from RNA-seq data. (B) Relative expression of *STX1A* mRNA among different BC subtypes. (C) Relative expression of *STX1A* mRNA between HER2-positive (HER2-enriched and luminal B) and HER2-negative (luminal A, basal and claudin-low) BC subgroups. Statistical analysis was performed using the Kruskal Wallis test (B) and U-Mann Whitney test (C). *** $p < 0.001$, **** $p < 0.0001$.

Then, *STX1A* expression among BC subtypes was assessed (*Figure 34B*). The results clearly showed that the highest expression of *STX1A* was in HER2-enriched BC subtype (M = 7.171, SEM = 0.044), followed by luminal B (M = 6.936, SEM = 0.025), luminal A (M=6.871, SEM = 0.019) basal (M = 6.700, SEM = 0.029) and claudin-low (M = 6.410, SEM = 0.040) BC subtypes.

Then, to replicate the results published in Fernández-Nogueira *et al.* (104) it was distinguished between HER2-positive BC tumours (HER2-enriched and luminal B) and HER2-negative BC tumours (luminal A, basal and claudin-low). The analysis of *STX1A* expression between both BC subgroups (Figure 34C) showed that HER2-positive BC tumours (M = 6.876, SEM = 0.03) expressed higher *STX1A* mRNA levels than HER2-negative ones (M = 6.612, SEM = 0.02). It is important to note that in HER2-positive BC subgroup all luminal B tumours were included, even though not all luminal B cancers overexpress HER2 receptor. This criterion was followed to replicate previous results obtained by Fernández-Nogueira *et al.* where no distinction between luminal B HER2-positive and luminal B HER2-negative was considered, and also because METABRIC database does not specify if luminal B tumours overexpress HER2 receptor or not. This analysis confirmed what was published in 2016 by which *STX1A* is overexpressed in HER2-positive in comparison to HER2-negative BC subtypes.

1.1.2. *SYNTAXIN-1A* EXPRESSION CORRELATES WITH WORSE PROGNOSIS AND TUMOUR PROGRESSION MARKERS

METABRIC BC cohort also included clinical data of BC patients. That fact made it possible to analyse *STX1A* expression in relation to several cancer progression parameters. First, it was analysed whether *STX1A* expression correlated with BC neoplasm histologic grade (graded from 1 to 3 where 1 is the less histologically aggressive and 3 is the most aggressive). The results determined that the higher the histologic grade, the higher the *STX1A* mRNA expression (grade 1: M = 6.535, SEM = 0.046; grade 2: M = 6.680, SEM = 0.022; grade 3: M = 6.759, SEM = 0.021) (Figure 35A).



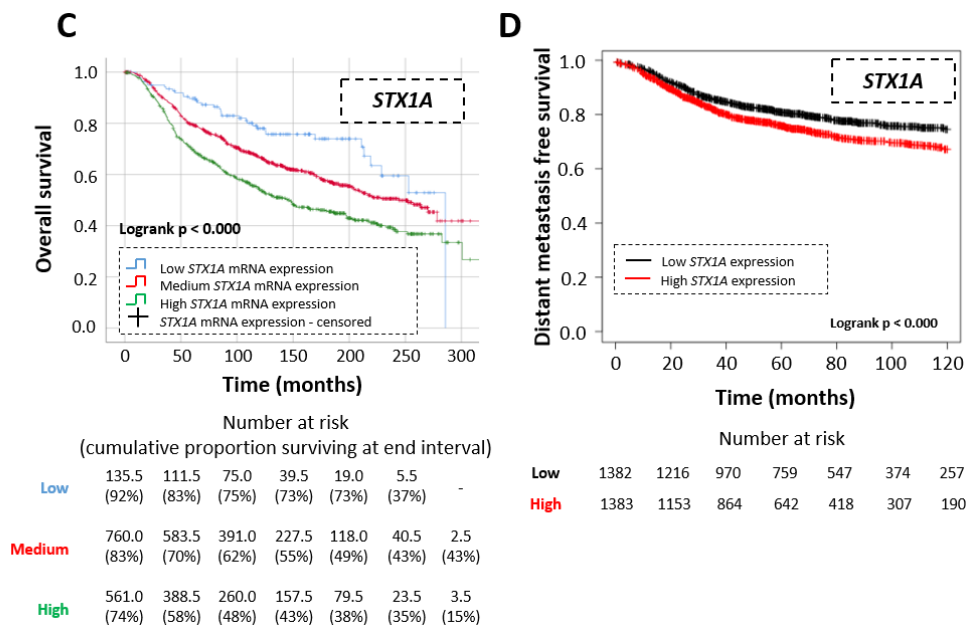


Figure 35 – Aggressive tumours overexpress *STX1A* and higher expression of *STX1A* is related to poor overall and distant metastasis free survival. (A) Graphical representation of relative *STX1A* mRNA expression grouped into different neoplasm histologic grade. (B) Decision tree diagram that shows how relative *STX1A* mRNA expression is grouped according to the patient survival status (deceased of the disease, dark green and living BC patients, light green). (C) On the top, overall survival Kaplan-Meier curve of BC tumours grouped according to *STX1A* expression. On the bottom survival table where the number at risk of BC patients and the cumulative proportion surviving at the end of the interval (in parenthesis) is shown. (D) Distant-metastasis free survival of BC patients grouped according to *STX1A* expression. Statistical analysis was performed by U-Mann-Whitney test (A), Chi-square test (B) and Logrank (C and D). *** $p < 0.001$, **** $p < 0.000$.

Next step was to classify BC tumours considering *STX1A* expression and the survival status of the patients. To do so, the decision tree algorithm which grouped *STX1A* mRNA expression according to the vital status of the patient (deceased of disease or living) at the end of the study was used. The output of the decision tree algorithm ($p > 0.000$) resulted in three statistically different groups: low *STX1A* mRNA expression (≤ 6.103), medium *STX1A* mRNA expression (between 6.103 and 6.674) and high *STX1A* expression (> 6.674) (Figure 35B).

Then, once these three groups were obtained, it was analysed clinical tumour parameters such as tumour volume, Nottingham prognostic index and number of mutations per tumour. The analysis of tumour volume determined that tumours within the group of high *STX1A* expression were the biggest ones ($M = 27.590$, $SEM = 0.563$) in comparison to the medium *STX1A* expression group ($M = 24.080$, $SEM = 0.430$) and the low *STX1A* expression group ($M = 24.200$, $SEM = 0.884$) (Annex figure 2B). Nottingham prognostic index analysis determined that tumours within the *STX1A* high expression group have the highest Nottingham prognostic index ($M = 4.142$, $SEM = 0.041$) in comparison to the middle and low *STX1A* expression group

($M = 3.969$, $SEM = 0.034$ and $M = 4.003$, $SEM = 0.090$, respectively) (*Annex figure 2C*). Surprisingly, analysis of mutation number per tumour showed that tumours within the group of low *STX1A* expression were the ones with a greater number of mutations per tumour ($M = 6.048$, $SEM = 0.135$), gradually decreasing in the medium ($M = 5.398$, $SEM = 0.107$) and in the highest *STX1A* expression groups ($M = 5.000$, $SEM = 0.335$) (*Annex figure 2D*).

It was used these *STX1A* mRNA classification to analyse if *STX1A* can become a prognostic factor considering the specific overall survival of the patients. The Kaplan-Meier results are shown in *Figure 35C*, where it is proved that higher expression of *STX1A* confer worse specific overall survival at 25 years (300 months) than medium or low levels of *STX1A* in BC patients ($p > 0.000$). Moreover, low levels of *STX1A* also correlated with better overall survival compared to patients with medium *STX1A* levels. More in detail, the difference between *STX1A* subgroups was clearly seen around 200 months where BC patients specific overall survival was less than 50% in medium and high *STX1A* expression group, whereas there were already more than 50% in the low *STX1A* expression group. Also, a correlation of *STX1A* expression was seen in distant-metastasis free survival. The Kaplan-Meier plotter from stratified two groups of BC patients (low and high) and the analysis resulted in a lower distant metastasis free period in patients with high levels of *STX1A* (*Figure 35D*).

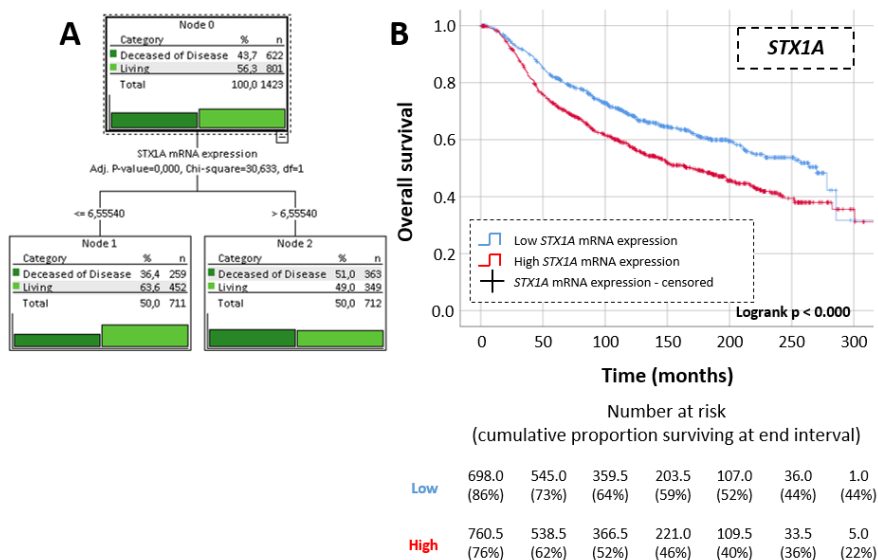


Figure 36 – Tumours with high *STX1A* have a lower overall survival. (A) Decision tree diagram that shows how relative *STX1A* mRNA expression is grouped according to the patient survival status (Deceased of the disease, dark green and living BC patients, light green). (B) On the top, overall survival Kaplan-Meier curve of BC tumours grouped according to *STX1A* expression. On the bottom survival table where the number at risk of BC patients and the cumulative proportion surviving at the end of the interval (in parenthesis) is shown. Statistical analysis was performed by Chi-square test (A) and Logrank test (B).

Finally, with the objective to facilitate further comparisons between STX1A expression and other SNARE genes, all the patients were re-grouped in two groups, high and low STX1A mRNA expression (*Figure 36A*). The previous analysis with the several clinical parameters were repeated and similar results were obtained (*Annex figure 3A-Annex figure 3C*), above all, tumours with high expression of STX1A have a decreased overall survival in comparison to tumour with low levels of the neurogene (*Figure 34B*).

1.1.3. STX1A EXPRESSION CORRELATES WITH THE EXPRESSION OF OTHER SYNTAXIN AND SNARE-RELATED GENES AND IMPROVES STX1A PROGNOSTIC VALUE

STX1A is a member of the Syntaxin family which at the same time is included in the SNARE family of proteins, this family includes SNAREs located into the cell membrane (t-SNARE) as STX1A, SNAREs located into cell vesicles (v-SNAREs) and soluble SNAREs proteins. In a cell, SNARE proteins do not work alone, they need other SNARE partners to form the SNARE complex to be functional. Having seen that *STX1A* expression correlates with poorer overall survival and worse clinical tumour progression parameters, the next step was to interrogate if other SNARE proteins, which work as *STX1A* partners, could also be good markers, alone or together with *STX1A*.

To do so, first of all it was analysed if there was a correlation in the mRNA expression of Syntaxin family members and other SNARE proteins (*Annex table 1*). The Spearman correlation analysis determined that other members of Syntaxin family such as *STX3* and *STX6*, the t-SNARE *SNAP-25*, and the soluble SNAREs *CPLX1*, *MUNC18-1*, *STXBP2* and *MUNC13* positively correlated with *STX1A* mRNA expression. Also, the t-SNARE *SNAP-23* and the v-SNAREs *VAMP-4* and *SYT1* negatively correlated with *STX1A* mRNA expression, whereas *STX1B*, *STX2*, *STX17*, *VAMP-1* and *VAMP-2* showed no correlation at all. It was also checked if there was a differential expression of a particular SNARE based on the low and high expression levels of *STX1A* (*Annex table 1*). This analysis showed that all SNARE genes that positively correlated with *STX1A* were highly expressed in high *STX1A* tumours. *SNAP-23* and *VAMP-4*, which negatively correlated with *STX1A*, showed higher expression in tumours with low *STX1A* expression, while no differences in *SYT1* were observed. It was also interesting to see, if as *STX1A*, these SNARE genes were differentially expressed based on HER2 status (*Annex table 1*). The results showed that *STX3*, *STX2*, *VAMP-2*, *VAMP-4*, *SYT1*, *STXBP2* and *MUNC13* were

overexpressed in HER2-positive BC subtypes, whereas *SNAP-23*, *SNAP-25*, *VAMP-1* and *MUNC18-1* were overexpressed in HER2-negative tumours.

Then, it was analysed if these SNAREs by themselves were able to predict the overall survival of the patients. First, each SNARE was subgrouped considering its tumour expression and their patient's vital status by a decision tree algorithm as previously done with *STX1A* (*data not shown*). Then a Kaplan-Meier curve for each SNARE gene was performed. All the correlation data is shown summarized in *Table 32*. Briefly, patients which tumours expressed high levels of *STX3* and *STX6* had a poor overall survival (*Figure 37A and Figure 37B, respectively*). Otherwise, low levels of *SNAP-23*, *VAMP-2* or *CPLX1* correlated with a poorer overall survival (*Figure 37C-Figure 37E*). No statistical difference was seen in the other SNAREs (*Table 32*).

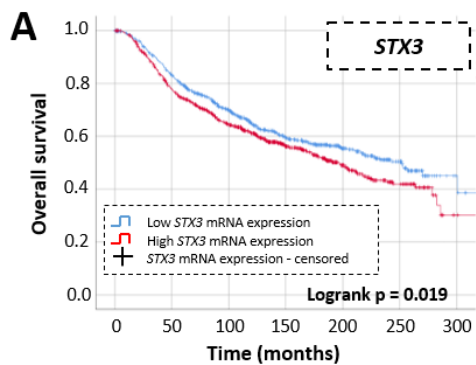
Finally, it was analysed if the expression of these SNARE genes could increase the prognostic value of *STX1A* expression. The pairings between SNAREs genes and *STX1A* were considered according to its correlation: if it was a positive correlation, high *STX1A* expression subgroup was paired with the other SNARE high expression subgroup, whereas low *STX1A* expression was paired with low SNARE expression group. On the other hand, if it was an inverse correlation, high expression of *STX1A* group was paired to low SNARE expression group, and inversely. The only exception was *CPLX1* gene, which considering that low expression of *CPLX1* correlated with poorer overall survival of BC patients, it was analysed the prognostic value of low *STX1A* and high *CPLX1* expression levels and inversely. The results are summarized in *Table 32*, *Figure 38* and *Annex figure 4*. Briefly, it was found that there were differences in the overall survival of BC patients in all the cases analysed except for the combination with *SNAP-25*. More in depth, even though the vast majority were statistically significant, only a few increased the prognosis in overall survival that already had *STX1A* alone (*Figure 36B*). The combination of *STX1A* and *STX1B* seemed to classify and to predict better the overall survival of the patients. As it can be seen in the Kaplan Meier graph (*Figure 38A*) *STX1A* combined with *STX1B* predicted better the overall survival of the patients between 100 and 250 months in comparison to *STX1A* alone (*Figure 36B*). Other two SNARE genes helped to increase the prognostic value of *STX1A*, *VAMP-2* and *CPLX1*. Low expression of *STX1A* and high expression of *VAMP-2* or *CPLX1* showed better overall survival than high *STX1A* and low *VAMP-2* or *CPLX1* expression (*Figure 38B and Figure 38C, respectively*). In these cases there were better prognostic value at the initial of the diagnosis to 100 months of the diagnosis

in comparison to *STX1A* marker alone (Figure 36B). Altogether these data show that, as *STX1A*, their SNARE partners could increase *STX1A* prognostic value.

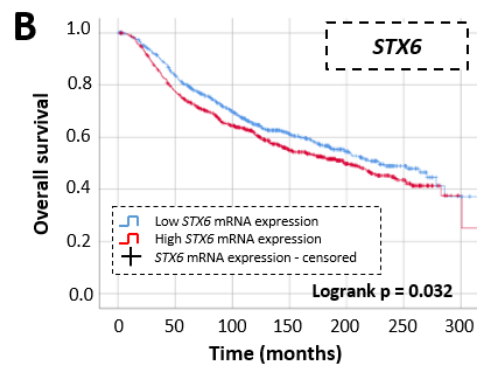
Table 32 – Summary of the study of other Syntaxins and SNARE genes in BC patients. Table shows the overall survival between tumours expressing high and low levels of *STX1A*, and the overall survival of other SNARE proteins together with *STX1A*. Also shows the distant metastasis free survival of syntaxins family and SNARE genes.

		Overall survival	Overall survival together with <i>STX1A</i> overall survival	Distant metastasis free survival
Syntaxin family	<i>STX1B</i>	There is no correlation (p = 0.056)	High <i>STX1A</i> and <i>STX1B</i> expression correlates with poor overall survival (p < 0.037)	There is no correlation (p = 0.390)
	<i>STX2</i>	There is no correlation (p = 0.464)	High <i>STX1A</i> and <i>STX2</i> expression correlates with poor overall survival (p < 0.000)	High <i>STX2</i> expression correlates with poor distant metastasis free survival (p < 0.000)
	<i>STX3</i>	High <i>STX3</i> expression correlates with poor overall survival (p = 0.019)	High <i>STX1A</i> and <i>STX3</i> expression correlates with poor overall survival (p < 0.000)	There is no correlation (p = 0.670)
	<i>STX6</i>	High <i>STX6</i> expression correlates with poor overall survival (p = 0.032)	High <i>STX1A</i> and <i>STX6</i> expression correlates with poor overall survival (p < 0.000)	High <i>STX6</i> expression correlates with poor distant metastasis free survival (p < 0.000)
	<i>STX17</i>	There is no correlation (p = 0.217)	High <i>STX1A</i> expression and low <i>STX17</i> expression correlates with poor overall survival (p < 0.000)	There is no correlation (p = 0.710)
t-SNAREs	<i>SNAP-23</i>	Low <i>SNAP-23</i> expression correlates with poor overall survival (p < 0.000)	High <i>STX1A</i> expression and low <i>SNAP-23</i> expression correlates with poor overall survival (p < 0.000)	There is no correlation (p = 0.088)
	<i>SNAP-25</i>	There is no correlation (p = 0.446)	There is no correlation (p = 0.446)	There is no correlation (p = 0.087)
v-SNAREs	<i>VAMP-1</i>	There is no correlation (p = 0.053)	High <i>STX1A</i> expression and low <i>VAMP-1</i> expression correlates with poor overall survival (p = 0.029)	There is no correlation (p = 0.037)
	<i>VAMP-2</i>	Low <i>VAMP-2</i> expression correlates with poor overall survival (p < 0.000)	High <i>STX1A</i> expression and low <i>VAMP-2</i> expression correlates with poor overall survival (p < 0.000)	Low <i>VAMP-2</i> expression correlates with poor distant metastasis free survival (p < 0.000)

	Overall survival	Overall survival together with <i>STX1A</i> overall survival	Distant metastasis free survival	
<i>VAMP-4</i>	There is no correlation (p = 0.102)	High <i>STX1A</i> expression and low <i>VAMP-4</i> expression correlates with poor overall survival (p < 0.000)	No data	
<i>SYT1</i>	There is no correlation (p = 0.084)	High <i>STX1A</i> expression and low <i>SYT1</i> expression correlates with poor overall survival (p < 0.000)	High <i>SYT1</i> expression correlates with poor distant metastasis free survival (p = 0.040)	
Soluble SNARES	<i>CPLX1</i>	Low <i>CPLX1</i> expression correlates with poor overall survival (p = 0.016)	No data	
	<i>MUNC18-1</i>	There is no correlation (p = 0.216)	There is no correlation (p = 0.290)	
	<i>STXBP2</i>	There is no correlation (p = 0.274)	High <i>STX1A</i> and <i>STXBP2</i> expression correlates with poor overall survival (p > 0.000)	Low <i>STXBP2</i> expression correlates with poor distant metastasis free survival (p = 0.004)
	<i>MUNC13</i>	There is no correlation (p = 0.221)	High <i>STX1A</i> and <i>MUNC13</i> expression correlates with poor overall survival (p < 0.000)	There is no correlation (p = 0.300)



	699.0	536.0	365.5	217.0	116.5	39.5	4.0
Low	(83 %)	(70%)	(85%)	(55%)	(50%)	(44%)	(33%)
High	775.5	544.5	358.5	206.0	100.0	30.0	2.0
	(78%)	(64%)	(56%)	(49%)	(42%)	(36%)	(18%)



	692.5	525.5	341.5	197.5	98.0	32.5	4.0
Low	(84 %)	(70%)	(61%)	(54%)	(48%)	(41%)	(31%)
High	762.0	555.0	382.5	225.5	118.5	37.0	2.0
	(78%)	(64%)	(55%)	(50%)	(44%)	(39%)	(20%)

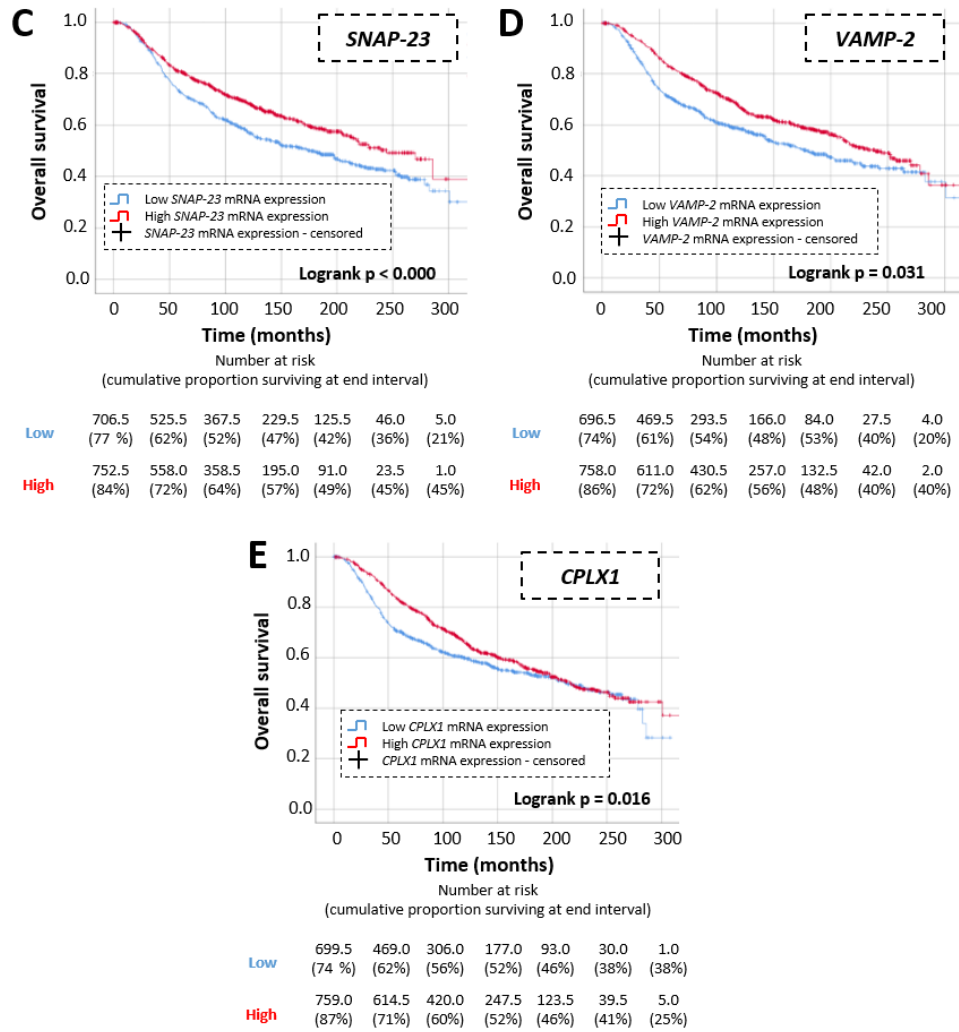
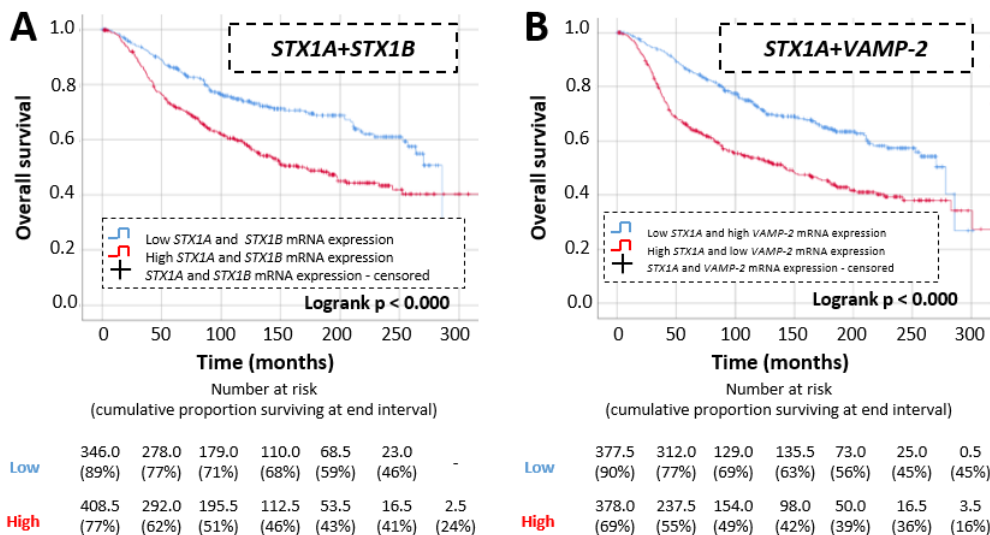


Figure 37 – Syntaxin family and SNARE-related gene expression correlates with BC overall survival. On the top of each figure, overall survival Kaplan-Meier curve of BC tumours grouped according to *STX3* (A), *STX6* (B), *SNAP-23* (C), *VAMP-2* (D), *CPLX1* (E) expression, classified according to the decision tree algorithm. On the bottom of each figure, survival table where the number at risk of BC patients and the cumulative proportion surviving at the end of the interval (in parenthesis) is shown. Statistical analysis was performed using the Logrank test.



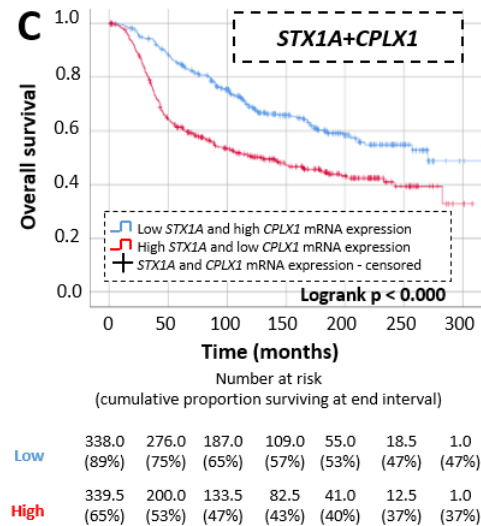
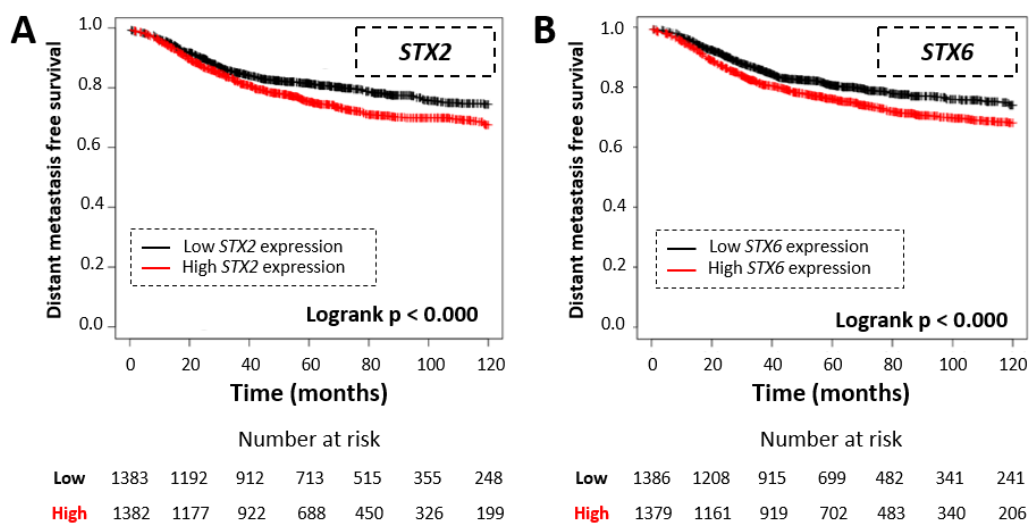


Figure 38 – *STX1A* together with Syntaxin family and SNARE related genes increases the overall survival prediction value in BC patients. On the top of each figure, overall survival Kaplan-Meier curve of BC tumours grouped according to *STX1A* and *STX1B* (A), *VAMP-2* (B), and *CPLX1* (C) expression, classified according to the decision tree algorithm. On the bottom of each figure, survival table where is shown the number at risk of BC patients and the cumulative proportion surviving at the end of the interval in parenthesis. Statistical analysis was performed using Logrank test.

Finally, it was looked for if the expression of these Syntaxin and SNARE-related genes correlated with distant metastasis free survival, using the Kaplan Meier plotter database. It resulted that high expression of *STX2* (Figure 39A), *STX6* (Figure 39B) and *SYT1* (Figure 39E) correlated with a shorter distant metastasis free period, whereas low expression of *VAMP-2* (Figure 39C) and *STXBP2* (Figure 39D) also correlated with a lower distant metastasis free period (Table 32).



Syntaxin-1A, a synaptic related protein in breast and head and neck cancer progression and prognosis

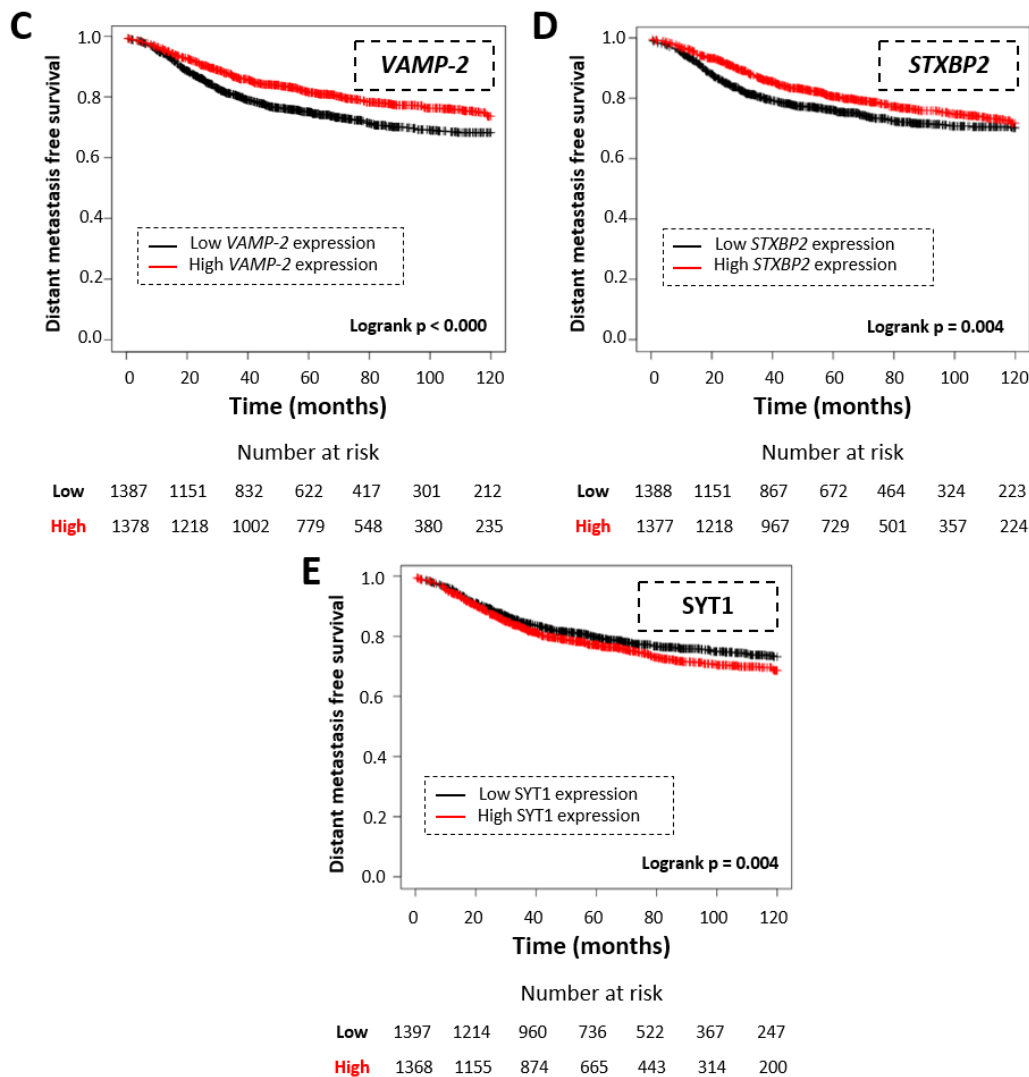


Figure 39 – Syntaxin and SNARE related genes correlate are able to predict distant metastasis free survival period. On the top of each figure, distant metastasis free survival Kaplan-Meier curve from Kaplan Meier plotter database of BC tumours grouped according low or high levels of *STX2* (A), *STX6* (B), *VAMP-2* (C), *STXBP2* (D) and *SYT1* (E). On the bottom of each figure, number at risk of BC patients. Statistical analysis was performed using the Logrank test.

1.2. SYNTAXIN-1A IN HER2-POSITIVE BREAST CANCER SUBTYPES

1.2.1. SYNTAXIN-1A EXPRESSION CORRELATES WITH WORSE PROGNOSIS IN HER2-POSITIVE TUMOURS

Considering that *STX1A* is overexpressed in HER2-positive BC subtype (HER2-enriched and luminal B) in comparison to HER2-negatives (luminal A, basal and claudin-low), it was continued by determining if *STX1A* could also work as a specific biomarker for HER2-positive BC subtypes.

First of all, it was analysed *STX1A* expression in the different neoplasm histologic grades (*Annex figure 5A*). No differences of *STX1A* expression were found among them. Then, as it was previously did, patient's tumours were grouped into high and low *STX1A* expression using the decision tree algorithm (*Annex figure 5B*). It resulted in a classification without statistical differences within *STX1A* groups. Even though it was still useful, considering that the main purpose of this stratification was to obtain two different groups. Analysis of tumour volume and Nottingham prognostic index did not show any difference among *STX1A*^{HIGH} and *STX1A*^{LOW} tumours (*Annex figure 5C and Annex figure 5D*). However, analysis of number of mutations per tumour resulted in an increase of mutations in tumours with high levels of *STX1A* in comparison to tumours with low levels of *STX1A* (M = 6.327, SEM = 0.231 and M = 5.831, SEM = 0.138, respectively) (*Annex figure 5E*), similarly to results found when considering all BC subtypes. Finally, it was analysed if the groups established were able to predict overall survival of the HER2-positive BC patients (*Figure 40A*). The analysis confirmed what described when analysed the outcome in all BC subtypes: there was a poorer overall survival in patients expressing high levels of *STX1A* in comparison to patients expressing low levels of *STX1A* (p = 0.043). Finally, it was analysed the distant metastasis free survival of HER2-positive BC patients using the Kaplan Meier plotter database. It resulted that, as it was previously seen in all BC patients, high levels of *STX1A* conferred a worse distant metastasis free survival in HER2-positive BC patients (*Figure 40B*).

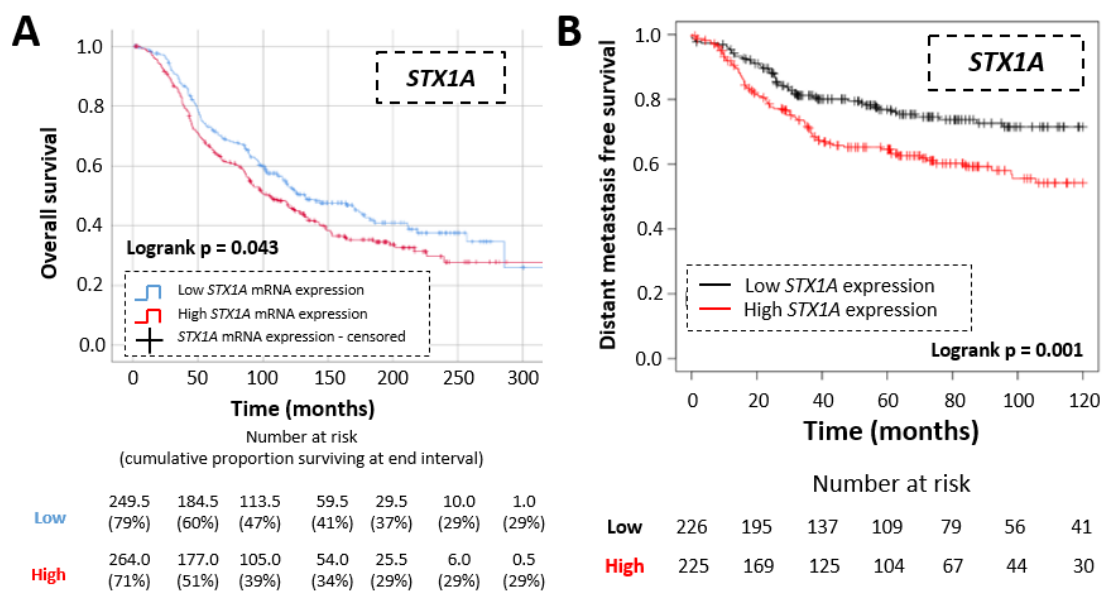


Figure 40 – HER2-positive patients with BC tumours with high *STX1A* expression have worse overall and distant metastasis free survival. (A) On the top, Kaplan-Meier plot representing the overall survival of HER2-positive BC patients considering tumours with low and high *STX1A* expression. On the bottom, number of HER2-positive BC patients at risk and in parenthesis the cumulative proportion surviving at the end of each interval. (B) On the top, Kaplan-Meier plot representing the distant metastasis free survival of HER2-positive BC patients considering tumours with low and high

STX1A expression. On the bottom, number of HER2-positive BC patients at risk. Statistical analysis was performed using the Logrank test.

1.2.2. SYNTAXIN-1A EXPRESSION CORRELATES WITH THE EXPRESSION OF OTHER SNARES AND EGFR/HER RECEPTORS GENES IN HER2-POSITIVE TUMOURS

It was also analysed, as it was previously did, if there was any correlation with other SNARE genes. Moreover, considering that BC tumours were split according to the expression of HER2, it was also interesting to determine if there was any type of relationship with the expression of genes encoding for the EGFR/HER family of receptors. Overall, the results presented in [Annex table 2](#) demonstrated that there was a direct correlation with *STX2* and *STX3* and SNARE genes *SNAP-25*, *MUNC18-1* and *MUNC13* and an inverse correlation among *STX1A* and *SNAP-23*, *VAMP-2*, *VAMP-4* and *SYT1*. Focusing on EGFR/HER family of receptors, expression of *STX1A* correlated positively with *EGFR*, *HER2* and *HER4*. Then, HER2-positive tumours were grouped according to *STX1A* expression levels to check if there was a differential expression of these SNARE and receptors between both subgroups ([Annex table 2](#)). The results stated that there was a higher expression of *SNAP-23*, *VAMP-2*, *VAMP-4*, *SYT1* and *HER2* in tumours that expressed low levels of *STX1A*. Otherwise, there was a higher expression of *STX2*, *STX3*, *SNAP-25*, *VAMP-1*, *MUNC18-1*, *EGFR*, *HER2* and *HER4* in tumours that expressed higher levels of *STX1A*.

Then, it was analysed if the expression of other members of the Syntaxin, the SNAREs and EGFR/HER receptors families could affect the overall survival of the BC patients by themselves ([Table 33](#)). Lower expression of *VAMP-2*, *VAMP-4* or *MUNC13* correlated with a poorer overall survival of the HER2-positive BC patients ([Figure 41B-Figure 41D](#)). Conversely, higher expression of *VAMP-1*, *EGFR* and *HER4* correlated with a worse overall survival ([Figure 41A](#), [Figure 41E and Figure 41F](#)).

Table 33 – Summary of the study of other Syntaxins, SNARE and EGFR/HER family receptor genes in HER2-positive BC patients. Overall survival of SNARE and EGFR/HER family receptor genes in HER2-positive BC tumours by themselves or adding *STX1A* and distant metastasis free survival of syntaxins family, SNARE and EGFR/HER family receptor genes.

		Overall survival	Overall survival together with <i>STX1A</i>	Distant metastasis free survival
Syntaxin family	<i>STX1B</i>	There is no correlation (p = 0.076)	High <i>STX1A</i> and <i>STX1B</i> expression correlate with poor overall survival (p = 0.006)	There is no correlation (p = 0.036)
	<i>STX2</i>	There is no correlation (p = 0.076)	There is no correlation (p = 0.150)	There is no correlation (p = 0.840)
	<i>STX3</i>	There is no correlation (p = 0.170)	High <i>STX1A</i> and <i>STX3</i> expression correlate with poor overall survival (p = 0.034)	There is no correlation (p = 0.540)
	<i>STX6</i>	There is no correlation (p = 0.399)	There is no correlation (p = 0.052)	There is no correlation (p = 0.730)
	<i>STX17</i>	There is no correlation (p = 0.415)	There is no correlation (p = 0.057)	There is no correlation (p = 0.270)
t-SNAREs	<i>SNAP-23</i>	There is no correlation (p = 0.138)	There is no correlation (p = 0.065)	There is no correlation (p = 0.280)
	<i>SNAP-25</i>	There is no correlation (p = 0.765)	There is no correlation (p = 0.243)	There is no correlation (p = 0.160)
v-SNAREs	<i>VAMP-1</i>	High <i>VAMP-1</i> expression correlates with poor overall survival (p = 0.004)	High <i>STX1A</i> and <i>VAMP-1</i> expression correlate with poor overall survival (p = 0.013)	There is no correlation (p = 0.760)
	<i>VAMP-2</i>	Low <i>VAMP-2</i> expression correlates with poor overall survival (p = 0.010)	High <i>STX1A</i> expression and low <i>VAMP-2</i> expression correlate with poor overall survival (p = 0.025)	Low <i>VAMP-2</i> expression correlates with poor metastasis free survival (p = 0.032)
v-SNAREs	<i>VAMP-4</i>	Low <i>VAMP-4</i> expression correlates with poor overall survival (p = 0.010)	High <i>STX1A</i> expression and low <i>VAMP-4</i> expression correlate with poor overall survival (p = 0.005)	No data
	<i>SYT1</i>	There is no correlation (p = 0.076)	High <i>STX1A</i> expression and low <i>SYT1</i> expression correlate with poor overall survival (p = 0.013)	There is no correlation (p = 0.110)

		Overall survival	Overall survival together with <i>STX1A</i>	Distant metastasis free survival
Soluble SNAREs	<i>CPLX1</i>	There is no correlation (p = 0.111)	High <i>STX1A</i> expression and low <i>CPLX1</i> expression correlate with poor overall survival (p = 0.032)	No data
	<i>MUNC18-1</i>	There is no correlation (p = 0.909)	There is no correlation (p = 0.148)	There is no correlation (p = 0.200)
	<i>STXBP2</i>	There is no correlation (p = 0.347)	High <i>STX1A</i> expression and low <i>STXBP2</i> expression correlate with poor overall survival (p = 0.032)	There is no correlation (p = 0.390)
	<i>MUNC13</i>	Low <i>MUNC13</i> expression correlates with poor overall survival (p < 0.000)	High <i>STX1A</i> and low <i>MUNC13</i> expression correlate with poor overall survival (p = 0.007)	There is no correlation (p = 0.410)
EGFR/HER family receptors	<i>EGFR</i>	High <i>EGFR</i> expression correlates with poor overall survival (p = 0.033)	High <i>STX1A</i> and <i>EGFR</i> expression correlate with poor overall survival (p = 0.043)	There is no correlation (p = 0.480)
	<i>HER2</i>	There is no correlation (p = 0.065)	High <i>STX1A</i> and <i>HER2</i> expression correlate with poor overall survival (p = 0.011)	There is no correlation (p = 0.220)
	<i>HER3</i>	There is no correlation (p = 0.936)	There is no correlation (p = 0.116)	There is no correlation (p = 0.660)
	<i>HER4</i>	High <i>HER4</i> expression correlates with poor overall survival (p = 0.032)	High <i>STX1A</i> and <i>HER4</i> expression correlate with poor overall survival (p = 0.009)	Low <i>HER4</i> expression correlates with poor metastasis free survival (p = 0.018)

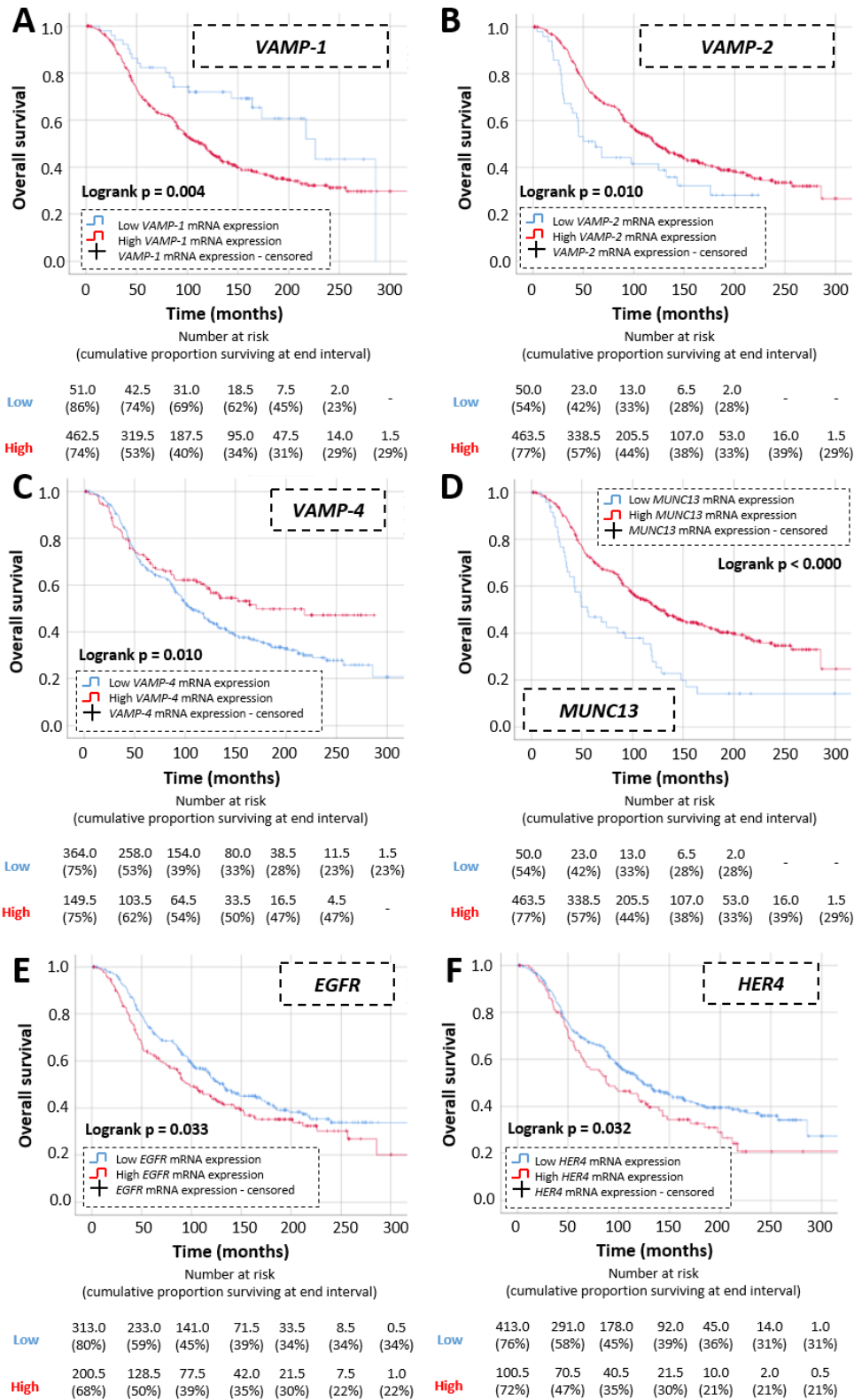
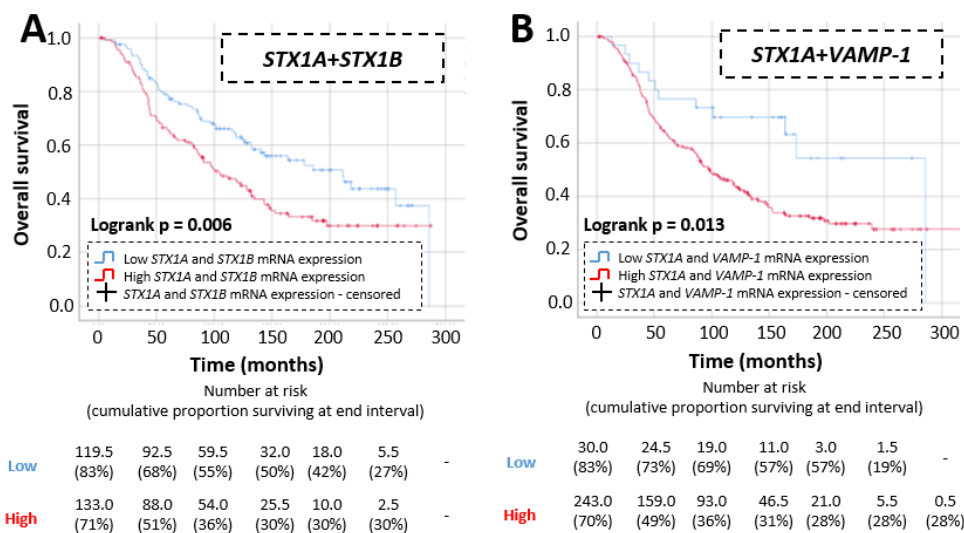
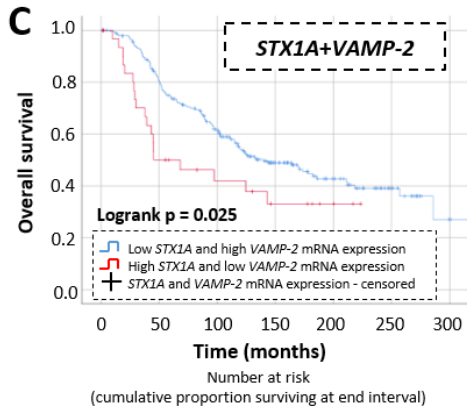


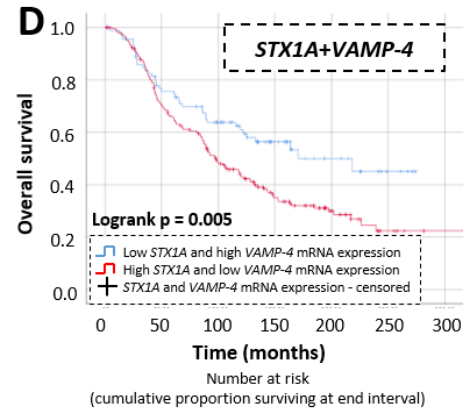
Figure 41– SNARE and EGFR/HER family of receptors genes expression correlate with HER2-positive BC overall survival. On the top of each figure, overall survival Kaplan-Meier curve of HER2-positive BC tumours grouped according to VAMP-1 (A), VAMP-2 (B), VAMP-4 (C), MUNC13 (D), EGFR (E), HER4 (F) expression, classified according to the decision tree algorithm. On the bottom of each figure, survival table where is shown the number at risk of BC patients and the cumulative proportion surviving at the end of the interval in parenthesis. Statistical analysis was performed using the Logrank test.

Finally, it was calculated if together with *STX1A*, the expression of these genes enhanced the *STX1A* prediction power of the overall survival (Table 33, Figure 42 and Annex figure 6). Analysing in depth of the results obtained, it was found that the combination of some SNARE genes and EGFR/HER family of receptors increased the predictive value of *STX1A* alone (Figure 40A). Among them, the combination of *STX1A* and *STX1B* resulted in a better prediction value (*STX1A* p = 0.043) from the 100th month to the 150th (Figure 42A). *STX1A* together with *VAMP-1* were able to increase the predictive value from the 50th month to 150th (Figure 42B). The consideration of the inverse correlation between *STX1A* with *VAMP-2* resulted in a better predictive value form the initial of the diagnosis until month 50th (Figure 42C). The inverse relationship between *STX1A* and *VAMP-4* also increased the predictive value on the outcome of HER2-positive patients from month 150th to 120th (Figure 42D). Similarly, the inverse correlation between *STX1A* and *SYT1* increased the predictive value from the 100th to 200th months (Figure 42E). *STX1A* together with the inverse expression of *STXBP2* resulted in an increase of better overall survival predictive value from month 50th to 100th, in comparison to *STX1A* alone (Figure 42F). Considering *STX1A* and *MUNC13*, their inverse correlation was able to predict the outcome of the patients from the initial time of diagnosis until month 100th (Figure 42G). Finally, considering the expression of *STX1A* together with *HER2* or *HER4*, there was an increase in predicting overall survival of HER2-positive BC patients from month 100th to 200th or 50th to 200th, respectively (Figure 42H and Figure 42I, respectively).

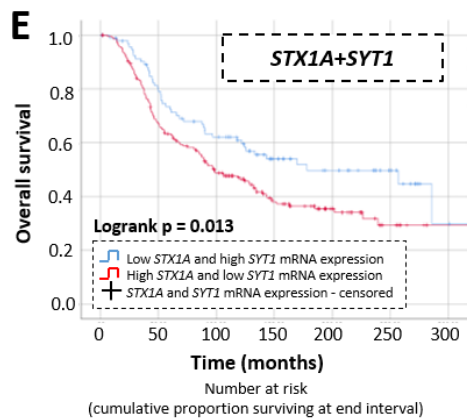




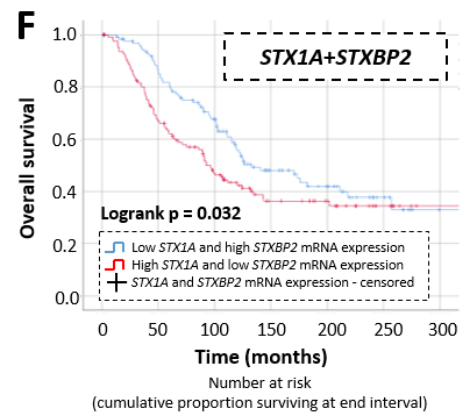
Low	230.5 (81%)	275.5 (61%)	109.5 (49%)	57.5 (43%)	29.0 (38%)	10.0 (31%)	1.0 (31%)
High	31.0 (52%)	13.5 (44%)	9.0 (34%)	4.5 (34%)	1.5 (34%)	-	-



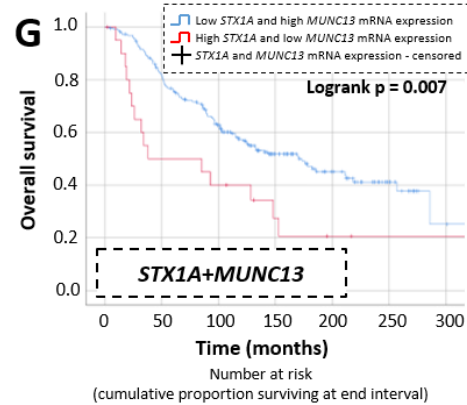
Low	91.0 (77%)	64.0 (64%)	40.0 (56%)	19.5 (50%)	8.5 (44%)	2.0 (44%)	-
High	205.5 (71%)	137.5 (49%)	80.0 (35%)	40.0 (30%)	17.5 (23%)	3.5 (23%)	0.5 (23%)



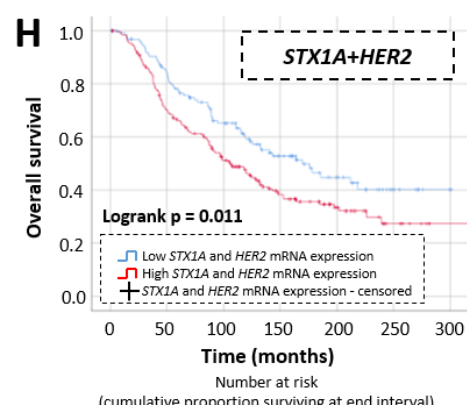
Low	92.0 (80%)	71.0 (62%)	45.5 (54%)	27.0 (50%)	16.5 (50%)	8.0 (38%)	1.0 (38%)
High	206.0 (67%)	131.0 (49%)	78.0 (39%)	41.0 (36%)	20.5 (31%)	5.0 (31%)	0.5 (31%)



Low	123.5 (87%)	99.0 (68%)	63.5 (47%)	31.5 (41%)	18.0 (37%)	6.0 (31%)	0.5 (31%)
High	125.5 (67%)	78.5 (48%)	44.5 (37%)	23.5 (37%)	14.5 (34%)	4.5 (34%)	0.5 (34%)



Low	221.0 (82%)	171.5 (63%)	105.5 (51%)	56.5 (45%)	28.0 (40%)	9.5 (32%)	1.0 (32%)
High	20.5 (51%)	10.0 (41%)	7.0 (29%)	3.5 (21%)	1.5 (21%)	1.0 (21%)	0.5 (21%)



Low	126.0 (85%)	99.5 (65%)	63.5 (53%)	35.0 (45%)	16.5 (40%)	4.5 (40%)	0.5 (40%)
High	191.0 (70%)	126.5 (51%)	77.5 (39%)	40.0 (34%)	19.0 (29%)	4.5 (29%)	0.5 (29%)

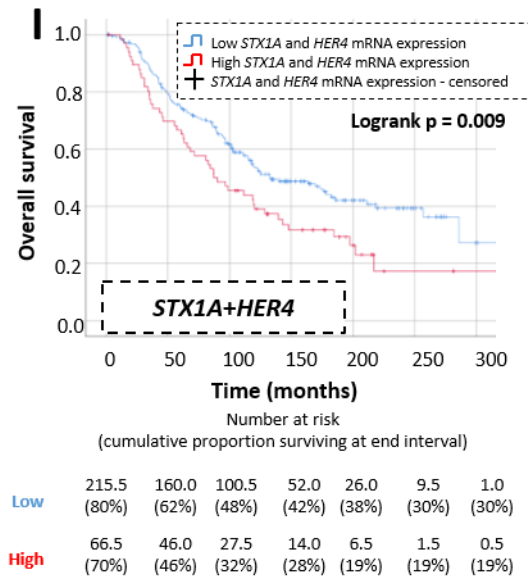


Figure 42 – *STX1A* together with Syntaxin, SNARE and EGFR/HER receptor families increases the overall survival prediction value in HER2-positive BC patients. On the top of each figure, overall survival Kaplan-Meier curve of HER2-positive BC tumours grouped according to *STX1A* and *STX1B* (A), *VAMP-1* (B), *VAMP-2* (C), *VAMP-4* (D), *SYT1* (E), *STXBP2* (F), *MUNC13* (G), *HER2* (H) and *HER4* (I) expression, classified according to the decision tree algorithm. On the bottom of each figure, survival table where the number at risk of HER2-positive BC patients and the cumulative proportion surviving at the end of the interval in parenthesis is shown. Statistical analysis was performed using Logrank test.

Finally, it was also analysed if other Syntaxins, SNARE or EGFR/HER family members could correlate with distant metastasis free survival in HER2-positive BC patients (Table 33). The analysis of Kaplan Meier plotter database resulted in that low expression of *VAMP-2* and *HER4* correlated with a worse distant metastasis free survival in comparison to higher levels of these genes (Figure 43A and Figure 43B, respectively).

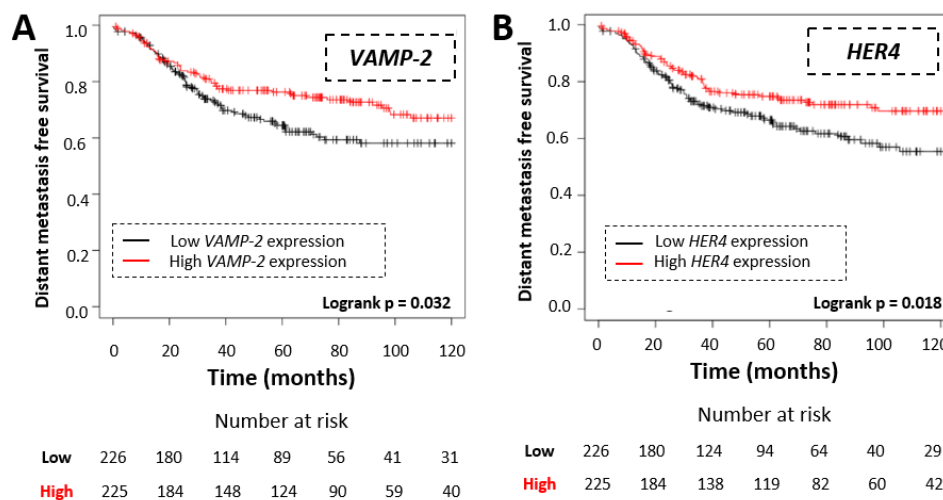


Figure 43 – *VAMP-2* and *HER4* are able to predict distant metastasis free survival period in HER2-positive BC patients. On the top of each figure, distant metastasis free survival Kaplan-Meier curve from Kaplan Meier plotter database of HER2-positive BC tumours grouped according low or high

levels of *VAMP-2* (A) and *HER4* (B). On the bottom of each figure, number at risk of HER2-positive BC patients. Statistical analysis was performed using the Logrank test.

1.2.3. G₂/M CHECKPOINT AND PI3K/AKT/mTOR SIGNALLING PATHWAYS ARE UP-REGULATED IN TUMOURS WITH *STX1A*^{HIGH}/*HER2*^{HIGH} HER2-POSITIVE BC TUMOURS

Next, to further characterize *STX1A* expression in HER2-positive BC tumours, it was performed a gene set enrichment analysis (GSEA). It was focused only in HER2-enriched BC subtype for two main reasons: a) HER2-positive BC subtype includes two very different subgroup in terms of clinical response and therapy and gene expression patterns, b) HER2-enriched subgroup is the one with the highest expression of *STX1A* gene (*Figure 34A*). Then, focusing on HER2-enriched tumours, *STX1A* expression was subgrouped considering the decision tree algorithm (*Annex figure 7A*) and using the GSEA software it was analysed tumours with high *STX1A* expression versus tumours with low *STX1A* expression. The results are shown in *Annex figure 7B*. Even though a lot of pathways were differentially expressed depending on *STX1A* expression level, none of them were statistically different (taking NOM p val ≤ 0.05 and FDR q val ≤ 0.25 as significant threshold). Then, considering that HER2-enriched tumours were analysed, it was thought to include *HER2* receptor since this gene is overexpressed in this particular subgroup and it positively correlates with *STX1A*, as well (*Annex table 2*). It was performed a GSEA analysis for HER2-enriched tumours with *HER2* high versus *HER2* low expression, grouped according to the division of the decision tree algorithm (*Annex figure 7C*). The results of the GSEA, shown in *Annex figure 7D*, determined that there were not any signalling pathways differentially expressed. Finally, it was decided to combine both genes, HER2-enriched tumours with *STX1A*^{HIGH} and *HER2*^{HIGH} in comparison to HER2-enriched tumours with *STX1A*^{LOW} and *HER2*^{LOW} (*Annex figure 7E*). It resulted in two differentially expressed signalling pathways, there was an up-regulation of the PI3K/AKT/mTOR and G₂/M checkpoint signalling pathways in tumours classified as *STX1A*^{HIGH} and *HER2*^{HIGH} (*Figure 44*). More in detail, it is possible to see in *Figure 44* the genes responsible for this differential expression of these signalling pathways.

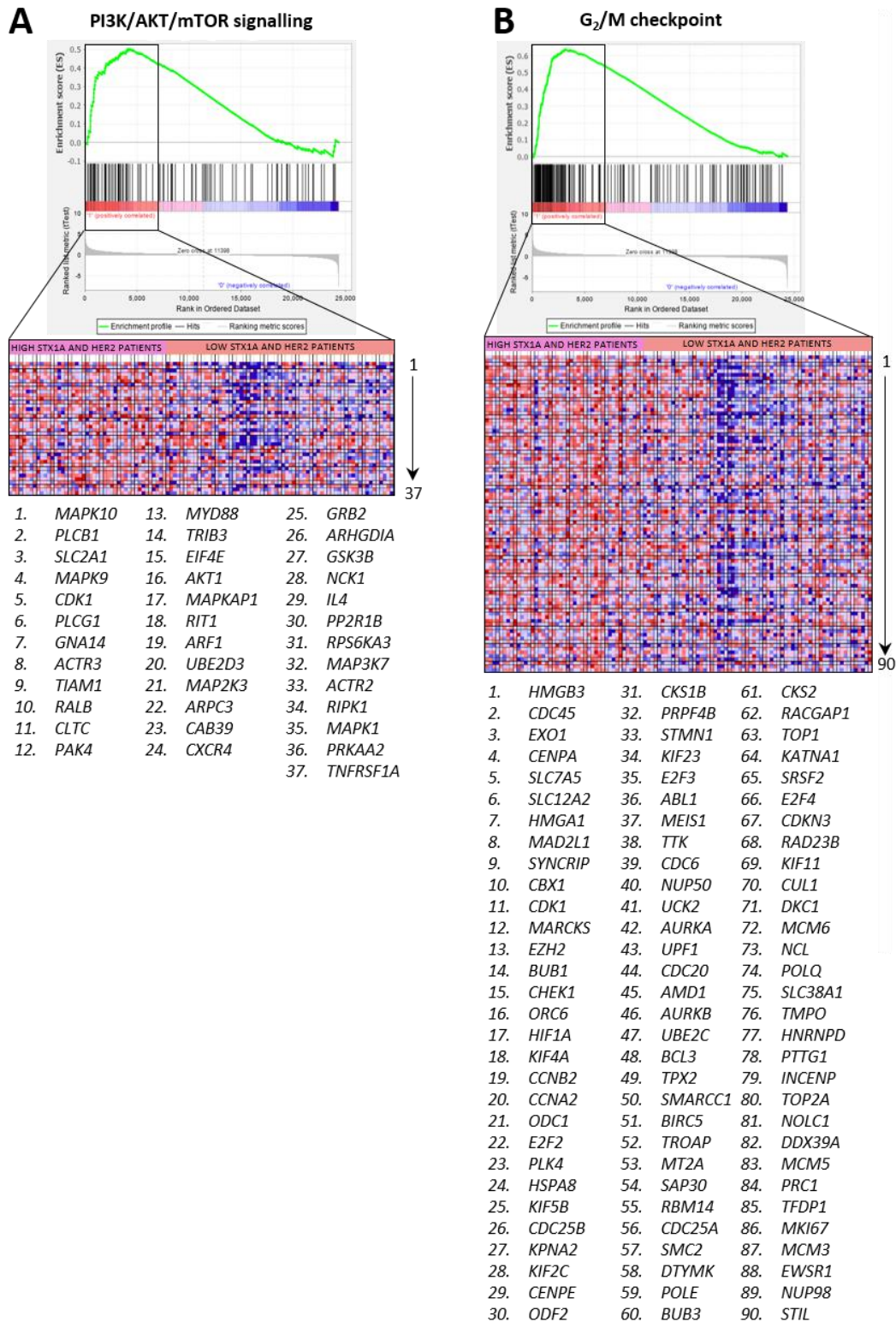
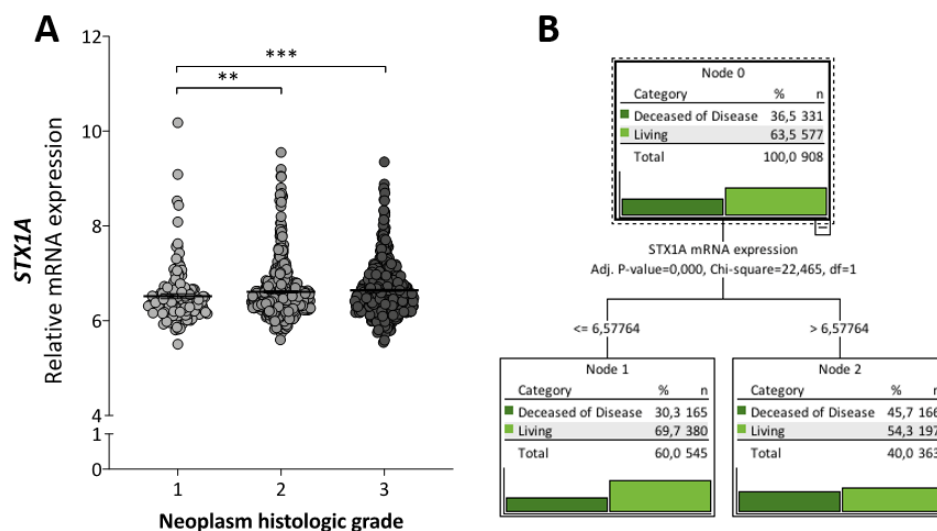


Figure 44 - HER2-enriched BC tumours with high levels of STX1A and HER2 upregulate PI3K/AKT/mTOR and G₂/M checkpoint signalling pathways. (A) GSEA of PI3K/AKT/mTOR signalling pathway and (B) of G₂/M checkpoint signalling pathway from STX1A^{HIGH} and HER2^{HIGH} HER2-enriched BC tumours. In the box, heat map with the genes responsible for the up-regulation of these pathways.

1.3. SYNTAXIN-1A IN HER2-NEGATIVE BREAST CANCER

1.3.1. SYNTAXIN-1A EXPRESSION CORRELATES WITH WORSE PROGNOSIS IN HER2-NEGATIVE BC TUMOURS

Even though *STX1A* was not such overexpressed in HER2-negative BC subtypes, it was also interesting to determine its likely role as a biomarker for prognosis in HER2-negative BC patients. First of all, it was determined if there was any difference in *STX1A* expression according to the neoplasm histological grade of HER2-negative BC subtypes (*Figure 45A*). The analysis demonstrated that the higher the neoplasm histologic grade, the higher the expression of *STX1A* gene (grade 1: M = 6.517, SEM = 0.049; grade 2: M = 6.609, SEM = 0.025; grade 3: M = 6.641, SEM = 0.024). HER2-negative BC patients were grouped following the decision tree algorithm (*Figure 45B*) and some clinical tumour markers were analysed. This study revealed that HER2-negative tumours with *STX1A*^{HIGH} correlated with poor prognosis markers, namely tumour volume, Nottingham prognostic index and mutation number. Regarding tumour volume (*Figure 45C*), HER2-negative tumours with high *STX1A* expression showed higher tumour volume (M = 26.100, SEM = 0.639 versus M = 25.060, SEM = 0.578). Moreover, tumours with high *STX1A* levels also had a higher Nottingham prognostic index (*Figure 45D*), (M = 3.971, SEM = 0.050 versus M = 3.811, SEM = 0.043) and more mutations per tumour (M = 5.870, SEM = 0.150 versus M = 5.185, SEM = 0.123) (*Figure 45E*). Also, if there were any differences in patient's overall survival was analysed as well. The Kaplan-Meier curve revealed that HER2-negative patients with high levels of *STX1A* had a poorer overall survival than patients with low *STX1A* expression levels (*Figure 45F*). Finally, it was checked, as it was previously did, if *STX1A* levels could correlate with metastasis disease free survival. The analysis demonstrated that HER2-negative BC patients had a lower metastasis free survival if their BC tumours had high levels of *STX1A* (*Figure 45G*).



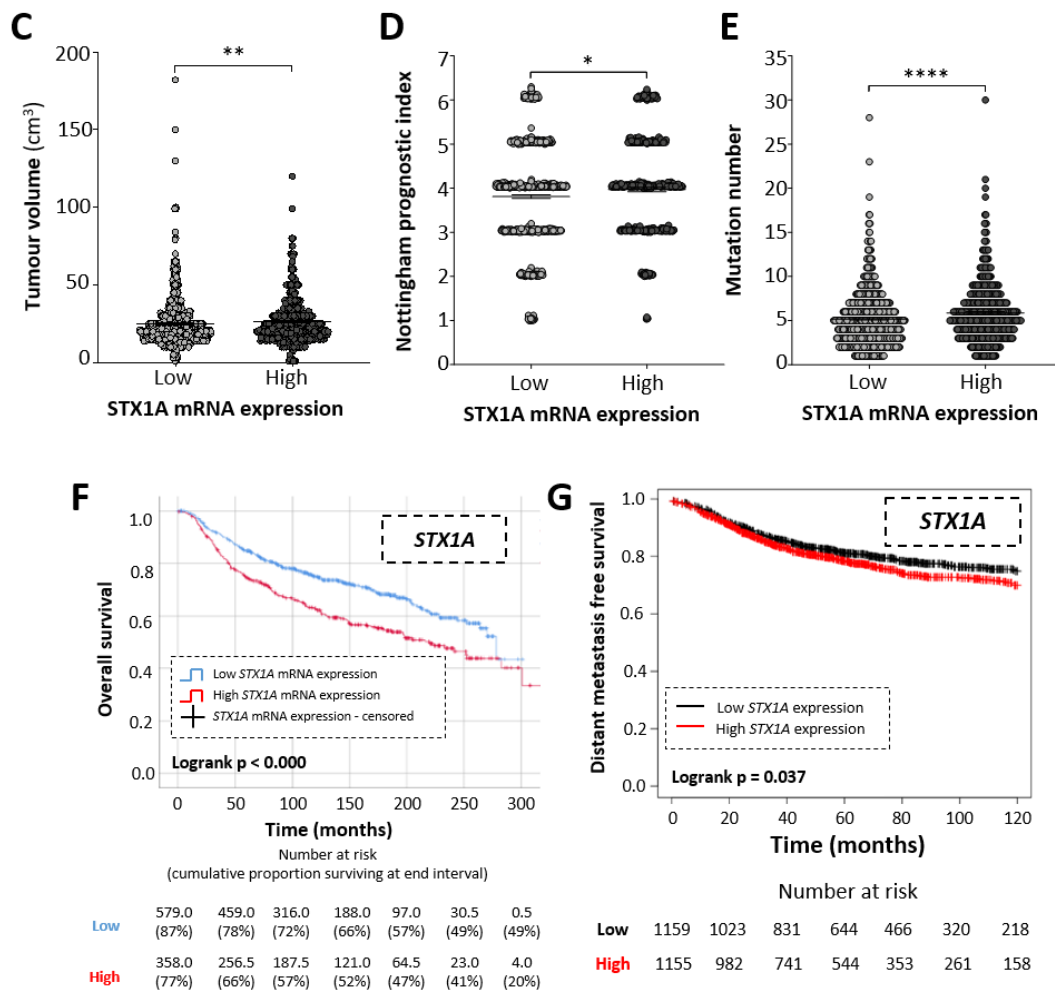


Figure 45 - Aggressive HER2-negative tumours overexpress *STX1A* and higher expression of *STX1A* is related to poor overall survival and distant metastasis free survival in HER2-negative BC subgroup. (A) Graphical representation of relative *STX1A* mRNA expression grouped into different neoplasm histologic grade in HER2-negative BC tumours. (B) Decision tree diagram that shows how relative *STX1A* mRNA expression is grouped according to the patient survival status (deceased of the disease, dark green and living HER2-negative BC patients, light green). (C) Graphical representation of HER2-negative BC tumour volume (cm³) in the different tumour subgroups classified according *STX1A* expression (low and high). (D) Graphical representation of Nottingham prognostic index in the different HER2-negative tumour subgroups classified according *STX1A* expression (low and high). (E) Graphical representation of HER2-negative BC mutation number in the different tumour subgroups classified according *STX1A* expression (low and high). (F) On the top, overall survival Kaplan-Meier curve of HER2-negative BC tumours grouped according to *STX1A* expression, grouped as shown in previous figure. On the bottom survival table where is shown the number at risk of HER2-negative BC patients and the cumulative proportion surviving at the end of the interval in parenthesis. (G) Distant-metastasis free survival of HER2-negative BC patients grouped according *STX1A* expression. Statistical analysis was performed by U-Mann-Whitney test (A, C-E), Chi-square test (B) and Logrank (Figure 2F and 2G). *p<0.05, **p<0.01, ***p<0.001, ****p<0.000.

1.3.2. SYNTAXIN-1A EXPRESSION CORRELATES WITH THE EXPRESSION OF OTHER SNARES AND EGFR/HER FAMILY MEMBERS IN HER2-NEGATIVE BC TUMOURS

Given that *STX1A* also correlates with a poorer overall survival in HER2-negative BC patients, it was interesting to determine if the joint analysis of their SNARE partners and also

EGFR/HER receptor family members could increase its predictive potential. First, it was determined if there was any correlation between *STX1A* and SNAREs or EGFR/HER receptor expression (*Annex table 3*). On one hand, the analysis of the Spearman coefficient correlation demonstrated that expression of SNAREs genes *STX3*, *SNAP-25*, *CPLX1*, *MUNC18-1* and *STXBP2* positively correlated with *STX1A* expression. On the other hand, the expression of SNARE genes *SNAP-23* and *VAMP-4* correlated negatively with *STX1A* gene expression. Regarding the family of EGFR/HER receptors, *HER2*, *HER3* and *HER4* positively correlated with *STX1A* gene expression, whereas *EGFR* negatively did. Next, it was determined if these genes were also differentially expressed amongst HER2-negative tumours regarding their *STX1A* levels. It turned out that tumours with low *STX1A* had an increased expression of *SNAP-23*, *VAMP-4* and *SYT1*, whereas tumours with high expression of *STX1A* had an increase expression of *SNAP-25*, *CPLX1*, *MUNC18-1*, *STXBP2*, *MUNC13*, *HER2* and *HER4* (*Annex table 3*).

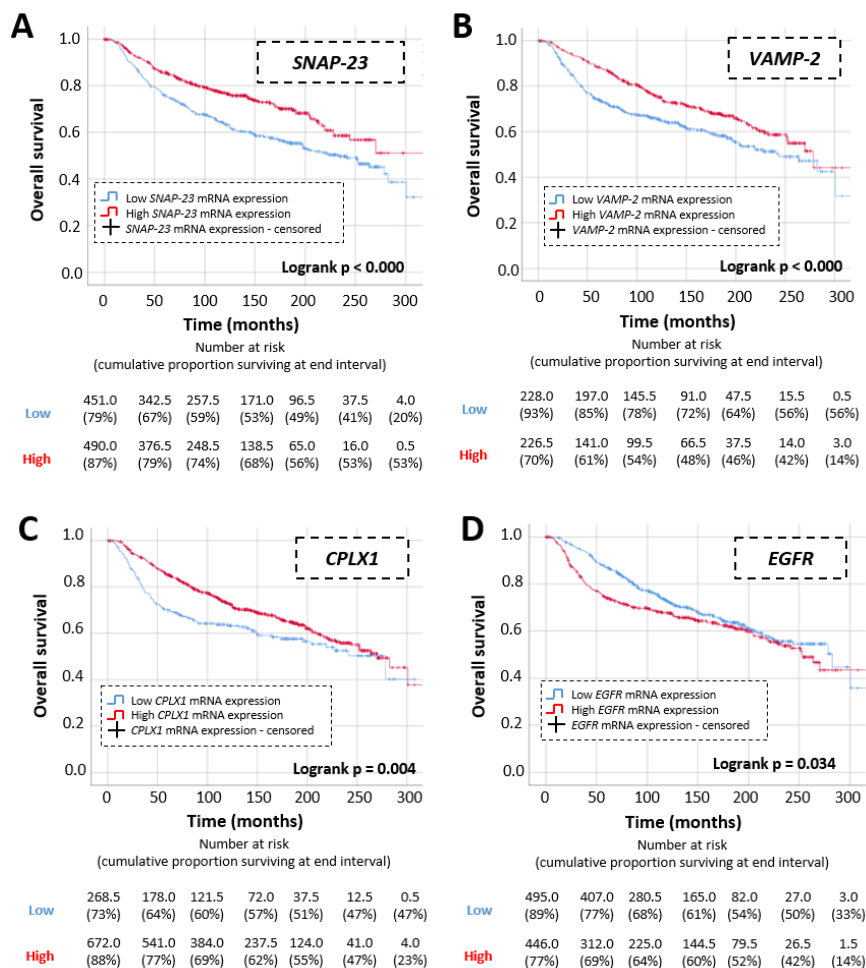


Figure 46 - SNARE and EGFR/HER family of receptors genes expression correlate with HER2-negative BC overall survival. On the top of each figure, overall survival Kaplan-Meier curve of HER2-negative BC tumours grouped according to *SNAP-23* (A), *VAMP-2* (B), *CPLX1* (C), *EGFR* (D) expression, classified according to the decision tree algorithm. On the bottom of each figure, survival table where is shown the number at risk of HER2-negative BC patients and the cumulative proportion surviving at the end of the interval in parenthesis. Statistical analysis was performed using Logrank test.

Table 34 – Summary of the study of other Syntaxins, SNARE and EGFR/HER family receptor genes in HER2-negative BC patients. In the table is shown the Spearman correlation of the genes with *STX1A*, the expression of the detrimental genes grouped among HER2-negative BC tumours expressing low or high levels of *STX1A*, the overall survival by themselves or adding *STX1A* and the distant metastasis free survival of syntaxins family, SNARE and EGFR/HER related genes.

		Overall survival	Overall survival together with <i>STX1A</i> overall survival	Distant metastasis free survival
Syntaxin family	<i>STX1B</i>	There is no correlation (p = 0.209)	High <i>STX1A</i> and <i>STX1B</i> expression correlate with poor overall survival (p < 0.000)	There is no correlation (p = 0.058)
	<i>STX2</i>	There is no correlation (p = 0.213)	High <i>STX1A</i> and <i>STX2</i> expression correlate with poor overall survival (p < 0.000)	High <i>STX2</i> expression correlates with poor distant metastasis free survival (p < 0.000)
	<i>STX3</i>	There is no correlation (p = 0.284)	High <i>STX1A</i> and <i>STX3</i> expression correlate with poor overall survival (p = 0.002)	There is no correlation (p = 0.130)
	<i>STX6</i>	There is no correlation (p = 0.449)	High <i>STX1A</i> and <i>STX6</i> expression correlate with poor overall survival (p = 0.003)	High <i>STX6</i> expression correlates with poor distant metastasis free survival (p = 0.005)
	<i>STX17</i>	There is no correlation (p = 0.241)	High <i>STX1A</i> and <i>STX17</i> expression correlate with poor overall survival (p = 0.001)	There is no correlation (p = 0.230)
t-SNAREs	<i>SNAP-23</i>	Low <i>SNAP-23</i> expression correlates with poor overall survival (p < 0.000)	High <i>STX1A</i> expression and low <i>SNAP-23</i> expression correlate with poor overall survival (p < 0.000)	Low <i>SNAP-23</i> expression correlates with poor distant metastasis free survival (p = 0.001)
	<i>SNAP-25</i>	There is no correlation (p = 0.272)	High <i>STX1A</i> and <i>SNAP-25</i> expression correlate with poor overall survival (p = 0.049)	There is no correlation (p = 0.270)
v-SNAREs	<i>VAMP -1</i>	There is no correlation (p = 0.408)	High <i>STX1A</i> expression and low <i>VAMP-1</i> expression correlate with poor overall survival (p = 0.042)	There is no correlation (p = 0.330)
	<i>VAMP -2</i>	Low <i>VAMP-2</i> expression correlates with poor overall survival (p > 0.000)	High <i>STX1A</i> expression and low <i>VAMP-2</i> expression correlate with poor overall survival (p < 0.000)	Low <i>VAMP-2</i> expression correlates with poor distant metastasis free survival (p < 0.000)
v-SNAREs	<i>VAMP-4</i>	There is no correlation (p = 0.101)	High <i>STX1A</i> expression and low <i>VAMP-4</i> expression correlate with poor overall survival (p = 0.015)	No data

		Overall survival	Overall survival together with <i>STX1A</i> overall survival	Distant metastasis free survival
	<i>SYT1</i>	There is no correlation (p = 0.066)	High <i>STX1A</i> expression and low <i>SYT1</i> expression correlate with poor overall survival (p < 0.000)	High <i>SYT1</i> expression correlates with poor distant metastasis free survival (p = 0.028)
Soluble SNAREs	<i>CPLX1</i>	Low <i>CPLX1</i> expression correlates with poor overall survival (p = 0.004)	High <i>STX1A</i> expression and low <i>CPLX1</i> expression correlate with poor overall survival (p < 0.000)	No data
	<i>MUNC18-1</i>	There is no correlation (p = 0.631)	High <i>STX1A</i> and <i>MUNC18-1</i> expression correlate with poor overall survival (p = 0.004)	There is no correlation (p = 0.220)
	<i>STXBP2</i>	There is no correlation (p = 0.763)	High <i>STX1A</i> and <i>STXBP2</i> expression correlate with poor overall survival (p = 0.007)	Low <i>STXBP2</i> expression correlates with poor distant metastasis free survival (p = 0.003)
	<i>MUNC13</i>	There is no correlation (p = 0.859)	High <i>STX1A</i> and <i>MUNC13</i> expression correlate with poor overall survival (p = 0.004)	There is no correlation (p = 0.290)
	<i>EGFR</i>	High <i>EGFR</i> expression correlates with poor overall survival (p = 0.034)	High <i>STX1A</i> and <i>EGFR</i> expression correlate with poor overall survival (p = 0.003)	Low <i>EGFR</i> expression correlates with poor distant metastasis free survival (p = 0.003)
EGFR/HER family receptors	<i>HER2</i>	There is no correlation (p = 0.969)	High <i>STX1A</i> and <i>HER2</i> expression correlate with poor overall survival (p = 0.010)	Low <i>HER2</i> expression correlates with poor distant metastasis free survival (p < 0.000)
	<i>HER3</i>	There is no correlation (p = 0.237)	There is no correlation (p = 0.077)	Low <i>HER3</i> expression correlates with poor distant metastasis free survival (p = 0.010)
	<i>HER4</i>	There is no correlation (p = 0.137)	High <i>STX1A</i> and <i>HER4</i> expression correlate with poor overall survival (p < 0.000)	Low <i>HER4</i> expression correlates with poor distant metastasis free survival (p < 0.000)

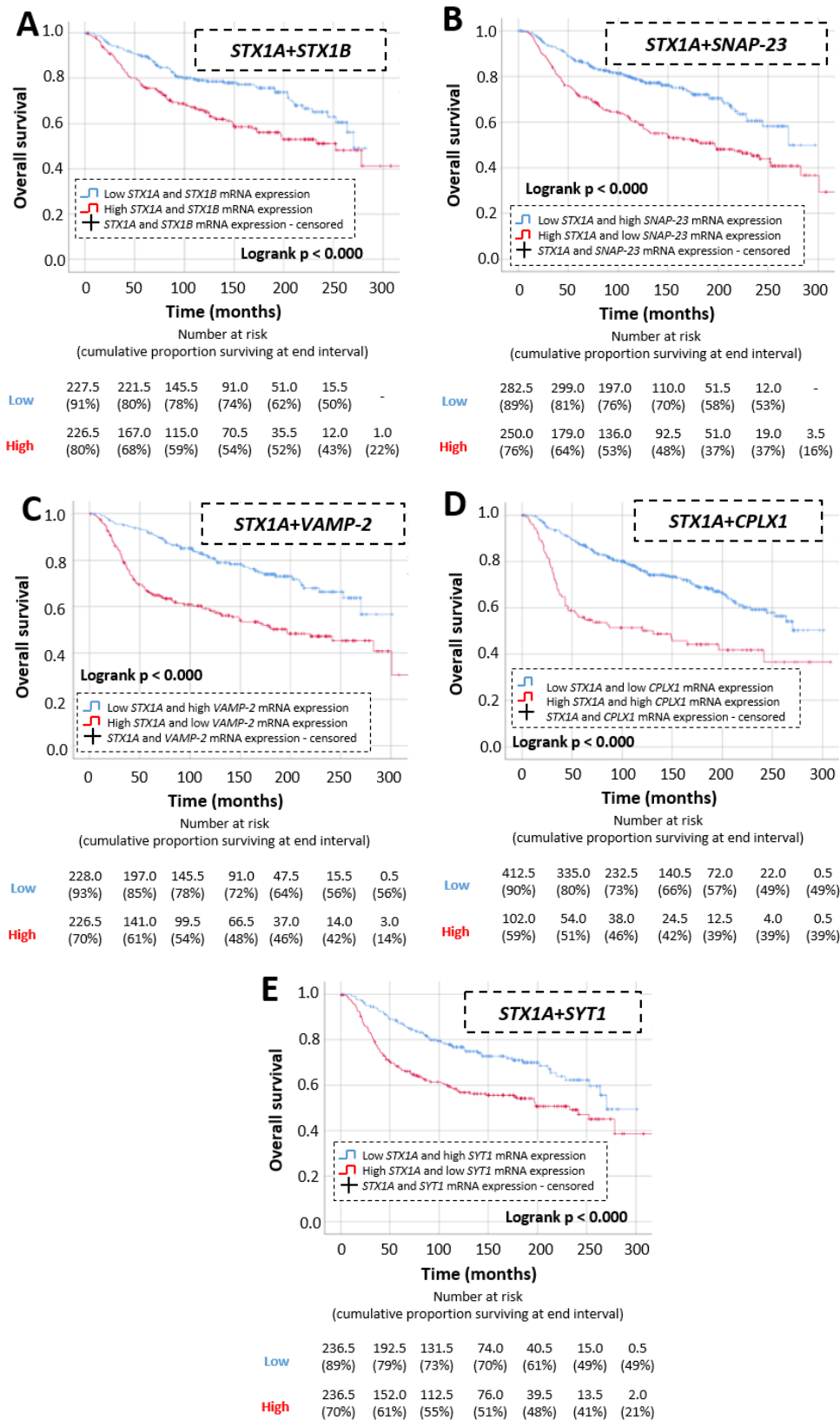
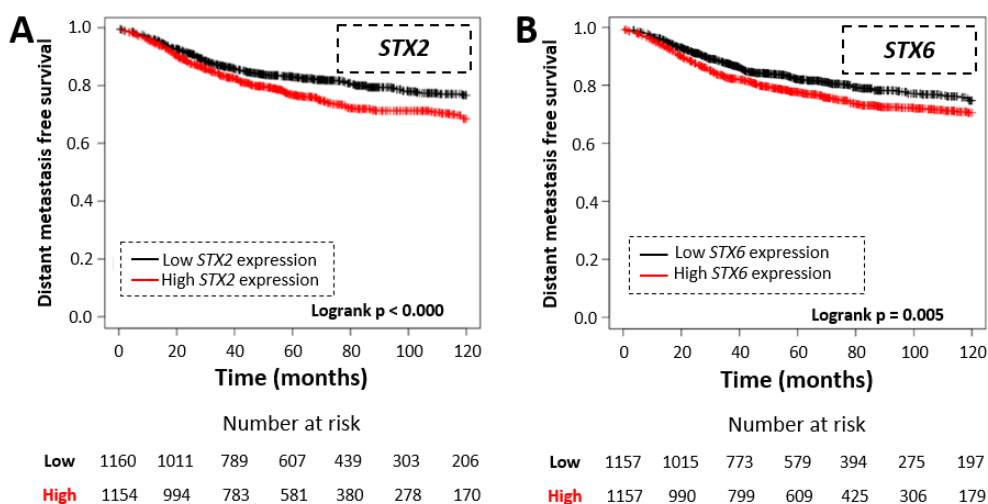
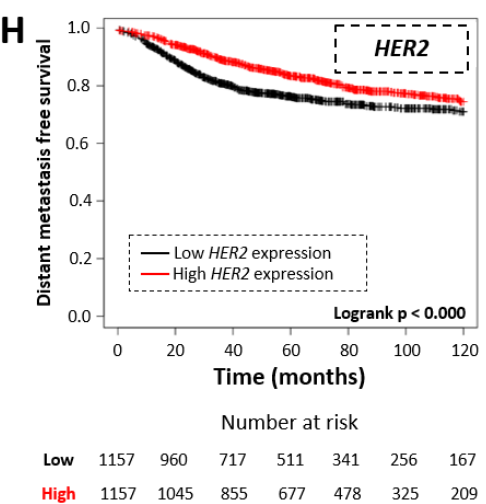
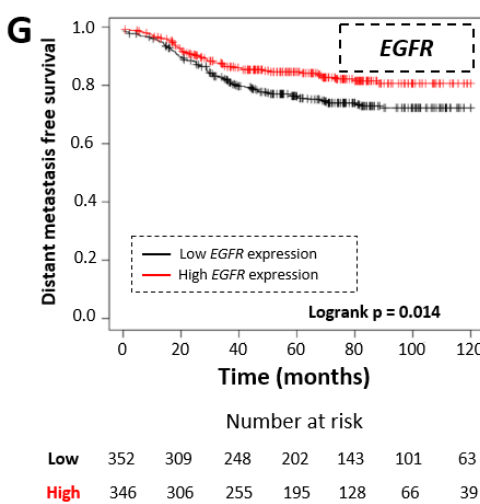
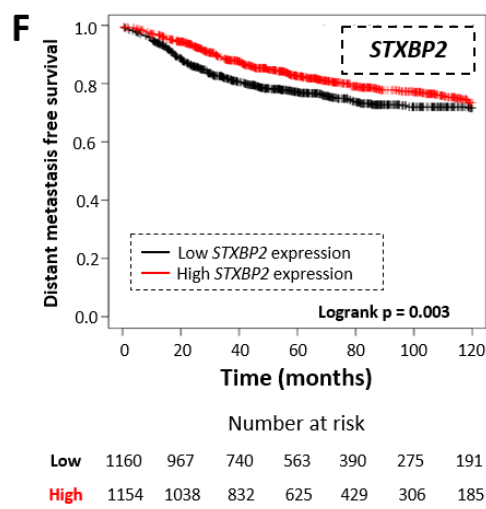
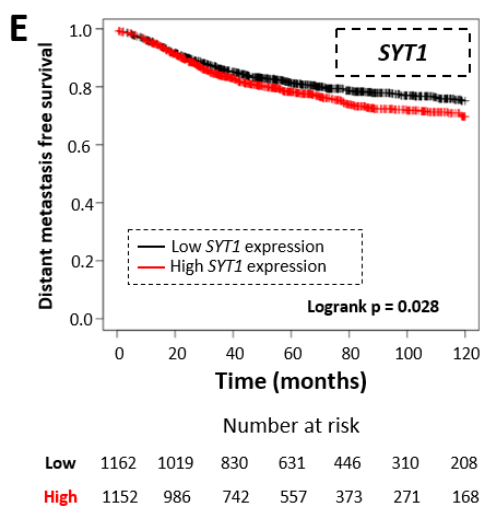
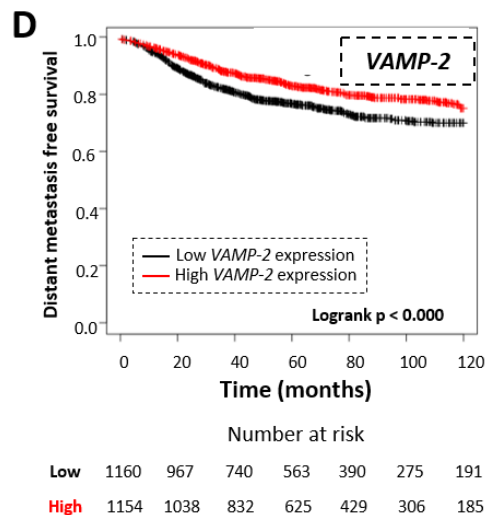
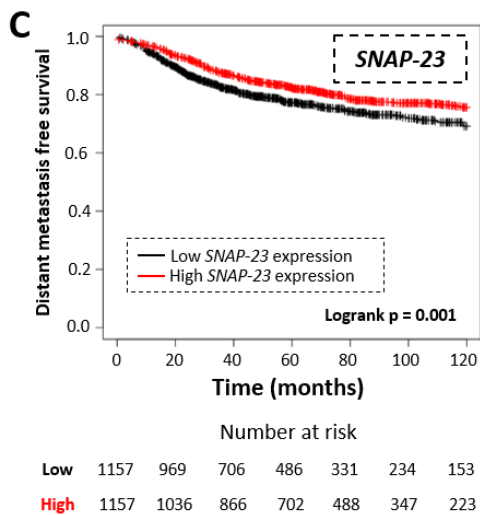


Figure 47 - STX1A together with other SNARE genes increases the overall survival prediction value in HER2-negative BC patients. On the top of each figure, overall survival Kaplan-Meier curve of BC tumours grouped according to *STX1A* and *STX1B* (A), *SNAP-23* (B), *VAMP-2* (C), *CPLX1* (D) and *SYT1* (E) expression, classified according to the decision tree algorithm. On the bottom of each figure, survival

table where is shown the number at risk of BC patients and the cumulative proportion surviving at the end of the interval in parenthesis. Statistical analysis was performed using Logrank test.

Then, it was analysed the potential of these SNARE and EGFR/HER receptors as biomarkers by themselves (*Table 34 and Figure 46*). Four of them were able to predict the overall survival of the HER2-negative patients: patients with low levels of *SNAP-23*, *VAMP-2* or *CPLX1* had a poorer overall survival (*Figure 46A-Figure 46C*), whereas high levels of *EGFR* gene expression correlated with a poorer overall survival for HER2-negative BC patients (*Figure 46D*). After that, it was determined if the co-expression of SNARE genes or EGFR/HER receptors together with *STX1A* increased significantly their individual prognostic value (summarized in *Table 34, Figure 47 and Annex figure 8*). However even though all of them were able to predict the overall survival of the HER2-negative BC patients, only five of them improved the overall survival together with *STX1A*. Specifically, *STX1A* together with *STXBP1* or the inverse expression of *SNAP-23* were better predictors than *STX1A* alone because together they increased the predictor overall survival power between month 100 and 200 after BC diagnosis (*Figure 47A and Figure 47B, respectively*). *STX1A* together with *VAMP-2* or *CPLX1* (considering that both have an indirect Spearman correlation with *STX1A*) increase the predictive overall survival at the beginning of the diagnosis until month 250 in comparison to *STX1A* alone (*Figure 47C and Figure 47D, respectively*). Finally, the inverse correlation between *STX1A* and *SYT1* also increased the predictive overall survival of *STX1A* alone between months 50 to 200 after the initial BC diagnosis (*Figure 47E*). Finally, it was also check whether expression of Syntaxin, SNARE and EGFR/HER family of receptors correlated with distant metastasis free survival (*Table 34 and Figure 48*). The Kaplan Meier plotter database analysis confirmed that some genes correlated with distant metastasis free survival: high expression of *STX2*, *STX6* and *SYT1* and low expression of *SNAP-23*, *VAMP-2*, *STXBP2*, *EGFR*, *HER2*, *HER3* and *HER4* correlated with worse overall survival (*Figure 48*).





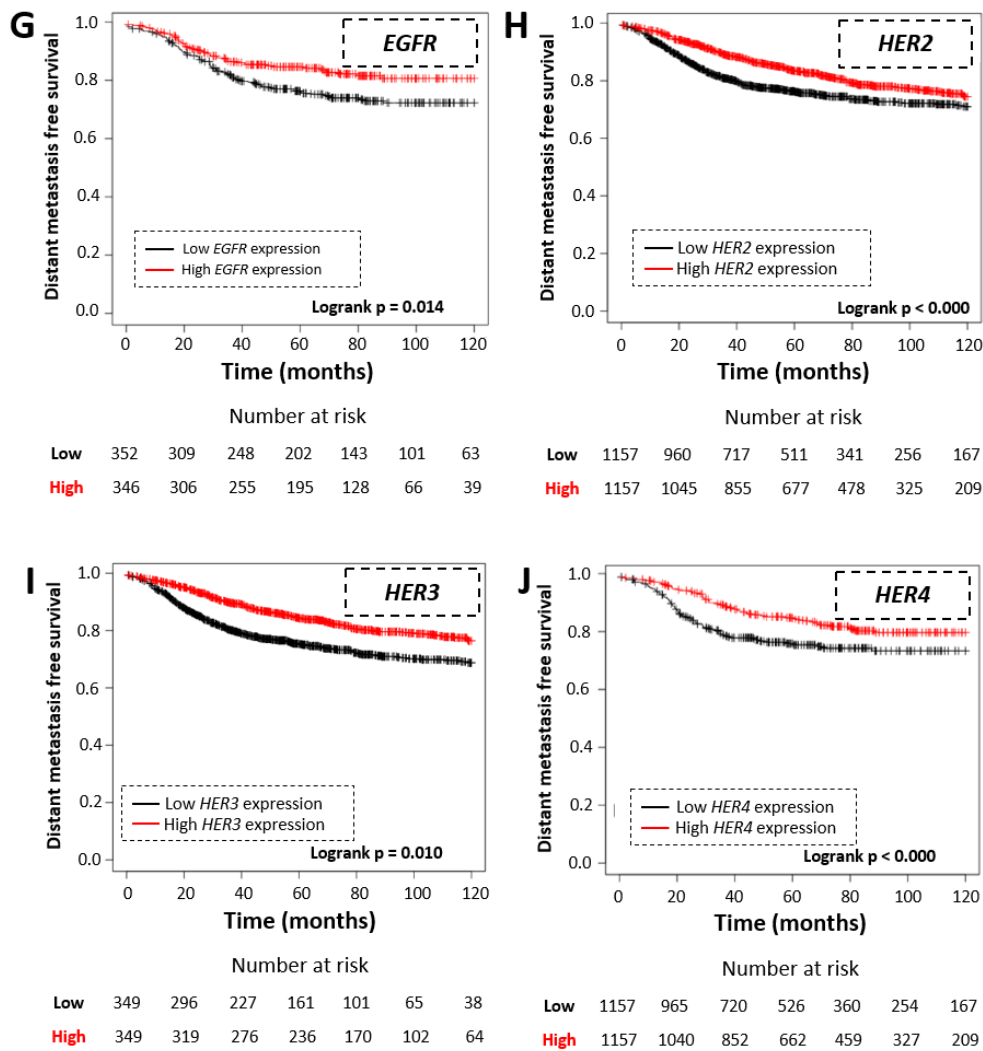
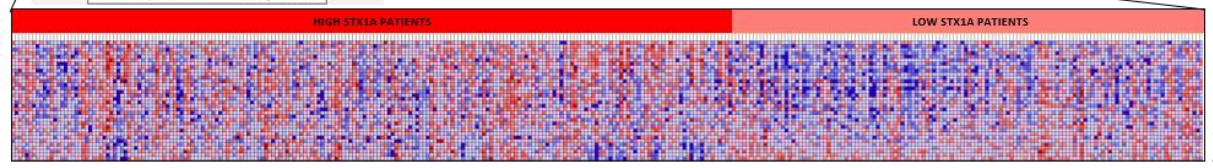
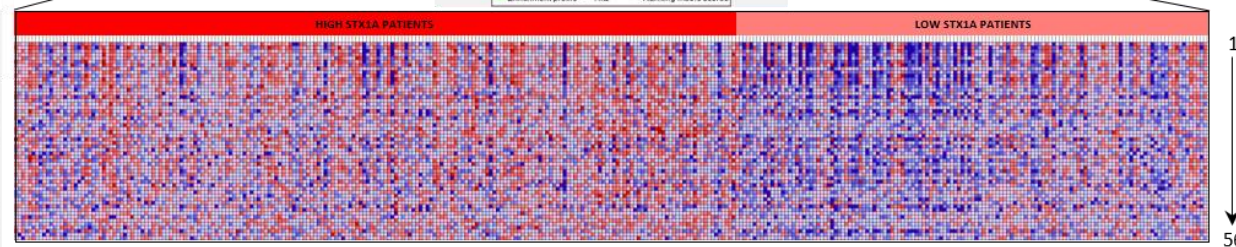
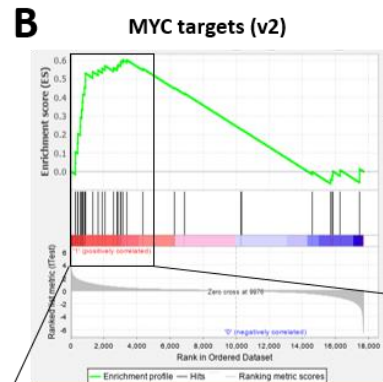
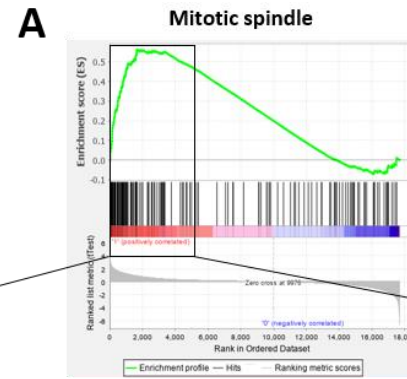


Figure 48 – Syntaxins, SNAREs and EGFR/HER family of receptors are able to predict distant metastasis free survival period in HER2-negative BC tumours. On the top of each figure, distant metastasis free survival Kaplan-Meier curve from Kaplan Meier plotter database of BC tumours grouped according low or high levels of *STX2* (A), *STX6* (B), *SNAP-23* (C), *VAMP-2* (D), *SYT1* (E), *STXBP2* (F), *EGFR* (G), *HER2* (H), *HER3* (I) and *HER4* (J). On the bottom of each figure, number at risk of BC patients. Statistical analysis was performed using the Logrank test.

1.3.3. *STX1A*^{HIGH} BASAL TUMOURS UP-REGULATE IMPORTANT SIGNALLING PATHWAYS

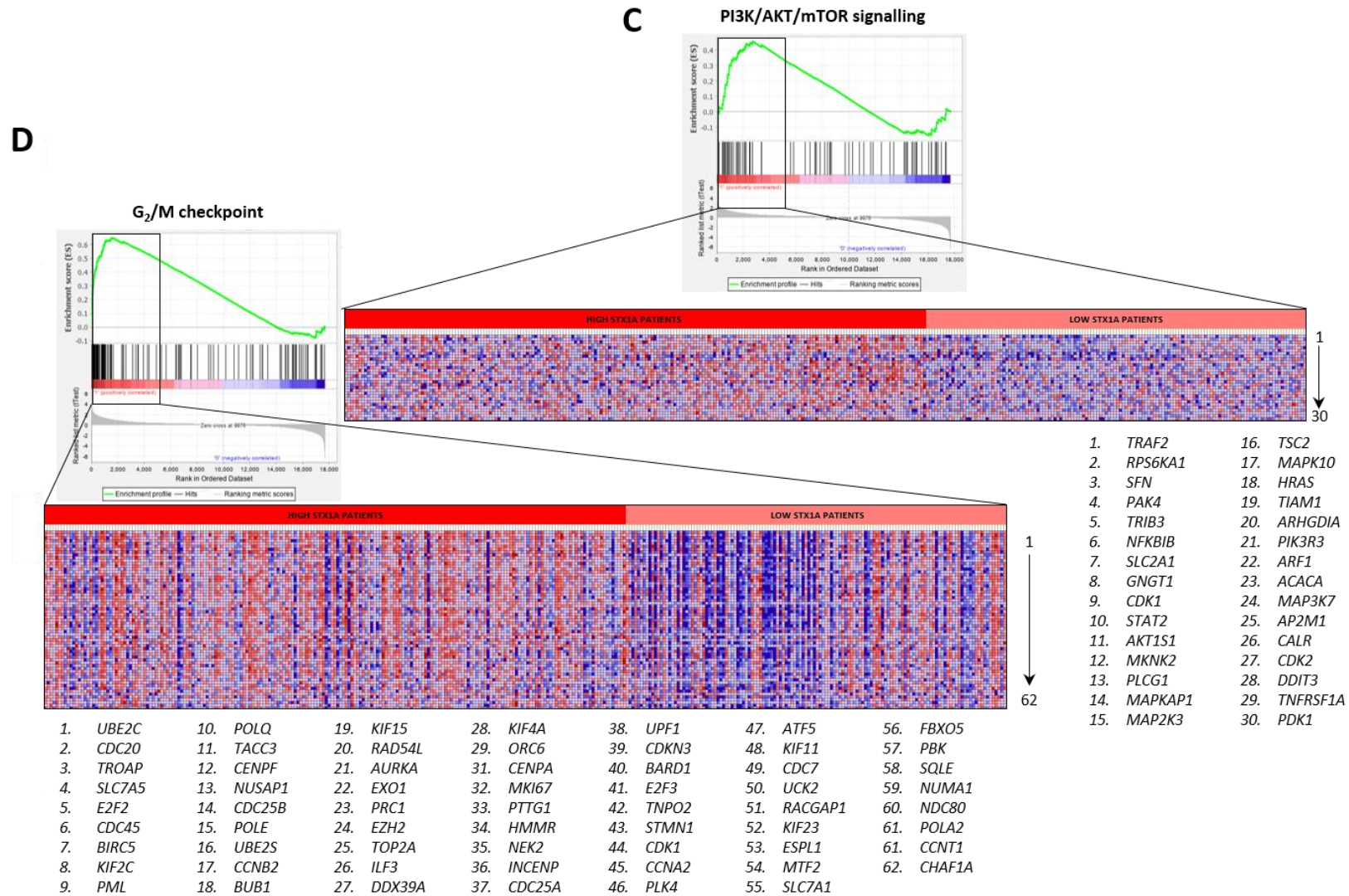
Then, as it was done for HER2-enriched tumours, it was performed a GSEA for a subgroup of HER2-negative BC tumours. In this case it was analysed the basal subgroup, considering that is the BC subgroup that has the lowest *STX1A* expression (*Figure 34A*), with the exception of the claudin-low subgroup.

First of all, basal tumours were classified as high and low expressing *STX1A* with the decision tree algorithm (*Annex figure 9A*). Then the GSEA analysis were run, graphically represented in *Annex figure 9B*. The analysis revealed that some signalling pathways were up-regulated in basal tumours expressing high levels of *STX1A*. These pathways were MYC targets (v2), mitotic spindle, PI3K/AKT/mTOR, G₂/M checkpoint, spermatogenesis, mTORC1, glycolysis and unfolded protein response signalling pathways. The detailed GSEA is represented in *Figure 49A - Figure 49H* along with the genes responsible for this up-regulation in *STX1A^{HIGH}* basal tumours. Then, another relevant gene was added to assess if it improved and narrowed the differences found in GSEA. In that case *EGFR* was chosen instead of *HER2* receptor because basal BC subtype did not overexpress *HER2* receptor at a relevant level, and also some tumours overexpressed *EGFR*. Moreover, it is the only EGFR/HER family of receptors that by himself correlated with patient's overall survival (*Annex table 3*). For these reasons it was considered jointly analysing basal tumours according *EGFR* and *STX1A* expressions. First of all, the relevance of the expression of *EGFR* alone was studied, dividing the cohort in two expression groups (*EGFR^{LOW}* and *EGFR^{HIGH}*) as shown in the decision tree algorithm (*Annex figure 9C*). The results determined a set of signalling pathways that were statistically differentially expressed in basal *EGFR^{HIGH}* BC tumours: mitotic spindle, glycolysis, E2F targets, mTORC1, PI3K/AKT/mTOR and G₂/M checkpoint signalling pathways (*Annex figure 9D*). The detailed GSEA analysis of each pathways and the genes responsible for the upregulation in *STX1A^{HIGH}* basal BC tumours are shown in *Annex figure 10*. Finally, it was performed the GSEA in order to compare tumours with high expression of *STX1A* and *EGFR* with tumours with low *STX1A* and *EGFR* expression (*Annex figure 9C*). The results demonstrated that there was an up-regulation of MYC targets (v2), mitotic spindle, PI3K/AKT/mTOR, G₂/M checkpoint, spermatogenesis and glycolysis signalling pathways in basal tumours with high expression of *STX1A* and *EGFR* (*Figure 50A-Figure 50E*). The genes involved in such up-regulation of the different pathways are remarked also in *Figure 50*.

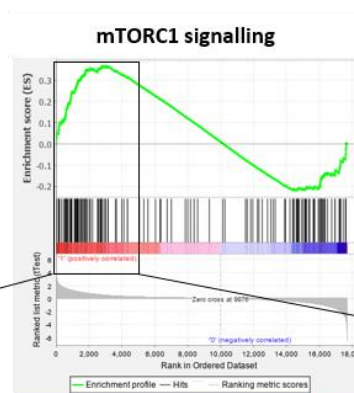


- | | | | |
|------------|-----------|------------|---------------|
| 1. MAP3K6 | 7. PA2G4 | 13. LAS1L | 19. IPO4 |
| 2. SLC19A1 | 8. NOC4L | 14. PLK1 | 20. UNG |
| 3. RRP12 | 9. NOP2 | 15. BYSL | 21. MPHOSPH10 |
| 4. PUS1 | 10. WDR74 | 16. NOP16 | 22. RRP9 |
| 5. FARSA | 11. NOP56 | 17. TMEM97 | |
| 6. CBX3 | 12. PLK4 | 18. MRTO4 | |

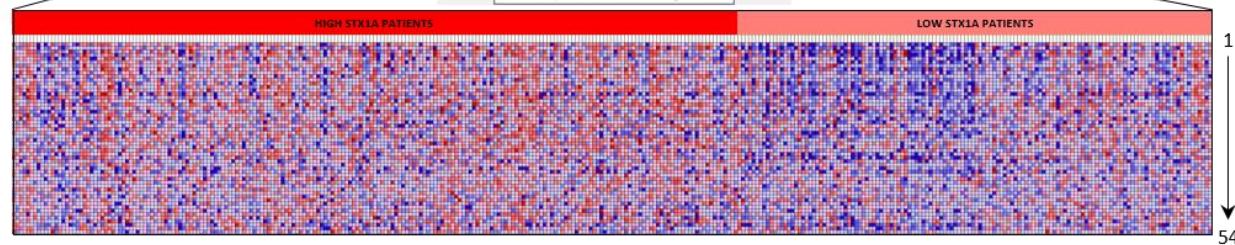
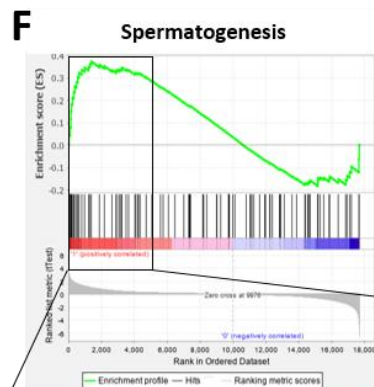
- | | |
|------------|-------------|
| 1. BIRC5 | 20. NEK2 |
| 2. KIF2C | 21. INCENP |
| 3. CENPF | 22. PLEKHG2 |
| 4. NUSAP1 | 23. CNTROB |
| 5. KNTC1 | 24. KLC1 |
| 6. CCNB2 | 25. MAP3K11 |
| 7. BUB1 | 26. BCAR1 |
| 8. TAOK2 | 27. RHOT2 |
| 9. KIF15 | 28. DLGAP5 |
| 10. AURKA | 29. ALMS1 |
| 11. PRC1 | 30. CDK1 |
| 12. TOP2A | 31. HDAC6 |
| 13. PIF1 | 32. TUBGCP2 |
| 14. MYO9B | 33. TUBA4A |
| 15. CLIP2 | 34. KIF11 |
| 16. KIF4A | 35. MAP1S |
| 17. TBCD | 36. RACGAP1 |
| 18. SAC3D1 | 37. KIF23 |
| 19. PCNT | 38. ESPL1 |



E



F



- | | | | |
|-----------------|-----------------|-------------------|-------------------|
| 1. <i>KIF2C</i> | 5. <i>AURKA</i> | 9. <i>NEK2</i> | 13. <i>PHKG2</i> |
| 2. <i>YBX2</i> | 6. <i>EZH2</i> | 10. <i>PCSK1N</i> | 14. <i>PCSK4</i> |
| 3. <i>CCNB2</i> | 7. <i>CNIH2</i> | 11. <i>CDKN3</i> | 15. <i>CRISP2</i> |
| 4. <i>BUB1</i> | 8. <i>CHFR</i> | 12. <i>CDK1</i> | 16. <i>MTOR</i> |

- | | | |
|-------------------|---------------------|-------------------|
| 1. <i>SLC7A5</i> | 19. <i>SCD</i> | 37. <i>ME1</i> |
| 2. <i>G6PD</i> | 20. <i>SRD5A1</i> | 38. <i>HSPA4</i> |
| 3. <i>BUB1</i> | 21. <i>MAP2K3</i> | 39. <i>AK4</i> |
| 4. <i>AURKA</i> | 22. <i>GAPDH</i> | 40. <i>GSR</i> |
| 5. <i>DDIT4</i> | 23. <i>IFRD1</i> | 41. <i>ACACA</i> |
| 6. <i>DDX39A</i> | 24. <i>DHCR24</i> | 42. <i>CALR</i> |
| 7. <i>ASNS</i> | 25. <i>P4HA1</i> | 43. <i>DDIT3</i> |
| 8. <i>CDC25A</i> | 26. <i>SQLE</i> | 44. <i>EIF2S2</i> |
| 9. <i>SHMT2</i> | 27. <i>NUP205</i> | 45. <i>LDLR</i> |
| 10. <i>TRIB3</i> | 28. <i>HMGCS1</i> | 46. <i>TMEM97</i> |
| 11. <i>NFKBIB</i> | 29. <i>SLC9A3R1</i> | 47. <i>PSPH</i> |
| 12. <i>SLC2A1</i> | 30. <i>ACLY</i> | 48. <i>PDK1</i> |
| 13. <i>TOMM40</i> | 31. <i>PHGDH</i> | 49. <i>ABCF2</i> |
| 14. <i>STIP1</i> | 32. <i>ARPC5L</i> | 50. <i>TFRC</i> |
| 15. <i>PSAT1</i> | 33. <i>PLK1</i> | 51. <i>SDF2L1</i> |
| 16. <i>TUBA4A</i> | 34. <i>STC1</i> | 52. <i>FADS2</i> |
| 17. <i>GPI</i> | 35. <i>PIK3R3</i> | 53. <i>UNG</i> |
| 18. <i>IFI30</i> | 36. <i>ADD3</i> | 54. <i>MLLT11</i> |

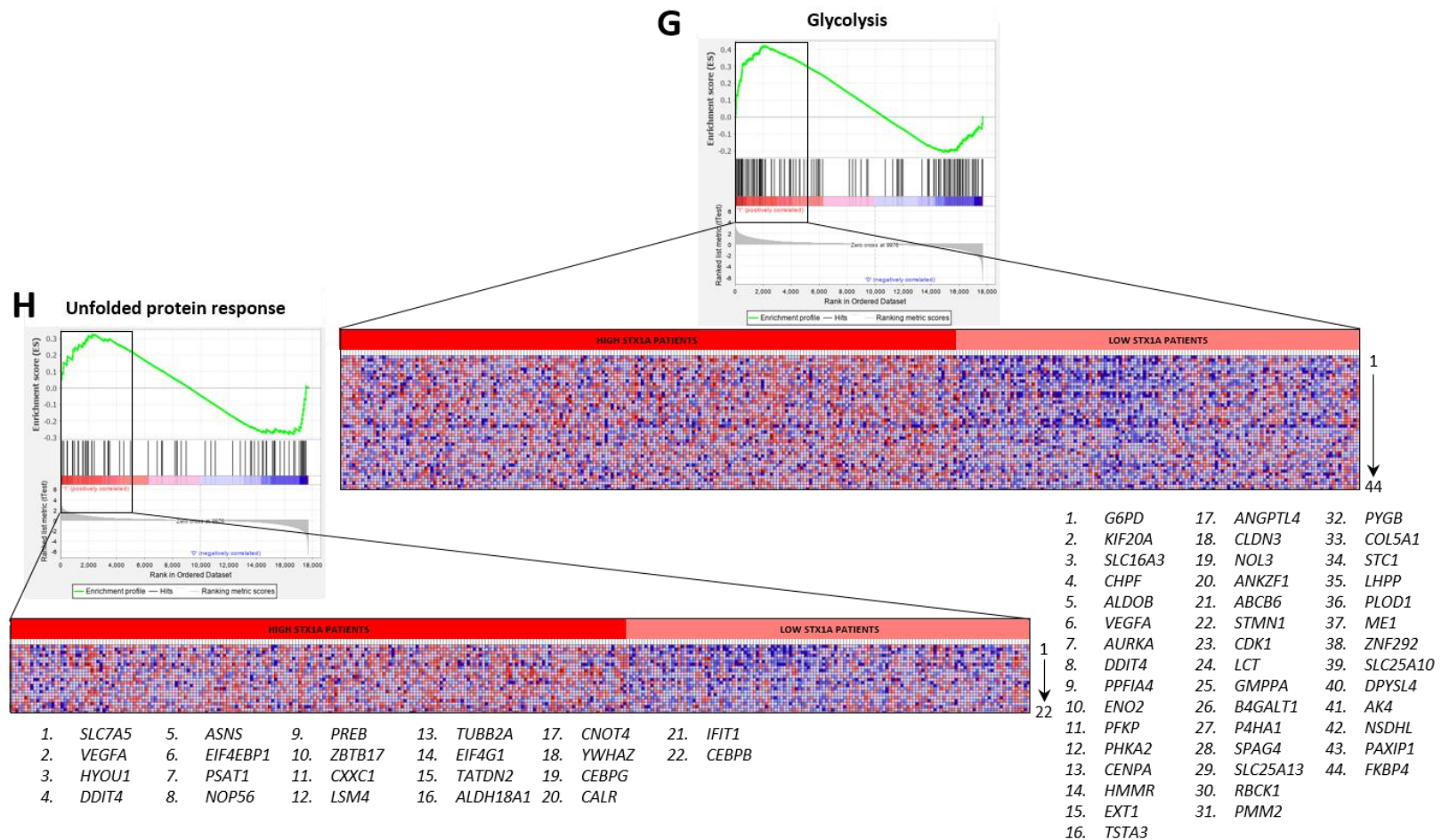
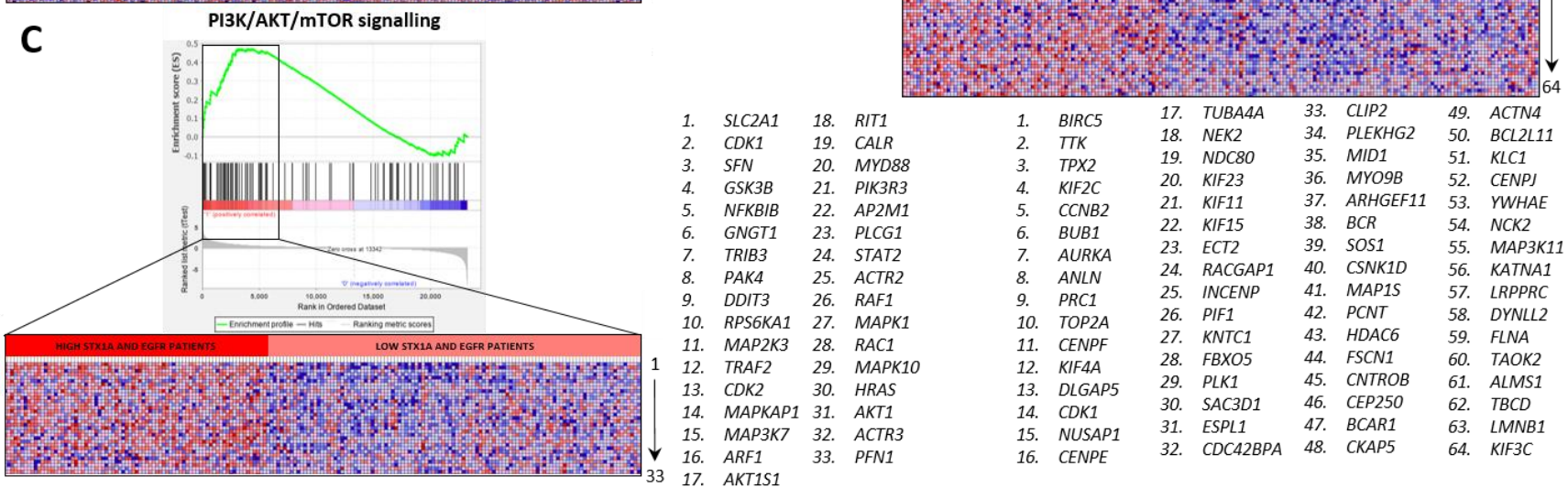
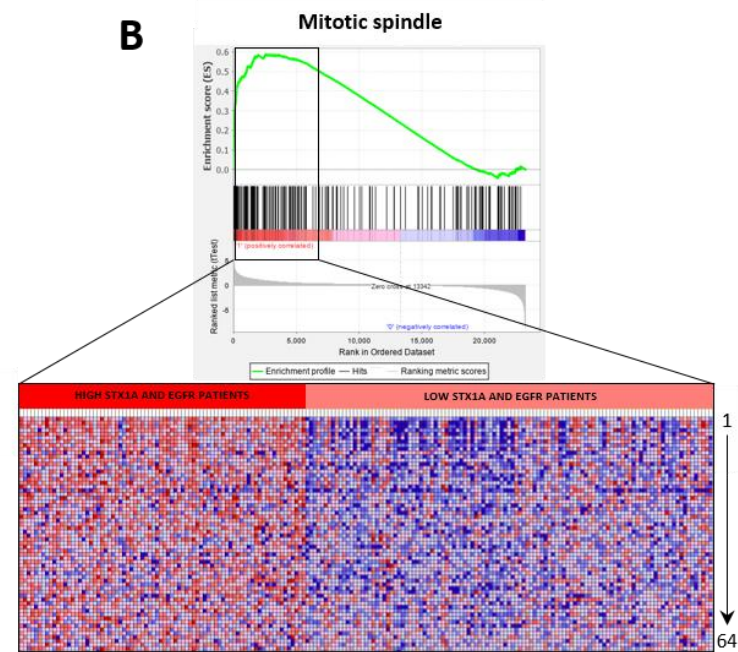
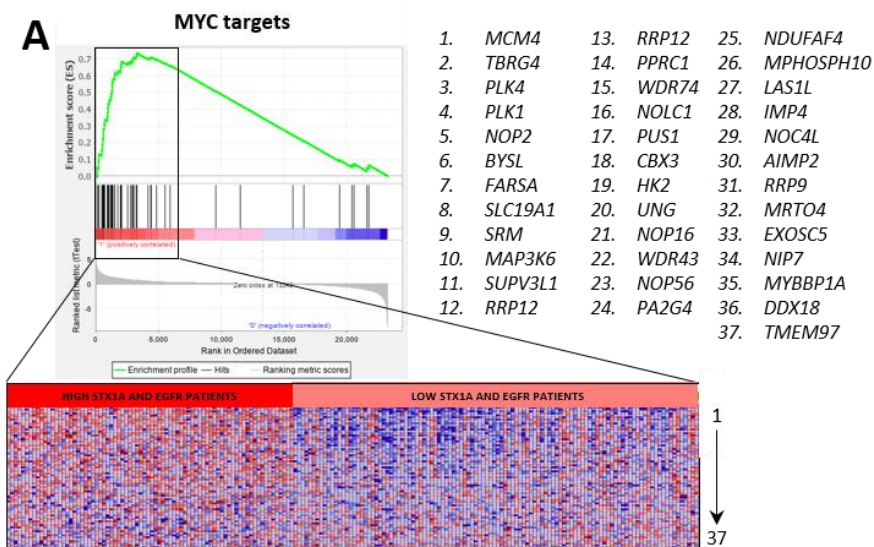


Figure 49 – Basal BC tumours with high levels of STX1A upregulate glycolysis and unfolded protein response signalling pathways. (A) GSEA of Mitotic spindle signalling pathway from STX1A^{HIGH} basal BC tumours. (B) GSEA of MYC targets (v2) from STX1A^{HIGH} basal BC tumours. (C) GSEA of PI3K/AKT/mTOR signalling pathway from STX1A^{HIGH} basal BC tumours. (D) GSEA of G₂/M checkpoint from STX1A^{HIGH} basal BC tumours. (E) GSEA of MTORC1 spindle signalling pathway from STX1A^{HIGH} basal BC tumours. (F) GSEA of Spermatogenesis from STX1A^{HIGH} basal BC tumours. (G) GSEA of glycolysis signalling pathway from STX1A^{HIGH} basal BC tumours. (H) GSEA of unfolded protein response from STX1A^{HIGH} basal BC tumours. On the bottom of each heat map, genes that are responsible for the up-regulation of these pathways.



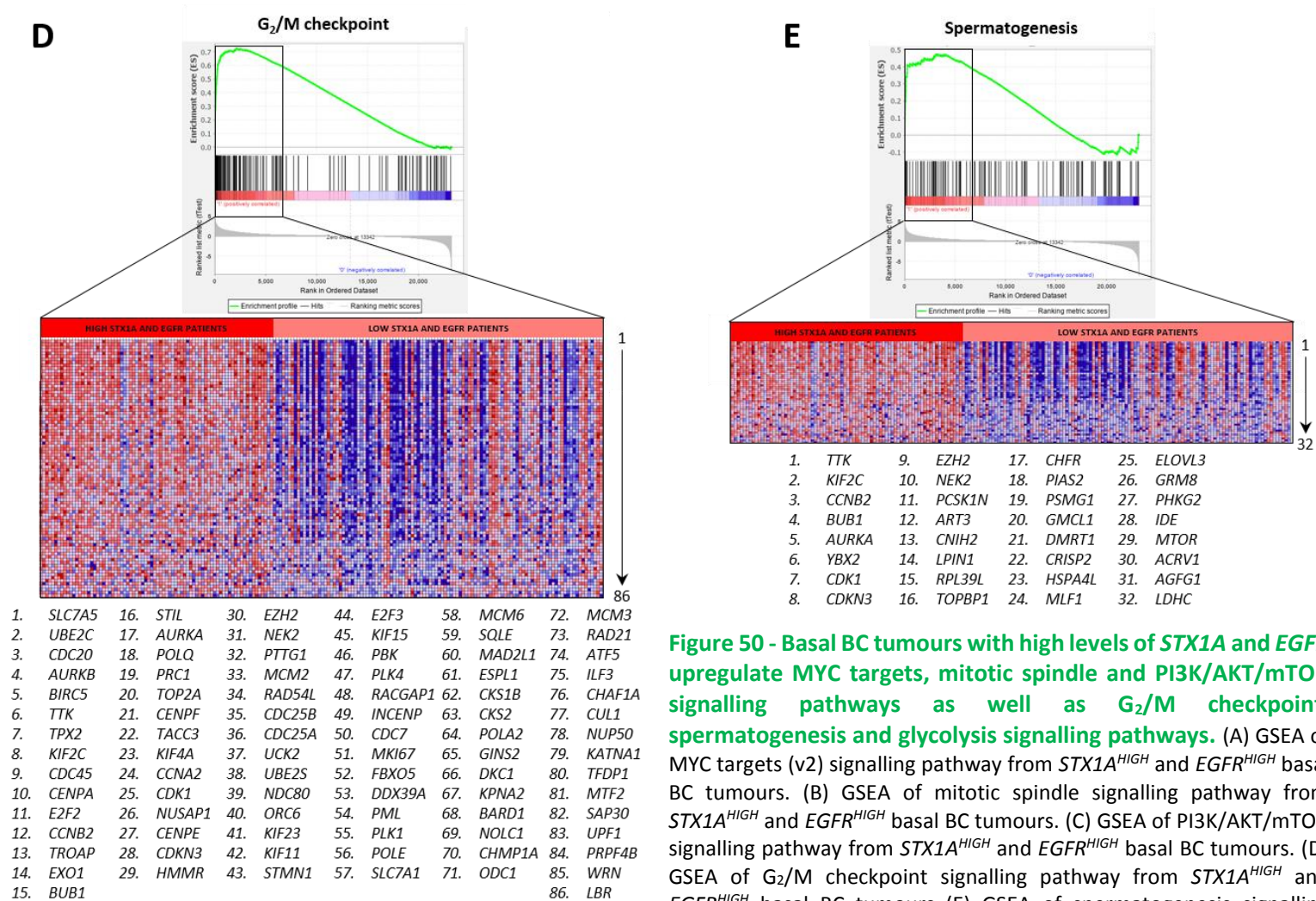


Figure 50 - Basal BC tumours with high levels of *STX1A* and *EGFR* upregulate *MYC* targets, mitotic spindle and *PI3K/AKT/mTOR* signalling pathways as well as *G₂/M* checkpoint, spermatogenesis and glycolysis signalling pathways. (A) GSEA of *MYC* targets (*v2*) signalling pathway from *STX1A*^{HIGH} and *EGFR*^{HIGH} basal BC tumours. (B) GSEA of mitotic spindle signalling pathway from *STX1A*^{HIGH} and *EGFR*^{HIGH} basal BC tumours. (C) GSEA of *PI3K/AKT/mTOR* signalling pathway from *STX1A*^{HIGH} and *EGFR*^{HIGH} basal BC tumours. (D) GSEA of *G₂/M* checkpoint signalling pathway from *STX1A*^{HIGH} and *EGFR*^{HIGH} basal BC tumours (E) GSEA of spermatogenesis signalling pathway from *STX1A*^{HIGH} and *EGFR*^{HIGH} basal BC tumours. On the bottom of each heat map, genes that are responsible for the up-regulation of these pathways.

1.3.4. SUMMARY OF THE RELATIONSHIP OF *SYNTAXIN-1A* EXPRESSION AND SYNTAXIN, SNARE AND EGFR/HER GENE EXPRESSION IN BC PATIENTS

After an exhaustive examination of the prognostic values of different Syntaxin, SNAREs and EGFR/HER gene expression in BC and their relationship with *STX1A* gene expression, all the important findings are summarized in [Table 35](#) and [Figure 51](#).

Highlighting the most important findings that were common between the three clusters studied (all BC subtypes, HER2-positive and HER2-negative subgroups) it was found that *STX1A* was a good overall survival biomarker considering that in all cases high expression of the gene conferred a poorer prognosis for BC patients, and also it was a good biomarker for distant metastasis free survival, where high expression of the gene conferred a worse prognosis. Then, if it was distinguished between tumours that expressed low levels of *STX1A* from the ones that expressed high levels, it was found that in all three groups *SNAP-23* and *VAMP-4* was overexpressed in tumours with low levels of *STX1A* and that *STX3* and *MUNC18-1* genes were up-regulated in high *STX1A* tumours. *SNAP-25*, *HER2* and *HER4* (only checked in HER2-positive and HER2-negative BC subgroups) were upregulated in tumours expressing high levels of *STX1A*.

Then, it was determined that low expression of *VAMP-2* conferred a worse prognosis in all the three clusters studied. After that, it was analysed if another SNARE-related or EGFR/HER family of receptors could increase the prognostic value. Among them, it was found that high expression of *STX1A* and *STX1B* and high expression of *STX1A* and low *VAMP-2* expression increased the overall survival of BC patients in all three groups of tumours studied. Finally, when it was checked if other genes could also predict metastasis free survival, it was found that high expression of *VAMP-2* and low expression of *HER4* correlated with poor metastasis free survival in HER2-positive and HER2-negative subgroups.

Table 35 – Summary of STX1A relationship with other syntaxin family, SNARE and EGFR/HER/ genes in BC prognosis. The table represents the several aspects discussed along the chapter regarding BC prognosis. It considers either all BC tumours, HER2-positive or HER2-negative BC tumours showing the overexpressed in HER2-positive and in HER2-negative BC subgroups (only for all BC tumours). It distinguishes for the genes overexpressed according to STX1A levels (low and high) and if the genes have an overall survival prognosis factor alone and in combination with STX1A expression (only represented the condition which confers a worse prognosis). Finally, if the genes inform of metastasis free survival prognosis (only represented the condition in which the prognosis is worse).

ALL BC TUMOURS						
HER2 status		STX1A status		Overall survival		Metastasis free survival (↓DMFS)
HER2-positive	HER2-negative	low STX1A	high STX1A	ALONE (↓OS)	+ OTHER SNAREs (↓OS)	
↑STX1A ↑STX3 ↑STX6 ↑VAMP-2 ↑VAMP-4 ↑SYT1 ↑STXBP2 ↑MUNC13	↑SNAP-23 ↑SNAP-25 ↑VAMP-1 ↑MUNC18-1	↑SNAP-23 ↑VAMP-2 ↑VAMP-4	↑STX3 ↑STX6 ↑SNAP-25 ↑CPLX1 ↑MUNC18-1 ↑STXBP2 ↑MUNC13	↑STX1A ↑STX3 ↑STX6 ↓SNAP-23 ↓VAMP-2 ↓CPLX1	↑STX1A + ↑STX1B ↑STX1A + ↓VAMP-2 ↑STX1A + ↓CPLX1	↑STX1A ↑STX2 ↑STX6 ↓VAMP-2 ↓STXBP2 ↑SYT1

HER2-POSITIVE BC SUBGROUP					HER2-NEGATIVE BC SUBGROUP				
STX1A status		Overall survival		Metastasis free survival (↓DMFS)	STX1A status		Overall survival		Metastasis free survival (↓DMFS)
low STX1A	high STX1A	ALONE (↓OS)	+ OTHER SNAREs (↓OS)		low STX1A	high STX1A	ALONE (↓OS)	+ OTHER SNAREs (↓OS)	
↑SNAP-23 ↑VAMP-2 ↑VAMP-4 ↑SYT1	↑STX2 ↑STX3 ↑SNAP-25 ↑VAMP-1 ↑MUNC18-1 ↑EGFR ↑HER2 ↑HER4	↑STX1A ↑VAMP-1 ↓VAMP-2 ↓VAMP-4 ↓MUNC13 ↑EGFR ↑HER4	↑STX1A + ↑STX1B ↑STX1A + ↑VAMP-1 ↑STX1A + ↓VAMP-2 ↑STX1A + ↓VAMP-4 ↑STX1A + ↓SYT1 ↑STX1A + ↓STXBP2 ↑STX1A + ↓MUNC13 ↑STX1A + ↑HER2 ↑STX1A + ↑HER4	↑STX1A ↓VAMP-2 ↓HER4	↑SNAP-23 ↑VAMP-4 ↑SYT1	↑STX3 ↑STX6 ↑STX17 ↑SNAP-25 ↑CPLX1 ↑MUNC18 ↑STXBP2 ↑MUNC13 ↑HER2 ↑HER4	↑STX1A ↓SNAP-23 ↓VAMP-2 ↓CPLX1 ↑EGFR	↑STX1A + ↑STX1B ↑STX1A + ↓SNAP-23 ↑STX1A + ↓VAMP-2 ↑STX1A + ↓CPLX1 ↑STX1A + ↓SYT1	↑STX1A ↑STX2 ↑STX6 ↓SNAP-23 ↓VAMP-2 ↑SYT1 ↓STXBP2 ↓EGFR ↓HER2 ↓HER3 ↓HER4

It was also analysed the differential expression of signalling pathways in *STX1A*^{HIGH} BC HER2-enriched and basal tumours by GSEA analysis. No differential pathways expression was found in *STX1A*^{HIGH} HER2-enriched BC tumours, but considering HER2 expression as well, it was found that G₂/M checkpoint and PI3K/AKT/mTOR signalling pathway were overactivated in HER2-enriched BC tumours. These two signalling pathways were also overactivated in *STX1A*^{HIGH} and *STX1A*^{HIGH}/*EGFR*^{HIGH} basal BC tumours. Moreover, in basal BC subtypes mitotic spindle, MYC target (v2), spermatogenesis, mTORC1, Glycolysis and unfolded protein response signalling pathway were overactivated in *STX1A*^{HIGH} basal BC tumours.

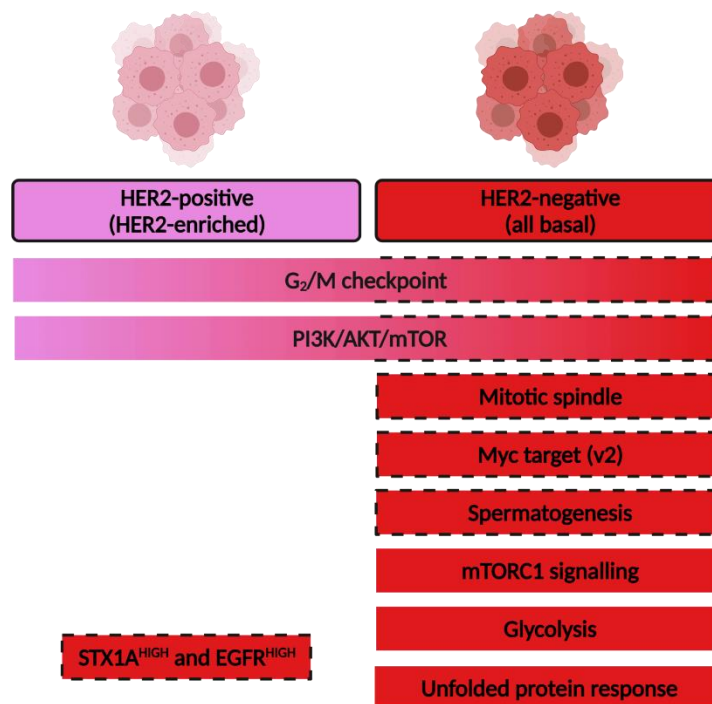


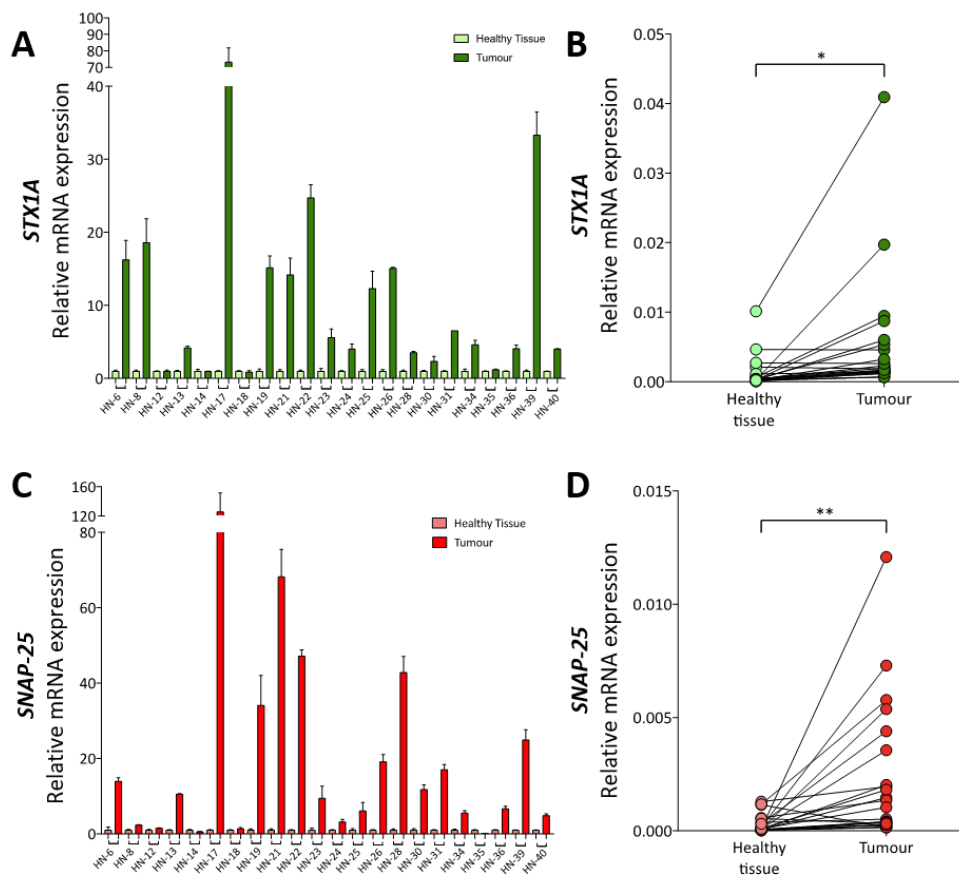
Figure 51 – GSEA common differential pathways in *STX1A*^{HIGH} BC tumours. Graphical representation of pathways differential expressed in *STX1A* and *HER2* high BC tumours, and in HER2-negative BC tumours with *STX1A* high and *EGFR* high (dotted line) tumours.

1.4. *SYNTAXIN-1A* IN HEAD AND NECK CANCER

1.4.1. *SYNTAXIN-1A* AND *SNAP-25* GENES ARE OVEREXPRESSED IN HEAD AND NECK TUMOURS

Throughout a collaboration with the Hospital Clínic de Barcelona otorhinolaryngologists we were able to obtain 22 clinical samples of paired healthy tissue and head and neck tumours. RNA from the tissues was extracted and analysed by q-PCR *STX1A* and *SNAP-25* mRNA expression within these tissues. The results, normalized with the healthy tissue, demonstrated that *STX1A* and *SNAP-25* were overexpressed in all tumour samples, in comparison to their corresponding surrounding healthy tissue (*Figure 52A and Figure 52C*). Moreover, grouping all

the samples of healthy tissue and all tumour samples and analysing *STX1A* or *SNAP-25* mRNA expression our findings were corroborated: in tumour samples *STX1A* and *SNAP-25* gene expression is overexpressed (Figure 52B and Figure 52D). *EGFR* is usually overexpressed in head and neck tumour samples, and since *STX1A* mRNA expression correlated with some those of *EGFR/HER* receptors in BC, *EGFR* expression was analysed in head and neck patient's tumour samples by q-PCR (Figure 52E). *EGFR* expression was higher in tumours than *STX1A* and *SNAP-25* expression, however, no statistically significant correlation was found in *STX1A/EGFR* or *SNAP-25/EGFR* correlation analysis (Table 36). Noteworthy, a strong correlation was found between *STX1A* mRNA levels and *SNAP-25* mRNA levels (Table 36).



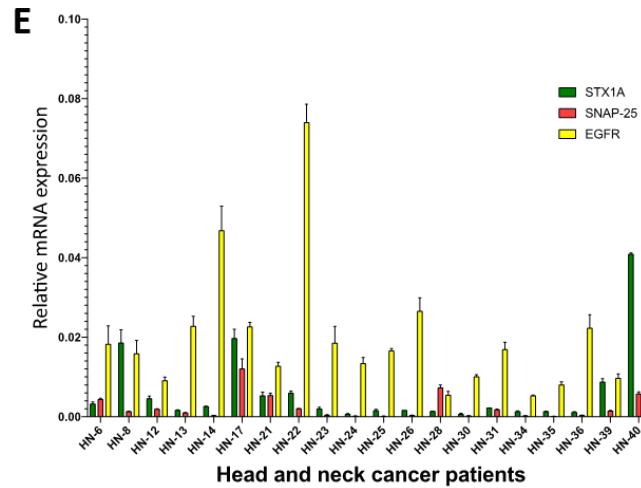


Figure 52 – Head and neck tumours overexpress *STX1A* and *SNAP-25* genes in comparison to surrounding healthy tissue. (A) Relative *STX1A* mRNA expression of Hospital Clínic de Barcelona HNSCC patients' cohort. Tumour samples (dark green) are relativized to its paired healthy tissue (light green). (B) *STX1A* mRNA expression comparison between all healthy patients' samples (light green) versus tumour patients' samples (dark green). (C) Relative *SNAP-25* mRNA expression of Hospital Clínic de Barcelona HNSCC patient's cohort. Tumour samples (dark red) are relativized to its paired healthy tissue (light red). (D) *SNAP-25* mRNA expression comparison between all healthy patients' samples (light red) versus tumour patients' samples (dark red). (E) *STX1A* (green), *SNAP-25* (red) and *EGFR* (yellow) mRNA expression among HNSCC patient tumours. Statistical analysis was performed using the paired t-test. * $p < 0.05$, ** $p < 0.01$, *** $p < 0.001$, **** $p < 0.000$.

Table 36 – *STX1A* correlates with *SNAP-25* expression. Pearson correlation among *STX1A*, *SNAP-25* and *EGFR* mRNA expression in tumour samples from Hospital Clínic cohort. Statistical analysis was performed using Spearman correlation.

	STX1A	SNAP-25
SNAP-25	$r = 1.000$ ($p > 0.000$)	
EGFR	$r = 0.033$ ($p = 0.887$)	$r = -0.04$ ($p = 0.863$)

1.4.2. HIGH SYNTAXIN-1A EXPRESSION CORRELATES WITH SHORTER RECURRENCE AND SPECIFIC OVERALL SURVIVAL AND *SNAP-25* EXPRESSION CORRELATES WITH LOCAL RECURRENCE

Thanks to another collaboration with the otorhinolaryngologists from the Hospital de la Santa Creu i Sant Pau (Barcelona), two different cohorts of HNSCC patients was studied. The first cohort, shown in [Figure 53](#) is from HNSCC patients that have undergone surgery and followed for 20 years. In this cohort, *STX1A* and *SNAP-25* mRNA expression levels were analysed by qPCR to determine if there was a correlation between these SNARE mRNA levels with HNSCC patient prognosis. Once the q-PCR for both genes in the several patients' tumour samples was performed, the expression of both genes was related to their clinical history. First of all, a decision tree was performed to see if it was possible to classify HNSCC patients

according to *STX1A* expression and vital status. The results clearly showed that it was possible to distinguish two groups of HNSCC patients, based on *STX1A* mRNA levels according to their vital status (Figure 53A). Then, these two groups were analysed if they had a prognostic power, and although it was not statistically significant ($p = 0.082$), patients with higher levels of *STX1A* had a clear tendency to a poorer specific overall survival (Figure 53B). Regarding *SNAP-25*, it was observed that it was possible to classify patients according to low and high *SNAP-25* mRNA expression levels and local recurrence (Figure 53C). The analysis of the Kaplan-Meier curve also determined that patients with low levels of *SNAP-25* had a significant ($p = 0.013$) increased risk of local recurrence in comparison to patients with high levels of *SNAP-25* (Figure 53D). Finally, it was also possible to classify head and neck tumours according to *SNAP-25* expression and distal metastasis (Annex figure 11A), although no statistical difference was shown in the metastasis-free survival curve (data not shown).

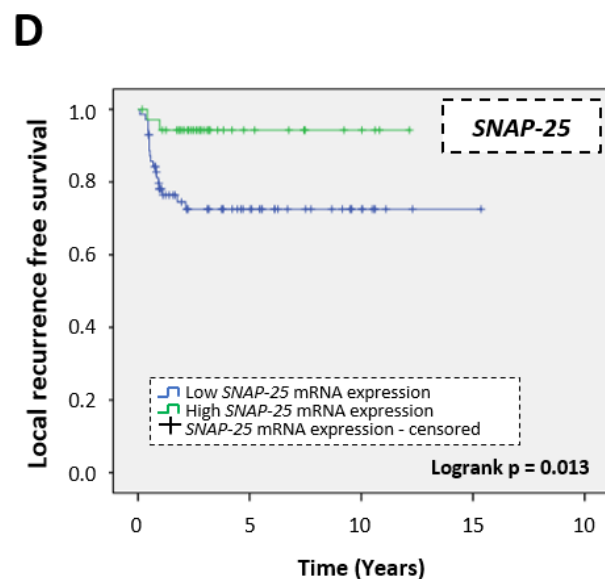
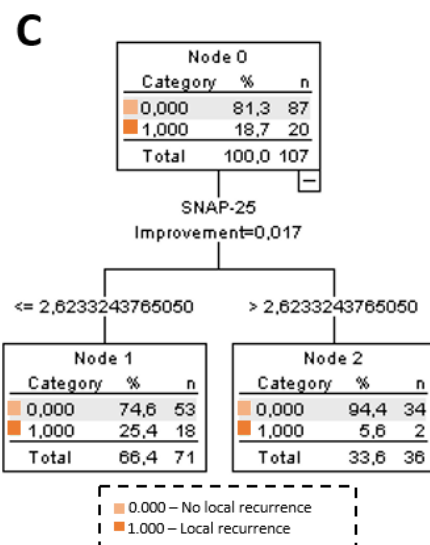
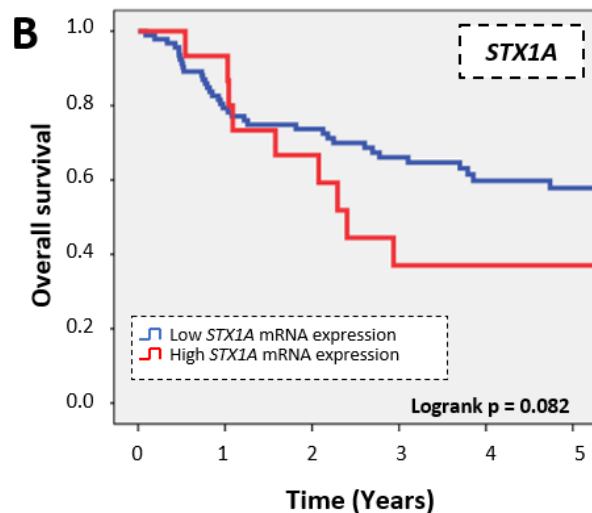
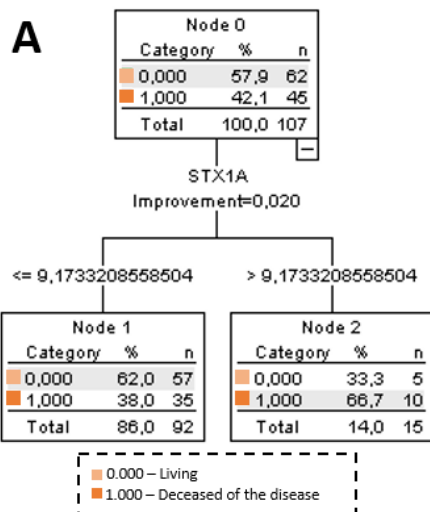
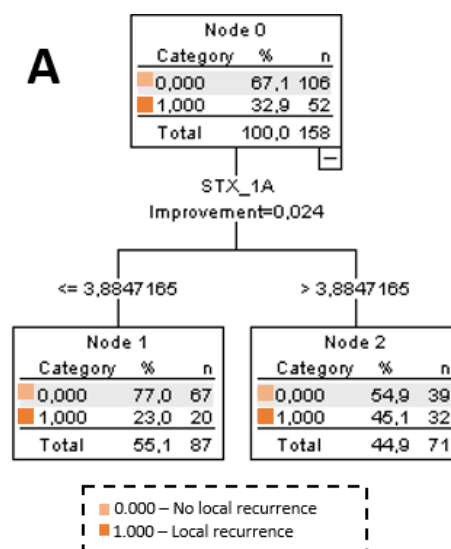


Figure 53- High *STX1A* mRNA expression correlates with poor specific overall survival and high *SNAP-25* mRNA expression correlates with worse local recurrence disease free survival in HNSCC patients. (A) Decision tree diagram that shows how relative *STX1A* mRNA expression is grouped according to the patient survival status (0: living, light orange and 1: deceased of the disease, dark orange) in HNSCC patients. (B) Overall survival Kaplan-Meier curve of HNSCC tumours grouped according to *STX1A* expression, grouped as shown in previous figure. (C) Decision tree diagram that shows how relative *SNAP-25* mRNA expression is grouped according to local recurrence status (0: no local recurrence, light orange and 1: local recurrence, dark orange) in HNSCC patients. (D) Local recurrence free survival Kaplan-Meier curve of HNSCC tumours grouped according to *SNAP-25* expression, grouped as shown in previous figure. Statistical analysis was performed by Chi-square test (A and C) and Logrank (B and D).

The second patient's cohort corresponded to HNSCC patients who were treated with radiotherapy or chemo-radiotherapy between 2004 and 2017. As in the previous cohort, *STX1A* and *SNAP-25* mRNA expression was determined. The analysis revealed that no differences in *STX1A* and *SNAP-25* mRNA levels between treatments. Then, patients were stratified by the decision tree algorithm, considering the tumour recurrence and *STX1A* or *SNAP25* expression, resulting in a significant stratification of HNSCC patients with *STX1A* levels of expression (*Figure 54A*), and no significant stratification for *SNAP-25* mRNA levels (*data not shown*). Considering these results, the analysis was only followed by the analysis of *STX1A*. The analysis of local recurrence free survival revealed that patients with high *STX1A* expression had a shorter recurrence free survival period (*Figure 54B*). Moreover, the analysis of its specific overall survival followed the same trend, patients with high levels of *STX1A* expression had poorer specific overall survival (*Figure 54C*).



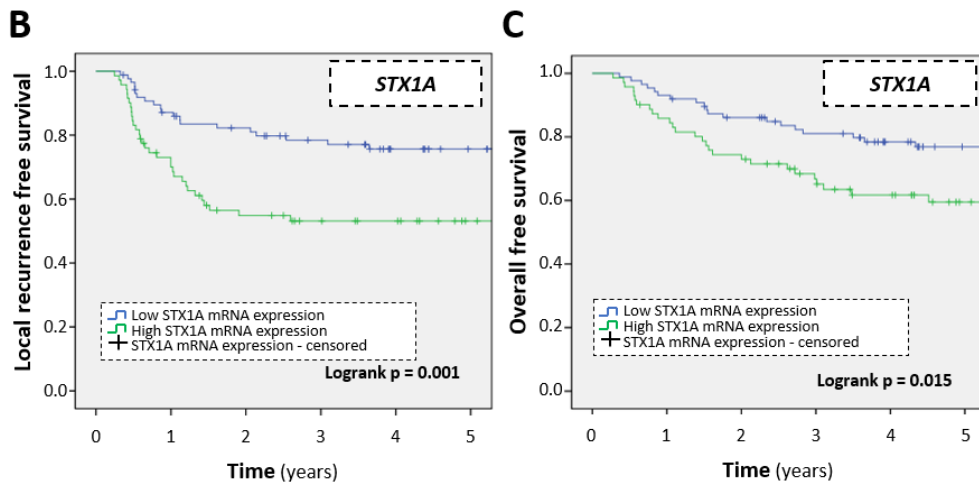
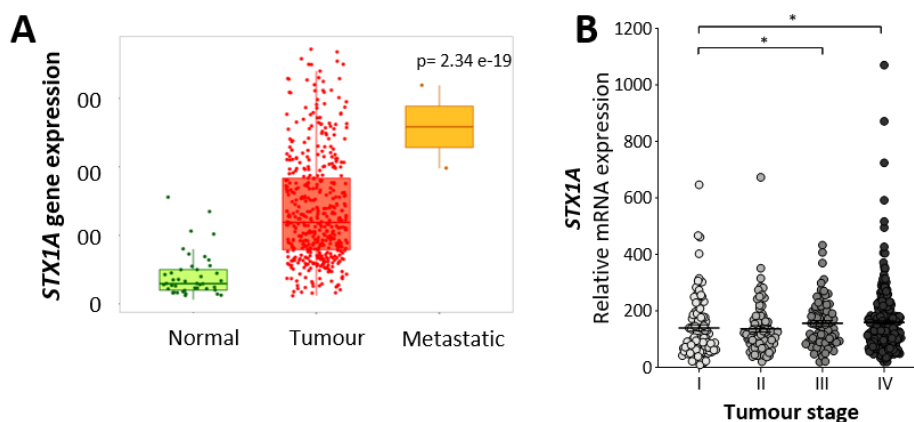


Figure 54 – *STX1A* expression correlates with a shorter recurrence free survival period and poorer specific overall survival in HNSCC patients. (A) Decision tree diagram that shows how relative *STX1A* mRNA expression is grouped according to the patient local recurrence status (0: no local recurrence, light orange and 1: local recurrence, dark orange) in HNSCC patients. (B) Local recurrence free survival Kaplan-Meier curve of HNSCC tumours grouped according to *STX1A* expression, grouped as shown in previous figure. (C) Specific overall survival of HNSCC tumours grouped according to *STX1A* expression. Statistical analysis was performed by Chi-square test (A) and Logrank (B and C).

1.4.3. HIGH *SYNTAXIN-1A* AND LOW *SNAP-25* GENE EXPRESSION CORRELATE WITH WORSE SPECIFIC OVERALL SURVIVAL

Finally, to increase the robustness of our findings in the different HNSCC cohorts two public HNSCC patient's database were analysed: TNM plot and TCGA. TNM plot corroborated the results found with Hospital Clínic cohort, by which head and neck tumour samples expressed higher levels of *STX1A* in comparison to healthy samples (*Figure 55A*). Data from metastatic samples was not considered due to there were only two samples.



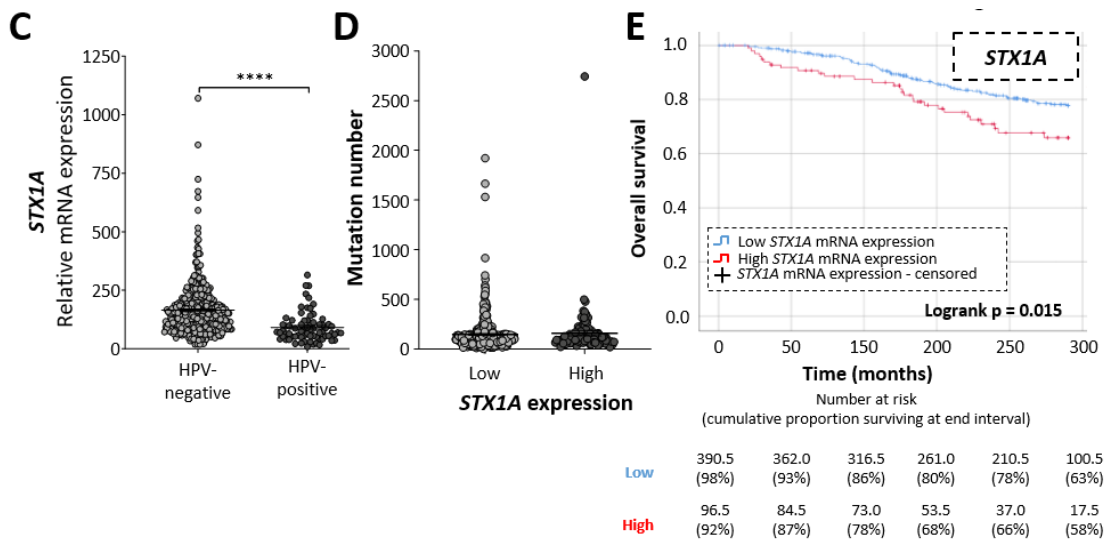


Figure 55 - Aggressive tumours overexpress *STX1A* and higher expression of *STX1A* is related to poor overall survival in HNSCC patients (TNM plot and TCGA public databases). (A) *STX1A* gene expression from healthy tissue, tumour and metastatic HNSCC. (B) Graphical representation of relative *STX1A* mRNA expression grouped into different neoplasm histologic grade. (C) Graphical representation of relative *STX1A* mRNA expression grouped according HPV status in HNSCC tumours. (D) Graphical representation of number of mutations per tumour grouped according to low or high levels of *STX1A*. (E) On the top, overall survival Kaplan-Meier curve of HNSCC tumours grouped according to *STX1A* expression. On the bottom survival table where the number at risk of HNSCC patients and the cumulative proportion surviving at the end of the interval in parenthesis is shown. Statistical analysis was performed by U-Mann-Whitney test and Kaplan Meier plots were analysed using Logrank test. * $p < 0.05$, **** $p < 0.000$.

Then, the TCGA public database was analysed, which collects more than 500 patients along with their clinical data and the genetic profile of their tumours. First of all, *STX1A* mRNA expression along the different tumour stages was checked (Figure 55B). An increase in *STX1A* mRNA expression was found as the tumour stage increases (I: $M = 139.200$, $SEM = 10.970$; II: $M = 136.400$, $SEM = 11.200$, III: $M = 156.300$, $SEM = 9.502$, IV: $M = 159.400$, $SEM = 7.280$). Then, considering that head and neck tumours are only subclassified according to HPV status, *STX1A* mRNA levels in both HNSCC subtypes was characterized (Figure 55C), which resulted that there was an increase of *STX1A* expression in HPV-negative head and neck subtypes in comparison to HPV-positive subtype ($M = 164.900$, $SEM = 5.566$ and $M = 91.540$, $SEM = 7.386$, respectively). Also, no difference was found determining the mutation number between low and high *STX1A* expression HNSCC tumours ($M = 147.200$, $SEM = 9.100$ and $M = 158.900$, $SEM = 27.44$, respectively) (Figure 55D). Moreover, it was investigated if, as in BC, high expression of *STX1A* correlated with a worse overall survival. To do that, two groups of tumours according to *STX1A* expression and the life status of the patients were established (Annex figure 11B). The analysis of the Kaplan-Meier graph showed that patients within the high *STX1A* expression group had a poorer 2-year overall survival than patients within the low *STX1A* expression group ($p = 0.015$) (Figure 55E). Difference in disease free survival were also analysed, but

STX1A expression did not show any prognostic value in this parameter ($p=0.746$) (*Annex figure 11C*).

As it was previously done with the Hospital Clínic HNSCC cohort, correlation between the expression of *STX1A* and *SNAP-25* and *EGFR* in the TCGA database was analysed. the positive correlation between *STX1A* and *SNAP-25* ($r = 0.107$) was corroborated while no correlation among *STX1A* and *EGFR* or *SNAP-25* and *EGFR* was found (*Table 37*); similarly, to data for the Hospital Clínic cohort. Therefore, *SNAP-25* expression was analysed in HNSCC as it was done for *STX1A*. As in Hospital Clínic HNSCC patient cohort, *SNAP-25* was overexpressed in tumours in comparison to healthy tissues. Although data from metastasis were also available, it was not considered because there were only two samples (*Figure 56A*). Analysing the TCGA database, *SNAP-25* expression did not differ along the tumour stages and no differences were detected between both HNSCC subtype (*Annex figure 12A and Annex figure 12B*). After differentiating two subgroups of tumours according *SNAP-25* expression (*Annex figure 12C*), it was analysed if there was any difference in number of mutations per tumours according to *SNAP-25* expression levels. It resulted that *SNAP-25* low expressing tumours displayed an increased mutation number, in comparison to tumours with high expression of *SNAP-25* (*Figure 56B*). Then, overall survival by a Kaplan-Meier curve was analysed and found no difference in overall survival according to *SNAP-25* gene expression levels ($p = 0.123$) (*Figure 56C*). Also, there were no differences in terms of disease-free survival ($p = 0.450$) (*Annex figure 12D*). Finally, when jointly considering *STX1A* and *SNAP-25* levels, in an attempt to increase the prediction power of *STX1A* in overall survival (*Figure 56D*), it was observed that patients with tumours with high levels of *STX1A* and low levels of *SNAP-25* had a poorer overall survival ($p = 0.001$) (*Figure 56D*). The same was done for disease free survival, but no statistical difference was found jointly analysing *STX1A* and *SNAP-25* mRNA expression (*Annex figure 12E*).

Table 37 - *STX1A* correlates with *SNAP-25* expression in HNSCC patients TCGA database. Spearman correlation among *STX1A*, *SNAP-25* and *EGFR* mRNA expression in tumour samples from HNSCC patients database.

	<i>STX1A</i>	<i>SNAP-25</i>
<i>SNAP-25</i>	$r = 0.107$ ($p = 0.015$)	
<i>EGFR</i>	$r = -0.10$ ($p = 0.813$)	$r = 0.014$ ($p = 0.759$)

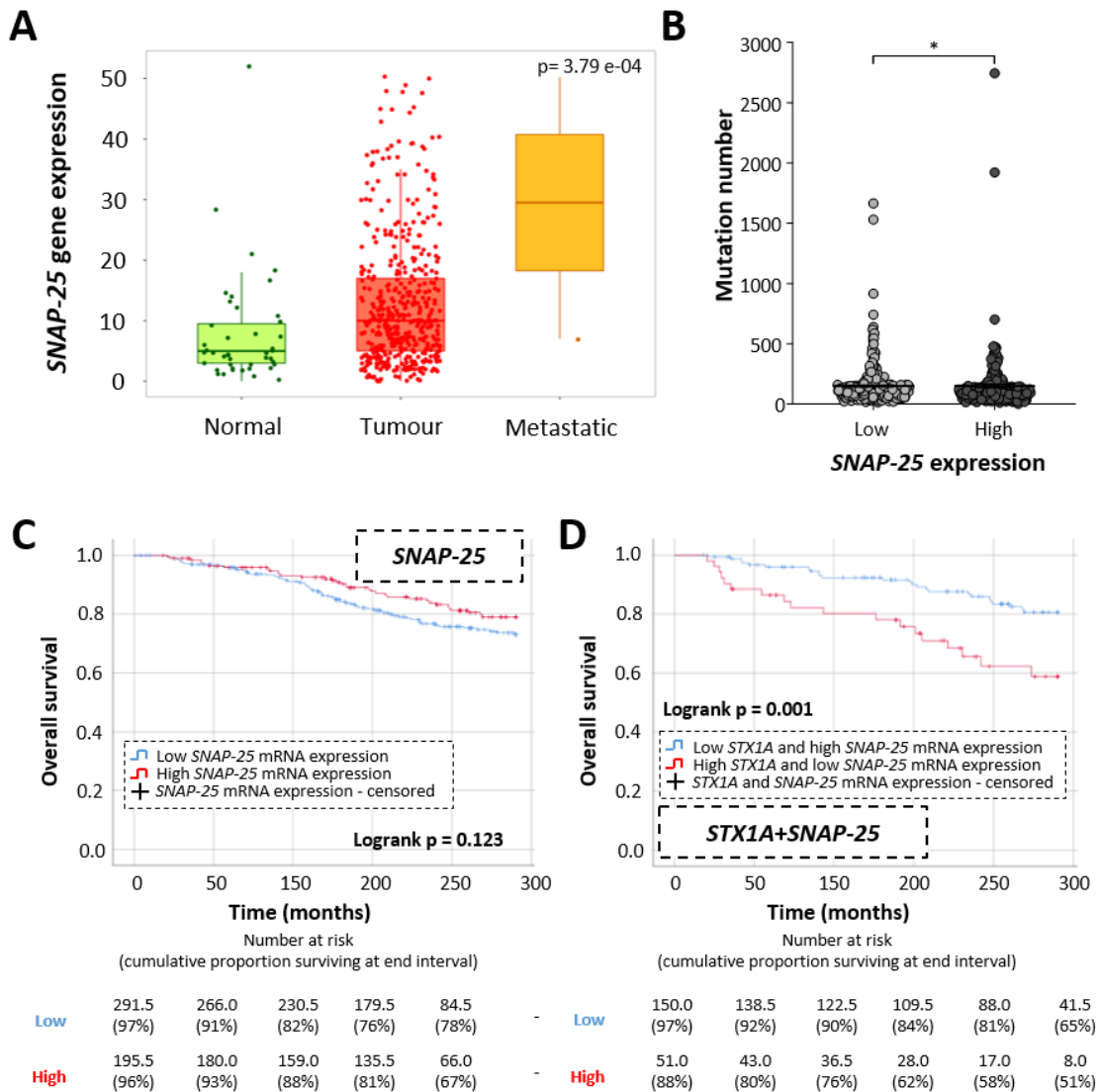


Figure 56 - High *STX1A* and low *SNAP-25* gene expression is related to poor overall survival in HNSCC patients (TNM plot and TCGA public databases). (A) *STX1A* gene expression from healthy head and neck tissue, tumour and metastatic HNSCC. (B) Graphical representation of number of mutations per tumour grouped in HNSCC tumours that did express low or high levels of *STX1A*. (C) On the top, overall survival Kaplan-Meier curve of HNSCC tumours grouped according to *SNAP-25* expression. On the bottom survival table where is shown the number at risk of HNSCC patients and the cumulative proportion surviving at the end of the interval in parenthesis. (D) On the top, overall survival Kaplan-Meier curve of HNSCC tumours grouped according to *STX1A* and *SNAP-25* expression. On the bottom survival table where is shown the number at risk of HNSCC patients and the cumulative proportion surviving at the end of the interval in parenthesis. Statistical analysis was performed by U-Mann-Whitney test and Kaplan Meier plots were analysed using Logrank test. * $p < 0.05$.

Altogether, our results in HNSCC patients demonstrate that *STX1A* and *SNAP-25* are overexpressed in HNSCC tumours, in comparison to healthy surrounding tissue. Also, the analysis of these neurogenes correlate high expression of *STX1A* or high expression of *SNAP-25* as predictors of local recurrence, while high expression of *STX1A* and low expression of *SNAP-25* are predictors of poor overall survival.

2. SYNTAXIN-1A CHARACTERIZATION IN BREAST AND HEAD AND NECK CANCER CELL LINES

Once confirmed that STX1A conferred a worse prognosis in BC and also in HNSCC based on patients' databases, we wanted to go further and study the mechanisms by which STX1A could contribute to BC and HNSCC progression. To do so, an online public database was interrogated, the Cancer Cell Line Encyclopedia (CCLE, The Broad Institute of MIT & Harvard), which has RNA-seq data from a wide panel of cancer cell lines. The wide panel of BC cell lines representative of BC subtypes and HNSCC cell lines available in our laboratory were also used. The essential step in this chapter is to assess and confirm our panel of cancer cell lines as good *in vitro* models for further studying the role of STX1A in BC and HNSCC.

2.1. SYNTAXIN-1A AND RELATED PROTEINS CHARACTERIZATION IN BREAST CANCER CELL LINES

2.1.1. SYNTAXIN-1A IS OVEREXPRESSED IN HER2-POSITIVE BREAST CANCER CELL LINES

First of all, *STX1A* expression in the online public database CCLE was analysed. Affymetrix data from *STX1A* gene in all cancer cell lines of the database was downloaded, however it was only used the BC cell lines. BC cell lines were grouped according to HER2 expression (HER2-positive and HER2-negative) and it resulted that HER2-positive BC cell lines overexpressed *STX1A* (Figure 57A) as it was previously demonstrated in BC tumours in other patients' public databases. Then, the focus was put on the BC cell lines available in our laboratory. *STX1A* expression was characterized at the mRNA level in our wide panel of BC cell lines classified according to their molecular profile: MCF-10A (non-transformed mammary epithelial cell); SK-BR-3, MDA-MB-453, HCC1954 (HER2-positive/HER2-enriched) BT-474 (HER2-positive/luminal B); T-47D, ZR-75-1 and MCF-7 (HER2-negative/luminal A,); MDA-MB-468, BT-549, MDA-MB-231, HCC70, Hs 578T (HER2-negative/ basal) (Figure 57B). The results showed that except for HCC1954, HER2-positive BC cell lines have higher *STX1A* mRNA levels, whereas most of the HER2-negative BC cell lines had similar or lower levels of *STX1A* to MCF-10A cells. Considering HER2 receptor status (HER2-positive and HER2-negative) there were no significant differences between both BC subtypes, when considering all BC cell lines (Figure 57C). However, MDA-MB-231 BC cell line (basal BC subtype, HER2-negative) displayed the highest *STX1A* expression of all BC cell lines, more than 4.5 times than the highest HER2-positive cell line. Therefore, if MDA-MB-231 BC cells were excluded, then HER2-positive BC cell lines overexpressed *STX1A* in comparison to HER2-negatives (Figure 57D), confirming the pattern previously seen in BC patients and cancer cell databases.

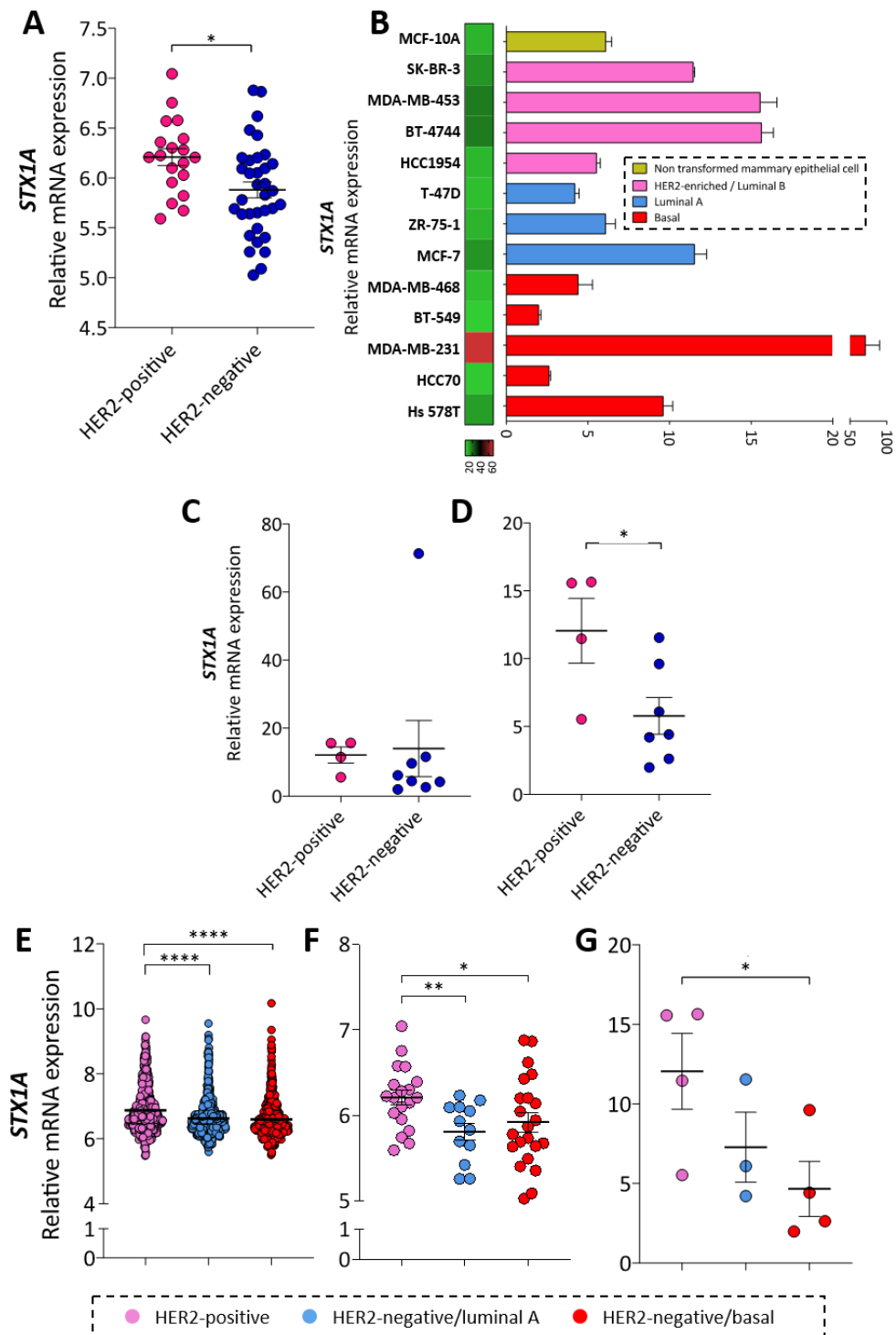


Figure 57 – *STX1A* is overexpressed in HER2-positive BC cell lines and BC tumours. (A) *STX1A* relative mRNA expression in CCLE database grouped according HER2-positive and HER2-negative subgroups. (B) On the left, heat map of *STX1A* expression of each BC cell line. On the right, representation in columns of *STX1A* mRNA relative expression in each BC cell line. (C) *STX1A* relative mRNA expression of lab BC cell lines grouped according HER2-positive and HER2-negative BC subgroup. (D) *STX1A* relative mRNA expression of lab BC cell lines, without considering the outlier MDA-MB-231, grouped according HER2-positive and HER2-negative BC subgroup. (E) *STX1A* relative mRNA expression in METABRIC BC patient database grouped according HER2-positive, HER2-negative/luminal A and HER2-negative/basal subgroups. (F) *STX1A* relative mRNA expression in CCLE database grouped according HER2-positive, HER2-negative/luminal A and HER2-negative/basal subgroups. (G) *STX1A*

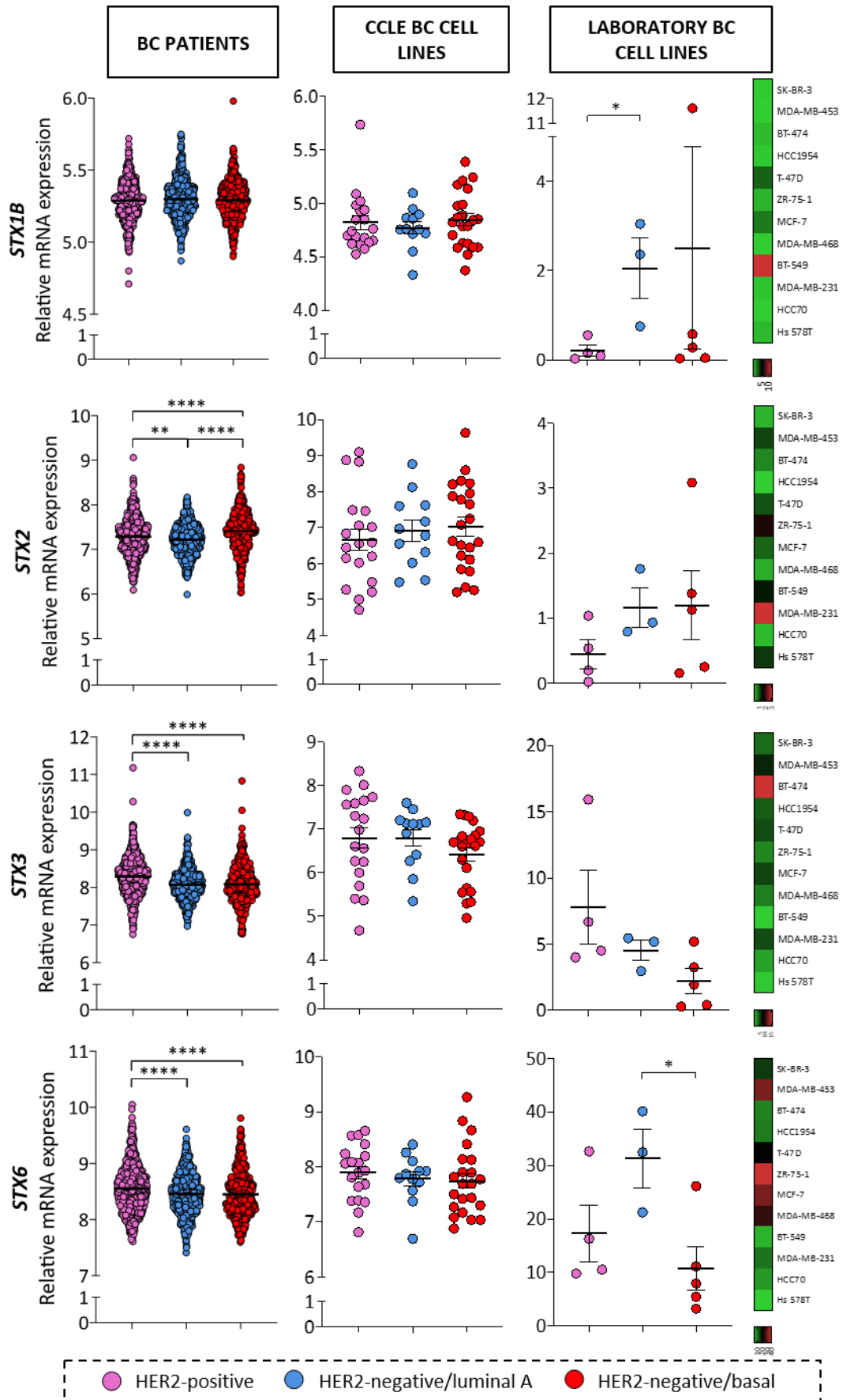
relative mRNA expression of lab BC cell lines, without considering the outlier MDA-MB-231, grouped according HER2-positive, HER2-negative/luminal A and HER2-negative/basal subgroups. Representative results of n=3 independent experiments performed in sextuplicate (qPCRs). Data presented as mean \pm SEM. Statistical analysis was performed using the U-Mann Whitney test for analysis of databases and Student's *t*-test for the statistic of lab BC cell lines. * $p < 0.05$, ** $p < 0.01$, **** $p < 0.000$.

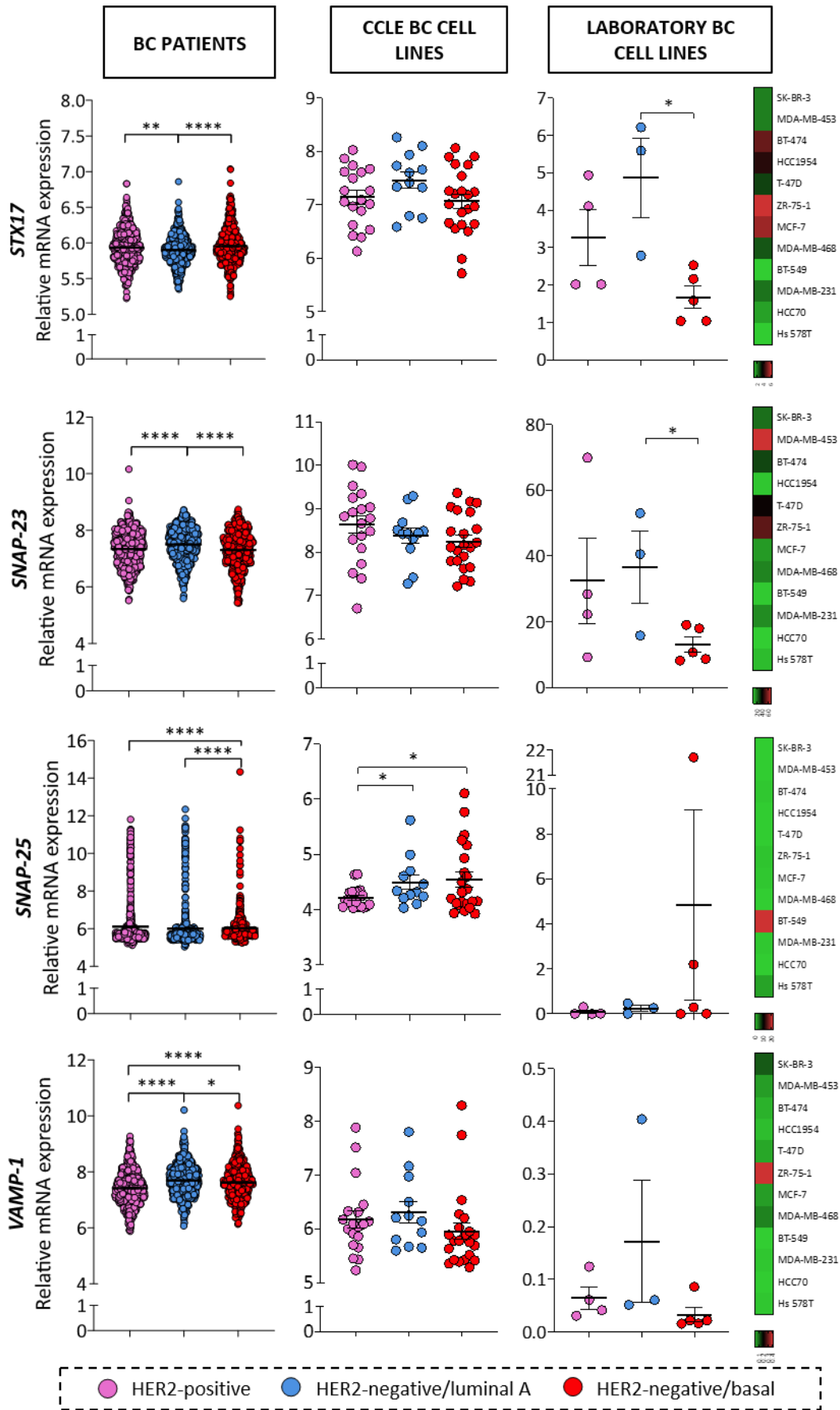
Then, taking into account that Luminal A and basal subtypes were included together in the HER2-negative subgroup and that, at the end, they were two complete clinically different BC subtypes which could lead us to misinterpretation of some data, *STX1A* expression was re-analysed considering three different subgroups: HER2-positive (HER2-enriched and luminal B BC subtypes), HER2-negative/luminal A and HER2-negative/basal BC subgroup (*Figure 57E-Figure 57G*). The re-analysis of the data resulted in an overexpression of *STX1A* in HER2-positive BC subtypes in comparison to the other two groups in METABRIC patient's database, and the same happened when analysing *STX1A* expression in CCLE database (*Figure 57F*). However, in our panel of BC cell lines it was only found that *STX1A* was overexpressed in HER2-positive BC cell lines in comparison to HER2-negative/basal BC cell lines. Even that, in HER2-negative/luminal A there was a clear tendency to express less *STX1A* levels in comparison to HER2-positive BC cell lines (*Figure 57G*).

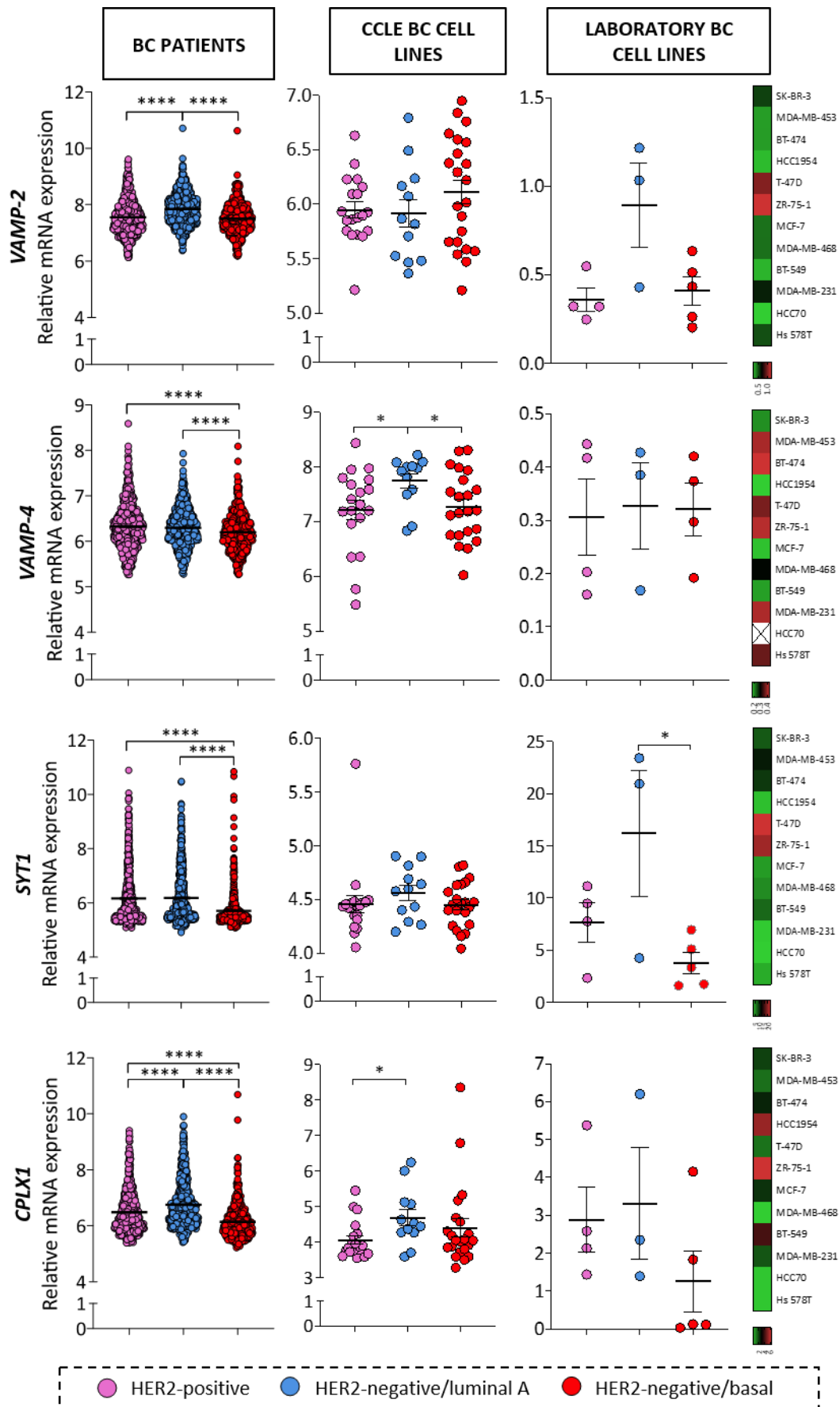
Altogether, this analysis indicate that BC cell lines resemble what it is found in BC patients' database, and also, that the BC cell lines that we have in our lab also recapitulate the *STX1A* expression pattern shown in patients and in cancer cell databases.

2.1.2. OTHER SNARES ARE DIFFERENTIALLY EXPRESSED AMONG BREAST CANCER SUBGROUPS

As it was previously done in BC patients database, the expression of other SNARE proteins in BC cell lines was also checked to confirm if they were a good model to continue the study of SNARE proteins in BC. First, the expression data available in CCLE of our genes of interest was analysed. Syntaxin and SNARE related genes expression was analysed considering two groups: HER2-positive and HER2-negative groups. The mRNA expression comparison with both groups resulted that only both SNAP-25 and STXB2 genes were overexpressed in HER2-negative BC subgroups (*Annex figure 13*). Then the same screening was performed in our wide panel of BC cell lines (*Annex figure 14*). There were no statistical differences, however some tendencies were detected.







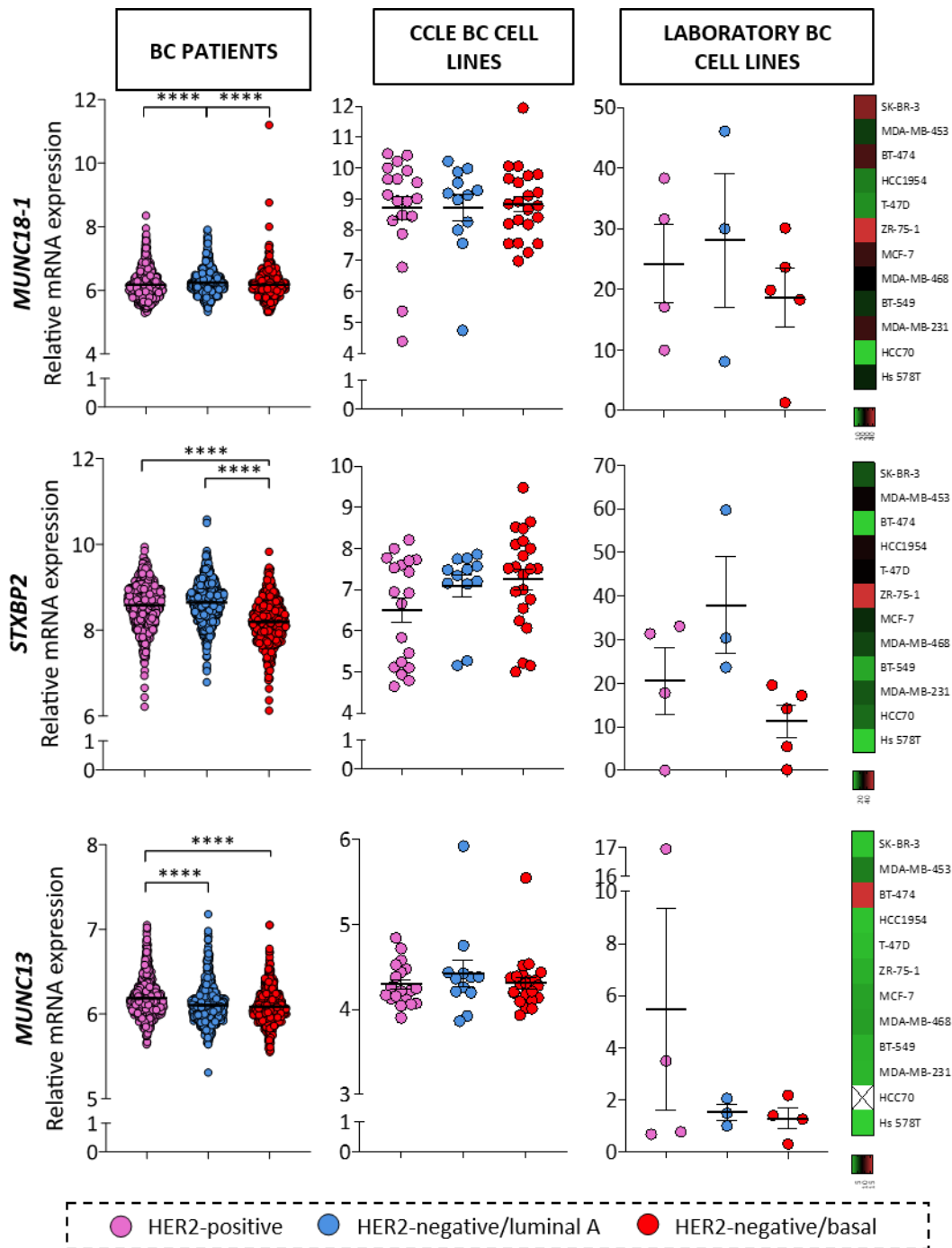


Figure 58 – Several Syntaxin and SNARE related genes are differentially expressed among BC subtypes. On the left, Syntaxin and SNARE related genes expression in METABRIC BC patients classified according to HER2-positive, HER2-negative/luminal A and HER2-negative/basal. In the middle, relative mRNA expression of the different genes in the BC CCLE database classified in the same subgroups. On the right, relative mRNA expression of Syntaxin and SNARE related genes in our lab BC cell lines classified in the same three BC subgroups and its correspondent heat map. Representative results of n=2 independent experiments (right panel) performed in sextuplicate. Data presented as mean \pm SEM. Statistical analysis was performed using the U-Mann Whitney test for analysis of databases and one-way ANOVA Sidak's test for the statistics of BC cell lines. *p<0.05, **p<0.01, **** p<0.0001.

Then, HER2-negative BC cell lines were divided between HER2-negative/luminal A and HER2-negative/basal and the expression of the Syntaxin and SNARE genes were analysed. First

BC tumours from METABRIC patients' databases were analysed (*Figure 58, left column*), but considering that there was a high amount of data, the results were summarized in *Table 38*. Briefly, *STX3*, *STX6* and *MUNC13* were overexpressed in HER2-positive BC subtypes; *SNAP-23*, *VAMP-1*, *VAMP-2*, *CPLX1* and *MUNC18-1* were overexpressed in HER2-negative/luminal A BC subgroup whereas *STX17* is under-expressed in this same BC subgroup. *STX2* was overexpressed in HER2-negative/basal BC subgroup and *VAMP-4*, *SYT1* and *STXBP2* were under-expressed in this subgroup.

Table 38 – Summary of the expression of Syntaxin and SNARE genes among BC subtypes in METABRIC BC patients. Mean and SEM, in parenthesis, of the relative mRNA Expression of the different Syntaxin and SNARE genes among BC subgroups (HER2-positive, HER2-negative/luminal A and HER2-negative/basal) and the BC subgroup where the particular gene is **overexpressed** or under-expressed.

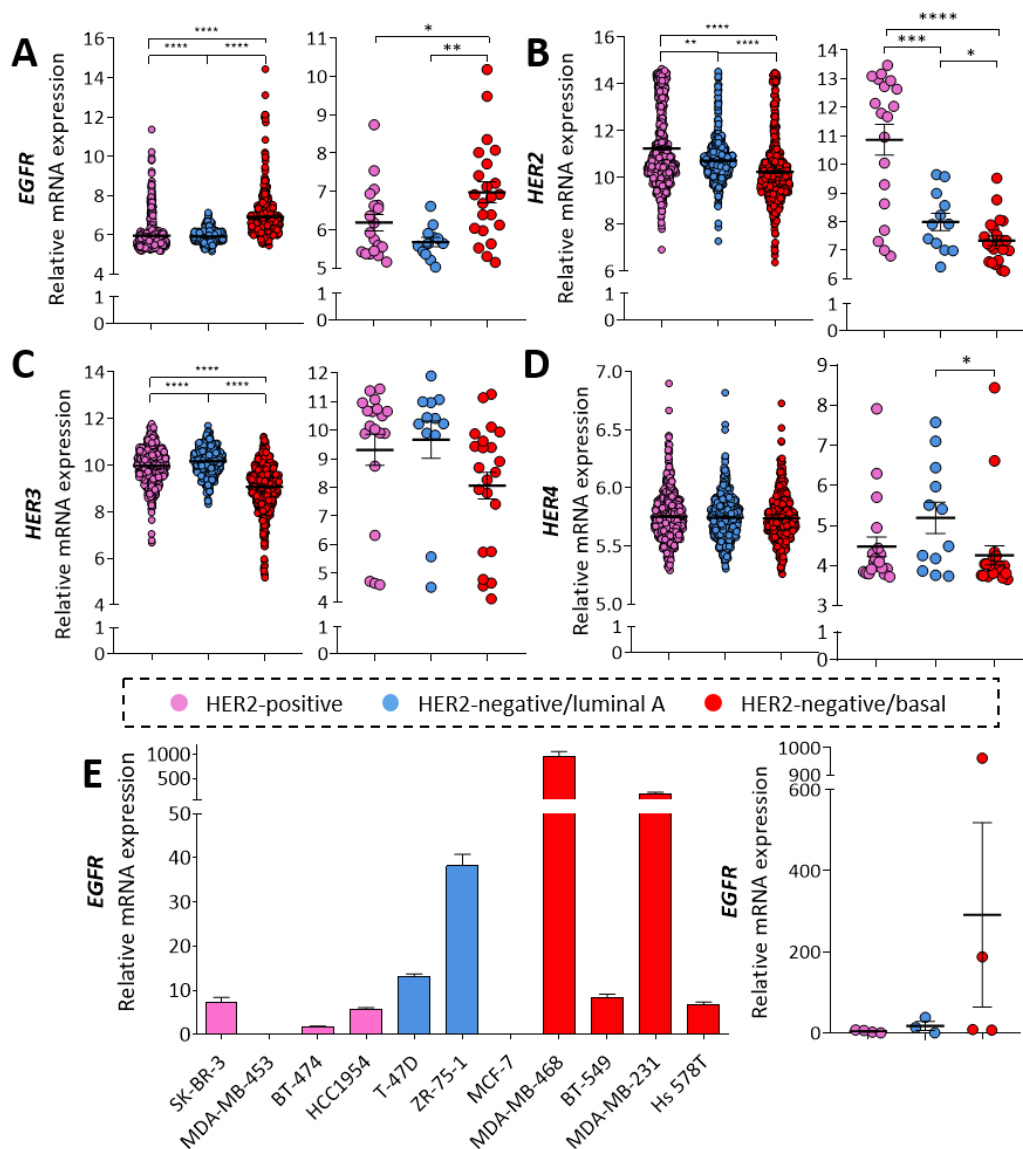
	HER2-positive	HER2-negative/luminal A	HER2-negative/basal	Differential expression
<i>STX1B</i>	5.288 (0.005)	5.298 (0.005)	5.292 (0.006)	No difference
<i>STX2</i>	7.288 (0.016)	7.218 (0.001)	7.409 (0.018)	Higher expression in basal > HER2-positive>luminal A
<i>STX3</i>	8.287 (0.019)	8.066 (0.014)	8.085 (0.020)	Overexpressed in HER2-positive
<i>STX6</i>	8.553 (0.015)	8.456 (0.013)	8.449 (0.017)	Overexpressed in HER2-positive
<i>STX17</i>	5.935 (0.009)	<u>5.903 (0.008)</u>	5.954 (0.011)	Underexpressed in HER2-negative/luminal A
<i>SNAP-23</i>	7.340 (0.023)	7.503 (0.021)	7.304 (0.027)	Overexpressed in HER2-negative/luminal A
<i>SNAP-25</i>	6.109 (0.047)	6.008 (0.042)	6.025 (0.035)	Underexpressed in HER2-negative/basal
<i>VAMP-1</i>	<u>7.418 (0.022)</u>	7.689 (0.020)	7.618(0.026)	Higher expression in luminal A >basal> HER2-positive
<i>VAMP-2</i>	7.550 (0.023)	7.847 (0.020)	7.499 (0.022)	Overexpressed in HER2-negative/luminal A
<i>VAMP-4</i>	6.325 (0.020)	6.298 (0.016)	<u>6.200 (0.017)</u>	Underexpressed in HER2-negative/basal
<i>SYT1</i>	6.165 (0.037)	6.181 (0.036)	<u>5.708 (0.028)</u>	Underexpressed in HER2-negative/basal
<i>CPLX1</i>	6.484 (0.028)	6.753 (0.030)	6.137 (0.025)	Higher expression in luminal A> HER2-positive>basal
<i>MUNC18-1</i>	6.176 (0.017)	6.241 (0.014)	6.175 (0.019)	Overexpressed in HER2-negative/luminal A
<i>STXBP2</i>	8.585 (0.019)	8.649 (0.017)	<u>8.198(0.002)</u>	Underexpressed in HER2-negative/basal
<i>MUNC13</i>	6.187 (0.009)	6.104 (0.008)	6.085 (0.009)	Overexpressed in HER2-positive

Considering that with the subclassification more differences among subgroups raised, the data from CCLE database was re-analysed (*Figure 58 middle column*). With this new distribution *SNAP-25* was found to be under-expressed in HER2-positive BC subgroups in comparison to both HER2-negative subgroups as it was previously described (*Annex figure 13*). Also, *VAMP-4* was overexpressed in HER2-negative/luminal A BC subgroup and *CPLX1* has higher expression in luminal A BC subtype comparing to HER2-positive subtype. Finally, re-analysing the mRNA expression of Syntaxins and SNARE gene expression of the laboratory BC cell lines *STX1B* was found to be underexpressed in HER2-positive subgroup compared to HER2-negative/luminal A. *STX6*, *STX17*, *SNAP-23* and *SYT1* had higher expression in HER2-negative/luminal A than HER2-negative/basal BC subgroup (*Figure 58 left column*).

After analysing all the Syntaxin and SNARE related genes it was detected that not all these genes followed the same trend when they were compared among the different data sources (BC patients data, BC cell lines from CCLE database and lab BC cell lines). However, even though most of the significant differences found in BC patients were not present when analysing BC cell lines, in some cases it is seen that the expression of certain Syntaxins and SNARE genes follows the same tendency. Among all, *STX1A* was the only one that was overexpressed in all the cohorts studied and overexpressed in the HER2-positive subgroup in comparison to HER2-negative subgroup (luminal A and basal), therefore our study was followed by mainly focusing on *STX1A*.

EGFR/HER family of receptors was also analysed in the METABRIC, CCLE database and in our panel of BC cell lines. First, *EGFR* was found to be overexpressed in HER2-negative BC cell lines while *HER2* and *HER3* were overexpressed in HER2-positive BC subtypes (*Annex figure 15, left column*). In contrast, in CCLE database analyses only *HER2* was found to be overexpressed in HER2-positive BC subgroup (*Annex figure 15*). As it was done for Syntaxin and SNARE gene expression HER2-negative BC subgroup was subdivided into two subgroups (HER2-negative/luminal A and HER2-negative/basal). The analysis of BC tumours revealed that EGFR receptor was overexpressed in HER2-negative/basal BC tumours, *HER2* overexpressed in HER2-positive tumours and *HER3* was overexpressed in HER2-negative/luminal A tumours (*Figure 59A-Figure 59D left graphs*). Then, analysing CCLE expression in these three BC subgroups, *EGFR* was overexpressed in HER2-negative/basal BC cell lines, *HER2* in HER2-positive BC cell lines and *HER4* was overexpressed in HER2-negative/luminal A BC cell lines (*Figure 59A-Figure 59D right graphs*). Then, focusing in our panel of BC cell lines, *EGFR* mRNA expression was analysed (*Figure 59E*). There were no statistical differences of *EGFR* expression

among HER2-positive and HER2-negative/luminal A or HER2-negative/basal BC subtypes, probably due to the high variability of *EGFR* expression in HER2-negative BC cell lines (Figure 59E). Then, focusing in the four receptors of the EGFR/HER family in HER2-positive BC cell lines, all receptors were found to be expressed and *HER2* receptor was clearly overexpressed in comparison to the others receptors of the family (Figure 59F). Then, the correlation between *STX1A* and EGFR/HER family of receptors in HER2-positive BC cell lines was analysed (Table 39), however, no correlation was found. Only a positive correlation between *EGFR* and *HER2* and a negative between *HER4* and *EGFR* and *HER2* were detected.



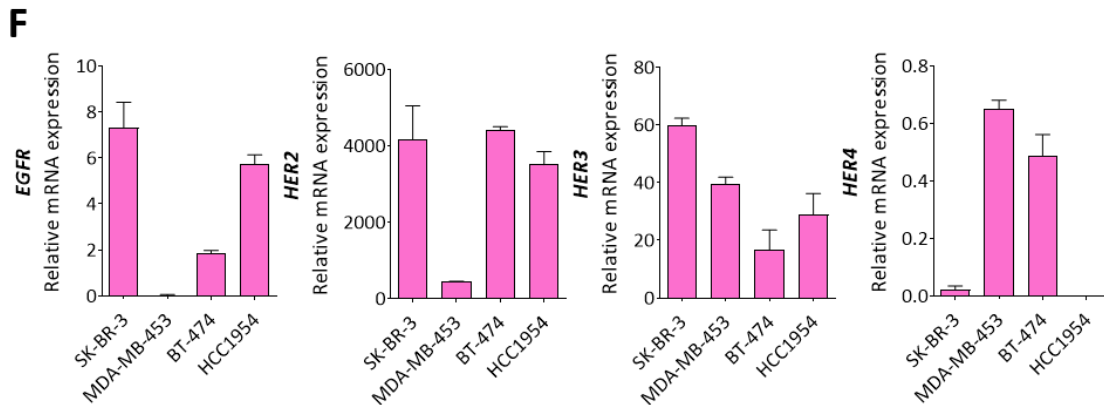


Figure 59 – EGFR/HER2 family of receptors expression in BC cell lines. (A-D) Left graphic, analysis of relative *EGFR* (A), *HER2* (B), *HER3* (C), *HER4* (D) expression in HER2-positive and HER2-negative BC tumours in METABRIC cohort. Right graphic, analysis of relative *EGFR* (A), *HER2* (B), *HER3* (C), *HER4* (D) expression in HER2-positive and HER2-negative BC cell lines in CLLE database (E) Left graphic, relative mRNA *EGFR* expression in our panel of BC cell lines. Right panel, mRNA *EGFR* expression of BC cell lines according to *HER2* expression. (F) Relative mRNA expression of *EGFR*, *HER2*, *HER3* and *HER4* in HER2-positive BC cell lines. Representative results of n=1 independent experiments (E and F) performed in sextuplicate. Data presented as mean ± SEM. Statistical analysis was performed using the U-Mann Whitney test for analysis of databases and one-way ANOVA test for the statistic of BC cell lines. *p<0.05, **p<0.01, ***p<0.001, **** p<0.000.

Table 39 – *STX1A* does not correlate with EGFR/HER mRNA expression. Pearson correlation analysis of *STX1A* and EGFR/HER family gene expression. The significant values (2-tailed) are highlighted in bold.

		<i>STX1A</i>			
<i>EGFR</i>	Correlation	0.488			
	p	0.512			
<i>HER2</i>	Correlation	0.468	0.996		
	p	0.532	0.004	<i>HER2</i>	
<i>HER3</i>	Correlation	-0.421	0.398	0.358	
	p	0.579	0.602	0.642	<i>HER3</i>
<i>HER4</i>	Correlation	-0.379	-0.981	-0.993	-0.379
	p	0.621	0.019	0.007	0.621

Finally, the expression of all genes and their possible relationship was analysed. To do that a bivariate analysis of the mRNA expression of each gene was performed and the Spearman correlation coefficient was performed between the BC cell lines from the CCLE database (Annex table 4). All significant expression correlation is shown in Figure 60. Among all the interactions we would like to highlight that *STX1A* correlated positively with *HER2* and *STX6*, which at the same time correlated positively between them. Then, focusing on these two genes (*HER2* and *STX6*) they both correlated positively with *HER3* and *STX3* and negatively with *STX2* and *EGFR*. Interestingly, all the correlations involving *EGFR* were negative correlations, except the correlation with *STXBP1*.

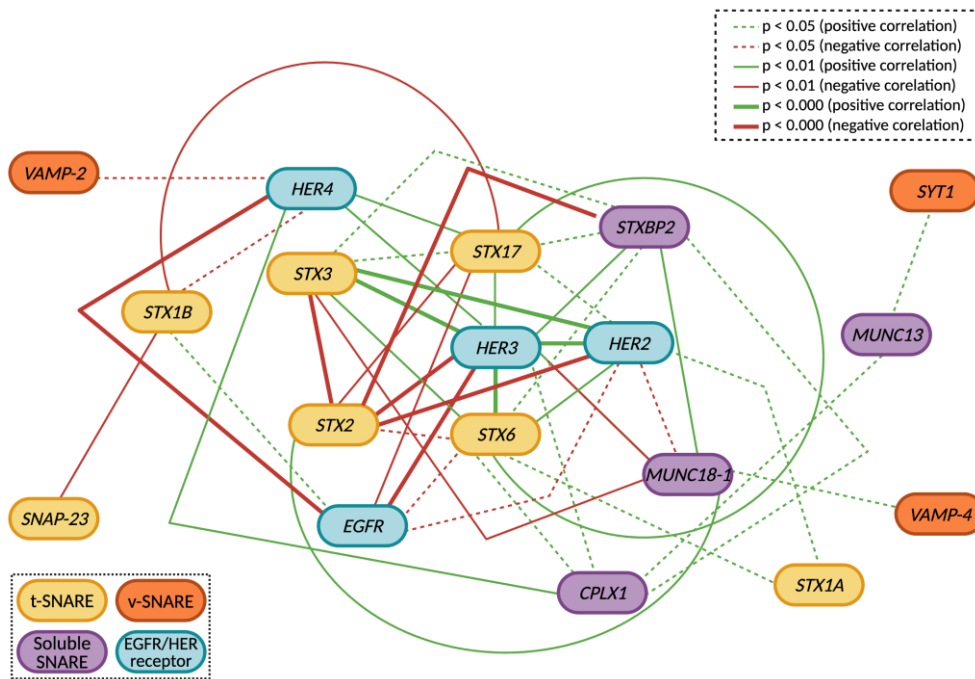


Figure 60 - Correlation and relationships among Syntaxin, SNARE and EGFR/HER family of receptors in all CCLE BC cell lines database. Graphical representation of positive and negative relationship among Syntaxin, SNARE and EGFR/HER family of receptors genes expression of CCLE BC cell lines database. The correlation values used are the Spearman correlation values from *Annex table 4*.

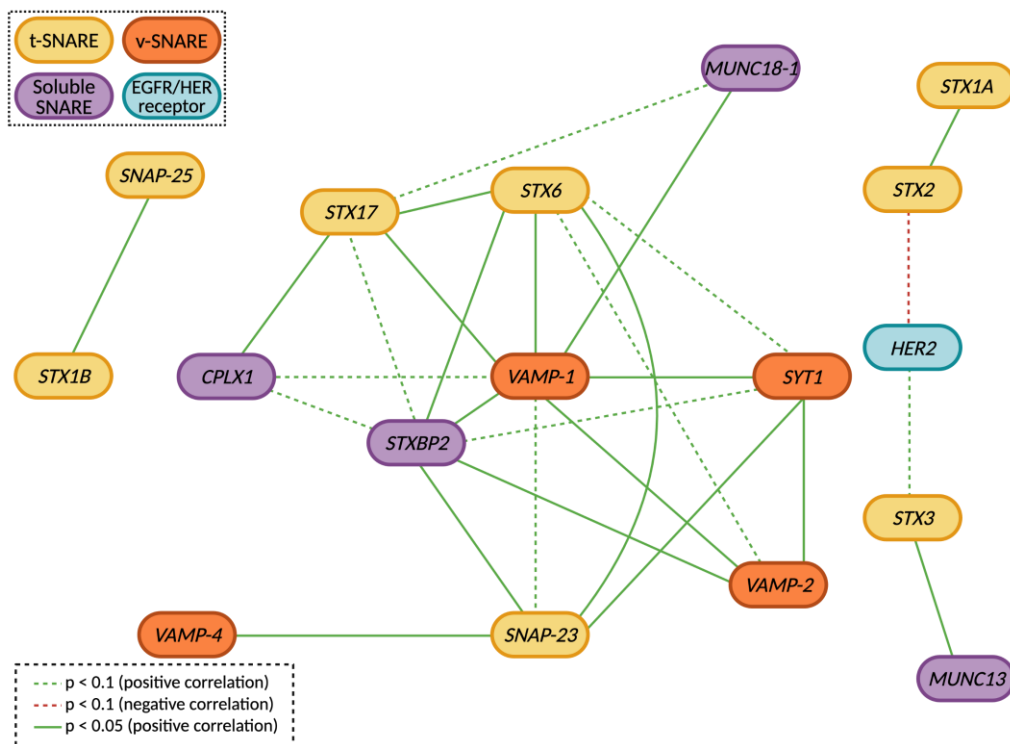


Figure 61 - Correlation and relationships among Syntaxin, SNARE and EGFR/HER family of receptors in our panel of BC cell lines. Graphical representation of positive and negative relationship among Syntaxin, SNARE and EGFR/HER family of receptors (only in HER2 positive BC cell

lines) genes expression of lab BC cell lines. The correlation values used are the Pearson correlation values from [Annex table 5](#).

Then, the same was done with the expression data from our lab BC cell lines. The Pearson correlation coefficient and its significance are shown in [Annex table 5](#). All the significant correlations found among them are depicted in Figure 61. Focusing on STX1A, it correlated positively with STX2 which in turn negatively correlated with HER2. It is important to note that this correlation is only determined in the HER2-positive BC cell lines of our lab. HER2 also correlates positively with STX3, similarly to data from CCLE BC cell lines. STX3 in turn positively correlated with MUNC13 in our BC cell lines.

2.1.3. SYNTAXIN-1A IS LOCALIZED INTO THE SMALL CLUSTERS IN BREAST CANCER CELL LINES

After confirming the *STX1A* overexpression in HER2-positive BC cell lines, to follow the study of *STX1A* role in BC, we had to narrow the number of BC cell lines that we were using. To do that, three HER2-positive BC cell lines (SK-BR-3, MDA-MB-453 and BT-474), two HER2-negative/luminal A BC cell lines (T-47D and ZR-75-1) and three HER2-negative/basal BC cell lines (MDA-MB-468, BT-549 and MDA-MB-231) were selected and protein expression of these cells was analysed. First, regarding *STX1A* protein expression ([Figure 62A](#)), there was higher expression in HER2-positive BC cell lines subgroup, even though it did not reach statistical significance ([Figure 62B left graphic](#)). Classifying *STX1A* expression in HER2-positive, HER2-negative/luminal A and HER2-negative/basal, *STX1A* was found under-expressed in luminal A subgroup of BC cell lines although it did not reach statistical significance either ([Figure 62B right graphic](#)). We were analysing MDA-MB-231 to have a higher number of cell lines, however considering that it had the highest expression of *STX1A*, it should be considered as an outlier, as previously did. MUNC18-1 protein expression was also analysed considering that this protein modulates *STX1A*, and SNAP-23 after seeing that it is down-regulated at mRNA levels in HER2-negative/basal BC cell lines ([Figure 58](#)). Focusing on MUNC18-1 protein expression ([Figure 62A](#)), no differences between HER2-negative and HER2-positive and no differences were neither detected among HER2-positive, HER2-negative/luminal A and HER2-negative/basal subgroups were detected ([Figure 62C](#)). Finally, SNAP-23 protein levels determination ([Figure 62A](#)) resulted in an overexpression of this protein in HER2-positive BC subgroup ([Figure 62D](#)).

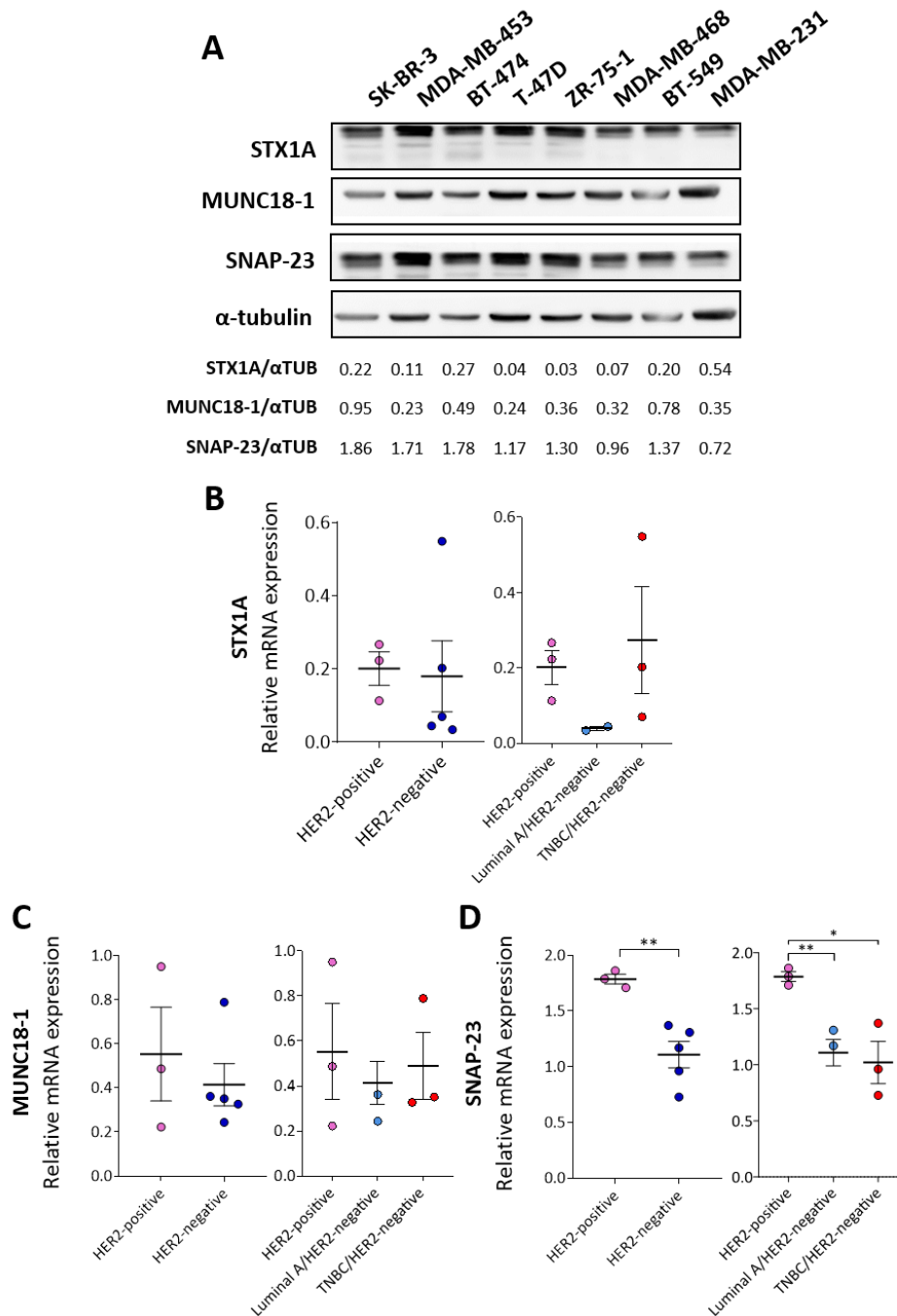
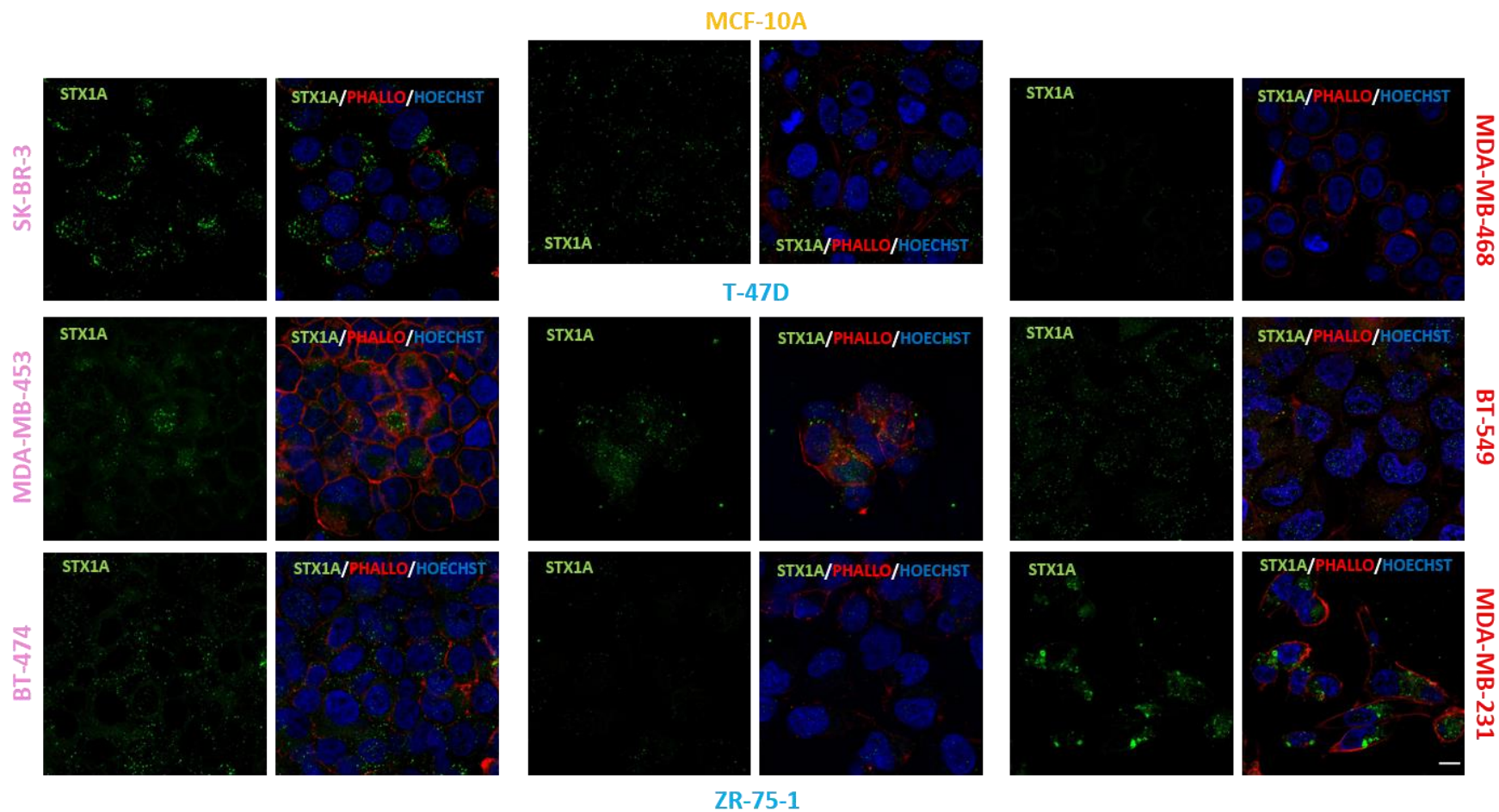


Figure 62 –SNAP-23 is upregulated in HER2-positive BC cell lines at protein levels. (A) Western blot analysis of STX1A expression among BC cell lines. α -tubulin was used as the internal control. On the bottom, Western blot quantification relative to α -tubulin. (B-D) On the left, STX1A (B), MUNC18-1 (C) and SNAP-23 (D) Western blot quantification of BC cell lines grouped according to HER2 status (HER2-positive and HER2-negative). On the right, STX1A (B), MUNC18-1 (C) and SNAP-23 (D) Western blot quantification of BC cell lines grouped according to HER2-positive, HER2-negative/luminal A and HER2-negative/basal. Representative results of $n=2$ independent experiments performed in triplicate. Data presented as mean \pm SEM. Statistical analysis was performed using Student's t-test or one-way ANOVA test. * $p < 0.05$, ** $p < 0.01$.



Non-transformed mammary epithelial cell HER2-positive HER2-negative/luminal A HER2-negative/basal

Figure 63 – STX1A is localized in intracellular clusters in non-epithelial mammary and BC cell lines. Immunofluorescence of STX1A and Phalloidin (Phallo) in non-transformed and BC cell lines grouped according to their BC subtype. Nuclei are counterstained with Hoechst. Scale bar = 50 μ M. Representative results of n=1 independent experiments performed in triplicate. At least 10 fields were considered in immunofluorescence images.

Then, to see STX1A localization in BC cell lines, STX1A expression by immunofluorescence was analysed in a confocal microscope (

Figure 63). MCF-10A cells were included to see if there was any difference in localization between a non-transformed mammary epithelial cell line and the other BC cell lines. As it can be seen in the immunofluorescence images, qualitatively, HER2-positive BC cell lines had higher intensity of STX1A in comparison to HER2-negative. Also, MDA-MB-231 was the BC cell line with the highest intensity for STX1A. Also, it seemed that STX1A rather than being localized into the cell membrane, its mainly expression was localized into the cytosol, forming intracellular clusters. It was also checked for phalloidin expression, which stained F-actin fibers, and it demonstrated that STX1A did not co-localize with F-actin fibers and that the majority of STX1A signal was localized into the cytosol.

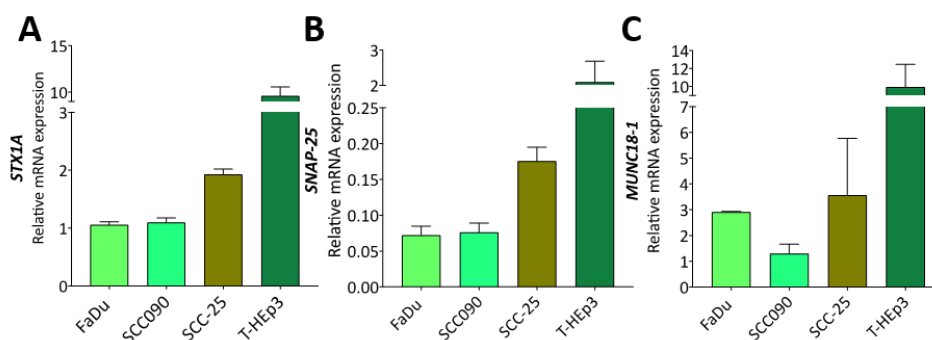
2.1. SYNTAXIN-1A CHARACTERIZATION IN HEAD AND NECK CANCER CELL LINES

2.1.1. SYNTAXIN-1A EXPRESSION IN HEAD AND NECK CANCER CELL LINES

First, *STX1A* expression at mRNA levels in HNSCC cells was checked (*Figure 64A*). All four HNSCC cell lines expressed *STX1A*, being the T-HEp3 cells the ones with the highest levels, followed by SCC-25, SCC090 and FaDu HNSCC cell lines. Then, *STX1A* expression at protein level by Western blot and immunofluorescence were also checked (*Figure 64D and Figure 64H*), and in all cases the pattern of mRNA expression was reflected at protein level as well. Also, expression of *STX1A* seemed not to be exclusive from the membrane because it was detected in clusters in the cytosol as well, as in BC cell lines (

Figure 63).

Expression levels of other SNARE proteins such as SNAP-25 and MUNC18-1 at mRNA and/or protein levels (*Figure 64B-Figure 64D*) were analysed. These genes were expressed at both mRNA and protein levels as well. Moreover, similarly to what was found in HNSCC patients, SNAP-25 expression in HNSCC cell lines positively correlated with *STX1A* expression and with MUNC18-1 at mRNA levels (*Table 40*).



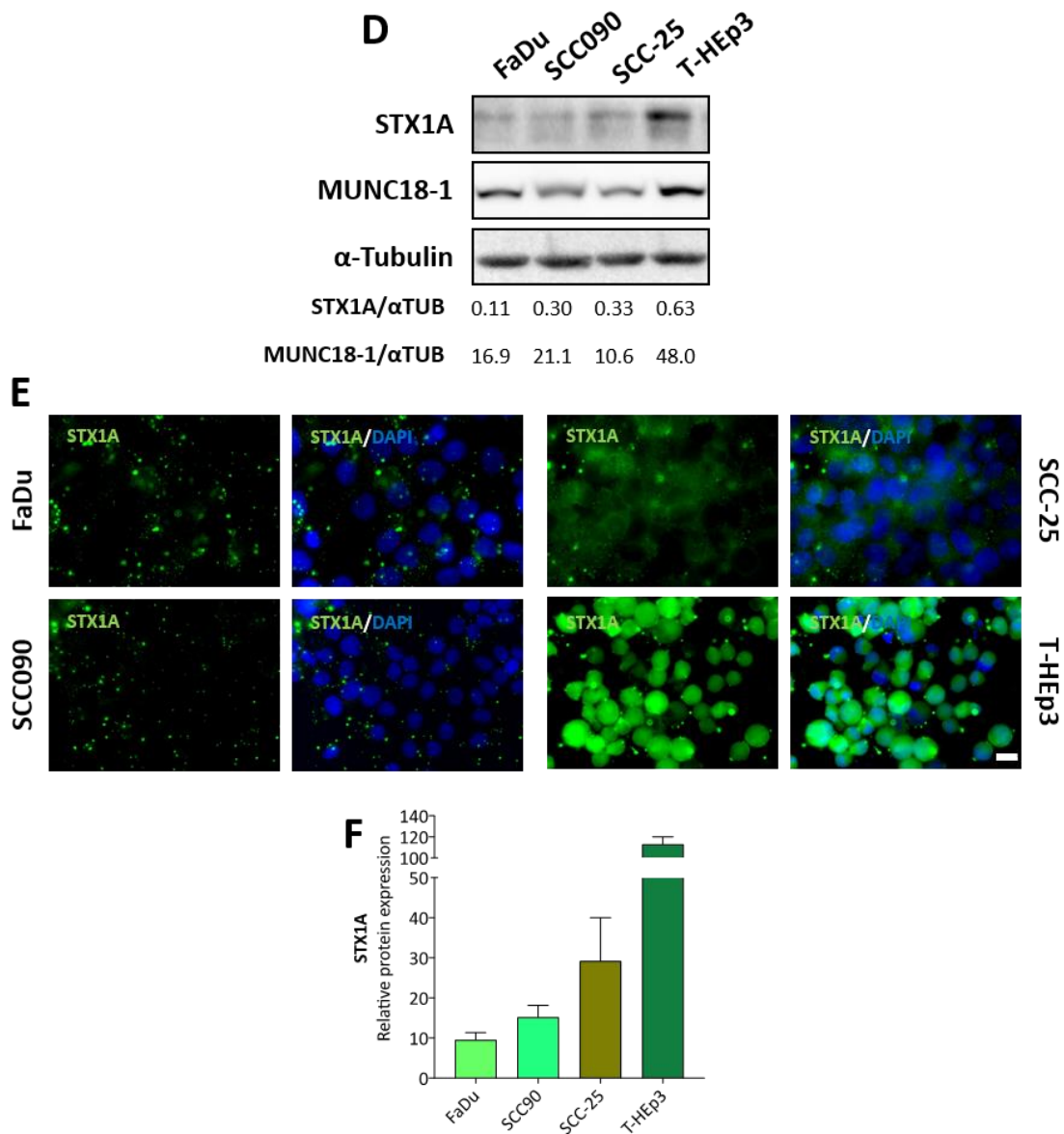


Figure 64 – HNSCC cell lines express STX1A. Relative mRNA expression of *STX1A* (A), *SNAP-25* (B) and *MUNC18-1* (C) in HNSCC cell lines. (D) Western blot analysis of *STX1A* and *MUNC18-1* among HNSCC cell lines. α -tubulin was used as the internal control. At the bottom, Western blot quantification relative to α -tubulin. (E) Immunofluorescence of *STX1A* in HNSCC cell lines. Nuclei are counterstained with Hoechst. Scale bar = 20 μ M. (F) Immunofluorescence intensity of *STX1A* quantification in HNSCC cell lines relative to Hoechst area. Representative results of n=1 independent experiments performed in triplicate. Data presented as mean \pm SEM. At least 10 fields were considered in immunofluorescence images.

Finally, EGFR/HER receptors family expression at mRNA levels was analysed (*Figure 65*). HNSCC cell lines expressed *EGFR*, *HER2* and *HER3*, but there was residual expression of *HER4*. Then, correlation between *STX1A* and these receptors was determined. It resulted that *STX1A* expression did not correlate with EGFR/HER family of receptors expression, however *HER2* and *HER3* expression positively correlate in HNSCC cell lines (*Table 40*).

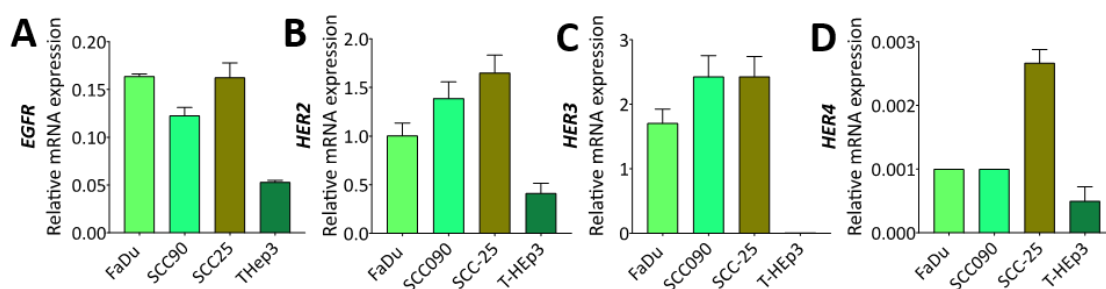


Figure 65 – HNSCC cell lines express EGFR/HER family of receptors. (A-D) Relative mRNA expression of *EGFR* (A), *HER2* (B), *HER3* (C) and *HER4* (D) in HNSCC cell lines. β -actin was used as internal control. Representative results of $n=1$ independent experiments performed in triplicate. Data presented as mean \pm SEM.

Table 40 – Correlation analysis of Syntaxins and SNAREs at mRNA level. Pearson correlation analysis of the different relative mRNA expression of *STX1A*, *SNAP-25*, *MUNC18-1* and EGFR/HER family of receptors. The significant values (2-tailed) are highlighted in bold.

		<i>STX1A</i>					
<i>SNAP25</i>	Correlation	.999**	<i>SNAP25</i>				
	p	0,001					
<i>MUNC18</i>	Correlation	.981*	.975*	<i>MUNC18</i>			
	p	0.019	0.025				
<i>EGFR</i>	Correlation	-0.91	-0.921	-0.813	<i>EGFR</i>		
	p	0.09	0.079	0.187			
<i>HER2</i>	Correlation	-0.825	-0.849	-0.82	0.784	<i>HER2</i>	
	p	0.175	0.151	0.18	0.216		
<i>HER3</i>	Correlation	-0.934	-0.946	-0.941	0.83	.965*	<i>HER3</i>
	p	0.066	0.054	0.059	0.17	0.035	
<i>HER4</i>	Correlation	-0.474	-0.517	-0.389	0.663	0.816	0.657
	p	0.526	0.483	0.611	0.337	0.184	0.343

2.2. SYNTAXIN-1A TRANSCRIPTIONAL MECHANISMS CHARACTERIZATION IN BREAST AND HEAD AND NECK CANCER CELL LINES

Next step was to understand how *STX1A* expression was regulated in BC and HNSCC cell lines. Looking for in the published bibliography, there were only three articles referring to *STX1A* regulation in neuronal and non-neuronal cell lines (232–234), so we wondered if *STX1A* could be regulated similarly as in PC-12 (rat adrenal gland cell line), FRSK (foetal rat skin keratinocyte) or 3Y1 (rat fibroblast) and also if epigenetic regulation could explain the differences in *STX1A* expression between HER2-positive and HER2-negative BC subtypes.

2.2.1. HUMAN SYNTAXIN-1A GENE REGULATORY ELEMENTS ARE SIMILAR TO THOSE IN THE RAT GENOME

Considering that the only information that existed about *STX1A* mechanisms of transcription was described in rat cell lines, we first analysed by bioinformatic software, such

as the Genome Browser, the human *STX1A* gene and its regulatory elements. The human genome GRCh37/hg17 assembly was used to characterize the gene and its regulatory elements. *STX1A* gene is found between 73,118,595-73,127,998 bp of the chromosome 7 (Figure 66). The regulatory elements described by Nakayama *et al.* (2016) (232) at the rat genome were represented by BLAT alignment in Figure 66 where enhancers, promoter region and transcription factor binding sites of *STX1A* gene should be. To analyse the possible regulatory elements of *STX1A* gene in human genome the DNase I Hypersensitivity Clusters track from the ENCODE project was used. The genome regions where their chromatin was more accessible to DNases were represented in darker colours which indicated possible regulatory regions, particularly promoters (Figure 66). Then, the CpG islands track was analysed as well. The presence of a CpG island is normally located near transcription start sites and usually associated with promoter regions. The Genome Browser indicated that, aligned with the DNase I cluster predicted, there was a CpG island (Figure 66).

To further characterize *STX1A* gene regulatory elements histone acetylation and methylation marks were investigated. Normally these signals are associated with open chromatin regions where promoters and enhancers are placed. The integrated regulation track from the ENCODE project was used. H3K4Me1, H3K4Me3 and H3K27Ac histone marks were aligned with the CpG island and a DNase I cluster placed at the beginning of the *STX1A* gene, indicating where the promoter regions of the gene could be (Figure 66). Then, from the GeneHancer track it was proved that the promoter/enhancer region was predicted to be where the acetylation and methylation histone marks were placed and also the CpG islands and DNase I clusters. Moreover, this track predicted some other enhancers that aligned with other CpG islands described and also the methylated histone mark H3K4Me1 (Figure 66). Also, the transcription starting site from the gene was also described (Figure 66). Finally, Nakayama and colleagues proved that the transcription factors SP1 regulated *STX1A* gene transcription, so another ENCODE track to predict the possible transcription factors that can bind into the DNA was used. Among others (*data not shown*), the transcription factor SP1 was predicted to bind into the *STX1A* gene, indicating that SP1 could control its expression (Figure 66).

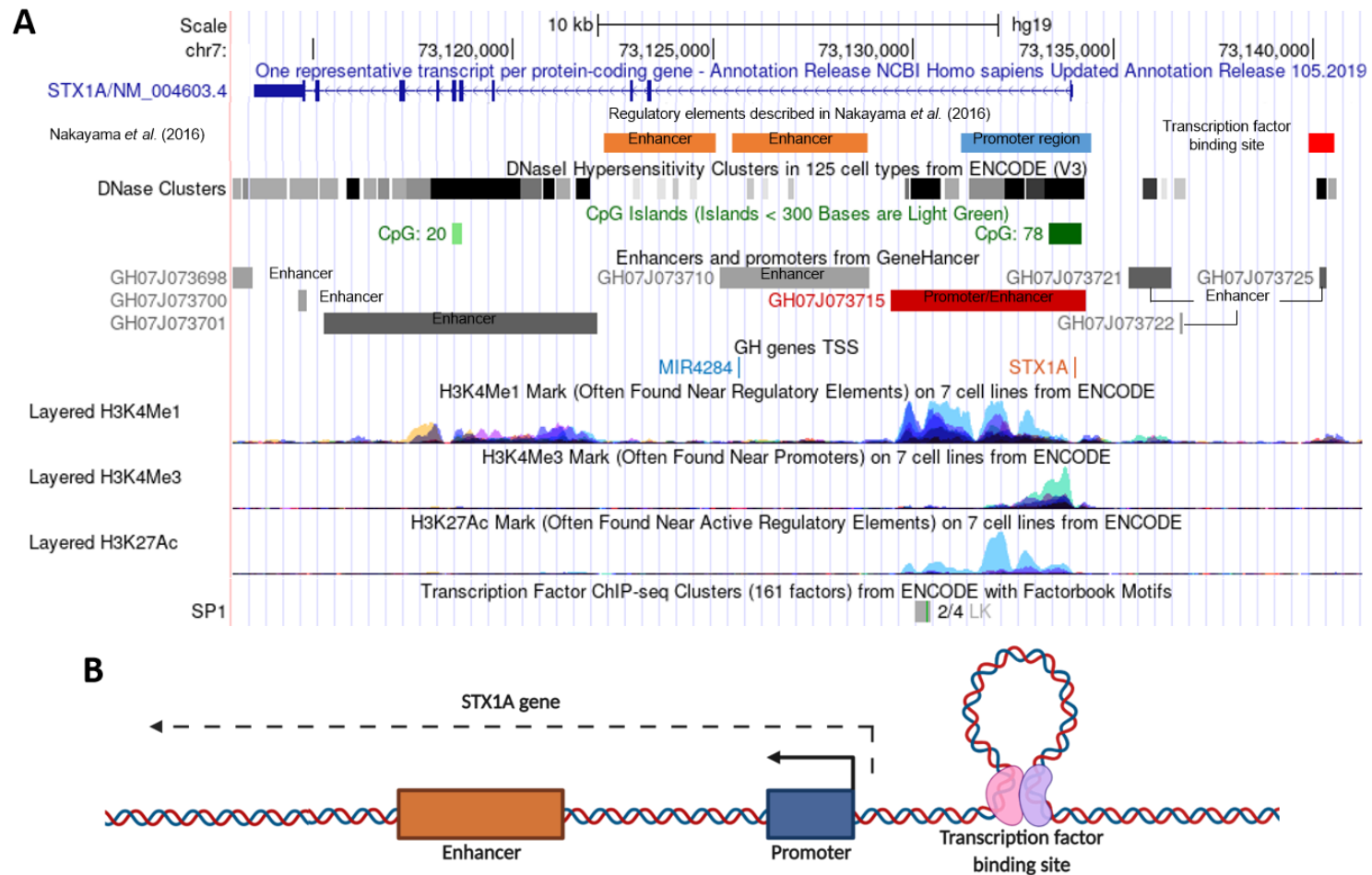
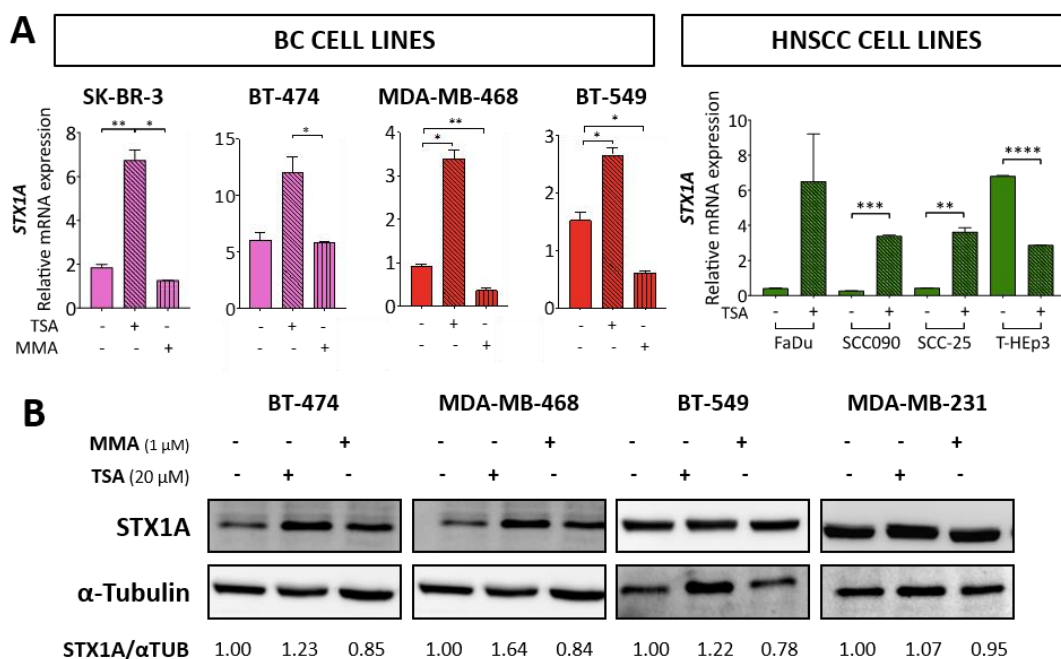


Figure 66 - Human STX1A gene is similar to those in rat genome. (A) Genome Browser data from different tracks used to study regulatory regions of *STX1A* in the human GRCh37/hg17 genome. From the top to the bottom, the represented tracks are: NCBI Reference Sequences (RefSeq), GeneHancer, Integrated regulation from ENCODE tracks (DNaseI hypersensitive clusters, H3K4Me1, H3K4Me3, H3K27Ac, Txn Factr ChIP E3). (B) Human *STX1A* gene schema according to the regulatory elements found in the Genome Browser

Together, this information made us conclude that *STX1A* gene regulatory elements are located similarly than in the *STX1A* rat gene, where it has a transcription factor binding site downstream to the promoter and an enhancer region upstream the promoter (Figure 66B). Moreover, the regulatory elements are located similarly, and are the same than the ones described by Nakayama *et al.* in the rat genome.

2.2.2. SYNTAXIN-1A TRANSCRIPTION IS REGULATED BY HISTONE DEACETYLASES IN BREAST AND HEAD AND NECK CANCER AND BY SP1 TRANSCRIPTION FACTOR AND PKA IN HER2-NEGATIVE BREAST CANCER SUBTYPE

Once characterized the gene in the human genome by bioinformatic tools, BC and HNSCC cell lines were treated with trichostatin A (TSA), a specific mammal class I and class II histone deacetylase inhibitor, as other authors did in PC12 cells (232,233). After 6 hours of treatment, the analysis of the mRNA expression resulted in a significant increase of *STX1A* mRNA in TSA-treated BC and HNSCC cell lines (Figure 67A). There was only one exception, HNSCC T-Hep3 cells treated with TSA down-regulated *STX1A* expression. Moreover, it was determined if the increased expression of *STX1A* mRNA was also translated into protein in BC cells. Accordingly, BC cells were treated with TSA for 6 hours and *STX1A* protein expression was analysed. As it can be seen in Figure 67B, inhibition of class I and class II histone deacetylases increased *STX1A* protein expression as well, except in the HER2-negative BC cell lines MDA-MB-231, the BC cell line with the highest expression of *STX1A*, where no *STX1A* modulation was found.



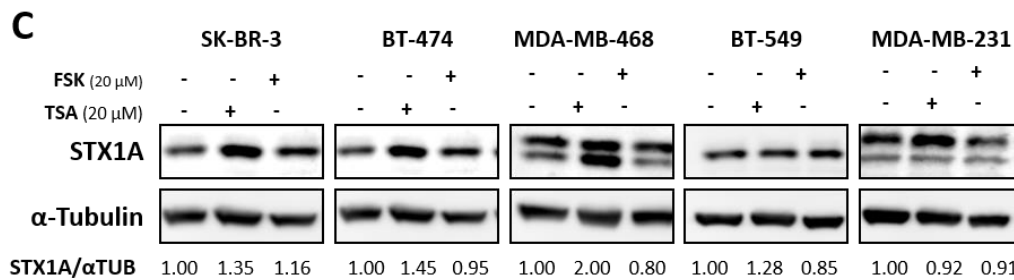


Figure 67 – *STX1A* is epigenetically regulated by histone deacetylases in BC and HNSCC cell lines, and in HER2-negative BC cell lines by SP1 transcription factor. (A) *STX1A* relative mRNA expression in BC cell lines treated with TSA (20 μ M) and MMA (1 μ M) for 6 hours and HNSCC cell lines treated with TSA (20 μ M) for 6 hours. β -actin was used as internal control. (B) Western blot analysis of BC cell lines treated with TSA (20 μ M) or MMA (1 μ M) for 6 hours, and on the bottom, Western blot quantification of *STX1A* expression relative to α -tubulin expression. (C) Western blot analysis of BC cell lines treated with TSA (20 μ M) or FSK (20 μ M) for 6 hours, and on the bottom, Western blot quantification of *STX1A* expression relative to α -tubulin expression. Representative results of n=2 independent experiments performed in triplicate (Western Blots) or sextuplicate (qPCR). Data presented as mean \pm SEM. Statistical analysis was performed using Student's *t*-test. *p<0.05, **p<0.01, ***p<0.001, **** p<0.000.

One of our objectives was to determine if there were any regulatory mechanisms that could explain the *STX1A* differential expression among HER2-positive and HER2-negative BC subtypes. However, the inhibition of class I and class II histone deacetylases did not show any differences between them. We continued by interrogating the transcription factor SP1, which was predicted to bind to *STX1A* promoter region and described to control *STX1A* gene transcription as well (232,233). Interestingly, 6 hours of treatment of BC cell lines with mithramycin A (MMA), an inhibitor of the SP1 binding to the DNA, resulted in no effect in *STX1A* transcription in HER2-positive BC cell lines, but a down-regulation of *STX1A* transcription in HER2-negative BC subtypes (Figure 67A). The effect of MMA at protein level was also analysed, however the effect was not so evident (Figure 67B). Finally, we wanted to know if protein kinase A (PKA) played a role in the transcriptional and epigenetic regulation of *STX1A* as described in the literature (233). To do so, HER2-positive and HER2-negative BC cell lines were treated with forskolin (FSK), a PKA activator and *STX1A* expression was analysed by Western blot assay (Figure 67C). The results showed a slight decrease of *STX1A* expression in HER2-negative BC cell line treated with FSK, whereas no homogenous effects were detected in HER2-positive BC cell lines.

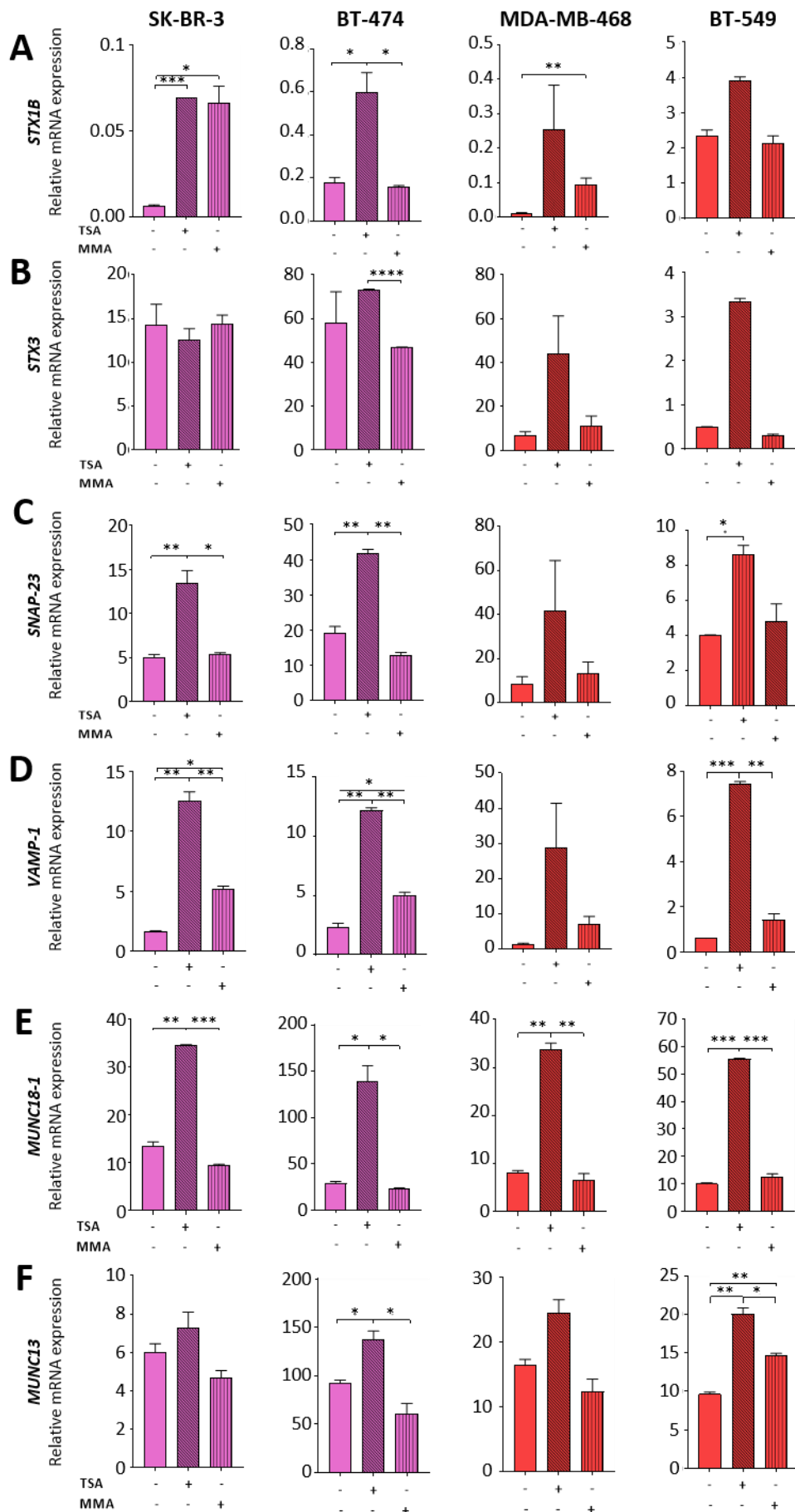


Figure 68 – Other SNARE genes are epigenetically regulated by histone deacetylases and VAMP-1 is also transcriptionally regulated by SP1 transcription factor in BC cell lines. *STX1B* (A), *STX3* (B), *SNAP-23* (C), *VAMP-1* (D), *MUNC18-1* (E), *MUNC13* (F) relative mRNA expression of BC cell lines treated with TSA (20 μ M) and MMA (1 μ M) for 6 hours. β -actin was used as internal control. Representative results of n=2 independent experiments performed in sextuplicate. Data presented as mean \pm SEM. Statistical analysis was performed using one-way ANOVA test. *p<0.05, **p<0.01, ***p<0.001, **** p<0.000.

The epigenetic regulation of other SNARE genes such as *SNAP-23*, *MUNC18-1*, *VAMP-1*, *MUNC13*, *STX1B* and *STX3* in BC cell lines and *SNAP-25* and *MUNC18-1* in HNSCC cell lines was also investigated (*Figure 68 and Figure 69*). What was common in all BC and HNSCC cell lines analysed was that TSA upregulated the expression of all SNAREs, independently of HER2 status in BC cell lines. However, when the effect of MMA in these SNAREs was analysed, it was only found that *VAMP-1* is negatively controlled by SP1 where it seemed that inhibition of SP1 binding into the DNA resulted in an increase of *VAMP-1* transcription in all HER2-positive and HER2-negative BC cell lines (*Figure 68*).

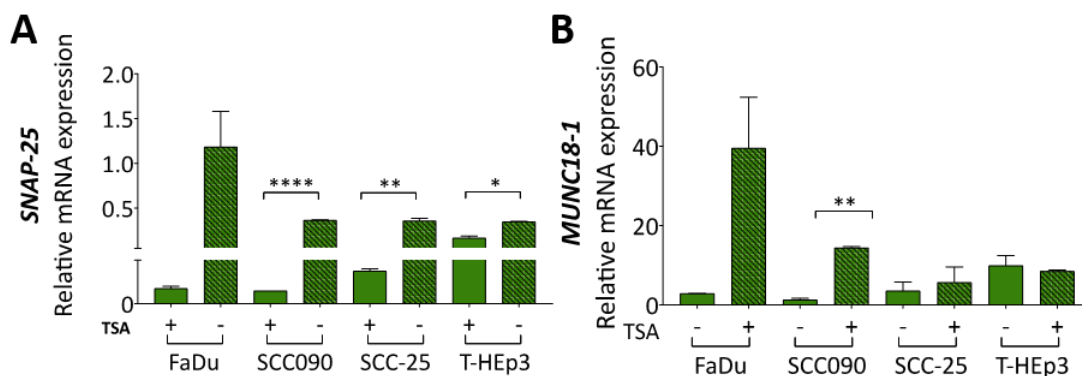


Figure 69 – SNAP-25 and MUNC18-1 are epigenetically regulated by histone deacetylases in HNSCC cell lines. (A) *SNAP-25* and (B) *MUNC18-1* relative mRNA expression of HNSCC cell lines treated with TSA (20 μ M) for 6 hours. β -actin was used as internal control. Representative results of n=2 independent experiments performed in sextuplicate. Data presented as mean \pm SEM. Statistical analysis was performed using Student's *t*-test for the statistic between paired HNSCC cell lines (control and treated). *p<0.05, **p<0.01, **** p<0.000.

Altogether these results clearly showed the transcriptomic and epigenetic regulation mechanisms of some SNARE proteins in BC and HNSCC cell lines. All SNARE proteins studied are regulated by histone deacetylases in BC and HNSCC cell lines and only *STX1A* and *VAMP-1* seems to be regulated by SP1 transcription factor in BC cell lines (*Figure 70*).

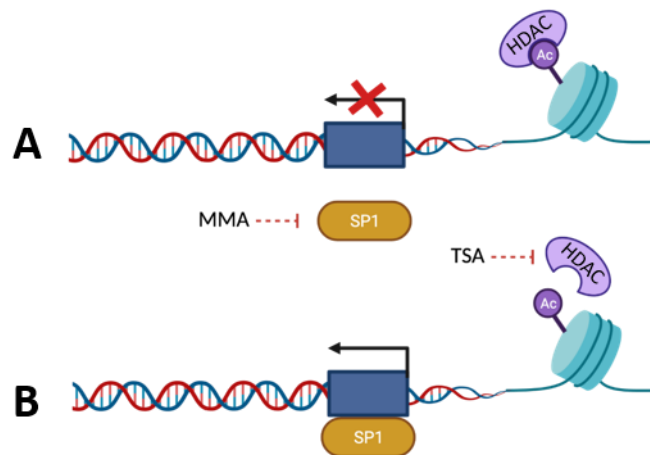


Figure 70 – Schematic representation of epigenetic and transcriptional regulation on *STX1A* gene. (A) *STX1A* gene transcription is repressed when HDAC are active and there is no binding of SP1. (B) *STX1A* gene transcription is activated when HDAC activity is blocked and SP1 transcription factor can bind to the promoter.

2.3. STRATEGIES TO IMPAIR SYNTAXIN-1A FUNCTION OR DOWN-REGULATE ITS EXPRESSION

To further study the role of *STX1A* in BC and HNSCC progression, it was necessary to establish an experimental model where *STX1A* was down-regulated at protein or at functional levels. To do that, several strategies were used, some of them specific for *STX1A* and others, even they mainly down-regulated or impaired function of *STX1A*, had also collateral effects on other proteins.

The first strategy that was used to inhibit *STX1A* function in BC cells was treating the cells with BoNTs, which were given by the collaboration with Dr. Eduardo Soriano's lab (Universitat de Barcelona). Following their protocol, HER2-positive BC cell lines (SK-BR-3, MDA-MB-453 and BT-474) and the BC cell line with the highest expression of *STX1A*, MDA-MB-231 (HER2-negative/basal subtype) were treated for 6 hours at a concentration of 20 units of BoNTs C1 and BoNT A. BoNT C1 cleaves specifically *STX1A* and SNAP-25 and BoNT A cleaves specifically SNAP-25 (*Figure 71A*). To confirm that these proteins were cut, the analysis of its effect was performed by Western blot assay, where if two protein bands should have appeared (*Figure 71B*). The results showed no *STX1A* cleavage in any of the BC cell lines, even though in MDA-MB-231 *STX1A* the band seemed more lightly, it was considered that there was not any inhibition because only one band was detected. Unfortunately, in this blot it was not possible to see SNAP-25 due to its low expression in BC cell lines, being not always detectable by

Western blot. Then, we focused only in one BC cell line (MDA-MB-453) and the effect of BoNT C1 treatment was analysed at different times. This time BoNT A was not used because we were not interested at that moment in the role of SNAP-25 in our *in vitro* model. After the treatment with BontC1 and the posterior analysis by Western blot, we did not see any effects of the neurotoxin either (*Figure 71C*).

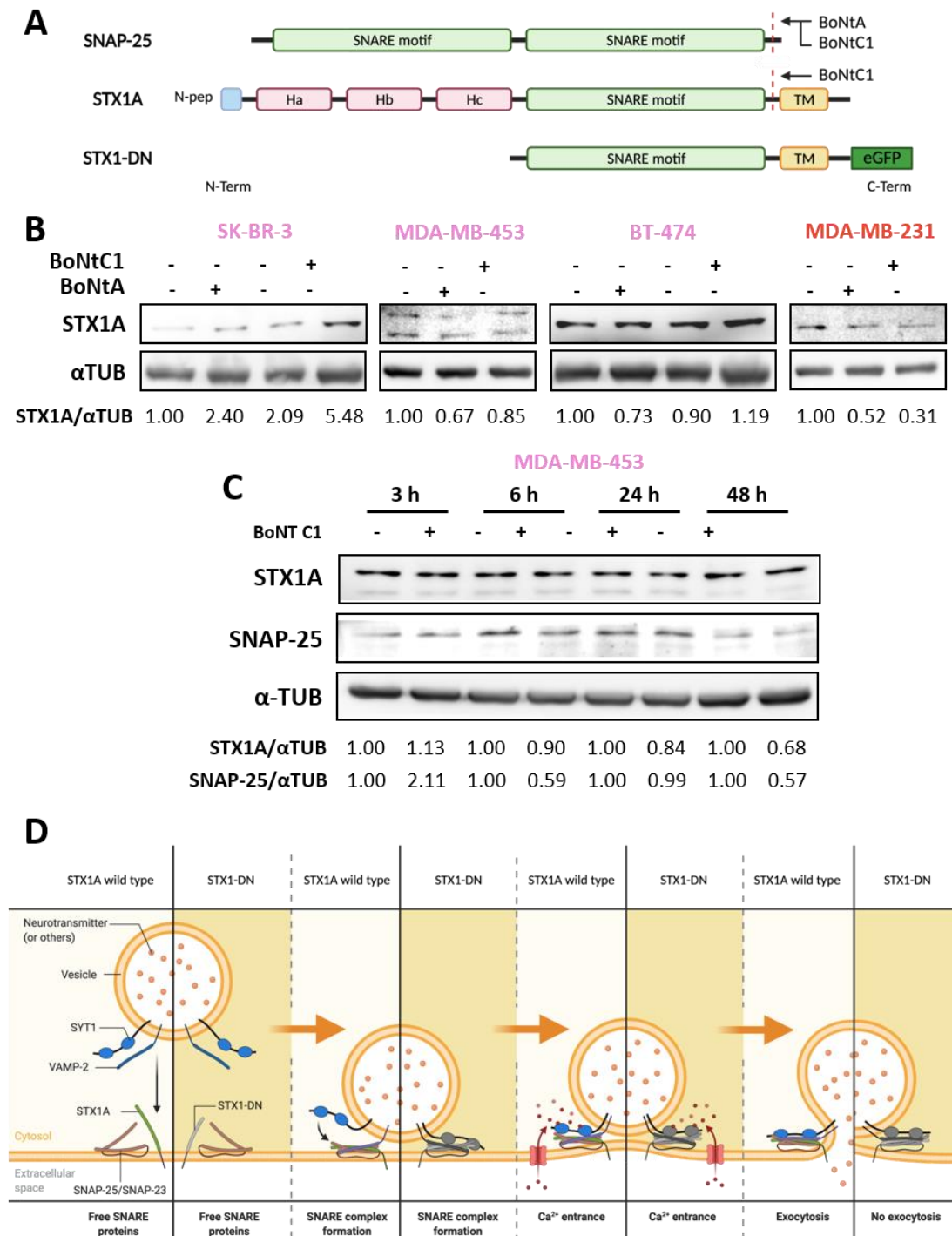


Figure 71 – BoNTs and STX1-DN as strategies to impair STX1A function. (A) Scheme of the cleavage site of BoNT A and BoNTC1 in SNAP-25, BoNT C1 in STX1A and the secondary protein sequence of STX1-DN. (B) On the top, analysis of STX1A by Western Blot of SK-BR-3, MDA-MB-453, BT-474 (HER2-positive BC cells) and MDA-MB-231 (HER2-negative/basal BC cells) treated for 6 hours with BoNT A or

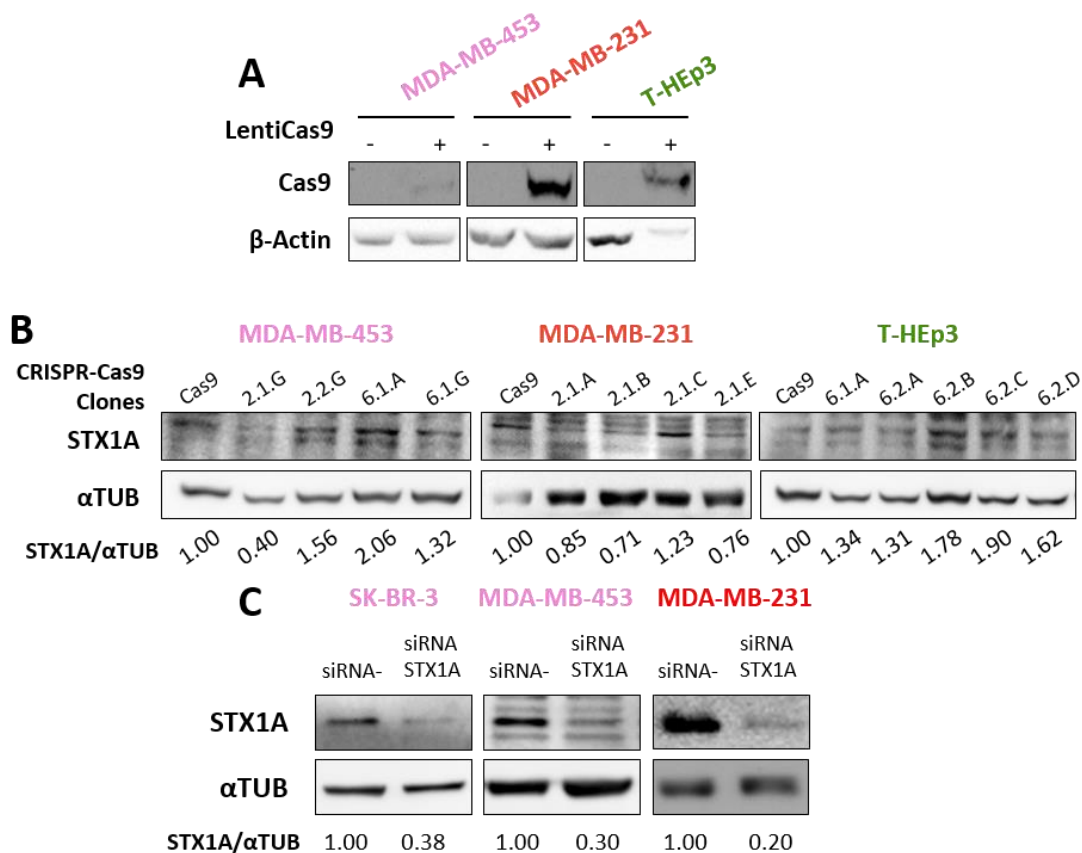
BoNT C1 (20 units). α -tubulin was used as internal control. On the bottom, relative quantification of protein expression (C). On the top, analysis of STX1A by Western Blot of MDA-MB-453 (HER2-positive BC cells) treated for 3, 6, 24 and 48 hours with BoNT C1 (20 units). α -tubulin was used as internal control. On the bottom, relative quantification of protein expression. (D) Scheme of how STX1-DN impairs STX1A and other SNARE function. Representative results of n=1 independent experiments.

At that point, the strategy to impair STX1A function was changed by using a Syntaxin-1 dominant negative (STX1-DN) plasmid kindly provided by our collaborator Dr. Eduardo Soriano, who already proved its efficacy and their function impairment in several research articles (84,242). The STX1-DN plasmid encodes for a protein that lacks the N-terminal fragment of the wild-type protein, which includes the Ha, Hb and Hc domains and the N-terminal peptide of STX1 (*Figure 71A*). The transfection of the plasmid and the consequent expression of the protein leads to a competition between STX1A wild-type and STX1-DN for their protein partners. Even though STX1-DN lacks its N-terminal domains, which works as a regulatory domain, this protein is still able to form the SNARE complex interacting with others t-SNAREs and v-SNAREs, but is not able to induce the fusion of the vesicle to the plasma membrane, hampering exocytosis of the vesicle content (*Figure 71D*). Several strategies were followed to work with the STX1-DN plasmid, first of all a transient expression plasmid was used, which was transfected to the cells of interest using lipofectamine 3000© and obtaining around 50% of efficiency of transfection (*Annex figure 16*). Given the fact that this was a transient expression, and that long-term experiments could not be done with this method, retroviral particles with the STX1-DN plasmid were produced in HEK-293 Phoenix cells, and after collecting them, HER2-positive BC cell lines (SK-BR-3 and MDA-MB-453), HER2-negative BC cell lines (BT-549 and MDA-MB-231) and HNSCC cell lines (FaDu and SCC090) were infected. The infected cells were selected according to their resistance to puromycin, and used to perform the long-term experiments. With this strategy it was able to impair STX1 function in a short (transfection) or long-term (cells infected with retroviral particles). However, it is important to have in mind that by using the STX1-DN cells not only the function of STX1A is impaired, but also STX1A partners, the ones that are forming the SNARE complex, as well to a certain extent.

2.3.1. SYNTAXIN-1A EXPRESSION WAS DOWN-REGULATED BY shRNA TECHNOLOGY

The main problem with the STX1-DN was that the possible differential effects seen in the experiments could not be specific to STX1A, but also to the impairment of the normal function of SNAP-23, VAMPs or others STX1A partners. To avoid this side effect, several strategies to specifically inhibit STX1A were tried. First of all, it was used the CRISPR-Cas9 technology

through a collaboration with Dr. Paloma Bragado's lab (UCM). She kindly provided the BC cell lines (MDA-MB453 and MDA-MB-231) and the T-HEp3 HNSCC cells already expressing the Cas9 protein (*Figure 72A*), which they were infected with lentiviral vectors bearing a gRNA against *STX1A* exon 2 or a gRNA against exon 6 (detailed in materials and methods in section 4.4). The infection was performed in duplicates for each exon and the non-target gRNA. After selecting the infected cells with puromycin *STX1A* expression was analysed by Western blot assay, however, no *STX1A* inhibition was achieved (*data not shown*). Afterwards, the subcloning protocol was started with the main objective to isolate single cells with *STX1A* gene deleted in a 96-multiwell dish and let them grow under puromycin selection pressure until they form a cell colony. Next, *STX1A* expression was analysed in the cells derived from the single colony. This procedure was done in all the cell lines infected, for both gRNA *STX1A* (exon 2 and exon 6) and once the colonies were big enough to perform a protein analysis by Western blot, we collected them. The results shown in (*Figure 72B*) determined that none of the clones were knock-out or knock-down for *STX1A*. Even though some clones seemed to show a slightly *STX1A* down-regulation such the clone 2.1G of the MDA-MB-453, after another Western blot analysis this down-regulation could not be confirmed (*data not shown*).



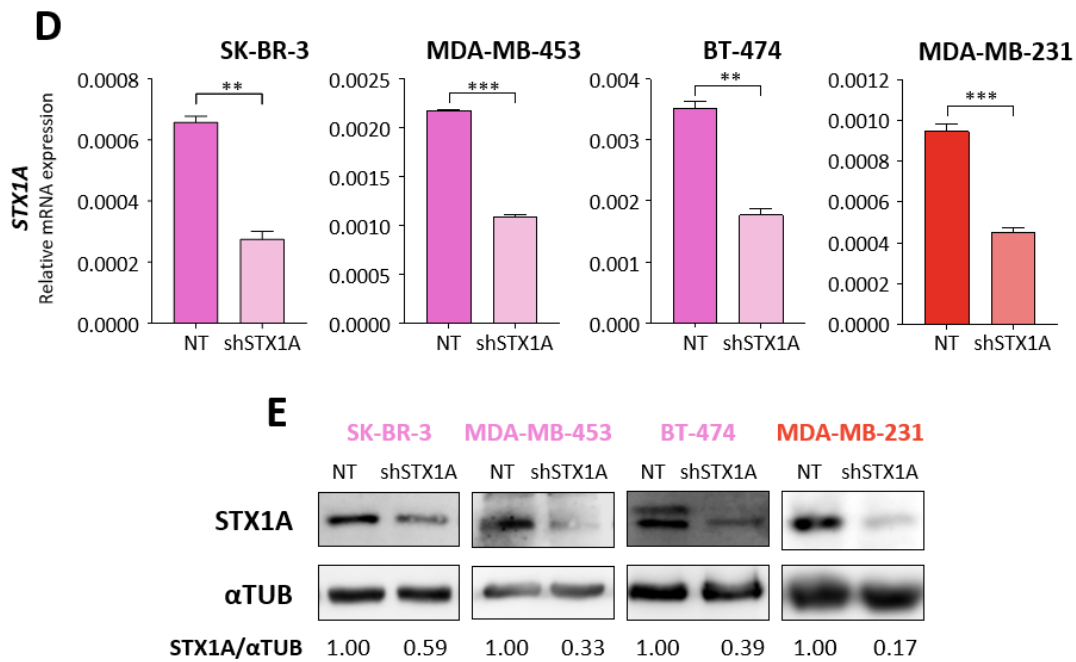


Figure 72 – Gene editing and siRNA/shRNA as strategies to specifically down-regulate *STX1A* at protein level. (A) Cas9 expression analysed by Western blot in MDA-MB-453 (HER2-positive BC cells), MDA-MB-231 (HER2-negative/basal BC cells) and T-HEp3 (HNSCC cells) transfected with Cas9. β -actin was used as internal control. (B) On the top, analysis of *STX1A* expression in CRISPR-Cas9 clones transfected with gRNA *STX1A* targeting exon 2 (clones starting with 2) and exon 6 (clones starting with 6). α -tubulin was used as internal control. On the bottom, quantification of protein expression. (C) On the top, analysis of *STX1A* after 72 hours of siRNA *STX1A* (50 nM) transfection in SK-BR-3 and MDA-MB-453 (HER2-positive) and MDA-MB-231 (HER2-negative/basal) BC cells. α -tubulin was used as internal control. On the bottom, quantification of protein expression. (D) Analysis of *STX1A* mRNA expression by qPCR in SK-BR-3, MDA-MB-453, BT-474 and MDA-MB-231 BC cells down-regulating *STX1A* by shRNA *STX1A*. β -actin was used as internal control. (E) On the top, analysis of *STX1A* expression in SK-BR-3, MDA-MB-453, BT-474 and MDA-MB-231 BC cells downregulating *STX1A* by shRNA *STX1A*. α -tubulin was used as internal control. On the bottom, quantification of protein expression. Representative results of at least $n=2$ independent experiments performed in sextuplicate (qPCR only). Data presented as mean \pm SEM. Statistical analysis was performed using Student's *t*-test. ** $p < 0.01$, *** $p < 0.001$.

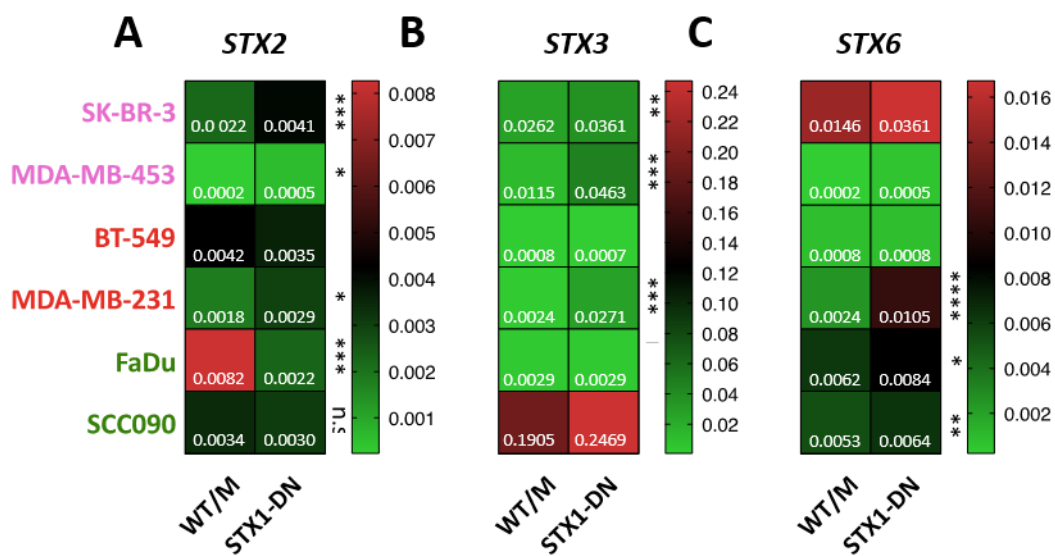
Then, transiently down-regulation of *STX1A* expression by siRNA was attempted instead of inhibiting *STX1A* by gene editing. After 72 hours of siRNA *STX1A* inhibition of BC cell, a down-regulation of the protein around 50% was detected (Figure 72C). Despite being able to perform several experiments with that strategy, a permanent inhibition of *STX1A* was looked for. Consequently, lentiviral particles bearing shRNA against *STX1A* was purchased, and then, infected into HER2-positive BC cell lines (SK-BR-3, MDA-MB-453 and BT-474) and in the HER2-negative BC cell line MDA-MB-231. After selecting the infected cells with G-418 (geneticin) the analysis of *STX1A* expression by qPCR was performed. It was detected around 50% of inhibition (Figure 72D), that was also translated into around 50% of *STX1A* protein down-regulation (Figure 72E). Thereafter, these cells were used to confirm, in some cases, if the effects seen in *STX1*-DN experiments were driven by *STX1A* impairment. It is important to mention that in

each experiment performed with these cell lines, *STX1A* expression was checked at protein or mRNA levels to ensure that *STX1A* was down-regulated.

2.3.2. SYNTAXIN-1 INFLUENCES THE TRANSCRIPTION OF ITS OTHER SNARE PARTNERS

Once stable BC and HNSCC cell lines expressing the STX1-DN protein were obtained, it was checked the transcriptional modulation of other SNAREs genes. Gene expression of several syntaxins (*STX2*, *STX3* and *STX6*) and other SNAREs (the t-SNARE *SNAP-23* and two v-SNAREs, *VAMP-2* and *VAMP-4*) were analysed, considering that they have been previously found overexpressed in tumours that were *STX1A^{LOW}* (*SNAP-23*, *VAMP-2* and *VAMP-4*) or overexpressed in tumours that were *STX1A^{HIGH}* (*STX2*, *STX3* and *STX6*) in the METABRIC BC bioinformatic analysis (section 1.3.4 of the results chapter).

The analysis by qPCR revealed that there were differences between MOCK cells and cells expressing STX1-DN. The results revealed that in BC cells with STX1-DN overexpress *STX2*, *STX3* and *STX6*, the t-SNARE *SNAP-23* and the v-SNAREs *VAMP-2* and *VAMP-4* (Figure 73). Focusing on HNSCC cell lines, the results demonstrate that these cells behave differently than BC downregulating *STX2* and *STX3* and only overexpressing *STX6*. Also downregulated *SNAP-23* t-SNARE and *VAMP-2* and *VAMP-4* v-SNAREs (Figure 73). Altogether, these results demonstrate that when STX1 is not functional there is also a modulation of other SNARE-related partners mRNA transcription.



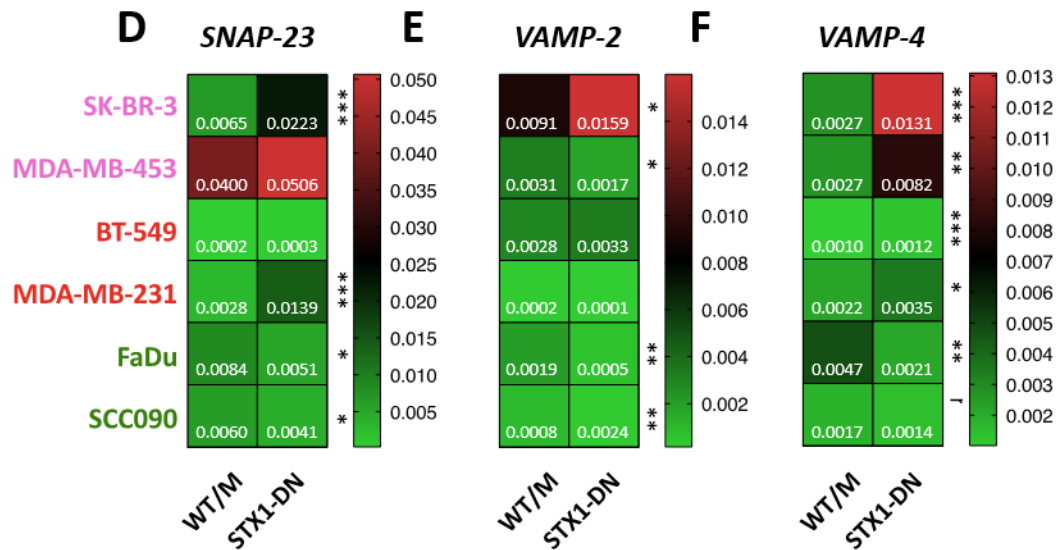


Figure 73 – Differential modulation of mRNA expression of SNARE-related genes in STX1-DN BC and HNSCC cell lines. Heat Maps of *STX2* (A), *STX3* (B), *STX6* (C), *SNAP-23* (D), *VAMP-2* (E) and *VAMP-4* (F), relative mRNA expression analysed by qPCR comparing wild-type (SK-BR-3 or MDA-MB-453) or MOCK (BT-549, MDA-MB-231, FaDu or SCC090) (M) versus STX1-DN cells (DN). β -actin was used as an internal control. Representative results of n=1 independent experiments performed in sextuplicate. Data presented as mean \pm SEM. Statistical analysis was performed using Student's *t*-test, comparing paired WT/M vs DN. ** $p < 0.01$, *** $p < 0.001$.

3. FUNCTIONAL CHARACTERIZATION OF SYNTAXIN-1A IN BREAST AND HEAD AND NECK CANCER MODELS

3.1. ROLE OF SYNTAXIN-1A IN BREAST AND HEAD AND NECK CANCER CELL PROLIFERATION

Once obtained the cells with down-regulated STX1A at protein level or functionality, these cells were used to further characterize STX1A role in BC and HNSCC cells in vitro. According to the results obtained from BC patients' databases, BC patients with tumours with high levels of STX1A overexpressed the G2/M checkpoint and PI3K/AKT/mTOR and mitotic spindle signalling pathways, which are closely related to cancer cell proliferation regulation. Based on these results, the study continued with the investigation of the role of STX1A in the regulation of proliferation in BC and HNSCC cells.

To decipherer the plausible role of STX1A in cell cycle regulation, STX1-DN BC and HNSCC cell lines and shRNA STX1A BC cell lines were used. The in vitro analysis performed to characterize the cell phenotype were MTT proliferation assays, cell cycle and clonogenics assays, accompanied by gene and protein expression determination to evaluate the implication of STX1A in cell cycle regulation.

3.1.1. SYNTAXIN-1A REPRESSES BC AND HNSCC CELL CYCLE PROGRESSION AND PROLIFERATION

According to the above-mentioned findings in BC patients' databases, BC tumours with high STX1A levels overactivated the PI3K/AKT/mTOR signalling pathway (*Figure 51*). Considering this result, characterization of AKT and ERK pathway activation by Western blot was performed. First, wild-type (SK-BR-3 and MDA-MB-453), MOCK (BT-549, MDA-MB-231, FaDu and SCC090) and their pairing STX1-DN cells were serum-starved overnight, following by the extraction of protein the next day and the correspondent Western blot analysis. The results, represented in *Figure 74A*, demonstrated that STX1A does not modulate AKT and ERK pathways in the same way in all the BC and HNSCC cell types, but in the vast majority, STX1A is involved in the activation or deactivation of AKT and ERK pathways. Concretely, STX1-DN HER2-positive BC cell lines (SK-BR-3 and MDA-MB-453), up-regulated ERK pathway whereas differential modulation was observed in AKT (down-regulated in SK-BR-3 and up-regulated in MDA-MB-453). STX1-DN HER2-negative/basal BC cell lines upregulated AKT pathway in comparison to their paired control. Nevertheless, they had a differential response regarding ERK activation: BT-549 STX1-DN cells activated ERK while it was down-regulated in MDA-MB-

231 STX1-DN cells. Finally, HNSCC (FaDu and SCC090) cells expressing STX1-DN down-regulated both AKT and ERK signalling pathways.

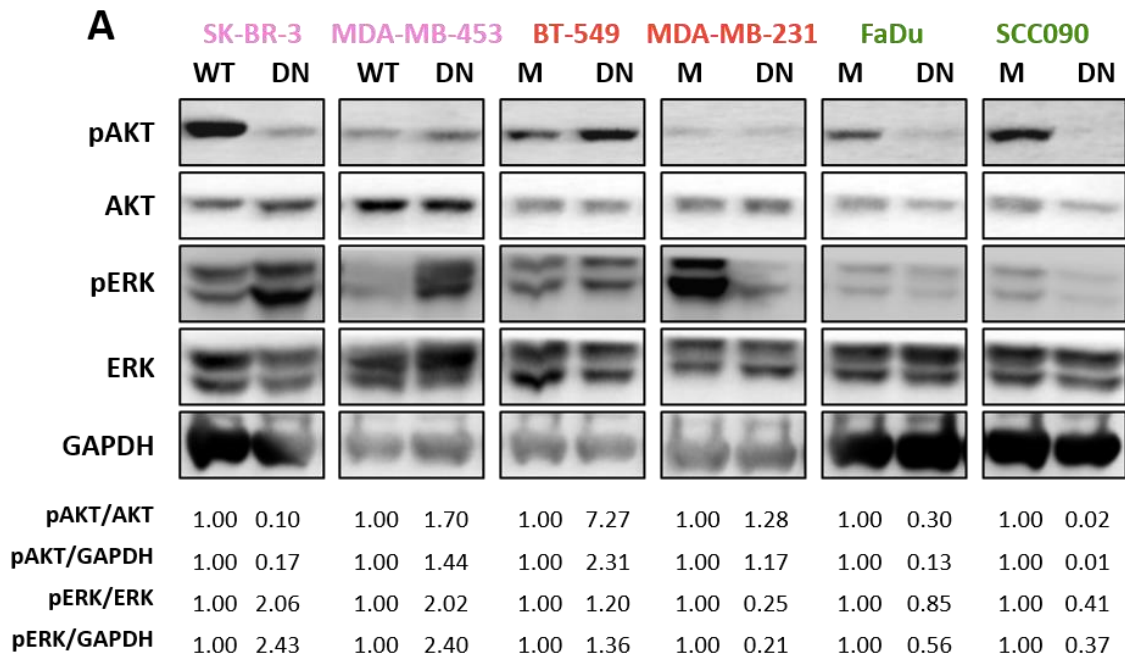


Figure 74 – Differential AKT and ERK activation state in BC and HNSCC STX1-DN cell lines. (A) On the top, a representative image of a Western blot analysis of pAKT, AKT, pERK and ERK between MOCK (M) or wild-type (WT) versus STX1-DN (DN) HER2-positive (SK-BR-3 and MDA-MB-453), HER2-negative/basal (BT-549 and MDA-MB-231) BC and HNSCC (FaDu and SCC090) cell lines. GAPDH was used as internal control. At the bottom, quantification of protein expression normalized to the control condition (mock or wild-type). Representative results of n=3 independent experiments.

Then, STX1-DN cells proliferation rate was checked, taking into account that STX1 function impairment is affecting AKT and ERK activation, which are proteins involved in pathways closely related to cell proliferation. To check for cell proliferation, MTT proliferation assays were performed, seeding the cells under restrictive conditions (media with 2% of FBS) and determining their proliferation rate along four days. The results displayed in [Figure 75](#), showed that functionally impaired STX1 cells have a higher proliferation rate than their controls, except for SCC090 and SK-BR-3 cells, in which no differences were found. Although other contributions cannot be ruled out, that could be explained, in part, because SK-BR-3 have a low proliferation rate, which make it difficult to detect differences between both conditions, and the opposite could have happened with SCC090 HNSCC cell lines, due to its high proliferation rate.

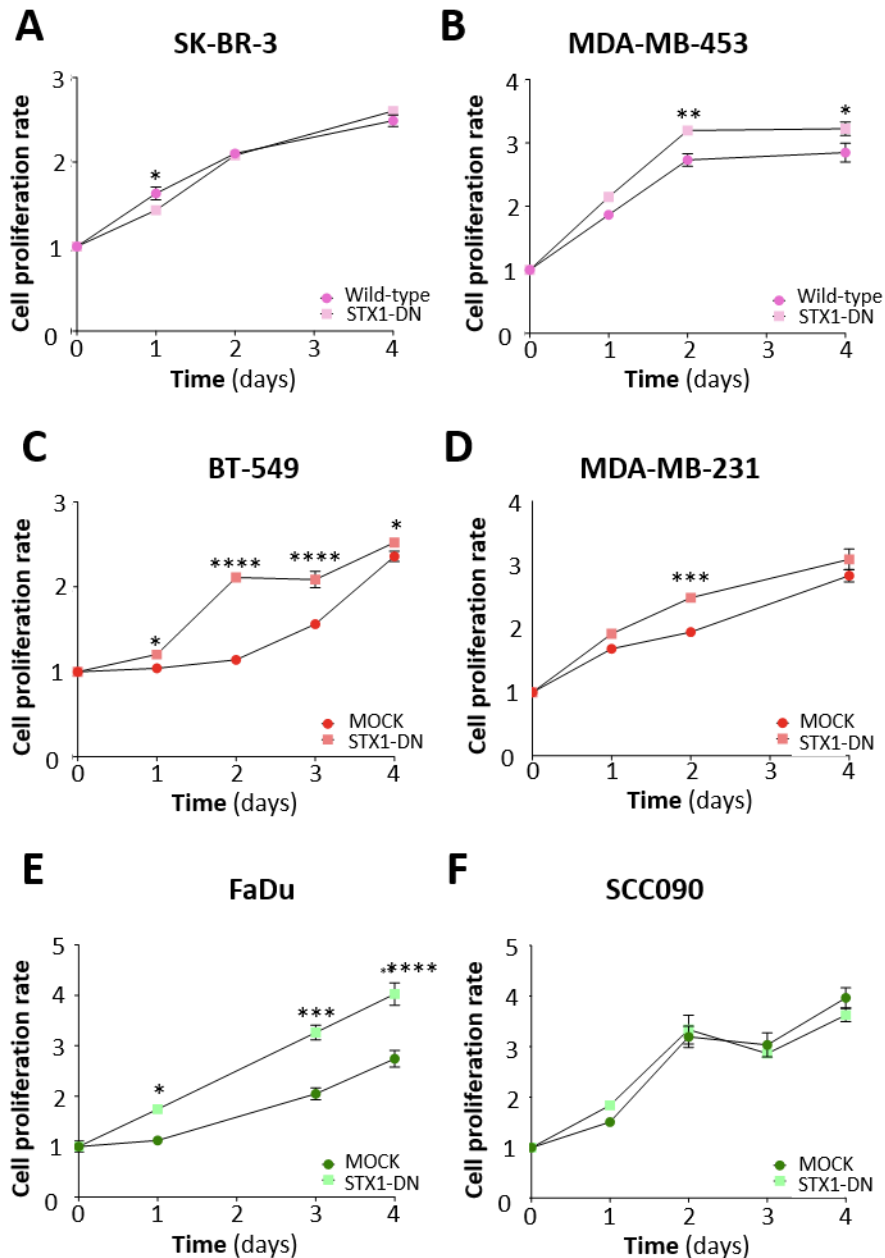


Figure 75 – Functional abrogation of STX1 confers a proliferative advantage. Representative proliferative MTT assays of SK-BR-3 (A), MDA-MB-453 (B) (HER2-positive BC cells), BT-549 (C), MDA-MB-231 (D) (HER2-negative/basal BC cells), FaDu (E) and SCC090 (F) (HNSCC cells) cultured at 2% FBS comparing proliferation rate of wild-type or MOCK versus STX1-DN cell lines for four days. Representative results of n=3 independent experiments performed in sextuplicate. Data presented as mean \pm SEM. Statistical analysis was performed using one-way ANOVA test comparing paired wild-type/MOCK vs STX1-DN cells. * p < 0.05, ** p < 0.01, *** p < 0.001.

To confirm that STX1-DN was stimulating the proliferation of BC and HNSCC cell lines, a cell-cycle assay was performed, also under a restrictive environment (cultured at 2% of FBS) for 24 hours. Data obtained showed that all STX1-DN cells except for MDA-MB-231, had a major proportion of cells in a proliferative state (phase S and G₂/M of the cell cycle) in comparison to their controls (*Figure 76, left graphics*). The mRNA levels of *Cyclin D1* (*CCND1*),

a cyclin involved in the transition from the phase G₁ to the S phase of the cell cycle were also checked. CCND1 was also overexpressed in almost all the STX1-DN cells (*Figure 76, right graphics*) explaining why cells with an impaired function of STX1 were found more proliferative in the MTT proliferation assays.

Altogether, these results demonstrate that STX1 is involved in cell cycle regulation, by repressing the transition from G₁ to S phase of the cell cycle, down-regulating somehow *CCND1* mRNA expression.

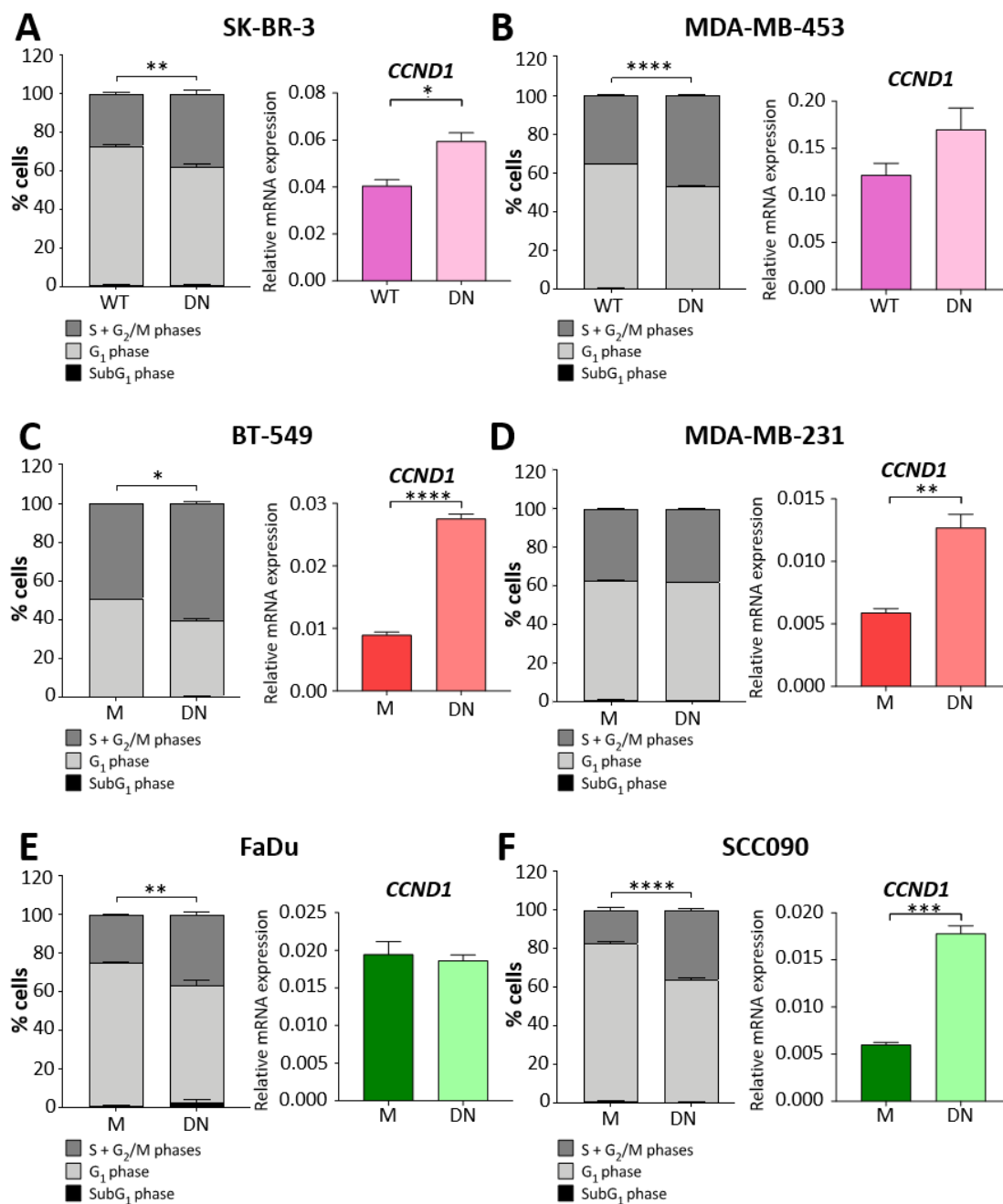
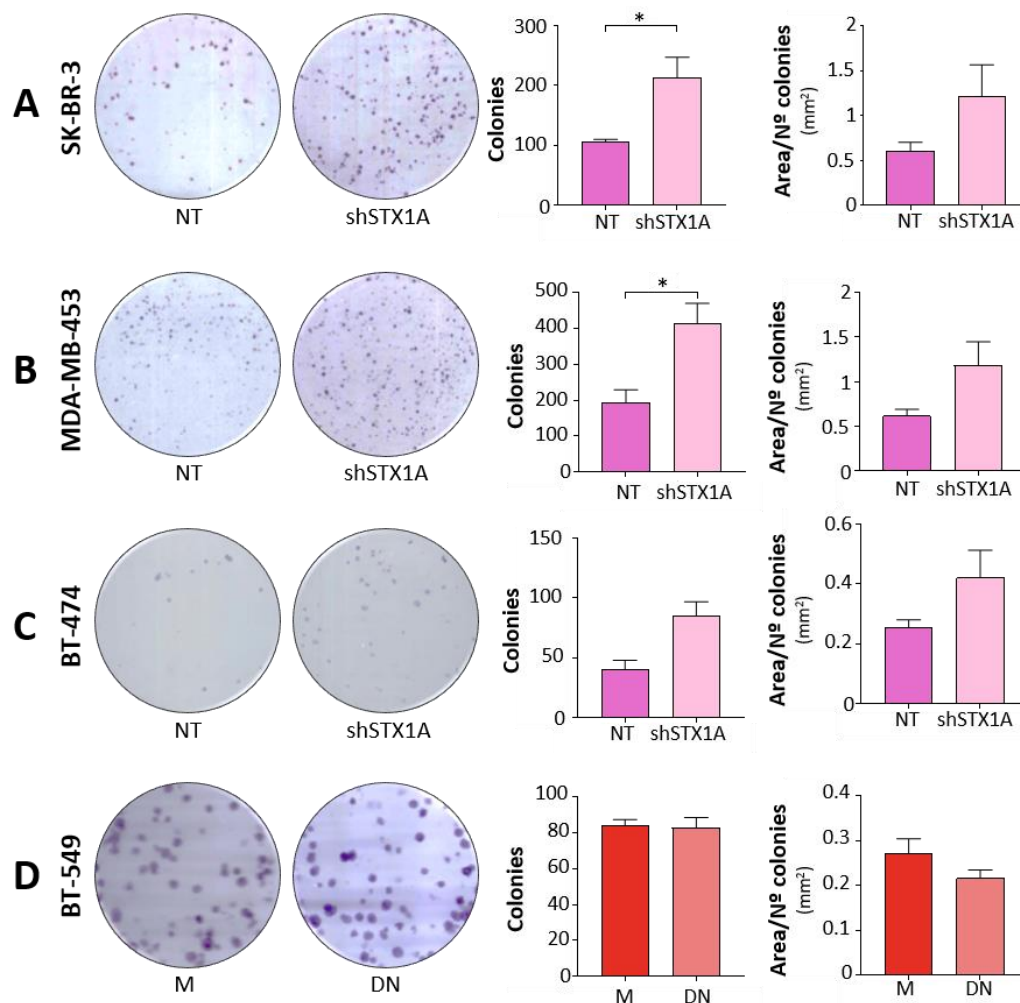


Figure 76 – Impairment of STX1 activity results in an increase of cells at S, G₂/M phase and of *CCND1* mRNA expression. On the left, representative cell cycle distribution of SK-BR-3 (A), MDA-

MB-453 (B) (HER2-positive BC cells), BT-549 (C), MDA-MB-231 (HER2-negative/basal BC cells), FaDu and SCC090 (HNSCC cells) comparing wild-type (WT) or MOCK (M) cells versus STX1-DN (DN) cells. On each respective right, qPCR analysis of *CCND1* mRNA expression in wild-type or MOCK versus STX1-DN cells (β -actin was used as an internal control). Representative results of at least $n=1$ independent experiment performed in duplicate (cell cycle) and sextuplicate (qPCR). Data presented as mean \pm SEM. Statistical analysis was performed using two-way ANOVA, Sidak's test (cell cycle) and Student's *t*-test (qPCR). ** $p < 0.01$, *** $p < 0.001$.

3.1.2. SYNTAXIN-1A INHIBITS BC AND HNSCC CLONOGENIC CAPACITY

After confirming that STX1 inhibits BC and HNSCC cancer cell proliferation, it was checked if it also played a role in regulating cell clonogenic capacity. To determine that, a clonogenic assay with shRNA STX1A cells (*STX1A* knock-down) and also with STX1-DN BC and HNSCC cell lines (functionally-impaired STX1A) was performed. The clonogenic results determined that STX1A was also involved in repressing BC and HNSCC clonogenic capacity. In most of the cell types studied knock-down and functionally-impaired STX1A cells displayed a significant increase in their clonogenic capacity (*Figure 77*), and in some cases, also they formed significant larger area of colonies (MDA-MB-231 and FaDu).



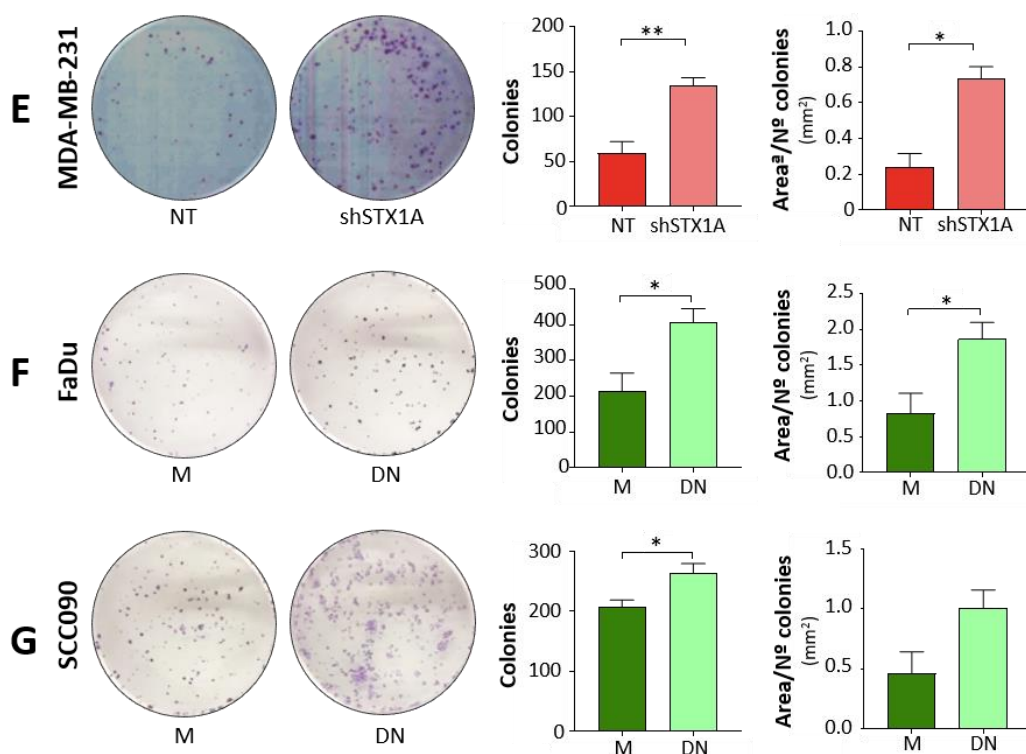


Figure 77 – Cells with down-regulated or functionally-impaired STX1A have higher clonogenic capacity. Representative images of clonogenic formation assay in SK-BR-3 (A), MDA-MB-453 (B), BT-474 (C) (HER2-positive BC cells), BT-549 (D), MDA-MB-231 (E) (HER2-negative/basal BC cells), FaDu (F) and SCC090 (G) (HNSCC cells) between shRNA Non-Target (NT) or MOCK (M) and shRNA STX1A (shSTX1A) or STX1-DN (DN), respectively. On the right, quantification of colony number and area/number of colonies. Representative results of at least n=3 independent experiments performed in triplicate. Data presented as mean \pm SEM. Statistical analysis was performed using Student's *t*-test comparing NT/M vs shSTX1A/DN. * $p < 0.05$, ** $p < 0.01$, *** $p < 0.001$, **** $p < 0$.

3.2. STUDY OF THE RELATIONSHIP BETWEEN SYNTAXIN-1A, THE EGFR/HER FAMILY OF RECEPTORS AND TREATMENT RESPONSES

Our initial data in BC patients databases point towards a possible functional relationship between STX1A and EGFR/HER family of receptors. Recapitulating, expression of *STX1A* positively correlated with higher expression of *EGFR*, *HER2* and *HER4* in HER2-positive BC subtypes (*Annex table 2*). Also, in HER2-negative BC subtypes *HER2*, *HER3* and *HER4* positively correlated, while *EGFR* presented an inverse correlation, with *STX1A* (*Annex table 3*). According to these findings we decided to study if a possible functional relationship between this family of receptors in BC and HNSCC cells could exist.

HER2-positive and HER2-negative BC and HNSCC cell lines were used. We focused on EGFR and HER2 receptors because among this receptor family, EGFR and HER2 are the most expressed among BC and HNSCC cell lines. Moreover, they are easier to study due to the fact that there are several specific tools to modulate their activity. However, it is important to note

that in the HER2-negative BC subtype HER2 is not overexpressed, therefore in this subtype we focused on EGFR.

3.2.1. EGFR, HER2 AND HER3 RECEPTORS ARE INVERSELY REGULATED IN BC AND HNSCC WHEN SYNTAXIN-1 FUNCTION IS IMPAIRED

The expression of *EGFR*, *HER2* and *HER3* was characterized in the BC and HNSCC cell lines stably expressing the STX1-DN form. First of all, it was analysed if there were differences at mRNA level. The qPCR analysis revealed that *EGFR* was significantly overexpressed in SK-BR-3, MDA-MB-231 and SCC090 STX1-DN cell lines (Figure 78A). Also in MDA-MB-453, although it did not reach statistical significance the *HER2* receptor was differentially modulated in cancer cells with STX1-DN, while the HER2-positive BC cell lines (SK-BR-3 and MDA-MB-453), the HER2-negative/basal BC cell line BT-549 and the HNSCC cancer cell line FaDu were down-regulating *HER2* mRNA transcription, MDA-MB-231 (HER2-negative/basal) and SCC090 (HNSCC) cells were overexpressing *HER2* receptor gene (Figure 78B). Finally, the mRNA expression analysis of *HER3* revealed that the cell lines analysed but FaDu increased *HER3* mRNA expression. The *HER3* receptor gene was found to be not expressed in BT-549 (Figure 78C).

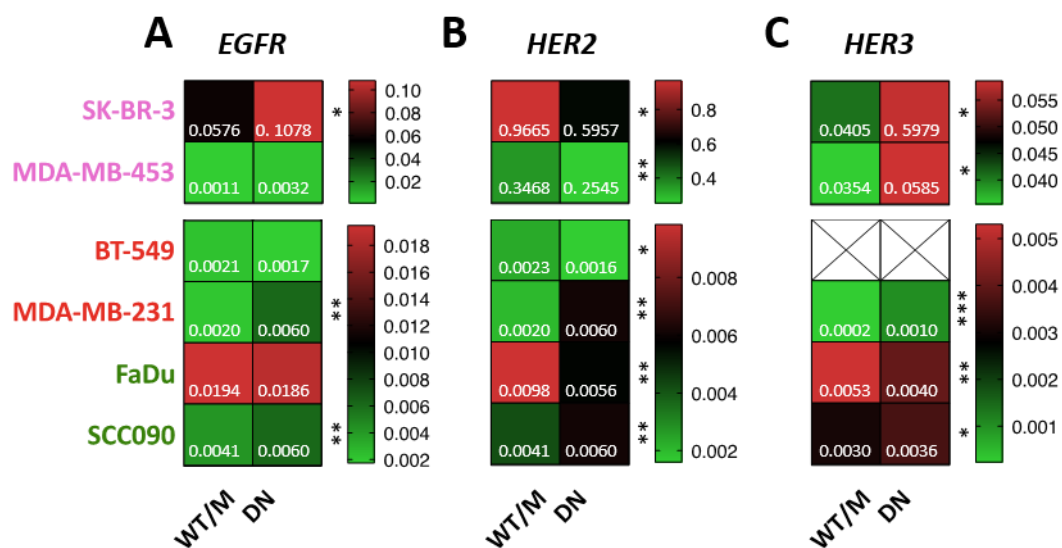
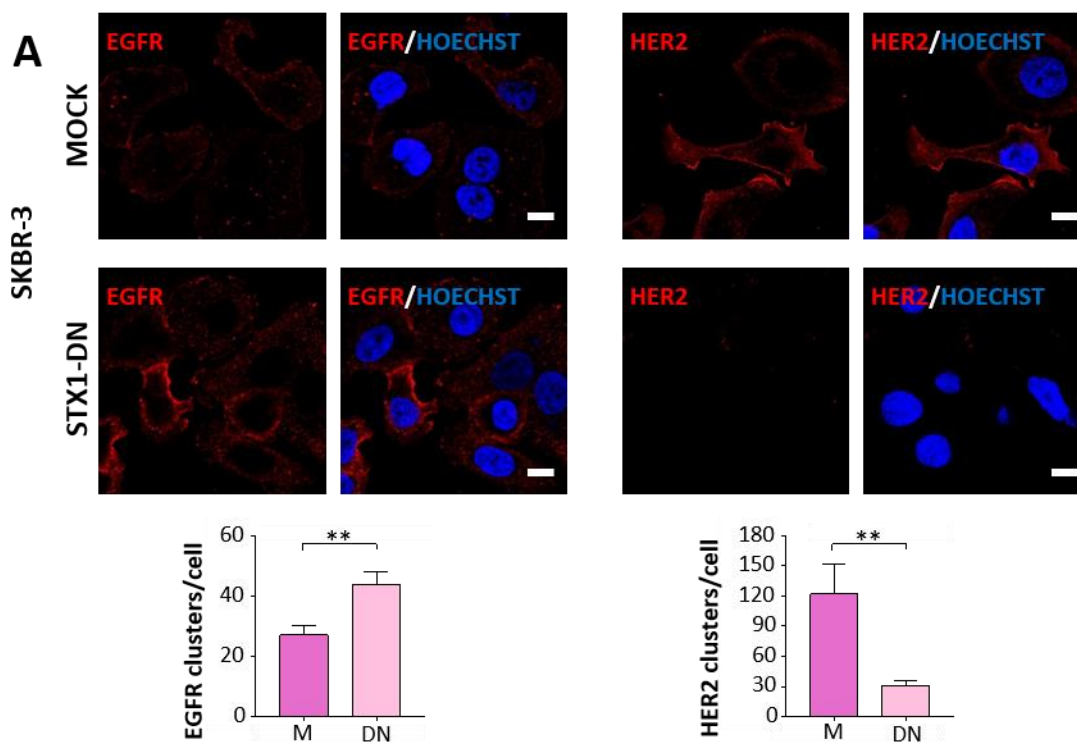
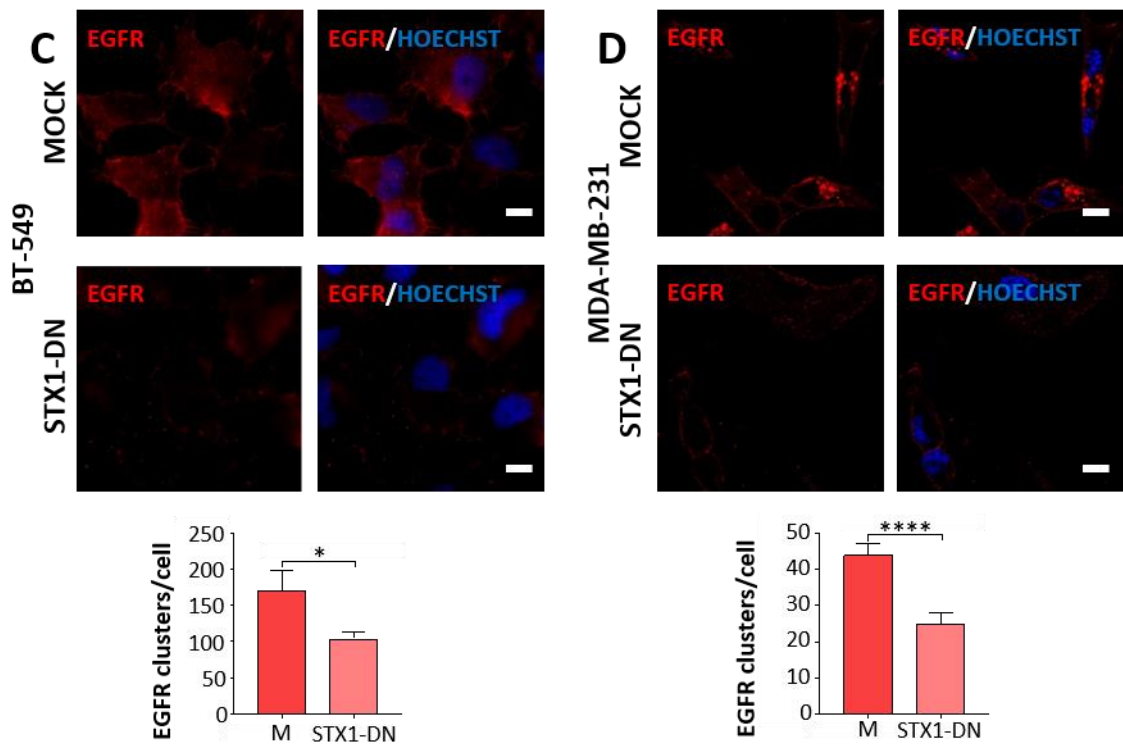
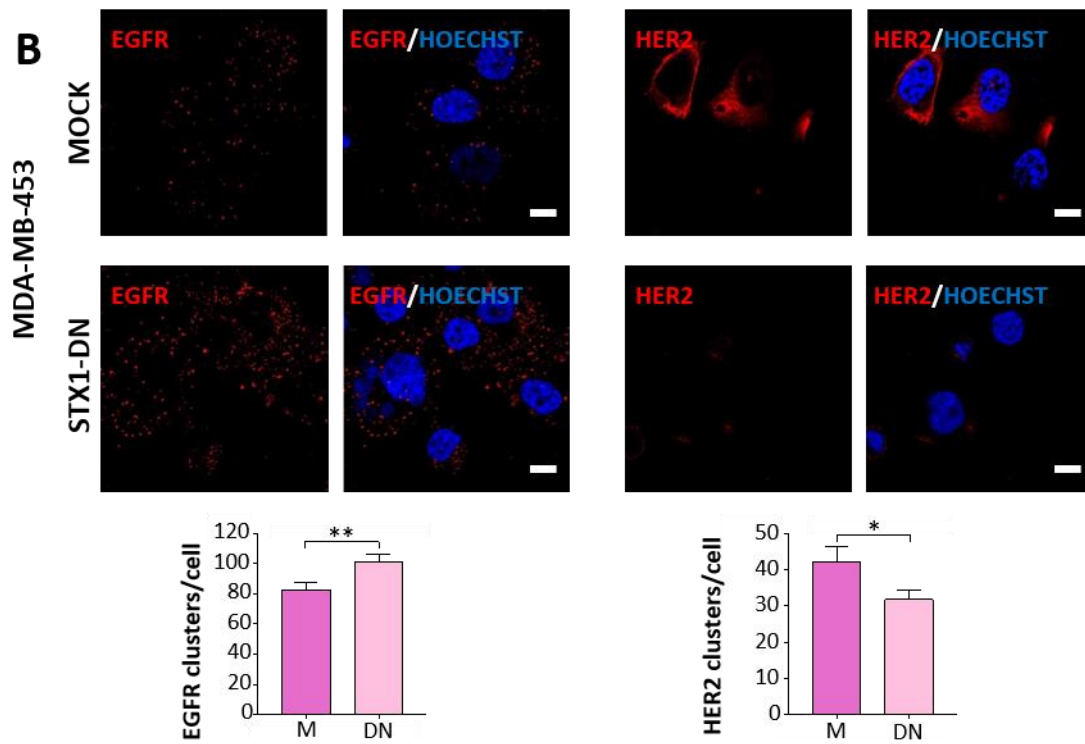


Figure 78 – Differential modulation of mRNA expression of EGFR/HER family of receptors in STX1A-DN BC and HNSCC cell lines. Heat Maps of *EGFR* (A), *HER2* (B) and *HER3* (C) relative mRNA expression analysed by qPCR comparing wild-type (WT) (SK-BR-3 or MDA-MB-453) or MOCK (M) (BT-549, MDAMB-231, FaDu or SCC090) versus STX1-DN cells (DN). β -actin was used as an internal control. Representative results of at n=1 independent experiments performed in triplicate. Data presented as mean. Statistical analysis was performed using Student's t-test comparing M/WT vs DN. * p < 0.05, ** p < 0.01, *** p < 0.001.

Then, to assess if the changes in the mRNA levels detected were translated to EGFR/HER family of receptors protein levels, and considering that these receptors are located mainly in

the plasma membrane, where they most often perform their function, membrane expression of EGFR and HER2 receptors in BC and HNSCC cells was checked (by non-permeabilized immunofluorescence). It was found that HER2-positive BC cells (SK-BR-3 and MDA-MB-453) overexpressed EGFR receptor and down-regulated HER2 expression at the plasma membrane when STX1 function was impaired (*Figure 79A and Figure 79B*). Then, considering that HER2-negative BC cell lines did not overexpress significant levels of HER2 receptor, only the presence of EGFR at the plasma membrane was checked, which resulted that cells with the STX1-DN had lower levels of this receptor (*Figure 79C and Figure 79D*). Finally, the expression of EGFR and HER2 receptors at the plasma membrane of HNSCC cells (FaDu and SCC090) resulted in an overexpression of EGFR in FaDu when STX1 function was impaired (*Figure 79E, left panel*), whereas no difference was detected in SCC090 (*Figure 79F, left panel*). Analysis of HER2 receptor resulted in a down-regulation in SCC090 STX1-DN (*Figure 79F, right panel*), and no differences were detected in STX1-DN FaDu cells (*Figure 79E, right panel*).





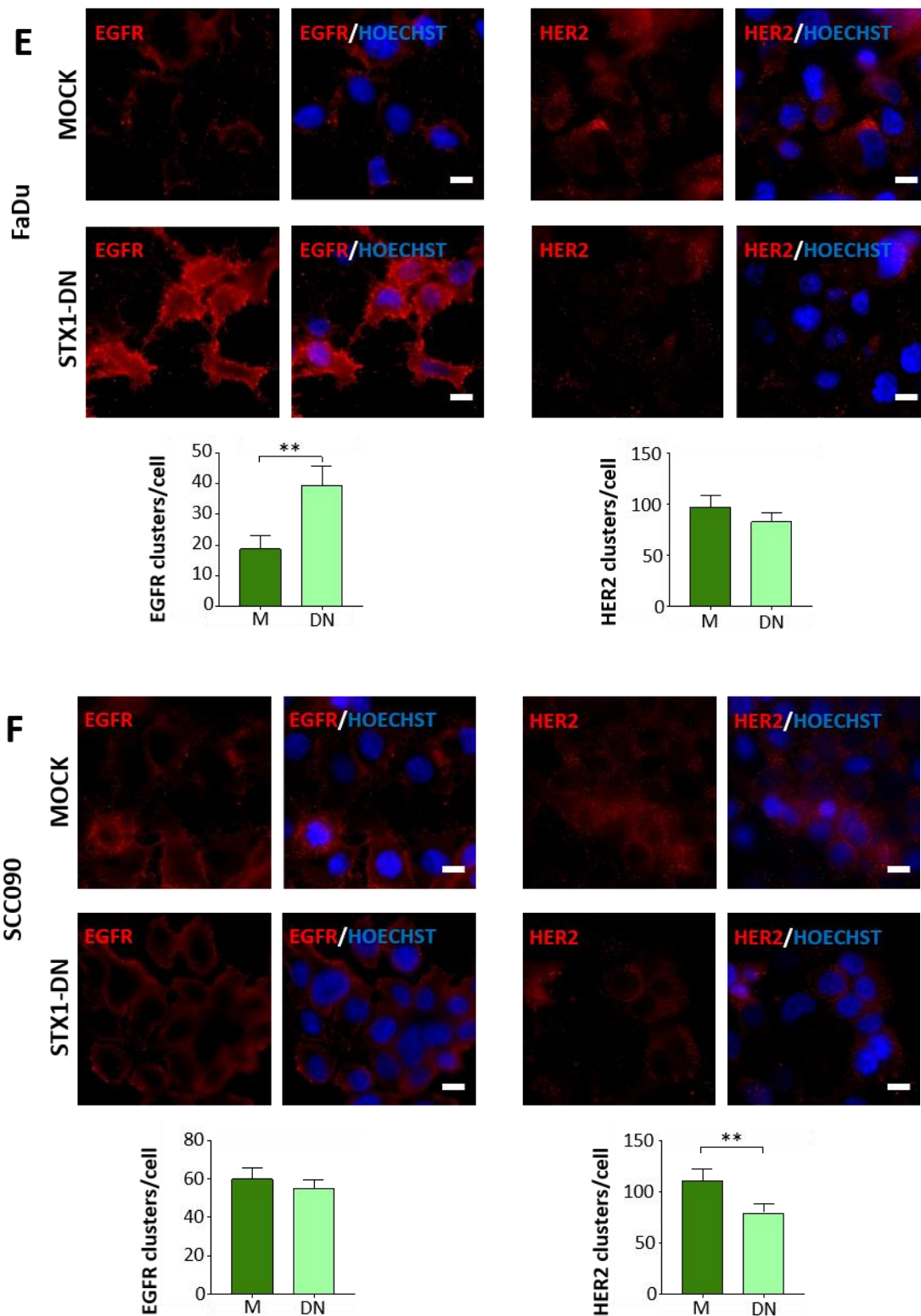
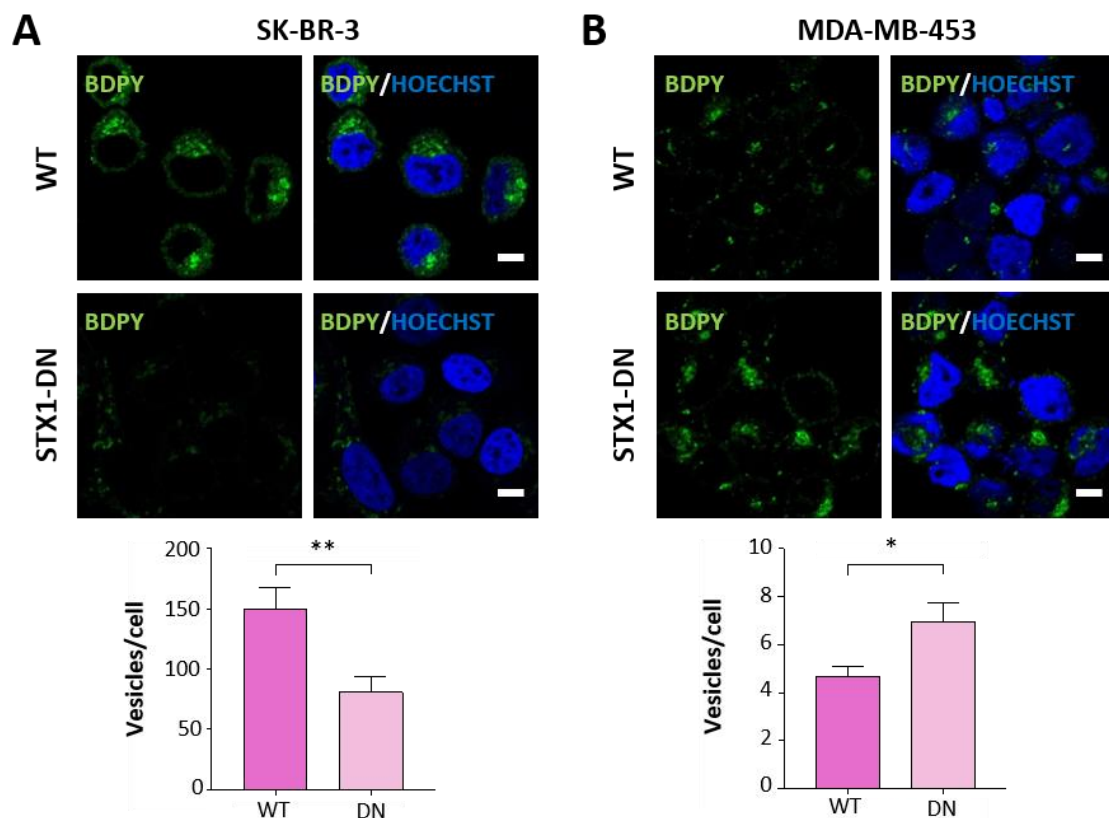


Figure 79 – Cells with non-functional STX1 have modified EGFR and HER2 levels at the plasma membrane. Representative immunofluorescence images of EGFR or HER2 without permeabilization in MOCK (M) or STX1-DN (DN) SK-BR-3 (A), MDA-MB-453 (B) (HER2-positive BC cells), BT-549 (C) and MDA-MB-231 (D) (HER2-negative/basal BC cells) or FaDu (E) and SCC090 (F) (HNSCC cells). Nuclei are counterstained with Hoechst. At the bottom immunofluorescence quantification. Scale bar = 10 μ m. Representative results of at least n=2 independent experiments performed in triplicate. Data presented as mean \pm SEM. At least 10 fields were considered in immunofluorescence images. Statistical analysis was performed using Student's *t*-test comparing M vs DN. * $p < 0.05$, ** $p < 0.01$, **** $p < 0.0001$.

Considering these differences in EGFR/HER family of receptors expression at the plasma membrane and the fact that STX1A is involved in vesicle trafficking and membrane exocytosis in neurons, the possibility that STX1A could be involved in membrane transport or endocytosis of these receptors in breast and HNSCC cells was investigated. Trying to answer that question, a BODIPY-ceramide assay was performed. BODIPY-ceramide is a lipid marker that preloads vesicular compartments, and the decrease in fluorescence signal of BODIPY-ceramide reflects exocytosis events in the cell. HER2-positive (SK-BR-3 and MDA-MB-453) BC cells, HER2-negative (MDA-MB-231) BC cells and HNSCC (FaDu and SCC090) cells were used, comparing wild-type or MOCK versus STX1-DN cells. The results are shown in [Figure 80](#) and in the case of MDA-MB-453, MDA-MB-231 and FaDu an increase in BODIPY-ceramide signal in the STX1-DN cells was found, indicating intracellular vesicles accumulation ([Figure 80B-Figure 80D](#)). Otherwise, in SK-BR-3 and SCC090 STX1-DN cells there was a decrease in intracellular vesicles, indicating that in these STX1-DN cells either more exocytic events could be taking place, or their rate of vesicle production is decreased ([Figure 80A and Figure 80E](#)).



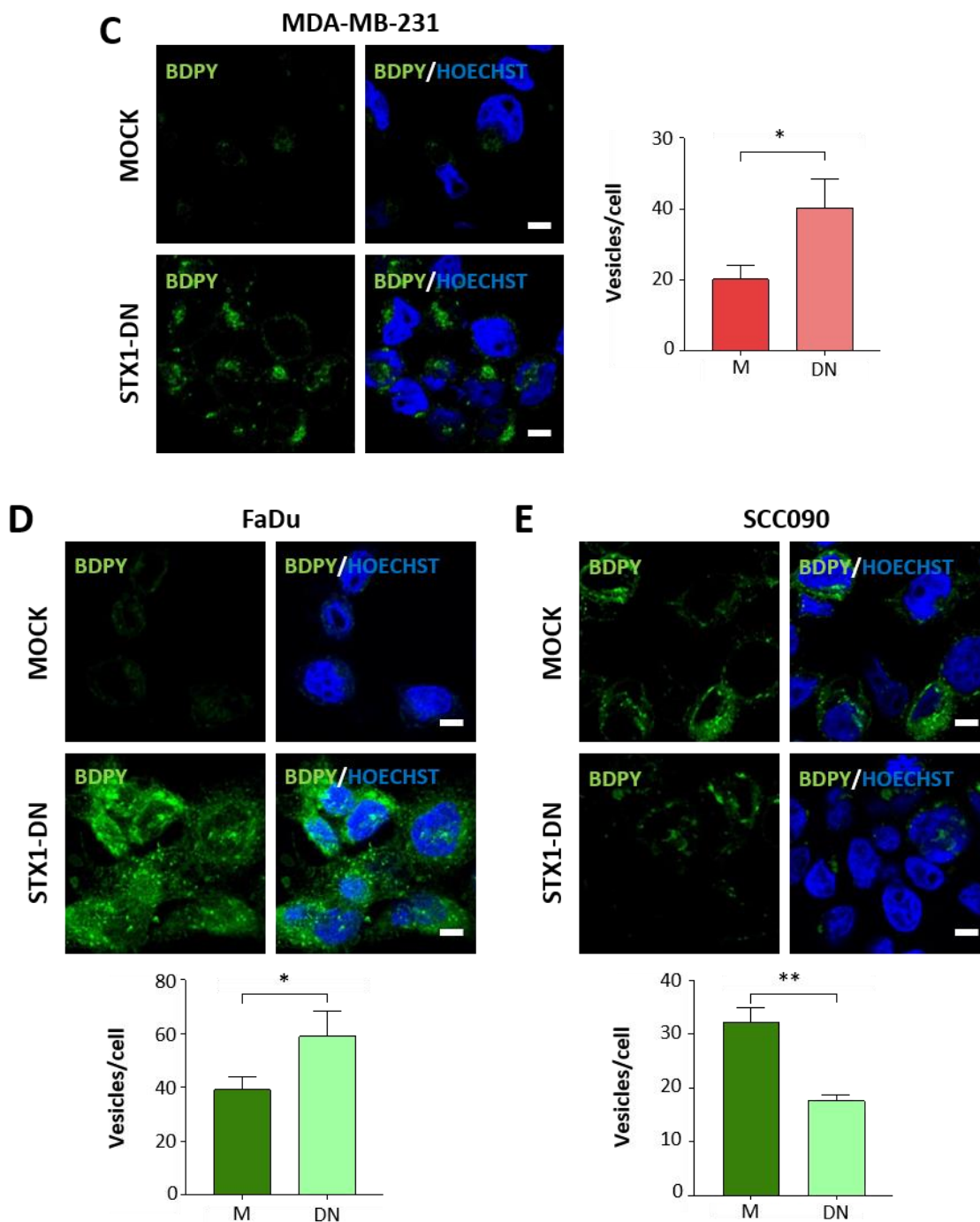
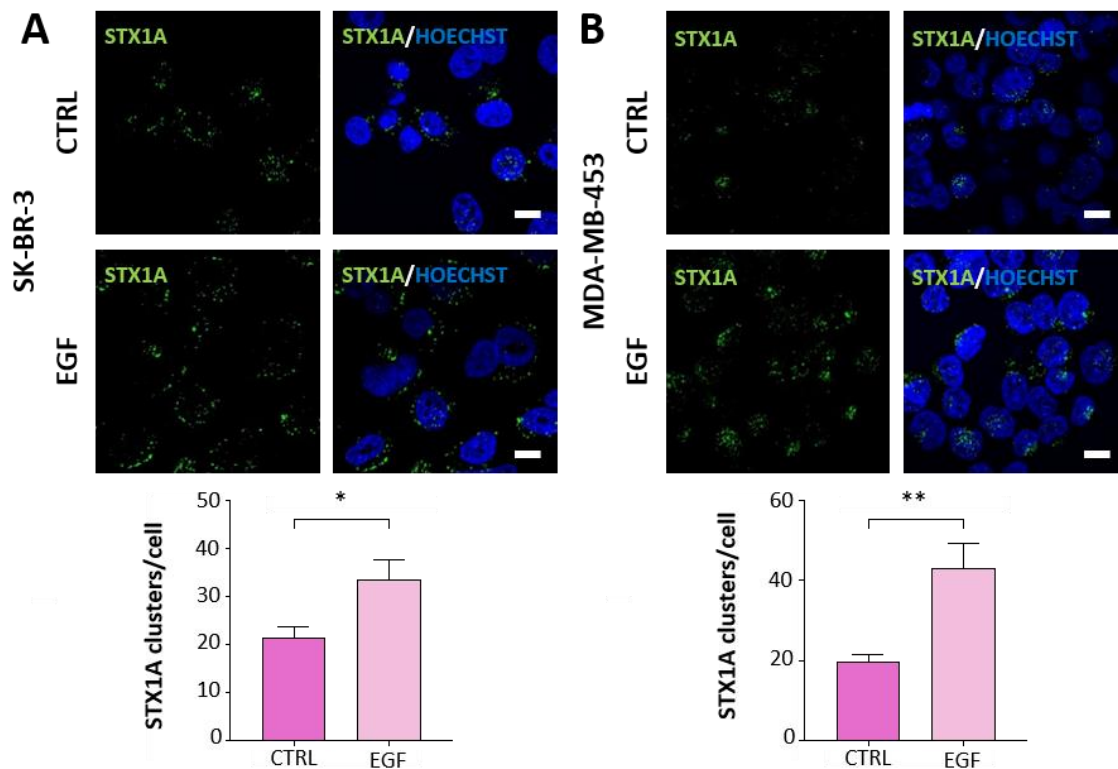


Figure 80 – STX1 function impairment results in alteration in vesicle transport/production in BC and HNSCC cells. Representative immunofluorescence images of SK-BR-3 (A), MDA-MB-453 (B) (HER2-positive BC cells), MDA-MB-231 (C) (HER2-negative/basal BC cells), FaDu (D) and SCC090 (E) (HNSCC cells) wild-type (WT) or MOCK (M) and STX1-DN (DN) cells treated with BODIPY-ceramide for 30 min and fixed after 3 hours of BODIPY-ceramide internalization. Nuclei are counterstained with Hoechst. At the bottom (or on the right in the case of MDA-MB-231 cells) representation of vesicle quantification per cell. Scale bar = 10 μ m. Representative results of at n=2 independent experiments performed in triplicate. Data presented as mean \pm SEM. At least 10 fields were considered in immunofluorescence images. Statistical analysis was performed using Student's *t*-test comparing M vs DN. * $p < 0.05$, ** $p < 0.01$.

Altogether, these results indicate that cells with non-functional STX1 have a different EGFR/HER family of receptors expression pattern at the plasma membrane, which could be explained according to an alteration of vesicle trafficking in STX1-DN BC and HNSCC cells.

3.2.2. EGF INDUCES SYNTAXIN-1A CLUSTERING IN BC AND HNSCC CELL LINES

Once proved that STX1 modulates EGFR and HER2 receptors presence at the plasma membrane, likely by regulating their turnover, it was wondered if the stimulation of these receptors would have any impact on STX1A cellular localization as well. To do that, wild-type BC and HNSCC cells were treated for two hours with EGF 100 nM, one of the natural ligands of the EGFR receptor. Then, the cells were fixed and permeabilized and an immunofluorescence against STX1A was performed, after that, cells were inspected under a confocal microscope. The results represented in [Figure 81](#) demonstrated that EGF-treated BC and HNSCC cells showed an increase of STX1A clusters at the cell membrane in all cases, except for the BT-549 HER2-negative/basal BC cell line. These results indicated that STX1A localisation was affected, directly or indirectly, by EGF. Probably, no differences were observed in BT-549 HER2-negative/basal BC cell line ([Figure 81C](#)) because, as previously described, this cell line have low STX1A protein levels ([Figure 62A](#)), which could make it difficult to appreciate a stimulation of STX1A clustering upon EGF treatment.



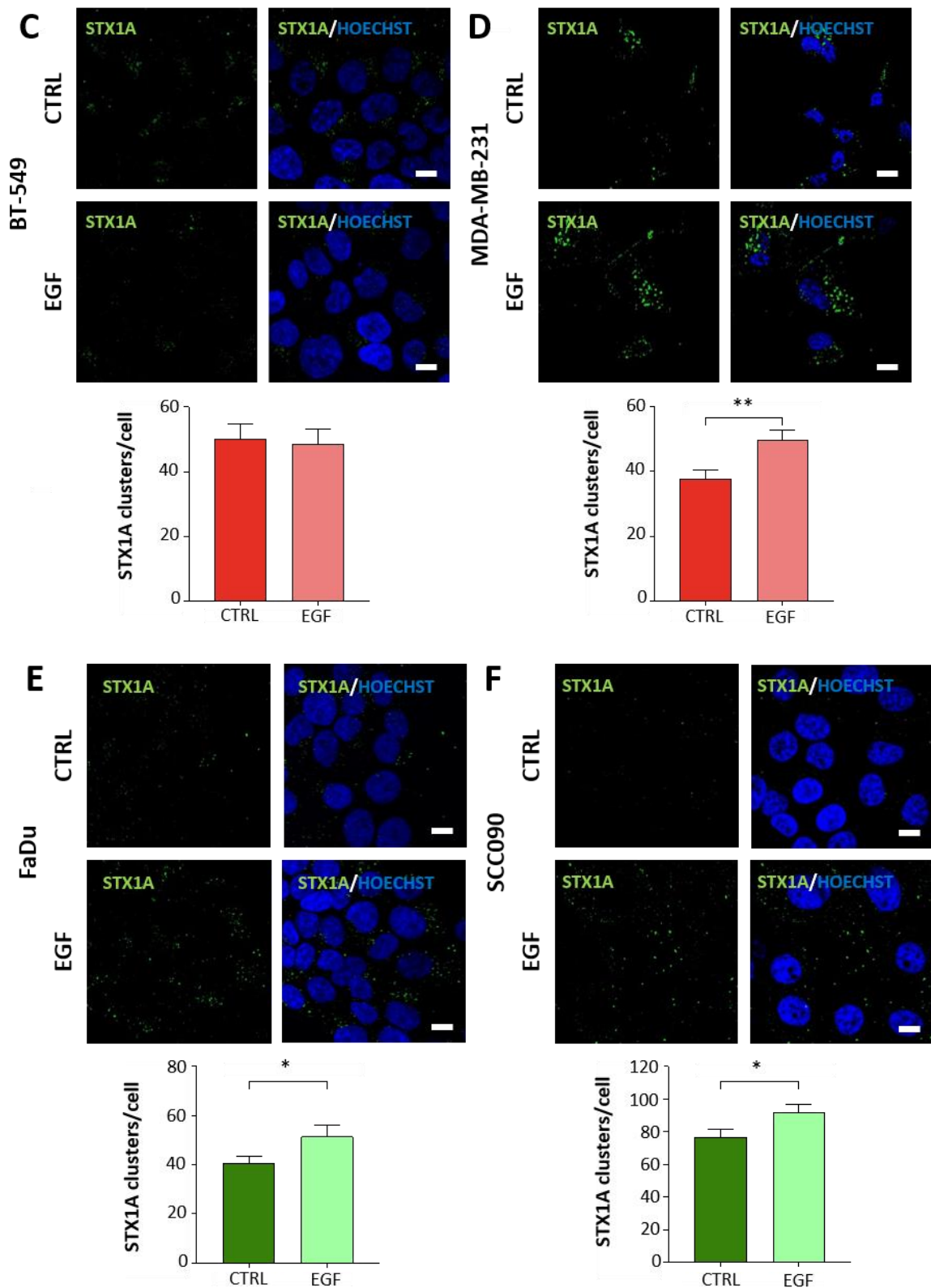


Figure 81 – EGF treatment induces STX1A clustering in BC and HNSCC cell lines. Representative permeabilizing immunofluorescence images of STX1A in SK-BR-3 (A), MDA-MB-453 (B) (HER2-positive BC cells), BT-549 (C) MDA-MB-231 (D) (HER2-negative/basal BC cells), FaDu (E) and SCC090 (F) (HNSCC cells) treated with EGF (100 nM) for 2 hours before fixation. Nuclei are counterstained with Hoechst. At the bottom of each immunofluorescence, representation of cluster quantification per cell. Scale bar = 10 μ m. Representative results of at n=3 independent experiments performed in triplicate. Data

presented as mean \pm SEM. At least 10 fields were considered in immunofluorescence images. Statistical analysis was performed using Student's *t*-test comparing CTRL vs EGF. * $p < 0.05$, ** $p < 0.01$.

After finding that STX1A cellular distribution responded to EGF stimulation, the effects of the stimulation of EGF/HER2 receptors by EGF, or its inhibition by a dual TKI, such as lapatinib, were investigated. *STX1A* gene transcription levels were analysed after 6 hours of treatment with EGF and an upregulation of *STX1A* mRNA levels in the HER2-positive SK-BR-3 BC cell line and in the HER2-negative BC cell line BT-549 was found. A clear tendency to be overexpressed was also seen in the MDA-MB-231 BC cell line (Figure 82A). Lapatinib treatment was only performed in HER2-positive BC cell lines because this BC subtype is the one usually treated with this drug. The dual inhibition of EGFR and HER2 receptors resulted in a slight decrease of *STX1A* mRNA in SK-BR-3 and MDA-MB-453 BC cell lines, although without reaching statistical power. Finally, even no changes were detected in *STX1A* mRNA expression levels after 6 hours of EGF treatment in the HER2-positive MDA-MB-453 BC cell line (Figure 82A), an upregulation of *STX1A* protein expression when the cells were treated with EGF for 24 hours was detected (Figure 82B).

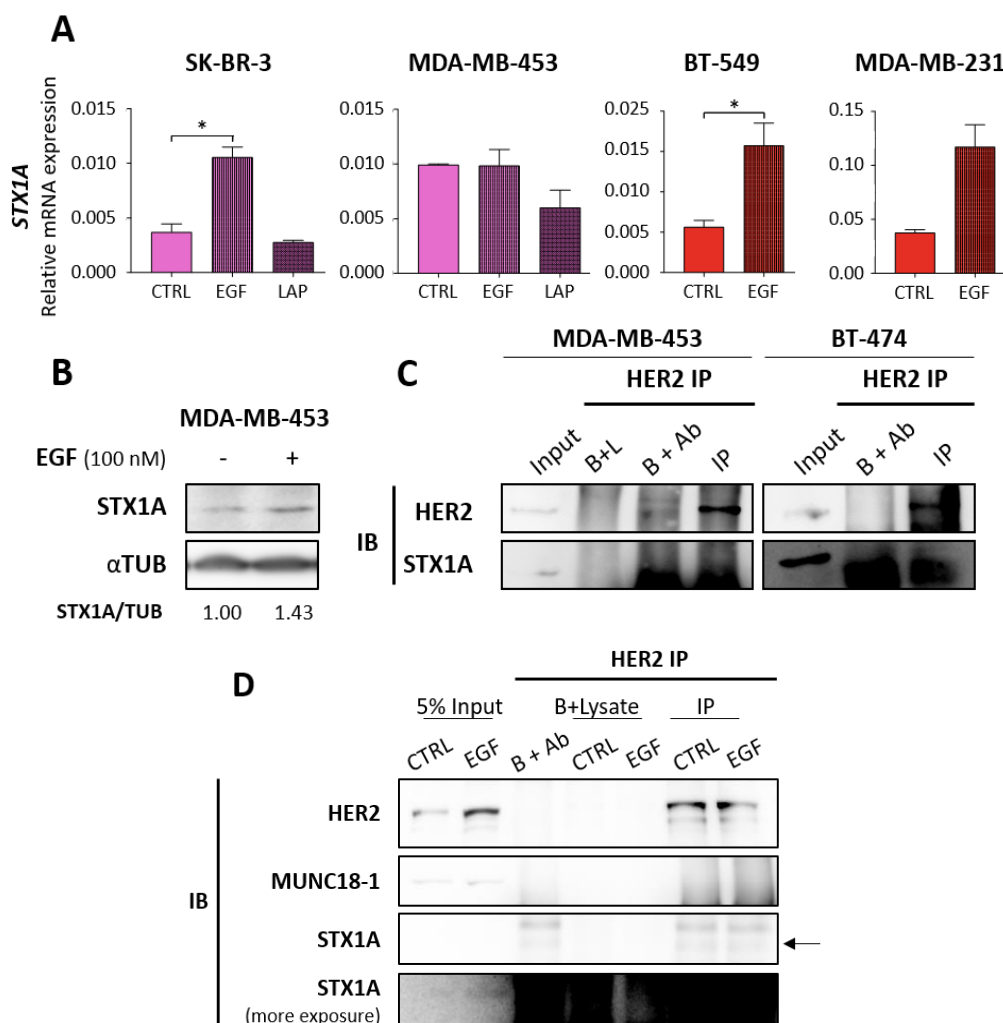


Figure 82 – EGF treatment promotes STX1A expression in BC cells. (A) Relative STX1A mRNA expression levels of SK-BR-3 and MDA-MB-453 treated with EGF (100 nM) or lapatinib (50 nM and 5 nM, respectively) for 6 hours and BT-549 and MDA-MB-231 treated with EGF (100 nM) for 6 hours. β -actin was used as an internal control. (B) Representative Western Blot analysis of STX1A in MDA-MB-453 cells treated with EGF (100 nM) for 24 hours. α TUB was used as internal control. On the bottom signal quantification of protein expression normalized to the control condition. (C) HER2 immunoprecipitation (IP) in HER2-positive MDA-MB-453 and BT-474 BC cells and immunoblotted (IB) for HER2 and STX1A detection. Beads + lysate (B+L), Beads + Antibody (B+Ab). (D) HER2 immunoprecipitation in MDA-MB-453 cells treated with EGF (100 nM) for 2 hours and immunoblotted for HER2, MUNC18-1 and STX1A detection. Representative results of n=2 independent experiments. Data presented as mean \pm SEM. Statistical analysis was performed using one-way ANOVA test (SK-BR-3 and MDA-MB-453) or Student's *t*-test (BT-549 and MDA-MB-231) comparing CTRL vs EGF or LAP. * $p < 0.05$.

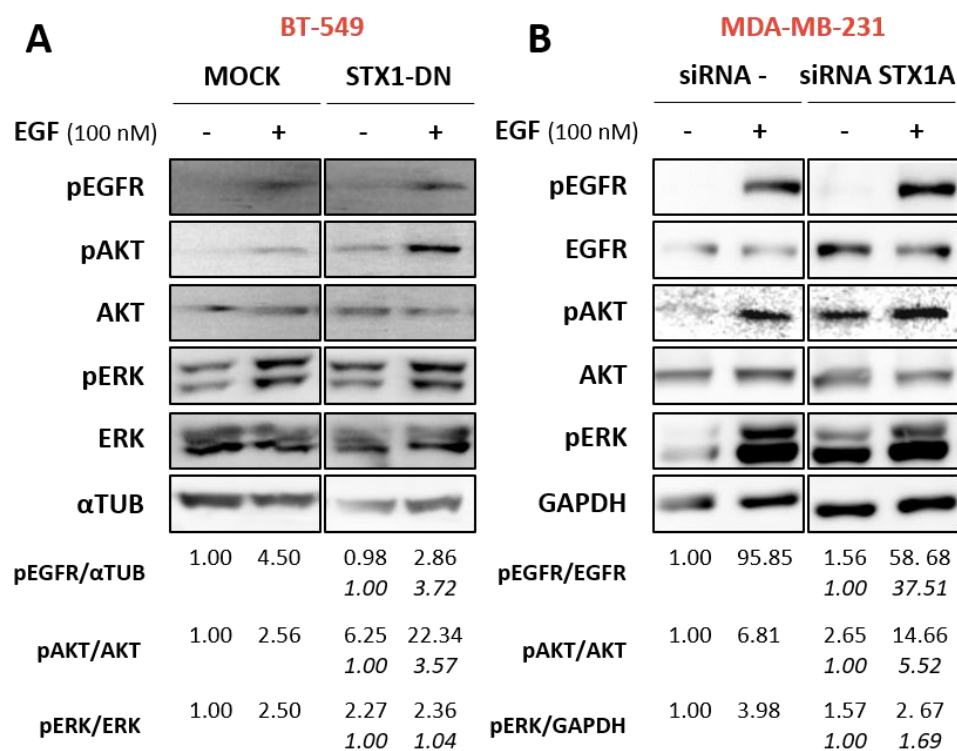
Going one step further, we checked whether STX1A was interacting with EGFR or HER2 receptors, which could explain why STX1A clustered when EGFR/HER2 were activated with EGF. First of all, HER2 receptor was immunoprecipitated in wild-type HER2-positive cells to determine if STX1A co-immunoprecipitated with this receptor. However, as it can be seen in [Figure 82C](#) no STX1A was pulled-down when HER2 receptor was immunoprecipitated in either cell line. Considering that STX1A clustering was induced when EGFR or HER2 receptors were stimulated with EGF, HER2-positive cells were treated with this growth factor, HER2 was immunoprecipitated and it was analysed if STX1A co-immunoprecipitated with it. No STX1A bands were found when HER2 was immunoprecipitated ([Figure 82D](#)). MUNC18-1 co-immunoprecipitation, a soluble SNARE that mediates STX1A SNARE complex formation, was also checked and no band was found when HER2 was immunoprecipitated either ([Figure 82D](#)). EGFR immunoprecipitation was also performed; however EGFR pull-down was not achieved ([data not shown](#)) and no further analysis could be done.

3.2.3. SYNTAXIN-1A MODULATES EGFR/HER FAMILY MEMBERS RESPONSIVENESS TO EGF AND LAPATINIB

Once demonstrated that STX1 modulates EGFR and HER2 abundance and distribution at the plasma membrane, and that EGF treatment induces STX1A clustering, it was explored whether the receptor down-stream signalling pathways were modulated by STX1A.

HER2-negative BC cell lines (BT-549 and MDA-MB-231), as this BC subtype is the one that overexpresses EGFR, and also HNSCC cell lines, which overexpress EGFR receptor as well, were treated with EGF 100 nM for 2 hours. After that time, the samples were collected to perform a Western blot to analyse EGFR down-stream signalling pathways. The results are shown in [Figure 83](#) and, as expected, MOCK or siRNA- cells, after EGF treatment, increased the

activation of EGFR, AKT and ERK signalling. Then, focusing on the treatment differences between MOCK/siRNA- and STX1-DN/siRNA STX1A it can be appreciated that in HER2-negative BC cell lines, even though EGFR was activated by EGF, this activation did not reach the MOCK or siRNA- activation levels. Then focusing on AKT and ERK activation upon EGF treatment the degree of ERK activation was lesser than that of the control cells, while no considerable modulation was detected in AKT (*Figure 83 A and Figure 83B*). In FaDu HNSCC cell line, treatment with EGF in STX1-DN cells resulted in a marked overactivation of EGFR and AKT, pERK levels increasing to a lesser extent (*Figure 83C*). Finally, in SCC090 HNSCC cell line treated with EGF, EGFR activation did not reach the same activation level in STX1-DN, as occurred with BC cell lines. However, they clearly overactivated AKT signalling, while little changes in ERK activation were detected (*Figure 83D*). It is worth to note that in all cases a parallel modulation of pEGFR and pERK was observed, whereas pAKT levels are found mostly increased in STX1-DN and siRNA cells treated with EGF.



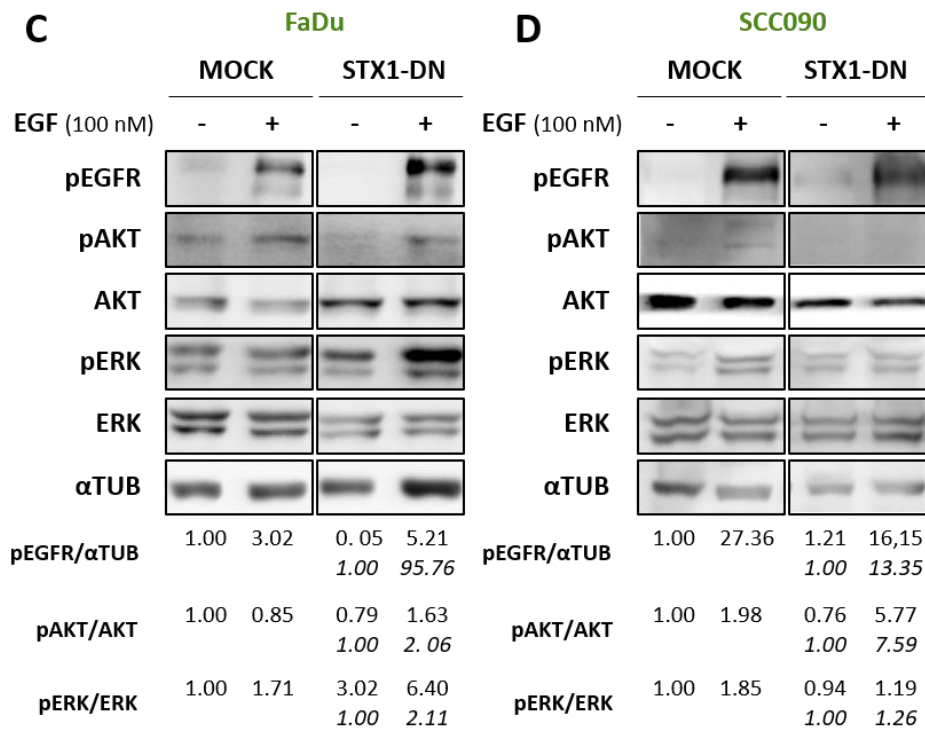


Figure 83 – STX1A function impairment affects HER2-negative/basal BC and HNSCC EGFR, AKT and ERK activation under EGF treatment. Representative Western blot analysis of EGFR, AKT and ERK activation in BT-549 (A), MDA-MB-231 (B), FaDu (C) and SCC090 (D) MOCK/siRNA - and STX1DN/siRNA STX1A cells treated with EGF (100 nM) for 2 hours. αTUB or GAPDH were used as internal controls. At the bottom, signal quantification of protein expression normalized to the control condition. Representative results of n=1 independent experiment.

HER2-positive BC and HNSCC cells were also treated with lapatinib for 2 hours, but each cell line at a different concentration, due to its different IC₅₀. Cells were collected after the treatment and AKT and ERK activation was analysed. Control BC cell lines upon lapatinib treatment down-regulated AKT and ERK signalling pathways, as expected (*Figure 84*). STX1-DN SK-BR-3 BC cell lines treated with lapatinib still showed activation of AKT signalling pathway (*Figure 84A*). The other HER2-positive BC cell line that was down-regulated for STX1A by shRNA, displayed similar results, AKT was less deactivated and ERK even slightly overactivated in comparison to the shRNA Non-Target treated with lapatinib (*Figure 84B*). Focusing on HNSCC cell lines, FaDu STX1-DN treated with lapatinib better maintained AKT pathway activation levels at both doses of lapatinib, and even a slight ERK activation was observed, when comparing with MOCK cells treated with lapatinib (*Figure 84C*). Less marked alterations were found in SCC090 cells (*Figure 84D*).

To summarize, until now these results demonstrate that STX1A activity positively modulates EGFR/HER family of receptors presence at the plasma membrane which in turn may

modify their activation state and of their main down-stream signalling pathways, in response to ligands and TKIs.

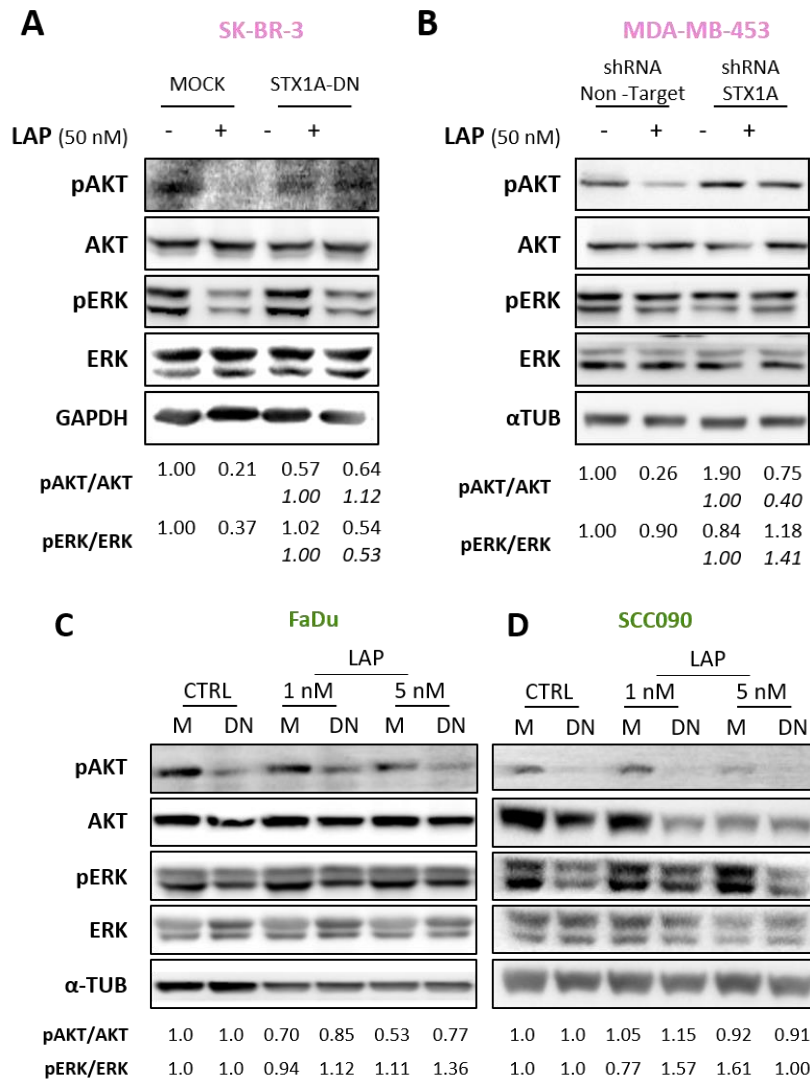
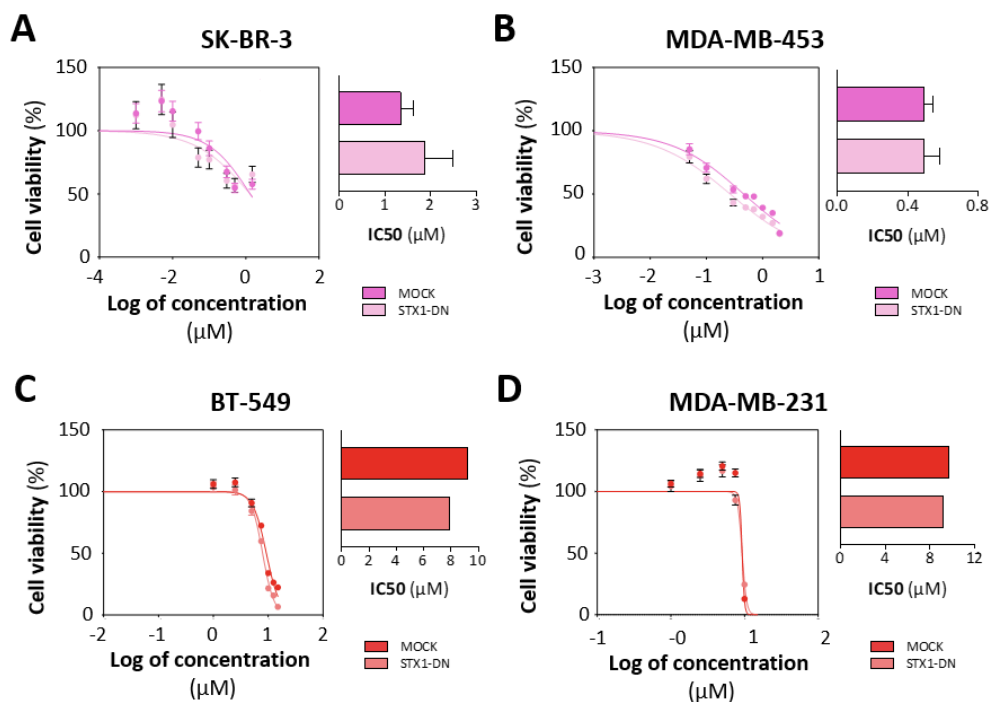


Figure 84 – STX1A function impairment affects BC and HNSCC cell signalling response to lapatinib treatment. Representative Western blot analysis of AKT and ERK activation in SK-BR-3 (A), MDA-MB-453 (B) (HER2-positive BC cells), FaDu (C) and SCC090 (D) (HNSCC cells) MOCK (M)/shRNA NonTarget and STX1-DN/shRNA STX1A cells treated with lapatinib (50 nM for SK-BR-3, 5 nM for MDA-MB-453 and 1 and 5 nM for FaDu and SCC090) for 2 hours. GAPDH or α TUB were used as internal controls. At the bottom signal quantification of protein expression normalized to the control (MOCK or shRNA Non-Target condition) or to each own control (MOCK CTRL or shRNA Non-Target CTRL and STX1DN CTRL or shRNA STX1A CTRL). Representative results of n=2 (BC cell lines) or n=1 (HNSCC cell lines) independent experiments.

3.2.4. HNSCC CELL LINES WITH NON-FUNCTIONAL SYNTAXIN-1A ARE MORE SENSITIVE TO LAPATINIB TREATMENT

The finding that BC and HNSCC cells with down-regulated STX1A or non-functional STX1 had a differential modulation of AKT and ERK activation after EGF and lapatinib treatment made us wonder if the STX1 loss-of-function could alter BC and HNSCC cells sensitivity to

lapatinib. To test possible differences in lapatinib sensitivity, MTT cytotoxic assays were performed, treating the cells with a range of lapatinib doses. First, HER2-positive BC cell lines (SK-BR-3 and MDA-MB-453) were checked, since lapatinib is used to treat this BC subtype. The results determined that neither STX1-DN SKBR-3 BC (*Figure 85A*) nor MDA-MB-453 BC cell line (*Figure 85B*) displayed an altered IC₅₀ to lapatinib. Even though lapatinib is not used to treat HER2-negative BC tumours, MTT cytotoxic assays were also performed in BT-549 and MDA-MB-231 to check if the loss of STX1 function sensitized these HER2-negative BC cell lines to lapatinib treatment. However, no difference in lapatinib sensitivity was detected either (*Figure 85C and Figure 85D*). Finally, and even though lapatinib is not usually used to treat HNSCC tumours, it was investigated for STX1-DN increase or decrease the sensitivity to lapatinib in HNSCC cell lines, since they usually overexpressed EGFR, one of the two lapatinib targets. Interestingly, it was found that STX1 function impairment resulted, as shown in *Figure 85E and Figure 85F*, in sensitization to lapatinib treatment. The IC₅₀ of both HNSCC cell lines were reduced 3 times: FaDu MOCK IC₅₀ being 6.133 μ M and reduced to 1.969 μ M when STX1 function was impaired (*Figure 85E*), whereas the initial IC₅₀ of SCC090 MOCK was 6.919 μ M and was reduced to 2.268 μ M in SCC090 STX1-DN cells (*Figure 85F*).



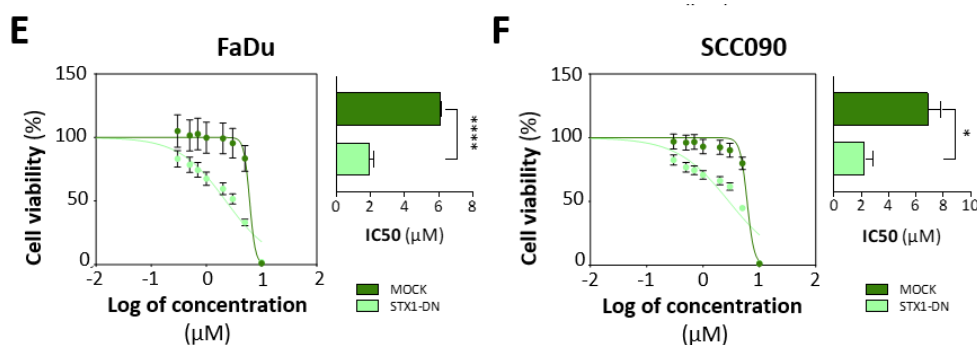


Figure 85 – HNSCC cells with STX1 function impairment are more sensitive to lapatinib treatment. MTTs of SK-BR-3 (A), MDA-MB-453 (B) (HER2-positive BC cells), BT-549 (C), MDA-MB-231 (D) (HER2-negative/basal BC cells), FaDu (E) and SCC090 (F) (HNSCC cells) MOCK and STX1-DN treated with different doses (0.001 – 1.5 μ M for SK-BR-3; 0.05 – 2 μ M for MDA-MB-453; 1 – 15 μ M for BT-549 and MDA-MB231 and 0.3 – 10 μ M for FaDu and SCC090) of lapatinib for 72 hours. On the right of each figure, IC₅₀ value representation. Representative results of n=3 or n=1 (HER2-negative/basal BC cell lines) independent experiments performed in sextuplicate. Data presented as mean \pm SEM. Statistical analysis was performed using Student's *t*-test comparing IC₅₀ value of M vs DN. * $p < 0.05$, **** $p < 0.0001$.

Then, to verify these results, a cell cycle assay was performed, treating STX1-DN BC and HNSCC cells with lapatinib for 24 hours to analyse possible differences in the cell cycle distribution. The results followed the same trend than the previous ones ([Figure 76](#)), STX1-DN cells were more proliferative with more cells going through S and G₂/M cell cycle phases. Then, focusing on the cells treated with lapatinib, the percentage of cells at G₁ phase was similar between both groups ([Figure 86A](#)). More in detail, when SK-BR-3 STX1-DN cells were treated with lapatinib, a major proportion of cells got arrested at the G₁ phase in comparison to its control, while no significant differences were detected in the MOCK cells treated with lapatinib. In the other HER2-positive BC cell line, MDA-MB-453, MOCK and STX1-DN cells both increased the cell proportion at G₁ phase when treated with lapatinib, however the increase was greater in STX1-DN cells. In HNSCC cells, FaDu MOCK cell cycle pattern did not change when cells were treated with lapatinib, while when the STX1-DN cells were treated the proportion of G₁ cells, proving the major sensitivity of these cells to the drug. Finally, considering SCC090 cells, no differences were detected when STX1-DN cells were treated with lapatinib, however in MOCK cells an increase on the proportion of cells at S and G₂/M cell cycle phase was detected.

Moreover, a clonogenic assay with the SK-BR-3 Non-Target and shRNA STX1A HER2-positive BC cells treated with lapatinib was performed to see if the cells with down-regulated STX1A decreased their colony formation capacity under the treatment. After three weeks of lapatinib treatment, it was found, as expected from the previous obtained results ([Figure 86B](#)),

that cells with down-regulated STX1A increased their colony formation capacity, but this was more sensitive to lapatinib treatment, in accordance to the cell cycle analysis findings.

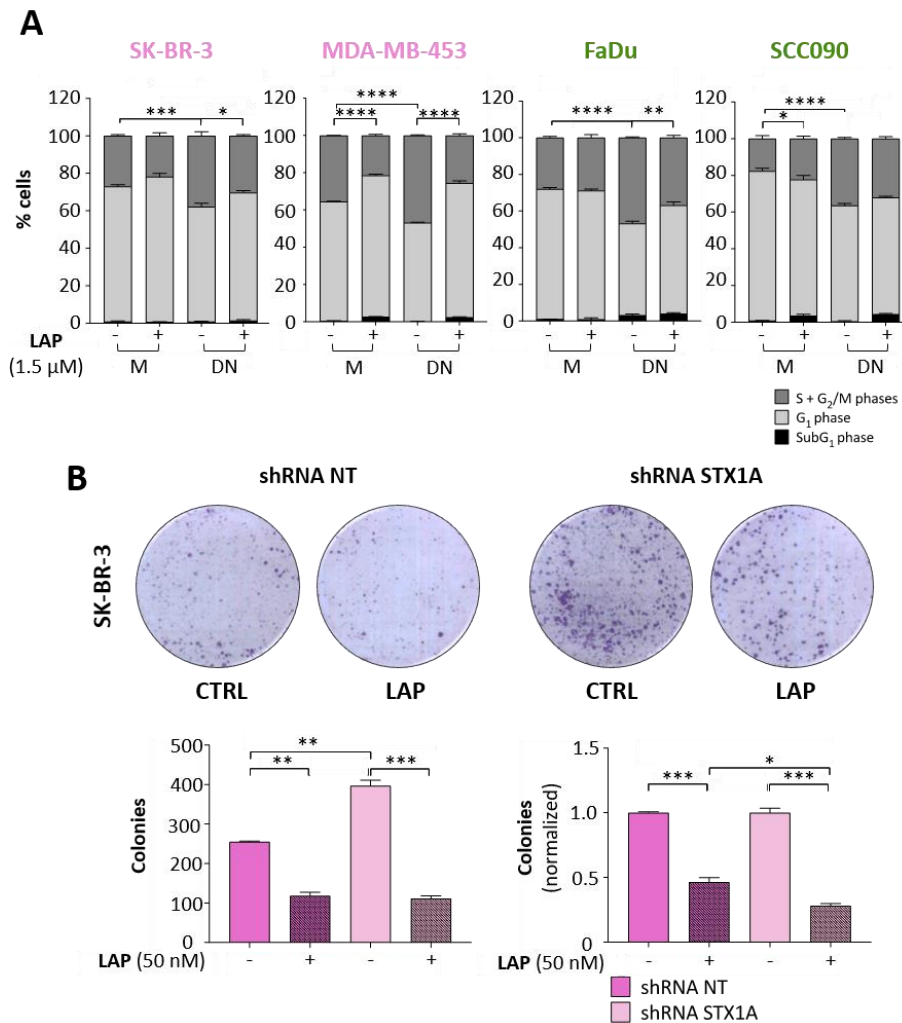


Figure 86 – Non-functional STX1 reduces proliferation of BC and HNSCC cells under lapatinib treatment. (A) Representation of MOCK (M) and STX1-DN (DN) SK-BR-3, MDA-MB-453 HER2-positive BC cells and FaDu and SCC090 HNSCC cells proliferation assay after 24 hours of 1.5 μ M lapatinib treatment. (B) Clonogenic assay of SK-BR-3 shRNA Non-target (shRNA NT) and shRNA STX1A treated with 50 nM lapatinib for 3 weeks. At the bottom, number of colonies for each condition and normalized according to each control shRNA NT or shRNA STX1A. Representative results of n=1 independent experiments performed in duplicates (cell cycle) or triplicates (clonogenics). Data presented as mean \pm SEM. Statistical analysis was performed using two-way ANOVA, Sidak's test (cell cycle) or one-way ANOVA (clonogenics). * p < 0.05, ** p < 0.01, *** p < 0.001, ****p < 0.0001.

An annexin V assay was performed in HNSCC cells since they were the most sensitized to lapatinib when STX1 function is impaired. First, the composition of the sample was analysed, selecting only the HNSCC singlets of the sample. As it is possible to see in [Figure 87A](#) and [Figure 87B](#), there was an increase of cells debris in the samples treated with 1.5 μ M lapatinib for 24 hours, but this increase was more notorious in the STX1-DN cells both in FaDu and SCC090 ([red arrows in Figure 87A](#) and [Figure 87B](#)), corroborating that STX1-DN cells were more sensitive to lapatinib. The analysis of the Annexin V and IP staining ([Figure 87C](#) and [Figure 87D](#)), revealed

no significant differences, considering the two apoptosis stages (early and late) and necrosis. However, the analysis of the total cell death events revealed that the percentage of STX1-DN cells treated with lapatinib was higher than the MOCK cells treated with lapatinib, as it was expected (*Figure 87C* and *Figure 87D*).

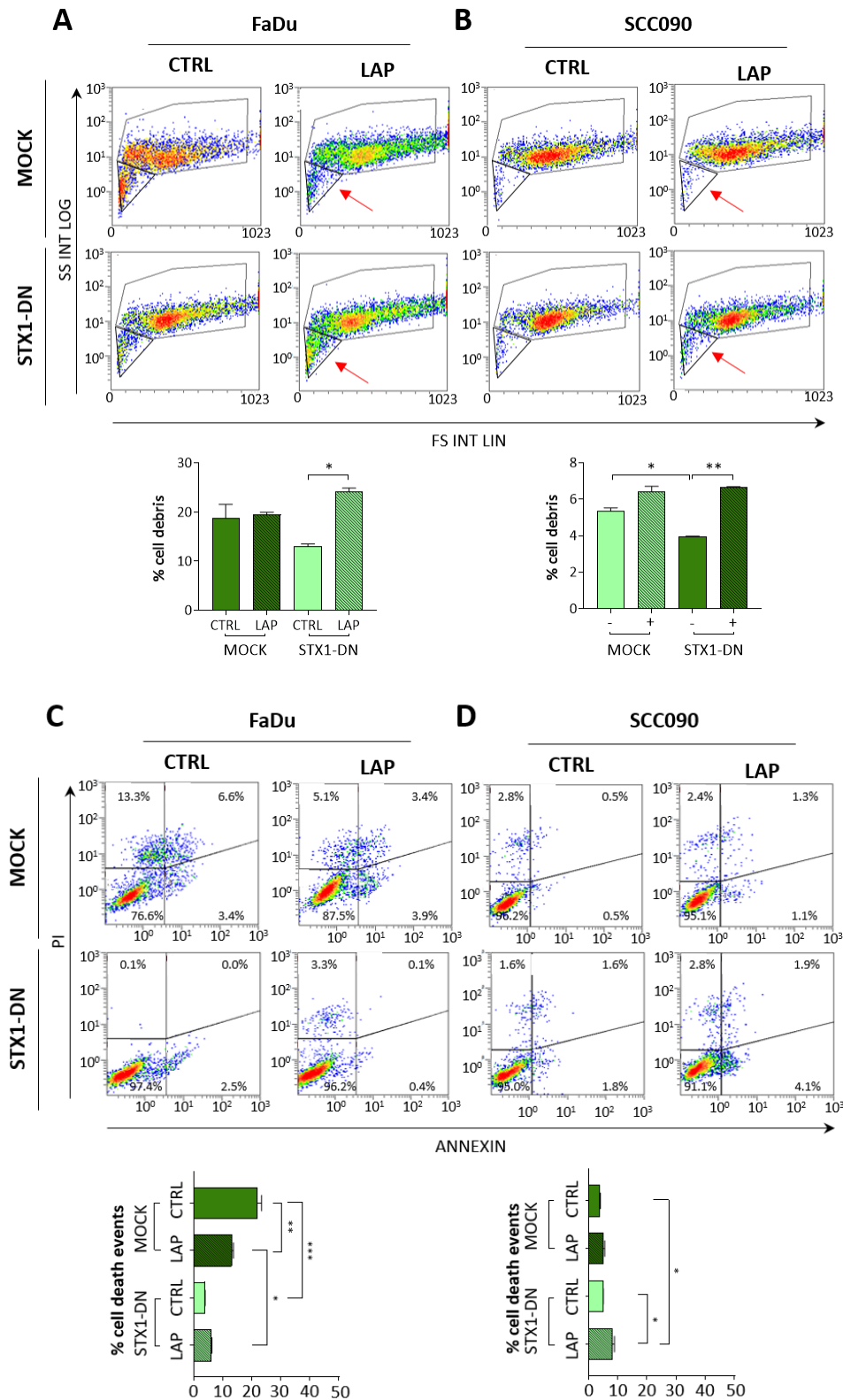


Figure 87 – Lapatinib treatment on STX1 function-impaired HNSCC cell lines results in an increase of cell debris. (A and B) On the top, panels representing side scatter (y axis) versus forward scatter (x axis) of FaDu (A) and SCC090 (B) HNSCC MOCK and STX1-DN cells treated with lapatinib 1.5 μ M for 24 hours. Red arrows indicate the cell debris fraction after lapatinib treatment in MOCK and STX1-DN HNSCC cells. At the bottom quantification of cells debris. (C and D) On the top, panels representing propidium iodide (PI) (y axis) versus Annexin V staining (x axis) of FaDu (C) and SCC090 (D) HNSCC cells treated with lapatinib 1.5 μ M for 24 hours. At the bottom, graphs representing the percentage of cell death events (PI-positive and/or Annexin V positive) shown in upper graphs. Representative results of n=1 independent experiments performed in duplicates. Data presented as mean \pm SEM. Statistical analysis was performed using two-way ANOVA Sidak's test. * $p < 0.05$, ** $p < 0.01$, *** $p < 0.001$.

The annexin V assay revealed that some cells died from apoptosis. However, focusing on the number of cells that entered to apoptosis and/or necrosis only around 10% of STX1-DN underwent apoptotic death. According to the MTT assays (*Figure 85E and Figure 85F*), cells should be dying, likely by apoptosis, considering IC_{50} and the lapatinib dose at which the cells were treated. This fact, together with the increase in cell debris when the STX1-DN cells were treated with lapatinib (*Figure 87A and Figure 87B*), opened the possibility that maybe the apoptotic pathway was not the main death pathway by which cells were dying. Bearing in mind that some syntaxins and other SNAREs proteins are involved in the autophagic pathway, it was decided to explore autophagy induction in HNSCC cells, treating them with 1.5 μ M lapatinib for 24 and 48 hours. The amount of the apoptotic marker BAX and the autophagic marker LC3 were detected by tracking the conversion of LC3-I to LC3-II by Western blot. The results in HNSCC FaDu and SCC090 revealed that no BAX expression was down-regulated in STX1-DN cells in comparison to MOCK cells and that no overexpression was detected after lapatinib treatment in FaDu cells. Only in SCC090 STX1-DN cells a slightly increase of BAX could be appreciated (*Figure 88*). Total LC3 content was increased in STX1-DN cells. An increase of LC3-II and in the LC3-II/LC3-I ratio was detected under lapatinib treatment, indicative of an induction of autophagy. Focusing on cells with impaired STX1 function, an increased LC3-II presence due to lapatinib treatment was found, increasing at the same time its LC3-II/LC3-I ratio. Besides, MOCK-treated cells also increased the LC3-II/LC3-I ratio, but it was not as marked as in STX1-DN cells, indicating that more STX1-DN cells were entering the autophagy process than MOCK FaDu and SCC090 cells under lapatinib treatment (*Figure 88*).

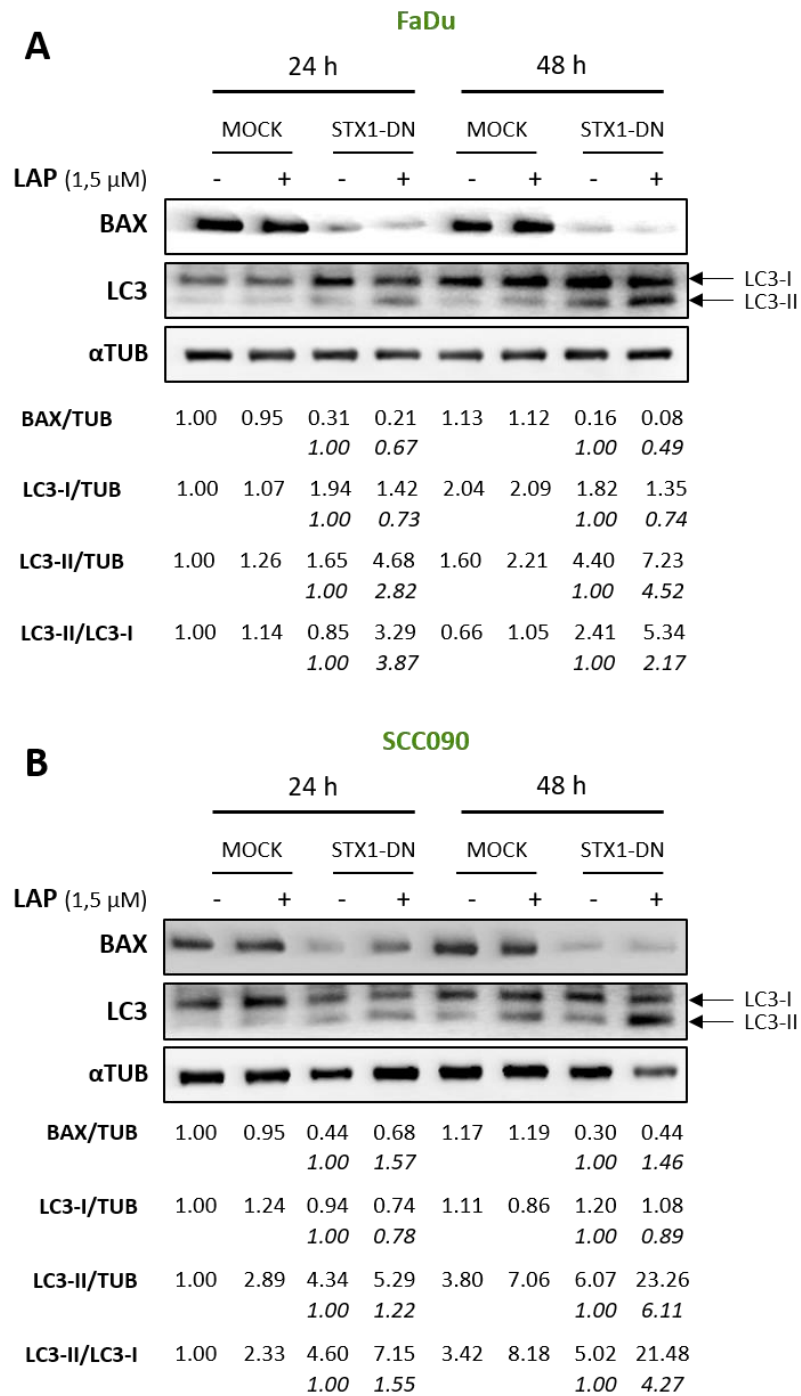
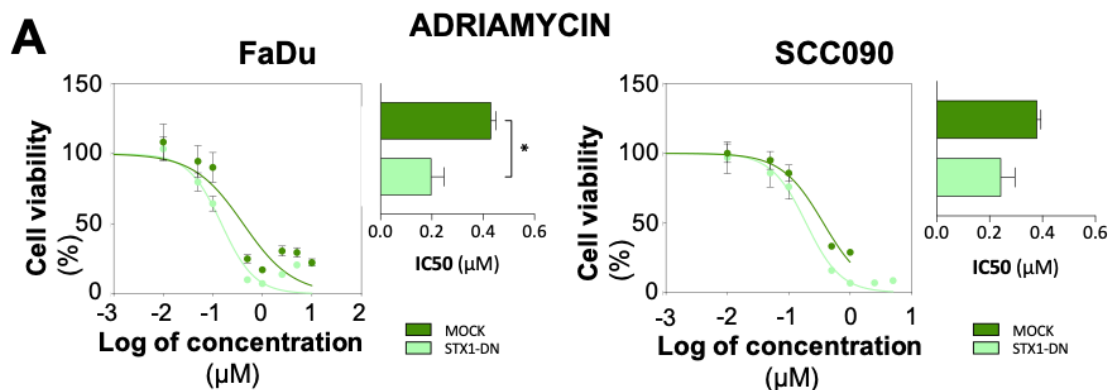


Figure 88 – Lapatinib treatment in HNSCC cells with functionality impaired STX1 results in an autophagy marker increase. Representative Western blot analysis of BAX and LC3 in FaDu (A) and SCC090 (B) MOCK and STX1-DN cells treated with lapatinib (1.5 μ M) for 24 or 48 hours. α TUB was used as internal control. On the bottom signal quantification of protein expression normalized to the control (MOCK) or to each own control (MOCK CTRL or STX1-DN CTRL). Representative results of n=2 independent experiments.

Overall, these results demonstrate that STX1 impairment of function sensitizes HNSCC cancer cells and HER2-positive BC cancer cells, to a lesser extent, by arresting the cell cycle at the G₁ phase and by inducing HNSCC cells autophagy.

3.2.5. HNSCC CELL LINES WITH DOWN-MODULATION OF SYNTAXIN-1 ACTIVITY ARE MORE SENSITIVE TO CISPLATIN TREATMENT

After demonstrating that HNSCC cells with impaired function of STX1 were more sensitive to lapatinib, it was studied if they were sensitized to other drugs, the most commonly used in HNSCC. First, a MTT cytotoxic assay with adriamycin, a drug that intercalates within the DNA strands inducing DNA breaks and inhibition of DNA and RNA synthesis, was performed. The MTT assay revealed that FaDu cells were significantly sensitized to adriamycin when STX1 was not functional (MOCK IC₅₀: 0.431 μM and STX1-DN IC₅₀: 0.199 μM) (*Figure 89A left*). SCC090 STX1-DN cells also increased their sensitivity to the drug and although IC₅₀ differences were not statistically significant, the IC₅₀ decreased from 0.380 μM to 0.244 μM (*Figure 89A right*). Secondly, the sensitivity to cisplatin, the gold standard therapy to treat HNSCC, was checked. HNSCC cells with impaired STX1 function were more sensitive to cisplatin than MOCK cells. In the case of FaDu, the MOCK IC₅₀ was significantly reduced from 23.73 μM to 14.97 μM for STX1-DN cells (*Figure 89B left*). Even though SCC090 IC₅₀ value decrease was not statistically significant, the cisplatin IC₅₀ of MOCK cells was reduced from 36.95 μM to 13.40 μM (*Figure 89B right*). The autophagy-induced pathway in FaDu HNSCC cells treated with cisplatin was also checked. After 48 hours of cisplatin treatment in MOCK and STX1-DN cells, no conclusive results were obtained. A slightly increase of the LC3-II/LC3-I ratio was detected in FaDu STX1-DN treated with cisplatin in comparison to its own control, however, the most notorious findings was the increase on LC3-I expression in STX1-DN treated with cisplatin, indicative of an increase of LC3-I production (*Figure 89C*).



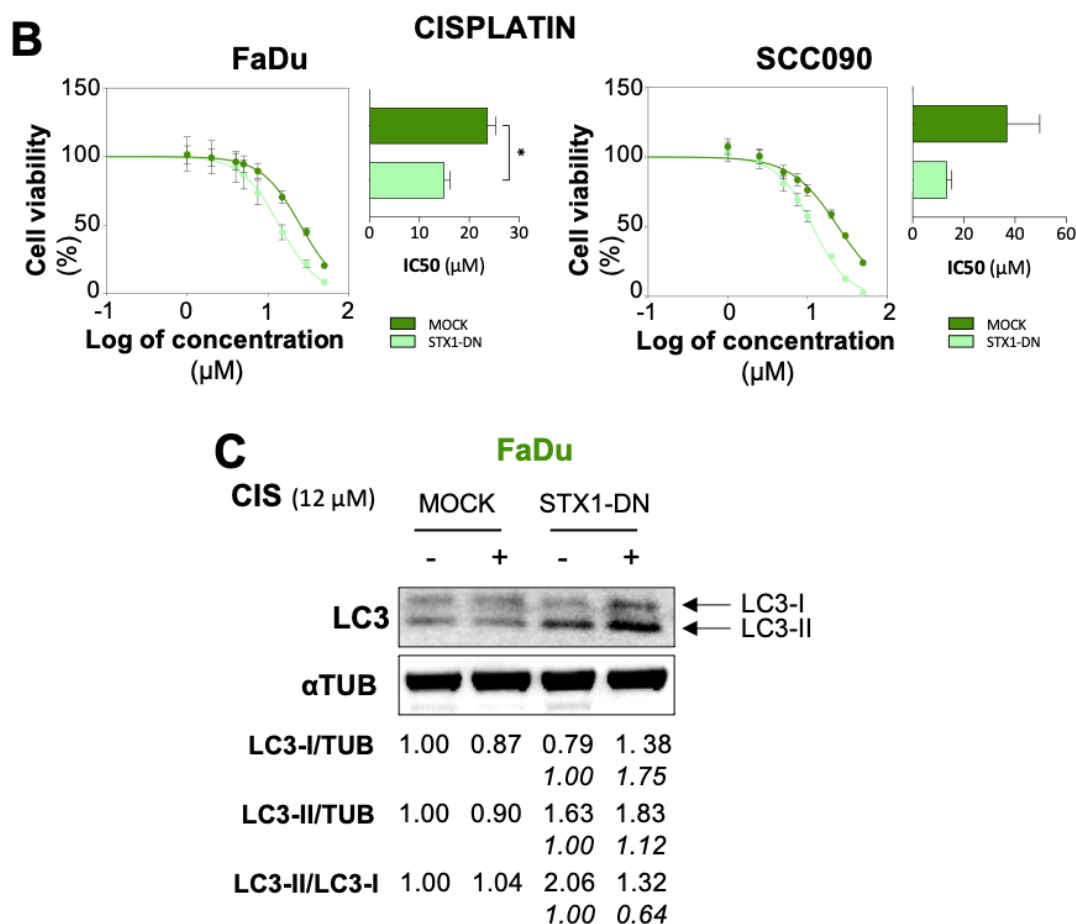


Figure 89 – HNSCC cells with impaired STX1 function are more sensitive to cisplatin treatment. MTTs of FaDu and SCC090 MOCK or STX1-DN treated with adriamycin (0.01-10 μM) for 72 hours (A), and cisplatin (1-50 μM) for 72 hours (B). On the right of each figure, IC₅₀ representation. (C) Representative Western blot analysis of LC3 in FaDu MOCK and STX1-DN HNSCC cells treated with cisplatin (12 μM) for 48 hours. αTUB was used as internal control. At the bottom signal quantification of protein expression normalized to the control (MOCK) or to each own control (MOCK CTRL or STX1-DN CTRL). Representative results of n=2 (MTTs) or n=1 (Western blot) independent experiments performed in sextuplicate (MTTs). Data presented as mean ± SEM. Statistical analysis was performed using Student's *t*-test comparing IC₅₀ value of M vs DN. * *p* < 0.05.

Given that STX1-DN HNSCC cells are more sensitive to lapatinib and cisplatin treatment, the ability of the combination of both drugs on increasing the sensitivity of STX1-DN cells was investigated. Several cytotoxic assays were performed on the HNSCC cells with a single dose of lapatinib or cisplatin (corresponding approximately at the 40% of the previous STX1-DN IC₅₀ for each drug) and different doses of cisplatin or lapatinib, respectively for 72 hours. The results obtained proved that the combination of the lapatinib at IC₄₀ with cisplatin reduced the IC₅₀ of cisplatin, and also that the treatment with the IC₄₀ of cisplatin with lapatinib, reduced the IC₅₀ of lapatinib, as well (*Figure 90A*). These results indicate that the combination of both drugs have a synergistic effect in HNSCC cancer cell lines. Moreover, the STX1-DN HNSCC cell lines were also more sensitive to the combination that MOCK cells (*Figure 90B*), confirming

that the combination is more effective while reducing the lapatinib and cisplatin doses in HNSCC cell lines.

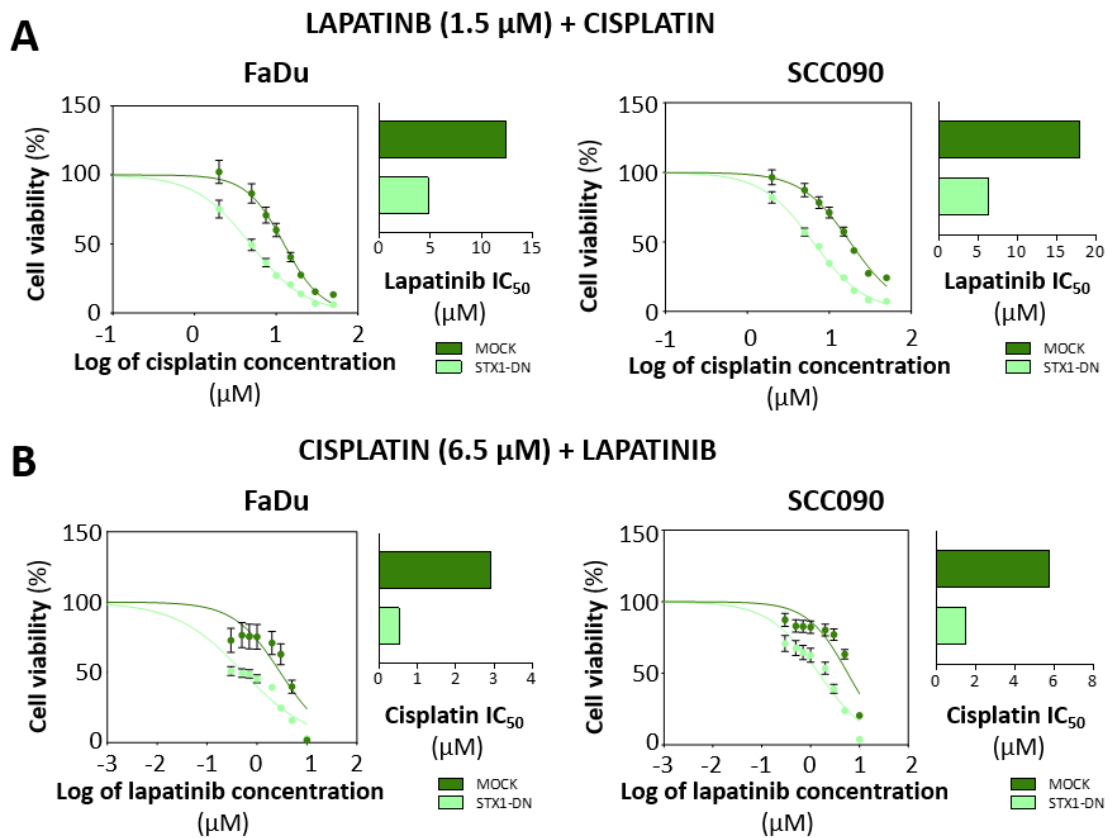


Figure 90 – Concurrent lapatinib and cisplatin treatment has a synergistic effect on HNSCC cells viability. (A-B) MTT cytotoxic assay of FaDu (A) and SCC090 (B) MOCK and STX1-DN cells treated for 72 hours with a single dose of lapatinib (1.5 μM) and a range-dose of cisplatin (2-50 μM). (C-D) MTT cytotoxic assay of FaDu (C) and SCC090 (D) MOCK and STX1-DN cells treated for 72 hours with a single dose of cisplatin (6.5 μM) and a range-dose of lapatinib (0.3-10 μM). Representative results of $n=1$ independent experiments performed in sextuplicate. Data presented as mean \pm SEM.

3.3. ROLE OF SYNTAXIN-1A IN BREAST AND HEAD AND NECK CANCER CELL MIGRATION AND INVASION

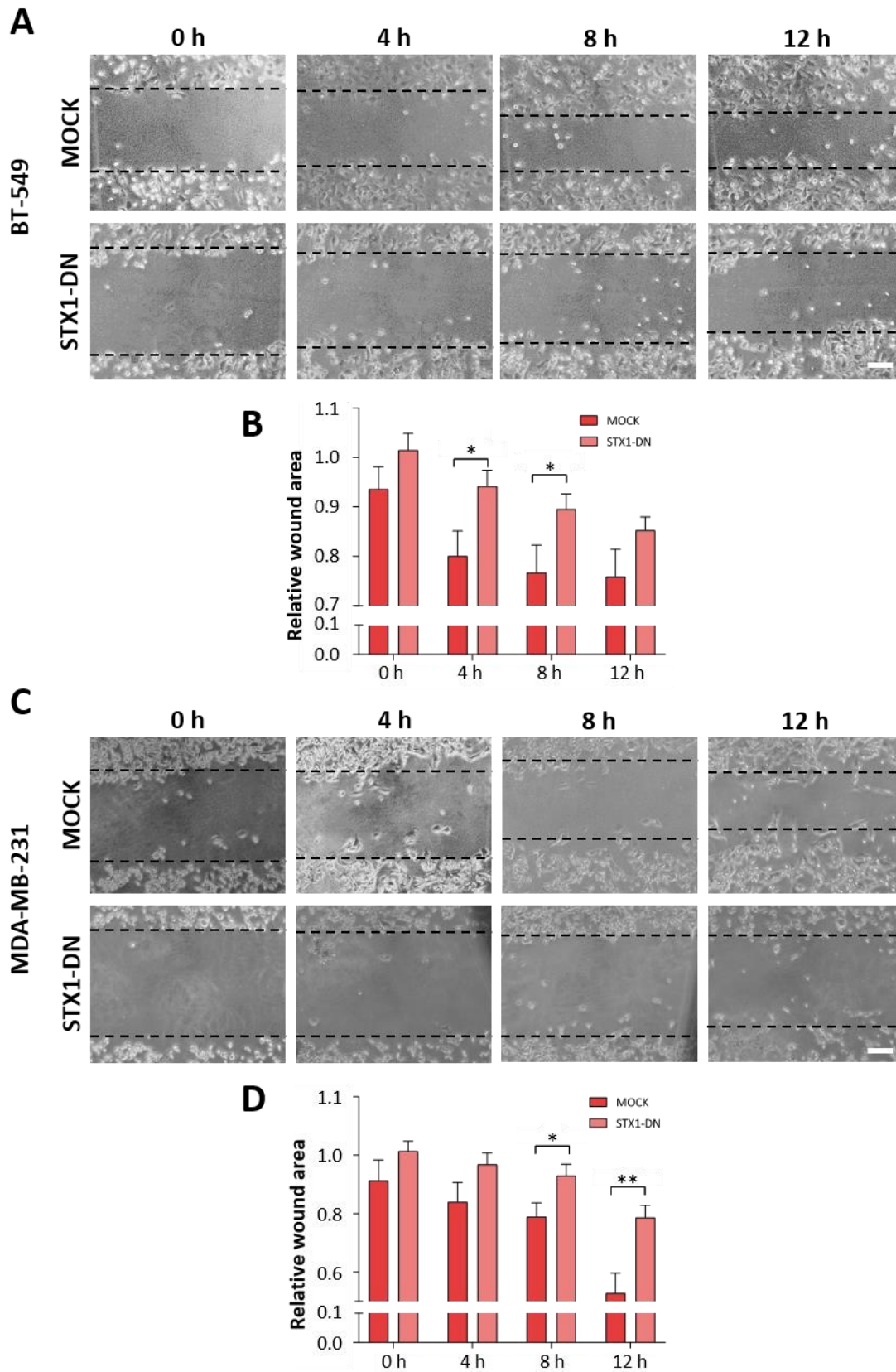
The results obtained from BC patients' databases determined that STX1A was involved in metastatic events. The analysis revealed that patients with high levels of this neuroprotein had a lower period of metastasis free survival (Table 38). Also, our collaborators from Dr. Soriano's lab found that impairment of the function of STX1 resulted in less invasion of glioblastoma cells into surrounding tissues. Altogether, this information encouraged us to assess STX1A in migration and invasion processes in BC and HNSCC.

To do that, HER2-negative/basal BC cell lines were used, since they are the most aggressive and the ones with higher migration and invasion capacities in comparison to the other BC subtypes. Moreover, even though they express lower levels of STX1A in comparison to HER2-positive BC cell lines, they still express STX1A at relevant levels. In parallel, HNSCC cell lines were used as it was done throughout all the project. Some functional assays, such as wound-healing or transwell invasion assays were performed accompanied by gene and protein expression determination to evaluate the possible role of STX1A in migration and invasion.

3.3.1. SYNTAXIN-1A PROMOTES MIGRATION IN BC AND HNSCC CELLS

First of all, to rapidly assess if STX1A was involved in migration events, wound healing assays in BC and HNSCC cell lines which stably expressed the non-functional form of STX1A (STX1-DN) were performed. Considering that each cell line had different migration rates, migration was assessed at different times according to the cell type. The results showed that HER2-negative/basal BT-549 and MDA-MB-231 BC cell lines expressing the STX1-DN form did not close the wound as fast as their respective MOCK partners (*Figure 91A-Figure 91D*), indicating that STX1 function impairment resulted in a lower migration rate of these BC cell lines. Similar results were seen in the HNSCC SCC090 cell line, 8 hours after the wound STX1-DN HNSCC cells had not migrated at the same rate than MOCK cells (*Figure 91E and Figure 91F*). The wound healing assay with FaDu MOCK and STX1-DN cells was also undertaken, however they use to grow in close contact and once the wound was performed all the cells detached from the plate as a film, making it impossible to monitor the wound closure.

Finally, considering that the STX1-DN was not specific from STX1A, STX1A was stably down-regulated by shRNA STX1A in MDA-MB-231 HER2-negative/basal BC cell line and repeated the wound-healing experiment repeated. The results shown in *Figure 91G* and *Figure 91H* reinforced our previous findings since specific down-regulation of STX1A also inhibited the migration capacity of this BC cells. Therefore, STX1A contributes to cell motility.



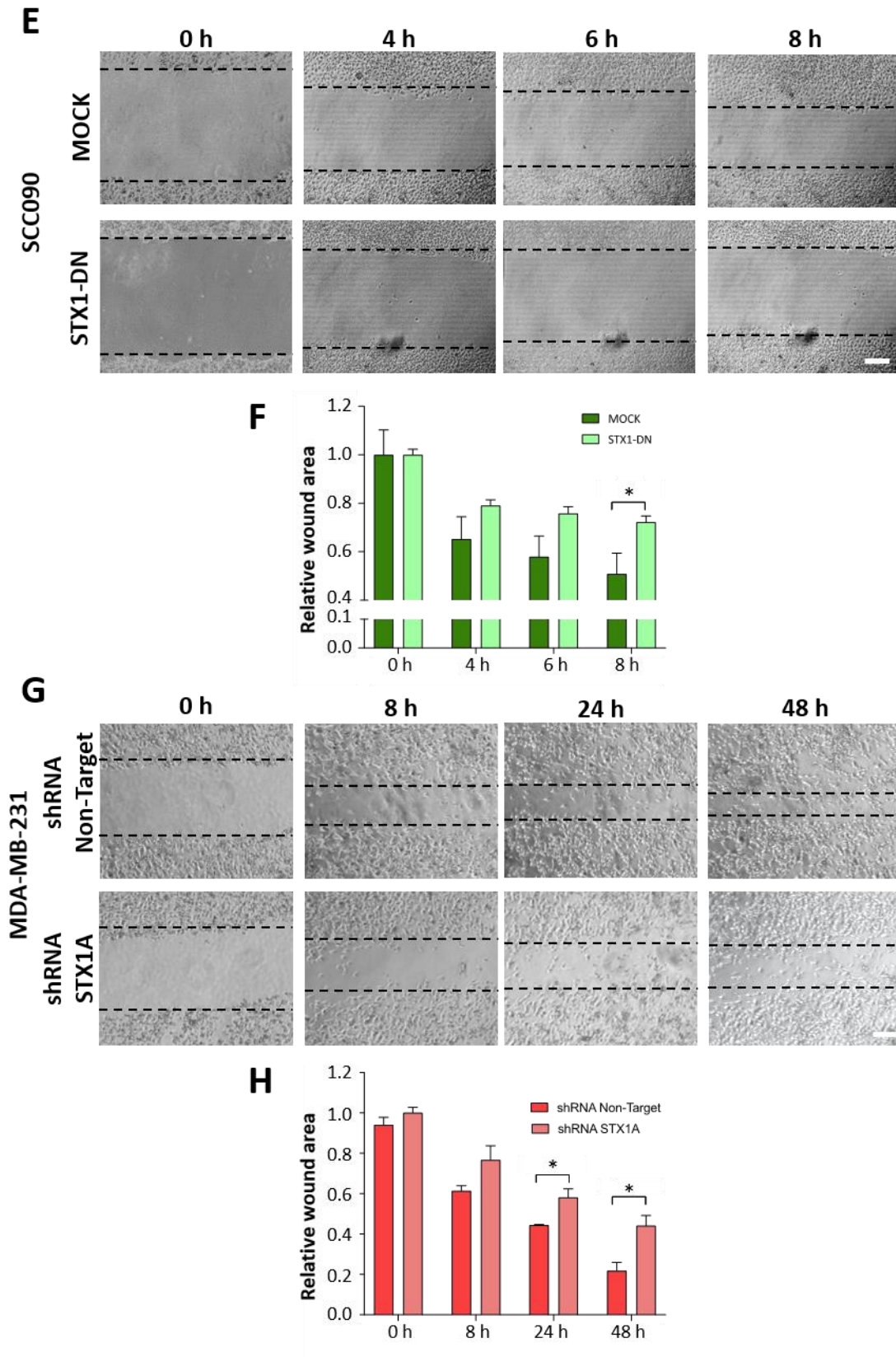


Figure 91 – STX1A inhibition results in lower migration rates of BC and HNSCC cell lines.

Representative images of wound-healing assays of MOCK and STX1-DN in BT-549 (A), MDA-MB-231 (C) HER2-negative BC cell lines and SCC090 (E) HNSCC cell line and shRNA Non-Target and shRNA STX1A MDA-MB-231 cells (G) at different time points (Scale bar = 100 μ m). In (B), (D), (F) and (H) quantitative representation of the relative wound area of a representative wound-healing experiment of the

corresponding cell line. Relative wound area is referred to its condition at time 0 h. Representative results of n=3 independent experiments performed in triplicate. Data presented as mean \pm SEM. Statistical analysis was performed using Student's *t*-test comparing MOCK vs STX1-DN or shRNA Non-Target vs shRNA STX1A for each time point. **p* < 0.05, ***p* < 0.01.

3.3.2. SYNTAXIN-1A PROMOTES CELL ADHESION AND SPREADING IN BC AND HNSCC CELL LINES

Once confirmed that STX1A contributes to cell migration, it was evaluated if STX1A also played a role in BC and HNSCC cell adhesion. To do that, cell adhesion assays were performed by detaching MOCK and STX1-DN cell lines and, then letting the cells to attach at the plate surface for 2 hours. After that time, cells were stained and counted. In BT-549 and MDA-MB-231 BC cell lines (*Figure 92A and Figure 92B, respectively*), it was found that STX1-DN cells had less adhesion capacity than their MOCK partners. The same results being found in the HNSCC cell lines as well (*Figure 92C and Figure 92D*).

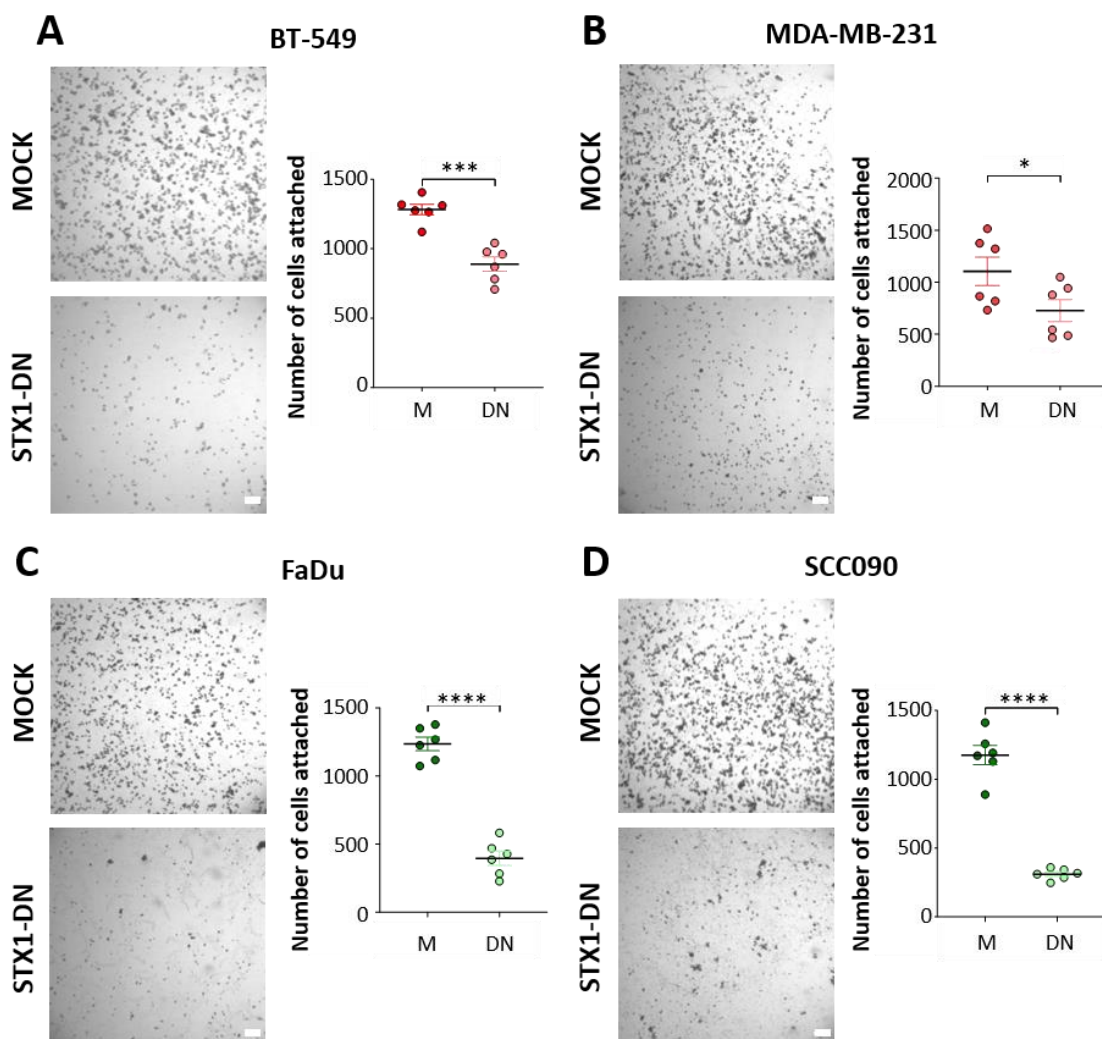
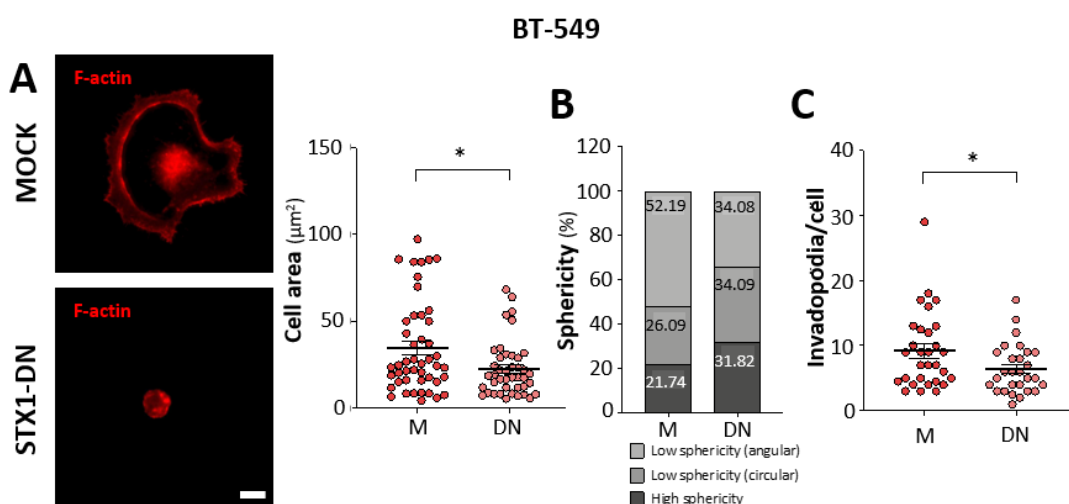
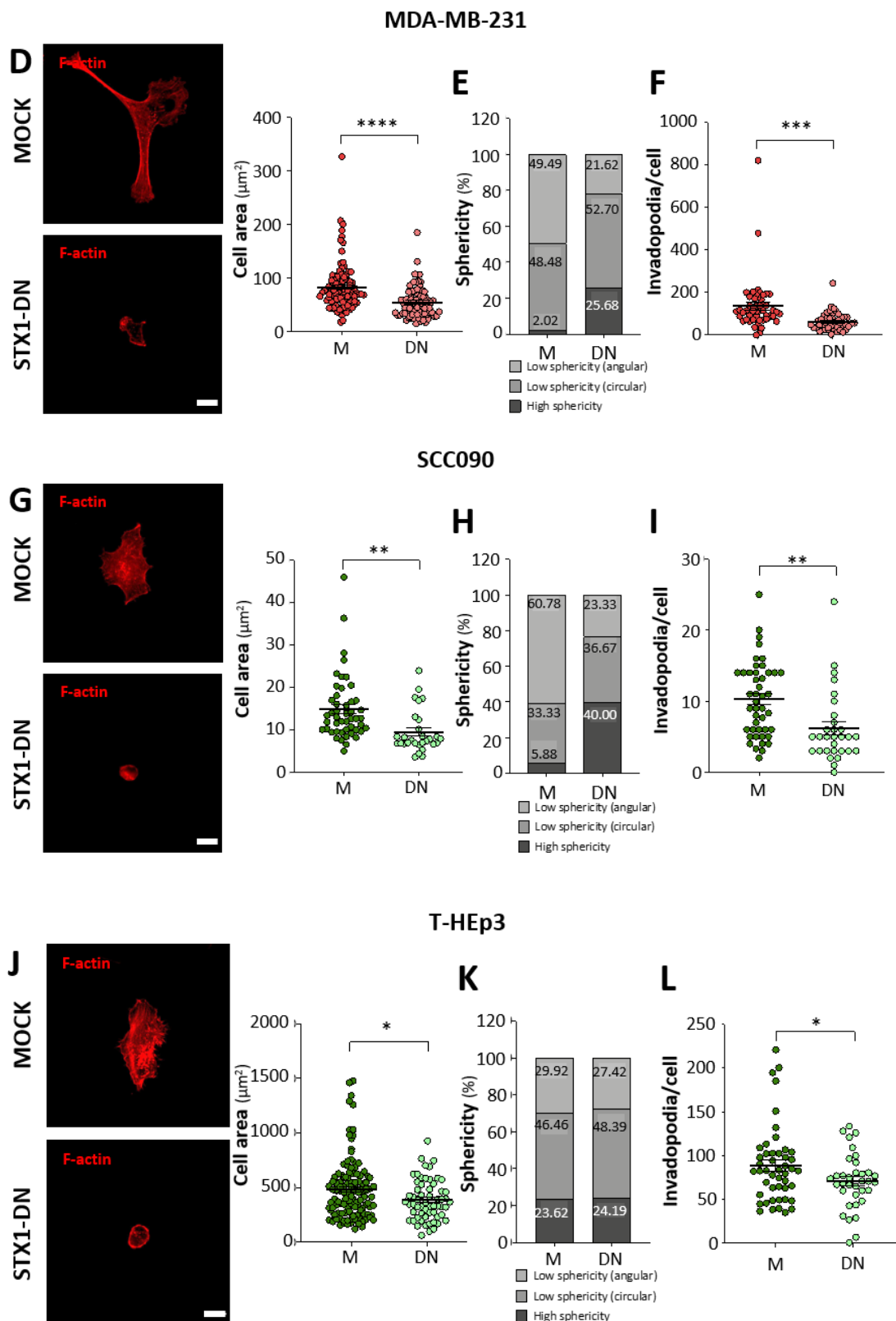


Figure 92 – BC and HNSCC cell lines with impaired STX1A function have a lower adhesion capacity. On the left, representative images of cell adhesion assays of BT-549 (A) and MDA-MB-231 (B)

BC cell lines and FaDu (C) and SCC090 (D) HNSCC cell lines (Scale bar = 100 μm). On the right, quantification of the number of cells attached in the plate surface from a representative experiment. Representative results of $n=3$ independent experiments performed in triplicate. Data presented as mean \pm SEM. At least 5 fields were considered in the cell adhesion assay. Statistical analysis was performed using Student's *t*-test comparing MOCK vs STX1-DN. * $p < 0.05$, *** $p < 0.001$, **** $p < 0.0001$.

Then, the research was focused in determining if STX1-DN cells that were attached to the plate were able to spread the same area than MOCK cells. To do that a cell spreading assay, that followed the same idea than the cell adhesion assay was performed, but in this case, cells were plated on fibronectin for 2 hours. After that time, cells were stained with phalloidin, a fluorescent-conjugated toxin that binds specifically to F-actin filaments. The results showed that STX1-DN BC cells had less spreading area than their correspondent MOCK cells (*Figure 93A and Figure 93D*). Similar results were seen in HNSCC cell lines (*Figure 93G and Figure 93J*). The sphericity of the cells was also analysed, considering that cellular protrusions can also give information about their migration abilities. The cellular morphology of MOCK and STX1-DN cells was classified according to three subgroups (see materials and methods for more information at section 7.3.4): high, low (circular) and low (angular) sphericity. The analysis showed that the cells with non-functional STX1 were more spherical than MOCK cells (except for T-HEp3 cells) (*Figure 93B, Figure 93E, Figure 93H and Figure 93K*), meaning that proper STX1 function is necessary for a cell to protrude correctly. Finally, invadopodia formation was also analysed, by considering invadopodia the F-actin punctae localized in the cell surface. The quantification of F-actin punctae showed that cells expressing the STX1-DN formed less invadopodia than MOCK cells (*Figure 93C, Figure 93F, Figure 93I and Figure 93L*), reinforcing the findings on the role of STX1A on promoting cell migration abilities.





quantification of cell morphology as percentage of cell sphericity according to high, low (circular) or low (angular). BT-549 (C), MDA-MB-231 (F), SCC090 (I) and THEp3 (L) quantification of invadopodia per each cell. Representative results of n=3 or n=1 (T-Hep3 cells) independent experiments performed in triplicate. Data presented as mean \pm SEM. At least 30 cells were considered per immunofluorescence slide. Statistical analysis was performed using Student's *t*-test comparing MOCK vs STX1-DN. * $p < 0.05$, ** $p < 0.01$, *** $p < 0.001$, **** $p < 0.0001$.

Following this line of research, during my internship at the University of Guelph (Guelph, Canada) under the supervision of Dr. Marc Coppolino, among other techniques, invadopodia formation in MDA-MB-231 cells and STX1A co-localization with invadopodia markers were checked. To do that a gelatin degradation assay was performed in which after 4 hours of cell plating over Alexa-fluor-594-labeled-gelatin coverslip, gelatin degradation and colocalization with STX1A in gelatin-degradation marks were looked for. Representative images can be seen in [Figure 94A](#) co-localization events being detected at some points. However, considering that the cells, once attached to the gelatin surface, can migrate, it was plausible that the colocalization of STX1A with gelatin degradation marks would be not-related. To address this issue, MDA-MB-231 cells were stained with an invadopodia marker, such as Integrin- $\beta 1$ (ITG $\beta 1$), and no co-localization was found between STX1A and ITG $\beta 1$ ([Figure 94B](#)). Another objective was to compare invadopodia formation capabilities between MOCK and STX1-DN or between shRNA Non-Target and shRNA STX1A cancer cell lines but this experiment could not be performed due to technical issues.

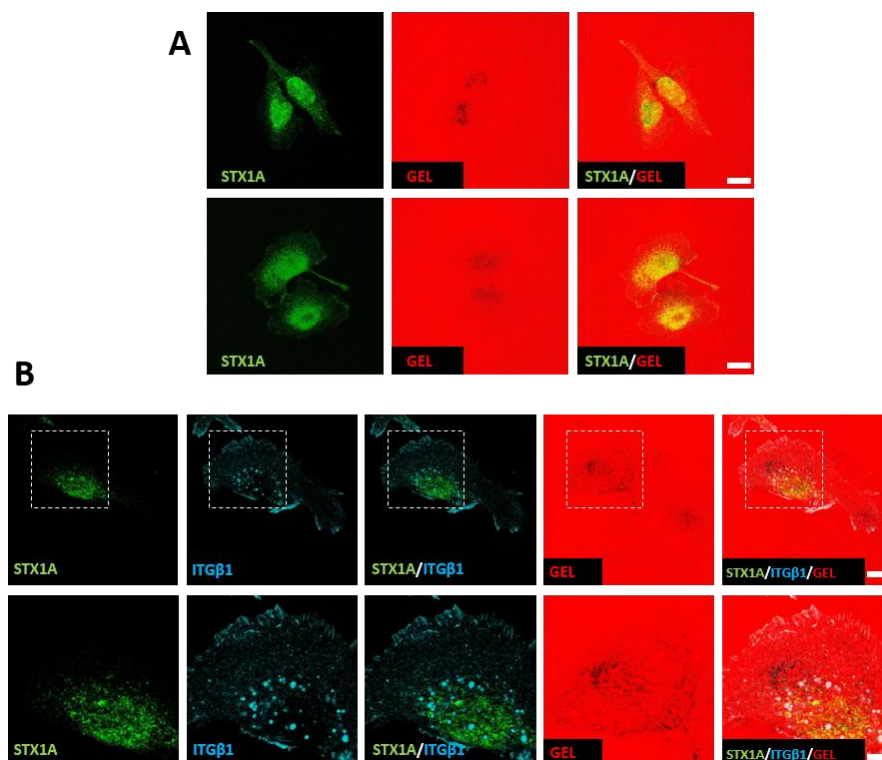
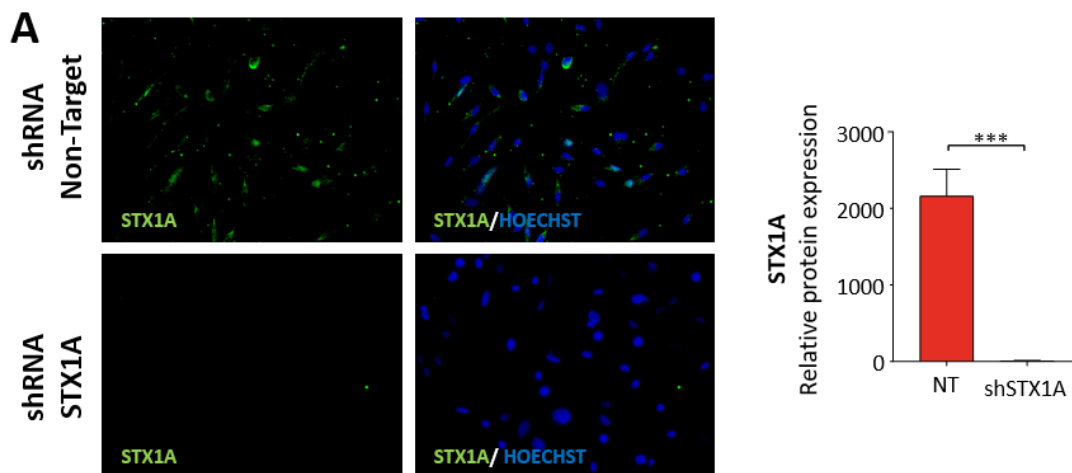


Figure 94 – STX1A and its relationship with invadopodia formation in MDA-MB-231 cell line.
(A) Two representative images of invadopodia formation assay after 4 hours of plating MDA-MB-231 BC

cells in Alexa-Fluor-594-labeled gelatin slides and stained with STX1A antibody (scale bar = 10 μ m). (B) Invadopodia formation assay after 4 hours of seeding MDA-MB-231 in Alexa-Fluor-594-labeled gelatin slides and stained for STX1A and ITG β 1. Bottom images correspond to an amplification from the upper image (region delimited with the white square). Scale bar upper images = 10 μ m; scale bar bottom images = 1 μ m. Representative results of n=2 independent experiments performed in triplicate.

To understand the mechanism by which STX1A was related to cell attachment and spreading in BC and HNSCC cells, SRC pathway activation, a pathway closely related to cell adhesion and invadopodia formation, was checked. MDA-MB-231 BC cell lines with STX1A down-regulated by shRNA STX1A were used (*Figure 95A*). A Western blot analysis of pSRC and SRC protein levels revealed that STX1A downregulated cells had a lower pSRC/SRC ratio in comparison to shRNA Non-Target ones (*Figure 95B*). Then, focusing on the described relationship between SRC pathway and integrin trafficking and focal adhesions turnover, integrin expression at the plasma membrane between shRNA Non-Target and shRNA STX1A MDA-MB-231 HER2-negative BC cells were compared. An immunofluorescence without cell permeabilization to determine cell surface ITG β 1 expression was performed. However, no differences between shRNA Non-Target cells and shRNA STX1A were found (*Figure 95C*). Then, the expression for ITG α 6 was checked. In that case it was found that STX1A down-regulated cells had ITG α 6 down-regulated as well (*Figure 95D*), indicative of the STX1A involvement of ITG α 6 trafficking into the plasma membrane, which could explain the decrease of cancer cell migration and adhesion signalling found in STX1A down-modulated cells.



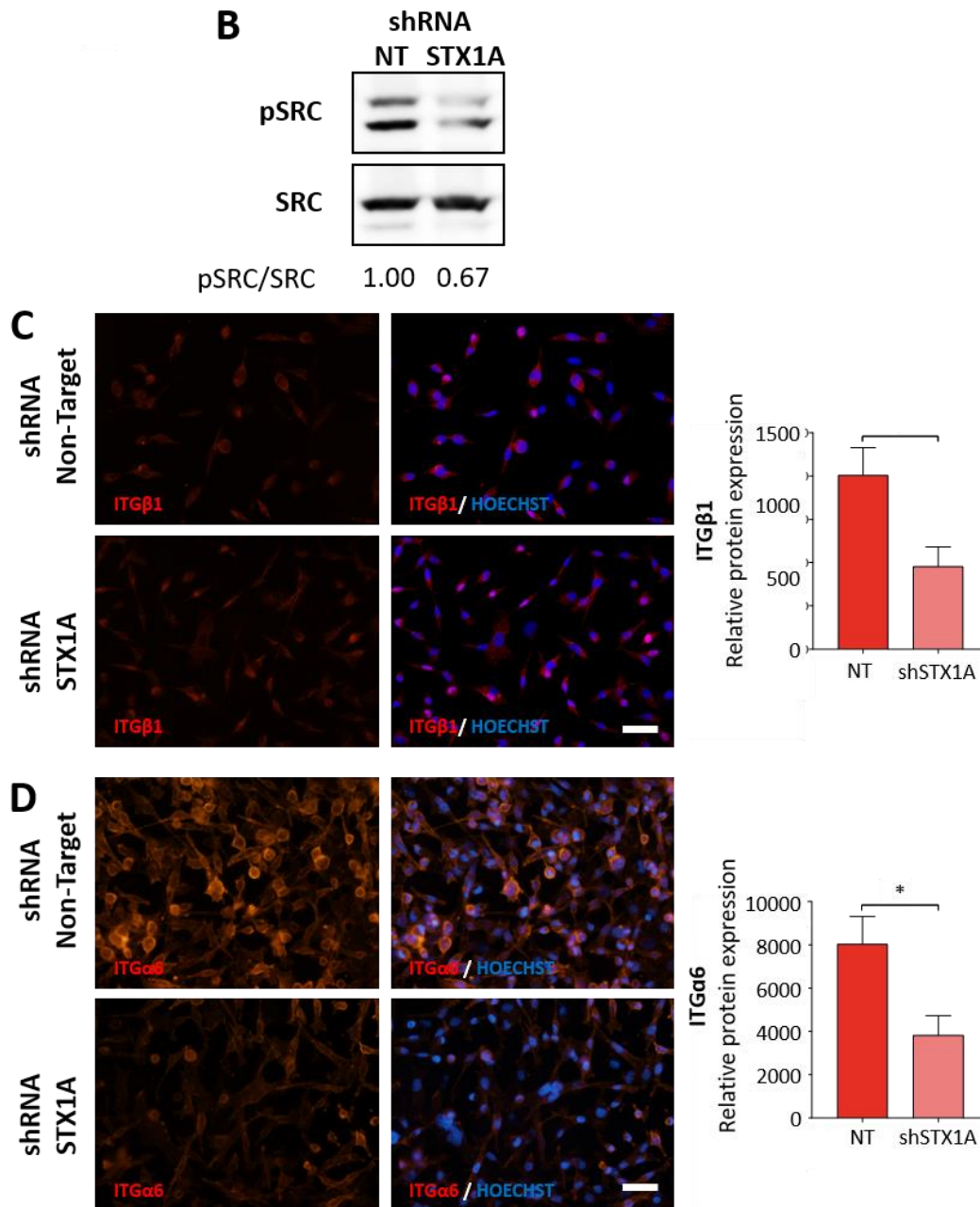
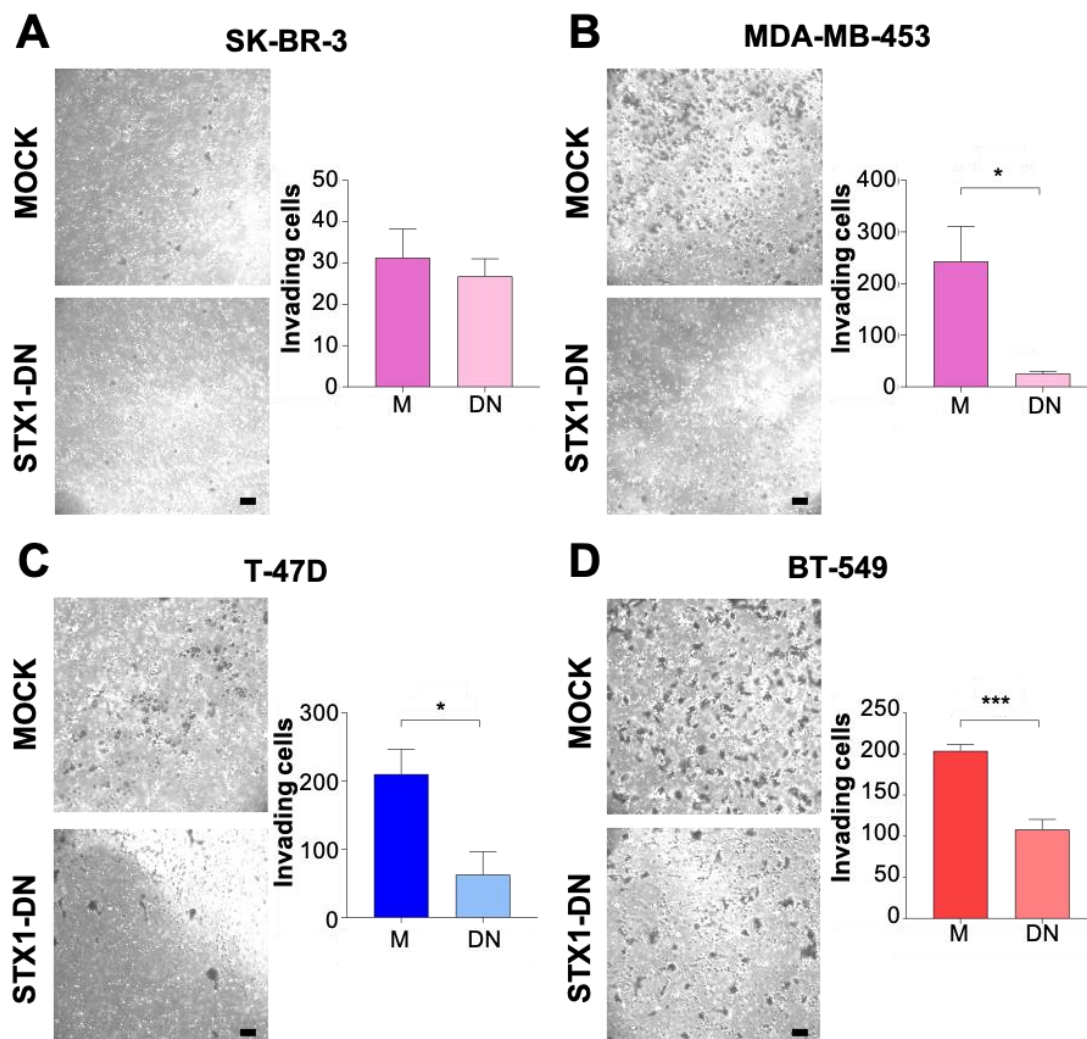


Figure 95 – SRC pathway and ITGα6 are down-regulated in the shRNA STX1A MDA-MB-231 BC cell line. (A) On the left, permeabilizing immunofluorescence of STX1A in shRNA Non-Target (NT) and shRNA STX1A (shSTX1A). Nuclei are counterstained with Hoechst. Scale bar = 25 μm. On the right, quantification of fluorescence intensity. (B) Representative Western blot assay of SRC and pSRC in the shRNA Non-Target (NT) and shRNA STX1A (STX1A) cells. Protein quantification is referred to shRNA NonTarget. (C and D) On the left, non-permeabilizing immunofluorescence of ITGβ1 (C) and ITGα6 (D) in shRNA Non-Target and shRNA STX1A cells. Nuclei are counterstained with Hoechst. Scale bar = 25 μm. On the right, quantification of fluorescence intensity. Representative results of n=2 independent experiments performed in triplicate. Data presented as mean ± SEM. At least 10 fields were considered in immunofluorescence images. Statistical analysis was performed using Student's *t*-test comparing NT vs shRNA STX1A. **p* < 0.05, ***p* < 0.01.

3.3.3. SYNTAXIN-1A PROMOTES CELL INVASION IN BC AND HNSCC CELL LINES

Being proved that STX1A plays an important role in cell migration, adhesion and spreading, next step was to determine if STX1A is also involved in invasion processes. To do that several transwell-invasion assays were performed with cells transiently transfected with MOCK or STX1-DN plasmid 24 hours before the assay. After the transfection, cells were seeded in serum-free media into transwells coated with Matrigel, and with complete media at the bottom of the well, and let the cells invade for 24 hours. This experiment was performed in HER2-positive (SK-BR-3, MDA-MB-453), HER2-negative/luminal A (T-47D) and HER2negative/basal (BT-549 and MDA-MB-231) BC cell lines and in SCC090, FaDu and T-HEp3 HNSCC cell lines. In all the cases, except for the low invading SK-BR-3 BC cell line, cells expressing STX1-DN displayed lower invasion rate than their controls (*Figure 96*). These findings corroborate that STX1A promotes BC and HNSCC migration and invasion processes.



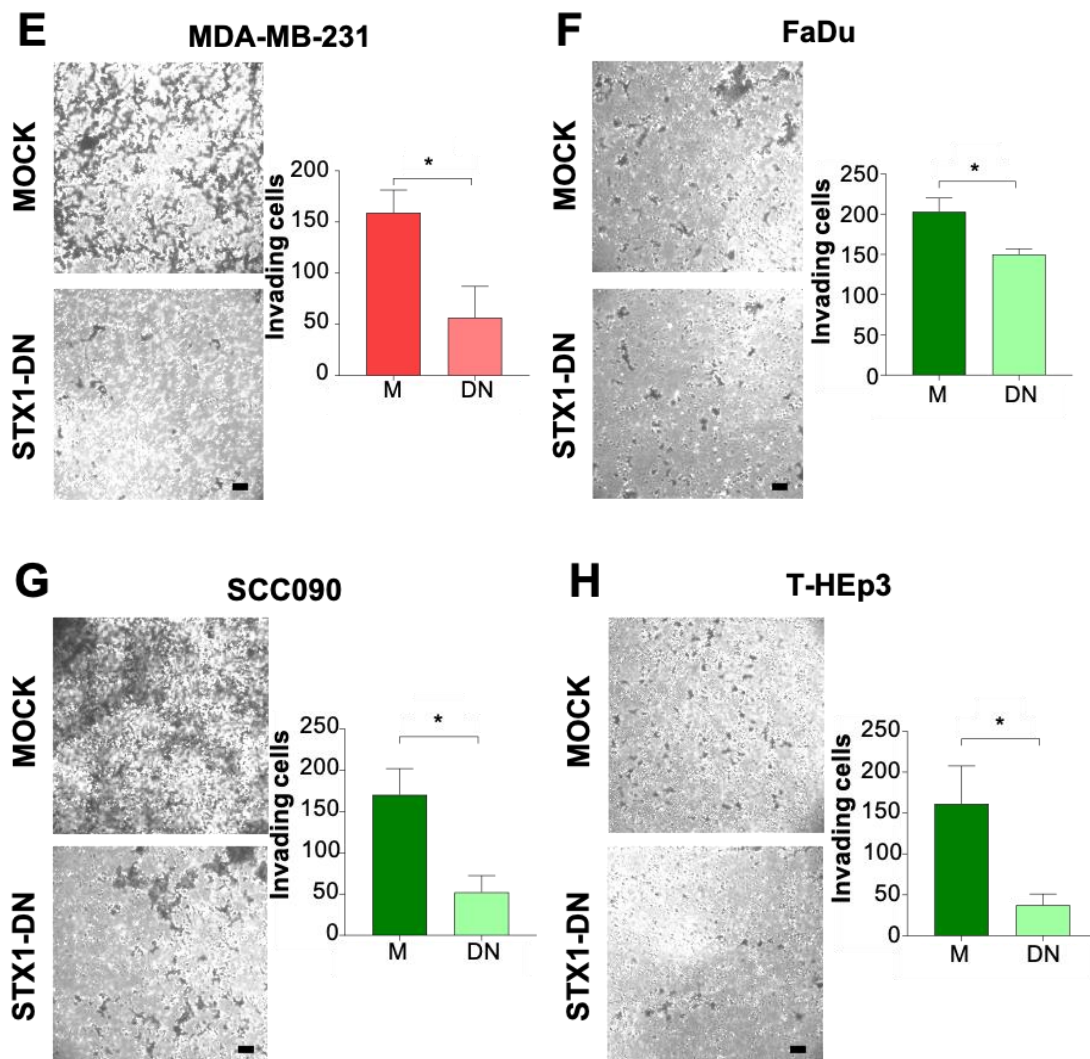


Figure 96 – BC and HNSCC cells transiently transfected with STX1-DN have a lower invasion rate than MOCK cells. On the left, representative transwell-invasion assay images of SK-BR-3 (A), MDA-MB-453 (B), T-47D (C), BT-549 (D) and MDA-MB-231 (E) BC cell lines and FaDu (E), SCC090 (G) and T-HEp3 (H) HNSCC cells after 24 hours of cell seeding in Matrigel (Scale bar = 100 μ m). On the right, quantification of number of invading cells. Representative results of n=2 or n=1 (T-Hep3) independent experiments performed in duplicate. Data presented as mean \pm SEM. At least 5 fields were considered in the transwell-invasion assay. Statistical analysis was performed using Student's *t*-test comparing MOCK vs STX1-DN. **p* < 0.05, ****p* < 0.001.

Then, considering that the cells with functionally impaired STX1A had a less invasive phenotype, EMT markers were determined. The analysis of their expression was done by qPCR in stably transfected cells (MOCK and STX1-DN), both in BC and HNSCC cell lines. In general, it was found that STX1-DN expressing cell lines had down-regulated several mesenchymal markers in comparison to MOCK cells (Figure 97). More in detail and focusing on BT-549, it was found that STX1-DN cells down-regulated *SNAI-2*, *TWIST-1* and *VIM* mesenchymal markers. There was no difference in *SNAI-1* expression, but it could be due to the really low expression of this transcription factor in this specific cell line (Figure 97A). Focusing on the other BC cell line analysed, MDA-MB-231 cells with impaired STX1A function had down-

regulated *SNAI-1*, *SNAI-2* and *VIM* EMT markers (Figure 97B), following the same trend than BT-549 BC cells. HNSCC cells behave similarly to BC cells regarding *TWIST-1*, *VIM*: FaDu and SCC090 STX1-DN cell lines had down-regulated these mesenchymal markers. Surprisingly, STX1-DN HNSCC cells upregulated *SNAI-2* expression and *SNAI-1* (only in FaDu), in an opposite way to what observed in BC cell lines (Figure 97C and Figure 97D, respectively).

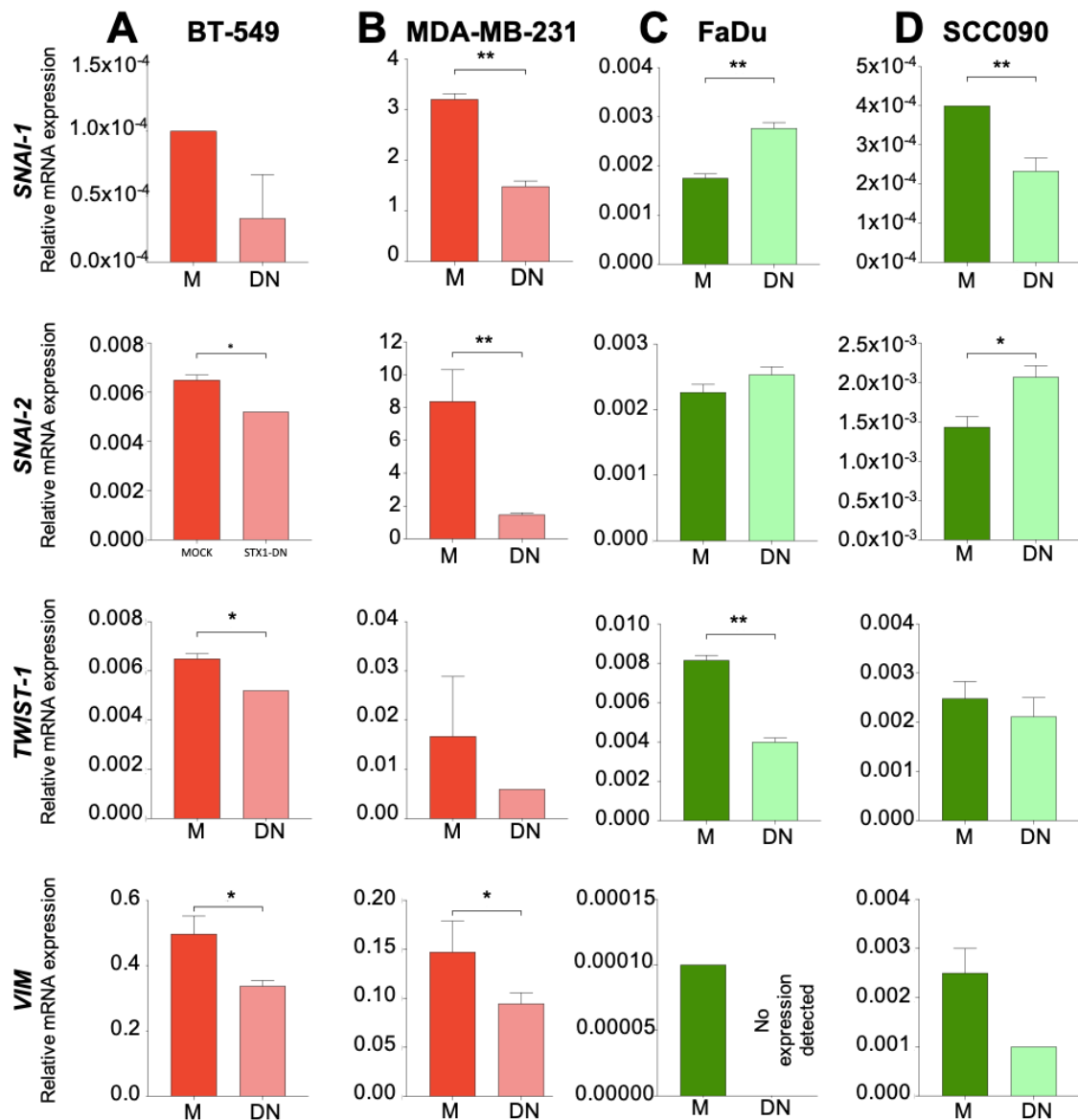


Figure 97 – STX1-DN BC and HNSCC cells down-regulate EMT expression markers. Analysis of *SNAI-1*, *SNAI-2*, *TWIST-1* and *VIM* mRNA expression by qPCR in MOCK (M) and STX1-DN (DN) BT-549 (A) and MDA-MB231 (B) HER2-negative BC cell lines and FaDu (C) and SCC090 (D) HNSCC cell lines. Representative results of n=2 independent experiments performed in sextuplicate. Data presented as mean ± SEM. Statistical analysis was performed using Student's t-test comparing MOCK vs STX1-DN. *p < 0.05, **p < 0.01.

After seeing that STX1-DN maintained a more epithelial phenotype, and that these cells did not invade, a zymogram was performed to determine if there were differences on the

activity of these proteases in the culture media of MOCK and STX1-DN MDA-MB-231 BC cells. It was possible to check for MMP-2 and MMP-9 activity between both cell types by a zymogram assay, but no differences in MMP2 and MMP9 protease activity were found (Figure 98A). MMPs protein expression was also checked in MDA-MB-231 culture media by Western blot, and no significant differences were found regarding MMP-7, MMP-14, MMP-2 and MMP-9 expression either (Figure 98B).

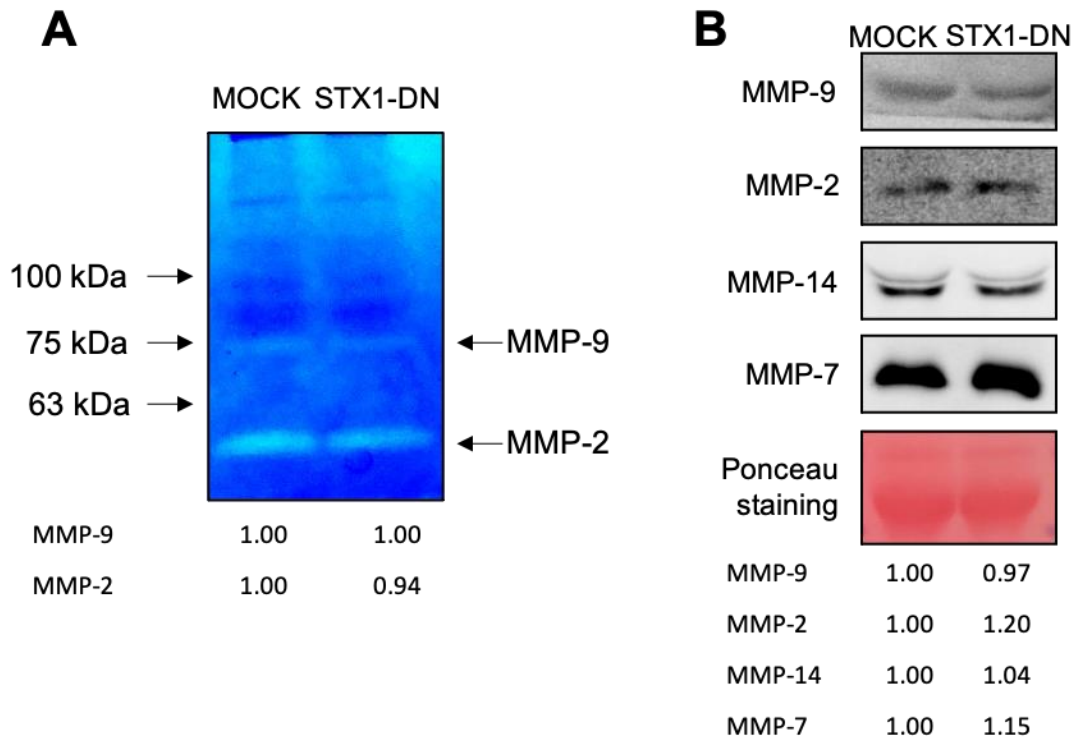


Figure 98 – STX1A is not involved in MMPs secretion in MDA-MB-231 BC cells. (A) Zymogram of MDA-MB-231 MOCK and STX1-DN supernatant collected after 48 hours of serum-free media culture. At the bottom, MMP9 and MMP-2 quantification referred to the MOCK cells. (B) Analysis by Western blot assay of MMP-9, MMP-2, MMP-14 and MMP-7 expression in MDA-MB-231 MOCK and STX1-DN supernatant after 48 hours of serum free media culture. Ponceau staining was used as loading control. At the bottom, MMPs quantification referred to the MOCK cells. Representative results of n=1 independent experiments.

Altogether these results indicate that STX1A is able to regulate invasion by switching the cell phenotype into a more mesenchymal one, without affecting MMPs secretion and activity in BC cells.

3.4. ROLE OF SYNTAXIN-1A IN TUMOUR GROWTH AND THERAPY RESISTANCE *IN VIVO*

Until now, part of our *in silico* data is confirmed by performing *in vitro* experiments which have proven that STX1A is involved in BC and HNSCC proliferation and in the regulation of EGFR/HER family of receptors expression at the plasma membrane, leading to a sensitization of HNSCC cells against some treatments such as lapatinib or cisplatin. Also, it has been proven that STX1A is involved in migration and invasion processes. Bearing these results in mind, next step was to translate our research from *in silico* and *in vitro* to *in vivo* models to corroborate the role of STX1A in these processes.

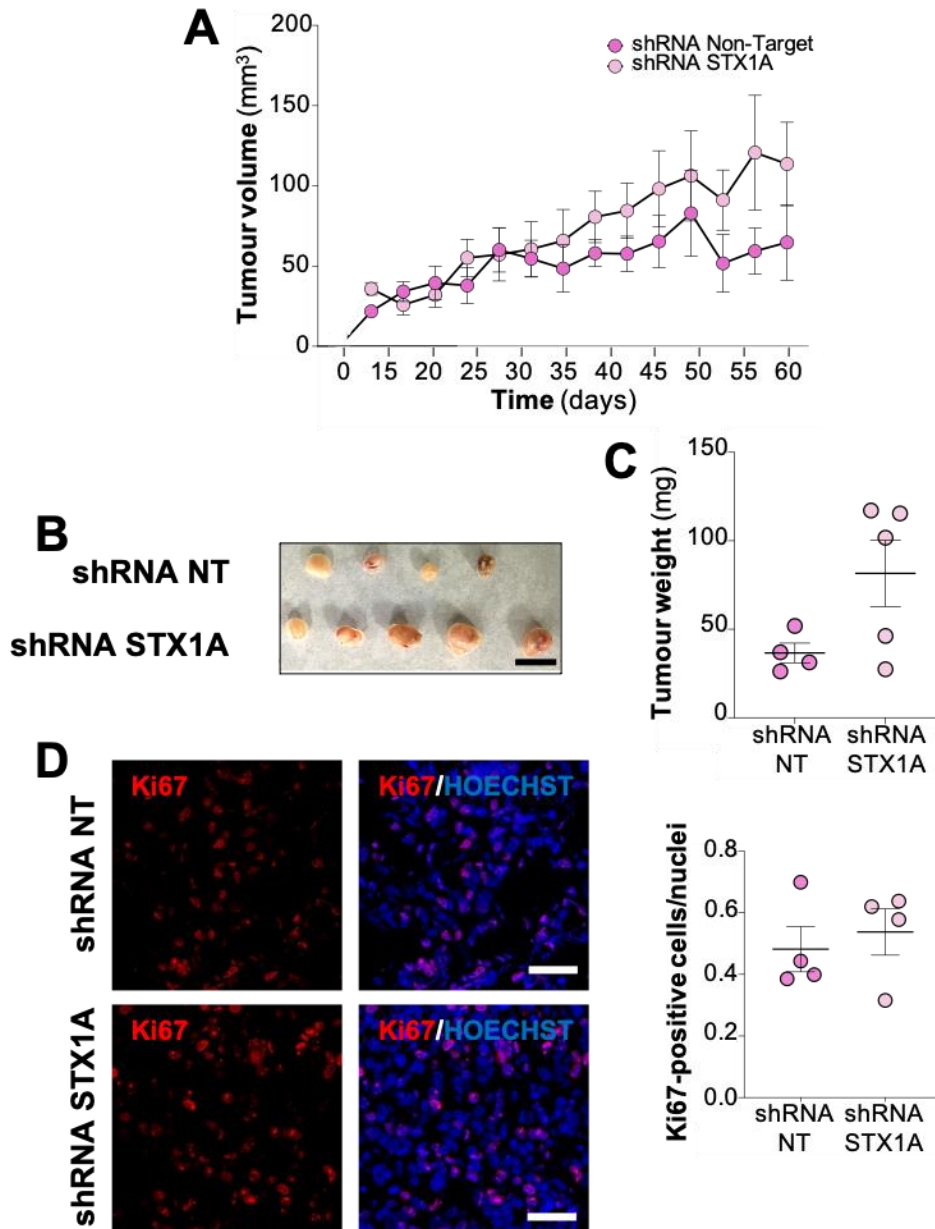
shRNA Non-Target and shRNA STX1A and MOCK and STX1-DN BC and HNSCC cells were used in two *in vivo* models, previously explained in materials and methods (section 8): immunodeficient nude mice and CAM model.

3.4.1. SYNTAXIN-1A SUPPRESSES TUMOUR GROWTH *IN VIVO*

To decipher the role of STX1A in tumour growth *in vivo*, BC cells with STX1A down-regulated by shRNA were orthotopically inoculated into the mammary fat pad of immunodeficient nude mice. shRNA STX1A paired to shRNA Non-target SK-BR-3, MDA-MB-453, BT-474 (HER2-positive) and MDA-MB-231 (HER2-negative/basal) BC cells were inoculated and once the tumours were palpable, their volume was continuously measured. When tumour volumes reached 100-200 mm³ or the quality of life of the mice were compromised, mice were sacrificed and the tumours excised for further analysis.

More in detail, three months after the orthotopically inoculation of Non-Target and shRNA STX1A SK-BR-3 BC cells, no tumour was detected, so it was proceeded to mice sacrifice and after the analysis of the mammary fat pads, only the remanent of cells inoculation was detected indicating that the cells did not grow properly (*data not shown*). Therefore, this experiment was discarded. Focusing on the other HER2-positive BC cells, MDA-MB-453 tumours grew better, however growth reached a steady state from day 60 after inoculation in both groups (*Figure 99A*), tumours with STX1A down-regulated showing a tendency to be bigger. After the tumour excision several days after, tumours were weighted and the tendency was confirmed, STX1A down-regulated tumours were bigger than their controls (*Figure 99A-Figure 99C*). Immunofluorescence staining for the proliferative marker Ki67 detected that there was a slightly but not significant increase in Ki67 positive cells in shRNA STX1A cells (*Figure 99D*). Also, considering the *in vitro* previous results in which cells with impaired

function of STX1A had lower levels of HER2 receptor at the plasma membrane (*Figure 79B*), HER2 levels at the plasma membrane of MDA-MB-453 tumours were checked as well. A non-permeabilizing immunofluorescence was performed and the results validated the previous *in vitro* findings, shRNA STX1A tumours had lower levels of HER2 receptor at the plasma membrane as well (*Figure 99E*), indicating that STX1A modulates the expression of HER2 at the plasma membrane of the tumour cell *in vivo*.



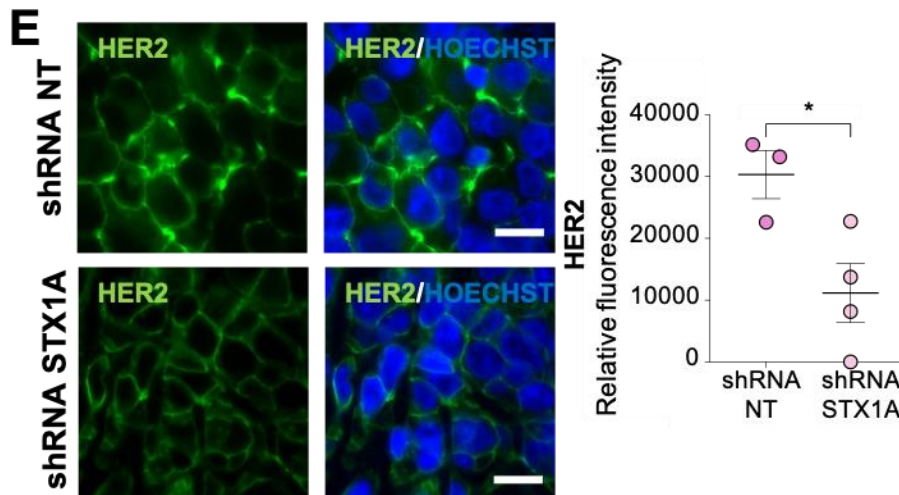


Figure 99 – MDA-MB-453 shRNA STX1A tumours are bigger and down-regulate HER2 membrane expression. (A) Orthotopic breast MDA-MB-453 shRNA Non-Target and shRNA STX1A tumour growth monitored over a period of 9 weeks. (B) Surgically removed MDA-MB-453 BC shRNA NT (shRNA Non-Target) and shRNA STX1A tumours from nude mice. Scale Bar = 1 cm. (C) Final tumour weight of MDA-MB-453 shRNA Non-Target and shRNA STX1A tumours. (D and E) On the left, representative immunofluorescent images of tumours permeabilized and stained against Ki67 (D) or non-permeabilized and stained against HER2 (E). Nuclei were counterstained with Hoechst. Scale bar = 50 μ m (D) and scale bar = 10 μ m (E). On the right, quantification of Ki67-positive cells related to nuclei (D) or fluorescence intensity related to total area of Hoechst staining (E). Representative results of n=1 independent experiments performed in triplicate. Data presented as mean \pm SEM. At least 10 fields were considered in immunofluorescence images. Statistical analysis was performed using Student's *t*-test comparing shRNA NT vs shRNA STX1A. **p* < 0.05.

Regarding the other HER2-positive BC model, BT-474 tumours grew faster and bigger than MDA-MB-453 tumours and also, probably due to the oestrogen pellet that was implanted in mice to sustain the oestrogen needs of BT-474 BC cells, their growth reduced mice quality of life. Therefore, they were sacrificed at day 40 after cell inoculation. During this period, tumour growth was monitored, which resulted in a clear tendency, as it was previously seen in MDA-MB-453 tumours, to form bigger tumours when STX1A was down-regulated (*Figure 100A*). This was confirmed once the tumours were excised and weighted (*Figure 100B and Figure 100C*), although it did not reach statistical significance. Ki67 proliferation marker was also analysed in these tumours, and it was found that tumours with down-regulated STX1A had significantly more Ki67 positive cells than their controls, indicating a proliferative advantage when STX1A was down-regulated (*Figure 100D*). HER2 receptor expression at the cell membrane was also checked, and once again, it proved that HER2 receptor was down-regulated in STX1A down-regulated BT-474 tumours (*Figure 100E*).

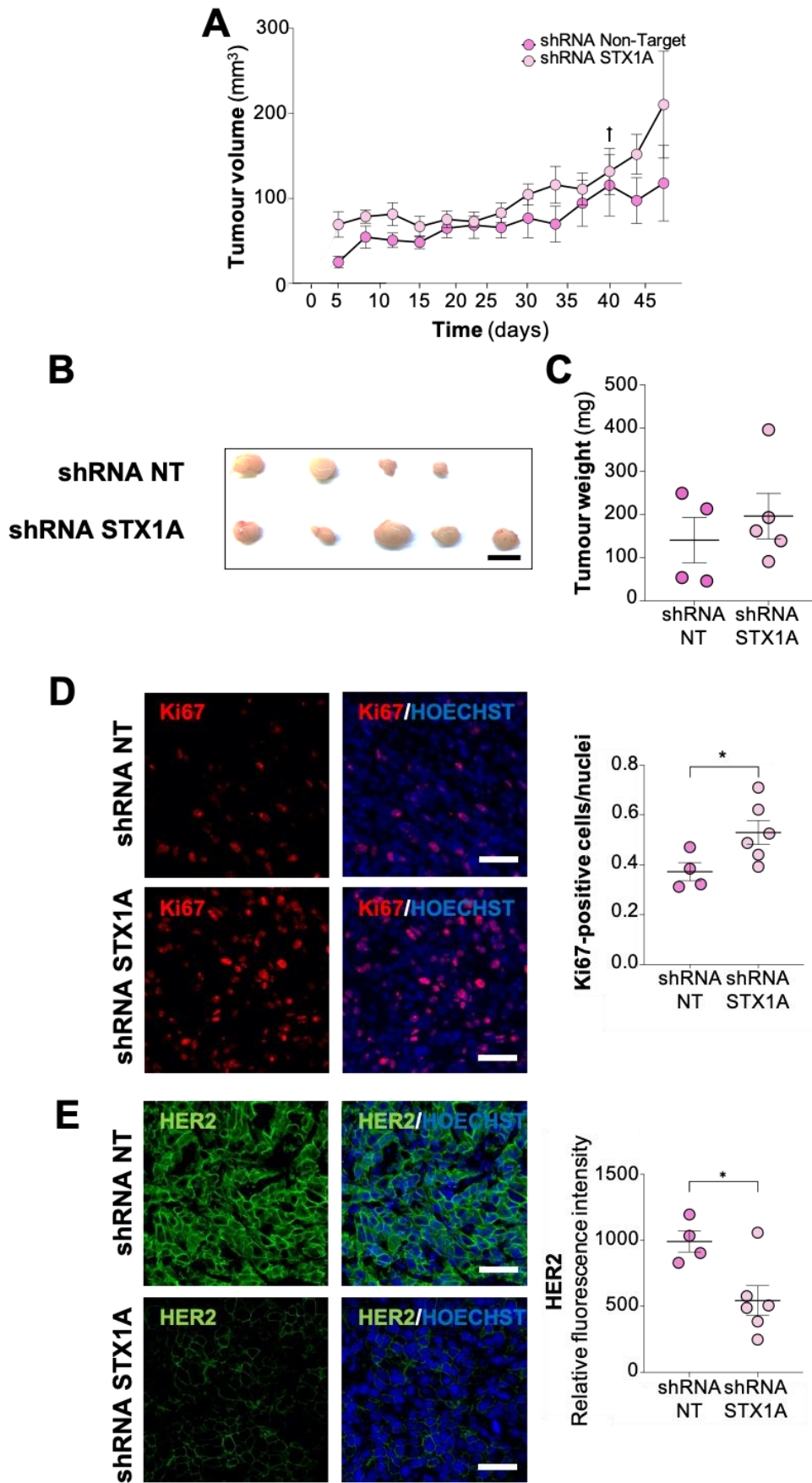
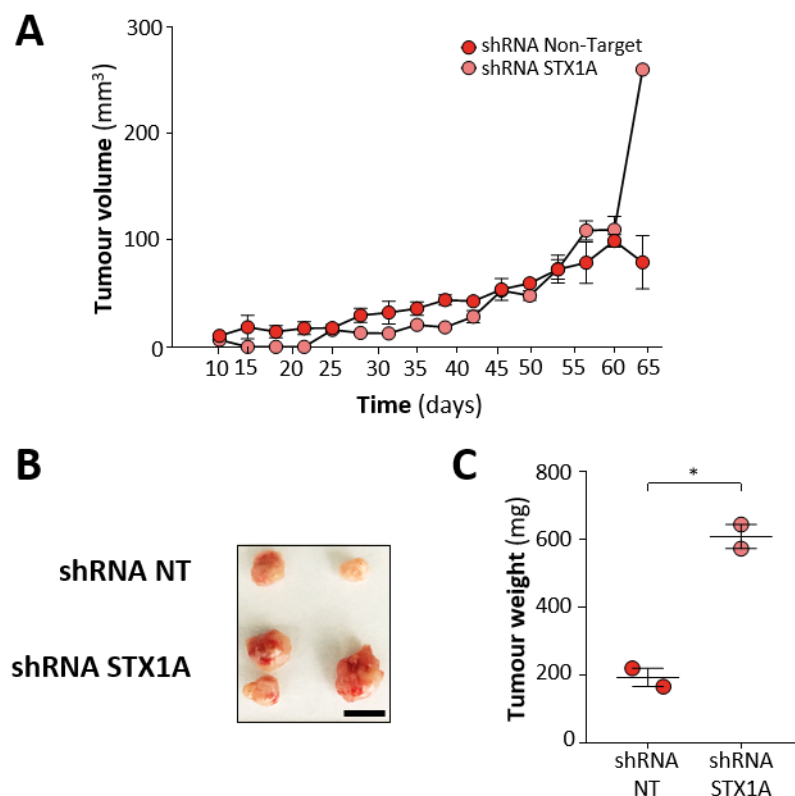


Figure 100 – BT-474 shRNA STX1A tumours are bigger and down-regulate HER2 membrane expression. (A) Orthotopic breast BT-474 shRNA Non-Target and shRNA STX1A tumour growth monitored over a period of 7 weeks. † indicates mice sacrifice from shRNA Non-Target and shRNA STX1A groups before the end point. (B) Surgically removed BT-474 HER2-positive BC shRNA NT (shRNA Non-Target) and shRNA STX1A tumours from nude mice. Scale Bar = 1 cm. (C) Final tumour weight of BT-474 shRNA Non-Target and shRNA STX1A tumours. (D and E) On the left, representative immunofluorescent images of BT-474 shRNA Non-Target and shRNA STX1A tumours permeabilized and stained against Ki67 (D) or non-permeabilized and stained against HER2 (E). Nuclei were counterstained with Hoechst. Scale bar = 50 µm. On the right, quantification of Ki67-positive cells related to nuclei (D) or fluorescence intensity related to total area of Hoechst staining(E). Representative results n=1 independent experiments performed in triplicate. Data presented as mean ± SEM. At least 10 fields were considered in immunofluorescence images. Statistical analysis was performed using Student's *t*-test comparing shRNA NT vs shRNA STX1A. **p* < 0.05.

Finally, tumours from shRNA Non-Target and shRNA STX1A MDA-MB-231 HER2-negative BC cells were analysed. Surprisingly, these tumours did not grow as expected and at the end of the experiment only two mice per condition developed tumour. Monitoring of tumour growth along the 65 days revealed that there were no differences in tumour size, until the last days, when the shRNA STX1A tumours started growing more than the shRNA Non-Target (*Figure 101A*). Once mice were sacrificed and tumours excised, it resulted that STX1A downregulated tumours were bigger than their controls (*Figure 101B and Figure 101C*). Then, Ki67 positive cells were also determined but no clear results were obtained due to the low number of samples (*Figure 101D*).



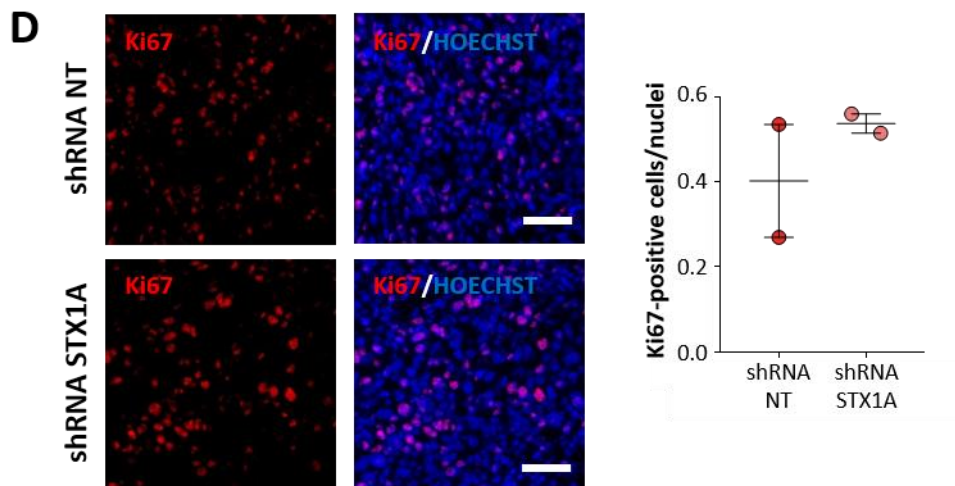


Figure 101 – MDA-MB-231 shRNA STX1A tumours are bigger. (A) Orthotopic breast MDA-MB-231 HER2-negative shRNA Non-Target and shRNA STX1A tumour growth monitored over a period of 9 weeks. (B) Surgically removed MDA-MB-231 BC shRNA NT (shRNA Non-Target) and shRNA STX1A tumours from nude mice. Scale Bar = 1 cm. (C) Final tumour weight of MDA-MB-231 shRNA Non-Target and shRNA STX1A tumours. (D) On the left, representative immunofluorescent images of MDA-MB-231 shRNA Non-Target and shRNA STX1A tumours permeabilized and stained against Ki67. Nuclei were counterstained with Hoechst. Scale bar = 50 μ m. On the right, quantification of Ki67-positive cells related to nuclei. Representative results n=1 independent experiments performed in triplicate. Data presented as mean \pm SEM. At least 10 fields were considered in immunofluorescence images. Statistical analysis was performed using Student's *t*-test comparing shRNA NT vs shRNA STX1A. **p* < 0.05.

After considering that MDA-MB-231 *in vivo* results were not conclusive since in our hands the tumours did not grow well in mice, the chicken CAM assay was used as another *in vivo* model. MDA-MB-231 shRNA Non-Target and shRNA STX1A MDA-MB-231 BC cell lines were inoculated in day 11 chicken embryo CAMs and let the cells form a tumour and grow for 7 days. After that time, the tumours were excised and weighted. Some shRNA STX1A tumours were bigger than shRNA Non-Target tumours (*Figure 102A and Figure 102B*), as previously observed in the mice model although not reaching statistical significance due to a high heterogeneity in tumour weights. When the tumours were histologically analysed, it was found by immunofluorescence that STX1A down-regulated tumours had more Ki67 positive cells than their controls, indicating that the absence of STX1A promoted proliferation of these tumours (*Figure 102C*). These results also demonstrated that this *in vivo* model was also useful and an alternative to mice *in vivo* models, and considering that the CAM model is less time consuming, more economic and easier to handle, the next *in vivo* experiments were performed using the CAM model.

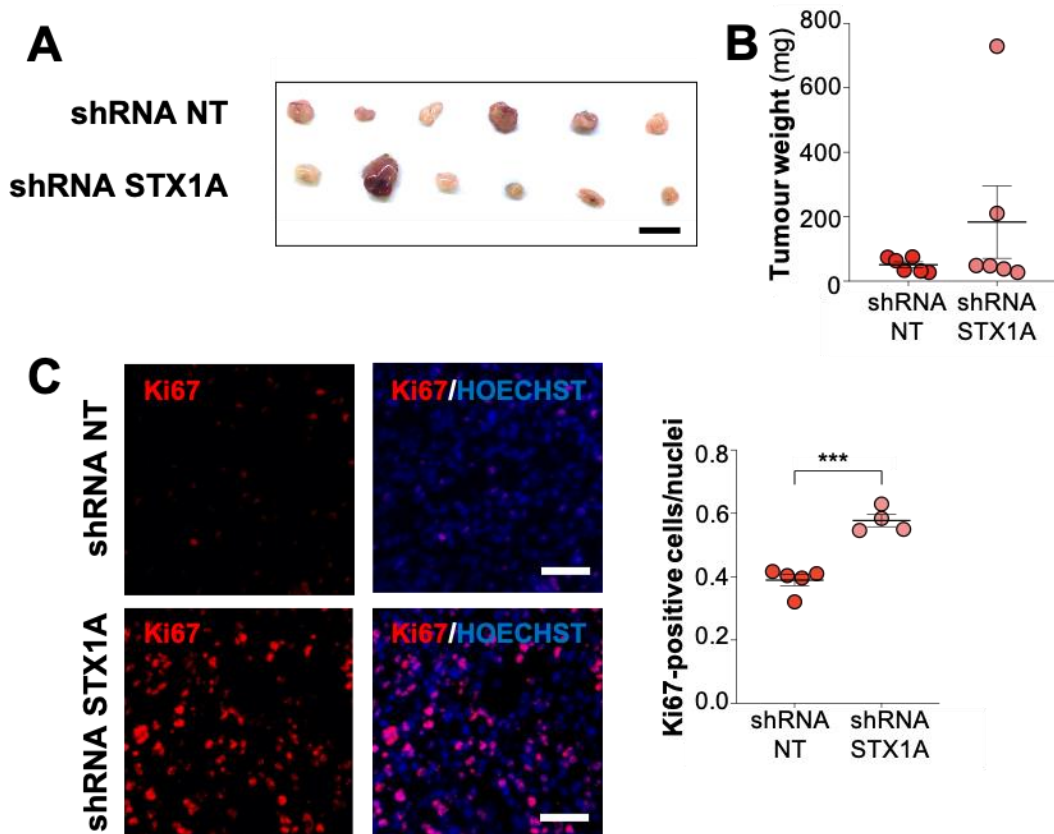
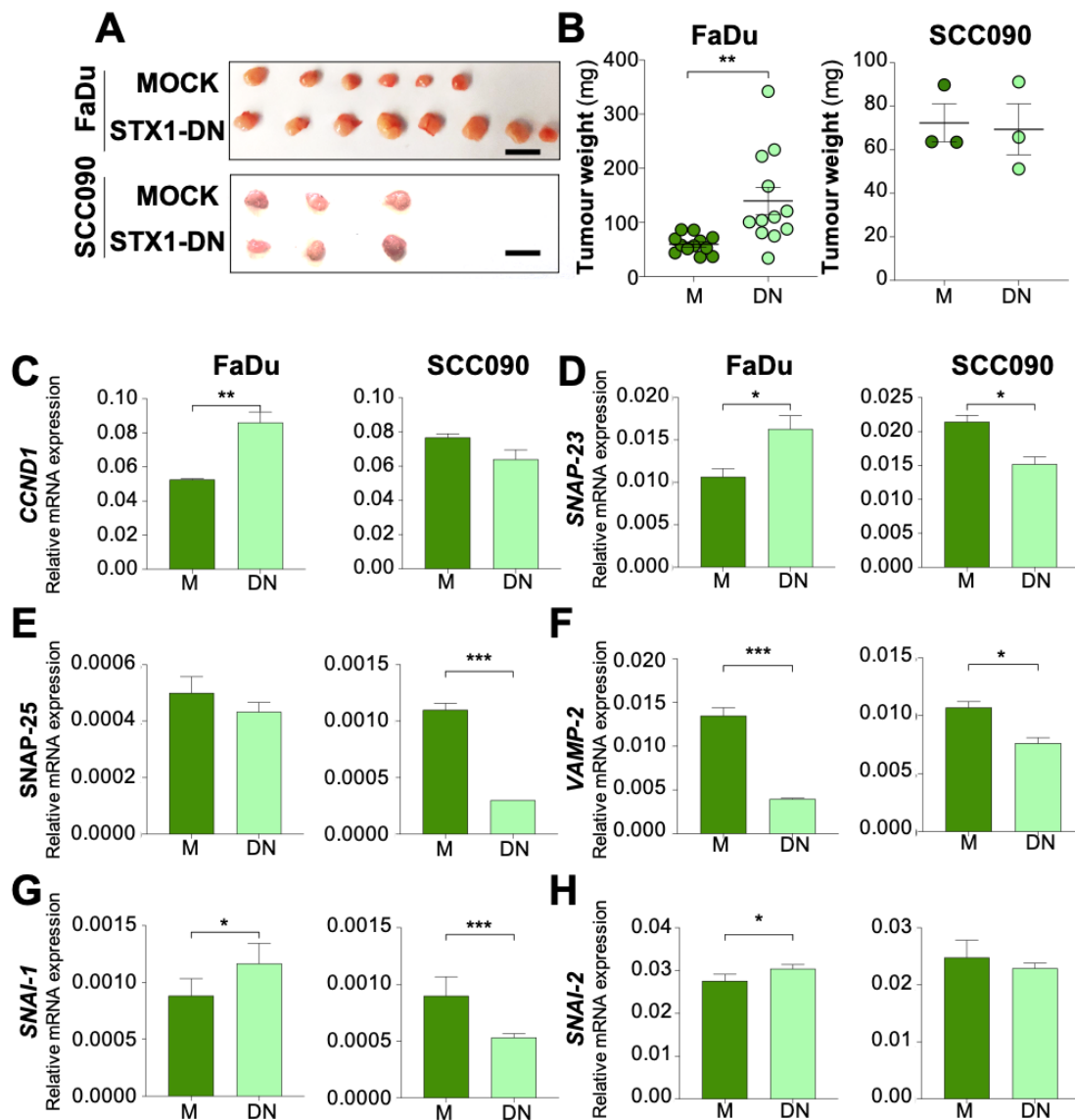


Figure 102 – MDA-MB-231 tumours with STX1A down-regulated grown in CAM have higher expression of the proliferative marker Ki67. (A) Representative images of MDA-MB-231 HER2-negative/basal BC shRNA Non-Target (shRNA NT) and shRNA STX1A tumours growth *in vivo* in CAM assay. Scale Bar = 1 cm. (B) Final tumour weight of MDA-MB-231 shRNA Non-Target and shRNA STX1A CAM tumours. (C) On the left, representative immunofluorescent images of MDA-MB-231 shRNA Non-Target and shRNA STX1A CAM tumours permeabilized and stained against Ki67. Nuclei were counterstained with Hoechst. Scale bar = 50 μ m. On the right, quantification of Ki67-positive cells related to nuclei. Representative results n=1 independent experiments performed in triplicate. Data presented as mean \pm SEM. At least 10 fields were considered in immunofluorescence images. Statistical analysis was performed using Student's *t*-test comparing shRNA NT vs shRNA STX1A. ****p* < 0.001.

Afterwards, *in vivo* CAM assays with the HNSCC FaDu and SCC090 MOCK and STX1-DN cells were performed. After 7 days of growth the tumours were excised and weighted. FaDu tumours with impaired STX1 function were bigger than MOCK tumours, while no difference in tumour weight was found between both groups of SCC090 tumours maybe because only three per condition grew (*Figure 103A and Figure 103B*). RNA from the tumours samples were extracted and it was analysed by qPCR. As it was done in the *in vitro* studies, *CCND1* expression was checked, finding that *CCND1* expression was upregulated in FaDu tumours with impaired STX1A function, while no differences were detected in SCC090 tumours in accordance with the weight results (*Figure 103C*). Then, other mRNA SNARE expression genes were checked and an up-regulation of *SNAP-23* in STX1-DN FaDu tumours was found, while it was down-

regulated in STX1-DN SCC090 tumours (*Figure 103D*). *SNAP-25* mRNA expression was also analysed in HNSCC tumours and it was down-regulated in SCC090 STX1-DN tumours (*Figure 103E*). v-SNARE *VAMP-4* expression was down-regulated in both FaDu and SCC090 STX1-DN tumours (*Figure 103F*). Several EMT markers were checked as well. *SNAI-1* mRNA expression was upregulated in FaDu tumours with impaired STX1 function, while it was down-regulated in SCC090 STX1-DN tumours (*Figure 103G*). The analysis of *SNAI-2* mesenchymal marker revealed that STX1-DN FaDu tumours had a significant upregulation, while no differences were found in SCC090 tumours (*Figure 103H*). *TWIST-1* transcription factor mRNA levels were found down-regulated in both STX1-DN HNSCC tumours (*Figure 103I*). Finally, *ITGa6* mRNA expression was analysed and no differences were found between any of the HNSCC tumour groups (*Figure 103J*).



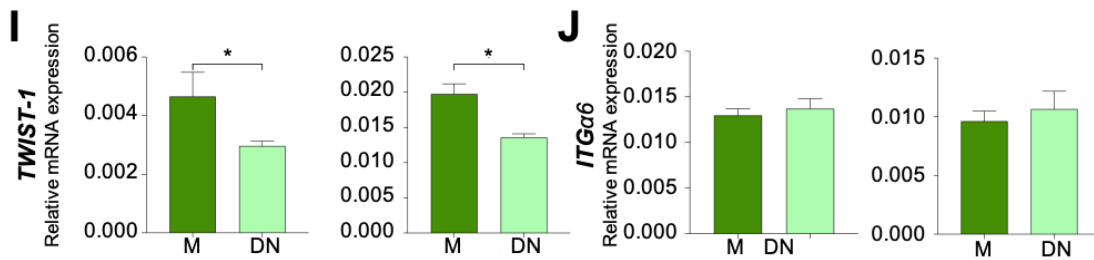


Figure 103 – FaDu tumours with impaired STX1A are bigger, overexpress *CCND1* and dysregulate EMT markers. (A) Representative images of FaDu and SCC090 HNSCC MOCK (M) and STX1-DN (DN) tumours from the *in vivo* CAM assay. Scale Bar = 1 cm. (B) Final tumour weight of FaDu (2 independent experiments) and SCC090 (1 experiment) MOCK and STX1-DN CAM tumours. (C-J) Relative *CCND1* (C), *SNAP-23* (D), *SNAP-25* (E), *VAMP-2* (F), *SNAI-1* (G), *SNAI-2* (H), *TWIST-1* (I) and *ITGα6* (J) mRNA expression levels of FaDu and SCC090 MOCK and STX1DN CAM tumours. β -actin was used as internal control. Representative results n=1 independent experiments performed in sextuplicate. Data presented as mean \pm SEM. Statistical analysis was performed using Student's *t*-test comparing shRNA MOCK vs STX1-DN. * $p < 0.05$. ** $p < 0.01$, *** $p < 0.001$.

Altogether these results confirmed the *in vitro* data: when STX1A is down-regulated or functionally impaired, tumour cells are able to proliferate more and form bigger breast and head and neck tumours with altered EMT markers expression. Therefore, STX1A is repressing tumour proliferation and migration *in vitro* and tumour growth *in vivo* in BC and HNSCC.

3.5.2. FUNCTION IMPAIRMENT OF SYNTAXIN-1A SENSITIZES BREAST AND HEAD AND NECK TUMOURS TO LAPATINIB

Then, considering our *in vitro* results by which BC and HNSCC cells with STX1-DN were more sensitive to lapatinib, two *in vivo* experiments with treatment with this drug were performed. MDA-MB-453 (HER2-positive) BC and FaDu (HNSCC) cell lines were used. However, since retroviral MDA-MB-453 MOCK cells were not possible to obtain, a transient MOCK and STX1-DN plasmid transfection was performed. Bearing in mind that transfection efficiency was relatively high and that the CAM experiments are short-time *in vivo* assays, it was not a major problem to use this approach. However, first a set-up experiment to check the optimal dose of lapatinib to treat MDA-MB-453 tumours had to be performed. Accordingly, MDA-MB-453 HER2-positive BC cells were inoculated in day 11 chicken embryo CAMs, the cells were let 48 hours to attach and grow and then the tumours were treated at different doses of lapatinib for 4 days. At day 6 after inoculation, the tumours were excised and weighted (*Figure 33*, *Figure 104A* and *Figure 104B*). Macroscopically, the analysis of tumour weight determined that even they only had been growing only for 6 days (normally our endpoint of the experiments

in CAM *in vivo* assay is at 7 days), the tumours were big enough to draw conclusions. No effect was perceived macroscopically in tumours treated with the lowest dose of lapatinib. However, tumours treated with 1, 2 and 5 μM lapatinib showed a lower tumour weight, although not reaching statistical significance (Figure 104A and Figure 104B). Then, tumour gene expression was analysed comparing the non-treated tumours with 2 μM lapatinib treated tumours. Treatment with lapatinib reduced *STX1A* expression (Figure 104C) as it was previously demonstrated *in vitro* (Figure 82A). Also, *SNAP-23* mRNA expression was decreased with lapatinib treatment (Figure 104D). The mRNA expression of *EGFR*, *HER2* and *HER3* was also checked. No changes were found in *EGFR* mRNA expression between groups, while *HER2* mRNA expression was reduced and *HER3* mRNA expression was significantly increased in lapatinib MDA-MB-453 treated tumours (Figure 104E and Figure 104G). Finally, the cell cycle regulator *CCND1* gene was analysed, and it was found that lapatinib-treated tumours did not decrease the expression of this cyclin (Figure 104H).

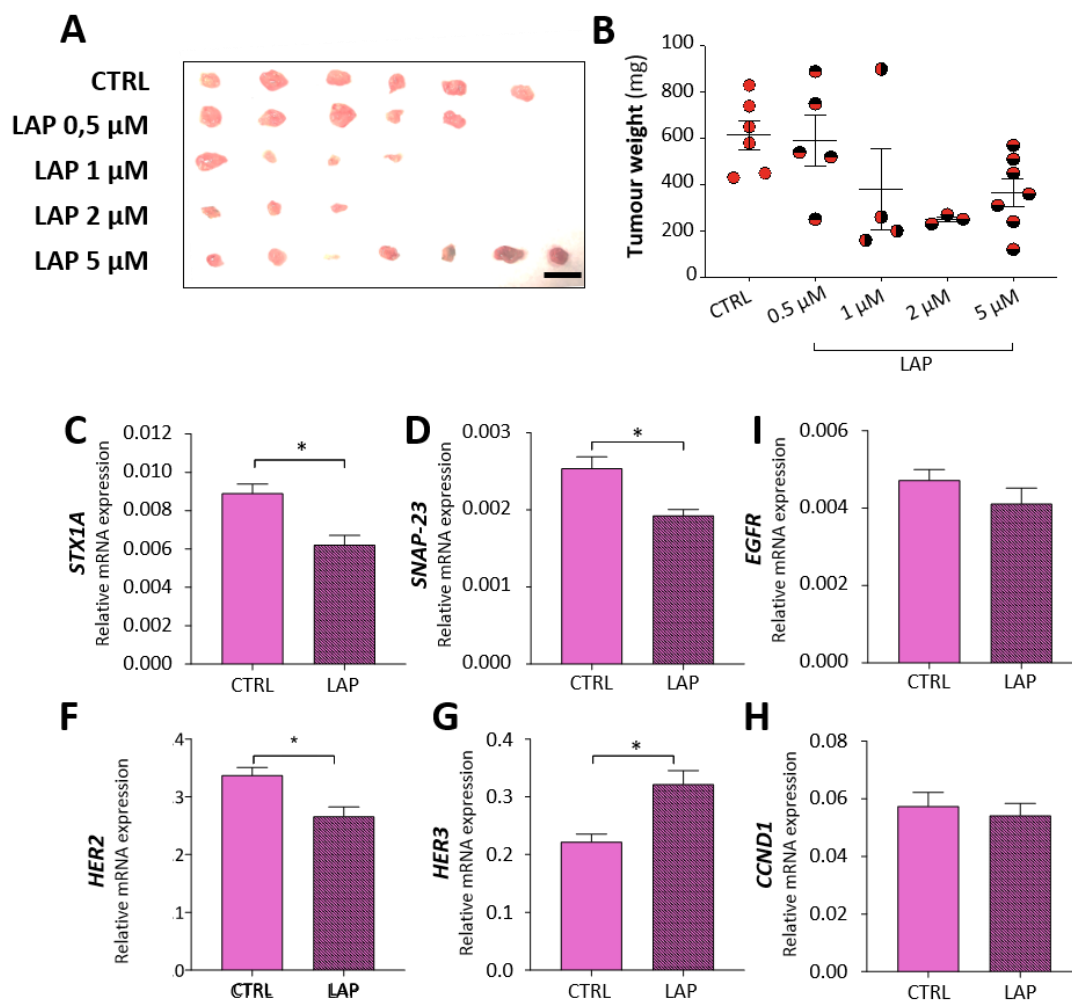
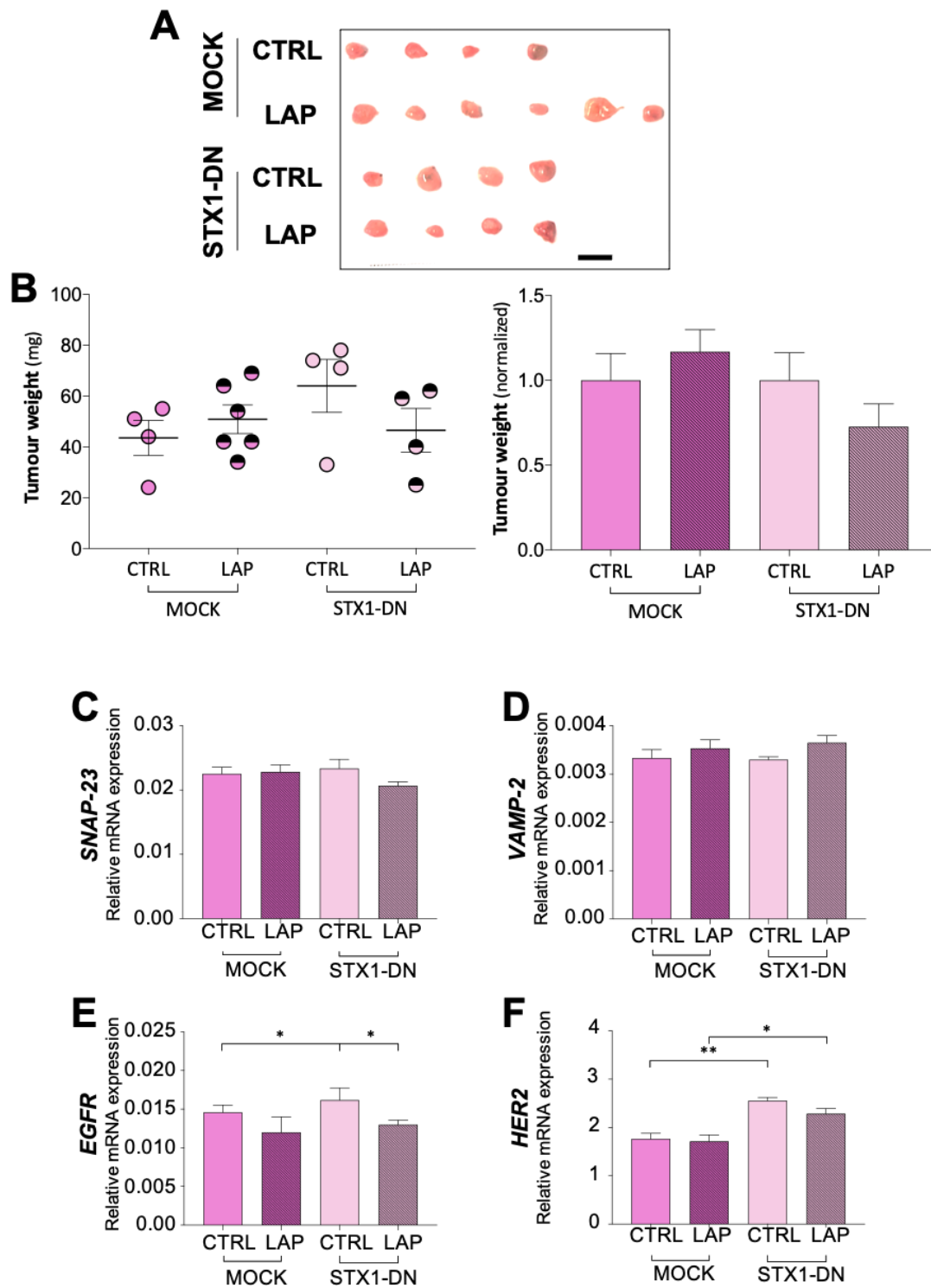


Figure 104 – MDA-MB-453 tumours treated with lapatinib decrease *STX1A*, *SNAP-23*, *HER2*- and *HER3* expression. (A) Representative images of MDA-MB-453 HER2-positive BC tumours treated at different doses of lapatinib for four days in CAM assay. Scale Bar = 1 cm. (B) Final tumour weight of

MDA-MB-453 tumours treated with lapatinib. (C-I) Relative *STX1A* (C), *SNAP-23* (D), *EGFR* (E), *HER2* (F) *HER3* (G) and *CCND1* (H)) mRNA expression levels of MDA-MB-453 CAM tumours treated with lapatinib (2 μ M). β -actin was used as an internal control. Representative results n=1 independent experiments performed in triplicate. Data presented as mean \pm SEM. Statistical analysis was performed using one-way ANOVA between CTRL and LAP treatments (B) and with Student's *t*-test comparing CTRL vs LAP (qPCR). * $p < 0.05$, ** $p < 0.01$.

According to the set-up experiment, it was decided to use a 2 μ M dose of lapatinib to treat the MDA-MB-453 tumours. It was the dose where the tumours were smaller in comparison to the control and with less deviation. The next step was to move on and to prove the *in vitro* results by treating MDA-MB-435 tumours with lapatinib. First of all, MDA-MB-453 cell lines were transfected with MOCK and STX1-DN plasmids 24 hours prior CAM cells inoculation, then they were inoculated into the CAM of chicken fertilized eggs, and as it was done in the set-up experiment, 48 hours after the cells had settled and started growing, the 2 μ M lapatinib treatment was started. Lapatinib treatment tested for 4 days and 6 days after the inoculation, the tumours were removed from the CAM and weighted (*Figure 33*). The tumour images and their correspondent weights are shown in *Figure 105A and Figure 105B*. STX1A-DN tumours were slightly bigger than MOCK MDA-MB-453 tumours, as it was previously seen in mice (*Figure 99A and Figure 99B*). Focusing on the effect of lapatinib treatment, unexpectedly no effect in MDA-MB-453 MOCK tumours, in contrast to the set-up experiment where lapatinib 2 μ M decreased three times the control tumour weight (*Figure 105A and Figure 105B*). However, an effect in STX1-DN MDA-MB-453 tumours, regarding tumour weight was detected since a 30% reduction in the weight of STX1-DN tumours was found, indicating a sensitization to lapatinib treatment when STX1 function was impaired. Tumour mRNA and protein expressions were also analysed. Regarding *SNAP-23* and *VAMP-2* mRNA quantification no statistical differences were found between MOCK and STX1-DN treated tumours (*Figure 105C-Figure 105D*). The analysis of *EGFR*, *HER2* and *HER3* mRNA receptors did not show any significant difference between MOCK and MOCK treated with lapatinib either (*Figure 105E-Figure 105G*). An increase in *EGFR*, *HER2* and *HER3* gene expression in STX1-DN was detected when comparing MOCK and STX1-DN groups. Then, focusing on the effect of lapatinib on STX1-DN tumours *EGFR* gene expression decreased due to the treatment (*Figure 105E*). It was also found that *CCND1* mRNA levels were upregulated in STX1-DN tumours in comparison to MOCK tumours (*Figure 105H*), a fact that could explain why tumours with STX1-DN were bigger than the MOCK ones. However, no statistical differences were observed under lapatinib treatment. Regarding the protein analysis, a Western blot analysis was performed to figure out if there were any differences in the activation of AKT and ERK signalling pathways. STX1-DN tumours overactivated the pAKT signalling pathway, as it had already been described *in vitro* (*Figure*

84B), and pAKT pathway was more markedly deactivated in lapatinib-treated STX1-DN tumours (*Figure 105J*). No evident changes on ERK activation were seen between groups (*Figure 105J*).



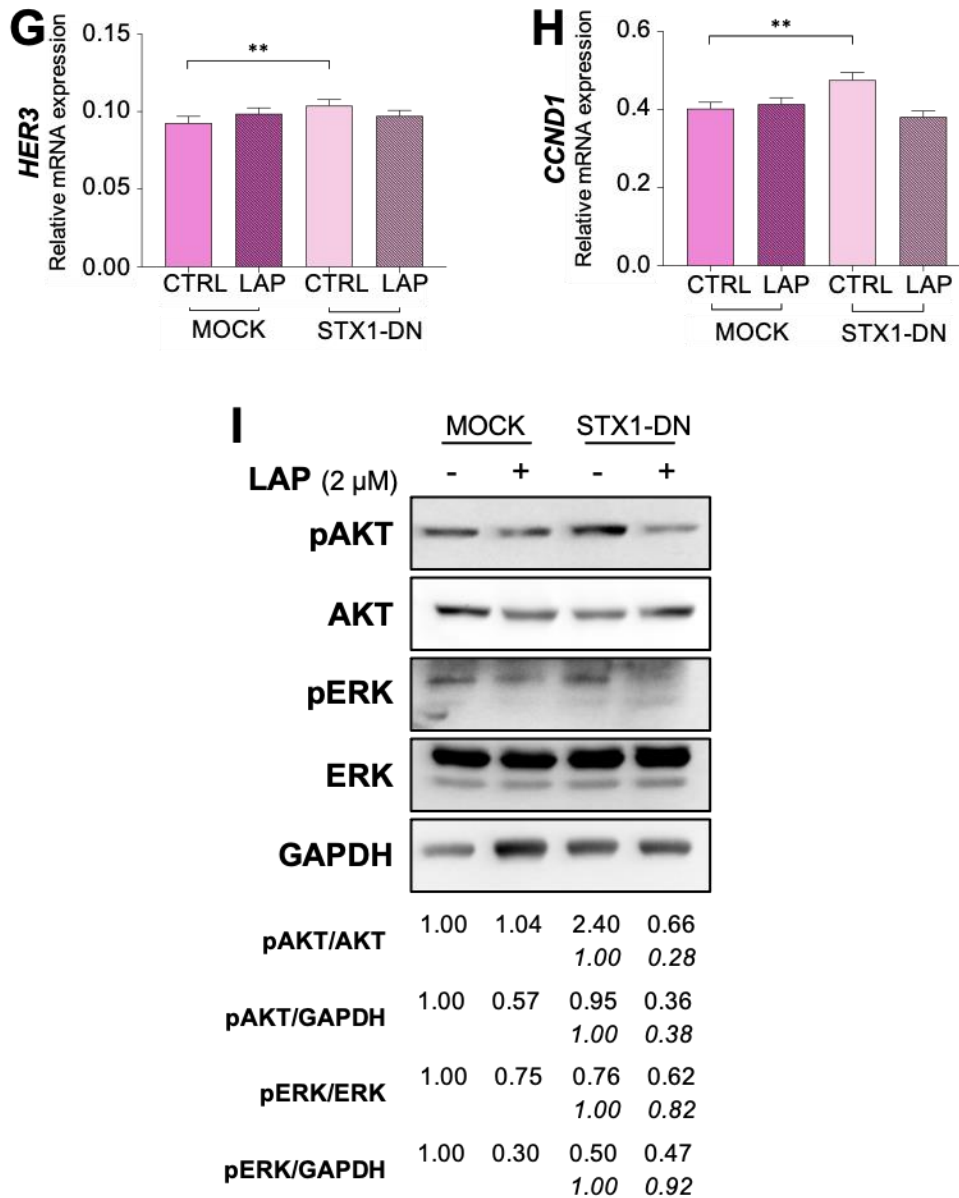
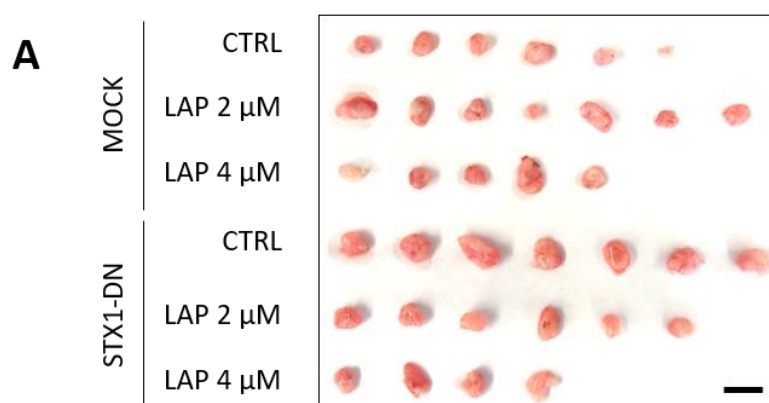
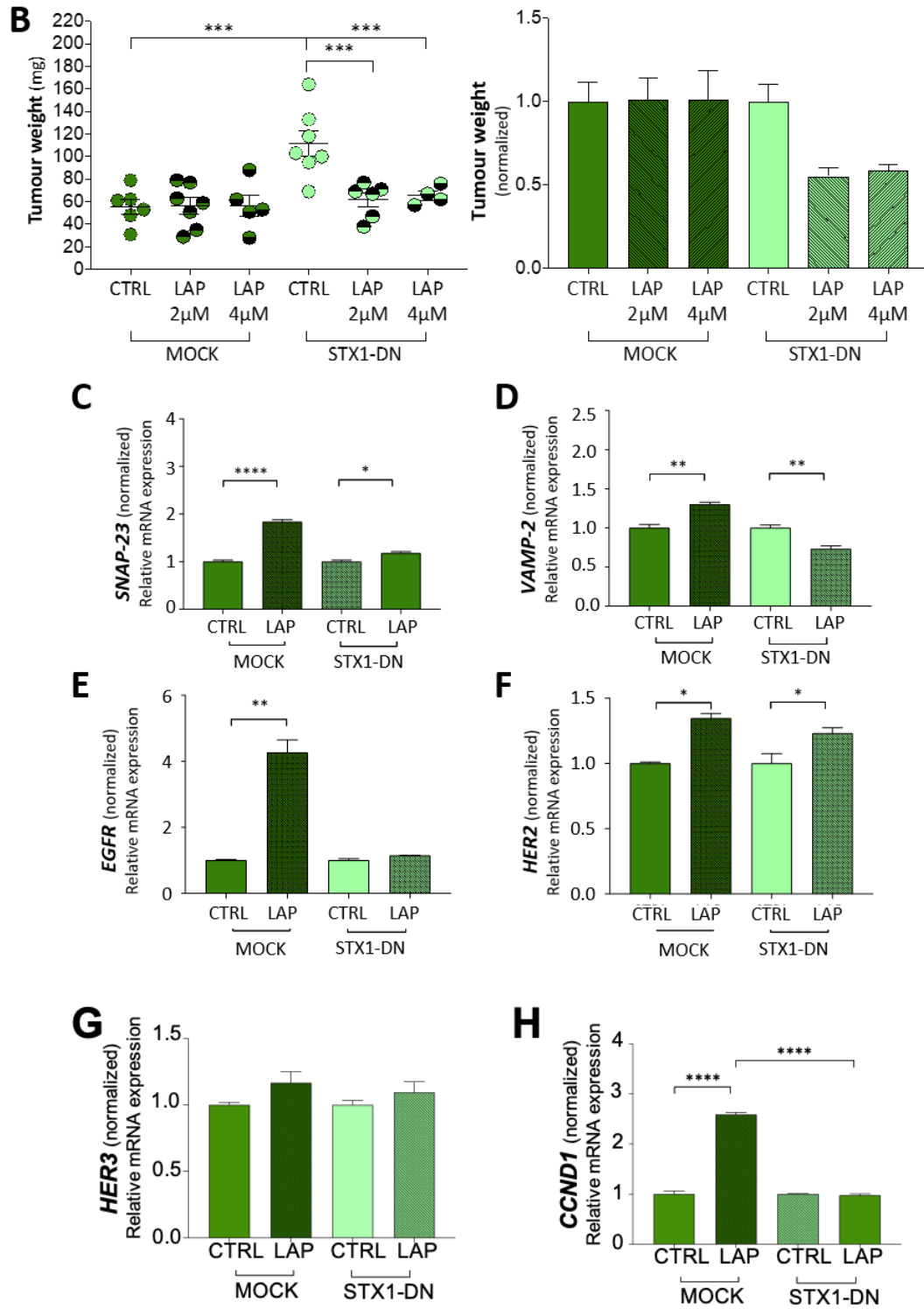


Figure 105 – MDA-MB-453 tumours with non-functional STX1A are more sensitive to lapatinib. (A) Representative images of MOCK and STX1-DN MDA-MB-453 HER2-positive BC tumours treated with lapatinib (2 μ M) for four days in CAM assay. Scale Bar = 1 cm. (B) On the left, final tumour weights. On the right, tumour weights normalized to its correspondent control situation. (C-H) Relative *SNAP-23* (C), *VAMP-2* (D), *EGFR* (E), *HER2* (F), *HER3* (G) and *CCND1* (H) mRNA expression levels of MOCK and STX1-DN MDA-MB-453 CAM tumours treated with lapatinib (2 μ M). β -actin was used as an internal control. (I) Representative Western blot analysis of AKT and ERK activation in MDA-MB-453 CAM tumours treated with lapatinib. GAPDH was used as internal control. At the bottom signal quantification of protein expression normalized to each control. Representative results n=1 independent experiments performed in sextuplicate (qPCR). Data presented as mean \pm SEM. Statistical analysis was performed using one-way ANOVA between CTRL M vs CTRL STX1-DN, LAP M vs LAP STX1-DN and CTRL STX1-DN vs LAP STX1-DN. * p < 0.05, ** p < 0.01.

Then, the focus was moved to the HNSCC FaDu cells impaired STX1A function, which were more sensitive to lapatinib, as described in the previous *in vitro* results (Figure 85). Taking advantage that FaDu cells stably expressing MOCK and STX1-DN constructs were obtained,

they could be used to form CAM *in vivo* tumours and treat them one more day. Therefore, the cells were set and grew into the chicken CAM for 2 days, and then tumours were treated with lapatinib (2 and 4 μM) for 5 days. Tumours were excised 7 days after inoculation (Figure 33). Tumours are shown in Figure 106A and their weights in Figure 106B. STX1-DN tumours were significantly bigger than MOCK tumours, as it was described in the previous *in vivo* FaDu CAM performed (Figure 103A and Figure 103B). There was no effect in tumour weight when MOCK tumours were treated with 2 or 4 μM of lapatinib, however in STX1-DN tumours there was a decrease of 50% of their weight (Figure 106B). These results clearly indicate that STX1 function impairment sensitizes FaDu tumours to lapatinib treatment. Then, the molecular analysis on the effect of STX1A function impairment and lapatinib treatment was performed. First, mRNA expression of *SNAP-23* was analysed. Lapatinib treatment increased *SNAP-23* mRNA expression in both groups, but more markedly in MOCK tumours (Figure 106C). An opposite pattern was detected for *VAMP-2*, increasing in MOCK and decreasing in STX1-DN tumours due to lapatinib treatment (Figure 106D). The analysis of *EGFR/HER* family of receptors expression highlighted that *EGFR* expression was increased in FaDu MOCK tumours treated with lapatinib, while no differences were seen in STX1-DN treated tumours (Figure 106E). *HER2* expression was similarly up-regulated in both groups treated with lapatinib (Figure 106F) and there were no differences regarding *HER3* expression in treated tumours (Figure 106G). Moreover, *CCND1* mRNA expression was also analysed. Surprisingly *CCND1* mRNA levels increased in lapatinib-treated MOCK tumours, while no differences were seen in STX1-DN tumours treated with lapatinib (Figure 106H).





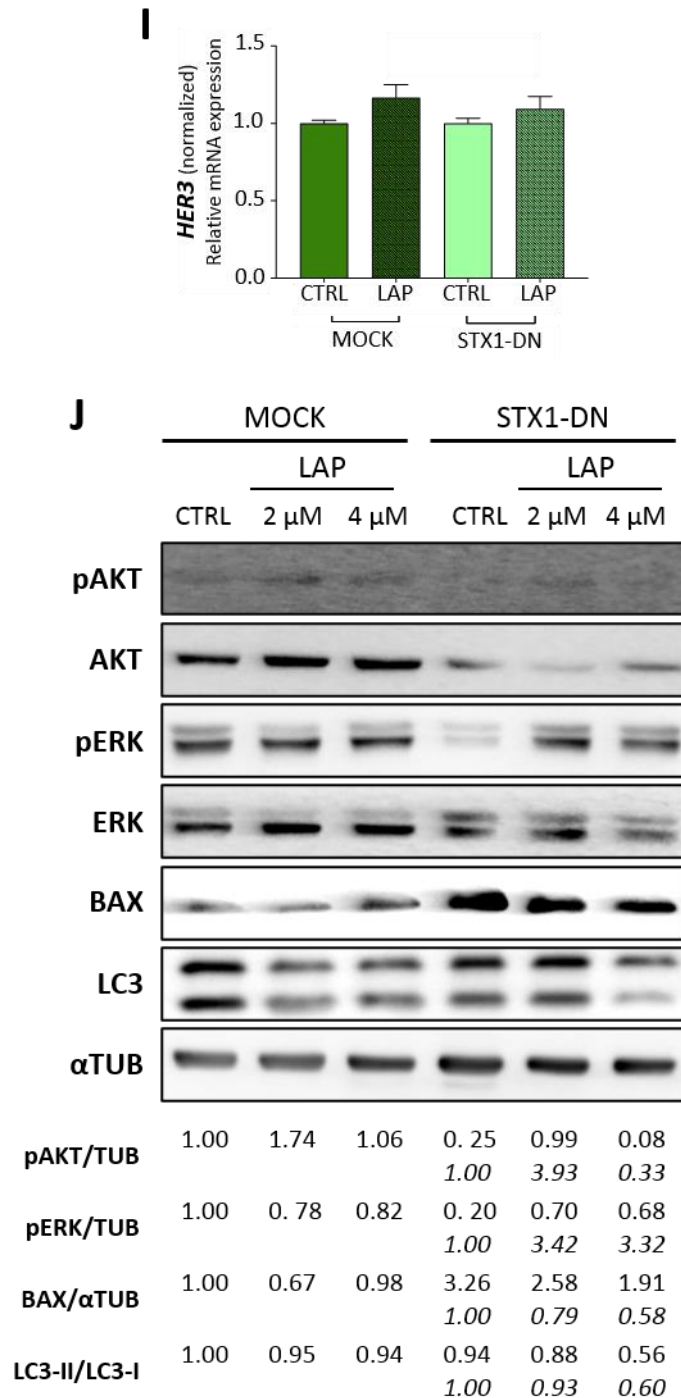


Figure 106 – FaDu tumours with non-functional STX1A are more sensitive to lapatinib. (A) Representative images of MOCK and STX1-DN FaDu HNSCC tumours treated with lapatinib (2 and 4 μ M) for five days in CAM assay. Scale Bar = 1 cm. (B) On the left, final tumour weight of MOCK and STX1-DN FaDu tumours treated with lapatinib. On the right, tumour weight normalized to its correspondent control situation. (C-F) Normalized mRNA expression of *SNAP-23* (C), *VAMP-2* (D), *CCND1* (E), *FOXO3* (F), *EGFR* (G), *HER2* (H) and *HER3* (I) mRNA expression levels of MOCK and STX1-DN FaDu CAM tumours treated with lapatinib (2 μ M). β -actin was used as an internal control. (J) Representative Western blot analysis of AKT and ERK activation, BAX and LC3 from FaDu CAM tumours treated with lapatinib. α TUB was used as internal control. At the bottom relative signal quantification of protein expression. Representative results n=1 independent experiments performed in sextuplicate (qPCR). Data presented as mean \pm SEM. Statistical analysis was performed using one-way ANOVA between CTRL M vs CTRL

STX1-DN, LAP M vs LAP STX1-DN and CTRL STX1-DN vs LAP STX1-DN. * $p < 0.05$, ** $p < 0.01$, **** $p < 0.0001$.

Finally, the protein analysis was performed by Western blot, analysing AKT and ERK pathway activation and BAX and LC3 protein levels (*Figure 106J*). AKT and ERK proteins were dephosphorylated in STX1-DN tumours in comparison to the MOCK ones, as it was previously seen *in vitro* (*Figure 84A*). In lapatinib-treated tumours and in both groups 2 μM lapatinib increased pAKT expression while with 4 μM pAKT levels were not altered in MOCK tumours but decreased in STX1-DN. There were no differences regarding ERK activation with lapatinib treatment in any group. Regarding BAX expression, a surprising result, compared to our *in vitro* findings was found (*Figure 88A*), with STX1-DN tumours expressed more BAX and it clearly decreased with lapatinib treatment. LC3 expression was also analysed and it was found unaltered in lapatinib-treated tumours. Surprisingly, LC3-II/LC3-I expression decreased with lapatinib treatment in STX1-DN tumours, contrarily to the *in vitro* results (*Figure 88A*).

Overall, these lapatinib-treatment *in vivo* results confirmed that MDA-MB-453 HER2-positive BC and FaDu HNSCC tumours were more sensitive to lapatinib when STX1A function is impaired, decreasing their tumour weight, in accordance to what was already demonstrated in the *in vitro* experiments.



Syntaxin-1A, a synaptic related protein in breast and head and neck cancer progression and prognosis

DISCUSSION

Syntaxin-1A, a synaptic related protein in breast and head and neck cancer progression and prognosis

Constant improvements and advances in research and technology provide researchers and oncologists with substantial scientific knowledge to be applied onto oncological clinical practice. However, in spite of these important advances, our society is still struggling against cancer. Cancer is the second current cause of death, the most relevant in terms of both clinical, social and economic burden (5,6). In particular, BC is an example of the major problem that cancer represents in our society. In 2020, the number of new cases of BC, that had been increasing in the last years, replaced lung cancer as the most common one, comprising 11.7% of all cancer cases (249). Moreover it is the first cause of cancer-related death in women, meaning that one in six cancer deaths will be of BC (249) in the next future. Although with a lower incidence than BC, HNSCC is the sixth more diagnosed cancer worldwide, but its incidence is expected to increase around 30% by 2030. In addition, HNSCC shows the second highest rate of cancer-related suicide, indicating the compromised quality of life these patients have (208). Hence, there is still a need to continue the research focused on early diagnose and on identification of specific targets to design direct oncology treatments. A better knowledge of how cancer works at molecular levels and which proteins regulate tumour main functions are the crucial steps to achieve these goals.

Cancer comprises multiple diseases, and some researchers consider tumours as organs. This means that research should not be limited to cancer cells themselves, but it has also to be extended to the comprehension of the environment where the tumour is located to finally understand these complex diseases. Nobody doubts that tumour microenvironment cells, ECM components and blood and lymphatic vessels play a pivotal role in tumour progression and invasion (19,22,33–35). However, little is known regarding the relationship between the nervous system and cancer, even though nerve fibres are found together with blood and lymphatic vessels within tumours.

During the past years, research about the influence of the nervous system and neural factors in tumour progression has evolved, and very interesting studies have been published revealing the huge impact of the crosstalk between nerves fibres and cancer cells on promoting nerve growth and cancer progression and metastasis. It has been proved that a direct correlation between neural infiltration and tumour stage exists in colon and prostate cancer, since several studies stress the impact of the inhibition (surgically or by chemical intervention) of the nervous system in gastric and prostate cancer resulting in a decrease of tumour growth and dissemination (41,53). This relationship could be explained considering soluble factors released by the nerves and by cancer cells. On one hand, cancer cells release

neural growth factors which induce nerve growth and infiltration within the tumours (44,45,68). On the other, nerves release neurotransmitters and/or neuromodulators which are able to promote tumour growth and metastasis and also affect the chemotherapeutic response (37,44,50). It is in this research field that our group has widely contributed. We have already proved that the neuromodulator substance P (SP) influences BC tumours (219,220). We have demonstrated that breast tumours express NK-1R, an SP receptor, highly expressed in HER2 primary breast tumours (in comparison to luminal and TNBC subtypes), whose expression correlates with poor prognosis. We have also proved that inhibition of NK-1R resulted in a decrease of tumour growth *in vivo* and in a down-regulation of EGFR and HER2 receptors, which are tightly linked to malignant progression and drug resistance (219,220). Back in 2016, we described seven neurogenes differentially expressed among BC subtypes, the expression of six of them (*STX1A*, *HRH1*, *NRP2*, *NGFR*, *APP* and *EFNB1*) correlating with overall survival of BC patients (104). Remarkably, we also published that treatment of basal BC subtype tumours and trastuzumab-resistant BC tumours with terfenadine, an HRH1 specific inhibitor, reduced tumour growth *in vivo* (224). As an aftermath of these seminal findings, two additional doctoral thesis besides the present one have been defended in 2021 in our lab, describing the role of NRP2 and SEMA3F in BC tumour progression and dissemination, highlighting the important role of the neurogenes expressed in tumour cells (222,223).

In the present project, our research is focused in *STX1A*, which is overexpressed in HER2-positive BC subtypes (HER2-enriched and luminal B) (104). However, considering that it is a member of the SNARE protein family, part of our research was extended to other SNARE partners, as well. We studied the role of these synaptic-related proteins in BC, taking advantage of the large experience our laboratory has in this field.. In spite of all the research done on BC, we still lack good biomarkers to predict patient overall survival, metastasis risk and therapy response. Moreover, even though there are many treatments available and target-specific for BC, with the exception of TNBC subtype where chemotherapy is still the gold-standard therapy, new therapeutical strategies arising from novel scientific approaches are still needed, due to the acquired resistance of BC tumours to current treatments.

Although BC was the primary focus of our project, the research field was also extended to HNSCC when some preliminary results appeared. Thus, an emergent collaboration with Dr. Vilaseca and Dr. Avilés otorhinolaryngologists from Hospital Clínic de Barcelona and Dr. León and Dr. Camacho otorhinolaryngologists from Hospital de la Santa Creu i Sant Pau was established. Although HNSCC is not as incident as BC, it is an aggressive and genetically

complex disease which lacks a proper molecular classification. Regarding HNSCC treatment, there is only one targeted therapy, cetuximab, the most common treatment options being surgery and radiotherapy, which results in an associated significant morbidity and reduction of quality of life. Therefore, HNSCC research is focused on identifying biomarkers able to stratify patients into clinically meaningful groups and to develop more effective targeted therapies (208,209,213).

In view of the above considerations, the main objective of this thesis has been to unravel the role of STX1A in BC and HNSCC progression and prognosis. Analysis of STX1A expression in BC and head and neck tumours have enabled us to evidence the relationship between STX1A gene expression and patient outcome, defining overexpression of STX1A as a bad prognosis marker. Moreover, STX1A may regulate the trafficking of EGFR/HER family of receptors into the plasma membrane. Consequently, STX1A lack of function results in the sensitization to EGFR- and HER2-targeted therapies in BC and HNSCC and to cisplatin and adriamycin in head and neck tumours. Finally, STX1A also promotes invasion and metastatic events in BC and HNSCC. Therefore, STX1A is proposed as an effective target to inhibit BC and HNSCC metastatic events, and also to increase the sensitivity to targeted therapies in BC and HNSCC and to HNSCC chemotherapy.

1. SYNTAXIN-1A, AND OTHER SNARE-RELATED GENES, AS NOVEL OVERALL SURVIVAL PREDICTORS IN BREAST AND HEAD AND NECK CANCERS

This project was initially based on the previous paper published by our group showing that *STX1A* is overexpressed in HER2-enriched and luminal B BC subtypes, and that high expression of this neurogene correlated with a poorer overall and distant metastasis free survival (104). *STX1A*, initially detected in neuronal tissues, is a member of the SNARE family, involved in vesicle-trafficking events. In particular, *STX1A* main role in neurons is to allow the fusion of vesicles containing neurotransmitters and/or neuromodulators with the plasma membrane, promoting their exocytosis in the synaptic cleft and triggering a response to the neighbouring neurons or other cell types (250). Even though the research in *STX1A* was focused in neurons, this protein and other SNAREs are also expressed in other tissues, with similar roles in vesicle trafficking. *STX1A* is also present in secretory cells, sperm or alveolar cells, among other cell types, where its function is to control membrane-fusing events such as the acrosome reaction or the fusion of insulin containing granules (116,125,132,134,251). Its role has also been linked to some ion channels modulation such as CFTR or ENaC in the lungs (122–124). Despite the

wide research in STX1A in neural and non-neuronal tissues, there are only a few articles looking for a possible role of STX1A in cancer (86,104,136,138–140), and none of them is focused on breast or head and neck cancer. There is no information in their corresponding healthy tissues, breast or oral cavity, pharynx or larynx, either.

Most of the articles that relate STX1A and cancer highlight the peculiarity that *STX1A* is overexpressed in tumours in comparison to healthy tissues with the exception of adamantinomatous craniopharyngioma, in which *STX1A* expression is down-regulated (103,137–140,225,252,253). As expected, tumours emerging from neural tissues, such as gliomas, express *STX1A* and it is overexpressed in comparison to healthy tissues (225). Moreover, in other neuroendocrine tumours, among them pulmonary neuroendocrine lung tumours, *STX1A* is found to be an excellent neuroendocrine marker (138,139,252,253). In addition, *STX1A* is overexpressed in tumours in which its function was not previously described, such as in bladder cancer, where *STX1A* is overexpressed together with *VAMP-2* (140) or in parathyroid carcinomas (103). The data presented in this thesis corroborate our previous findings in BC, *STX1A* is overexpressed in tumours in comparison to breast healthy tissues (*Figure 34A*). Besides, we have also extended this same conclusion to HNSCC patient tumour samples, confirming that *STX1A* is overexpressed in tumoural tissue (*Figure 52A and Figure 52B*), the same results being found in public patient databases (*Figure 55A*). The expression of *SNAP-25*, an *STX1A* partner, was analysed and the same trend was found in HNSCC patients (*Figure 52C and Figure 52D*). Overexpression of *SNAP-25* has been recently documented also in colon cancer (254).

Further analysis of BC patient METABRIC database corroborated the overexpression of *STX1A* in HER2-positive (HER2-enriched and Luminal B) BC subgroup versus HER2-negative BC subgroup (Luminal A and basal) (*Figure 34C*), as published by Fernández-Nogueira *et al.* (104). The analysis of mRNA expression in a BC cell line database (*Figure 57A*), and from our panel of BC cell lines (*Figure 57C*) also sustained the results. In addition, *STX1A* analysis at protein level confirmed the same tendency, where HER2-positive BC cells have higher expression of *STX1A* (*Figure 62A and Figure 62B*).

Differential expression of other SNAREs, partners of *STX1A*, is detected between HER2-positive and HER2-negative BC subtypes (*Annex table 1*). *STX3*, *STX6*, *VAMP-2*, *VAMP-4*, *SYT1*, *MUNC18-1*, *STXBP2* and *MUNC13*, as *STX1A*, are overexpressed in HER2-positive BC tumours, while *SNAP-23*, *SNAP-25*, *VAMP-1* and *MUNC18-1* are overexpressed in HER2-negative

tumours. However, although the differences between BC subtypes are statistically significant, they should be treated as merely descriptive, considering that the mean values are very similar, in some cases, between both subtypes, and the significance could be influenced by the high number of tumours in each group. Further analyses stratified BC tumours considering *STX1A* expression into BC tumours with *STX1A*^{HIGH} and *STX1A*^{LOW} mRNA expression groups (*Annex table 1*). This classification highlights possible relationships between *STX1A* and other SNARE genes. *STX3*, *SNAP-25* and *MUNC18-1* are overexpressed in *STX1A*^{HIGH} BC tumours while *SNAP-23* and *VAMP-4* are overexpressed in *STX1A*^{LOW} BC tumours. More in detail, overexpression of *STX2* and *VAMP-1* was detected in *STX1A*^{HIGH} HER2-positive in comparison to *STX1A*^{LOW} HER2-positive BC tumours (*Annex table 2*). Overexpression of *VAMP-2* and *SYT1* is detected in HER2-positive *STX1A*^{LOW} BC tumours. On the other hand, *STX6*, *STX17*, *CPLX1*, *STXBP2* and *MUNC13* are overexpressed in *STX1A*^{HIGH} HER2-negative tumours and *SYT1* is overexpressed in *STX1A*^{LOW} HER2-negative BC tumours (*Annex table 3*). Even though, as previously mentioned, in some cases even if there is a significant difference, the mean is very similar. This data can lead to the conclusion that *STX1A* SNARE partners could be diverse depending on the BC subgroups, although the meaning and/ or relevance of these correlations still remains to be elucidated.

After considering possible interactions between SNAREs in BC cells, a correlation and relationship map was built, just considering SNARE expression correlation between pairs of SNARE and EGFR/HER family of receptors genes (*Figure 60 and Figure 61*). This map, given the impossibility of taking into consideration the high number of interactions found in the BC patient databases, is built considering the expression values from BC cells database and the expression of SNARE proteins in the BC cell lines available in our lab. Focusing on *STX1A* first, it has a direct expression correlation with *HER2* and *STX6* in the BC cells database, and with *STX2* in our BC cell lines (*Figure 60 and Figure 61, respectively*). It seems difficult for *STX1A* to have a direct interaction with *STX2* or *STX6*, but some articles state that *STX6* could be part of the same SNARE interactome as *STX1A* (255), meaning that even though they do not directly interact, their expression could be interdependent. There is no information regarding *STX1A*-*STX2* interaction but an article describes that *STX2* could mimic *STX1A* function by binding to granuphilin when *STX1A* is not present in β -cells (256). This fact makes it feasible that in BC cells *STX1A* interacts, possibly, indirectly with other syntaxins. Finally, it is also seen that not only *STX1A*, but also the mRNA expression of other SNARE genes correlates positively or negatively with the expression of some members of the EGFR/HER family of receptors. It is not the first time that this relationship is described. For example, in BC *VAMP-8* expression is

regulated by HER2 (257). Also, *VAMP-2-NRG* fusion gene is seen to activate HER2 and HER3 heterodimer in non-small cell lung adenocarcinoma (258) and an interaction between STX1A and HER3 has been predicted in non-small cell lung cancer (259). To summarize all the information gathered about correlations found in the analysis of BC cells database and in the expression analysis of the lab cells and to avoid possible meaningless apparent results, only correlations that are present in both analyses considered to be further discussed. By doing this, the triple correlation among *STX6-STX17-STXBP2* stands among any other one, *STXBP2* positively correlating with *CPLX1*, as well. Besides, *HER2* also correlates directly with *STX3* and indirectly with *STX2* (Figure 107). It is worth mentioning that this map could have been improved if more bioinformatic resources and knowledge would have been available, but at least it is useful to illustrate an idea of possible relationship among SNARE genes between themselves or with the EGFR/HER family of receptors.

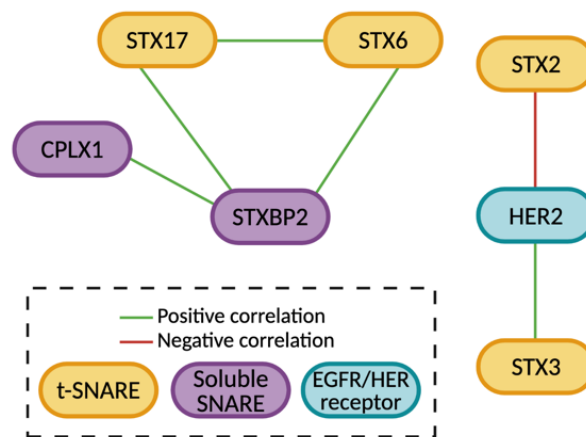


Figure 107 – Correlation and relationships among SNARE proteins and EGFR/HER family of receptors. Graphical representation of positive and negative relationship among SNARE and EGFR/HER family of receptors that are common between BC cells databases (Figure 60) and BC cells from our lab (Figure 61).

These data are merely descriptive, considering that differences between subgroups are not adding any clinical relevance to the patients. Clinically, what is more interesting is the possible prognostic value that these SNARE proteins could have. Kaplan-Meier analyses of the neurogenes in all METABRIC BC subtypes revealed promising biomarkers able to predict patient overall survival. In BC, as in glioblastoma (225) or in undifferentiated carcinoma of the colon and rectum (226), high expression of STX1A correlates with a worse overall survival. This same correlation is seen with the analysis of all BC tumours (Figure 35C and Figure 36B) or separately analysing its expression in HER2-positive (Figure 40A) or HER2-negative BC subgroups (Figure 45F). These results corroborate the ones published by Fernández-Nogueira *et al.* (104) and also add the prognostic value of STX1A for the HER2-negative subgroup. This

data is supported with the analysis of STX1A mRNA expression along tumour stages in BC tumours. High grade tumours have higher STX1A expression, in all BC tumour types (*Figure 35A*) and in HER2-negative BC subgroup specifically (*Figure 45B*), as it is seen in bladder cancer (140). Other bad prognosis markers, such as the number of mutations per tumour or the Nottingham prognostic value, are increased in tumours with high STX1A levels (*Annex figure 2A - Annex figure 2D and Figure 45B-Figure 45E*).

We had the opportunity to collaborate with otorhinolaryngologists from Hospital de la Santa Creu i Sant Pau de Barcelona which had access to tumour samples and clinical history from two different HNSCC patient cohorts. Data analysis detected that patients with *STX1A*^{HIGH} tumours have a poorer overall survival (*Figure 53B*), the same being detected in TCGA HNSCC patient database (*Figure 54E*). Moreover, high levels of *STX1A* result in a shorter recurrence free survival period (*Figure 53C*). Altogether, these results confirmed the fact that *STX1A* is a marker of bad prognosis in breast and head and neck cancer.

However, not only *STX1A* has been linked to poor prognosis in cancer patients. This thesis provides evidence for other SNAREs being linked to patient prognosis as well. Considering all BC subtypes, high expression of *STX3* or *STX6* confer a poorer prognosis, while low expression of *SNAP-23*, *VAMP-2* or *CPLX1* is related to a poorer overall survival in BC patients (*Table 35*). *STX3* has been previously described as a bad prognostic factor in BC, confirming our results (102). However, the expression of this syntaxin family member has been recently found down-regulated in lung cancer tumour samples and high expression relates to a better overall survival of lung cancer patients (260). *STX6* is also a marker of poor prognosis in gastric cancer and papillary renal cell carcinoma (261,262), as it is found in BC. Interestingly, *SNAP-23* expression in cervical carcinoma follows the same trend as in BC, low expression of this v-SNARE correlates with poorer clinical markers (263). Nevertheless, in ovarian cancer it is the high expression of *SNAP-23* which correlates with poorer outcomes (89), revealing that the role of *SNAP-23* could be cancer-specific or partner-dependent. Finally, published data of *VAMP-2* regarding overall survival of cancer patients goes against our findings, pointing out that in bladder and lung cancer and in undifferentiated carcinoma of the colon and rectum the high expression of *VAMP-2* correlates with worse overall survival (226,264,265). No information is found regarding *CPLX1* in cancer, our findings being the first to relate that low expression of *CPLX1* is a marker of bad prognosis in BC. However, its homolog *Complexin-2* (*CPLX2*) has already been related to be increased in patients with poor prognosis in lung high

grade neuroendocrine tumours (266) while low expression of *CPLX2* reduce life expectancy in glioma patients (267).

Even though these SNARE genes could be used as independent predictive markers, it was evaluated if the combination of *STX1A* expression with another SNARE gene could increase the predictive value of *STX1A* alone, which has never been done before. Most SNAREs that were not predictive by themselves, when evaluated in combination with *STX1A* expression, reached the significance threshold. However, these proteins have been considered only if they improved the predictive capacity of *STX1A* alone. Overall, the best predictive marker sets are the combination between *STX1A* and *STX1B* (Table 38A), or the inverse relationship of *STX1A* and *VAMP-2* (Table 38B), both able to predict the overall survival in BC patients, but also between HER2-positive and HER2-negative subgroups. Both partners of markers are good prognostic markers, but *STX1A-STX1B* partnership is better to predict overall survival at middle-long term, and *STX1A-VAMP-2* is better for the initial-middle term after diagnosis. Also, *STX1A* together with *CPLX1* is a prognostic marker for all BC patients and HER2-negative BC patients. The final analysis is summarized in Table 38C, in which more putative markers are described.

To summarize this first part, our research confirms *STX1A* as a neurogene able to predict the overall survival of BC and HNSCC patients, whose combination with other SNARE genes can increase its predictive value in BC patients. However, more research is needed to validate these findings and propose them as biomarkers for predicting patient prognosis. In addition, better bioinformatical and statistical analyses are needed to confirm and validate these results, considering that only one patient database was used in this study.

2. STX1A CHARACTERIZATION IN BREAST AND HEAD AND NECK CANCER CELL LINES

The bioinformatical analysis gives important clues about the importance of *STX1A* and other SNARE genes, in breast and head and neck cancer, up to the point to postulate it as a biomarker to predict BC and HNSCC overall survival. However, to deepen in the role of *STX1A* in BC and HNSCC, the validation of the *STX1A* role in *in vitro* and *in vivo* models is required. As it has been previously mentioned BC cell lines follow the same pattern of *STX1A* expression found in BC patient database and published by Fernández-Nogueira *et al.* (104): HER2-positive (HER2-enriched and luminal B) BC cell lines overexpress *STX1A* at mRNA levels (Figure 56D) in comparison to HER2-negative BC (luminal A and basal) cell lines. Regarding HNSCC cell lines,

they also express *STX1A* at mRNA levels, indicating that they are a good model to study *STX1A* role in HNSCC, as well (*Figure 64A*). This is the first time *STX1A* is characterized in BC and HNSCC cell lines, endorsing the lack of information that is present in the literature about the role of this neurogene in BC and HNSCC.

Due to the impossibility to perform *in vitro* and *in vivo* experiments with all available BC cell lines, the BC cell line panel was narrowed to eight cell lines, three HER2-positive (SK-BR-3, MDA-MB-453 and BT-474) two HER2-negative/luminal A BC cell lines (T-47D and ZR-75-1) and three HER2-negative/basal BC cell lines (MDA-MB-468, BT-549 and MDA-MB-231) which follow the same *STX1A* expression trend: it is more expressed in the HER2-positive BC subgroup (*Figure 62A*). Regarding HNSCC cell lines, two were mainly used, FaDu and SCC090 (*Figure 64D*).

The BC cell lines are fully validated by the characterization of other SNARE partners comparing the levels of expression in patients and in the CCLE database (*Figure 58*). As it happens with *STX1A*, there is no literature supporting our characterization, which means that our findings are completely original in the BC field. These results demonstrate that *STX1A* and several SNARE genes are differentially expressed in BC subtypes (*Table 38*). Sometimes, even though statistical differences are found when analysing BC patients, they are not seen in the CCLE database or in our BC cell lines, due to the small number of samples. However, *STX3* and *MUNC13* are overexpressed in the HER2-positive BC subgroup, as a clear tendency is shown in CCLE database and in lab BC. *STX6* is also overexpressed in HER2-positive BC subgroup but not in lab BC cell lines, where it was overexpressed in HER2-negative/luminal A subtype. These are interesting findings that can point out that these three SNARE proteins can be involved in vesicle trafficking in HER2-positive BC subtypes as *STX1A* seems to be. There is no literature relating *MUNC13* and *STX3* or *STX6*, but it is well described that *MUNC13* opens *STX1A* conformation in neurons and other tissues, which can indicate its role in BC (80). Also, considering that *STX3* and *STX6* are overexpressed in this subtype, it can be feasible that they exert a role in vesicle trafficking through the TGN to the plasma membrane in cancer cells, as it is described in Riggs *et al.* (94). It is not the first time *STX3* expression has been checked in BC, despite the lack of a wide characterization between subtypes, since the soluble form of *STX3* is found to be down-regulated in TNBC tumours, indicating that it should be more expressed in HER2-positive, which supports our findings (268).

STX17, *SNAP-23*, *VAMP-1*, *VAMP-2*, *CPLX1* and *MUNC18-1* are found to be overexpressed in luminal A BC subtypes (*Table 38*). Luminal A BC subtypes are characterized, among other aspects, because they are PR and ER positive (183). It can be feasible that these SNARE proteins could display some kind of relationship with ER or PR considering that some articles have described that some SNARE proteins such as *SNAP-25*, *VAMP-1* and *VAMP-2* are modulated by oestrogen in rat brain or in the pituitary gland (269–271). Finally, *SNAP-25*, *VAMP-4*, *SYT1* and *STXBP2* are found to be down-regulated in basal BC subtypes (*Table 38*), and as happened before there is no information regarding the implication of these SNARE proteins in BC. The results are summarized in *Figure 108*.

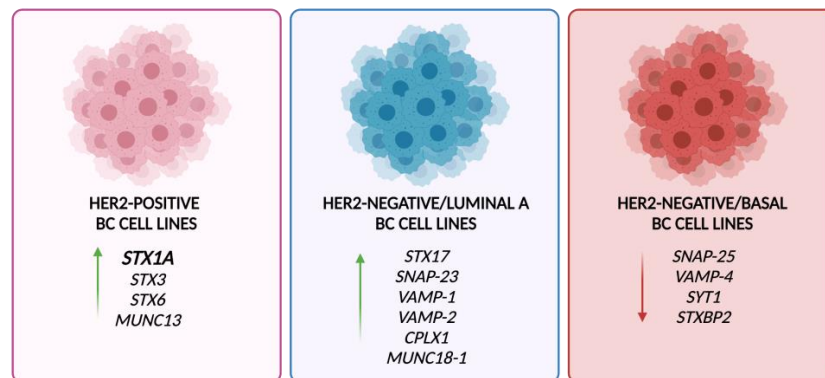


Figure 108 – Differential expression of SNARE genes in BC tumours and cell lines. Schematic representation of the SNARE genes that are upregulated in HER2-positive BC cell lines and HER2-negative/luminal A BC cell lines and the genes that are downregulated in HER2-negative/basal BC cell lines.

3. EPIGENETICALLY MODULATION OF SNARE GENES

Considering the differential expression of SNARE genes among BC subtypes, it was worthwhile to continue the research with the mechanisms that could regulate this differential expression in BC and HNSCC and among BC subgroups. Bearing in mind that the focus was on gene expression, the starting point was the bioinformatical characterization of *STX1A* gene. *STX1A* is a TATA-less gene with several transcription start sites (TSS) with a 204 bp upstream core promoter region (CPR) located at chromosome 7 (232). Analysis of *STX1A* gene in genome browser confirmed what Nakayama *et al.* (66) found experimentally, the promoter region of *STX1A* gene matches with DNase I hypersensitivity clusters and with H3 methylation and acetylation marks (H3K4Me1, H3K4Me3 and H3K27Ac), typical of promoter regions (*Figure 66*). Also, the enhancer regions found experimentally by Nakayama *et al.* (232) are similar to the ones predicted by GeneHancer track. Moreover, in two different articles Nakayama *et al.* also stressed the importance of SP1 transcription factor in promoting *STX1A* transcription

(232,233), which analysis of the ENCODE track also highlighted the binding site of this transcription factor into the promoter region of *STX1A* gene (Figure 66).

STX1A is also found to be transcriptionally regulated by histone acetylation marks, which promote *STX1A* transcription in neural and non-neural cells (232–234). Our findings confirm that inhibition of histone deacetylases promotes *STX1A* transcription in BC cell lines, without differences between BC subtypes (Figure 67A - Figure 67C). HNSCC cells, as BC cells, treated with an unspecific inhibitor of histone deacetylases (TSA) upregulated *STX1A* mRNA expression (Figure 67A). Interestingly, when the binding of SP1 transcription factor to the DNA is impaired, the transcription of *STX1A* in HER2-negative BC cell lines is also impaired, while no effects are seen in HER2-positive BC cell lines (Figure 67A and Figure 67B). These findings point out the importance of SP1 transcription factor in HER2-negative BC cell lines, which can be one possible explanation of the differential expression of *STX1A* between BC subgroups. Nakayama *et al.* also demonstrated that protein kinase A (PKA) regulated *STX1A* expression in non-neural cells (232,233), however our preliminary results seem to indicate that PKA activation results in the repression of *STX1A* expression in HER2-negative BC cell lines (Figure 67C). Recently, an article from the same authors revealed that Yin-Yang 1 (YY1) transcription factor binds to the CPR of *STX1A* in cells that do not express this SNARE gene. After treatment with TSA, *STX1A* are expressed and YY1 is unbound from the CPR (234). Putting all this information together, it becomes interesting to analyse *SP1* and *YY1* expression levels in the different BC subtypes, to determine if a differential expression of these transcription factors among BC subtypes can also be related to *STX1A* expression. In fact, a more definitive approach would be CHIP experiments with different BC cell lines to determine if these transcription factors are bound in *STX1A* CPR regions, and if there are differences between HER2-positive and HER2-negative BC subgroups.

Finally, we describe for the first time the epigenetic regulation of *SNAP-23*, *MUNC18-1*, *VAMP-1*, *MUNC13*, *STX1B* and *STX3* genes (Figure 68A-Figure 68B). As it is found for *STX1A*, these genes are also regulated by histone deacetylases and acetylation marks. In all the cases, when these deacetylase enzymes are inhibited, there is an increase of transcription in these SNARE genes. More controversial is the regulation by the SP1 transcription factor. It seems that only *VAMP-1* is regulated by SP1, and its regulation is the opposite as seen in HER2-negative BC cell lines (Figure 68D). In this case, when SP1 is not bound to the promoter region of *VAMP-1* is when its transcription is promoted. Therefore, SP1 seems a negative regulator of

VAMP-1 transcription. In HNSCC *SNAP-25* and *MUNC18-1* are positively regulated by histone deacetylases, as well (Figure 69A and Figure 69B).

However, more research is needed, since our preliminary results highlight the importance of histone deacetylases in *STX1A* transcriptional regulation in BC and HNSCC cell lines, as in other SNARE genes as well. These findings suggest possible mechanisms that would explain the differential regulation of *STX1A* in BC subgroups: it can be through a differential expression of SP1 binding factor or through a different sensibility to PKA between HER2-positive and HER2-negative BC subgroups. Moreover, it is important to consider the recent finding involving YY1 transcription factor in repressing *STX1A* transcription in HER2-negative BC cell lines (Figure 109).

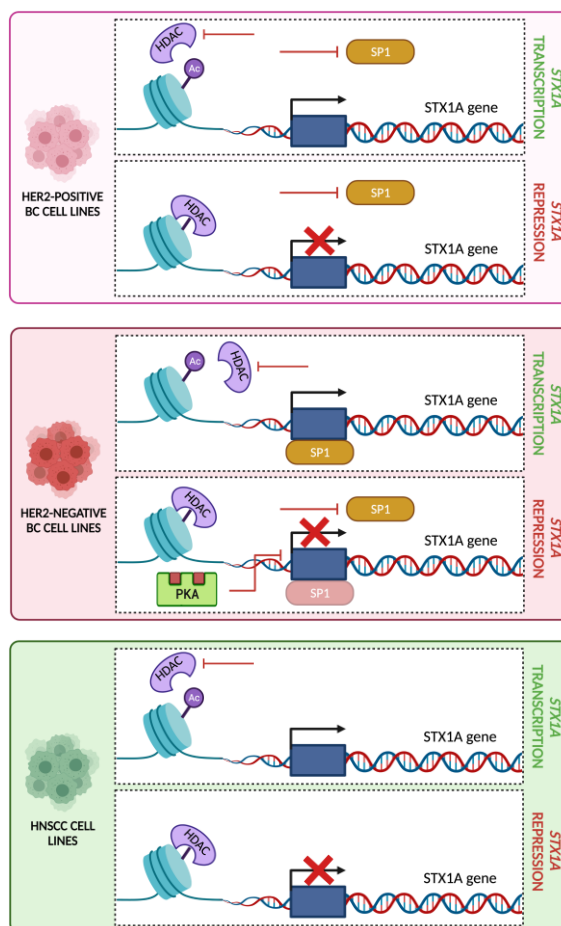


Figure 109 – Schematic representation of *STX1A* epigenetic modulation in BC and HNSCC cell lines. *STX1A* transcription in HER2-positive BC cell lines is regulated by histone acetylation which promotes *STX1A* transcription. If HDAC enzymes remove acetylation marks, *STX1A* transcription is repressed. SP1 does seem to control *STX1A* transcription in this BC subtype. In HER2-negative BC cell lines, acetylation marks are required as in HER2-positive BC cell lines, but binding of SP1 is also necessary. When this transcription factor is not bound to the *STX1A* promoter, there is no *STX1A* transcription. PKA seems to be a *STX1A* transcription repressor in HER2-negative BC subtype, as it could

be YY1 according to the literature (marked in light red because it is not proved experimentally in our model). *STX1A* transcription in HNSCC is controlled by H3 acetylation marks as it is for BC cell lines.

4. STRATEGIES TO INHIBIT STX1A EXPRESSION OR TO IMPAIR ITS FUNCTION

We have also attempted to further understand the role of STX1A and its SNARE partners in both types of cancer. To address this goal, cells with down-regulation of STX1A or with a functionally impaired protein were needed. To this purpose several strategies have been used to down-regulate or prevent STX1A function. The first one was the treatment of BC cells with BoNTs, which cleave specifically SNAP-25 (BoNT A and C) and STX1A (BoNT C). However, no effect of the BoNTs are seen at the protein level (*Figure 71B*), since if the BoNTs approach would have worked two additional bands should have appeared (242,272) that do not show. After some attempts to optimize this inhibition method we moved to another strategy.

Next, a STX1-DN was used to impair STX1A function. The plasmid was kindly provided by Dr. Eduardo Soriano's. The activity of the STX1-DN had been already shown in several articles (84,242). As it has been explained before, its main function is to compete with wild-type STX1 for their natural ligands and SNARE partners but resulting in no final exocytosis (*Figure 71D*). The STX1-DN does not have its N-terminal part (it lacks the Habc domains and the N-peptide) so it does not have the capacity to fuse the vesicles to the cytoplasmic membrane, among other functions in which STX1 is involved (*Figure 71A*) (86,242). It is important to bear in mind for all the following discussion that this dominant negative is not specific for STX1A but for all STX1 forms. In addition, the effects described are not only caused by STX1A lack of function but by the impairment of the formation of the SNARE complex, meaning that the function of other SNARE complex proteins could be affected as well (84,242).

The abovementioned strategy is really useful to impair STX1 and other SNARE functions but is not specific for STX1A. To further elucidate if the effects seen in STX1-DN cells are specific for STX1A, we looked for different strategies to specific down-regulate STX1A. After trying different siRNA transfections, this strategy resulted in a short-time down-regulation not fully reliable, since not all the experiments achieved a 50% down-regulation (*Figure 72C*). Another option was infecting BC cells with shRNA STX1A lentiviral particles (*Figure 72D and Figure 72E*). This strategy worked very well for the first four weeks after transfection, however even though the cells were kept under antibiotic selection pressure, no STX1A down-regulation was found anymore. After looking at the literature and scientific forums what could have been happening, some researchers found that the CMV promoter of the shRNA could be

methyated and therefore the shRNA expression would be inhibited (273). Knowing the limitations of this down-regulation techniques enabled us to perform experiments in this time frame, but longer-term experimental planning was complex. This realization made us move forward to yet another inhibition technique.

Finally, with the collaboration of Dr. Paloma Bragado, from UCM, Faculty of pharmacy, Madrid, the CRISPR-Cas9 technology was used to inhibit STX1A expression in our BC and HNSCC cells. After infection of lentiviral particles bearing gRNA complementary to a specific part of exon 2 or exon 6 of STX1A gene, and after following the subcloning protocol, no inhibition or down-regulation of STX1A was detected (*Figure 72B*). After several attempts and with different cell lines, the same result was obtained. Maybe the deletion of part of exon 2 or exon 6 resulted in no impairment of the STX1A mRNA and as a consequence the protein was fully translated. Also, there could be problems in the Cas9/gRNA abundance or in Cas9 PAM recognition of the genomic sequence target of gRNA (274). Considering all these facts and the time granted to present this thesis, it was decided not to continue with CRISPR/Cas9 experiments and focus our experimental efforts on STX1-DN and shRNA STX1A cells.

5. STX1A ACTS AS A GROWTH REPRESSOR IN BREAST AND HEAD AND NECK CANCER

SNARE proteins have been linked to tumour growth. SNAP-23, for example, represses tumour growth in cervical cancer by regulating the cell cycle (263), and STX3 plays an opposite role in BC through the activation of the PI3K/AKT/mTOR signalling pathway (102). Moreover, there is already one published study proving that STX1A is involved in tumour growth, promoting proliferation (86). Our bioinformatical analyses have revealed that *STX1A^{high}* and *HER2^{high}* HER2-enriched tumours and *STX1A^{high}* HER2-negative tumours have an overactivation of PI3K/AKT/mTOR and G₂/M checkpoint signalling pathways (*Figure 44A and Figure 44B; Figure 49C and Figure 49D*), among others. Due to these findings, it was hypothesized that probably STX1A is regulating BC and also HNSCC cancer cell proliferation as well. Proliferation assays in BC and HNSCC cells show that functionally impaired STX1 cells are more proliferative than their controls (*Figure 75A-Figure 75F*), corroborating the bioinformatic analysis, but contradictory to the described STX1A role in glioblastoma, where cells without STX1A proliferate less (86). STX1A also seems to be involved in BC and HNSCC clonogenic capacity, since it suppresses the capacity to initiate colonies (*Figure 77A-Figure 77G*), as its partner SNAP-23 does in cervical cancer (263). These results are further confirmed with mice and CAM *in vivo* experiments, where BC tumours with STX1A down-regulated are slightly bigger (in the HER2-positive MDA-MB-453 and BT-474 BC tumours) (*Figure 99C and Figure 100C*,

respectively) or significantly bigger in the HER2-negative MDA-MB-231 tumours (*Figure 101C*). Furthermore, the CAM models for HNSCC tumours also confirmed the *in vitro* data, since HNSCC tumours with STX1-DN are bigger than their controls (*Figure 103B*). In addition, the molecular analysis of the tumours revealed an up-regulation of the proliferative markers Ki67 (*Figure 100D and Figure 102C*) or *CCND1* (*Figure 103C*) in STX1A down-regulated or functionally-impaired tumours, indicative of the growth repressing activity of STX1A in our BC and HNSCC models.

Since phenotypically STX1A seems to be a growth suppressor in our BC and HNSCC models, we tried to further elucidate its mechanistic role. The cell cycle analysis of BC and HNSCC cells with non-functional STX1 revealed that there is an increase of cells at phases S and G₂/M of the cell cycle together with an increased expression of *CCND1* (*Figure 76*). It is not the first time that a SNARE protein has been linked to cell cycle regulation, SNAP-23 has also been proposed as a cell cycle repressor in cervical cancer, by inhibiting cyclin B1 and promoting p21 transcription (263).

Considering that *CCND1* modulates the transition from G₁ to S phase, therefore regulating the cell cycle progression (275), it was further investigated how the cells with non-functional STX1A could control the transcription of this cyclin. AKT and ERK signalling pathways are known to promote cancer cell proliferation at different levels, one of them, by the activation of this cyclin (276). Interestingly, in HER2-negative BC cell lines and in HER2-positive MDA-MB-453 BC cell line AKT is overactivated; in HER2-positive BC cell lines and in BT-549 HER2-negative/basal BC cell line ERK is overactivated (*Figure 74*). Our data could indicate that these signalling pathways could be inducing *CCND1* transcription. However, in HNSCC cell lines and in SK-BR-3 (HER2-positive BC cell line) AKT is down-regulated; in MDA-MB-231 (HER2-negative/basal BC cell line) ERK signalling is down-regulated as well. These data could indicate that proliferation through *CCND1* activation can be driven by AKT and/or ERK signalling pathways in a cancer-specific manner. Furthermore, it must be noticed that other signalling pathways such as β -catenin or MYC can be also altered in these STX1 impaired cells, leading to *CCND1* transcription, as well (277,278). In addition, the differential expression of receptors at the plasma membrane could play an important role on the impact of the impairment of STX1A may cause (*Figure 79*). Even though this issue will be further discussed in the next section, it is important to consider that nuclear EGFR can interact with the promoter of the *CCND1* gene, activating its transcription. Therefore, given that some BC cells with STX1-DN overexpressed EGFR at the plasma membrane, this could lead to the activation and the

transcription of the *CCND1* gene (279). Besides, some articles have described that endosomal EGFR signalling is able to promote survival pathways which could lead to *CCND1* activation (280,281).

Summarizing, it is demonstrated for the first time that STX1A acts as a tumour growth suppressor in breast and head and neck cancers. It inhibits cell cycle progression through the repression of *CCND1* transcription. However, more research is needed to clarify how STX1A controls *CCND1* transcription, being either through AKT and/or ERK activation, differential plasma membrane receptors profile or by any other altered signalling pathways.

6. SYNTAXIN-1A CONTROLS EGFR/HER FAMILY OF RECEPTORS TRAFFICKING INTO THE PLASMA MEMBRANE

Cancer cells, as well as normal cells, respond to signals from their microenvironment through the activation of intracellular signalling that will end up triggering a biological response. Part of this microenvironment response is mediated by plasma membrane receptors which are able to bind to external factors and transfer signals intracellularly (282). A particularly interesting group of these membrane receptors, involved in intracellular signalling and cancer progression, is the EGFR/HER2 family of receptors, which are found to be overexpressed in some tumours, mainly HER2 receptor in BC and EGFR in head and neck tumours (143,208). Besides the fact that STX1A is overexpressed in HER2-positive BC tumours (*Figure 34C*) (104), it has also been proved that there is a direct positive association between the expression of *STX1A* and different members of the EGFR/HER family of receptors in HER2-positive and HER-negative BC tumours (*Annex table 2 and Annex table 3*).

In some cases, trafficking of EGFR/HER family of receptors into/from the plasma membrane has been described to be driven by SNARE proteins. It is the case of STX9, which binds to EGFR in skin hair follicle epithelium promoting its internalization (283). Other members of the syntaxin family such as STX4 or STX12, and other SNARE family members such as MUNC18c or SNAP-23 have also been linked to EGFR trafficking in the formation of MDA-MB-231 BC invadopodia (284,285). Focusing on STX1A, it has been proved that isolated STX1A is not enough to trigger membrane granule or vesicle fusion. It is necessary a STX1A cluster and also the initial interaction with MUNC18-1 to induce the SNARE complex formation by the latter association with SNAP-25 and MUNC13 and the consequent docking of the granule or vesicle in pancreatic β -cells (107,108). EGF stimulation of our BC and HNSCC cancer cells induces STX1A clustering into the plasma membrane (*Figure 81A-Figure 81F*) and *STX1A*

transcription, whereas inhibition of EGFR and HER2 receptors by lapatinib suppresses *STX1A* transcription in HER2-negative BC cell lines (*Figure 82A*), confirming the functional relationship between *STX1A* and EGFR/HER family of receptors and reinforcing the idea of the regulatory role of *STX1A* on EGFR/HER2 signalling.

EGF also induces EGFR clustering into the cell membrane (286,287), and as a consequence also HER2 clustering, considering that the formation of homodimers or heterodimers is needed to induce intracellular signalling (168). Normally, EGFR and HER2 clustering induce coupling of the intracellular signalling proteins, such as AKT, in the intracellular part of the receptors tyrosine kinase receptors (168). Moreover, it is worth mentioning that these receptors are usually found in lipid rafts, facilitating their dimerization. In the literature it has been described that this dimerization, and as a consequence the coupling of the intracellular proteins, is stabilized by flotillin-1, which at the same time promotes the intracellular signalling transmission (286,288,289). SNARE proteins, in particular *STX1A*, have been described to be located in lipids rafts co-localizing with flotillin-1 (169), indicating that *STX1A* and EGFR-HER2 heterodimers can be found in the same regions. Taken all together, it seems that if *STX1A* responds to EGF stimulation as EGFR/HER2 receptors do, clustering of *STX1A* could be involved in EGFR/HER2 localization or in triggering their intracellular signalling. From our immunoprecipitation assays, HER2 does not seem to directly interact with *STX1A*, since no co-immunoprecipitation of *STX1A* is detected when HER2 is pulled-down in the control situation or in MDA-MB-453 HER2-positive BC cells stimulated with EGF (*Figure 82C-Figure 82D*). However, it cannot be ruled out a possible interaction with EGFR or even the possibility that *STX1A* influences the presence of EGFR/HER2 family of receptors at the plasma membrane, by controlling the fusion of the vesicles that transport these receptors.

Overall, our results confirm that *STX1A* transcription and clustering is induced under EGF stimulation, a process in which other proteins of the SNARE complex could be involved. Taking into consideration that it has been described that *STX1A*, EGFR and HER2 receptors are localized in lipid raft domains together with flotillin-1, *STX1A* could be involved in EGFR and HER2 heterodimerization, trafficking of these receptors into/from the plasma membrane or even in triggering their signalling (*Figure 110*).

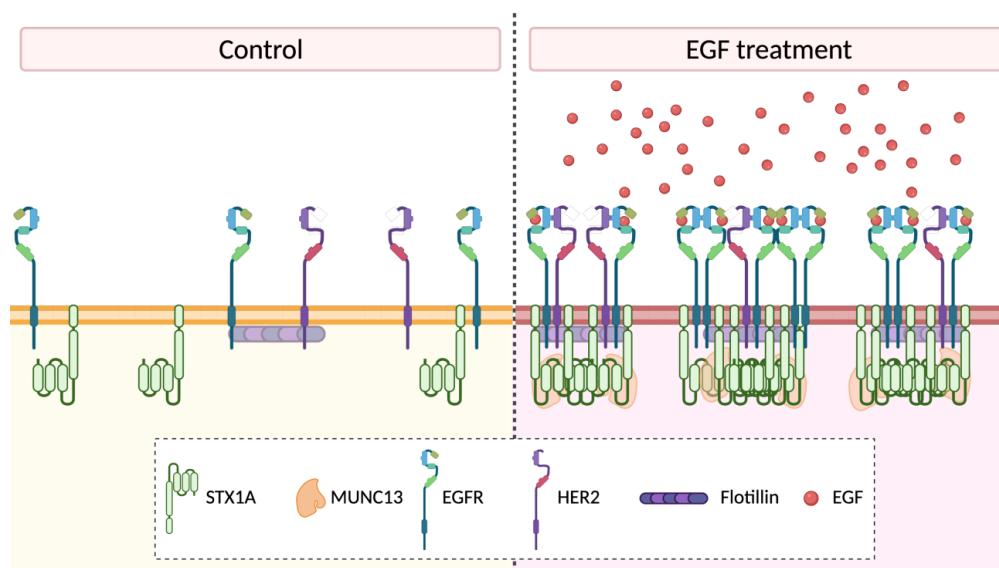


Figure 110 – Proposed model of EGF-induced STX1A clustering in BC and HNSCC plasma membranes. EGF induces STX1A and also HER2 and EGF clustering in the plasma membrane. Flotillin and MUNC13 (light coloured), as well as other SNARE proteins, could be involved in this process, which is not proved experimentally.

HER2 receptor expression is mainly restricted to the plasma membrane where orchestrates the oncogenic intracellular signalling, while little is found in intracellular compartments, usually in early endosomes (168–170,290). However, HER2 trafficking is still a process poorly understood. Several hypotheses are being considered due to discrepant results, since some studies defend that HER2 is resistant to internalization (291,292) while others support that HER2 suffers a rapid recycling in the early endosomes and is returned back to the plasma membrane (293–295). Our studies demonstrate that STX1A inhibition is able to downregulate HER2 expression in HER2-positive BC and in HNSCC cell lines in vitro and in vivo (*Figure 79A-Figure 79F*). Moreover, our preliminary data show that cells expressing the STX1-DN have an accumulation of intracellular vesicles (*Figure 80A-Figure 80E*). These findings do not support either HER2 trafficking hypotheses, since they could contribute to both. On one side, STX1A could be contributing to the stabilization of HER2 into the plasma membrane by inhibiting its endocytosis. As a consequence of STX1A function impairment, STX1A would thus not be inhibiting the endocytic signal, with flotillin-1 playing an important role, as we had hypothesised before. In consequence, STX1A would be regulating flotillin-1 HER2 mediated-endocytosis, and the absence of STX1A could trigger the endocytic mechanism, resulting in the increase of the intracellular vesicles found in our experiments with STX1-DN cells. On the other side, however, it could also be that HER2 receptors have a rapid recycling cycle in which STX1A is involved by promoting the fusion of HER2-containing vesicles to the plasma membrane, closing the recycling process. In this scenario, absence or impairment of function of STX1A

would result in the impossibility to fuse the HER2-containing vesicles, which would then accumulate intracellularly without fusing with the plasma membrane. This would consequently reduce HER2 levels at the plasma membrane, as we have also proved. In view of the results obtained, it is clear that STX1A is involved in HER2 turnover, however more research is needed to clarify how this SNARE protein is involved in such process.

Moreover, a possible compensatory response is seen in HER2-positive BC and HNSCC cells: while HER2 is down-regulated by STX1A-DN, plasma membrane EGFR and *HER3* mRNA expression are increased (*Figure 79A-Figure 79F and Figure 78C*). It is not the first time that a compensatory mechanism is seen regarding EGFR/HER family of receptors, since it has been described that down-regulation of HER2 in glioblastoma cell lines resulted in an increase of *EGFR* mRNA expression, and EGFR down-regulation results in an increase of HER2 protein and mRNA expression (296). In BC cell lines, treatment with lapatinib, which down-regulates both EGFR and HER2 activity, results in an up-regulation of HER3 receptor (297), confirming our findings.

Interestingly, in HER2-negative BC cell lines EGFR is the one down-regulated at the plasma membrane (*Figure 79C and Figure 79D*). HER2 receptor was not checked at the plasma membrane, considering that these cells do not overexpress it at relevant levels, however no conclusive result is found analysing *HER2* mRNA levels, since one HER2-negative/basal BC cell line down-regulated (BT-549) and other up-regulated it (MDA-MB-231) (*Figure 78B*). These findings may reflect that the regulation exerted by STX1A over the EGFR/HER family of receptors is subtype specific in BC cell lines. The expression of EGFR into the plasma membrane is also reflected at their activation levels (*Figure 83*), under stimulation of EGF HER2-negative/basal BC cell lines and SCC090 that express STX1-DN do not activate EGFR at the same level than MOCK cells, likely as a result of the consequent EGFR down-regulation at the plasma membrane. ERK signalling followed the same trend that EGFR activation. Surprisingly, STX1-DN cells overactivated the AKT pathway under EGF stimulation, indicating that this signalling pathway is being stimulated by another tyrosine kinase distinct from EGFR. EGF not only induces EGFR activation but it can also activate other receptors such as MET by EGFR-mediated transactivation (122). As a result, MET activation can compensate EGFR inhibition by activating AKT (298,299), providing a feasible explanation by which AKT could be overactivated even though EGFR is under-expressed in the plasma membrane of STX1-DN cells.

To summarize, our findings prove that STX1A can modulate EGFR/HER family of receptors trafficking to/from the plasma membrane in BC and HNSCC cell lines. Probably, because of this

modulation, there is a change in EGFR activation and AKT and ERK signalling pathways which need further research to fully elucidate possible compensatory mechanisms with clinical relevance potential.

7. SYNTAXIN-1A PROMOTES LAPATINIB, AN EGFR/HER2 TARGETED THERAPY, RESISTANCE IN BREAST CANCER

As previously mentioned, 25-30% of BC subtypes overexpress HER2 and 90% of HNSCC tumours overexpress EGFR (143,208), suggesting that these tumour types may be dependent on these TK receptors. This belief induced researchers to develop several EGFR/HER2 targeted therapies. More efforts to develop anti-EGFR/HER2 targeted therapies have been assayed against BC than against HNSCC, and some of them have been approved, such as trastuzumab or lapatinib, which have dramatically improved the outcome of HER2-positive BC patients (143,179). Interestingly, even though HNSCC tumours overexpress EGFR and several anti-EGFR therapies have been developed and tested, they only resulted in a slight overall survival improvement. The monoclonal antibody cetuximab is normally used as a radiation sensitizer, alone or in combination with chemotherapy, for the treatment of patients with recurrent or metastatic disease (207,208). Unfortunately, if the tumour is not intrinsically resistant to these therapies, it ends up developing an adaptive resistance to the specific agent due to the selective pressure. This fact makes extremely important to understand the mechanisms underlying this resistance and to develop strategies to sensitize tumours.

Considering that STX1A could be modulating EGFR/HER2 membrane trafficking and abundance, it was thought that this differential expression could have an impact in lapatinib treatment, a TKI of both receptors. Our preliminary results on lapatinib cytotoxicity in HER2-positive BC cell lines showed no differences in sensitivity (*Figure 85A and Figure 85B*), measured as IC₅₀, but lapatinib induced an increase of cells arrested at the G₁ phase of the cell cycle in STX1-DN cells (*Figure 86A*), indicating that cells with intact STX1 are more resistant to lapatinib action. *In vivo* results confirm that MDA-MB-453 tumours with non-functional STX1 are more sensitive to lapatinib, showing a marked reduction in tumour volume (*Figure 104B*).

The *in vitro* analysis of the differential activation or deactivation of signalling pathways reveal that cells that are STX1A deficient (with STX1A either down-regulated or functionally impaired) have a delayed lapatinib response (*Figure 84A and Figure 84B*). While control cells treated with lapatinib downregulate AKT and ERK activity after 2 hours treatment, HER2-positive BC cell lines with STX1 impaired do not show a decrease in AKT or ERK activity. A

possible explanation could be based on the previously described down-regulation of HER2 receptors at the plasma membrane of non-functional STX1 cells, which would difficult the interaction of lapatinib with its target. After a long-term treatment, such as in the *in vivo* CAM assay, a decrease of AKT activation is found (*Figure 105I*), indicating that the down-regulation of this pro-survival pathway could lead to the increase of lapatinib sensitivity to HER2-positive BC tumours. Although not demonstrated experimentally, a possible hypothesis could be that even though there is a down-regulation of HER2 expression in the plasma membrane in cells with STX1A impaired, HER2 is still accumulated in endosomes waiting to reach the plasma membrane. As it happens with EGFR, which signals even through receptors that are located in the endosomes (280,281), HER2 could still be signalling down-stream. If this is the case, a higher concentration of receptors would be located into the endosomes, being more accessible for lapatinib, and therefore the TKI would be more efficient.

Regarding EGFR, it is detected a higher expression of EGFR at the plasma membrane in HER2-positive BC cell lines with non-functional STX1 (*Figure 79A and Figure 79B*), indicating that its higher expression could lead to an increase of lapatinib resistance, however our findings reveal that the cells are more sensitive *in vitro*. Zhang *et al.* already proved that inhibition of EGFR by specific siRNA in BT-474 and SK-BR-3 (HER2-positive) BC cells resulted in no difference in lapatinib sensitivity (300), following the same trend as our findings and indicating that even though in our model EGFR is overexpressed, it is not really involved in HER2-positive BC lapatinib sensitivity. Noteworthy, *EGFR* mRNA is downregulated after lapatinib treatment in MDA-MB-453 STX1-DN tumours (*Figure 105E*), indicating that lapatinib is able to reduce the overexpression of EGFR to the same levels as MOCK tumours.

Overall, these results confirm that STX1A is involved in lapatinib sensitivity in HER2-positive BC tumours. The resistance mechanism by which STX1A is involved is still preliminarily depicted, but it seems that is related to the modulation of the trafficking and presence of EGFR/HER family of receptors into the plasma membrane of the cell.

8. SYNTAXIN-1A PROMOTES LAPATINIB RESISTANCE IN HEAD AND NECK CANCER

It has been proved that STX1 increases the resistance to lapatinib in HER2-positive BC cells *in vitro* and *in vivo*. Then, considering that lapatinib is targeting both EGFR and HER2 and that HNSCC tumours usually overexpress EGFR, it was worth wondering if STX1A could be involved in HNSCC sensitivity to lapatinib as well, after being confirmed that SCC090 HNSCC cells with STX1-DN down-regulate HER2 receptors (*Figure 79F*).

Surprisingly, the results are more significant than in BC. The cytotoxic assay of HNSCC cell lines reveal that the IC₅₀ for lapatinib in cells that do not have a functional STX1 is three times lower than their MOCK partners (*Figure 85E and Figure 85F*). Also, as it happens in HER2-positive BC cells, HNSCC STX1-DN cells treated with lapatinib are arrested at the G₁ phase in higher percentage than MOCK cells treated with the drug (*Figure 86A*), confirming that STX1 is involved in decreasing the sensitivity of HNSCC cells to lapatinib. These results are further confirmed by an *in vivo* CAM assay, in which FaDu MOCK tumours do not respond to lapatinib treatment, while tumours with STX1 functionally impaired halve their growth (*Figure 106B*), clearly indicating that tumours that do not have a functional STX1A are more sensitive to lapatinib treatment. The obtained results confirm that STX1 inhibition sensitize BC and HNSCC cells to lapatinib treatment. After these somehow unexpected results it was also tried to decipher the mechanisms by which HNSCC cells with STX1-DN were more sensitive to this TKI.

As in BC, the analysis of AKT and ERK activation in STX1-DN HNSCC cells after 2 hours of lapatinib treatment did not reveal any significant differences (*Figure 84C and Figure 84D*). AKT activation is slightly modified in STX1-DN cells, while MOCK cells down-regulate AKT activation, in STX1-DN cells its downregulation is slightly lower indicating, as found in BC, that lapatinib-induced response is delayed. On the contrary, ERK signalling pathway is upregulated in MOCK cells treated with lapatinib and even more overactivation is detected in STX1-DN cells, but this effect is only detected in cells resistant to lapatinib (301). In our model, ERK may be activated for other reasons, ranging from cell stress-related proteins to proteins involved in autophagy, such an increase of LC3-II (302,303). To further analyse this response, it is checked the role of apoptosis in this cell death by Annexin V staining. Surprisingly, only a 10% of cell death was detected by Annexin V and IP staining in cells with STX1 function impaired (*Figure 87C and Figure 87D*), while around 40% of the cells were dying at the same dose in the cytotoxic assay (*Figure 85E and Figure 85F*). This result, together with an increase of cell debris in STX1-DN cells treated with lapatinib (*Figure 87A and Figure 87B*), made us suspect that lapatinib was not solely triggering the apoptotic pathway. Literature describes that lapatinib can induce death by the apoptotic pathway, but can also do it by increasing autophagy (304,305). LC3 is a cytosolic protein used as a marker to monitor this cell process. When autophagy is triggered in a cell, LC3-I is lipid-conjugated with phosphatidylethanolamine (PE) and moved to isolated membranes, autophagosomes and, to a minor extent, autolysosomes. The LC3 lipidated form is designed as LC3-II and is a marker of autophagy (306). After 24 and 48 hours of lapatinib treatment in HNSCC cells with non-functional STX1 there is an increase of LC3-II/LC3-I ratio (*Figure 88A and Figure 88B*), indicating that these cells are accumulating autophagosomes,

explaining why there are more debris and more dead cells in STX1-DN HNSCC cells treated with lapatinib. However, it is important to be careful with the interpretation of the LC3-II results, because an increase of this autophagic marker could indicate that there is an upregulation of the autophagosome formation, but also that there is a blockage of the autophagic degradation (306). To correctly interpret our results, it would be necessary to use lysosome protease inhibitors. In any case, this increase in LC3-II could explain the overactivation of ERK pathway commented before (303). Moreover, it is important to consider that an increase in autophagosome content can also induce cell death (304,305) and fits our results with lapatinib treatment. The link between STX1A and autophagy is not studied, but worth exploring. Several articles proved the relationship of other syntaxins to autophagy. The most studied is STX17 which is shown to be involved in the fusion of the autophagosome with the lysosome via interaction with other SNAREs such as SNAP-29 and the lysosomal SNARE VAMP-8 (307,308). Also STX16 has been involved in lysosome and autophagosome fusion with a redundant role for STX17 (309).

The results demonstrate that STX1 is involved in HNSCC lapatinib sensitivity, as well as in BC. Our findings suggest that STX1 is controlling the distribution of EGFR/HER2 receptors at the plasma membrane and, therefore the accessibility of lapatinib to its targets. Lapatinib would have more difficulties to interact with HER2 receptors which accumulate in vesicles/endosomes. As a consequence, AKT downregulation would be delayed in comparison to MOCK cells, but after a longer time, it would increase due to the higher sensitization of STX1-DN cells to lapatinib. Also, an increase in ERK signalling due to autophagy induction, proved by the increase of LC3-II, would have been taking place under lapatinib treatment (*Figure 111*).

It is demonstrated that lapatinib is more effective in HNSCC tumours that have STX1A functionally impaired, making it feasible to be used it as an adjuvant treatment to HNSCC patients with low levels of STX1A, which should be more sensitive. However, lapatinib is not currently used as an HNSCC standard treatment. Some clinical studies already investigated its effect and did not find any significant differences between patients treated with lapatinib or the approved standard therapy (310,311). However, these results could be improved by a stratification of the HNSCC patients according to a gene-signature. Unfortunately, this has not been done yet. A possible improvement could be stratifying patients according to STX1A levels. As it derives from our results, patients with low STX1A levels could be more sensitive to lapatinib and the treatment with the TKI could be beneficial for their outcome.

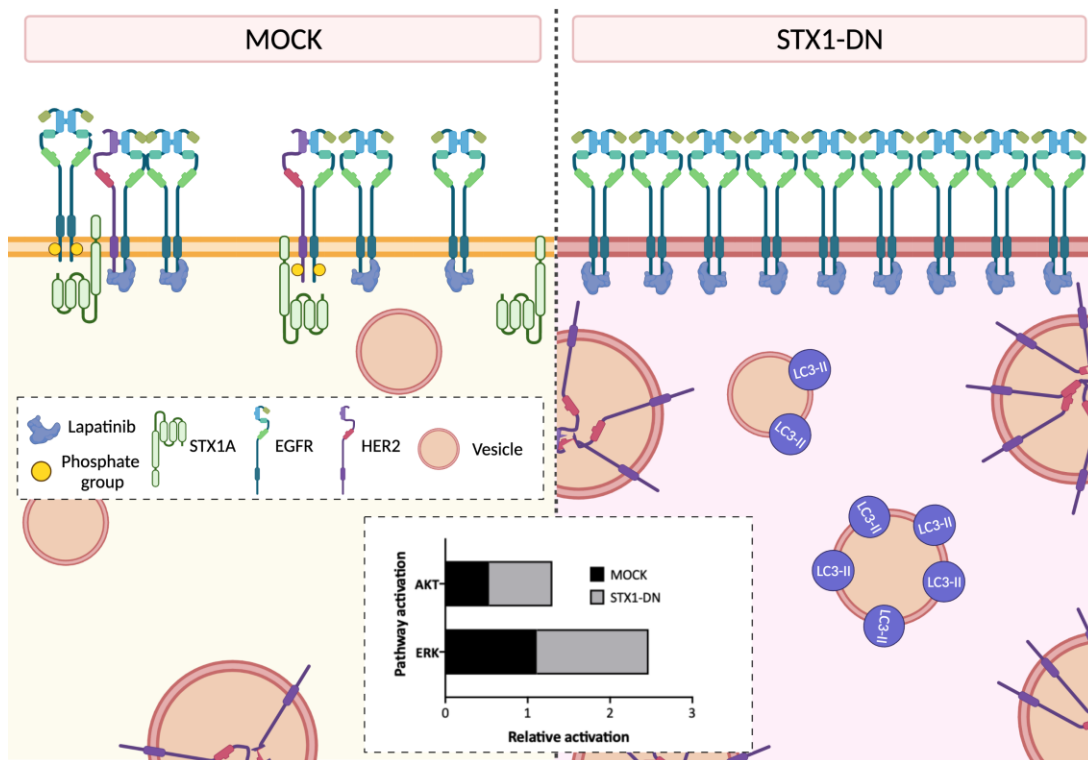


Figure 111 – STX1A promotes lapatinib resistance in HER2-positive BC and in HNSCC cell lines. Schematic representation of STX1 involvement in MOCK (left) and STX1-DN (right) situations when cells are treated with lapatinib. On the middle box, relative activation of AKT and ERK proteins. Cells with STX1A function impaired have more EGFR into the plasma membrane, while HER2 receptor are found in intracellular vesicles. In addition, there is an increase of AKT and ERK activation and an overactivation of LC3-II production (only checked in HNSCC cells).

9. SYNTAXIN-1A PROMOTES CISPLATIN AND ADRIAMYCIN RESISTANCE IN HEAD AND NECK CANCER

Considering that our findings on HNSCC response to lapatinib had a difficult clinical application since it is not an approved treatment, we also focused on other drugs that are currently used to treat HNSCC patients, such as adriamycin and cisplatin. Adriamycin is an anthracycline that intercalates into the DNA helix causing oxidative damage and inducing the formation of covalent topoisomerase-DNA complexes, leading the cell to enter into apoptosis. Our cytotoxicity assays showed that treating STX1-DN HNSCC cell lines with adriamycin results in an increase of sensitivity to the drug (*Figure 89A*). These are preliminary results that need further investigation, but it points out that STX1 could be involved also in adriamycin sensitivity. One hypothesis could be that STX1 is influencing adriamycin sensitivity by regulating the expression in the plasma membrane of the P-glycoprotein (P-gp) protein responsible of removing xenobiotics like adriamycin (312,313). This protein is located in lipid rafts, where STX1A is also located, therefore STX1A could be promoting its translocation into the membrane. Consequently, HNSCC cells with impaired STX1 function could be down-

regulating P-gp membrane expression and avoiding drug efflux, resulting in an increased adriamycin cytotoxicity.

Cisplatin is another chemotherapeutic drug that induces the crosslink between purine bases on the DNA and interferes with DNA repair mechanisms, causing DNA damage and, as a consequence, inducing cell death. Cisplatin is widely used as a chemotherapeutic drug to radiosensitize HNSCC tumours (208,214). Our results point out that STX1 is also involved in sensitization of HNSCC cells to cisplatin, as the cytotoxic assay demonstrate (Figure 89B). HNSCC cells expressing the STX1-DN are more sensitive to cisplatin, by decreasing 50% the IC₅₀ value with respect to MOCK cells. Besides, there is an upregulation of the autophagic signalling pathway as demonstrated by an increase of the LC3-II/LC3-I ratio (Figure 89C). The entry and exit of cisplatin into the cell are regulated, in addition to passive diffusion, by two transporters. The human copper transporter 1 (hCTR1) regulates its entry, while the ATP7B transporter regulates its exit (314,315). In conclusion, STX1 is able to modulate both the activity and the expression at the cell membrane of receptors and transporters, so it could be regulating the expression of one or both transporters, indirectly controlling the sensitivity of HNSCC cells to cisplatin.

Finally, considering that HNSCC cells with impaired STX1 function are more sensitive to lapatinib and cisplatin, we checked the effect of combining both drugs. The cytotoxicity assay demonstrates that STX1-DN cells are more sensitive to the drug combination, and there is also an increase of the autophagy response after 48 hours of treatment. Even though these are all preliminary results, they are really promising since the combination of both drugs could lead to a better response in patients that do not have high levels of STX1. Some previous *in vitro* research confirmed that the combination of lapatinib and cisplatin had synergistic effects in HNSCC cells (316,317). Moreover, some clinical trials have been developed investigating the combination effects of cisplatin and lapatinib in HNSCC patients. However, controversial results have been found. Administration of lapatinib as a postoperative adjuvant drug and concurrent chemoradiotherapy, followed by lapatinib maintenance in high-risk HNSCC patients resulted in no clinical benefits and had additional toxicity in comparison to patients that have been treated with placebo instead of lapatinib (310). In another clinical trial the effects of lapatinib combined with cisplatin and administration of lapatinib as a maintenance therapy were analysed. This trial was successful, in fact patients in the treated arm have increased their progression-free survival and overall survival at 18 months in comparison to the placebo arm (318). Finally, another clinical trial investigated the effects of lapatinib in

combination with carboplatin and paclitaxel as a neoadjuvant therapy, followed by tumour resection and, if it was needed, by radiotherapy and cisplatin administration as adjuvant therapy. The study concluded with a high response rate and excellent long-term outcomes of the patients (319). These clinical trials proved that the combination of lapatinib and cisplatin is clinically relevant in HNSCC patients, although some parameters should be revised. Stratifying HNSCC patients according to STX1A expression status could help to improve their response to this therapy, indicating that this is a promising research line which should be further explored.

Overall, our results confirmed that STX1, besides of lapatinib, is also involved in adriamycin and cisplatin sensitivity in HNSCC, increasing its therapeutic effect when lapatinib and cisplatin are combined. The mechanism by which STX1 influences drug sensitivity needs further investigation, however our results point out that HNSCC cells are more sensitive to autophagy induction when treated with cisplatin and/or lapatinib and STX1 function is impaired.

10. SYNTAXIN-1A PROMOTES INVASION AND MIGRATION OF BREAST AND HEAD AND NECK CANCER CELLS

Migration and invasion events are very coordinated cellular processes with the final objective to spread tumour cells through the tissues. These mechanisms are tightly coordinated and involve several molecular mechanisms such as cytoskeleton remodelling, trafficking of adhesion receptors, activation of tyrosine kinase receptors, adapter and signalling proteins and secretion of proteolytic mechanisms, among others (14). The SNARE family of proteins are also involved in the regulation of this complex scenario (320). Initially, SNARE proteins have emerged as important factors for regulating neuronal migration and growth cone extension and migration, but recently, SNAREs have been linked to cancer cell invasion and migration processes, whereas its role in BC and HNSCC is still poorly understood.

Only one article has described STX1A as a potential key factor affecting metastasis overall survival in osteosarcoma (136), while Ulloa *et al.* proved that STX1A down-regulation resulted in less glioblastoma cell invasion (86), indicating its potential role in metastatic events. Our group has already proposed *STX1A* as a marker of metastasis free survival, where high expression of the neurogene resulted in a poorer overall survival of BC patients (*Figure 35D*) (104). However more detailed analysis demonstrate that it is also a good marker for predicting metastasis free survival within HER2-positive and HER2-negative BC subgroups (*Figure 40B and Figure 45G*).

Regarding the other SNARE genes, the results presented in this thesis are the first to describe them as good markers for BC metastasis free survival ([Table 35](#)). Considering all BC subtypes, *STX2*, *STX6*, *VAMP-2*, *STXBP2* and *SYN1* are useful markers for metastasis-free survival. Independently, *HER4* is also a good marker of metastasis-free survival in HER2-positive BC subtypes, while *SNAP-23* is a good marker for metastasis predictor but only in the HER2-negative BC subgroup. *STX2* has been previously related to metastatic events, since high expression of this syntaxin correlates with a poorer metastasis free survival in colorectal cancer (321). Also, a positive correlation between *STX6* and poor disease free metastasis outcome is found in HNSCC (322), confirming our results found in BC. Interestingly *VAMP-2* is described as a metastasis promoter, opposite to our findings showing that low levels of this v-SNARE correlate with a shorter metastasis free period. The same situation is found for *SNAP-23*, where down-regulation in ovarian cancer results in less cell invasion (89). No literature regarding *STXBP2* and tumour invasion and metastasis is found, indicating the novelty of our findings.

The bioinformatic analysis confirmed that SNARE genes are involved in BC metastasis reinforcing the importance of the research in this field. However, this thesis is essentially focused on the study of *STX1A* and its role in invasion and migration, even though the study of other SNAREs with invasion and metastatic is promising as well.

Currently, *STX1A* has been associated to migration events, predominantly in neurons. Dr. Soriano's group, with whom we are currently collaborating, described *STX1A* as necessary in neuronal migration through direct interaction with Netrin-1 and DCC receptor, and also by regulating TrkB receptor activity (83,84,242). The same research group, working with glioblastoma, demonstrated that *STX1A* is also involved in promoting glioblastoma cells invasiveness (86). Our experiments point out at the same direction, confirming that functionally impaired *STX1* HER2-negative/basal BC and SCC090 HNSCC cells migrate less in comparison to the controls ([Figure 91A-Figure 91F](#)). Using the *STX1*-DN cells it is proved that the formation of the SNARE complex is essential for the tumour cell migration as Cotrufo *et al.* proved in neurons (83,242). Our results also prove that the effect seen in *STX1*-DN cells is *STX1A*-specific by repeating the same experiment with MDA-MB-231 down-regulated by shRNA *STX1A* ([Figure 91G-Figure 91H](#)). Phenotypically, it is demonstrated that *STX1A* is essential in migration processes, however we went a step forward by evidencing that it could be caused by the impairment of the cell attachment and cell spreading machinery. When *STX1* function is impaired, BC and HNSCC cancer cells are not able to attach ([Figure 92A-Figure 92D](#))

and they spread less (*Figure 93A, Figure 93D, Figure 93G and Figure 93J*), maintaining their sphericity (*Figure 93B, Figure 93E, Figure 93H and Figure 93K*). This is not the first time that the SNARE complex has been involved in cell adhesion and expansion processes, but it is the first time that STX1 has been associated with these cell functions. Its SNARE partner, SNAP-23, is found to form a SNARE complex with STX12 and VAMP-3 in CHO cells during cell adhesion, which reinforces the fact that SNARE complexes are essential for this cell process (323). More in detail, SNAP-23 and the SNARE modulator NSF have been found to be involved in activating FAK at the early time point of adhesion, and also have been involved in the cellular localization of Src, the same STX1A partner closely related to focal adhesion turnover (99). Considering that SNAP-23 and also VAMP proteins are putative STX1A partners in BC and HNSCC cancer cells, it is feasible that they could control together focal adhesion turnover in these BC and HNSCC cells.

The cell spreading assay offers an insight into the role of STX1 in invadopodia formation (*Figure 93C, Figure 93F, Figure 93I and Figure 93L*). Despite being aware that more accuracy in the assay would be needed to confirm this statement, co-localization between F-actin punctae and an invadopodia marker, such as TKS5 (324), allow us to think that STX1 is involved. The experiments demonstrate that cells expressing STX1-DN have less F-actin punctae when plated into fibronectin slides. This finding is not surprising according to the growing amount of literature relating SNARE involvement in invadopodia formation. Other SNARE proteins, such as SNAP-23, STX4, STX12, VAMP-7, TI-VAMP or MUNC18c have been already described as invadopodia inducers (96,284,285,325), however our data are the first to describe STX1 involvement in regulating invadopodia formation. We tried to further characterize STX1A role in invadopodia formation by a gelatin degradation assay (*Figure 94A and Figure 94B*), but due to technical problems it has not been possible yet.

Focal adhesions and invadopodia formation are controlled by Src signalling pathway and both require integrin trafficking to the plasma membrane (99,285). STX1A down-regulation is associated with down-regulation of Src activation which could be related with the decrease seen in cell adhesion and migration (*Figure 95B*). CCND1 is described to play an important role in focal adhesion and cell spreading as well. In particular, it has been demonstrated that macrophages, fibroblasts and BC cells with down-regulation of CCND1 increased their adhesion and cell spreading, the same results found in BC cells and in fibroblasts (326,327). Our results point out that cells with STX1-DN have more expression of CCND1 (*Figure 76A-Figure 76F*), which could explain, in part, the reduction in cell adhesion and spreading.

Moreover, SNARE proteins are involved in integrin trafficking, focusing on this role, it was discarded the involvement of STX1A in ITG β 1 trafficking since no differential ITG β 1 expression into the plasma membrane was detected (*Figure 95C*). These data differ from the findings from Karla *et al.* describing that SNAP-23 and STX12 are involved in ITG β 1 trafficking into the invadopodia (285). However, it could still be possible that SNAP-23 and STX12 SNARE complex is specific for ITG β 1 trafficking, whereas STX1A is specific for ITG α 6 membrane trafficking, considering that down-regulation of this SNARE protein resulted in less membrane expression of ITG α 6 in MDA-MB-231 BC cells (*Figure 95D*). ITG α 6 has already been linked to metastasis and invasion events, in BC and HNSCC themselves and in pancreatic cells it has been proved that inhibition of this integrin results in less cell migration and invasion (328–330). Also, a link between ITG α 6 levels and AKT activation is described in pancreatic cancer cells, in which inhibition of ITG α 6 expression results in down-regulation of AKT signalling pathway activation (330). HNSCC cells with non-functional STX1 also downregulate this signalling pathway (*Figure 74*), however we think that it can be attributed to STX1 lack of function instead of the down-regulation of ITG α 6. Certainly, the lack of ITG α 6 at the plasma membrane is mostly attributable to a reduction in membrane trafficking events, as the BODIPY experiments indicate (*Figure 80*) by an accumulation of intracellular vesicles in BC and HNSCC cell lines.

These changes in migration and invasion capabilities probably result in changes of cell phenotype, from a mesenchymal-like into an epithelial-like phenotype. STX4, another member of the syntaxin family has been linked to EMT processes in normal breast morphogenesis. It has been proved that STX4 binds to E-cadherin and down-regulates its presence at the plasma membrane by avoiding E-cadherin-laminin interaction, leading the cell into a mesenchymal phenotype, inducing the morphogenesis of the breast (101). Our results demonstrate that impairment of STX1A function results into a down-regulation of mesenchymal transcription factors mRNA expression such as *SNAI-1*, *SNAI-2*, *TWIST-1* and *VIM* in BC and HNSCC cell lines (*Figure 97*). However, it is important to note that in FaDu, non-functional STX1A induces an overexpression of *SNAI-1* transcription factor and an overexpression of *SNAI-2* is detected in SCC090, as well. This partial EMT characteristics, already described in HNSCC cells (331), are also seen in *in vivo* CAM FaDu and SCC090 tumours (*Figure 103G - Figure 103I*). The scenario described in HNSCC cells *in vitro* and *in vivo* seems to indicate a process of partial EMT, characterized by an intermediate transition step sharing both epithelial and mesenchymal properties which give migration and metastatic advantages to the cell (331). However, it is very important to bear in mind the cancer cell phenotype: when STX1A is inhibited or its function impaired, cells migrate and invade less than their control partners. These functional

results hint at the complex pleiotropic network that control these processes, where even though some EMT transcription factors are surprisingly up-regulated, BC and HNCC cells with STX1A impaired migrate and invade less.

Finally, considering that one of the characteristics of invading cells is the secretion of MMPs, and also the link that exists between the secretion of these proteases and SNARE proteins (14,15,96,284,332), their secretion and activity into the media of these cells were analysed. Preliminary results of MMPs secretion (*Figure 98B*) and activity (*Figure 98A*) do not show any differences, indicating that STX1A is not involved in the secretion of these proteases. Our results do not follow the same trend as the ones obtained in Coppolino's lab, in which the SNARE proteins STX4, STX12, VAMP-3, VAMP-7, STX12, SNAP-23 and MUNC18c are clearly involved in the secretion of MMPs in the invadopodia of invading cells (96,284,332).

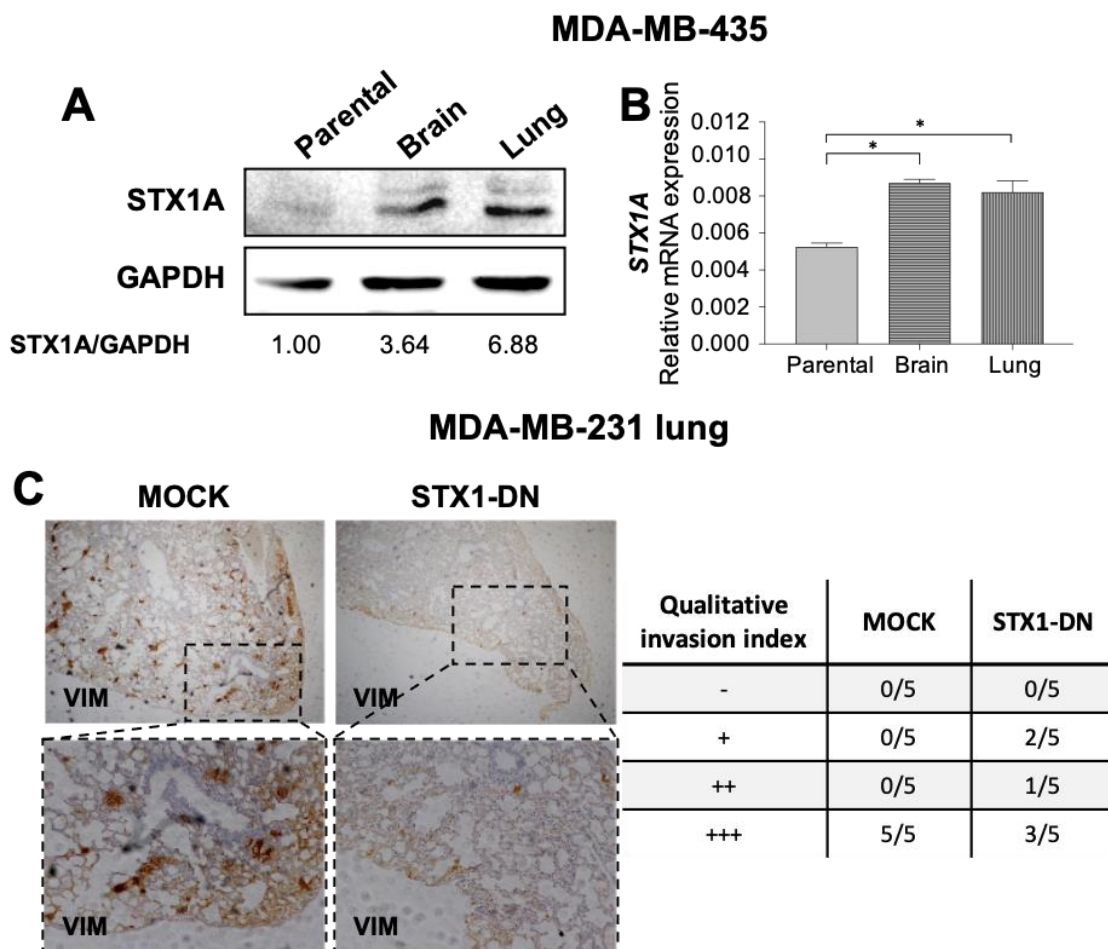


Figure 112 – STX1A expression is increased in metastasis and its inhibition results in less lung metastases. (A) On the top, Western blot of STX1A expression in parental MDA-MB-435 cell lines and their brain and lung derived metastases. GAPDH was used as internal control. At the bottom, relative quantification of STX1A protein expression. (B) Analysis of STX1A mRNA expression by qPCR in parental MDA-MB-435 cell lines and their brain and lung derived metastases. (C) On the left, representative

images of lungs from mice inoculated with MDA-MB-231-Lu MOCK or STX1-DN cells. On the right qualitative invasion index of the five lungs from each condition. Dr. Soriano's lab unpublished results. * $p < 0.05$ comparing parental versus brain or lung using one-way ANOVA test.

The potential metastatic capacity of STX1A is further exemplified in our unpublished results with the MDA-MB-435 melanoma cell line. Cell lines were obtained from parental orthotopic tumours, lung metastasis and brain metastasis. STX1A protein and mRNA expression were determined and STX1A was found overexpressed in the metastatic cell lines (*Figure 112A and Figure 112B*). In addition, our collaborators from Dr. Soriano's lab performed an *in vivo* experiment with MDA-MB-231 cells with specific metastatic tropism to lungs (MDA-MB-231-Lu) (*unpublished results*). They did an intracardiac injection of MDA-MB-231-Lu cells expressing STX1-DN and after three weeks mice were sacrificed and the lungs were histologically analysed. The results show that mice injected with MDA-MB-231-Lu STX1-DN have less lung metastasis than their controls (*Figure 112C*). All these results confirm our findings that STX1A acts as a metastatic promoter.

Altogether our results confirm the important role of STX1A in migration and invasion in BC and HNSCC cancer cells *in vitro* and describe some of the mechanisms by which STX1A facilitates these capabilities (*Figure 113*). However, more research is needed to further clarify the molecular processes by which STX1A drives metastasis in BC and HNSCC cells.

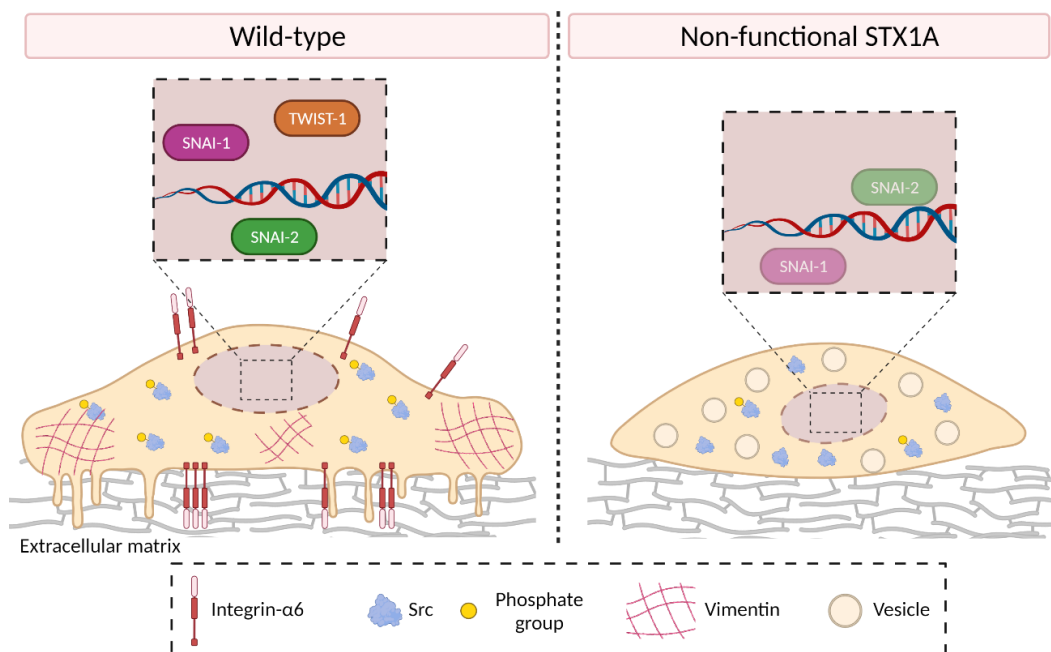


Figure 113 – Scheme of the influence of STX1A on migration and invasion in BC and HNSCC cell lines. On the left, a BC or HNSCC cell with normal STX1A expression. The cell interacts with the ECM components by integrins, in this case ITG α 6 and form invadopodia. There is also

activation of the Src signalling pathway, presence of vimentin and the mesenchymal transcription factors SNAI-1, SNAI-2 and TWIST-1 are activated. On the right, a cell with impaired STX1A function. The morphology of the cell is more spheric, Src signalling pathway is not activated and there is no ITG α 6 at the plasma membrane, being probably accumulated in the vesicles which, due to the STX1A lack of function, cannot fuse to and vehicle ITG α 6 into the plasma membrane. EMT transcription factors, with the exception of SNAI-1 or SNAI-2 in HNSCC cells, are not upregulated.

11. STX1A IS A PROMISING TARGET TO INCREASE OVERALL AND METASTASIS FREE SURVIVAL OF BREAST AND HEAD AND NECK CANCER PATIENTS

Our work has demonstrated that STX1A and other SNARE proteins are predictive factors for overall and distant metastasis free survival in BC and also that STX1A is a good overall survival predictor in HNSCC patients. These promising results, even though they need further validation, indicate that a possible stratification of breast and head and neck tumours based on STX1A or SNARE levels could be useful in the clinical to predict the overall survival and the possibility of distant recurrence of the tumour. Moreover, it can also be useful in predicting the type of treatment that should be more beneficial for the patient. Considering our results, it is found that impairment of STX1A results in a sensitization of BC and HNSCC tumours to lapatinib, so patients with low levels of this synaptic-related protein can be more sensitive to this TKI treatment. In HNSCC it can also be interesting to treat STX1^{low} patients with cisplatin or adriamycin, as our preliminary results have pointed out. Moreover, after more research, therapy combination can be also considered.

It is proved that STX1A down-regulation or its function impairment by using a STX1-DN form inhibits migration and invasion processes of the tumour cells, besides from sensitizing the tumour to several therapies. These results open the possibility of considering the inhibition or the impairment of STX1A function as a possible BC and HNSCC treatment to prevent metastases to distal organs or as a neoadjuvant therapy in lapatinib treatment in BC. In HNSCC this strategy can also be considered to chemosensitize tumours, besides to lapatinib, to cisplatin or adriamycin treatments. In fact, there is already a strategy to cleave STX1A and to inhibit its function by the treatment with BoNTs, more specifically type C1 which specifically cleaves STX1A and SNAP-25. Currently, BoNT A and B are vastly used in the clinic to treat hyperkinetic movement disorders, symptoms caused by glandular hyperactivity (sialorrhea and hyperhidrosis), bladder dysfunction or for treatment of spasticity in diseases such as stroke, cerebral palsy, multiple sclerosis and cerebral and spinal cord injury (63). However, research in BoNT and cancer is very limited, mainly focused on relieving the cancer-related pain raised from cancer mass pressure or from neuropathic pain at the site of cancer surgery

or radiation. Normally BoNTs are more used in HNSCC where, in addition to be used as pain-relievers, they are also used to alleviate possible side effects such as gustatory hyperhidrosis caused by parotid or oral surgery in cancer patients. However, only few research articles have proved their anticancer effect *in vitro* and *in vivo*. The most notorious research articles in this sense are the experiments conducted by Zhao *et al.* in which they demonstrated that injection of BoNT A in the stomach results in a pharmacological denervation of the organ, reducing tumour incidence and progression and enhances therapeutical effects of systemic chemotherapy (53). *In vivo*, denervation of the pancreas by the injection of BoNT A resulted in less pancreatic tumour growth (333) and also the same results are obtained in prostate cancer (218). Interestingly, in a clinical trial where prostate cancer patients were treated with BoNT A on one side of the prostate and with saline injection on the contralateral side, after six weeks, histological studies demonstrated atrophy and degenerative features (reduced cytoplasm and pyknotic nuclei) where seen in the side where BoNT A was administered, highlighting the promising effects of BoNT A in prostate cancer treatment (218). Finally, in a case patient report with metastatic prostate cancer BoNT A injection was tested and the injection improved its clinical parameters by reducing the primary tumour mass (334).

To the best of our knowledge, no more research or clinical trials have been developed with other BoNT serotypes and more research is needed to finally use this strategy to treat cancer patients. It is important to mention that these strategies are focused mainly on the tumour microenvironment and the histological analyses are focused only in tumour innervation. In our case, BoNT C1 could be proposed to treat directly breast and head and neck cancer tumour cells. This fact implies that more specific strategies must be considered to apply this toxin. To increase the sensitivity of the neurotoxin to our chosen cancer cell type and to enhance the entrance of BoNT into the cell, it could be possible to replace the normal neuronal binding domain of the BoNT with a targeting domain, for example for an EGFR/HER family of receptor ligand, to increase its ability to bind to the tumour cell and direct its SNARE-specific cleavage. Examples of this strategy are already found in the literature, where Somm *et al.* developed a recombinant protein consisting of the GH-releasing hormone peptide ligand domain bound to the light chain of the BoNT serotype A, which specifically targeted pituitary somatotrophs cells and inhibited the GH/IGF1 axis (335). Another BoNT construct, coupled with EGF, targeted specifically neuroendocrine cells and inhibited vesicle release (336). This BoNT construct reinforces our hypothesis that constructing a recombinant protein between the protease domain of BoNT C1 and EGF, which will target EGFR and also HER2 due to EGFR-HER2 heterodimerization, could be technically approachable and worth exploring.

Finally, another strategy is already developed to specifically inhibit the SNARE protein SNAP-25. Peptides mimicking the N-end of SNAP-25 are already proved to inhibit exocytosis in neurons by disrupting the interaction with STX1 and therefore, inhibiting the formation of SNARE complexes, acting as a competitive antagonist of SNAP-25 (337). On that account, these peptides could be useful to inhibit the SNARE formation in our breast and head and neck cancer models and as a consequence inhibit STX1A function, or also, specific peptides targeting also the N-terminal of STX1A could be designed.

Overall, our findings suggest that targeting STX1A could be useful, at expenses of increase local tumour growth, to reduce BC and HNSCC metastasis events and to sensitize HER2-positive BC tumours to lapatinib and HNSCC cells to lapatinib, cisplatin and adriamycin (Figure 114). Even though more research is needed, several pharmacological strategies currently exist, such as recombination of BoNTs or SNARE peptides, which could be suitable to inhibit STX1A and/or SNARE complex formation. Moreover, we present *STX1A*, among other SNARE genes, as a biomarker to predict overall and metastasis free survival in BC and HNSCC.

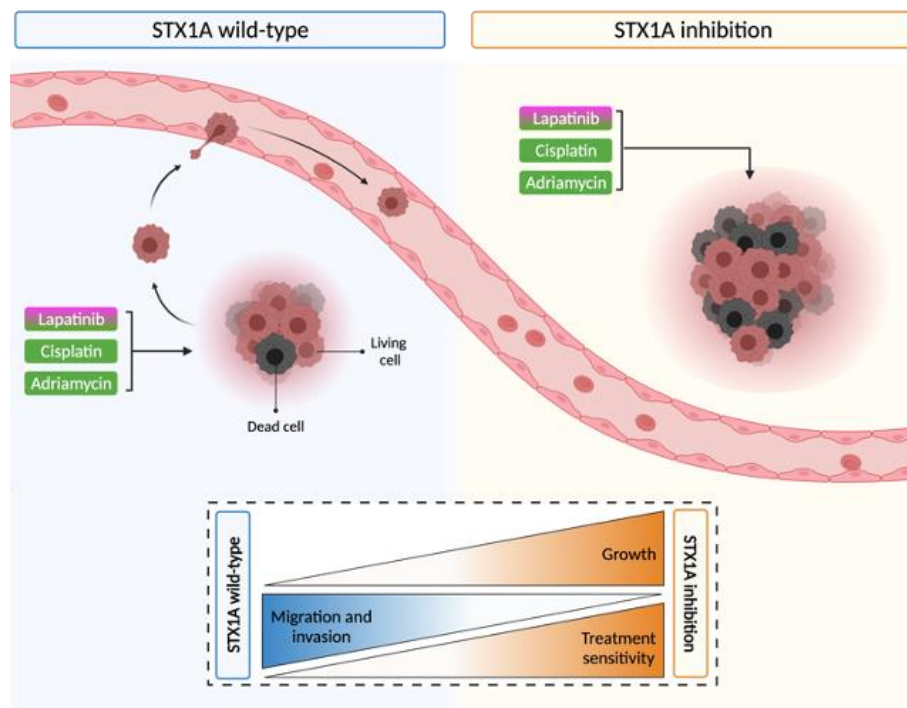


Figure 114 – Summary of STX1A inhibition effects in breast and head and neck tumours. The picture represents, on the left, wild-type breast and head and neck tumours treated with lapatinib (HER2-positive and HNSCC), cisplatin (HNSCC) or adriamycin (HNSCC) and, on the right, both tumours without functional STX1A. In the middle box the main distinguishable characteristics of tumours with impaired function of STX1A are described: tumours tend to be bigger but with less migration and invasion capacities and more responsive to lapatinib (HER2-positive BC tumours and HNSCC tumours) and, in the case of HNSCC tumour to cisplatin and adriamycin.

Syntaxin-1A, a synaptic related protein in breast and head and neck cancer progression and prognosis

CONCLUSIONS

Syntaxin-1A, a synaptic related protein in breast and head and neck cancer progression and prognosis

1. High levels of *STX1A* expression in BC and HNSCC tumours correlate with a poor clinical prognosis, so *STX1A*, either alone or in conjunction with some *SNARE* family members, is proposed as a biomarker to predict overall survival of BC and HNSCC patients and distant-metastasis free survival in BC patients.
2. Analysis of mRNA and protein expression of *STX1A* and other *SNAREs* in our BC and HNSCC cell lines follow the same expression pattern seen in BC patients and in the cancer cell line database, confirming that our BC and HNSCC cell line panel is a good *in vitro* model to further study the role of these proteins in BC and HNSCC.
3. The differential expression of *STX1A* between HER2-positive and HER2-negative BC subgroups can be due to a differential response to transcription factors: histone acetylation promotes *STX1A* transcription in all BC and HNSCC cell lines, while SP1 binding is crucial and necessary only in HER2-negative BC cell lines.
4. *STX1A* acts as a proliferative suppressor, up-regulating G₂/M checkpoint and also reducing *CCND1* expression and, as a consequence, restraining BC and HNSCC tumour growth.
5. *STX1A* and the EGFR/HER family of receptors are functionally related. *STX1A* clusters in response to EGF and *STX1A* function impairment results in an inverse regulation of plasma membrane levels of both EGFR (up) and HER2 (down) in BC and HNSCC, likely related to an altered vesicle transport. These events may explain the direct correlation between the high levels of both *STX1A* and HER2 found in patients.
6. *STX1A* also modulates signal transduction and response to treatments. *STX1A* function impairment sensitizes BC and HNSCC tumours to lapatinib, therefore, concomitant treatment of lapatinib and anti-*STX1A* drugs could be worth exploring.
7. *STX1A* function impairment also sensitizes HNSCC cells to adriamycin and cisplatin by inducing autophagy, and concurrent lapatinib and cisplatin treatment has a synergistic effect on HNSCC cells cytotoxicity. Therefore, lapatinib is proposed as a worth exploring treatment for *STX1A*^{low} HNSCC tumours, alone or in combination with cisplatin.

8. STX1A promotes migration and invasion in BC and HNSCC cell lines. It facilitates cell adhesion, spreading and invasion *in vitro* by inducing the EMT program.

Therefore, considering all the results compiled in this thesis, we propose STX1A as a prognosis biomarker in BC and HNSCC patients and as a metastasis biomarker in BC. In addition, STX1A might be also considered as an attractive target for advanced BC and HNSCC tumours. Blocking STX1A activity should inhibit metastatic events and sensitize BC and HNSCC tumours to lapatinib, and HNSCC tumours to adryamicin and cisplatin, as well.

Syntaxin-1A, a synaptic related protein in breast and head and neck cancer progression and prognosis

BIBLIOGRAPHY

Syntaxin-1A, a synaptic related protein in breast and head and neck cancer progression and prognosis

1. Um P. Cancer, Definition. In: Highlander SK, Rodriguez-Valera F, White BA, editors. *Encyclopedia of Metagenomics: Environmental Metagenomics* [Internet]. Boston, MA: Springer US; 2015. p. 65. Available from: https://doi.org/10.1007/978-1-4899-7475-4_106
2. Hanahan D, Weinberg RA. Hallmarks of cancer: The next generation. *Cell* [Internet]. 2011;144(5):646–74. Available from: <http://dx.doi.org/10.1016/j.cell.2011.02.013>
3. Hanahan D, Weinberg RA. The Hallmarks of Cancer. *Cell*. 2000;100:57–70.
4. Floor SL, Dumont JE, Maenhaut C, Raspe E. Hallmarks of cancer: Of all cancer cells, all the time? *Trends Mol Med*. 2012;18(9):509–15.
5. Mattiuzzi C, Lippi G. Current Cancer Epidemiology. *J Epidemiol Glob Health*. 2019;9(4):217–22.
6. Ritchie H, Roser M. Causes of death [Internet]. *Our World in data*. 2020. Available from: <https://ourworldindata.org/causes-of-death>
7. World Health Organization. Globocan.
8. Siegel RL, Miller KD, Fuchs HE, Jemal A. Cancer Statistics, 2021. *CA Cancer J Clin*. 2021;71(1):7–33.
9. Welch HG, Schwartz LM. Are Increasing 5-Year Survival Rates. 2017;283(22):2975–8.
10. Feitelson MA, Arzumanyan A, Kulathinal RJ, Blain SW, Holcombe RF, Mahajna J, et al. Sustained proliferation in cancer: therapeutic targets. *Semin Cancer Biol*. 2016;35:25–54.
11. Nahta R, Al-Mulla F, Al-Temaimi R, Amedei A, Andrade-Vieira R, Bay S, et al. Mechanisms of environmental chemicals that enable the cancer hallmark of evasion of growth suppression. *Carcinogenesis*. 2015;36:S2–18.
12. Lei X, Lei Y, Li JK, Du WX, Li RG, Yang J, et al. Immune cells within the tumor microenvironment: Biological functions and roles in cancer immunotherapy. *Cancer Lett* [Internet]. 2020;470(November 2019):126–33. Available from: <https://doi.org/10.1016/j.canlet.2019.11.009>
13. O'Donnell JS, Teng MWL, Smyth MJ. Cancer immunoeediting and resistance to T cell-based immunotherapy. *Nat Rev Clin Oncol* [Internet]. 2019;16(3):151–67. Available from: <http://dx.doi.org/10.1038/s41571-018-0142-8>
14. Fares J, Fares MY, Khachfe HH, Salhab HA, Fares Y. Molecular principles of metastasis: a hallmark of cancer revisited. *Signal Transduct Target Ther* [Internet]. 2020;5(1). Available from: <http://dx.doi.org/10.1038/s41392-020-0134-x>
15. Suhail Y, Cain MP, Vanaja K, Kurywchak PA, Levchenko A, Kalluri R, et al. Systems Biology of Cancer Metastasis. *Cell Syst* [Internet]. 2019;9(2):109–27. Available from: <https://doi.org/10.1016/j.cels.2019.07.003>
16. Pastushenko I, Blanpain C. EMT Transition States during Tumor Progression and Metastasis. *Trends Cell Biol* [Internet]. 2019;29(3):212–26. Available from: <https://doi.org/10.1016/j.tcb.2018.12.001>
17. Murata M. Inflammation and cancer. *Environ Health Prev Med*. 2018;23(1):1–8.
18. Hayashi MT, Cesare AJ, Teresa R, Jan K. Cell Death During Crisis Is Mediated by Mitotic Telomere Deprotection. *Nature* [Internet]. 2015;522:492–6.
19. Hida K, Maishi N, Annan DA, Hida Y. Contribution of tumor endothelial cells in cancer progression. *Int J Mol Sci*. 2018;19(5):1–12.
20. Lee JK, Choi Y La, Kwon M, Park PJ. Mechanisms and Consequences of Cancer Genome Instability: Lessons from Genome Sequencing Studies. *Annu Rev Pathol Mech Dis*. 2016;11:283–312.
21. Sharma A, Boise LH, Shanmugam M. Cancer metabolism and the evasion of apoptotic cell death. *Cancers (Basel)*. 2019;11(8):1–20.
22. Balkwill FR, Capasso M, Hagemann T. The tumor microenvironment at a glance. *J Cell Sci*. 2012;125(23):5591–6.
23. Whiteside TL. The tumor microenvironment and its role in promoting tumor growth. *Oncogene*. 2008 Oct;27(45):5904.ss. *Oncogene*. 2008;27(45):5904–12.
24. Laplane L, Duluc D, Bikfalvi A, Larmonier N, Pradeu T. Beyond the tumour microenvironment. *Int J Cancer*. 2019;145(10):2611–1618.
25. LeBleu VS, Kalluri R. A peek into cancer-associated fibroblasts: Origins, functions and translational impact. *DMM Dis Model Mech*. 2018;11(4):1–9.
26. Shiga K, Hara M, Nagasaki T, Sato T, Takahashi H, Takeyama H. Cancer-associated fibroblasts: Their characteristics and their roles in tumor growth. *Cancers (Basel)*. 2015;7(4):2443–58.
27. Dumas JF, Brisson L. Interaction between adipose tissue and cancer cells: role for cancer progression. *Cancer Metastasis Rev*. 2020;
28. Zhao C, Wu M, Zeng N, Xiong M, Hu W, Lv W, et al. Cancer-associated adipocytes: Emerging supporters in breast cancer. *J Exp Clin Cancer Res*. 2020;39(1):1–17.
29. Pickup MW, Mouw JK, Weaver VM. The extracellular matrix modulates the hallmarks of cancer.

- EMBO Rep. 2014;15(12):1243–53.
30. Walker C, Mojares E, Del Río Hernández A. Role of extracellular matrix in development and cancer progression. Vol. 19, International Journal of Molecular Sciences. 2018.
 31. Fernández-Nogueira P, Mancino M, Fuster G, Bragado P, Prats de Puig M, Gascón P, et al. Breast Mammographic Density: Stromal Implications on Breast Cancer Detection and Therapy. *J Clin Med*. 2020;9(3):776.
 32. Murphy DA, Courtneidge SA. The “ins” and “outs” of podosomes and invadopodia: Characteristics, formation and function. *Nat Rev Mol Cell Biol* [Internet]. 2011;12(7):413–26. Available from: <http://dx.doi.org/10.1038/nrm3141>
 33. Rajabi M, Mousa SA. The role of angiogenesis in cancer treatment. *Biomedicines*. 2017;5(2).
 34. Petrova T V., Koh GY. Biological functions of lymphatic vessels. *Science* (80-). 2020;369(6500).
 35. Stacker SA, Williams SP, Karnezis T, Shayan R, Fox SB, Achen MG. Lymphangiogenesis and lymphatic vessel remodelling in cancer. *Nat Rev Cancer* [Internet]. 2014;14(3):159–72. Available from: <http://dx.doi.org/10.1038/nrc3677>
 36. Jobling P, Pundavela J, Oliveira SMR, Roselli S, Walker MM, Hondermarck H. Nerve-cancer cell crosstalk: A novel promoter of tumor progression. *Cancer Res*. 2015;75(9):1777–81.
 37. Arese M, Bussolino F, Pergolizzi M, Bizzozero L, Pascal D. Tumor progression: the neuronal input. *Ann Transl Med*. 2018;6(5):89–89.
 38. Zubeldia-Plazaola A, Recalde-Percaz L, Moragas N, Alcaraz M, Chen X, Mancino M, et al. Glucocorticoids promote transition of ductal carcinoma in situ to invasive ductal carcinoma by inducing myoepithelial cell apoptosis. *Breast Cancer Res*. 2018;20(1):1–16.
 39. Ayala GE, Dai H, Powell M, Li R, Ding Y, Wheeler TM, et al. Cancer-related axonogenesis and neurogenesis in prostate cancer. *Clin Cancer Res*. 2008;14(23):7593–603.
 40. Zahalka AH, Frenette PS. Nerves in cancer. *Nat Rev Cancer* [Internet]. 2020;20(3):143–57. Available from: <http://dx.doi.org/10.1038/s41568-019-0237-2>
 41. Magnon C, Hall SJ, Lin J, Xue X, Gerber L, Freedland SJ, et al. Autonomic Nerve Development Contributes to Prostate Cancer Progression. *Science*. 2013;341(6142):1–10.
 42. Servick K. How body’s nerves become accomplices in the spread of cancer [Internet]. *Science*. 2019. Available from: <https://www.sciencemag.org/news/2019/09/how-body-s-nerves-become-accomplices-spread-cancer>
 43. Entschladen F, Palm D, Lang K, Drell IV TL, Zaenker KS. Neoneurogenesis: Tumors may initiate their own innervation by the release of neurotrophic factors in analogy to lymphangiogenesis and neoangiogenesis. *Med Hypotheses*. 2006;67(1):33–5.
 44. Mancino M, Ametller E, Gascón P, Almendro V. The neuronal influence on tumor progression. *Biochim Biophys Acta - Rev Cancer*. 2011;1816(2):105–18.
 45. Pundavela J, Demont Y, Jobling P, Lincz LF, Roselli S, Thorne RF, et al. ProNGF correlates with Gleason score and is a potential driver of nerve infiltration in prostate cancer. *Am J Pathol* [Internet]. 2014;184(12):3156–62. Available from: <http://dx.doi.org/10.1016/j.ajpath.2014.08.009>
 46. Entschladen F, Palm D, Niggemann B, Zaenker KS. The cancer’s nervous tooth: Considering the neuronal crosstalk within tumors. *Semin Cancer Biol*. 2008;18(3):171–5.
 47. Noguera-Castells A, Fernández-Nogueira P, Fuster G, Recalde-Percaz L, Moragas N, López-Plana A, et al. Histamine receptor 1 inhibition enhances antitumor therapeutic responses through extracellular signal-regulated kinase (ERK) activation in breast cancer. *Cancer Lett* [Internet]. 2018; Available from: <http://linkinghub.elsevier.com/retrieve/pii/S0304383518302052>
 48. Bauman J, McVary K. Autonomic nerve development contributes to prostate cancer progression. *Asian J Androl*. 2013;15(6):713–4.
 49. Li X, Dun MD, Faulkner S, Hondermarck H. Neuroproteins in Cancer: Assumed Bystanders Become Culprits. *Proteomics*. 2018;18(14):1–6.
 50. Voss MJ, Entschladen F. Tumor interactions with soluble factors and the nervous system. *Cell Commun Signal*. 2010;8:1–6.
 51. Zänker KS. The Neuro-Neoplastic Synapse : Does it Exist ? 2007;39:154–61.
 52. Kuol N, Stojanovska L, Apostolopoulos V, Nurgali K. Role of the nervous system in cancer metastasis. *J Exp Clin Cancer Res*. 2018;37(1):1–12.
 53. Zhao CM, Hayakawa Y, Kodama Y, Muthupalani S, Westphalen CB, Andersen GT, et al. Denervation suppresses gastric tumorigenesis. *Sci Transl Med*. 2014;6(250):1–13.
 54. Kamiya A, Hayama Y, Kato S, Shimomura A, Shimomura T, Irie K, et al. Genetic manipulation of autonomic nerve fiber innervation and activity and its effect on breast cancer progression. *Nat*

- Neurosci [Internet]. 2019;22(8):1289–305. Available from: <http://dx.doi.org/10.1038/s41593-019-0430-3>
55. Bao W, Qiu H, Yang T, Luo X, Zhang H, Wan X. Upregulation of TrkB Promotes Epithelial-Mesenchymal Transition and Anoikis Resistance in Endometrial Carcinoma. Vol. 8, PLoS ONE. 2013.
 56. Akil H, Perraud A, Jauberteau MO, Mathonnet M. Tropomyosin-related kinase B/brain derived-neurotrophic factor signaling pathway as a potential therapeutic target for colorectal cancer. *World J Gastroenterol*. 2016;22(2):490–500.
 57. Okada Y, Eibl G, Guha S, Duffy JP, Reber HA, Hines OJ. Nerve growth factor stimulates MMP-2 expression and activity and increases invasion by human pancreatic cancer cells. *Clin Exp Metastasis*. 2004;21(4):285–92.
 58. Okada Y, Eibl G, Duffy JP, Reber HA, Hines OJ. Glial cell-derived neurotrophic factor upregulates the expression and activation of matrix metalloproteinase-9 in human pancreatic cancer. *Surgery*. 2003;134(2):293–9.
 59. Yang E V., Sood AK, Chen M, Li Y, Eubank TD, Marsh CB, et al. Norepinephrine up-regulates the expression of vascular endothelial growth factor, matrix metalloproteinase (MMP)-2, and MMP-9 in nasopharyngeal carcinoma tumor cells. *Cancer Res*. 2006;66(21):10357–64.
 60. Hsieh YH, Chan HL, Lin CF, Liang SHY, Lu ML, McIntyre RS, et al. Antipsychotic use is inversely associated with gastric cancer risk: A nationwide population-based nested case-control study. *Cancer Med*. 2019;8(9):4484–96.
 61. Walker AJ, Card T, Bates TE, Muir K. Tricyclic antidepressants and the incidence of certain cancers: A study using the GPRD. *Br J Cancer*. 2011;104(1):193–7.
 62. Pottegard A, Rodríguez LAG, Rasmussen L, Damkier P, Friis S, Gaist D. Use of tricyclic antidepressants and risk of glioma: A nationwide case-control study. *Br J Cancer*. 2016;114(11):1265–8.
 63. Mittal SOM, Jabbari B. Botulinum neurotoxins and cancer—a review of the literature. *Toxins (Basel)*. 2020;12(1):1–14.
 64. Meng J, Wang J. Role of SNARE proteins in tumourigenesis and their potential as targets for novel anti-cancer therapeutics. *Biochim Biophys Acta - Rev Cancer* [Internet]. 2015;1856(1):1–12. Available from: <http://dx.doi.org/10.1016/j.bbcan.2015.04.002>
 65. Pirazzini M, Rossetto O, Eleopra R, Montecucco C. Botulinum neurotoxins: Biology, pharmacology, and toxicology. *Pharmacol Rev*. 2017;69(2):200–35.
 66. Chen S, Barbieri JT. Multiple pocket recognition of SNAP25 by botulinum neurotoxin serotype E. *J Biol Chem* [Internet]. 2007;282(35):25540–7. Available from: <http://dx.doi.org/10.1074/jbc.M701922200>
 67. Guo J, Chan EWC, Chen S. Mechanism of substrate recognition by the novel Botulinum Neurotoxin subtype F5. *Sci Rep*. 2016;6(October 2015):1–9.
 68. Meng J, Wang J. Role of SNARE proteins in tumourigenesis and their potential as targets for novel anti-cancer therapeutics. *Biochim Biophys Acta - Rev Cancer* [Internet]. 2015;1856(1):1–12. Available from: <http://dx.doi.org/10.1016/j.bbcan.2015.04.002>
 69. Shu-Heng J, Li-Peng H, Xu W, Jun L, Zhi-Gang Z. Neurotransmitters: emerging targets in cancer. *Oncogene*. 2020;39:503–15.
 70. Chiodoni C, Di Martino MT, Zazzeroni F, Caraglia M, Donadelli M, Meschini S, et al. Correction to: Cell communication and signaling: How to turn bad language into positive one (Journal of Experimental and Clinical Cancer Research DOI: 10.1186/s13046-019-1122-2). *J Exp Clin Cancer Res*. 2019;38(1):1–11.
 71. Jahn R, Scheller RH. SNAREs - Engines for membrane fusion. *Nat Rev Mol Cell Biol*. 2006;7(9):631–43.
 72. Han J, Pluhackova K, Böckmann RA. The multifaceted role of SNARE proteins in membrane fusion. *Front Physiol*. 2017;8(JAN).
 73. Hong WJ, Lev S. Tethering the assembly of SNARE complexes. *Trends Cell Biol* [Internet]. 2014;24(1):35–43. Available from: <http://dx.doi.org/10.1016/j.tcb.2013.09.006>
 74. Baker RW, Hughson FM. Chaperoning SNARE assembly and disassembly. *Nat Rev Mol Cell Biol*. 2016;17(8):465–79.
 75. Wang T, Li L, Hong W. SNARE proteins in membrane trafficking. *Traffic*. 2017;18(12):767–75.
 76. Hong W. SNAREs and traffic. *Biochim Biophys Acta*. 2005;1744(3):493–517.
 77. Rizo J, Xu J. The Synaptic Vesicle Release Machinery. *Annu Rev Biophys* [Internet]. 2015;44(1):339–67. Available from: <http://www.annualreviews.org/doi/10.1146/annurev-biophys-060414-034057>
 78. Risselada HJ, Mayer A. SNAREs, tethers and SM proteins: How to overcome the final barriers to

- membrane fusion? *Biochem J.* 2020;477(1):243–58.
79. Brunger AT, Choi UB, Lai Y, Leitz J, White KI, Zhou Q. The pre-synaptic fusion machinery. *Curr Opin Struct Biol* [Internet]. 2019;54:179–88. Available from: <https://doi.org/10.1016/j.sbi.2019.03.007>
 80. Wang S, Li Y, Gong J, Ye S, Yang X, Zhang R, et al. Munc18 and Munc13 serve as a functional template to orchestrate neuronal SNARE complex assembly. *Nat Commun* [Internet]. 2019;10(1). Available from: <http://dx.doi.org/10.1038/s41467-018-08028-6>
 81. Spessott WA, Sanmillan ML, McCormick ME, Kulkarni V V., Giraudo CG. SM protein Munc18-2 facilitates transition of Syntaxin 11-mediated lipid mixing to complete fusion for T-lymphocyte cytotoxicity. *Proc Natl Acad Sci U S A.* 2017;114(11):E2176–85.
 82. Bennett MK, Whiteheart SW, Scheller RH, Rothman JE, Söllner TH. A protein assembly-disassembly pathway in vitro that may correspond to sequential steps of synaptic vesicle docking, activation, and fusion. *Cell* [Internet]. 1993;75(3):409–18.
 83. Cotrufo T, Andrés RM, Ros O, Pérez-Brangulí F, Muhaisen A, Fuschini G, et al. Syntaxin 1 is required for DCC/Netrin-1-dependent chemoattraction of migrating neurons from the lower rhombic lip. *Eur J Neurosci.* 2012;36(9):3152–64.
 84. Fuschini G, Cotrufo T, Ros O, Muhaisen A, Andrés R, Comella JX, et al. Syntaxin-1/TI-VAMP SNAREs interact with Trk receptors and are required for neurotrophin-dependent outgrowth. *Oncotarget.* 2018;9(89):35922–40.
 85. Song SJ, Kim SJ, Song MS, Lim DS. Aurora B-mediated phosphorylation of RASSF1A maintains proper cytokinesis by recruiting syntaxin16 to the midzone and midbody. *Cancer Res.* 2009;69(22):8540–4.
 86. Ulloa F, González-Juncà A, Meffre D, Barrecheguren PJ, Martínez-Mármol R, Pazos I, et al. Blockade of the SNARE protein syntaxin 1 inhibits glioblastoma tumor growth. *PLoS One.* 2015;10(3):1–10.
 87. Chen Y, Meng D, Wang H, Sun R, Wang D, Wang S, et al. VAMP8 facilitates cellular proliferation and temozolomide resistance in human glioma cells. *Neuro Oncol.* 2015;17(3):407–18.
 88. Wang L, Brautigan DL. α -SNAP inhibits AMPK signaling to reduce mitochondrial biogenesis and dephosphorylates Thr172 in AMPK α in vitro. *Nat Commun* [Internet]. 2013;4:1559. Available from: <http://dx.doi.org/10.1038/ncomms2565>
 89. Sun Q, Huang X, Zhang Q, Qu J, Shen Y, Wang X, et al. SNAP23 promotes the malignant process of ovarian cancer. *J Ovarian Res* [Internet]. 2016;9(1):1–9. Available from: <http://dx.doi.org/10.1186/s13048-016-0289-9>
 90. Fader CM, Sánchez DG, Mestre MB, Colombo MI. TI-VAMP/VAMP7 and VAMP3/cellubrevin: two v-SNARE proteins involved in specific steps of the autophagy/multivesicular body pathways. *Biochim Biophys Acta - Mol Cell Res* [Internet]. 2009;1793(12):1901–16. Available from: <http://dx.doi.org/10.1016/j.bbamcr.2009.09.011>
 91. Thorburn A, Morgan MJ. Autophagy and cancer therapy. *Autophagy and Cancer.* 2013;(June):191–204.
 92. Itakura E, Kishi-Itakura C, Mizushima N. The hairpin-type tail-anchored SNARE syntaxin 17 targets to autophagosomes for fusion with endosomes/lysosomes. *Cell* [Internet]. 2012;151(6):1256–69. Available from: <http://dx.doi.org/10.1016/j.cell.2012.11.001>
 93. Moreno-Smith M, Halder JB, Meltzer PS, Gonda TA, Mangala LS, Rupaimoole R, et al. ATP11B mediates platinum resistance in ovarian cancer. *J Clin Invest.* 2013;123(5):2119–30.
 94. Riggs KA, Hasan N, Humphrey D, Raleigh C, Nevitt C, Corbin D, et al. Regulation of integrin endocytic recycling and chemotactic cell migration by syntaxin 6 and VAMP3 interaction. *J Cell Sci.* 2012;125(16):3827–39.
 95. Brasher MI, Martynowicz DM, Grafinger OR, Hucik A, Shanks-Skinner E, Uniacke J, et al. Interaction of Munc18c and syntaxin4 facilitates invadopodium formation and extracellular matrix invasion of tumor cells. *J Biol Chem.* 2017;292(39):16199–210.
 96. Williams KC, McNeilly RE, Coppolino MG. SNAP23, Syntaxin4, and vesicle-associated membrane protein 7 (VAMP7) mediate trafficking of membrane type 1-matrix metalloproteinase (MT1-MMP) during invadopodium formation and tumor cell invasion. *Mol Biol Cell.* 2014;25(13):2061–70.
 97. Grafinger OR, Gorshtein G, Stirling T, Brasher MI, Coppolino MG. β 1 integrin-mediated signaling regulates MT1-MMP phosphorylation to promote tumor cell invasion. *J Cell Sci.* 2020;133(9).
 98. Gonon EM, Skalski M, Kean M, Coppolino MG. SNARE-mediated membrane traffic modulates RhoA-regulated focal adhesion formation. *FEBS Lett.* 2005;579(27):6169–78.
 99. Skalski M, Sharma N, Williams K, Kruspe A, Coppolino MG. SNARE-mediated membrane traffic is required for focal adhesion kinase signaling and Src-regulated focal adhesion turnover. *Biochim Biophys Acta - Mol Cell Res* [Internet]. 2011;1813(1):148–58. Available from:

- <http://dx.doi.org/10.1016/j.bbamcr.2010.09.008>
100. Hirose Y, Shirai K, Hirai Y. Membrane-tethered syntaxin-4 locally abrogates E-cadherin function and activates Smad signals, contributing to asymmetric mammary epithelial morphogenesis. *J Cell Biochem*. 2018;119(9):7525–39.
 101. Shirai K, Hagiwara N, Horigome T, Hirose Y, Kadono N, Hirai Y. Extracellularly Extruded Syntaxin-4 Binds to Laminin and Syndecan-1 to Regulate Mammary Epithelial Morphogenesis. *J Cell Biochem*. 2017;118(4):686–98.
 102. Nan H, Han L, Ma J, Yang C, Su R, He J. STX3 represses the stability of the tumor suppressor PTEN to activate the PI3K-Akt-mTOR signaling and promotes the growth of breast cancer cells. *Biochim Biophys Acta - Mol Basis Dis* [Internet]. 2018;1864(5):1684–92. Available from: <https://doi.org/10.1016/j.bbadis.2018.01.031>
 103. Lu M, Forsberg L, Höög A, Juhlin CC, Vukojević V, Larsson C, et al. Heterogeneous expression of SNARE proteins SNAP-23, SNAP-25, Syntaxin1 and VAMP in human parathyroid tissue. *Mol Cell Endocrinol*. 2008;287(1–2):72–80.
 104. Fernández-Nogueira P, Bragado P, Almendro V, Ametller E, Rios J, Choudhury S, et al. Differential expression of neurogenes among breast cancer subtypes identifies high risk patients. *Oncotarget*. 2016;7(5):5313–26.
 105. Giudicessi BA, Ackerman A. Determinants of incomplete penetrance and variable expressivity in heritable cardiac arrhythmia syndromes. *Trans Res*. 2013; 161(1):1–14. Available from: <https://www.ncbi.nlm.nih.gov/pmc/articles/PMC3624763/pdf/nihms412728.pdf>
 106. Teng FYH, Wang Y, Tang BL. The syntaxins. *Genome Biol*. 2001;2(11):1–7.
 107. Yin P, Gandasi NR, Arora S, Omar-Hmeadi M, Saras J, Barg S. Syntaxin clusters at secretory granules in a munc18-bound conformation. *Mol Biol Cell*. 2018;29(22):2700–8.
 108. Gandasi NR, Barg S. Contact-induced clustering of syntaxin and munc18 docks secretory granules at the exocytosis site. *Nat Commun*. 2014;5(May).
 109. Zhou P, Pang ZP, Yang X, Zhang Y, Rosenmund C, Bacaj T, et al. Syntaxin-1 N-peptide and H abc - domain perform distinct essential functions in synaptic vesicle fusion. *EMBO J*. 2013;32(1):159–71.
 110. Ramakrishnan NA, Drescher MJ, Drescher DG. The SNARE complex in neuronal and sensory cells. *Mol Cell Neurosci* [Internet]. 2012;50(1):58–69. Available from: <http://dx.doi.org/10.1016/j.mcn.2012.03.009>
 111. Yang B, Steegmaier M, Gonzalez LC, Scheller RH. nSec1 binds a closed conformation of syntaxin1A. *J Cell Biol*. 2000;148(2):247–52.
 112. Burkhardt P, Hattendorf DA, Weis WI, Fasshauer D. Munc18a controls SNARE assembly through its interaction with the syntaxin N-peptide. *EMBO J*. 2008;27(7):923–33.
 113. Fletcher AI, Shuang R, Giovannucci DR, Zhang L, Bittner MA, Stuenkel EL. Regulation of exocytosis by cyclin-dependent kinase 5 via phosphorylation of Munc18. *J Biol Chem*. 1999;274(7):4027–35.
 114. Lee S, Shin J, Jung Y, Son H, Shin J, Jeong C, et al. Munc18-1 induces conformational changes of syntaxin-1 in multiple intermediates for SNARE assembly. *Sci Rep* [Internet]. 2020;10(1):1–8. Available from: <https://doi.org/10.1038/s41598-020-68476-3>
 115. Stepien KP, Prinslow EA, Rizo J. Munc18-1 is crucial to overcome the inhibition of synaptic vesicle fusion by α SNAP. *Nat Commun* [Internet]. 2019;10(1):1–18. Available from: <http://dx.doi.org/10.1038/s41467-019-12188-4>
 116. Ramalho-Santos J, Moreno RD, Sutovsky P, Chan AWS, Hewitson L, Wessel GM, et al. SNAREs in mammalian sperm: Possible implications for fertilization. *Dev Biol*. 2000;223(1):54–69.
 117. Mayorga LS, Tomes CN, Belmonte SA. Acrosomal exocytosis, a special type of regulated secretion. *IUBMB Life*. 2007;59(4–5):286–92.
 118. Schulz JR, Sasaki JD, Vacquier VD. Increased association of synaptosome-associated protein of 25 kDa with syntaxin and vesicle-associated membrane protein following acrosomal exocytosis of sea urchin sperm. *J Biol Chem*. 1998;273(38):24355–9.
 119. Tsai PS, De Vries KJ, De Boer-Brouwer M, Garcia-Gil N, Van Gestel RA, Colenbrander B, et al. Syntaxin and VAMP association with lipid rafts depends on cholesterol depletion in capacitating sperm cells. *Mol Membr Biol*. 2007;24(4):313–24.
 120. Rodríguez F, Zanetti MN, Mayorga LS, Tomes CN. Munc18-1 controls SNARE protein complex assembly during human sperm acrosomal exocytosis. *J Biol Chem*. 2012;287(52):43825–39.
 121. Ganeshan R, Di A, Nelson DJ, Quick MW, Kirk KL. The interaction between syntaxin 1A and cystic fibrosis transmembrane conductance regulator Cl⁻ channels is mechanistically distinct from syntaxin 1A-SNARE interactions. *J Biol Chem* [Internet]. 2003;278(5):2876–85. Available from:

- <http://dx.doi.org/10.1074/jbc.M211790200>
122. Peters KW, Qi J, Johnson JP, Watkins SC, Frizzell R. Role of snare proteins in CFTR and ENaC trafficking. *Pflugers Arch Eur J Physiol*. 2001;443(SUPPL. 1):65–9.
 123. Von Kanel T, Stanke F, Weber M, Schaller A, Racine J, Kraemer R, et al. Clinical and molecular characterization of the potential CF disease modifier syntaxin 1A. *Eur J Hum Genet*. 2013;21(12):1462–6.
 124. Naren AP, Quick MW, Collawn JF, Nelson DJ, Kirk KL. Syntaxin 1A inhibits CFTR chloride channels by means of domain-specific protein-protein interactions. *Proc Natl Acad Sci U S A*. 1998;95(18):10972–7.
 125. Sheu L, Pasyk EA, Ji J, Huang X, Gao X, Varoqueaux F, et al. Regulation of insulin exocytosis by Munc13-1. *J Biol Chem*. 2003;278(30):27556–63.
 126. Ohara-Imaizumi M, Nishiwaki C, Nakamichi Y, Kikuta T, Nagai S, Nagamatsu S. Correlation of syntaxin-1 and SNAP-25 clusters with docking and fusion of insulin granules analysed by total internal reflection fluorescence microscopy. *Diabetologia*. 2004;47(12):2200–7.
 127. Dong Y, Wan Q, Yang X, Bai L, Xu P. Interaction of Munc18 and Syntaxin in the regulation of insulin secretion. *Biochem Biophys Res Commun*. 2007;360(3):609–14.
 128. Leung YM, Kang Y, Xia F, Sheu L, Gao X, Xie H, et al. Open form of syntaxin-1A is a more potent inhibitor than wild-type syntaxin-1A of Kv2.1 channels. *Biochem J*. 2005;387(1):195–202.
 129. Leung YM, Kang Y, Gao X, Xia F, Xie H, Sheu L, et al. Syntaxin 1A binds to the cytoplasmic C terminus of Kv2.1 to regulate channel gating and trafficking. *J Biol Chem*. 2003;278(19):17532–8.
 130. Cui N, Kang Y, He Y, Leung YM, Xie H, Pasyk EA, et al. H3 domain of syntaxin 1A inhibits KATP channels by its actions on the sulfonylurea receptor 1 nucleotide-binding folds-1 and -2. *J Biol Chem*. 2004;279(51):53259–65.
 131. Kang Y, Huang X, Pasyk EA, Ji J, Holz GG, Wheeler MB, et al. Syntaxin-3 and Syntaxin-1A inhibit L-type calcium channel activity, insulin biosynthesis and exocytosis in beta-cell lines. *Diabetologia*. 2002;45(2):231–41.
 132. Lam PPL, Leung YM, Sheu L, Ellis J, Tsushima RG, Osborne LK, et al. Transgenic mouse overexpressing syntaxin-1A as a diabetes model. *Diabetes*. 2005;54(9):2744–54.
 133. Communication S. Syntaxin-1a is a Direct Target of miR-29a in Insulin-producing β -Cells. :463–6.
 134. Nagamatsu S, Nakamichi Y, Yamamura C, Matsushima S, Watanabe T, Ozawa S, et al. Decreased expression of t-SNARE, syntaxin 1, and SNAP-25 in pancreatic β -cells is involved in impaired insulin secretion from diabetic GK rat islets: Restoration of decreased t-SNARE proteins improves impaired insulin secretion. *Diabetes*. 1999;48(12):2367–73.
 135. Tsunoda K, Sanke T, Nakagawa T, Furuta H, Nanjo K. Single nucleotide polymorphism (D68D, T to C) in the syntaxin 1A gene correlates to age at onset and insulin requirement in Type II diabetic patients. *Diabetologia*. 2001;44(11):2092–7.
 136. Diao CY, Guo HB, Ouyang YR, Zhang HC, Liu LH, Bu J, et al. Screening for metastatic osteosarcoma biomarkers with a DNA microarray. *Asian Pacific J Cancer Prev*. 2014;15(4):1817–22.
 137. Yang J, Hou Z, Wang C, Wang H, Zhang H. Gene expression profiles reveal key genes for early diagnosis and treatment of adamantinomatous craniopharyngioma. *Cancer Gene Ther [Internet]*. 2018;25(9–10):227–39. Available from: <http://dx.doi.org/10.1038/s41417-018-0015-4>
 138. Kővári B, Turkevi-nagy S, Báthori Á, Fekete Z, Krenács L. Syntaxin 1: A novel robust immunophenotypic marker of neuroendocrine tumors. *Int J Mol Sci*. 2020;21(4):1–13.
 139. Graff L, Castrop F, Bauer M, Höfler H, Gratzl M. Expression of vesicular monoamine transporters, synaptosomal-associated protein 25 and syntaxin1: A signature of human small cell lung carcinoma. *Cancer Res*. 2001;61(5):2138–44.
 140. Raja SA, Abbas S, Shah STA, Tariq A, Bibi N, Yousuf A, et al. Increased expression levels of syntaxin 1a and synaptobrevin 2/vesicle-associated membrane protein-2 are associated with the progression of bladder cancer. *Genet Mol Biol*. 2019;42(1):40–7.
 141. Ribes J, Esteban L, Clèries R, Galceran J, Marcos-Gragera R, Gispert R, et al. Cancer incidence and mortality projections up to 2020 in Catalonia by means of Bayesian models. *Clin Transl Oncol*. 2014;16(8):714–24.
 142. Koczkodaj P, Sulowska U, Gotlib J, Mańczuk M. Breast cancer mortality trends in Europe among women in perimenopausal and postmenopausal age (45+). *Arch Med Sci*. 2020;16(1):146–56.
 143. Harbeck N, Penault-Llorca F, Cortes J, Gnant M, Houssami N, Poortmans P, et al. Breast cancer. Vol. 5, *Nature Reviews Disease Primers*. 2019.
 144. Viale G. The current state of breast cancer classification. *Ann Oncol*. 2012;23(SUPPL. 10).

145. Malhotra GK, Zhao X, Band H, Band V. Histological, molecular and functional subtypes of breast cancers. *Cancer Biol Ther*. 2010;10(10):955–60.
146. van Seijen M, Lips EH, Thompson AM, Nik-Zainal S, Futreal A, Hwang ES, et al. Ductal carcinoma in situ: to treat or not to treat, that is the question. *Br J Cancer* [Internet]. 2019;121(4):285–92. Available from: <http://dx.doi.org/10.1038/s41416-019-0478-6>
147. Widomska Justyna. HHS Public Access. *Physiol Behav*. 2017;176(5):139–48.
148. Luveta J, Parks RM, Heery DM, Cheung K-L, Johnston SJ. Invasive Lobular Breast Cancer as a Distinct Disease: Implications for Therapeutic Strategy. *Oncol Ther* [Internet]. 2020;8(1):1–11. Available from: <https://doi.org/10.1007/s40487-019-00105-0>
149. McCart Reed AE, Kutasovic JR, Vargas AC, Jayanthan J, Al-Murrani A, Reid LE, et al. An epithelial to mesenchymal transition programme does not usually drive the phenotype of invasive lobular carcinomas. *J Pathol*. 2016;238(4):489–94.
150. Szymiczek A, Lone A, Akbari MR. Molecular intrinsic versus clinical subtyping in breast cancer: A comprehensive review. *Clin Genet*. 2020;(November):1–25.
151. Reis-Filho JS, Pusztai L. Gene expression profiling in breast cancer: Classification, prognostication, and prediction. *Lancet*. 2011;378(9805):1812–23.
152. Perou CM, Sørlie T, Eisen MB, Rijn M Van De, Jeffrey SS, Rees CA, et al. Molecular portraits of human breast tumours. *letters to nature* 748. *Nature* [Internet]. 2000;533(May):747–52. Available from: www.stanford.edu/molecularportraits/
153. Sørlie T, Perou CM, Tibshirani R, Aas T, Geisler S, Johnsen H, et al. Gene expression patterns of breast carcinomas distinguish tumor subclasses with clinical implications. *Proc Natl Acad Sci U S A*. 2001;98(19):10869–74.
154. Bernard PS, Parker JS, Mullins M, Cheung MCU, Leung S, Voduc D, et al. Supervised risk predictor of breast cancer based on intrinsic subtypes. *J Clin Oncol*. 2009;27(8):1160–7.
155. Koboldt DC, Fulton RS, McLellan MD, Schmidt H, Kalicki-Veizer J, McMichael JF, et al. Comprehensive molecular portraits of human breast tumours. *Nature*. 2012;490(7418):61–70.
156. Eroles P, Bosch A, Alejandro Pérez-Fidalgo J, Lluch A. Molecular biology in breast cancer: Intrinsic subtypes and signaling pathways. *Cancer Treat Rev* [Internet]. 2012;38(6):698–707. Available from: <http://dx.doi.org/10.1016/j.ctrv.2011.11.005>
157. Prat A, Pineda E, Adamo B, Galván P, Fernández A, Gaba L, et al. Clinical implications of the intrinsic molecular subtypes of breast cancer. *Breast*. 2015;24:S26–35.
158. Prat A, Perou CM. Deconstructing the molecular portraits of breast cancer. *Mol Oncol*. 2011;5(1):5–23.
159. Fernández-Nogueira P, Bragado P, Almendro V, Ametller E, Rios J, Choudhury S, et al. Differential expression of neurogenes among breast cancer subtypes identifies high risk patients. *Oncotarget* [Internet]. 2015;7(5). Available from: <http://www.ncbi.nlm.nih.gov/pubmed/26673618>
160. Dedić Plavetić N, Kulić A, Vrbanc D. Role of HER2 signaling pathway in breast cancer: Biology, detection and therapeutical implications. *Period Biol*. 2012;114(4):505–10.
161. Roskoski R. The ErbB/HER family of protein-tyrosine kinases and cancer. *Pharmacol Res* [Internet]. 2014;79:34–74. Available from: <http://dx.doi.org/10.1016/j.phrs.2013.11.002>
162. Roepstorff K, Grøvdal L, Grandal M, Lerdrup M, Van Deurs B. Endocytic downregulation of ErbB receptors: Mechanisms and relevance in cancer. *Histochem Cell Biol*. 2008;129(5):563–78.
163. Moore M, Cook N, Frese K. Assessing the role of the EGF receptor in the development and progression of pancreatic cancer. *Gastrointest Cancer Targets Ther*. 2014;23.
164. Vu T, Claret FX. Trastuzumab: Updated mechanisms of action and resistance in breast cancer. *Front Oncol*. 2012;2 JUN(May).
165. Sorkin A, Goh LK. Endocytosis and intracellular trafficking of ErbBs. *Exp Cell Res*. 2008;314(17):3093–106.
166. Fry WHD, Simion C, Sweeney C, Carraway KL. Quantity Control of the ErbB3 Receptor Tyrosine Kinase at the Endoplasmic Reticulum. *Mol Cell Biol*. 2011;31(14):3009–18.
167. Sak MM, Breen K, Rønning SB, Pedersen NM, Bertelsen V, Stang E, et al. The oncoprotein ErbB3 is endocytosed in the absence of added ligand in a clathrin-dependent manner. *Carcinogenesis*. 2012;33(5):1031–9.
168. Jeong J, Kim W, Kim LK, Van Houten J, Wysolmerski JJ. HER2 signaling regulates HER2 localization and membrane retention. *PLoS One*. 2017;12(4):1–16.
169. Bertelsen V, Stang E. The mysterious ways of ErbB2/HER2 trafficking. *Membranes (Basel)*. 2014;4(3):424–46.

170. Helfand BT, Mendez MG, Pugh J, Delsert C, Goldman RD. Maintaining the Shape of Nerve Cells □. *Mol Biol Cell*. 2003;14(December):5069–81.
171. Worthylake R, Opresko LK, Wiley HS. ErbB-2 amplification inhibits down-regulation and induces constitutive activation of both ErbB-2 and epidermal growth factor receptors. *J Biol Chem* [Internet]. 1999;274(13):8865–74. Available from: <http://dx.doi.org/10.1074/jbc.274.13.8865>
172. Meric-Bernstam F, Johnson AM, Ileana Dumbrava EE, Raghav K, Balaji K, Bhatt M, et al. Advances in HER2-targeted therapy: Novel agents and opportunities beyond breast and gastric cancer. *Clin Cancer Res*. 2019;25(7):2033–41.
173. Wang J, Xu B. Targeted therapeutic options and future perspectives for her2-positive breast cancer. *Signal Transduct Target Ther* [Internet]. 2019;4(1). Available from: <http://dx.doi.org/10.1038/s41392-019-0069-2>
174. Ménard S, Balsari A, Pupa SM, Tagliabue E, Campiglio M. Activity and resistance of trastuzumab according to different clinical settings. *Cancer Treat Rev* [Internet]. 2011;38(3):212–7. Available from: <http://dx.doi.org/10.1016/j.ctrv.2011.06.002>
175. Gajria D, Chandarlapaty S. HER2-amplified breast cancer: Mechanisms of trastuzumab resistance and novel targeted therapies. *Expert Rev Anticancer Ther*. 2011;11(2):263–75.
176. Oh DY, Bang YJ. HER2-targeted therapies — a role beyond breast cancer. *Nat Rev Clin Oncol* [Internet]. 2020;17(1):33–48. Available from: <http://dx.doi.org/10.1038/s41571-019-0268-3>
177. De Placido S, Rosa R, Raimondo L, D’Amato V, Giuliano M, Bianco R, et al. Mechanisms of lapatinib resistance in HER2-driven breast cancer. *Cancer Treat Rev*. 2015;41(10):877–83.
178. Di Modica M, Tagliabue E, Triulzi T. Predicting the Efficacy of HER2-Targeted Therapies: A Look at the Host. *Dis Markers*. 2017;2017(subdomain II).
179. D’Amato V, Raimondo L, Formisano L, Giuliano M, De Placido S, Rosa R, et al. Mechanisms of lapatinib resistance in HER2-driven breast cancer. *Cancer Treat Rev* [Internet]. 2015;41(10):877–83. Available from: <http://dx.doi.org/10.1016/j.ctrv.2015.08.001>
180. Chen FL, Xia W, Spector NL. Acquired resistance to small molecule ErbB2 tyrosine kinase inhibitors. *Clin Cancer Res*. 2008;14(21):6730–4.
181. Eiermann W. Symposium article Trastuzumab combined with chemotherapy for the treatment of. *Ann Oncol* [Internet]. 2001;12:57–62. Available from: https://doi.org/10.1093/annonc/12.suppl_1.S57
182. Nahta R, Esteva FJ. HER2 therapy: Molecular mechanisms of trastuzumab resistance. *Breast Cancer Res*. 2006;8(6):1–8.
183. Gao JJ, Swain SM. Luminal A Breast Cancer and Molecular Assays: A Review. *Oncologist*. 2018;23(5):556–65.
184. Hilton HN, Clarke CL, Graham JD. Estrogen and progesterone signalling in the normal breast and its implications for cancer development. Vol. 466, *Molecular and Cellular Endocrinology*. 2018. p. 2–14.
185. Saha T, Makar S, Swetha R, Gutti G, Singh SK. Estrogen signaling: An emanating therapeutic target for breast cancer treatment. *Eur J Med Chem* [Internet]. 2019;177:116–43. Available from: <https://doi.org/10.1016/j.ejmech.2019.05.023>
186. Cenciarini ME, Proietti CJ. Molecular mechanisms underlying progesterone receptor action in breast cancer: Insights into cell proliferation and stem cell regulation. *Steroids*. 2019;152(June).
187. Brisken C. Progesterone signalling in breast cancer: A neglected hormone coming into the limelight. *Nat Rev Cancer*. 2013;13(6):385–96.
188. Thomas C, Gustafsson JÅ. Progesterone receptor-estrogen receptor crosstalk: A novel insight. *Trends Endocrinol Metab*. 2015;26(9):453–4.
189. Haque MM, Desai K V. Pathways to Endocrine Therapy Resistance in Breast Cancer. *Front Endocrinol (Lausanne)*. 2019;10(August):1–7.
190. Li F, Dou J, Wei L, Li S, Liu J. The selective estrogen receptor modulators in breast cancer prevention. *Cancer Chemother Pharmacol*. 2016;77(5):895–903.
191. Nathan MR, Schmid P. A Review of Fulvestrant in Breast Cancer. *Oncol Ther*. 2017;5(1):17–29.
192. Hanker AB, Sudhan DR, Arteaga CL. Overcoming Endocrine Resistance in Breast Cancer. *Cancer Cell*. 2020;37(4):496–513.
193. Ali S, Rasool M, Chaoudhry H, Pushparaj PN, Jha P, Hafiz A, et al. Molecular mechanisms and mode of tamoxifen resistance in breast cancer. *Bioinformation* [Internet]. 2016;12(3):135–9. Available from: <https://www.ncbi.nlm.nih.gov/pmc/articles/PMC5267957/pdf/97320630012135.pdf>
194. Yin L, Duan JJ, Bian XW, Yu SC. Triple-negative breast cancer molecular subtyping and treatment

- progress. *Breast Cancer Res.* 2020;22(1):1–13.
195. Macdonald S, Oncology R, General M. Breast Cancer [Internet]. Vol. 70, *Journal of the Royal Society of Medicine.* 2016. 515–517 p. Available from: <https://www2.tri-kobe.org/nccn/guideline/breast/english/breast.pdf>
 196. Kumar P, Aggarwal R. An overview of triple-negative breast cancer. *Arch Gynecol Obstet.* 2016;293(2):247–69.
 197. da Silva JL, Cardoso Nunes NC, Izetti P, de Mesquita GG, de Melo AC. Triple negative breast cancer: A thorough review of biomarkers. *Crit Rev Oncol Hematol* [Internet]. 2020;145(August 2019):102855. Available from: <https://doi.org/10.1016/j.critrevonc.2019.102855>
 198. Prat A, Guo H, Ganesan P, Parker JS, Gao M, Moulder S, et al. Phenotypic and molecular characterization of the claudin-low intrinsic subtype of breast cancer. *Breast Cancer Res* [Internet]. 2010;12(5):68–86. Available from: <http://breast-cancer-research.com/content/12/5/R68%0ARESEARCH>
 199. Lehmann BD, Bauer JA, Chen X, Sanders ME, Chakravarthy AB, Shyr Y, et al. Identification of human triple-negative breast cancer subtypes and preclinical models for selection of targeted therapies. *J Clin Invest.* 2011;121(7):2750–67.
 200. Lehmann BD, Jovanović B, Chen X, Estrada M V., Johnson KN, Shyr Y, et al. Refinement of triple-negative breast cancer molecular subtypes: Implications for neoadjuvant chemotherapy selection. *PLoS One.* 2016;11(6):1–22.
 201. Lyons TG. Targeted Therapies for Triple-Negative Breast Cancer. *Curr Treat Options Oncol.* 2019;20(11).
 202. Waks AG, Winer EP. Breast Cancer Treatment: A Review. *JAMA - J Am Med Assoc.* 2019;321(3):288–300.
 203. Jafari SH, Saadatpour Z, Salmaninejad A, Momeni F, Mokhtari M, Nahand JS, et al. Breast cancer diagnosis: Imaging techniques and biochemical markers. *J Cell Physiol.* 2018;233(7):5200–13.
 204. Yilmaz MT, Elmali A, Yazici G. Abscopal Effect, From Myth to Reality: From Radiation Oncologists' Perspective. *Cureus.* 2019;11(1):9–13.
 205. Shagufta, Ahmad I. Tamoxifen a pioneering drug: An update on the therapeutic potential of tamoxifen derivatives. Vol. 143, *European Journal of Medicinal Chemistry.* 2018. p. 515–31.
 206. Chen A. PARP inhibitors: its role in treatment of cancer. *Chin J Cancer.* 2011;30(7):463–71.
 207. Bose P, Brockton NT, Dort JC. Head and neck cancer: From anatomy to biology. *Int J Cancer.* 2013;133(9):2013–23.
 208. Johnson DE, Burtness B, Leemans CR, Lui VWY, Bauman JE, Grandis JR. Head and neck squamous cell carcinoma. *Nat Rev Dis Prim.* 2020;6(1).
 209. Leemans CR, Snijders PJF, Brakenhoff RH. The molecular landscape of head and neck cancer. *Nat Rev Cancer.* 2018;18(5):269–82.
 210. Asociación Española Contra el Cáncer. Datos Cáncer de Mama 2019. *Asoc Española Contra el Cáncer* [Internet]. 2020;1–5. Available from: https://www.aecc.es/sites/default/files/content-file/Datos-cancer-mama_2019_0.pdf
 211. Asociación Española Contra el Cáncer. Observatorio AECC.
 212. Yang D, Shi Y, Tang Y, Yin H, Guo Y, Wen S, et al. Effect of HPV infection on the occurrence and development of laryngeal cancer: A review. *J Cancer.* 2019;10(19):4455–62.
 213. Alshafi E, Begg K, Amelio I, Raulf N, Lucarelli P, Sauter T, et al. Clinical update on head and neck cancer: molecular biology and ongoing challenges. *Cell Death Dis.* 2019;10(8).
 214. Marur S, Forastiere AA. Head and Neck Squamous Cell Carcinoma: Update on Epidemiology, Diagnosis, and Treatment. *Mayo Clin Proc* [Internet]. 2016;91(3):386–96. Available from: <http://dx.doi.org/10.1016/j.mayocp.2015.12.017>
 215. Karam SD, Raben D. Radioimmunotherapy for the treatment of head and neck cancer. *Lancet Oncol* [Internet]. 2019;20(8):e404–16. Available from: [http://dx.doi.org/10.1016/S1470-2045\(19\)30306-7](http://dx.doi.org/10.1016/S1470-2045(19)30306-7)
 216. Longley DB, Harkin DP, Johnston PG. 5-Fluorouracil: Mechanisms of action and clinical strategies. *Nat Rev Cancer.* 2003;3(5):330–8.
 217. Weaver BA. How Taxol/paclitaxel kills cancer cells. *Mol Biol Cell.* 2014;25(18):2677–81.
 218. Coarfa C, Florentin D, Putluri NR, Ding Y, Au J, He D, et al. Influence of the neural microenvironment on prostate cancer. *Prostate.* 2018;78(2):128–39.
 219. Garcia-Recio S, Pastor-Arroyo EM, Marín-Aguilera M, Almendro V, Gascón P. The transmodulation of HER2 and EGFR by substance P in breast cancer cells requires c-Src and metalloproteinase activation. *PLoS One.* 2015;10(6):1–15.

220. Garcia-Recio S, Fuster G, Fernandez-Nogueira P, Pastor-Arroyo EM, Park SY, Mayordomo C, et al. Substance P autocrine signaling contributes to persistent HER2 activation that drives malignant progression and drug resistance in breast cancer. *Cancer Res.* 2013;73(21):6424–34.
221. Mayordomo C, García-Recio S, Ametller E, Fernández-Nogueira P, Pastor-Arroyo EM, Vinyals L, et al. Targeting of substance P induces cancer cell death and decreases the steady state of EGFR and Her2. *J Cell Physiol.* 2012;227(4):1358–66.
222. Recalde-Percaz L. Neuropilin-2 role in the regulation of disseminated tumour cells dormancy and metastasis in breast and head and neck cancer. *Universitat de Barcelona*; 2021.
223. Moragas-Garcia N. Paper dels factors neuronals SEMA3F i NTN1 en la transició de càncer de mama in situ a invasiu. *Universitat de Barcelona*; 2021.
224. Fernández-Nogueira P, Noguera-Castells A, Fuster G, Recalde-Percaz L, Moragas N, López-Plana A, et al. Histamine receptor 1 inhibition enhances antitumor therapeutic responses through extracellular signal-regulated kinase (ERK) activation in breast cancer. *Cancer Lett.* 2018;424:70–83.
225. Luo X, Tu T, Zhong Y, Xu S, Chen X, Chen L, et al. ceRNA Network Analysis Shows That lncRNA CRNDE Promotes Progression of Glioblastoma Through Sponge mir-9-5p. *Front Genet.* 2021;12(March):1–15.
226. Grabowski P, Schönfelder J, Ahnert-Hilger G, Foss HD, Heine B, Schindler I, et al. Expression of neuroendocrine markers: A signature of human undifferentiated carcinoma of the colon and rectum. *Virchows Arch.* 2002;441(3):256–63.
227. Curtis C, Shah SP, Chin SF, Turashvili G, Rueda OM, Dunning MJ, et al. The genomic and transcriptomic architecture of 2,000 breast tumours reveals novel subgroups. *Nature.* 2012;486(7403):346–52.
228. Pereira B, Chin SF, Rueda OM, Vollan HKM, Provenzano E, Bardwell HA, et al. The somatic mutation profiles of 2,433 breast cancers refines their genomic and transcriptomic landscapes. *Nat Commun.* 2016;7(May).
229. Hoadley KA, Yau C, Hinoue T, Wolf DM, Lazar AJ, Drill E, et al. Cell-of-Origin Patterns Dominate the Molecular Classification of 10,000 Tumors from 33 Types of Cancer. *Cell.* 2018;173(2):291-304.e6.
230. Subramanian A, Tamayo P, Mootha VK, Mukherjee S, Ebert BL, Gillette MA, et al. Gene set enrichment analysis: A knowledge-based approach for interpreting genome-wide expression profiles. *Proc Natl Acad Sci U S A.* 2005;102(43):15545–50.
231. Ringnér M, Fredlund E, Häkkinen J, Borg Å, Staaf J. GOBO: Gene expression-based outcome for breast cancer online. *PLoS One.* 2011;6(3):1–11.
232. Nakayama T, Mikoshiba K, Akagawa K. The cell- and tissue-specific transcription mechanism of the TATA-less syntaxin 1A gene. *FASEB J.* 2016;30(2):525–43.
233. Nakayama T, Akagawa K. Transcription regulation mechanism of the syntaxin 1A gene via protein kinase A. *Biochem J* [Internet]. 2017;474(14):2465–73. Available from: <http://biochemj.org/lookup/doi/10.1042/BCJ20170249>
234. Nakayama T, Fukutomi T, Terao Y, Akagawa K. Syntaxin 1A gene is negatively regulated in a cell/tissue specific manner by YY1 transcription factor, which binds to the –183 to –137 promoter region together with gene silencing factors including histone deacetylase. *Biomolecules.* 2021;11(2):1–10.
235. Ghandi M, Huang FW, Jané-Valbuena J, Kryukov G V., Lo CC, McDonald ER, et al. Next-generation characterization of the Cancer Cell Line Encyclopedia. *Nature* [Internet]. 2019;569(7757):503–8. Available from: <http://dx.doi.org/10.1038/s41586-019-1186-3>
236. Pruitt KD, Tatusova T, Maglott DR. NCBI Reference Sequence (RefSeq): A curated non-redundant sequence database of genomes, transcripts and proteins. *Nucleic Acids Res.* 2005;33(DATABASE ISS.):501–4.
237. Fishilevich S, Nudel R, Rappaport N, Hadar R, Plaschkes I, Iny Stein T, et al. GeneHancer: genome-wide integration of enhancers and target genes in GeneCards. *Database (Oxford).* 2017;2017:1–17.
238. Gardiner-Garden M, Frommer M. CpG islands in vertebrate genomes. *J Mol Biol.* 1987;196:261–82.
239. Dunham I, Kundaje A, Aldred SF, Collins PJ, Davis CA, Doyle F, et al. An integrated encyclopedia of DNA elements in the human genome. *Nature.* 2012;489(7414):57–74.
240. Ossowski L, Russo H, Gartner M, Wilson EL. Growth of a human carcinoma (HEp3) in nude mice: Rapid and efficient metastasis. *J Cell Physiol.* 1987;133(2):288–96.
241. Dai X, Cheng H, Bai Z, Li J. Breast cancer cell line classification and Its relevance with breast tumor subtyping. *J Cancer.* 2017;8(16):3131–41.

242. Cotrufo T, Pérez-Brangulí F, Muhaisen A, Ros O, Andrés R, Baeriswyl T, et al. A signaling mechanism coupling netrin-1/deleted in colorectal cancer chemoattraction to SNARE-mediated exocytosis in axonal growth cones. *J Neurosci*. 2011;31(41):14463–80.
243. Dharmacon. DharmaFECT™ Transfection Reagents siRNA Transfection Protocol. siRNA Transfection Protoc. 2014;4.
244. Uder S, George H, Boedeker B. MISSION™ shRNA Library: Next Generation RNA Interference. Order [Internet]. 1998;6:1–6. Available from: http://www.sigmaaldrich.com/etc/medialib/docs/Sigma/General_Information/vol6_iss2_mission_shrna.Par.0001.File.tmp/vol6_iss2_mission_shrna.pdf
245. Jiang F, Doudna JA. CRISPR – Cas9 Structures and Mechanisms. 2017;505–31.
246. Gupta D, Bhattacharjee O, Mandal D, Sen MK, Dey D, Dasgupta A, et al. CRISPR-Cas9 system: A new-fangled dawn in gene editing. *Life Sci* [Internet]. 2019;232(June):116636. Available from: <https://doi.org/10.1016/j.lfs.2019.116636>
247. Bartha Á, Gyórfy B. Tnmplot.Com: A web tool for the comparison of gene expression in normal, tumor and metastatic tissues. *Int J Mol Sci*. 2021;22(5):1–12.
248. Sciences HA of. Kaplan-Meier Plotter [Internet]. 2010. Available from: <http://kmplot.com/analysis/>
249. World Health Organisation. Latest global cancer data: Cancer burden rises to 19.3 million new cases and 10.0 million cancer deaths in 2020. *Int Agency Res Cancer*. 2020;(december):13–5.
250. Chang XS, Arancillo M, Wu XY, Trimbuch XT, Rosenmund XC. Distinct Functions of Syntaxin-1 in Neuronal Maintenance , Synaptic Vesicle Docking , and Fusion in Mouse Neurons. 2016;36(30):7911–24.
251. Bagge A, Dahmcke CM, Dalgaard LT. Syntaxin-1a is a Direct Target of miR-29a in Insulin- producing β -Cells. *Horm Metab Res*. 2013;45(6):463–6.
252. Zombori T, Turkevi-Nagy S, Sejben A, Juhász-Nagy G, Cserni G, Furák J, et al. The panel of syntaxin 1 and insulinoma-associated protein 1 outperforms classic neuroendocrine markers in pulmonary neuroendocrine neoplasms. *Apmis*. 2021;129(4):186–94.
253. David P, El Far O, Martin-Mouto N, Poupon MF, Takahashi M, Seagar MJ. Expression of synaptotagmin and syntaxin associated with N-type calcium channels in small cell lung cancer. *FEBS Lett*. 1993;326(1–3):135–9.
254. Zou J, Duan D, Yu C, Pan J, Xia J, Yang Z, et al. Mining the potential prognostic value of synaptosomal-associated protein 25 (SNAP25) in colon cancer based on stromal-immune score. *PeerJ*. 2020;8:1–18.
255. Tang BL, Gee HY, Lee MG. The Cystic Fibrosis Transmembrane Conductance Regulator’s Expanding SNARE Interactome. *Traffic*. 2011;12(4):364–71.
256. Wang H, Ishizaki R, Kobayashi E, Fujiwara T, Akagawa K, Izumi T. Loss of granuphilin and loss of syntaxin-1A cause differential effects on insulin granule docking and fusion. *J Biol Chem* [Internet]. 2011;286(37):32244–50. Available from: <http://dx.doi.org/10.1074/jbc.M111.268631>
257. Bollig-Fischer A, Dewey TG, Ethier SP. Oncogene activation induces metabolic transformation resulting in insulin-independence in human breast cancer cells. *PLoS One*. 2011;6(3).
258. Jung Y, Yong S, Kim P, Lee HY, Jung Y, Keum J, et al. VAMP2-NRG1 fusion gene is a novel oncogenic driver of non-small-cell lung adenocarcinoma. *J Thorac Oncol* [Internet]. 2015;10(7):1107–11. Available from: <http://dx.doi.org/10.1097/JTO.0000000000000544>
259. Lau SK, Boutros PC, Pintilie M, Blackhall FH, Zhu CQ, Strumpf D, et al. Three-gene prognostic classifier for early-stage non-small-cell lung cancer. *J Clin Oncol*. 2007;25(35):5562–9.
260. Chen Y, Shen L, Chen B, Han X, Yu Y, Yuan X, et al. The predictive prognostic values of CBFA2T3, STX3, DENR, EGLN1, FUT4, and PCDH7 in lung cancer. *Ann Transl Med*. 2021;9(10):843–843.
261. Huan M, Peijun W, Yuan L, Yan Y, Shuhui Z, Yuqiang G. Decreased expression of serum miR-647 is associated with poor prognosis in gastric cancer. *Int J Clin Exp Pathol*. 2019;12(7):2552–8.
262. Peak TC, Su Y, Chapple AG, Chyr J, Deep G. Syntaxin 6: A novel predictive and prognostic biomarker in papillary renal cell carcinoma. *Sci Rep* [Internet]. 2019;9(1):1–11. Available from: <http://dx.doi.org/10.1038/s41598-019-39305-z>
263. Lu E, Ren B, Zheng X, Wu Y, Xu L, Luo J, et al. SNAP23 suppresses cervical cancer progression via modulating the cell cycle. *Gene* [Internet]. 2018;673(May):217–24. Available from: <https://doi.org/10.1016/j.gene.2018.06.028>
264. Zhang N, Zhang SW. Identification of differentially expressed genes between primary lung cancer and lymph node metastasis via bioinformatic analysis. *Oncol Lett*. 2019;18(4):3754–68.
265. Khawaja A, Yousuf A, Tariq A, Mehmood A, Shah STA, Khan MJ, et al. Increased expression levels

- of Syntaxin 1A and Synaptobrevin 2/Vesicle-Associated Membrane Protein-2 are associated with the progression of bladder cancer. *Genet Mol Biol.* 2019;47:40–7.
266. Komatsu H, Kakehashi A, Nishiyama N, Izumi N, Mizuguchi S, Yamano S, et al. Complexin-2 (CPLX2) as a potential prognostic biomarker in human lung high grade neuroendocrine tumors. *Cancer Biomarkers.* 2013;13(3):171–80.
267. Wei B, Wang R, Wang L, Du C. Prognostic factor identification by analysis of the gene expression and DNA methylation data in glioma. *Math Biosci Eng.* 2020;17(4):3909–24.
268. Giovannone AJ, Winterstein C, Bhattaram P, Reales E, Low SH, Baggs JE, et al. Soluble syntaxin 3 functions as a transcriptional regulator. *J Biol Chem.* 2018;293(15):5478–91.
269. Manca P, Mameli O, Caria MA, Torrejón-Escribano B, Blasi J. Distribution of SNAP25, VAMP1 and VAMP2 in mature and developing deep cerebellar nuclei after estrogen administration. *Neuroscience.* 2014;266:102–15.
270. Weiss JM, Hüller H, Polack S, Friedrich M, Diedrich K, Treeck O, et al. Estradiol differentially modulates the exocytotic proteins SNAP-25 and munc-18 pituitary gonadotrophs. *J Mol Endocrinol.* 2007;38(1–2):305–14.
271. Jacobsson G, Razani H, Ögren SO, Meister B. Estrogen down-regulates mRNA encoding the exocytotic protein SNAP-25 in the rat pituitary gland. *J Neuroendocrinol.* 1998;10(3):157–63.
272. Stahl AM, Ruthel G, Torres-Melendez E, Kenny TA, Panchal RG, Bavari S. Primary cultures of embryonic chicken neurons for sensitive cell-based assay of botulinum neurotoxin: Implications for therapeutic discovery. *J Biomol Screen.* 2007;12(3):370–7.
273. Hsu CC, Li HP, Hung YH, Leu YW, Wu WH, Wang FS, et al. Targeted methylation of CMV and E1A viral promoters. *Biochem Biophys Res Commun* [Internet]. 2010;402(2):228–34. Available from: <http://dx.doi.org/10.1016/j.bbrc.2010.09.131>
274. Wu X, Kriz AJ, Sharp PA. Target specificity of the CRISPR-Cas9 system. *Quant Biol.* 2014;2(2):59–70.
275. Montalto FI, De Amicis F. Cyclin D1 in Cancer: A Molecular Connection for Cell Cycle Control, Adhesion and Invasion in Tumor and Stroma. *Cells.* 2020;9(12):1–15.
276. Zhou Y, Liu L, Liu Y, Zhou P, Yan Q, Yu H, et al. Implication of human endogenous retrovirus W family envelope in hepatocellular carcinoma promotes MEK/ERK-mediated metastatic invasiveness and doxorubicin resistance. *Cell Death Discov* [Internet]. 2021;7(1). Available from: <http://dx.doi.org/10.1038/s41420-021-00562-5>
277. Yang CM, Ji S, Li Y, Fu LY, Jiang T, Meng FD. β -Catenin promotes cell proliferation, migration, and invasion but induces apoptosis in renal cell carcinoma. Vol. 10, *OncoTargets and Therapy.* 2017. p. 711–24.
278. García-Gutiérrez L, Delgado MD, León J. Myc oncogene contributions to release of cell cycle brakes. *Genes (Basel).* 2019;10(3).
279. Lin SY, Makino K, Xia W, Matin A, Wen Y, Kwong KY, et al. Nuclear localization of EGF receptor and its potential new role as a transcription factor. *Nat Cell Biol.* 2001;3(9):802–8.
280. Huang CC, Lee CC, Lin HH, Chang JY. Cathepsin S attenuates endosomal EGFR signalling: A mechanical rationale for the combination of cathepsin S and EGFR tyrosine kinase inhibitors. *Sci Rep* [Internet]. 2016;6(June):1–12. Available from: <http://dx.doi.org/10.1038/srep29256>
281. Wang Y, Pennock S, Chen X, Wang Z. Endosomal Signaling of Epidermal Growth Factor Receptor Stimulates Signal Transduction Pathways Leading to Cell Survival. *Mol Cell Biol.* 2002;22(20):7279–90.
282. Parachoniak CA, Park M. Dynamics of receptor trafficking in tumorigenicity. *Trends Cell Biol* [Internet]. 2012;22(5):231–40. Available from: <http://dx.doi.org/10.1016/j.tcb.2012.02.002>
283. Wang Y, Foo LY, Guo K, Gan BQ, Zeng Q, Hong W, et al. Syntaxin 9 is enriched in skin hair follicle epithelium and interacts with the epidermal growth factor receptor. *Traffic.* 2006;7(2):216–26.
284. Brasher MI, Martynowicz DM, Grafinger OR, Hucik A, Shanks-Skinner E, Uniacke J, et al. Interaction of Munc18c and syntaxin4 facilitates invadopodium formation and extracellular matrix invasion of tumor cells. *J Biol Chem.* 2017;292(39):16199–210.
285. Williams KC, Coppolino MG. SNARE-dependent interaction of Src, EGFR and α 1 integrin regulates invadopodia formation and tumor cell invasion. *J Cell Sci.* 2014;127(8):1712–25.
286. Gaoa J, Wangb Y, Caia M, Pana Y, Xu H, Jianga J, et al. Mechanistic Insights into EGFR Membrane Clustering Revealed by Super-resolution Imaging. *Nanoscale* [Internet]. 2015;7(6):2511–9. Available from: <http://xlink.rsc.org/?DOI=C5TC02043C>
287. Ichinose J, Murata M, Yanagida T, Sako Y. EGF signalling amplification induced by dynamic clustering of EGFR. *Biochem Biophys Res Commun.* 2004;324(3):1143–9.

288. Amaddii M, Meister M, Banning A, Tomasovic A, Mooz J, Rajalingam K, et al. Flotillin-1/Reggie-2 protein plays dual role in activation of receptor-tyrosine kinase/mitogen-activated protein kinase signaling. *J Biol Chem* [Internet]. 2012;287(10):7265–78. Available from: <http://dx.doi.org/10.1074/jbc.M111.287599>
289. Banning A, Kurrle N, Meister M, Tikkanen R. Flotillins in Receptor Tyrosine Kinase Signaling and Cancer. *Cells*. 2014;3(1):129–49.
290. Hao M, Yeo SK, Turner K, Harold A, Yang Y, Zhang X, et al. Autophagy Blockade Limits HER2+ Breast Cancer Tumorigenesis by Perturbing HER2 Trafficking and Promoting Release Via Small Extracellular Vesicles. *Dev Cell* [Internet]. 2021;56(3):341–355.e5. Available from: <https://doi.org/10.1016/j.devcel.2020.12.016>
291. Haslekås C, Breen K, Pedersen KW, Johannessen LE, Stang E, Madshus IH. The inhibitory effect of ErbB2 on epidermal growth factor induced formation of clathrin-coated pits correlates with retention of epidermal growth factor receptor-ErbB2 oligomeric complexes at the plasma membrane. *Mol Biol Cell*. 2005;16(December):5832–42.
292. Hommelgaard AM, Lerdrup M, van Deurs B. Association with membrane protrusions makes ErbB2 an internalization-resistant receptor. *Mol Biol Cell*. 2004;15(April):1557–67.
293. Harari D, Yarden Y. Molecular mechanisms underlying ErbB2/HER2 action in breast cancer. *Oncogene*. 2000;19(53):6102–14.
294. Austin CD, De Mazière AM, Pisacane PI, van Dijk SM, Eigenbrot C, Sliwkowski MX, et al. Endocytosis and sorting of ErbB2 and the site of action of cancer therapeutics trastuzumab and geldanamycin. *Mol Biol Cell*. 2004;15(December):5268–5282.
295. Pietilä M, Sahgal P, Peuhu E, Jäntti NZ, Paatero I, Närvä E, et al. SORLA regulates endosomal trafficking and oncogenic fitness of HER2. *Nat Commun*. 2019;10(1).
296. Wichmann H, Güttler A, Bache M, Taubert H, Rot S, Kessler J, et al. Targeting of EGFR and HER2 with therapeutic antibodies and siRNA: A comparative study in glioblastoma cells. *Strahlentherapie und Onkol*. 2015;191(2):180–91.
297. Garrett JT, Olivares MG, Rinehart C, Granja-Ingram ND, Sánchez V, Chakrabarty A, et al. Transcriptional and posttranslational up-regulation of HER3 (ErbB3) compensates for inhibition of the HER2 tyrosine kinase. *Proc Natl Acad Sci U S A*. 2011;108(12):5021–6.
298. Dulak AM, Gubish CT, Stabile LP, Henry C, Siegfried JM. HGF-independent potentiation of EGFR action by c-Met. *Oncogene*. 2011;30(33):3625–35.
299. Wang Q, Yang S, Wang K, Sun SY. MET inhibitors for targeted therapy of EGFR TKI-resistant lung cancer. *J Hematol Oncol*. 2019;12(1):1–11.
300. Zhang D, Pal A, Bornmann WG, Yamasaki F, Esteva FJ, Hortobagyi GN, et al. Activity of lapatinib is independent of EGFR expression level in HER2-overexpressing breast cancer cells. *Mol Cancer Ther*. 2008;7(7):1846–50.
301. Gayle SS, Castellino RC, Buss MC, Nahta R. MEK Inhibition Increases Lapatinib Sensitivity Via Modulation of FOXM1. *Curr Med Chem*. 2013;777(777):1–14.
302. Guo Y, Pan W, Liu S, Shen Z, Xu Y, Hu L. ERK/MAPK signalling pathway and tumorigenesis (Review). *Exp Ther Med*. 2020;1997–2007.
303. Martinez-Lopez N, Athonvarangkul D, Mishall P, Sahu S, Singh R. Autophagy proteins regulate ERK phosphorylation. *Nat Commun*. 2013;4:1–14.
304. Zhu X, Wu L, Qiao H, Han T, Chen S, Liu X, et al. Autophagy stimulates apoptosis in HER2-overexpressing breast cancers treated by lapatinib. *J Cell Biochem*. 2013;114(12):2643–53.
305. Chen YJ, Chi CW, Su WC, Huang HL. Lapatinib induces autophagic cell death and inhibits growth of human hepatocellular carcinoma. *Oncotarget*. 2014;5(13):4845–54.
306. Mizushima N, Yoshimori T. How to interpret LC3 immunoblotting. *Autophagy*. 2007;3(6):542–5.
307. Itakura E, Mizushima N. Syntaxin 17: The autophagosomal SNARE. *Autophagy*. 2013;9(6):917–9.
308. Kumar S, Gu Y, Abudu YP, Bruun JA, Jain A, Farzam F, et al. Phosphorylation of Syntaxin 17 by TBK1 Controls Autophagy Initiation. *Dev Cell* [Internet]. 2019;49(1):130–144.e6. Available from: <https://doi.org/10.1016/j.devcel.2019.01.027>
309. Tang BL. Syntaxin 16's Newly Deciphered Roles in Autophagy. *Cells*. 2019;8(12):25–9.
310. Harrington K, Temam S, Mehanna H, D'Cruz A, Jain M, D'Onofrio I, et al. Postoperative adjuvant lapatinib and concurrent chemoradiotherapy followed by maintenance lapatinib monotherapy in high-risk patients with resected squamous cell carcinoma of the head and neck: A phase III, randomized, double-blind, placebo-controlled study. *J Clin Oncol*. 2015;33(35):4202–9.
311. Weiss JM, Bagley S, Hwang W-T, Bauml J, Olson JG, Cohen RB, et al. Capecitabine and lapatinib for

- the first-line treatment of metastatic/recurrent head and neck squamous cell carcinoma. *Cancer*. 2016;15:2350–5.
312. Alves AC, Magarkar A, Horta M, Lima JLFC, Bunker A, Nunes C, et al. Influence of doxorubicin on model cell membrane properties: Insights from in vitro and in silico studies. *Sci Rep*. 2017;7(1):1–11.
313. Bao L, Haque A, Jackson K, Hazari S, Moroz K, Jetly R, et al. Increased expression of p-glycoprotein is associated with doxorubicin chemoresistance in the metastatic 4T1 breast cancer model. *Am J Pathol* [Internet]. 2011;178(2):838–52. Available from: <http://dx.doi.org/10.1016/j.ajpath.2010.10.029>
314. Inoue Y, Matsumoto H, Yamada S, Kawai K, Suemizu H, Gika M, et al. ATP7B expression is associated with in vitro sensitivity to cisplatin in non-small cell lung cancer. *Oncol Lett*. 2010;1(2):279–82.
315. Gupta A, Lutsenko S. Human copper transporters: mechanism, role in human diseases and therapeutic potential. *Future Med Chem*. 2009;1(6):1125–42.
316. Schrader C, Boehm A, Reiche A, Diet A, Mozet C, Wichmann G. Combined effects of lapatinib and cisplatin on colony formation of head and neck squamous cell carcinoma. *Anticancer Res*. 2012;32(8):3191–9.
317. Kondo N, Tsukuda M, Ishiguro Y, Kimura M, Fujita K, Sakakibara A, et al. Antitumor effects of lapatinib (GW572016), a dual inhibitor of EGFR and HER-2, in combination with cisplatin or paclitaxel on head and neck squamous cell carcinoma. *Oncol Rep*. 2010;23:957–63.
318. Harrington K, Berrier A, Robinson M, Remenar E, Housset M, De Mendoza FH, et al. Randomised Phase II study of oral lapatinib combined with chemoradiotherapy in patients with advanced squamous cell carcinoma of the head and neck: Rationale for future randomised trials in human papilloma virus-negative disease. *Eur J Cancer*. 2013;49(7):1609–18.
319. Weiss JM, Grilley-Olson JE, Deal AM, Zevallos JP, Chera BS, Paul J, et al. Phase 2 trial of neoadjuvant chemotherapy and transoral endoscopic surgery with risk-adapted adjuvant therapy for squamous cell carcinoma of the head and neck. *Cancer*. 2018;124(14):2986–92.
320. Wolf K, Friedl P. Molecular mechanisms of cancer cell invasion and plasticity. *Br J Dermatol*. 2006;154 Suppl:11–5.
321. Wang Y, Xu H, Jiao H, Wang S, Xiao Z, Zhao Y, et al. STX2 promotes colorectal cancer metastasis through a positive feedback loop that activates the NF- κ B pathway. *Cell Death Dis* [Internet]. 2018;9(6). Available from: <http://dx.doi.org/10.1038/s41419-018-0675-x>
322. Du J, Liu X, Wu Y, Zhu J, Tang Y. Essential role of STX6 in esophageal squamous cell carcinoma growth and migration. *Biochem Biophys Res Commun* [Internet]. 2016;472(1):60–7. Available from: <http://dx.doi.org/10.1016/j.bbrc.2016.02.061>
323. Skalski M, Yi Q, Kean MJ, Myers DW, Williams KC, Burtnik A, et al. Lamellipodium extension and membrane ruffling require different SNARE-mediated trafficking pathways. *BMC Cell Biol*. 2010;11.
324. Baik M, French B, Chen YC, Byers JT, Chen KT, French SW, et al. Identification of invadopodia by TKS5 staining in human cancer lines and patient tumor samples. *MethodsX* [Internet]. 2019;6:718–26. Available from: <https://doi.org/10.1016/j.mex.2019.03.024>
325. Steffen A, Le Dez G, Poincloux R, Recchi C, Nassoy P, Rottner K, et al. MT1-MMP-Dependent Invasion Is Regulated by TI-VAMP/VAMP7. *Curr Biol*. 2008;18(12):926–31.
326. Neumeister P, Pixley FJ, Xiong Y, Xie H, Wu K, Ashton A, et al. Cyclin D1 governs adhesion and motility in macrophages. *Mol Biol Cell*. 2003;14(May):2005–15.
327. Li Z, Wang C, Jiao X, Lu Y, Fu M, Quong AA, et al. Cyclin D1 Regulates Cellular Migration through the Inhibition of Thrombospondin 1 and ROCK Signaling. *Mol Cell Biol*. 2006;26(11):4240–56.
328. Brooks DLP, Schwab LP, Krutilina R, Parke DN, Sethuraman A, Hoogewijs D, et al. ITGA6 is directly regulated by hypoxia-inducible factors and enriches for cancer stem cell activity and invasion in metastatic breast cancer models. *Mol Cancer* [Internet]. 2016;15(1):1–19. Available from: <http://dx.doi.org/10.1186/s12943-016-0510-x>
329. Kwon J, Lee TS, Lee HW, Kang MC, Yoon HJ, Kim JH, et al. Integrin alpha 6: A novel therapeutic target in esophageal squamous cell carcinoma. *Int J Oncol*. 2013;43(5):1523–30.
330. Wu Y, Tan X, Liu P, Yang Y, Huang Y, Liu X, et al. ITGA6 and RPSA synergistically promote pancreatic cancer invasion and metastasis via PI3K and MAPK signaling pathways. *Exp Cell Res* [Internet]. 2019;379(1):30–47. Available from: <https://doi.org/10.1016/j.yexcr.2019.03.022>
331. Pal A, Barrett TF, Paolini R, Parikh A, Puram S V. Partial EMT in head and neck cancer biology: a spectrum instead of a switch. *Oncogene* [Internet]. 2021; Available from: <http://dx.doi.org/10.1038/s41388-021-01868-5>

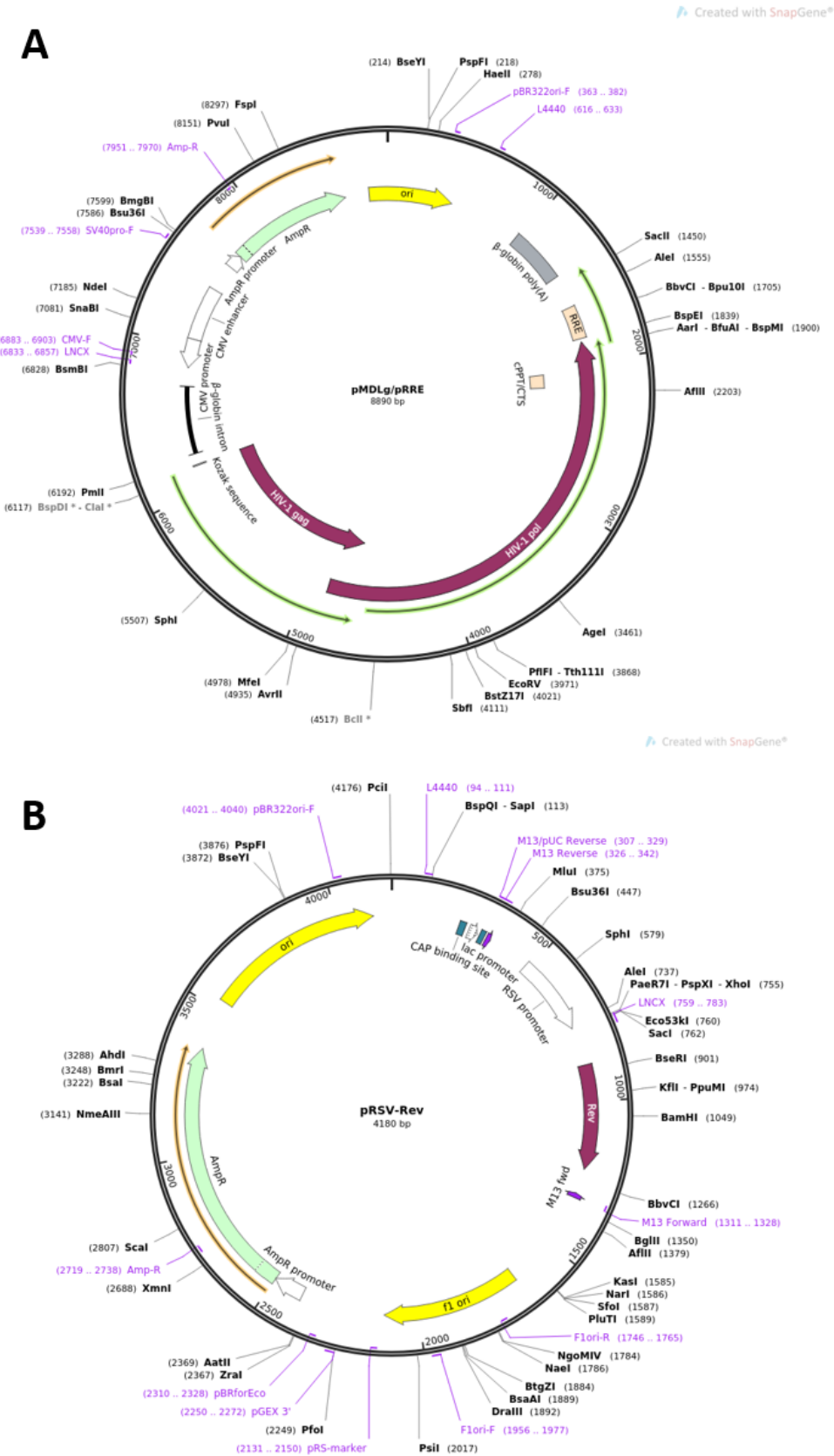
332. Kean MJ, Williams KC, Skalski M, Myers D, Burtnik A, Foster D, et al. VAMP3, syntaxin-13 and SNAP23 are involved in secretion of matrix metalloproteinases, degradation of the extracellular matrix and cell invasion. *J Cell Sci* [Internet]. 2009;122(22):4089–98. Available from: <http://jcs.biologists.org/cgi/doi/10.1242/jcs.052761>
333. He D, Manzoni A, Florentin D, Fisher W, Ding Y, Lee MJ, et al. Biologic effect of neurogenesis in pancreatic cancer. *Hum Pathol* [Internet]. 2016;52:182–9. Available from: <http://dx.doi.org/10.1016/j.humpath.2016.02.001>
334. Vezdrevanis K. Prostatic carcinoma shrunk after intraprostatic injection of botulinum toxin. *Urol J*. 2011;8(3):239–41.
335. Somm E, Bonnet N, Martinez A, Marks PMH, Cadd VA, Elliott M, et al. A botulinum toxin - Derived targeted secretion inhibitor downregulates the GH/IGF1 axis. *J Clin Invest*. 2012;122(9):3295–306.
336. Arsenault J, Ferrari E, Niranjana D, Cuijpers SAG, Gu C, Vallis Y, et al. Stapling of the botulinum type A protease to growth factors and neuropeptides allows selective targeting of neuroendocrine cells. *J Neurochem*. 2013;126(2):223–33.
337. Blanes-Mira C, Merino JM, Valera E, Fernández-Ballester G, Gutiérrez LM, Viniegra S, et al. Small peptides patterned after the N-terminus domain of SNAP25 inhibit SNARE complex assembly and regulated exocytosis. *J Neurochem*. 2004;88(1):124–35.

Syntaxin-1A, a synaptic related protein in breast and head and neck cancer progression and prognosis

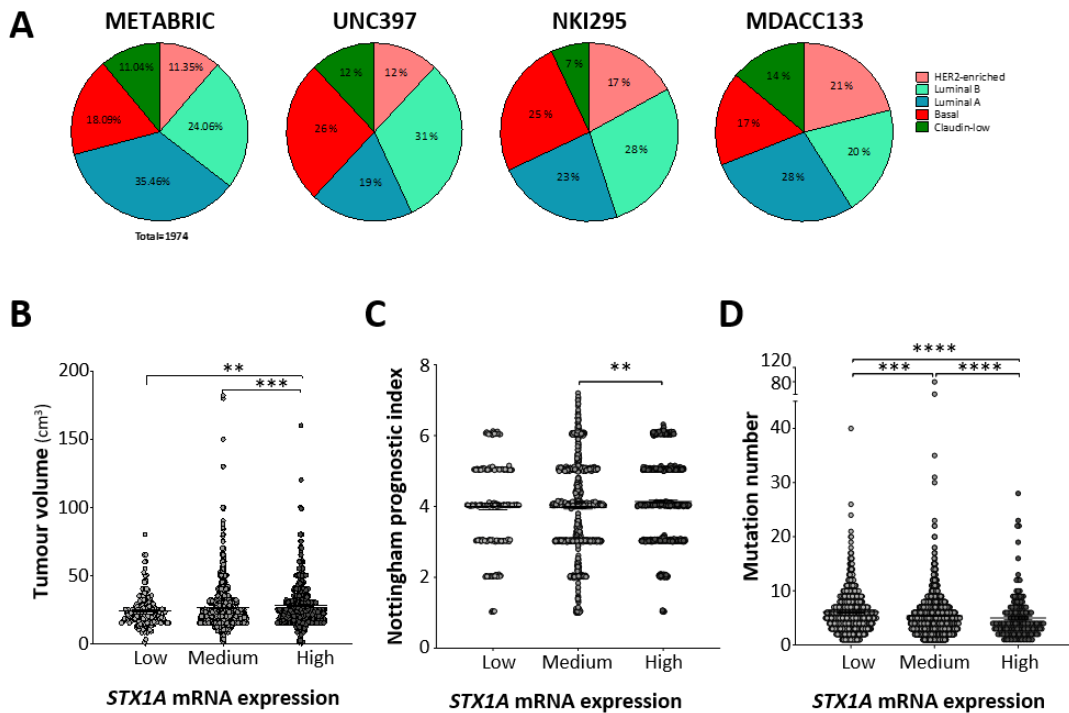
ANNEX

Syntaxin-1A, a synaptic related protein in breast and head and neck cancer progression and prognosis

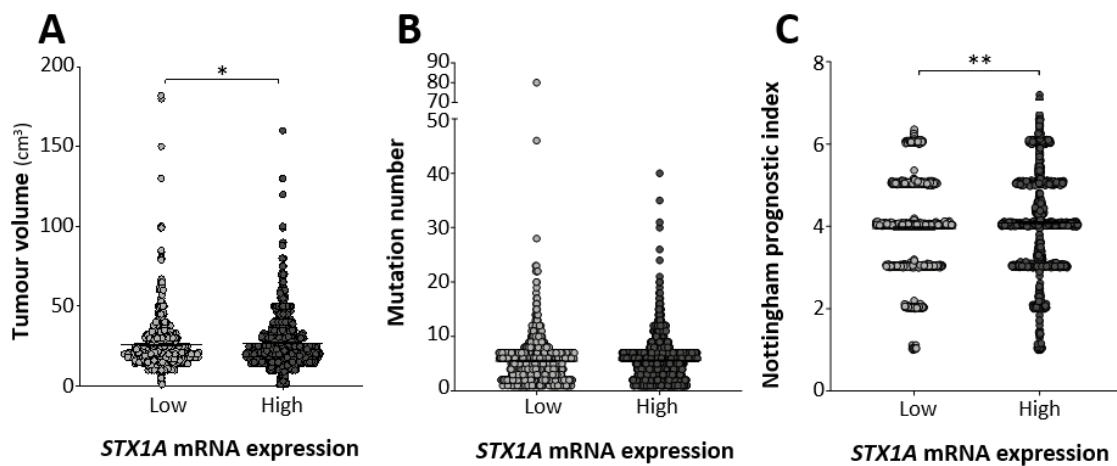
1. FIGURES



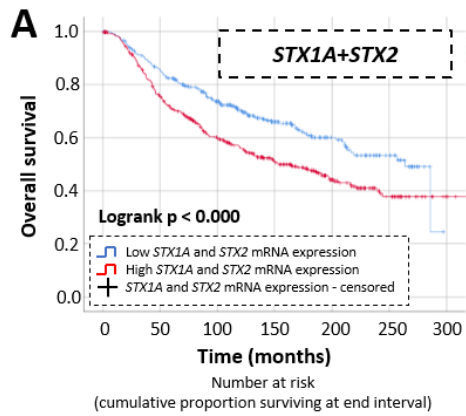
Annex figure 1 – Schematic representation of pMDLg/pRRE plasmid (Addgene, #12251) (A) and pRSV-Rev (Addgene, #12253) plasmid (B).



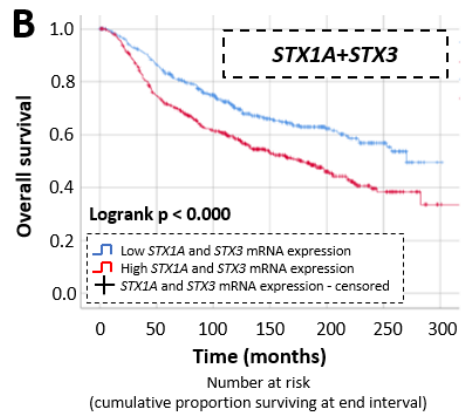
Annex figure 2 – (A) Frequency of BC subtypes in different public databases: METABRIC, UNC397, NKI295 and MDACC133. (B) Graphical representation of BC tumour volume (cm³) in the different tumour subgroups classified according *STX1A* expression (low, medium and high). (C) Graphical representation of Nottingham prognostic index in the different tumour subgroups classified according *STX1A* expression (low, medium and high). (D) Graphical representation of BC mutation number in the different tumour subgroups classified according *STX1A* expression (low, medium and high). Statistical analysis was performed using the U-Mann Whitney test. *p<0.05, **p<0.01, ***p<0.001, ****p<0.000.



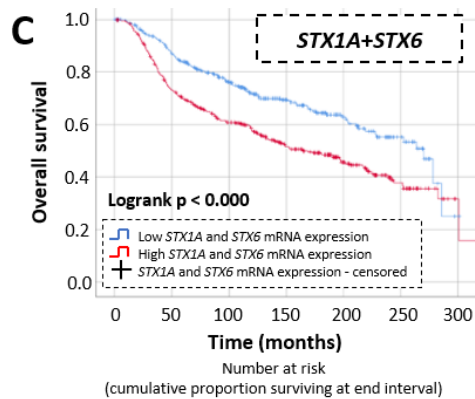
Annex figure 3 – (A) Graphical representation of BC tumour volume (cm³) in the different tumour subgroups classified according *STX1A* expression (low and high). (B) Graphical representation of Nottingham prognostic index in the different tumour subgroups classified according *STX1A* expression (low and high). (C) Graphical representation of BC mutation number in the different tumour subgroups classified according *STX1A* expression (low and high). Statistical analysis was performed using U-Mann Whitney test. *p<0.05, **p<0.01.



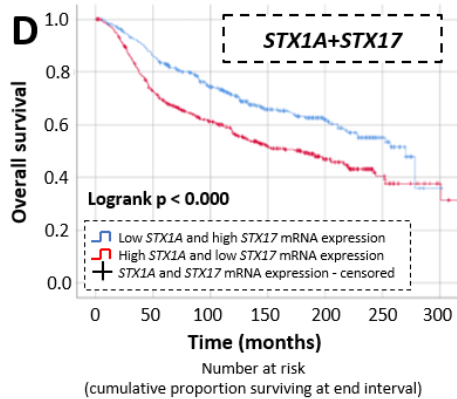
Low	423.0 (87%)	355.0 (75%)	226.5 (66%)	131.0 (62%)	70.5 (56%)	23.5 (49%)	0.5 (49%)
High	482.5 (75%)	335.5 (61%)	226.5 (53%)	133.5 (46%)	63.5 (39%)	17.0 (37%)	1.5 (12%)



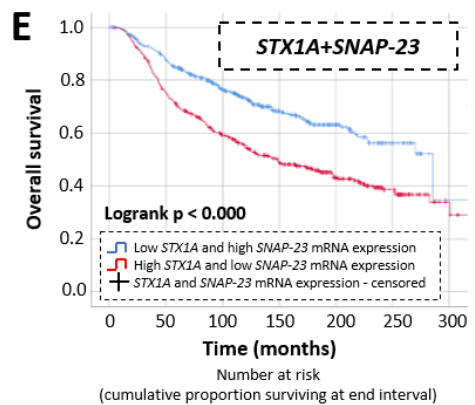
Low	354.5 (86%)	279.0 (74%)	180.5 (66%)	99.5 (60%)	54.0 (52%)	18.5 (44%)	-
High	414.0 (76%)	293.5 (60%)	198.0 (51%)	123.0 (44%)	61.5 (39%)	18.5 (39%)	2.0 (39%)



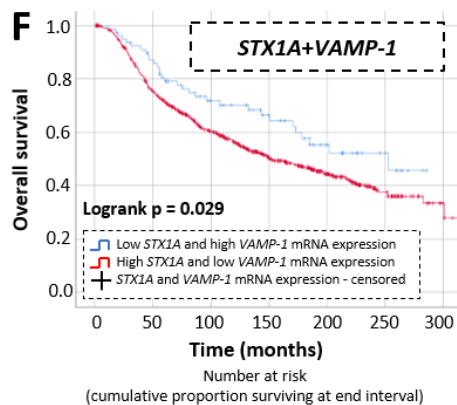
Low	370.0 (87%)	287.5 (76%)	189.5 (69%)	109.5 (62%)	57.0 (53%)	19.0 (39%)	0.5 (39%)
High	436.0 (73%)	298.5 (61%)	123.5 (52%)	131.5 (52%)	68.5 (39%)	20.0 (33%)	1.5 (11%)



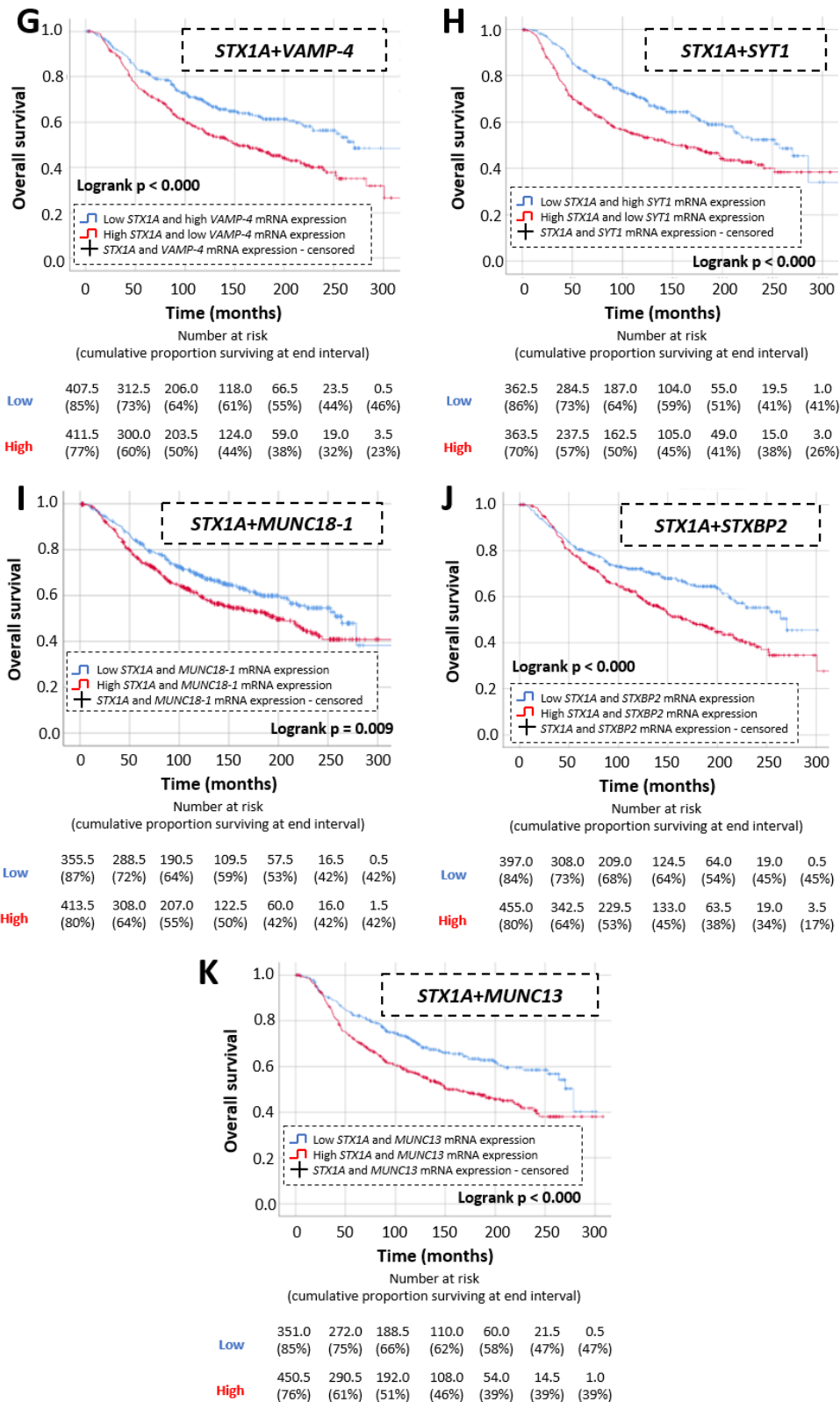
Low	362.0 (86%)	285.0 (74%)	192.0 (66%)	113.5 (62%)	62.0 (54%)	19.5 (43%)	0.5 (43%)
High	421.0 (73%)	283.5 (61%)	201.5 (52%)	122.5 (47%)	62.5 (41%)	19.0 (37%)	4.0 (18%)



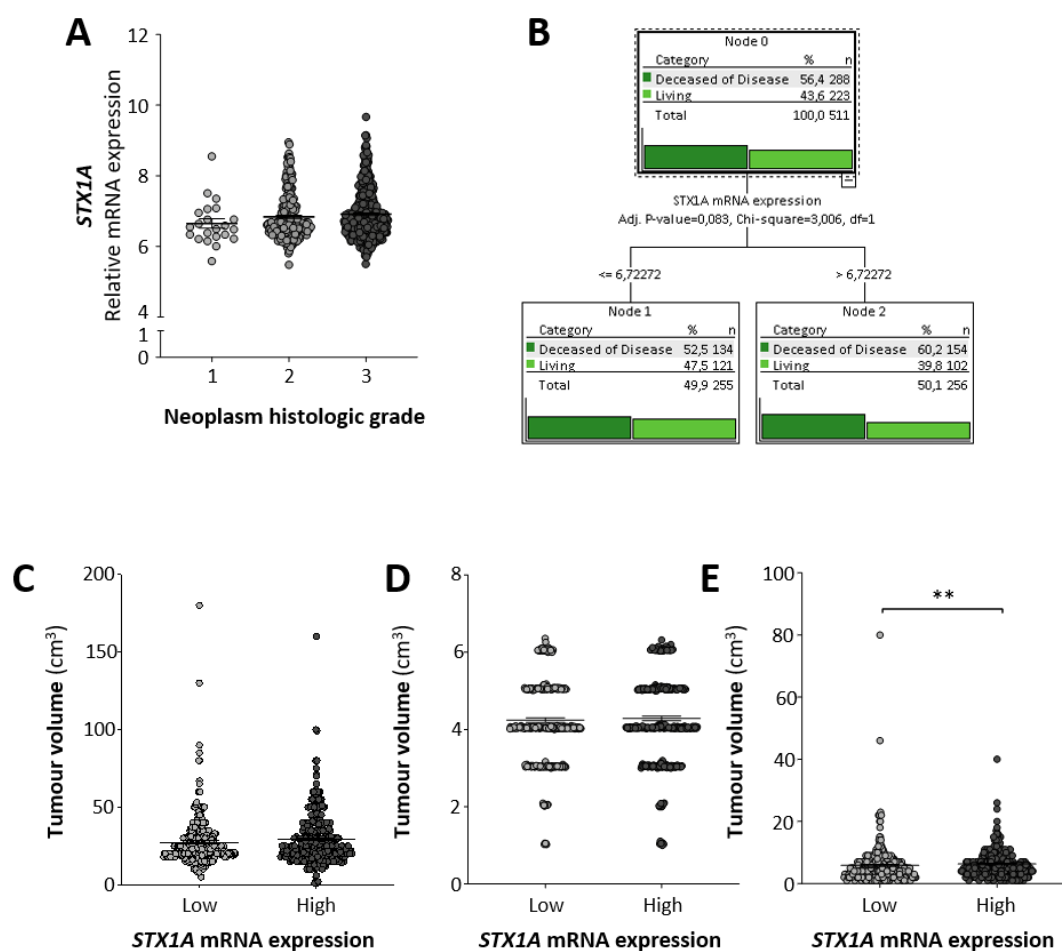
Low	442.0 (88%)	344.0 (76%)	219.0 (68%)	119.0 (62%)	58.5 (55%)	16.5 (48%)	0.5 (48%)
High	450.5 (75%)	324.5 (59%)	227.0 (49%)	145.0 (43%)	76.5 (39%)	26.5 (39%)	4.5 (19%)



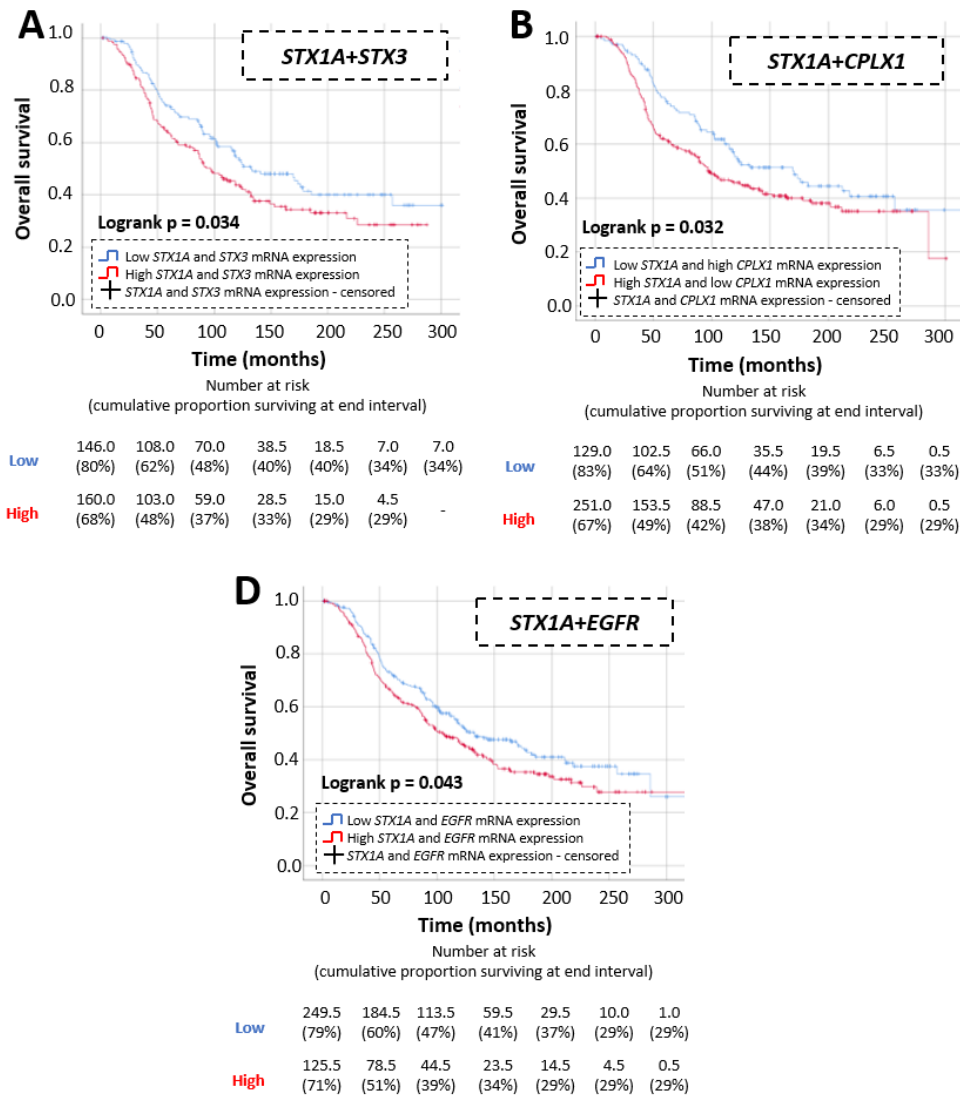
Low	78.5 (87%)	61.5 (72%)	40.5 (66%)	29.0 (55%)	15.0 (51%)	5.0 (41%)	-
High	696.5 (75%)	488.5 (60%)	327.5 (50%)	194.5 (44%)	97.5 (38%)	29.0 (34%)	4.0 (17%)



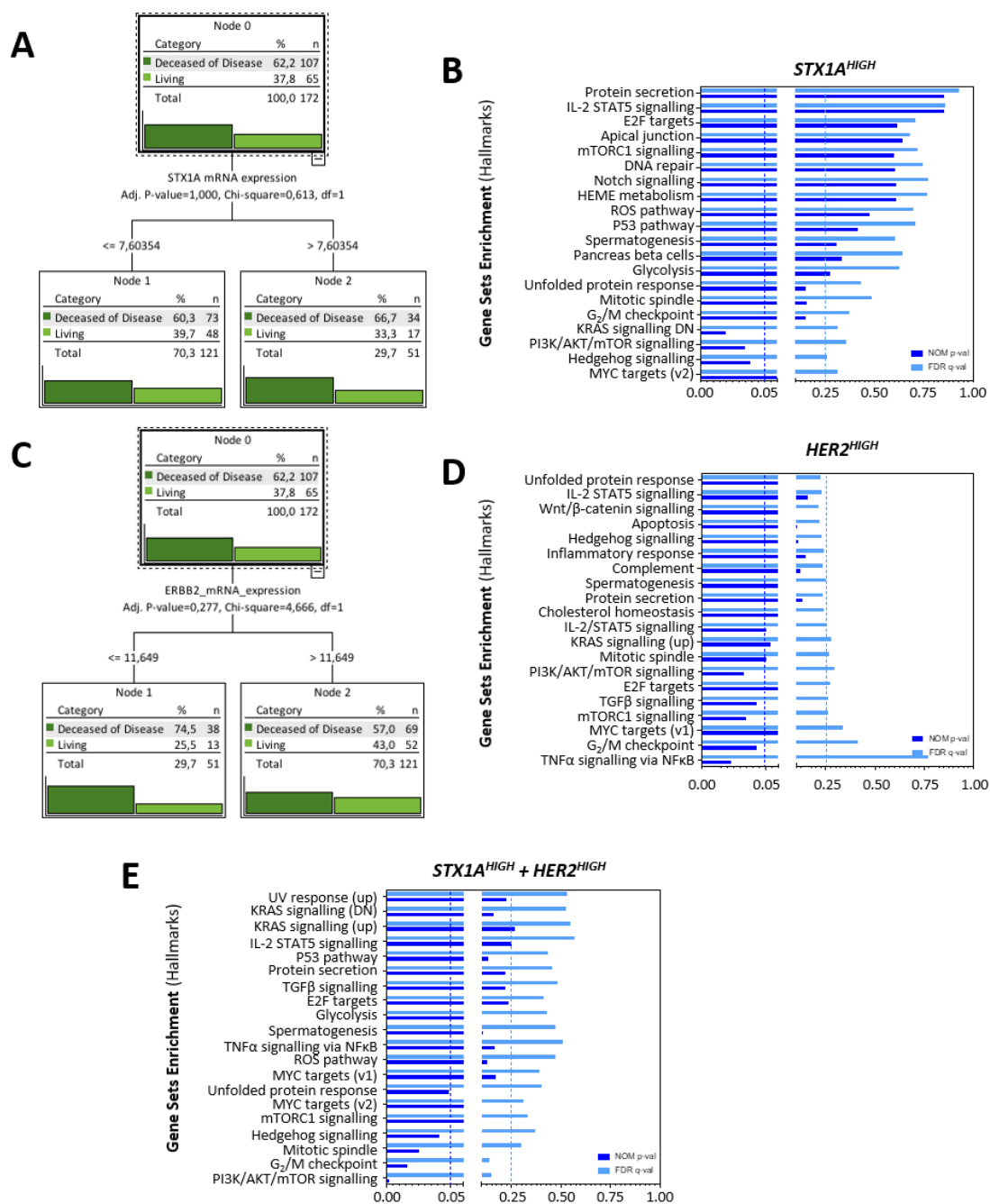
Annex figure 4 – On the top of each figure, overall survival Kaplan-Meier curve of BC tumours grouped according to *STX1A* and *STX2* (A), *STX3* (B), *STX6* (C), *STX17* (D), *SNAP-23* (E), *VAMP-1* (F), *VAMP-4* (G), *SYT1* (H), *MUNC18-1* (I), *STXBP2* (J) or *MUNC13* (K) expression, classified according to the decision tree algorithm. On the bottom of each figure, survival table where the number at risk of BC patients and the cumulative proportion surviving at the end of the interval in parenthesis is shown. Statistical analysis was performed using Logrank test.



Annex figure 5 – (A) Graphical representation of relative *STX1A* mRNA expression grouped into different neoplasm histologic grade HER2-positive BC tumours. (B) Decision tree diagram that shows how relative *STX1A* mRNA expression is grouped according to the patient survival status (deceased of the disease, dark green and living BC patients, light green) in HER2-positive BC patients. (C) Graphical representation of HER2-positive BC tumour volume (cm³) in the different tumour subgroups classified according to *STX1A* expression (low and high). (D) Graphical representation of Nottingham prognostic index in the different HER2-positive tumour subgroups classified according to *STX1A* expression (low and high). (E) Graphical representation of HER2-positive BC mutation number in the different tumour subgroups classified according to *STX1A* expression (low and high). Statistical analysis was performed using the U-Mann Whitney test and Chi-square test for the decision tree algorithm. **p<0.01.

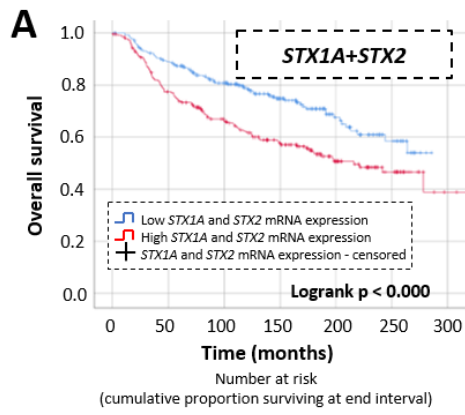


Annex figure 6 – On the top of each figure, overall survival Kaplan-Meier curve of HER2-positive BC tumours grouped according to *STX1A* and *STX3* (A), *CPLX1* (B) and *EGFR* (C) expression, classified according to the decision tree algorithm. On the bottom of each figure, survival table where is shown the number at risk of BC patients and the cumulative proportion surviving at the end of the interval in parenthesis. Statistical analysis was performed using Logrank test.

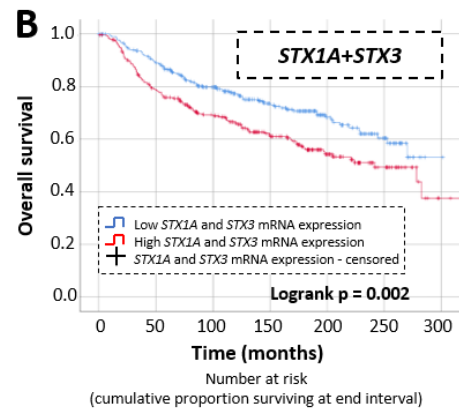


Annex figure 7 – (A) Decision tree diagram that shows how relative *STX1A* mRNA expression is grouped according to the patient survival status (Deceased of the disease, dark green, and living BC patients, light green) in *HER2*-enriched BC patients. (B) GSEA of differential pathways expressed in *STX1A^{HIGH}* *HER2*-enriched BC tumours. Dark blue lines correspond to NOM p-value which threshold is $p < 0.05$ and light blue correspond to FDR q-value which threshold is 0.25. (C) Decision tree diagram that shows how relative *HER2* mRNA expression is grouped according to the patient survival status (deceased of the disease, dark green and living BC patients, light green) in *HER2*-enriched BC patients. (D) GSEA of differential pathways expressed in *HER2^{HIGH}* *HER2*-enriched BC tumours. Dark blue lines correspond to NOM p-value which threshold is $p < 0.05$ and light blue correspond to FDR q-value which threshold is 0.25. (E) GSEA of differential pathways expressed in *STX1A^{HIGH}* and *HER2^{HIGH}* *HER2*-enriched BC tumours. Dark blue lines correspond to NOM p-value which threshold is $p < 0.05$ and light blue correspond to FDR q-value which threshold is 0.25.

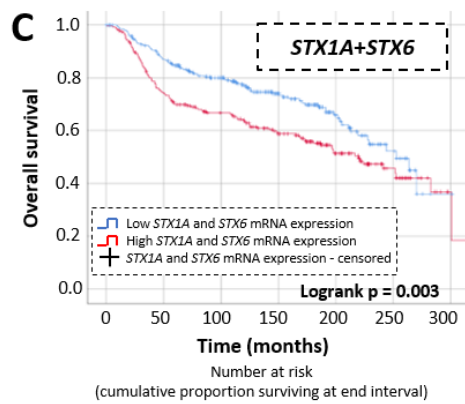
Syntaxin-1A, a synaptic related protein in breast and head and neck cancer progression and prognosis



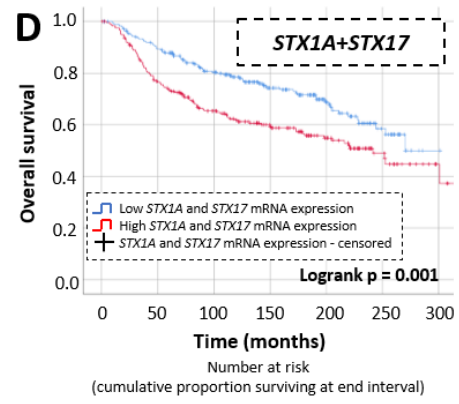
Low	270.5 (89%)	219.0 (81%)	151.5 (75%)	86.5 (68%)	42.5 (58%)	12.5 (54%)	-
High	223.0 (78%)	160.5 (66%)	118.5 (58%)	77.0 (51%)	39.0 (47%)	14.0 (44%)	1.5 (44%)



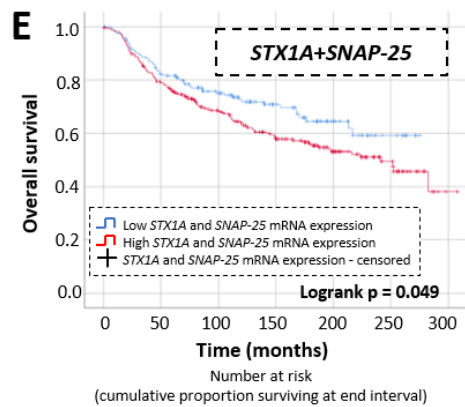
Low	314.0 (89%)	254.5 (80%)	178.5 (73%)	108.5 (68%)	58.0 (60%)	19.0 (54%)	0.5 (54%)
High	267.0 (79%)	193.5 (69%)	141.0 (61%)	90.0 (54%)	45.5 (50%)	15.0 (43%)	1.5 (14%)



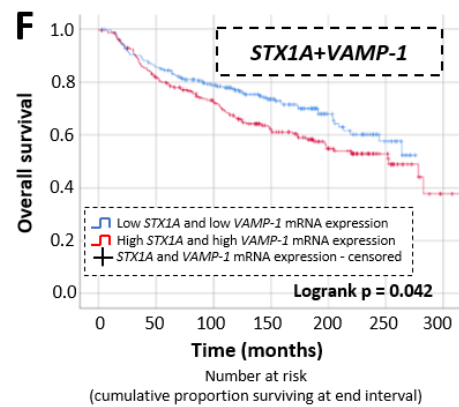
Low	284.5 (87%)	223.0 (80%)	155.5 (74%)	89.5 (66%)	43.0 (52%)	12.0 (39%)	0.5 (39%)
High	240.5 (74%)	167.5 (67%)	133.0 (59%)	91.0 (52%)	46.5 (46%)	15.0 (37%)	1.5 (12%)



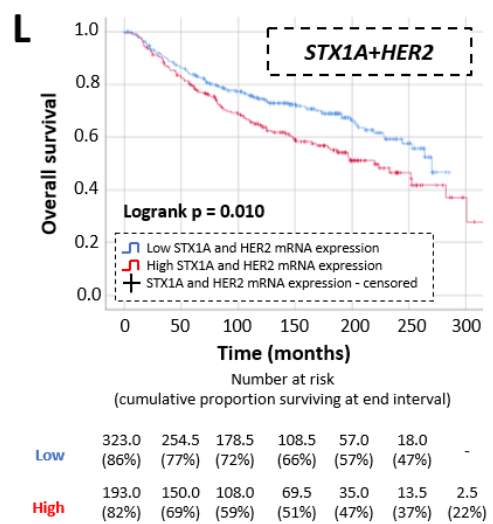
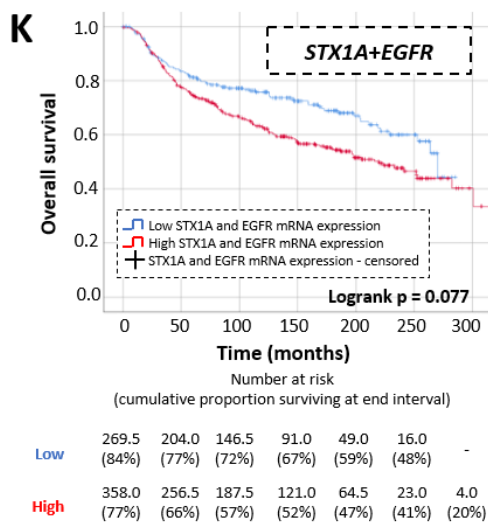
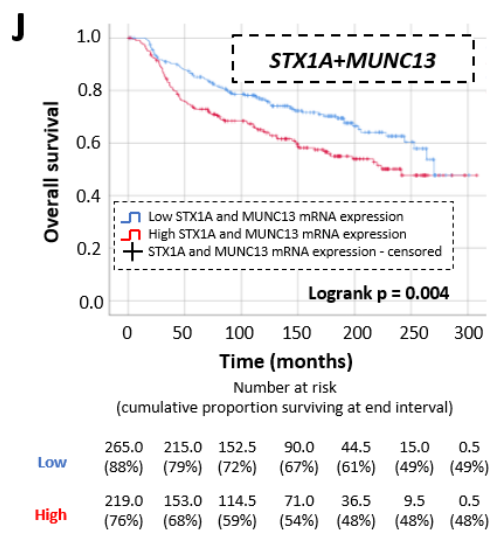
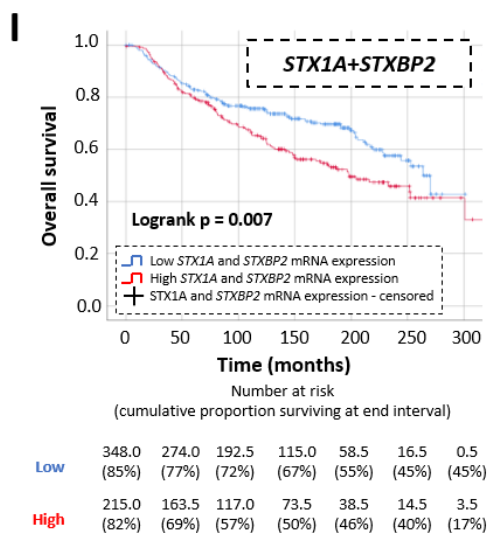
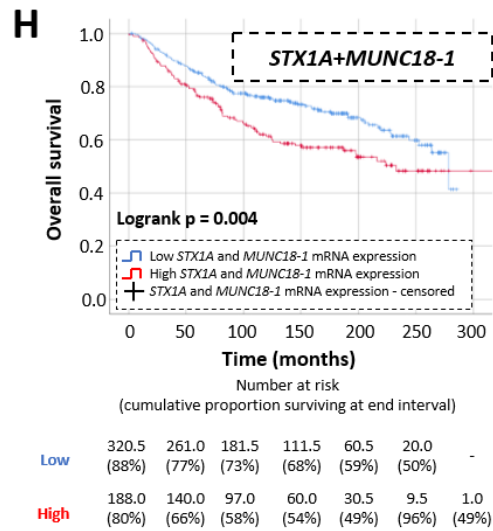
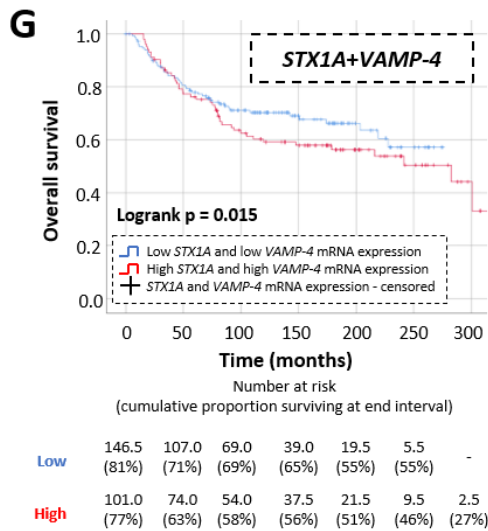
Low	281.5 (89%)	230.0 (80%)	161.0 (74%)	96.5 (69%)	50.0 (58%)	14.5 (50%)	0.5 (50%)
High	234.0 (76%)	165.0 (65%)	117.5 (59%)	79.0 (55%)	44.5 (49%)	16.5 (43%)	4.0 (21%)

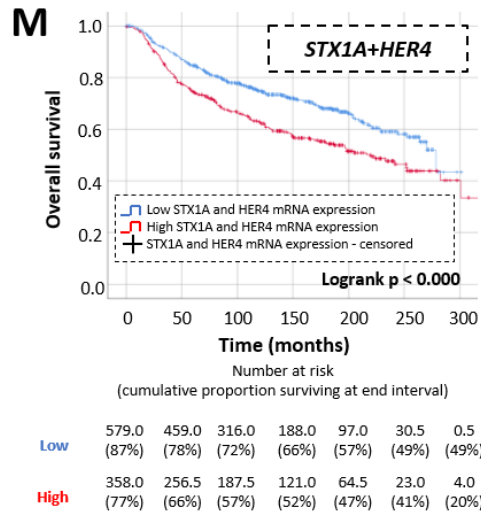


Low	169.5 (82%)	126.5 (75%)	85.0 (71%)	47.5 (63%)	21.0 (57%)	5.5 (57%)	-
High	260.0 (79%)	189.0 (68%)	139.5 (58%)	90.5 (53%)	48.5 (50%)	16.0 (41%)	0.5 (41%)

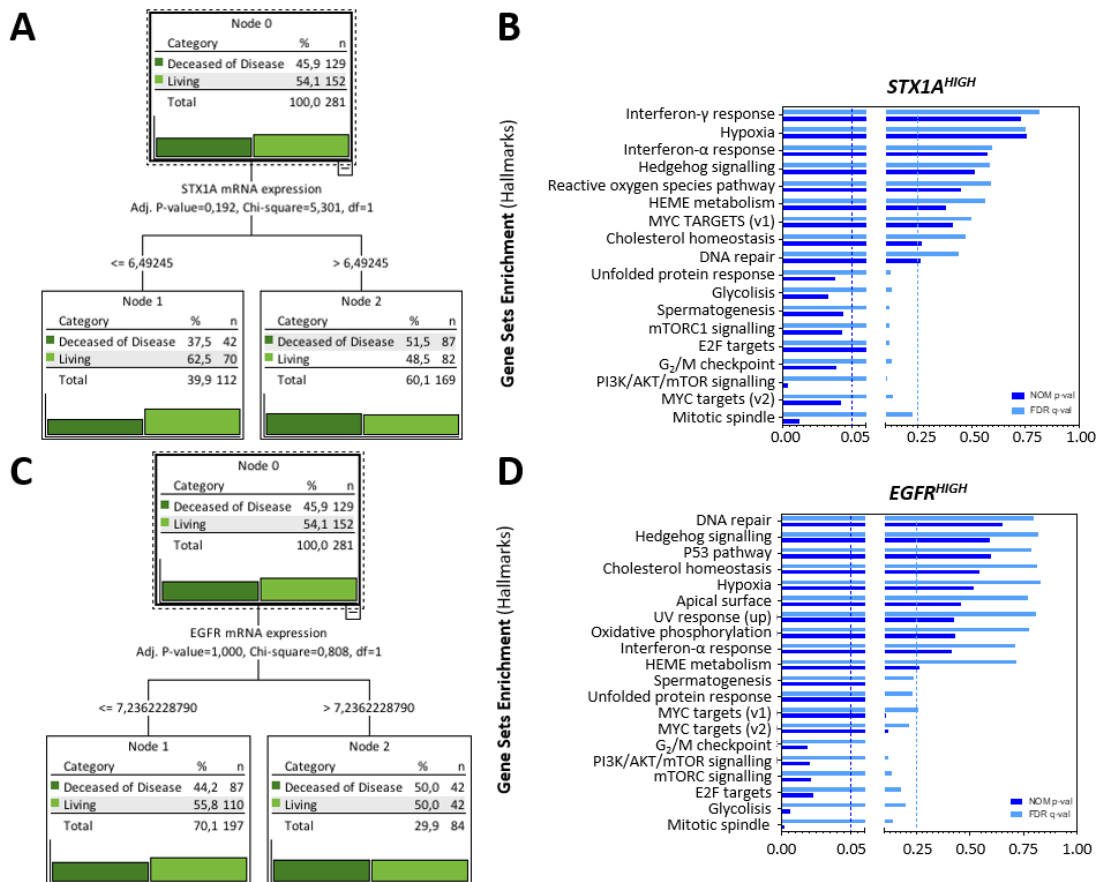


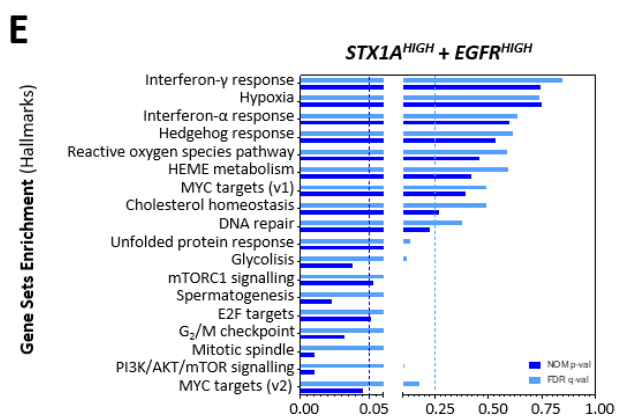
Low	272.0 (86%)	212.5 (79%)	151.5 (74%)	88.5 (68%)	42.0 (56%)	11.0 (51%)	-
High	224.5 (82%)	170.5 (72%)	129.5 (62%)	84.5 (55%)	45.5 (53%)	17.5 (41%)	1.5 (41%)



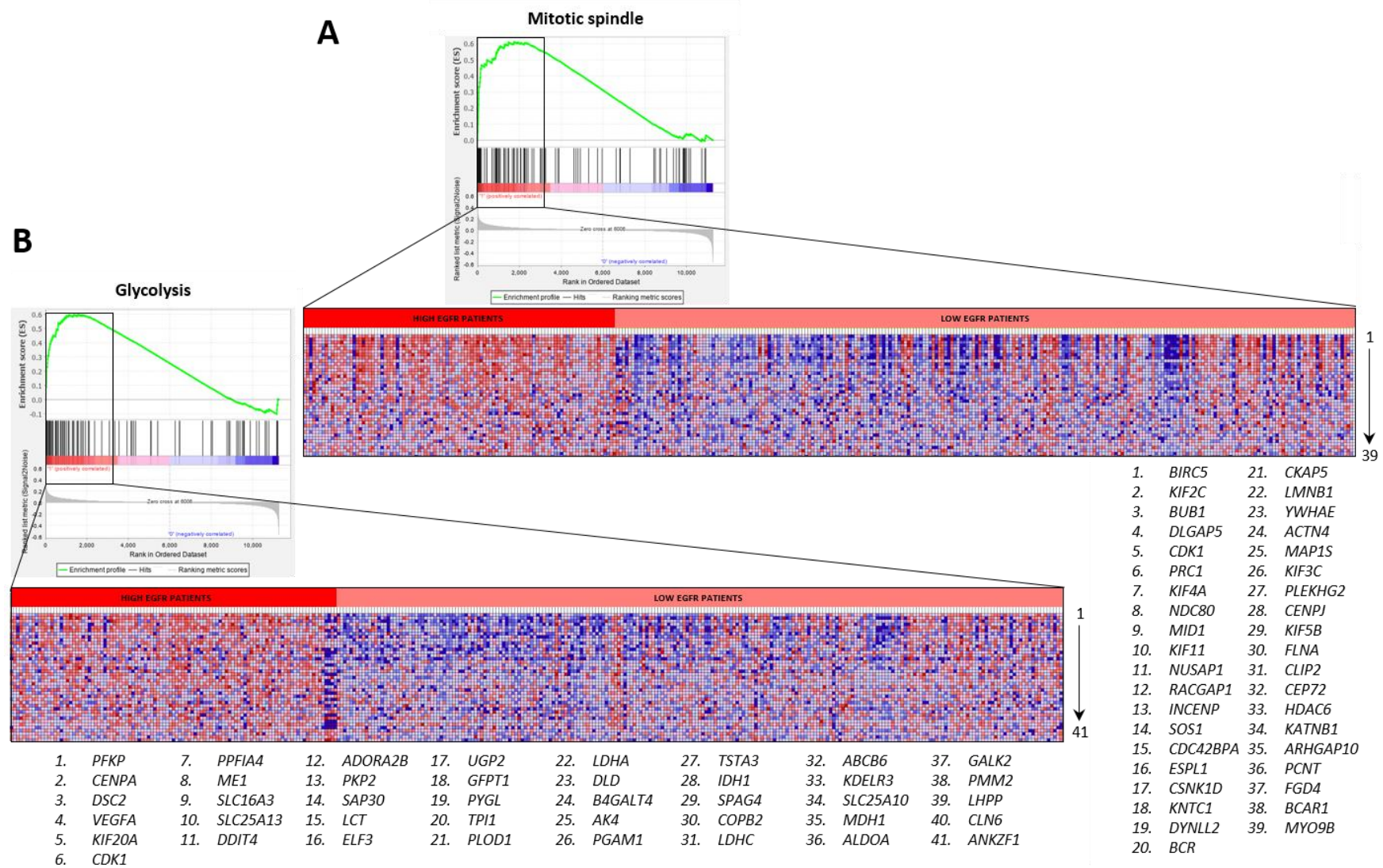


Annex figure 8 – On the top of each figure, overall survival Kaplan-Meier curve of HER2-negative BC tumours grouped according to *STX1A* and *STX2* (A), *STX3* (B), *STX6* (C), *STX17* (D), *SNAP-25* (E), *VAMP-1* (F), *VAMP-4* (G), *MUNC18-1* (H), *STXBP2* (I), *MUNC13* (J), *EGFR* (K), *HER2* (L) and *HER4* (M) expression, classified according to the decision tree algorithm. On the bottom of each figure, survival table where the number at risk of BC patients and the cumulative proportion surviving at the end of the interval in parenthesis is shown. Statistical analysis was performed using Logrank test.



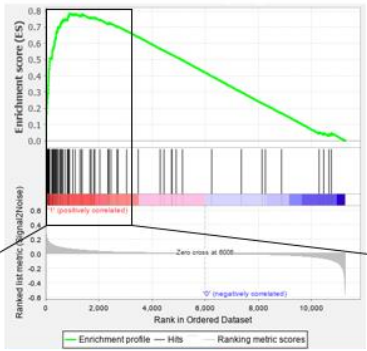


Annex figure 9 – (A) Decision tree diagram that shows how relative *STX1A* mRNA expression is grouped according to the patient survival status (Deceased of the disease, dark green, and living BC patients, light green) in basal BC patients. (B) GSEA of differential pathways expressed in *STX1A*^{HIGH} basal BC tumours. Dark blue lines correspond to NOM p-value which threshold is $p < 0.05$ and light blue correspond to FDR q-value which threshold is 0.25. (C) Decision tree diagram that shows how relative *EGFR* mRNA expression is grouped according to the patient survival status (deceased of the disease, dark green and living BC patients, light green) in basal BC patients. (D) GSEA of differential pathways expressed in *EGFR*^{HIGH} basal BC tumours. Dark blue lines correspond to NOM p-value which threshold is $p < 0.05$ and light blue correspond to FDR q-value which threshold is 0.25. (E) GSEA of differential pathways expressed in *STX1A*^{HIGH} and *EGFR*^{HIGH} basal BC tumours. Dark blue lines correspond to NOM p-value which threshold is $p < 0.05$ and light blue correspond to FDR q-value which threshold is 0.25.



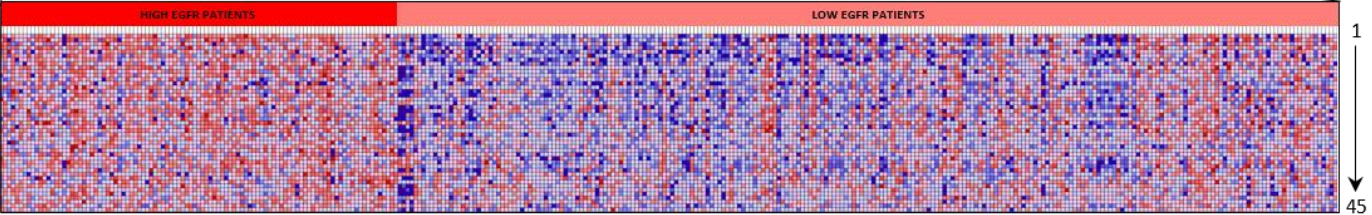
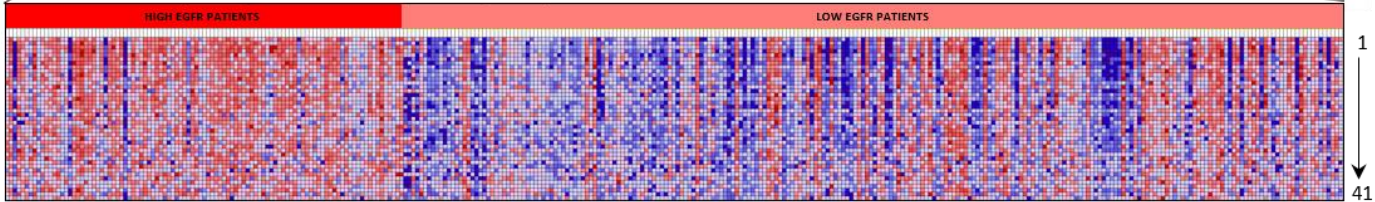
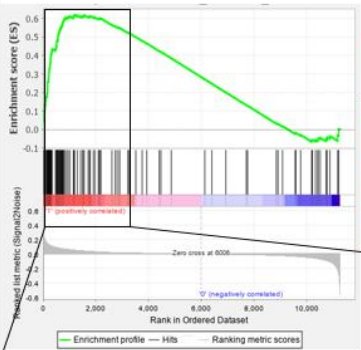
C

E2F targets



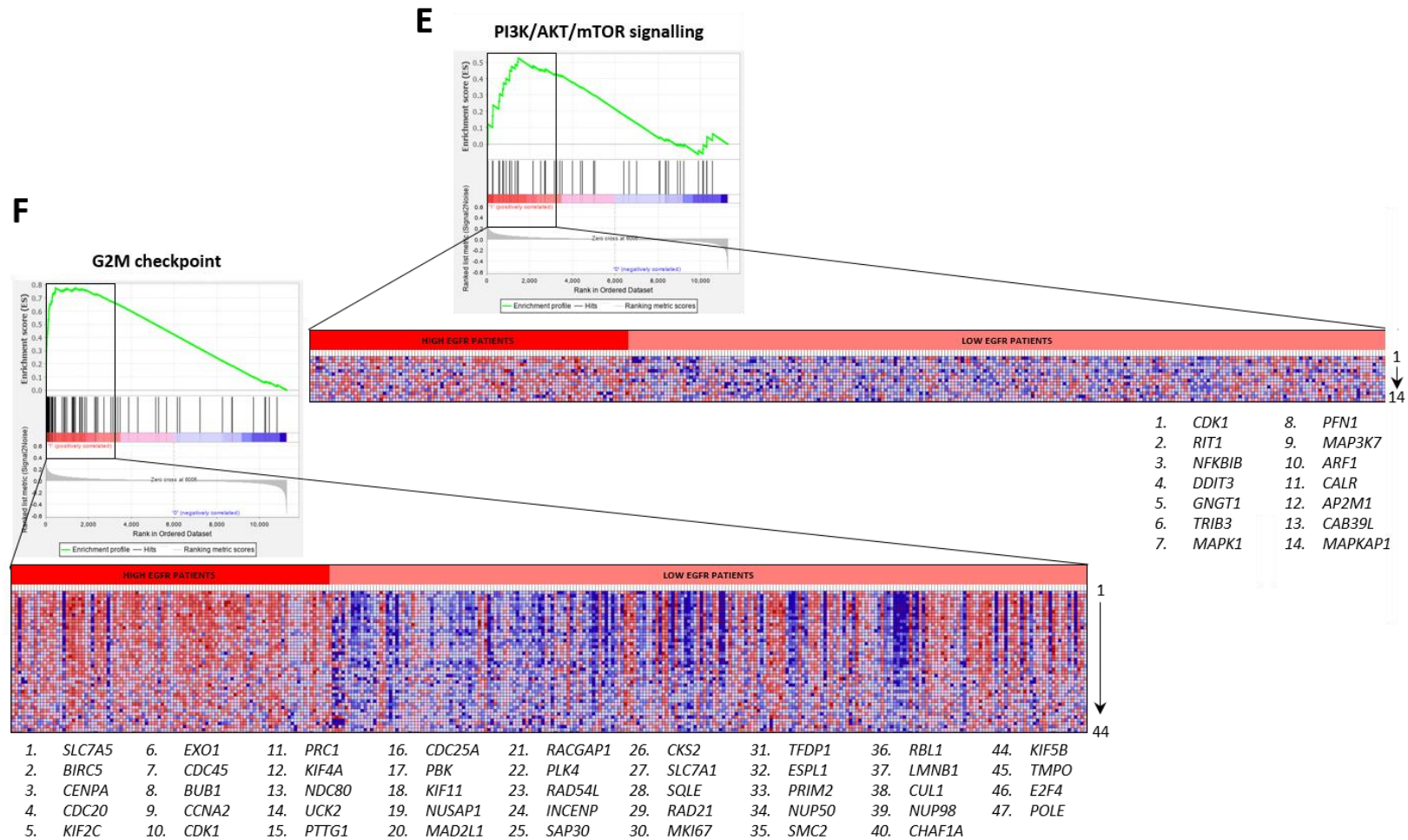
D

MTORC1 signalling

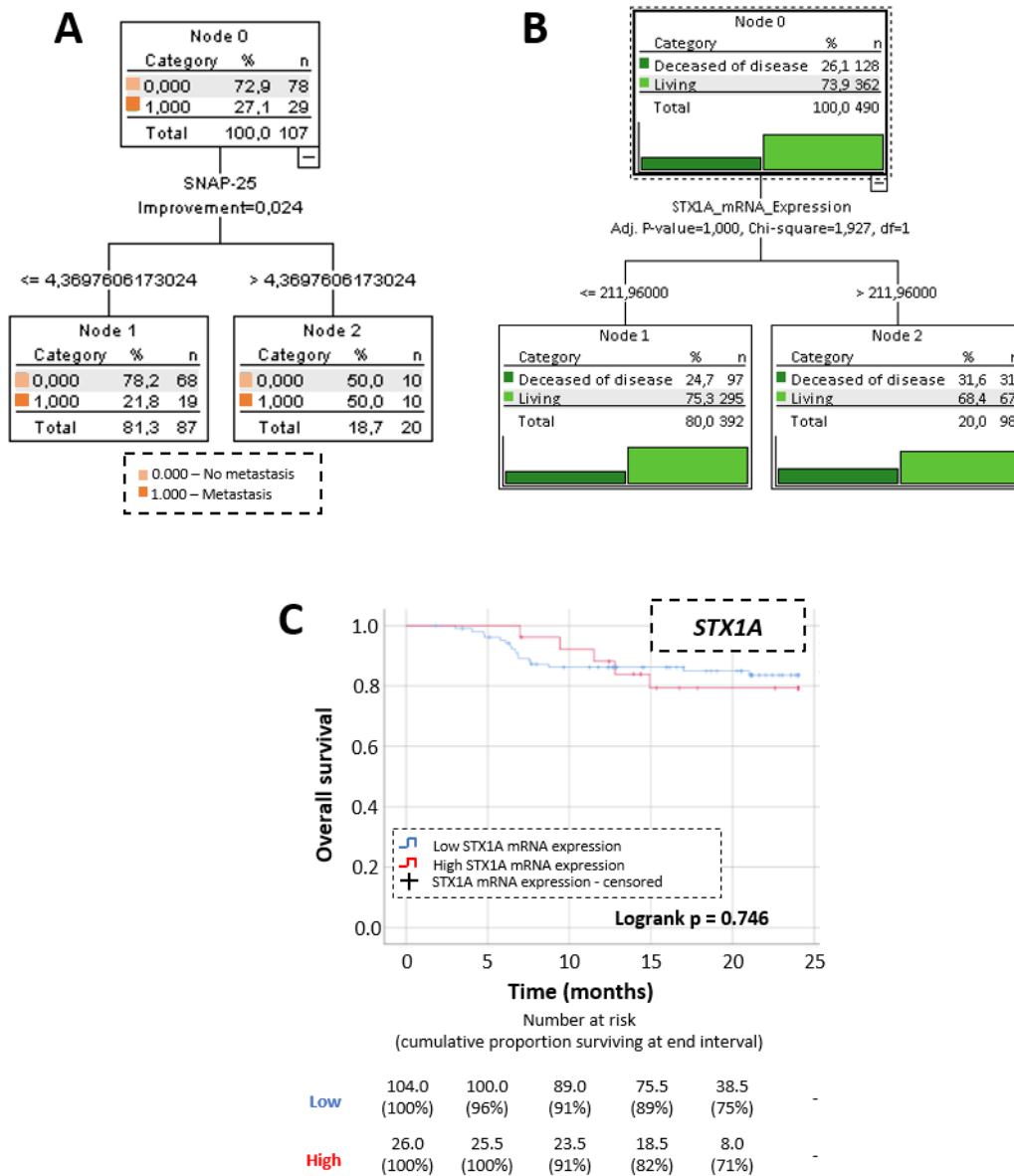


- | | | | | | | | |
|------------------|-------------------|-------------------|-------------------|-------------------|-------------------|-------------------|-------------------|
| 1. <i>SLC7A5</i> | 7. <i>IFRD1</i> | 13. <i>FADS2</i> | 19. <i>SQLE</i> | 25. <i>TP11</i> | 31. <i>AK4</i> | 36. <i>TRIB3</i> | 41. <i>TXNRD1</i> |
| 2. <i>BUB1</i> | 8. <i>DDIT4</i> | 14. <i>ASNS</i> | 20. <i>CACYBP</i> | 26. <i>FADS1</i> | 32. <i>SHMT2</i> | 37. <i>INSIG1</i> | 42. <i>RPA1</i> |
| 3. <i>SRD5A1</i> | 9. <i>PGM1</i> | 15. <i>RRM2</i> | 21. <i>NUP205</i> | 27. <i>EEF1E1</i> | 33. <i>STIP1</i> | 38. <i>LDLR</i> | 43. <i>LGMN</i> |
| 4. <i>PHGDH</i> | 10. <i>UCHL5</i> | 16. <i>RIT1</i> | 22. <i>NAMPT</i> | 28. <i>DDIT3</i> | 34. <i>TOMM40</i> | 39. <i>IDH1</i> | 44. <i>CALR</i> |
| 5. <i>ME1</i> | 11. <i>PSMG1</i> | 17. <i>GAPDH</i> | 23. <i>IFI30</i> | 29. <i>EIF2S2</i> | 35. <i>TFRC</i> | 40. <i>ATP2A2</i> | 45. <i>PITPNB</i> |
| 6. <i>CDC25A</i> | 12. <i>MLLT11</i> | 18. <i>NFKBIB</i> | 24. <i>PSMD14</i> | 30. <i>LDHA</i> | | | |

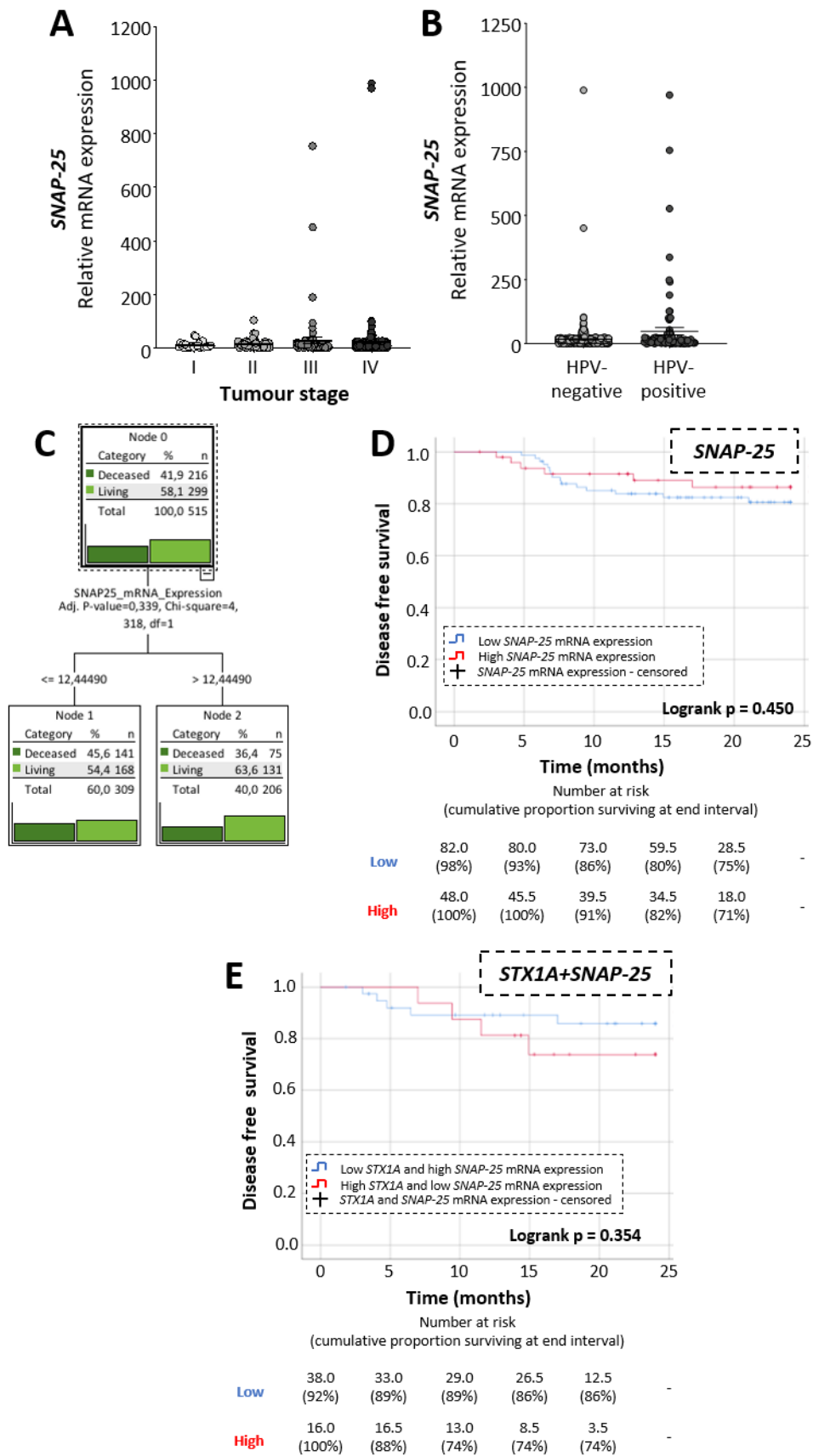
- | | |
|--------------------|-------------------|
| 1. <i>BIRC5</i> | 22. <i>RAD21</i> |
| 2. <i>MELK</i> | 23. <i>MKI67</i> |
| 3. <i>CDC20</i> | 24. <i>NUP205</i> |
| 4. <i>KIF2C</i> | 25. <i>MCM7</i> |
| 5. <i>DLGAP5</i> | 26. <i>GINS4</i> |
| 6. <i>CDK1</i> | 27. <i>POLD1</i> |
| 7. <i>KIF4A</i> | 28. <i>GINS3</i> |
| 8. <i>DONSON</i> | 29. <i>ESPL1</i> |
| 9. <i>PTTG1</i> | 30. <i>PRIM2</i> |
| 10. <i>UBE2T</i> | 31. <i>PRKDC</i> |
| 11. <i>CDC25A</i> | 32. <i>AK2</i> |
| 12. <i>NCAPD2</i> | 33. <i>ZW10</i> |
| 13. <i>ATAD2</i> | 34. <i>RFC3</i> |
| 14. <i>ASF1B</i> | 35. <i>POP7</i> |
| 15. <i>MAD2L1</i> | 36. <i>TFRC</i> |
| 16. <i>RACGAP1</i> | 37. <i>PRDX4</i> |
| 17. <i>PLK4</i> | 38. <i>DNMT1</i> |
| 18. <i>SPC25</i> | 39. <i>SNRNP</i> |
| 19. <i>USP1</i> | 40. <i>LMNB1</i> |
| 20. <i>RRM2</i> | 41. <i>XRCC6</i> |
| 21. <i>CKS2</i> | |



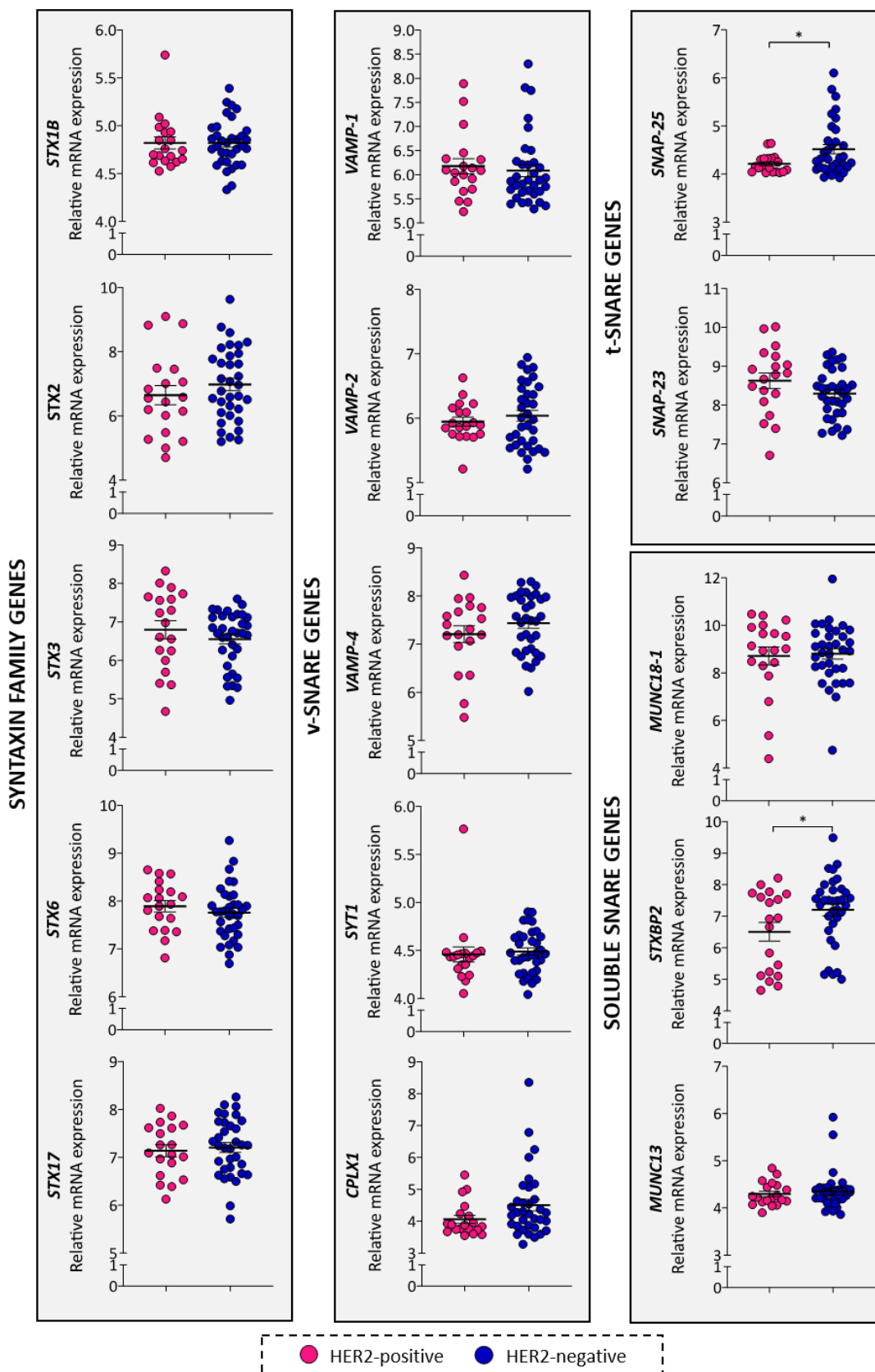
Annex figure 10 – (A) GSEA of mitotic spindle signalling pathway from EGFR^{HIGH} basal BC tumours. (B) GSEA of glycolysis signalling pathway from EGFR^{HIGH} basal BC tumours. (C) GSEA of E2F targets signalling pathway from EGFR^{HIGH} basal BC tumours. (D) GSEA of MTORC1 signalling pathway from EGFR^{HIGH} basal BC tumours. (E) GSEA of PI3K/AKT/mTOR signalling pathway from EGFR^{HIGH} basal BC tumours. (F) GSEA of G₂/M checkpoint signalling pathway from EGFR^{HIGH} basal BC tumours. In the boxes, heatmap with genes responsible for the up-regulation of these pathways.



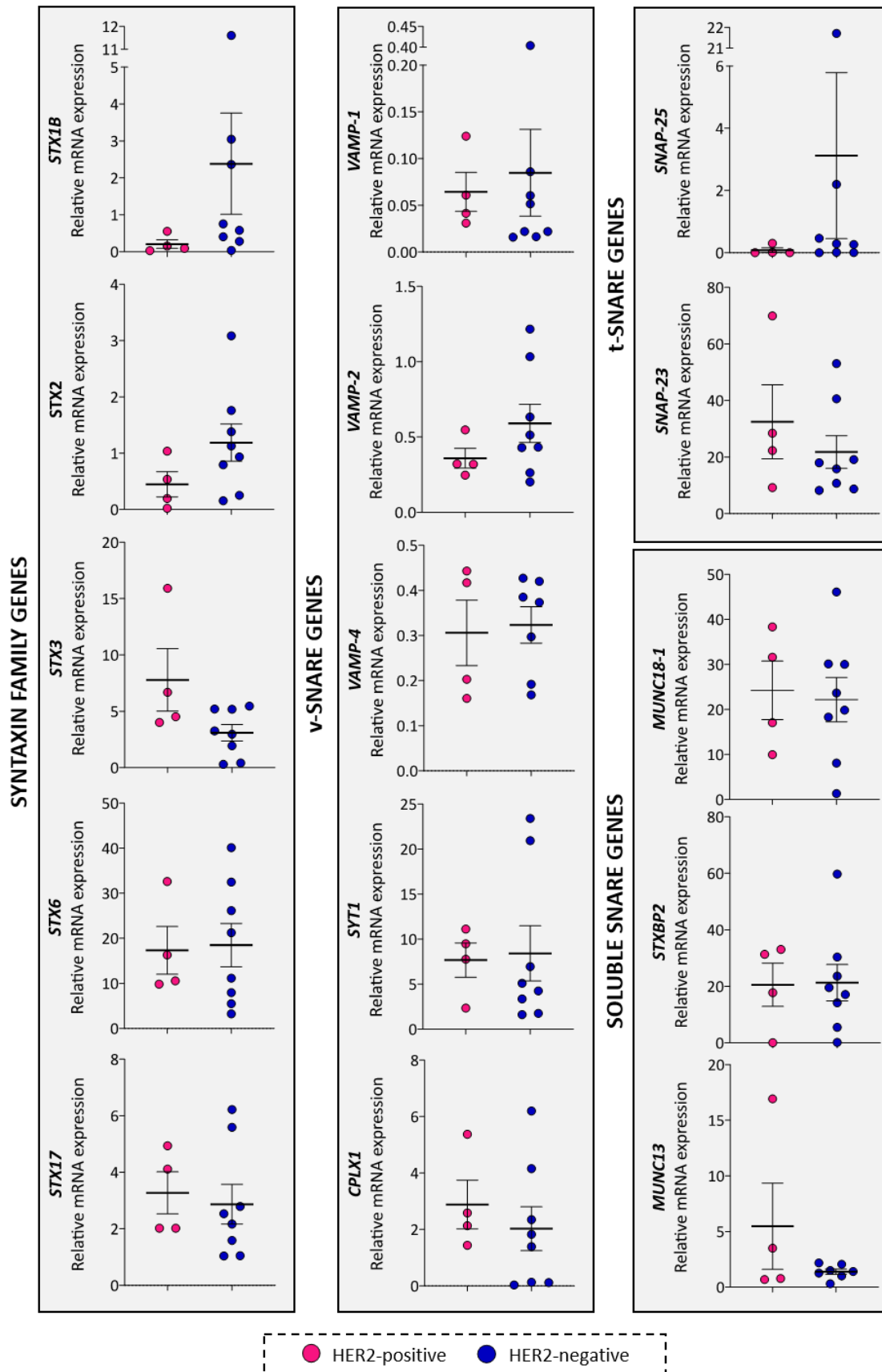
Annex figure 11 – (A) Decision tree diagram that shows how relative *SNAP-25* mRNA expression is grouped according to the distant metastasis (0: no metastasis, light orange; and 1: metastasis, dark orange) in HNSCC patients (Hospital de la Santa Creu i Sant Pau cohort). (B) Decision tree diagram that shows how relative *STX1A* mRNA expression is grouped according to the patient survival status (deceased of the disease, dark green, and living patients, light green) in HNSCC patients (TCGA public database). (C) On the top, disease free survival Kaplan-Meier curve of HNSCC tumours grouped according to *STX1A* expression, grouped as shown in previous figure. On the bottom survival table where the number at risk of HNSCC patients and the cumulative proportion surviving at the end of the interval in parenthesis is shown. Statistical analysis was performed using Logrank test.



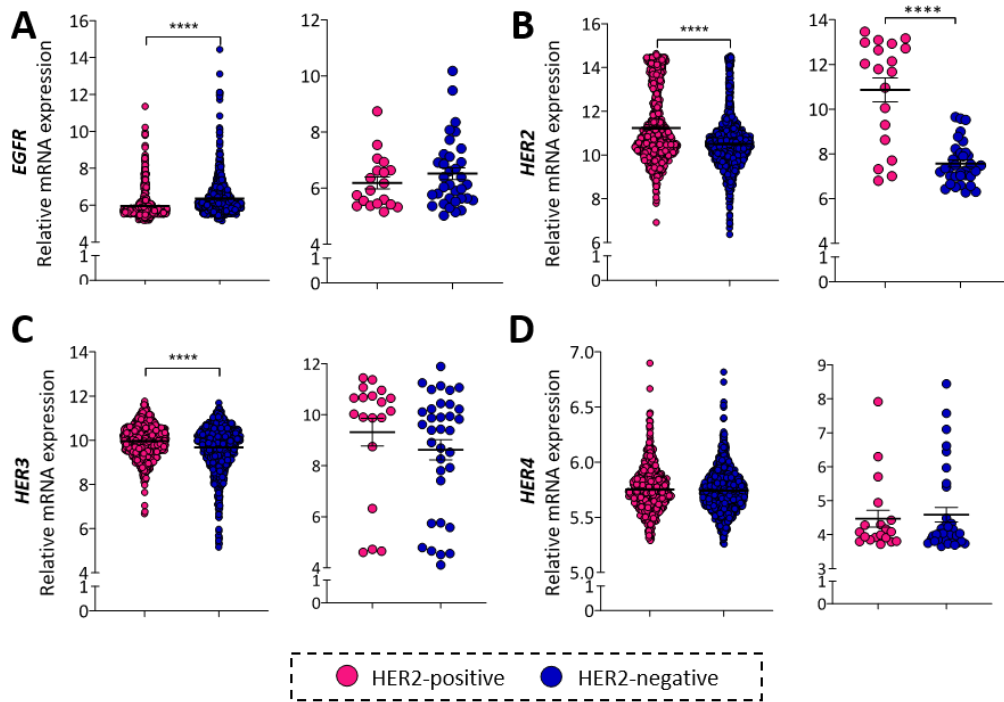
Annex figure 12 – (A) Graphical representation of relative *SNAP-25* mRNA expression according to neoplasm histologic grade. (B) Graphical representation of relative *SNAP-25* mRNA expression according to HPV status in HNSCC tumours. (C) Decision tree diagram that shows relative *SNAP-25* mRNA expression according to the patient survival status (deceased of the disease, dark green; and living patients, light green) in HNSCC patients. (D) On the top, disease free survival Kaplan-Meier curve of HNSCC tumours grouped according to *SNAP-25* expression. On the bottom survival table where the number at risk of HNSCC patients and the cumulative proportion surviving at the end of the interval in parenthesis is shown. (E) On the top, disease free survival Kaplan-Meier curve of HNSCC tumours grouped according to *STX1A* and *SNAP-25* expression. On the bottom survival table where the number at risk of HNSCC patients and the cumulative proportion surviving at the end of the interval in parenthesis is shown. Statistical analysis was performed using the U-Mann Whitney test, Chi-square test for the decision tree algorithm and Logrank test for D and E.



Annex figure 13 – Syntaxin and SNARE relative mRNA expression from CCLE database grouped according to HER2-positive and HER2-negative BC subtypes. Statistical analysis was performed using the U-Mann Whitney test. *p<0.05, **p<0.01, ***p<0.001, **** p<0.000.

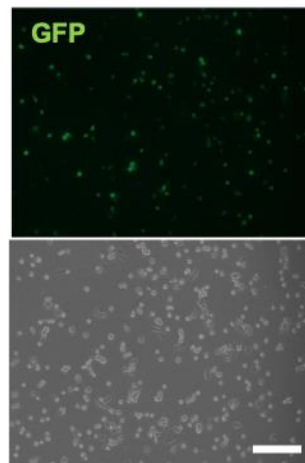


Annex figure 14 – Syntaxin and SNARE relative mRNA expression from lab BC cell lines database grouped according to HER2-positive and HER2-negative BC subtypes. Statistical analysis was performed using the student's *t*-test. * $p < 0.05$, ** $p < 0.01$, *** $p < 0.001$, **** $p < 0.000$.



Annex figure 15 – (A-D) Left graphic, analysis of relative *EGFR* (A), *HER2* (B), *HER3* (C) and *HER4* (D) expression in HER2-positive and HER2-negative BC tumours in METABRIC cohort. Right graphic, analysis of relative *EGFR*, *HER2*, *HER3* or *HER4* expression in HER2-positive and HER2-negative BC cell lines in CLLE database. Statistical analysis was performed using the U-Mann Whitney test.

MDA-MB-231



Annex figure 16 – STX1-DN plasmid transfection efficiency in MDA-MB-231 HER2-negative BC cells. On the top GFP fluorescence of the transfected cells, on the bottom image of the total of cells in the microscopic field. Scale bar = 100 μ m.

2. TABLES

Annex table 1 - Table shows the Spearman correlation of the genes with *STX1A*, the expression of the SNARE genes grouped among BC tumours expression low or high levels of *STX1A*, the expression of the studied genes among BC subtypes (HER2-positive and HER2-negative).

	Spearman correlation	Differential expression among <i>STX1A</i> BC subtypes		Differential expression among BC subtypes	
		Low <i>STX1A</i>	High <i>STX1A</i>	HER2-positive	HER2-negative
Syntaxin family	<i>STX1B</i>	5.293 (SEM = 0.004)	5.292 (SEM = 0.004)	5.288 (SEM=0.005)	5.295 (SEM = 0.004)
		(p = 0.541)	(p = 0.677)	(p = 0.266)	
	<i>STX2</i>	7.287 (SEM = 0.013)	7.307 (SEM = 0.013)	7.288 (SEM = 0.019)	7.302 (SEM = 0.012)
		(p = 0.062)	(p = 0.274)	(p = 0.446)	
	<i>STX3</i>	8.042 (SEM = 0.014)	8.254 (SEM = 0.015)	8.286 (SEM = 0.018)	8.075 (SEM = 0.012)
(p < 0.000)		(p < 0.000)	(p < 0.000)		
<i>STX6</i>	8.451 (SEM = 0.012)	8.525 (SEM = 0.015)	8.554 (SEM = 0.015)	8.453 (SEM = 0.010)	
	(p < 0.000)	(p < 0.000)	(p < 0.000)		
<i>STX17</i>	5.924 (SEM = 0.007)	5.993 (SEM = 0.008)	5.935 (SEM = 0.009)	5.926 (SEM = 0.006)	
	(p = 0.428)	(p = 0.374)	(p = 0.398)		
t-SNARES	<i>SNAP-23</i>	7.566 (SEM = 0.018)	7.214 (SEM = 0.019)	7.340 (SEM=0.023)	7.415 (SEM = 0.017)
		(p < 0.000)	(p < 0.000)	(p = 0.045)	
<i>SNAP-25</i>	5.816 (SEM = 0.015)	6.275 (SEM = 0.047)	6.016 (SEM = 0.028)	6.109 (SEM = 0.047)	
	(p < 0.000)	(p < 0.000)	(p = 0.002)		
v-SNARES	<i>VAMP-1</i>	7.583 (SEM = 0.019)	7.563 (SEM = 0.019)	7.418 (SEM=0.022)	7.658 (SEM = 0.016)
		(p = 0.460)	(p = 0.338)	(p < 0.000)	
	<i>VAMP-2</i>	7.660 (SEM = 0.017)	7.625 (SEM = 0.020)	6.325 (SEM = 0.019)	6.255 (SEM = 0.012)
		(p = 0.088)	(p = 0.032)	(p < 0.000)	
	<i>VAMP-4</i>	6.368 (SEM = 0.014)	6.192 (SEM = 0.014)	6.320 (SEM = 0.018)	6.248 (SEM = 0.011)
(p < 0.000)		(p < 0.000)	(p = 0.009)		
<i>SYT1</i>	6.047 (SEM = 0.029)	6.037 (SEM = 0.030)	6.166 (SEM = 0.038)	5.972 (SEM = 0.025)	
	(p = 0.018)	(p = 0.135)	(p < 0.000)		

	Spearman correlation	Differential expression among <i>STX1A</i> BC subtypes		Differential expression among BC subtypes		
		Low <i>STX1A</i>	High <i>STX1A</i>	HER2-positive	HER2-negative	
Soluble SNAREs	<i>CPLX1</i>	0.142	6.381 (SEM = 0.021)	6.582 (SEM = 0.028)	6.481 (SEM = 0.022)	6.484 (SEM = 0.028)
		(p < 0.000)	(p < 0.000)		(p = 0.762)	
	<i>MUNC18-1</i>	0.166	6.147 (SEM = 0.011)	6.248 (SEM = 0.016)	6.174 (SEM = 0.017)	6.212 (SEM = 0.011)
		(p < 0.000)	(p = 0.001)		(p = 0.002)	
<i>STXBP2</i>	0.182	8.423 (SEM = 0.016)	8.570 (SEM = 0.017)	8.584 (SEM = 0.019)	8.449 (SEM = 0.015)	
	(p < 0.000)	(p < 0.000)		(p < 0.000)		
<i>MUNC13</i>	0.095	6.112 (SEM = 0.006)	6.144 (SEM = 0.008)	6.186 (SEM = 0.008)	6.096 (SEM = 0.006)	
	(p < 0.000)	(p = 0.040)		(p < 0.000)		

Annex table 2 – Table shows the Spearman correlation of the genes with *STX1A*, the expression of the SNARE genes low or high levels of *STX1A* in HER2-positive BC tumours.

		Spearman correlation	Differential expression among <i>STX1A</i> BC subtypes	
			Low	High
Syntaxin family	<i>STX1B</i>	-0.004	5.286 (SEM = 0.007)	5.291 (SEM = 0.007)
		(p = 0.917)	(p = 0.762)	
	<i>STX2</i>	0.109	7.245 (SEM = 0.020)	7.334 (SEM = 0.023)
		(p = 0.005)	(p = 0.008)	
	<i>STX3</i>	0.210	8.192 (SEM = 0.026)	8.387 (SEM = 0.026)
(p < 0.000)		(p < 0.000)		
<i>STX6</i>	0.059	8.527 (SEM = 0.021)	8.582 (SEM = 0.023)	
	(p = 0.125)	(p = 0.054)		
<i>STX17</i>	-0.210	5.935 (SEM = 0.012)	5.935 (SEM = 0.014)	
	(p = 0.588)	(p = 0.688)		
t-SNAREs	<i>SNAP-23</i>	-0.288	7.500 (SEM = 0.030)	7.170 (SEM = 0.033)
		(p < 0.000)	(p < 0.000)	
	<i>SNAP-25</i>	0.263	5.771 (SEM = 0.024)	6.469 (SEM = 0.090)
		(p < 0.000)	(p < 0.000)	
v-SNAREs	<i>VAMP-1</i>	0.180	7.367 (SEM = 0.030)	7.507 (SEM = 0.035)
		(p = 0.641)	(p = 0.034)	
	<i>VAMP-2</i>	-0.800	7.592 (SEM = 0.029)	7.507 (SEM = 0.035)
		(p = 0.037)	(p = 0.006)	
v-SNAREs	<i>VAMP-4</i>	-0.299	6.440 (SEM = 0.025)	6.202 (SEM = 0.027)
		(p < 0.000)	(p < 0.000)	
	<i>SYT1</i>	-0.244	6.266 (SEM = 0.053)	6.258 (SEM = 0.053)
		(p < 0.000)	(p < 0.000)	
Soluble SNAREs	<i>CPLX1</i>	0.067	6.542 (SEM = 0.047)	6.429 (SEM = 0.033)
		(p = 0.079)	(p = 0.845)	
	<i>MUNC18-1</i>	0.167	6.098 (SEM = 0.020)	6.258 (SEM = 0.028)
		(p < 0.000)	(p < 0.000)	
<i>STXBP2</i>	0.160	8.594 (SEM = 0.029)	8.577 (SEM = 0.027)	
	(p = 0.678)	(p = 0.773)		
<i>MUNC13</i>	0.103	6.162 (SEM = 0.010)	6.212 (SEM = 0.014)	
	(p = 0.007)	(p = 0.800)		
EGFR/HER family	<i>EGFR</i>	0.205	5.790 (SEM = 0.032)	6.131 (SEM = 0.046)
		(p < 0.000)	(p < 0.000)	
	<i>HER2</i>	0.304	10.760 (SEM = 0.069)	11.750 (SEM = 0.096)
		(p < 0.000)	(p < 0.000)	
<i>HER3</i>	-0.640	9.998 (SEM = 0.038)	9.924 (SEM = 0.040)	
	(p = 0.095)	(p = 0.109)		
<i>HER4</i>	0.145	5.724 (SEM = 0.009)	5.785 (SEM = 0.012)	
	(p < 0.000)	(p = 0.001)		

Annex table 3 – Table shows the Spearman correlation of the genes with *STX1A*, the expression of the SNARE genes low or high levels of *STX1A* in HER2-negative BC tumours.

	Spearman correlation	Differential expression among <i>STX1A</i> BC subtypes	
		Low	High
Syntaxin family	<i>STX1B</i>	-0.001 (p = 0.982)	5.295 (SEM = 0.005) 5.296 (SEM = 0.005) (p = 0.986)
	<i>STX2</i>	0.012 (p = 0.682)	7.305 (SEM = 0.016) 7.300 (SEM = 0.016) (p = 0.895)
	<i>STX3</i>	0.232 (p < 0.000)	7.983 (SEM = 0.017) 8.159 (SEM = 0.016) (p < 0.000)
	<i>STX6</i>	0.047 (p = 0.103)	8.417 (SEM = 0.009) 8.486 (SEM = 0.015) (p < 0.000)
	<i>STX17</i>	0.021 (p = 0.467)	5.917 (SEM = 0.009) 5.934 (SEM = 0.009) (p = 0.243)
t-SNAREs	<i>SNAP-23</i>	-0.365 (p < 0.000)	7.574 (SEM = 0.210) 7.194 (SEM = 0.270) (p < 0.000)
	<i>SNAP-25</i>	0.113 (p < 0.000)	5.835 (SEM = 0.017) 6.266 (SEM = 0.062) (p = 0.001)
v-SNAREs	<i>VAMP -1</i>	0.033 (p = 0.253)	7.658 (SEM = 0.023) 7.658 (SEM = 0.024) (p = 0.876)
	<i>VAMP -2</i>	0.026 (p = 0.370)	7.684 (SEM = 0.021) 7.701 (SEM = 0.024) (p = 0.995)
v-SNAREs	<i>VAMP-4</i>	-0.256 (p < 0.000)	6.326 (SEM = 0.015) 6.156 (SEM = 0.018) (p < 0.000)
	<i>SYT1</i>	-0.44 (p = 0.125)	5.974 (SEM = 0.034) 6.251 (SEM = 0.019) (p < 0.000)
Soluble SNAREs	<i>CPLX1</i>	0.188 (p < 0.000)	6.364 (SEM = 0.024) 6.643 (SEM = 0.040) (p < 0.000)
	<i>MUNC18-1</i>	0.104 (p < 0.000)	6.173 (SEM = 0.012) 6.267 (SEM = 0.022) (p = 0.010)
	<i>STXBP2</i>	0.244 (p < 0.000)	8.368 (SEM = 0.019) 8.562 (SEM = 0.024) (p = 0.010)
	<i>MUNC13</i>	0.031 (p = 0.277)	6.091 (SEM = 0.008) 6.971 (SEM = 0.036) (p = 0.010)
EGFR/HER family receptors	<i>EGFR</i>	-0.062 (p = 0.030)	6.299 (SEM = 0.026) 6.432 (SEM = 0.049) (p = 0.117)
	<i>HER2</i>	0.187 (p < 0.000)	10.340 (SEM = 0.037) 10.730 (SEM = 0.056) (p < 0.000)
	<i>HER3</i>	0.069 (p = 0.016)	9.632 (SEM = 0.037) 9.742 (SEM = 0.039) (p = 0.167)
	<i>HER4</i>	0.161 (p < 0.000)	5.716 (SEM = 0.006) 5.772 (SEM = 0.009) (p < 0.000)

Annex table 4 – Correlation analysis of Syntaxins, SNAREs and EGFR/HER2 family of receptors. Spearman correlation analysis of the different relative mRNA expression of Syntaxins, SNAREs and EGFR/HER family gene expression. The significant values (2-tailed) are highlighted in bold.

		STX1A																							
STX1B	Correlation	0,14																							
	p	0,318																							
STX2	Correlation	-0,01	STX1B																						
	p	0,946	0,67																						
STX3	Correlation	0,108	0,139	STX2																					
	p	0,441	0,321	-0,577**	0																				
STX6	Correlation	,324*	-0,159	-0,337*	,354**	STX3																			
	p	0,018	0,255	0,014	0,009	STX6																			
STX17	Correlation	-0,104	-,325*	-,364**	,346*	,362**	STX17																		
	p	0,459	0,018	0,007	0,011	0,008	SNAP23																		
SNAP23	Correlation	0,01	-,397**	0,144	-0,089	0,004	0,054	SNAP-25																	
	p	0,941	0,003	0,304	0,528	0,979	0,699	SNAP-25																	
SNAP25	Correlation	0,084	-0,08	0,263	-0,23	0,006	-0,018	-0,007	SNAP-25																
	p	0,548	0,567	0,057	0,098	0,967	0,9	0,96	SNAP-25																
VAMP1	Correlation	-0,092	-0,103	-0,211	0,127	-0,211	0,251	-0,018	0,058	VAMP-1															
	p	0,512	0,461	0,13	0,366	0,129	0,069	0,9	0,681	VAMP-1															
VAMP2	Correlation	0,172	0,135	0,125	-0,147	-0,103	-0,13	-0,093	0,144	-0,043	VAMP-2														
	p	0,217	0,334	0,372	0,292	0,463	0,352	0,506	0,305	0,761	VAMP-2														
VAMP4	Correlation	0,244	0,016	0,133	0,036	0,261	0,232	0,104	0,228	-0,055	0,067	VAMP-4													
	p	0,078	0,911	0,341	0,796	0,059	0,094	0,46	0,1	0,693	0,636	VAMP-4													
SYN1	Correlation	0,072	0,202	0,147	-0,157	-0,172	-0,244	-0,175	0,187	-0,008	0,17	0,038	SYN1												
	p	0,606	0,146	0,292	0,261	0,219	0,078	0,211	0,181	0,956	0,222	0,787	SYN1												
CPLX1	Correlation	-0,039	0,011	-0,26	0,123	,333*	0,225	0	-0,174	-0,099	-0,088	0,193	-0,194	CPLX1											
	p	0,781	0,937	0,06	0,382	0,015	0,105	0,998	0,214	0,479	0,532	0,167	0,165	CPLX1											
MUNC18-1	Correlation	0,071	-0,174	,417**	-,348*	0,097	-0,09	0,046	0,132	0,03	0,141	,272*	0,044	-0,037	MUNC18-1										
	p	0,614	0,213	0,002	0,011	0,488	0,522	0,742	0,346	0,83	0,314	0,049	0,756	0,795	MUNC18-1										
STXBP2	Correlation	-0,191	0,051	-,549**	,285*	,305*	,279*	-0,203	-0,187	0,032	0,043	-0,124	-0,218	,323*	-,418**	STXBP2									
	p	0,17	0,718	0	0,039	0,027	0,043	0,145	0,181	0,819	0,762	0,375	0,117	0,018	0,002	STXBP2									
MUNC13	Correlation	0,245	0,235	-0,061	0,055	0,195	-0,124	-0,173	0,146	-0,119	0,122	0,013	,271*	,327*	-0,124	0,048	MUNC13								
	p	0,077	0,09	0,664	0,694	0,163	0,376	0,215	0,296	0,395	0,382	0,925	0,05	0,017	0,375	0,733	MUNC13								
EGFR	Correlation	-0,132	,301*	-0,046	-0,209	-,341*	-,430**	-0,096	-0,102	-0,141	0,201	-0,254	0,14	-0,178	0,016	0,125	0,065	EGFR							
	p	0,345	0,029	0,743	0,134	0,012	0,001	0,492	0,468	0,315	0,149	0,067	0,317	0,202	0,911	0,373	0,643	EGFR							
HER2	Correlation	,281*	-0,045	-,490**	,486**	,421**	,284*	0,238	-0,239	0,095	-0,187	-0,069	-0,199	0,13	-,299*	0,177	0,041	-,311*	HER2						
	p	0,041	0,752	0	0	0,002	0,039	0,086	0,085	0,498	0,18	0,621	0,153	0,354	0,03	0,205	0,773	0,023	HER2						
HER3	Correlation	0,159	-0,155	-,508**	,529**	,476**	,373**	0,099	-0,264	0,092	-0,192	0,027	-0,081	,348*	-,353**	,350*	0,104	-,515**	,731**	HER3					
	p	0,255	0,268	0	0	0	0,006	0,482	0,057	0,512	0,169	0,849	0,563	0,011	0,01	0,01	0,457	0	0	HER3					
HER4	Correlation	-0,015	-,272*	-0,13	0,27	0,255	,424**	0,157	-0,094	0,141	-,298*	0,076	-0,201	,387**	-0,013	-0,068	0,024	-,525**	0,256	,430**	HER4				
	p	0,913	0,049	0,354	0,05	0,065	0,002	0,26	0,502	0,314	0,03	0,59	0,149	0,004	0,925	0,627	0,863	0	0,064	0,001	HER4				

Annex table 5 – Correlation analysis of Syntaxins and SNAREs in our panel of BC cell lines. Pearson correlation analysis of the different relative mRNA expression of Syntaxins and SNAREs gene expression. The significant values (2-tailed) are highlighted in bold.

		<i>STX1A</i>															
<i>STX1B</i>	Correlation	-0,229															
	p	0,475															
<i>STX2</i>	Correlation	,757**	0,179														
	p	0,004	0,578														
<i>STX3</i>	Correlation	0,21	-0,303	-0,096													
	p	0,511	0,338	0,766													
<i>STX6</i>	Correlation	-0,121	-0,231	0,07	0,083												
	p	0,708	0,47	0,829	0,799												
<i>STX17</i>	Correlation	-0,082	-0,238	-0,03	0,476	,591*											
	p	0,801	0,457	0,927	0,118	0,043											
<i>CPLX1</i>	Correlation	-0,1	0,283	0,154	0,046	0,23	,585*										
	p	0,757	0,373	0,632	0,888	0,472	0,046										
<i>SYT1</i>	Correlation	-0,275	0,106	0,122	0,153	0,54	0,349	0,302									
	p	0,388	0,744	0,705	0,634	0,07	0,267	0,341									
<i>VAMP1</i>	Correlation	-0,165	-0,172	0,173	-0,086	,684*	,581*	0,544	,593*								
	p	0,609	0,593	0,591	0,79	0,014	0,048	0,068	0,042								
<i>VAMP2</i>	Correlation	0,08	-0,098	0,437	-0,099	0,507	0,372	0,27	,787**	,719**							
	p	0,804	0,762	0,156	0,759	0,093	0,234	0,396	0,002	0,008							
<i>VAMP4</i>	Correlation	0,365	-0,36	0,491	0,383	0,152	0,047	-0,224	0,447	0,244	0,455						
	p	0,27	0,276	0,125	0,244	0,656	0,891	0,508	0,168	0,469	0,16						
<i>SNAP-23</i>	Correlation	-0,007	-0,224	0,193	0,306	,711**	0,269	0,145	,722**	0,509	0,474	,609*					
	p	0,982	0,484	0,547	0,333	0,01	0,398	0,653	0,008	0,091	0,12	0,047					
<i>SNAP-25</i>	Correlation	-0,187	,950**	0,183	-0,364	-0,356	-0,367	0,269	-0,068	-0,184	-0,239	-0,338	-0,287				
	p	0,56	0	0,568	0,244	0,256	0,24	0,398	0,833	0,567	0,454	0,31	0,366				
<i>MUNC13</i>	Correlation	0,024	-0,126	-0,175	,907**	-0,125	0,349	-0,012	0,05	-0,113	-0,266	0,393	0,139	-0,113			
	p	0,945	0,712	0,608	0	0,715	0,292	0,972	0,884	0,742	0,429	0,232	0,683	0,741			
<i>MUNC18-1</i>	Correlation	0,273	-0,127	0,352	0,225	0,434	0,504	0,378	0,211	,669*	0,444	0,179	0,253	-0,1	0,188		
	p	0,39	0,693	0,261	0,482	0,159	0,094	0,226	0,509	0,017	0,149	0,599	0,428	0,757	0,58		
<i>STXBP2</i>	Correlation	-0,107	-0,233	0,123	-0,132	,784**	0,556	0,549	0,572	,761**	,628*	0,089	,591*	-0,328	-0,361	0,245	
		0,74	0,467	0,704	0,682	0,003	0,061	0,065	0,052	0,004	0,029	0,794	0,043	0,298	0,275	0,444	



